JOURNAL OF POLYMER SCIENCE: PART A VOL. 1, PP. 1473–1482 (1963)

Preparation and Properties of Copolymers of Maleic Anhydride and 2,2-Dimethylaminoethyl Methacrylate*

W. D. TAYLOR and A. E. WOODWARD, *College of Chemistry and Physics, The Pennsylvania State University, University Park, Pennsylvania*

Synopsis

Preparation of copolymers by reaction of *N,N*-dimethylaminoethyl methacrylate with maleic anhydride in an excess of the latter and the presence of water is described. The reaction products have been characterized by elemental analysis, by conductiometric titrations with acid and with base, and by specific viscosity determinations and light-scattering measurements in dilute solution. Although there is evidence that a 1:1 copolymer is formed, the results of the titrations and viscosity measurements indicate that this reaction product is a polyacid and not a polyampholyte. Light-scattering measurements indicate that aggregation occurs in aqueous solutions of this polymer. Attempts to prepare regularly alternating polyampholytes from other monomer combinations are described.

INTRODUCTION

In the course of an investigation concerned with the preparation of a polyampholyte with a regular alternation of acid and base groups along the chain and the study of its dilute solution properties, some copolymers of *N,N*-dimethylaminoethyl methacrylate (DMAEM) and maleic anhydride (acid) (MA) were prepared and characterization studies carried out. Although there was strong evidence which indicated the formation of a 1:1 copolymer, the expected ampholytic behavior was not observed, these polymers having the characteristics of polyacids instead.

Since copolymers formed from these monomers have not been described previously, the purpose of this paper is to present and discuss some details concerning the preparation, analysis, and dilute solution properties of such polymers.

EXPERIMENTAL

A. Reagents

Maleic anhydride (Eastman) was recrystallized from a chloroform - ligroin mixture. DMAEM (Monomer-Polymer) was vacuum-distilled at 4 cm. Hg, the liquid coming over at 70–73°C. being used. Crotonic acid

* This investigation was supported in part by research grant A-270 from the National Institute of Arthritis and Metabolic Diseases, Public Health Service.

(Eastman) was recrystallized from water. Allylamine (Monomer-Polymer) was vacuum-distilled at low pressures. Benzoyl peroxide (Bz_2O_2) (Eastman), 2,2-azobisisobutyronitrile (ABIN) (Eastman), and all solvents (reagent grade) were used as received.

B. Apparatus and Procedures

1. General Polymerization Techniques

All polymerizations were carried out in $^1/_2$ in. diameter Pyrex glass tubes sealed under vacuum following mixing of the ingredients and outgassing with prepurified nitrogen gas. The tubes were placed in an oil bath thermostatted to ± 0.5°C. Isolation of polymer was carried out by precipitation in a nonsolvent. Unless otherwise noted, the polymer obtained was purified further by dialysis against water and then freeze-dried.

2. Conductiometric Titrations

The apparatus consisted of a Hewlett-Packard (1000 cycle/sec.) audiogenerator, an oscilloscope, a Leeds and Northrup a.c. bridge, and black platinum dipping electrodes. All measurements were made with the cell placed in a water bath held at 25° ± 0.5°C. NaOH solutions 0.01–0.04M and HCl solutions 0.009–0.04M were employed, polymer concentrations being 0.005 to 0.02 g. in a total volume of 300 cc. To exclude CO_2, the titrations were carried out under a nitrogen atmosphere. Repeated titrations of solutions of maleic acid, of DMAEM, and of poly(methacrylic acid) gave experimental values within 1% of those expected.

3. Solution Viscosity

These measurements were carried out in three different viscometers, a Schurz-Immergut trigradient viscometer (flow times for water at 25 ± 0.2°C. of 361, 427, and 359 sec. for the three bulbs), an Ubbelohde dilution viscometer (flow time for water of 94 sec.), and a Cannon-type Ostwald viscometer (flow time for water of 63.2 sec.). The trigradient viscometer was calibrated with water and n-butanol at 25°C. and the other two viscometers with water at 0 and 25°C. In all cases the corrections were small compared with the reproducibility of the experiments, and the viscosities were assumed to be proportional to the flow times. The viscometers were suspended in a constant temperature water bath at 25 ± 0.02°C. Solutions were made up in doubly distilled water and passed through a fine sintered glass filter directly into the viscometer. Flow times were converted to specific viscosity (η_{sp}) in the usual manner: $\eta_{sp} = (t_{soln} - t_{solv})/t_{solv}$.

4. Light Scattering

These measurements were made with a Brice-Phoenix light-scattering photometer in a constant temperature room at 25 ± 1°C., blue light (4358 A.) being used. Both dissymmetry- and erlenmeyer-type cells were

employed, with measurements being made at about 10° angular increments from 45° to 135°. The erlenmeyer-type cell was tested with a fluoroscein solution and the Rayleigh ratio, R_θ, found to be constant when plotted versus $\sin^2 \theta/2$. This cell was calibrated with the use of doubly distilled water with the scattering at 90° taken to be 6.8×10^{-6} cm.$^{-1}$. Solutions were clarified by passing them through either fine or ultrafine sintered glass filters, as indicated in the next section, directly into the cell. Polymer solutions containing salt were prepared by dialysis against a salt solution of the molarity indicated.

Refractive index increments at 25°C. were obtained with a Brice-Phoenix differential refractometer. Calibration of this instrument was carried out with KCl solutions.

C. Polymer Preparations

1. Attempted Copolymerizations of MA and DMAEM in Organic Solvents

Copolymerizations were attempted in the following solvents: acetone, benzene, dioxane, and toluene. The weight ratio of MA/DMAEM was 6.8:1, the monomer/solvent weight ratio being 1:1 with Bz_2O_2 as initiator. At 30°C. a yellow color was observed immediately, and after 12 hr. the mixture was black, no detectable polymer being formed. These experiments were repeated in acetone and in glacial acetic acid with ABIN as initiator with the same results.

2. MA–DMAEM Copolymer A

This polymer was prepared in water containing suspended Bz_2O_2, the ratio on a weight basis of MA:DMAEM:H_2O:Bz_2O_2 being 8:2.5:20:0.01. After 24 hr. at 47°C. the polymer was precipitated in acetone, dialyzed, and freeze-dried, a yield of 8% being obtained. Elemental analysis gave 55.21%C, 7.57%H, 30.08%O, and 6.55%N by weight.

For this and similar reaction mixtures it was found that upon mixing the anhydride and the amine in water the reaction container became warm to the touch. This was not observed when organic solvents only were used, when maleic acid or crotonic acid were used in place of the anhydride, when the anhydride was dissolved in water alone, or when the base was added to water alone.

3. MA–DMAEM Copolymer B

This polymer was prepared at 25°C. in the absence of an added initiator, using a weight ratio of 3:1:5 of MA:DMAEM:H_2O with a 36-hr. reaction time, a 1% yield being obtained.

4. MA–DMAEM Copolymer C

The polymerization charge was initially 7.9:1:8:0.02 by weight in MA:DMAEM:H_2O:Bz_2O_2. After 24 hr. at 47°C. little viscosity increase was noted, so the tubes were opened, additional Bz_2O_2 added, and the ratio of

MA:DMAEM decreased to 6.8:1. After an additional 4 hr. at 45°C. the viscosity had increased markedly, and the polymer was then precipitated in acetone. Parts of this polymer were given the following treatments. C1 was precipitated three times from water into acetone and dried in a vacuum oven at 40°C. C3 was extracted with acetone and vacuum dried. C4 was dialyzed first against a HCl solution and then against a NaOH solution until no salt was detected in the solution outside the dialysis bag using $AgNO_3$. However, following recovery of C4 by freeze drying, elemental analysis gave 54.35%C, 8.10%H, 25.2%O, and 7.18%N, the remaining presumably being inorganic material. Further dialysis led to a polymer (C4ii) with 54.5%C, 8.53%H, 27.44%O, and 6.91%N, while still further dialysis yielded a polymer (C4iii) with 57.03%C, 6.95%H, 28.85%O, and 6.65%N. The total yield for copolymer C was 10–20%.

5. MA–DMAEM Copolymer D

Tubes containing MA, DMAEM, H_2O, acetone and Bz_2O_2 in weight proportions of 25:1.8:20:15.8:0.005 were heated for 5 hr. at 40°C. The polymer was precipitated with ether, dialyzed, and freeze-dried, a yield of 3% being obtained (54.7%C, 7.7%H, 31.1%O, 6.55%N).

6. MA–DMAEM Copolymer E

The reaction was carried out with 20:1.8:20:0.005 weight ratio of MA: DMAEM:0.1*N* HCl solution: Bz_2O_2 at 40°C. for 5 hr. The polymer was isolated by twice repeated precipitation in acetone, dissolving in water, and adding NaOH until the pH equalled 6, and then dialyzing versus water until the pH was constant (four days). The yield was 2%; 51.51%C, 8.98%H, 6.68%N, 32.83%O (by difference).

7. MA–DMAEM Copolymer F

A mixture of MA, DMAEM, H_2O, acetone and ABIN in the ratio 20:3.6:60:1.6:0.04 was heated for seven days at 65°C. The resulting polymer was precipitated in an ether–acetone mixture, dialyzed, and freeze-dried. The yield was 7%; 52.96%C, 7.53%H, 5.33%N, 34.18%O (by difference).

8. Control of Experiments

A 50:50 wt.-% solution of MA in water in the presence of suspended Bz_2O_2 was heated at 45°C. for 72 hr.; no polymer was obtained. This experiment was repeated with some triethylamine added, and again no polymer was formed.

A ~10 wt.-% solution of DMAEM in water plus suspended Bz_2O_2 yielded no polymer after heating at 45°C. for 24 hr. Heating for one week at 56°C. of 15 g. DMAEM, 20 g. acetone, 3 g. malonic acid, and ~0.004 g. Bz_2O_2 led to ~2% yield of polymer, 60.0%C, 9.4%H, 21.3%O, 9.0%N (calc: 61.2%C, 9.6%H, 20.4%O, 8.9%N). Conductiometric ti-

tration with acid accounted for 90% of the base groups, the product being assumed to be poly(DMAEM).

9. Additional Copolymerization Attempts

a. Maleic Anhydride and Allylamine (AA). Reaction of these monomers present in mixtures of 12:1:13:~0.002 g. of MA:AA:solvent:Bz_2O_2 after 12 hr. at 30°C. with acetone or dioxane as solvent and after one week at 45°C. with water as solvent did not yield polymer. Repeating the latter experiment at 56°C. led to a small amount (<1% yield) of brown material.

b. Crotonic Acid (CA) and DMAEM. With CA, DMAEM, acetone, water, and Bz_2O_2 in the weight ratio of 6:2:7.9:10:0.001 a 6% yield of polymer after five days at 60°C. was found. Similar results were obtained with the use of either ethyl acetate or acetone in place of the water–acetone mixture. Conductiometric titration indicated the presence of base groups in amounts of 60–90% of those expected for pure poly(DMAEM). With dioxane as solvent and ABIN as initiator, two experiments were performed in which the amounts of CA and DMAEM were varied from 1:2 to 5:1 by weight, the solvent weight being kept approximately constant at ~60%. Heating was carried out for three weeks at 60°C., the polymer then being precipitated in ether, followed by dialysis and freeze drying. Although conductiometric titrations indicated the presence of both acid and base functional groups, and elemental analysis showed that both types of monomer units were present, it was concluded from viscosity results that these polymers were polybases. Using benzene as solvent led to similar results for a 7:1 CA:DMAEM weight ratio.

c. Crotonic Acid and Allyamine. Reactions carried out in water plus suspended Bz_2O_2 at 56°C. (17:3 by weight of acid/base) led to small amounts (<1% yield) of brown material after one week.

RESULTS AND DISCUSSION

The results of conductiometric titrations on the various MA–DMAEM reaction products are summarized in Table I; in addition, empirical formulae for some of these polymers, as obtained from elemental analysis, are given. It is seen that the total number of titratable groups for all nine polymers is essentially the same, being $(7 \pm 1) \times 10^{-3}$ moles/g. With two exceptions, the number of basic groups appear to be zero within the sensitivity of the method, leading to the conclusion that these polymers are polyacids. That the analytical method could detect base groups if they were available is demonstrated by the results for poly(DMAEM) and for the DMAEM–crotonic acid reaction products (see experimental). The high result for basic groups in C4 can be explained as due to the presence of NaOH on the polymer as a consequence of the dialysis versus a solution of this reagent. If the number of acidic groups are taken as the total number of groups as found by back titration, then there is a constancy in this number in going from one preparation to another with the possible exception of poly-

mer F. The elemental analysis for F also differs from that of the others. In light of the elemental analysis results for C4, it is believed that further dialysis of E would also lead to a formula more in agreement with those for A, C4iii and D. Therefore, except for polymer F, it appears that all preparations have an empirical formula of $C_{10}H_{16}O_4N$, an acid group content of 7×10^{-3} moles/g. polymer, and a zero base group content.

TABLE I
Maleic Anhydride–*N*,*N*-Dimethylaminoethyl Methacrylate Copolymers

Designation	Empirical formula	Functional groups, moles/g. $\times 10^3$				
		Forward titration			Back titration	
		Acidic	Basic	Total	Base	Acid
A	$C_{10}H_{16}O_4N$	5.5	1.7 ± 0.02[a]	7.2	8.2	—
B		8.5	0	8.5	—	8.9
C1		8.4	0[a]	8.4	8.5	—
C3		7.1	0	7.1	6.4	—
C4i	$C_9H_{16}O_2N$	2.7	3.4	6.1	7.9 ± 1.3	—
C4ii	$C_9H_{17}O_{3.5}N$					
C4iii	$C_{10}H_{15}O_4N$					
D	$C_{10}H_{16.5}O_4N$	4.6 ± 0.05[a]	0	4.6	7.3	7.2 ± 0.5[a]
E	$C_9H_{19}O_4N$	—	0	—	8.1	—
F	$C_{11.5}H_{20}O_{5.5}N$	4.0	0	4.0	4.3	6.3
		6 ± 2	0.6 ± 0.6	6.6 ± 1.4	7.2 ± 1.1	7.5 ± 1.0

[a] Mean of two determinations.

Plots of η_{sp}/c versus concentration c for polymer D in pure water and for polymer E in 0.005, 0.050, and 0.500M NaCl solutions are given in Figure 1. The upward swing of the curve for polymer D with decreasing polymer concentration and the shift to lower η_{sp}/c values of the plots with increasing salt concentration for polymer E are both characteristic of polyelectrolytes in solution.[1] The viscosity η_{sp} of a 0.168 g./100 cc. solution of polymer F containing $1.3 \times 10^{-3}M$ NaOH was 1.2 times higher than that for a similar solution in pure water. On the other hand, η_{sp} of two 0.12 g./100 cc. solutions of polymer F containing 5.48×10^{-3} and $11.2 \times 10^{-3}M$ HCl, respectively, was 1.3 and 1.5 times lower than that for the pure polymer in water. This behavior is characteristic of a polyacid and is therefore in agreement with the titration results. The specific viscosity of a 0.23 g./100 cc. solution of polymer D in water was found to decrease from 1.32 to 1.12 after standing at 25°C. for 14 days under nitrogen, indicating the loss of the higher molecular weight material, possibly by precipitation.

Various light-scattering measurements were carried out on solutions of polymer D. The first measurements were made in 0.1M NaCl solutions, initially clarified by centrifugation at 40,000 rpm for 1 hr., then by filtration through a fine filter, at three concentrations from 0.37 to 0.10 g./100 cc. at angles of 45°, 90°, and 135°. Extrapolation of the dissymmetry ($R_{45°}/R_{135°}$) and $Kc/R_{90°}$ versus concentration plots to $c = 0$ yielded a root-mean-

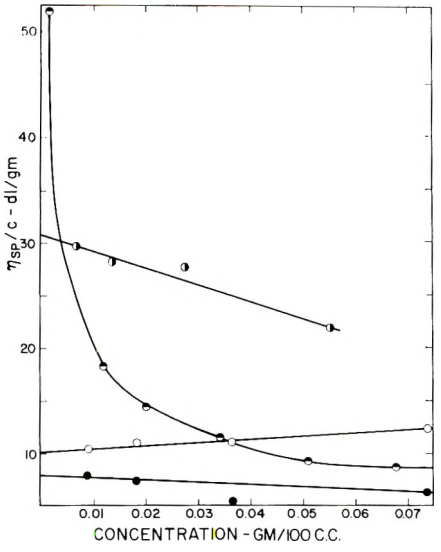

Fig. 1. η_{sp}/c vs. concentration c for maleic anhydride (acid)–*N,N*-dimethylaminoethyl methacrylate copolymers: (◓) copolymer D in water; (◑) copolymer E in 0.005*M* NaCl; (○) copolymer E in 0.05*M* NaCl; (●) copolymer E in 0.5*M* NaCl.

square end-to-end distance $\langle\sqrt{r^2}\rangle_z$ of 915 A. and a weight-average molecular weight $\bar{M}_w$ of 2×10^6. However, upon making measurements in the erlenmeyer cell at concentrations of 0.02–0.002 g./100 cc. in aqueous solutions containing 0–0.5*M* NaCl, clarification being carried out with fine filters, twisted Zimm plots[2] were obtained, and extrapolation of these to zero concentration and zero angle gave negative intercepts. In addition, dissymmetries of ~10 and ~3 were found for the solutions in pure water and 0.1*M* NaCl, respectively. These results indicate either an extreme polydispersity or the presence of particulate matter. Following several weeks storage under nitrogen, precipitates were observed in all of the solutions. Two angular runs were made on solutions in pure water made up separately but both clarified by an ultrafine filter, concentrations of 0.08–0.005 g./100 cc. being used. Zimm plots, such as that shown in Figure 2, were obtained with positive zero angle line slopes and negative zero concentration line slopes, thereby have dissymmetries less than one.

Angular behavior such as this was reported earlier by Ehrlich and Doty[3] for a synthetic polyampholyte in pure water. However, a negative zero angle line slope was found which is not in agreement with the present behavior. Also, it was noted in this study that a decrease by a factor of two or more in the Kc/R_θ value at all angles took place when the solution was made 0.005*M* in NaCl; addition of more salt (0.05*M*) caused further decreases. Ehrlich and Doty found an increase in similar experiments. However, in both studies the slope of the plot of Kc/R_θ versus $\sin^2\theta/2$ plot becomes positive, and therefore the dissymmetry becomes greater than unity upon addition of salt. The light-scattering results for polymer D

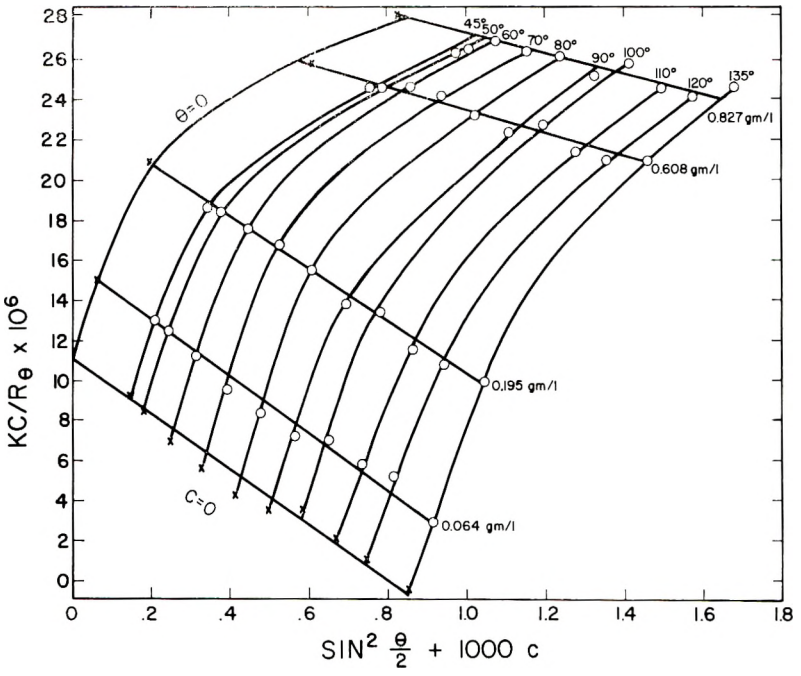

Fig. 2. Light-scattering (Zimm) plot for maleic anhydride (acid)–*N*,*N*-dimethylaminoethyl methacrylate copolymer D in water.

in water using ultrafine filtration were also found to be time-dependent, $^1/R_{90}$ for a 0.2 g./100 cc. solution decreasing in three days by a factor of 25% but staying essentially constant over the next nine days; $R_{45°}/R_{135°}$ increased from a value of 2.7 to 4.3 after three days and reached a value of 5.6 in twelve days. This latter result is a further indication that aggregation is occurring leading to very high molecular weight species. It does not appear that the light-scattering results for polymer D can be explained as typical polyelectrolyte behavior,[4,5] although few data on polyelectrolytes in pure water are available.

Since under the conditions used for the copolymerizations, maleic anhydride (or acid) does not form high polymer and DMAEM polymerizes little, if at all, a 1:1 (monobase–diacid) copolymer is expected as the reaction product due to the large amounts of acid present. Such a product would have an empirical formula of $C_{12}H_{19}O_6N$ and would contain 7.4×10^{-3} moles of acid and 3.7×10^{-3} moles of base groups per gram of polymer, respectively. It is readily apparent that this hypothetical reaction product does not have the characteristics found experimentally for polymers A–F. Although the number of acid groups correspond approximately, the absence of titratable base groups and the high amount of N in the analyses indicate the presence of another structure.

One possible reaction which would lead to loss of amine groups with retention of the nitrogen is amide formation. In the present case this could

occur by reaction of the amine group with an anhydride or acid unit either in the polymer or before polymerization occurs, resulting in lactam formation and the production of methanol. The apparent necessity of having the anhydride present initially instead of the acid clearly indicates that reaction of the base with the anhydride (and water) takes place immediately upon mixing the monomers in water. Assuming that a 1:1 copolymer is formed in the polymerization an empirical formula of $C_{11}H_{15}O_5N$ and an acid group titer of 4.1×10^{-3} moles/g. of polymer results. This appears to be in approximate agreement with the results for polymer F but does not completely explain the results for the other polymers. Formulae similar to those for polymers A, D, and C4iii can be obtained for a copolymer containing two base units to one acid ($C_{10}H_{17}O_4N$) or for a 1:1 copolymer with CH_3 and CO_2 split out ($C_{10}H_{16}O_4N$), the latter presumably involving a methyl unit from the base monomer and one of the carboxyl groups on the diacid monomer unit. However, the acid titer would be 4.7×10^{-3} and 4.4×10^{-3} moles/g. polymer, respectively, and there would also be the same numbers of base groups present. Therefore, due to discrepancies between the results of elemental analysis and conductiometric titrations, it is not possible to elucidate completely at this time the reactions that are occurring in this system.

We are grateful to Dr. Shintaro Sugai for help with some of the experimental work given herein.

References

1. Fuoss, R. M., and U. P. Strauss, *J. Polymer Sci.*, **3**, 246 (1948); R. M. Fuoss, *Discussions Faraday Soc.*, **11**, 125 (1951).
2. Muus, L. T., and F. W. Billmeyer, Jr., *J. Am. Chem. Soc.*, **79**, 5079 (1957).
3. Ehrlich, G., and P. Doty, *J. Am. Chem. Soc.*, **76**, 3764 (1954).
4. Oth, A., and P. Doty, *J. Phys. Chem.*, **56**, 43 (1952).
5. Schneider, N. S., and P. Doty, *J. Phys. Chem.*, **58**, 762 (1954).

Résumé

On décrit la préparation de copolymères de méthacrylate de *N,N*-diméthylaminoéthyle et d'anhydride maléique avec un excès de ce dernier et en présence d'eau. On caractérise les produits de réaction par analyse élémentaire, partitrations conductimétriques d'acide et de base, et par déterminations de viscosité spécifique et mesures de diffusion lumineuse en solution diluée. Bien que la formation d'un polymère 1:1 soit évidente, les résultats des titrations et des mesures de viscosité montrent que le produit de réaction est un polyacide et non un polyampholyte. Les mesures de diffusion lumineuse indiquent qu'il y a formation d'aggrégats en solution aqueuse de ce polymère. On décrit les essais de préparations de polyampholytes alternants de façon régulière à partir d'autres combinaisons de monomères.

Zusammenfassung

Die Darstellung von Copolymeren durch Reaktion von *N,N*-Dimethylaminoäthylmethacrylat mit Maleinsäureanhydrid im Überschuss und in Gegenwart von Wasser wird beschrieben. Die Reaktionsprodukte wurden durch Elementaranalyse, durch konduktometrische Titration mit Säure und Base sowie durch Bestimmung der spezifischen Vis-

kosität und Lichtstreuungsmessungen in verdünnter Lösung charakterisiert. Obgleich Hinweise auf die Bildung eines 1:1-Copolymeren bestehen, zeigen die Ergebnisse der Titrationen und Viskositätsmessungen, dass das Reaktionsprodukt eine Polysäure und nicht ein Polyampholyt ist. Lichtstreuungsmessungen sprechen für das Auftreten einer Aggregation in der wässrigen Lösung dieses Polymeren. Versuche zur Darstellung regelmässig alternierender Polyampholyte aus anderen Monomerkombinationen werden beschrieben.

Received February 19, 1962

JOURNAL OF POLYMER SCIENCE: PART A VOL. 1, PP. 1483–1490 (1963)

Dynamic Shear Behavior of Poly(γ-benzyl L-Glutamate), Poly(D,L-Propylene Oxide), and Poly(ethyl Vinyl Ether)*

R. G. SABA, J. A. SAUER, and A. E. WOODWARD, *Department of Physics, The Pennsylvania State University, University Park, Pennsylvania*

Synopsis

The dynamic mechanical properties in shear have been studied for poly(γ-benzyl-L-glutamate), poly(D,L-propylene oxide), and poly(ethyl vinyl ether) in the 95–100° to 240–340°K. region by use of a torsional pendulum in free decay at frequencies of 0.05–1 cycles/sec. Poly (γ-benzyl L-glutamate) exhibits a prominent loss maximum at 288°K. (0.18 cycles/sec.) attributed to reorientational motions principally of the side chains. For poly(D,L-propylene oxide) two loss peaks are found at ~120°K. (0.59 cycles/sec.) and 211°K. (0.37 cycle/sec.), being attributed to motion in the amorphous regions of a small (3–4) and large number of segments, respectively. In the case of poly(ethyl vinyl ether) the principal dispersion region is found at $\gtrsim$230°K., while a secondary loss maximum is located at ~100°K. This behavior is similar to that reported for polypentene-1 and polybutene-1, except that the two motional processes are shifted to lower temperatures.

I. INTRODUCTION

Previous studies of the dynamic mechanical properties of polypeptides have been limited to wool[1] and silk,[2] only a narrow temperature range being covered. To obtain further information about the properties of such compounds, it was felt that a study of some synthetic polypeptides would prove of interest. Due to difficulties in sample preparation, it has been possible thus far to make mechanical loss and storage modulus measurements on only one such polymer poly(γ-benzyl L-glutamate)

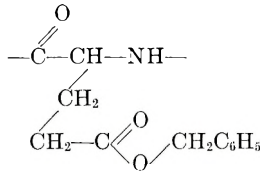

The data obtained are presented and discussed herein.

Dynamic mechanical studies have been reported for the linear poly-

* Supported in part by research grant G14143 from the National Science Foundation.

(alkylene oxides), $[-O-(CH_2)_x-]_n$, where the alkylene group was methylene,[3-6] ethylene,[5,6] trimethylene,[7] and tetramethylene.[7] The latter two compounds exhibit a secondary mechanical loss peak at ~160°K. (~100 cycles/sec.). There is also evidence[4] for the presence of such a maximum for the first member of the series, polyoxymethylene, although at low frequencies it may be part of the principal amorphous transformation region. In order to investigate this secondary maximum further, the dynamic mechanical properties of poly(D,L-propylene oxide), $[-OCH_2-CH(CH_3)-]_n$ were studied by use of a torsional pendulum, as described below.

One dynamic mechanical investigation at low frequencies of poly(ethyl vinyl ether), $[-CH-CH_2(OCH_2CH_3)-]_n$, has been previously reported.[8] However, the data were not given, only peak positions being reported. Further data were deemed desirable for this polymer and, as described below, these have been obtained in the 96°–240°K. region at a frequency which varied from 0.9 to 0.4 cycles/sec.

II. EXPERIMENTAL

A. Sample

Poly(γ-benzyl L-glutamate), *P*γBLG, was obtained through the courtesy of Dr. E. K. Blout of the Polaroid Corporation. This polymer was reported to have a reduced specific viscosity of 1.29 at a concentration of 0.2% in dichloroacetic acid, giving a weight-average molecular weight of 2×10^5.

Poly(D,L-propylene oxide), PDLPO, was furnished by the Dow Chemical Company. The poly(ethyl vinyl ether), PEVE, was supplied by Union Carbide Plastics Company.

Films of the three polymers for the dynamic mechanical measurements were prepared by evaporation from a solution. The experimental dimensions, the densities, and the solvents used in the preparation of the films are given in Table I. Densities were measured at 20°C. by a displacement technique, the fluid employed being distilled water.

No preferred orientation was observed when the PγBLG specimens were examined with a 1200× polarizing microscope.

TABLE I

Polymer	Width, in.	Thickness, in.	Length, in.	Density, g./cc.	Solvent
PγBLG					
1	0.125	0.0045	1.5	1.177	Chloroform
2	0.125	0.0105	1.5	—	
PDLPO	0.117	0.013	2.0	1.212	Acetone
PEVE					
1	0.125	0.017	2.0	0.944	Ether
2	0.250	0.017	2.5	—	

B. Apparatus and Procedures

The dynamic mechanical measurements were carried out in shear by use of a free decay-type torsional pendulum. The sample, in the form of a strip of film, was held vertically between two clamps. The upper clamp, supporting the system, was attached to a rigid support rod and the lower clamp was attached to a freely suspended torque bar. The amplitude of the oscillations was obtained visually using a small telescope which focused on the image of an illuminated scale reflected by a mirror attached to the torque bar. This suspension system was surrounded by a hollow, double-walled copper cylinder through which a coolant was circulated. In order to maintain a uniform warming rate throughout the entire temperature range, a heating element, consisting of Nichrome wire wound about the outside surface of the cylindrical cryostat, was employed from approximately 240°K. to temperatures at which flow of the polymer took place. This entire assembly was contained within a steel chamber which could be evacuated.

The specimen was clamped in place, the chamber evacuated, and then dry nitrogen gas was introduced to facilitate heat exchange within the chamber. The sample was then cooled by circulation of liquid nitrogen. Measurements were made at intervals of about 2°C. as the sample warmed up, the rate of warming being 0.1°C./min.

The usual procedures were used for obtaining the logarithmic decrement (log dec) and the storage modulus (G'), a correction being made in the latter quantity to account for the effect of the tensile load. Complete details of the apparatus and procedures are given elsewhere.[9,10]

III. RESULTS AND DISCUSSION

A. Poly(γ-benzyl L-Glutamate)

The dynamic mechanical results for PγBLG as a function of temperature from 100 to 310°K. are given in Figure 1 in terms of the logarithmic decrement and the shear storage modulus for the 0.0045 in. thick specimen. At a temperature of 310°K. coinciding with the upswing in logarithmic decrement, the sample was observed visually to undergo extension. With the sample of 0.0105 in. thickness an upswing in damping was also obtained, but no change of length was evident.

The data of Figure 1 show that this polymer exhibits a sizeable loss maximum at 288°K. (0.18 cycle/sec.) which has associated with it a modulus decrease of about two decades. A proton magnetic resonance study of a similar compound has shown that a line-narrowing process, involving considerable side chain motion at frequencies of 10^4–10^5 cycles/sec. and above, has been found[11] at $\geq$300°K. It is believed that the mechanical process is a consequence of the same type of motion, its occurrence at a lower temperature being due to the lower frequency of the mechanical method.

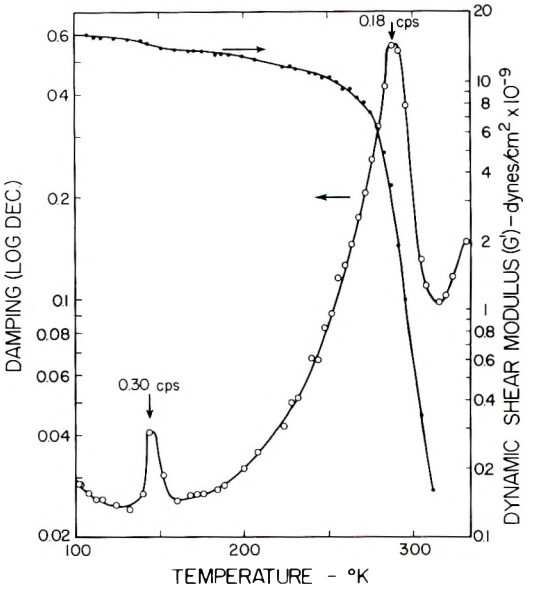

Fig. 1. Damping (log dec) and dynamic shear modulus (G') vs. temperature for poly-(γ-benzyl L-glutamate).

The data also show that a small sharp loss peak, and an accompanying modulus dispersion, occurs at 143°K. (0.30 cycles/sec.) in addition to an upswing in logarithmic decrement as the temperature is decreased from 125 to 100°K. Both of these effects are reproducible, but their causes are not at present known.

B. Poly(D,L-propylene Oxide)

As is evident from the experimental data in Figure 2, PDLPO is found to have two loss maxima, one of low strength, γ, (117–124°K.; 0.59 cycle/sec.) and the other much more prominent, β, (211°K.; 0.37 cycle/sec.), with associated modulus dispersions of small and large magnitudes, respectively.

The β peak is believed to be due to segmental motion involving a large number of chain units in the amorphous regions accompanying the glass transition. A value of 195°K. for T'_g has been given previously[12] for an amorphous sample of low molecular weight. The γ peak is tentatively ascribed to the cooperative motion of a limited number of segments, possibly three or four, in the amorphous regions.

A proton magnetic resonance study[13] of PDLPO indicates the presence of the main amorphous transformation process at ~210–250°K. (10^4–10^3 cycles/sec.). In addition, the single component of the spectra was found to slowly narrow in width in going from $\leq$77 to 190°K.

For polypropylene two mechanical loss maxima corresponding to those found for PDLPO have been reported by a number of investigators.[7,14–20]

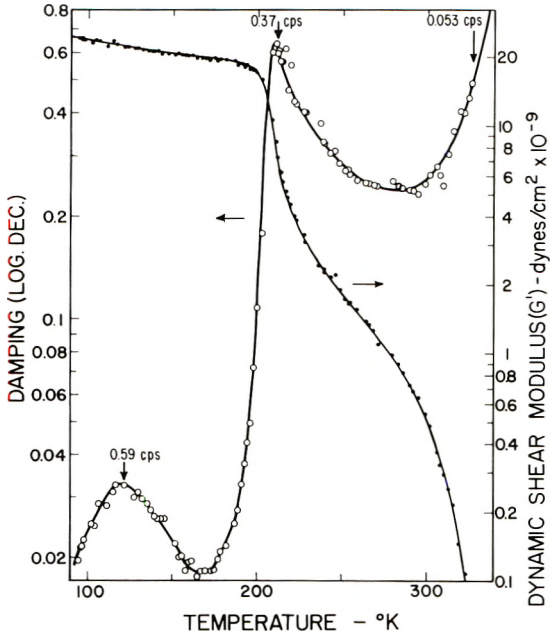

Fig. 2. Damping (log dec) and dynamic shear modulus (G') vs. temperature for poly-(D,L-propylene oxide).

With the present apparatus with a sample of annealed (125°C. for 3 hr.) polypropylene film having a density at 23°C. of 0.909 g./cc. these maxima were found to be located at 200–220°K. (0.32 cycle/sec.; $[\log \text{dec}]_{\max} = 0.03$) and at 272°K. (0.25 cycle/sec.; $[\log \text{dec}]_{\max} = 0.22$). Assuming these maxima to have the same molecular origin as the two found for PDLPO, it is seen that the introduction of an —O— unit in the backbone chain leads to a considerable reduction in the temperature at which both maxima appear. The changes in crystallinity, chain configuration, and chain conformation accompanying this change in composition might account at least partially for this shift.

The final upswing in damping and drop in modulus starting at ~290°K. is attributed to the increased chain mobility as a consequence of crystalline melting, the melting point for such a polymer being reported as 345–347°K.[21]

C. Poly(ethyl Vinyl Ether)

The damping and dynamic storage modulus in shear are given in Figure 3 for PEVE. The principal amorphous transition is seen as an upswing in damping and a drop in modulus which become very sharp at temperatures above 230°K. The low temperature peak evident at ~100°K. (0.90 cycle/sec.) is due to cooperative motion of three or four segments, most probably including those in the side chain.

High frequency (2×10^6 cycles/sec.) dielectric measurements[22] gave a

secondary loss maximum at ~230°K., while two small mechanical loss peaks were found[22] at the same frequency at ~230 and ~190°K., in addition to the two questionable ones reported earlier[8] at ~160 and ~200°K. at 8 cycles/sec.

Comparison of the plot of logarithmic decrement versus temperature for PEVE with that for the α-olefin analog polypentene-1, [—CH_2—CH-($CH_2CH_2CH_3$)—]$_n$, would be of interest, but unfortunately no data at this frequency have been published. However, at higher frequencies (~10^3 cycles/sec.) a partially crystalline (~30%) polypentene-1 sample was found[23] to have two peaks at 145°K. (2350 cycles/sec.) and 290°K. (430 cycles/sec.), behavior similar to that for PEVE. Since it was shown[23] that polypentene-1 and polybutene-1 had almost identical mechanical

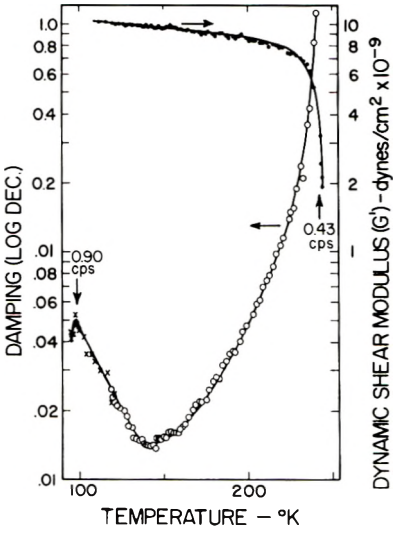

Fig. 3. Damping (log dec) and dynamic shear modulus (G') vs. temperature for poly-(ethyl vinyl ether): (×) sample no. 1; (●,○) sample no. 2.

loss–temperature plots below 300°K. at frequencies of ~10^3 cycles/sec., a comparison of the data for PEVE with that for a polybutene-1 sample (ρ = 0.898 g./cc. at 21°C.; crystallinity = 40%) obtained with the present apparatus, should be of interest. Such a test has been run on the polybutene-1 sample. The data show a damping peak at 257°K. (0.42 cycle/sec.; log dec = 1.3) and an upswing in logarithmic decrement with decreasing temperature starting at about 160°K. (log dec = 0.023); at the lowest temperature employed, 128°K., the logarithmic decrement had increased to a value of 0.097. Therefore it appears that the substitution of —O— for —CH_2— in the side chain leads to a shift of both motional processes to lower temperatures. However, changes of crystallinity and tacticity as well as composition are also involved and may account for at least a portion of these changes.

We are grateful to Drs. E. K. Blout of Polaroid Corporation, H. W. McCormick of the Dow Chemical Company and H. F. Wakefield of Union Carbide Plastics Company for supplying samples.

References

1. Mackay, R. H., and J. G. Downes, *J. Appl. Polymer Sci.*, **2**, 32 (1959).
2. Fujino, K., H. Kawai, and T. Horino, *Textile Res. J.*, **25**, 722 (1955).
3. Ishida, Y., M. Matsuo, H. Ito, M. Yoshino, F. Irie, and M. Takayanagi, *Kolloid-Z.*, **174**, 162 (1961); Y. Ishida, *Kolloid-Z.*, **171**, 149 (1960).
4. Thurn, H., *Carl Würster Anniversary Publication*, Badische Anilin and Soda Fabrik, December 7, 1960, pp. 321–33.
5. Read, B. E., and G. Williams, *Polymer*, **2**, 239 (1961).
6. McCrum, N. G., *J. Polymer Sci.*, **54**, 561 (1961).
7. Willbourn, A. H., *Trans. Faraday Soc.*, **54**, 717 (1958).
8. Schmieder, K., and K. Wolf, *Kolloid-Z.*, **134**, 149 (1953).
9. Wolf, J., Ph.D. Dissertation, The Pennsylvania State University, 1960.
10. Saba, R. G., M. S. Thesis, The Pennsylvania State University, 1962.
11. Kail, J. A., J. A. Sauer, and A. E. Woodward, *J. Phys. Chem.*, **66**, 1292 (1962).
12. St. Pierre, L. E., and C. C. Price, *J. Am. Chem. Soc.*, **78**, 3432 (1956).
13. Slichter, W. P., *Makromol. Chem.*, **34**, 67 (1959).
14. Sauer, J. A., R. A. Wall, N. Fuschillo, and A. E. Woodward, *J. Appl. Phys.*, **29**, 1385 (1958).
15. Muus, L. T., N. G. McCrum, and F. C. McGrew, *SPE Journal*, **15**, 368 (1959).
16. Staverman, A. J., and I. J. Heijboer, *Kunststoffe*, **50**, 23 (1960).
17. Wada, Y., H. Hirose, H. Umebayashi, and M. Otomo, *J. Phys. Soc. Japan*, **15**, 2324 (1960).
18. Lewis, A. F., and M. C. Tobin, paper presented before the Polymer Division, 139th Meeting of the American Chemical Society, St. Louis, Mo., March 1961.
19. Oberst, H., and L. Bohn, *Rheol. Acta*, **1**, 608 (1961).
20. Illers, K. H., *Rheol. Acta*, **1**, 616 (1961).
21. Price, C. C., M. Osgan, R. E. Hughes, and C. Shambelan, *J. Am. Chem. Soc.*, **78**, 690 (1956); C. K. Price and M. Osgan, *J. Am. Chem. Soc.*, **78**, 4787 (1956.)
22. Thurn, H., and K. Wolf, *Kolloid-Z.*, **148**, 16 (1956).
23. Woodward, A. E., J. A. Sauer, and R. A. Wall, *J. Polymer Sci.*, **50**, 117 (1961).

Résumé

On a étudié les propriétés dynamiques mécaniques au cisaillement au moyen d'un pendule à torsion en chute libre, aux fréquences de 0.05–1 cycle/sec., dans le cas du poly-(γ-benzyl-L-glutamate), du poly(D,L-oxyde de propylène) et de l'éther polyéthyl vinylique dans la région de 95–100° à 240–340°K. On observe un maximum isolé bien marqué pour le poly(γ-benzyl-L-glutamate) à une température de 288°K. (0.18 cycle/sec.), attribué aux mouvements de réorientation, principalement des chaines latérales. Pour le poly-(D,L-oxyde de propylène) on trouve deux sommets isolés à ~120°K. (0.59 cycle/sec.) et 211°K. (0.37 cycle/sec.), attribués aux mouvements dans les régions amorphes respectivement d'un petit (3–4) et d'un grand nombre de segments Dans le cas de l'éther poly-éthyl vinylique, la principale région de dispersion fut trouvée à $\gtrsim$230°K., tandis qu'un second maximum isolé se trouve à ~100°K. Le comportement est le mème que celui décrit pour le polypentène-1 et le polybutène-1; les deux processus de réorintation se retrouvent toutefois à des température plus basses.

Zusammenfassung

Die dynamisch-mechanischen Scherungseigenschaften von Poly-γ-benzylglutamat, Poly-D,L-propylenoxyd und Polyäthylvinyläther wurden im Bereich von 95–100° bis

240–340°K. unter Benützung eines Torsionspendels bei Frequenzen von 0,05 bis 1 Hz untersucht. Poly-γ-benzyl glutamat zeigt bei 288°K. (0,18 Hz) ein ausgeprägtes Verlustmaxima, das auf Reorientierungsbewegungen, hauptsächlich der Seitenketten, zurückgeführt wird. Bei Poly-D,L-propylenoxyd werden zwei Verlustmaxima bei ~120°K. (0,59 Hz) und 211°K. (0,37 Hz) festgestellt, die der Bewegung einer kleinen (3–4) bzw. grossen Zahl von Segmenten in den amorphen Bereichen zugeschrieben werden. Im Falle des Polyäthylvinyläthers liegt das Hauptidispersionsbereich bei $\gtrsim$ 230°K. und ein sekundäres Verlustmaximum bei ~100°K. Dieses Verhalten ist ähnlich dem bei Polypenten-1 und Polybuten-1 gefundenen, mit dem Unterschied, dass die beiden Bewegungsvorgänge zu tieferer Temperatur verschoben sind.

Received March 5, 1962

JOURNAL OF POLYMER SCIENCE: PART A VOL. 1, PP. 1491–1499 (1963)

Cyclopolymerization. I. Structure of Polyacrylic Anhydride*

J. MERCIER and G. SMETS, *Laboratoire de Chimie Macromoléculaire, University of Louvain, Belgium*

Synopsis

The structure of the cyclopolymers of acrylic anhydride has been examined by infrared spectrometry (cyclized units) and by chemical analysis (bromometry for vinyl unsaturation). The infrared analysis was based on the study of the two carbonyl absorption bands at about 1750 and 1810 cm.$^{-1}$; two types of cyclized hexaatomic anhydrides, different in their stereochemical structure, have been shown to be present. By comparison with the *meso* and racemic varieties of α,α'-dimethyl glutaric anhydride, the syndiotactic structure (racemic) has been assigned to the polyanhydride obtained at 35°C. in cyclohexanone. By heating, or in the presence of traces of acid this variety isomerizes into the isotactic form (*meso*). Pentaatomic cyclized units are formed only by polymerization at high temperatures, e.g., 115°C. (bands at 1780 and 1860 cm.$^{-1}$). On the other hand, residual unsaturation has always been found on the basis of the vinyl absorption band at 1625 cm.$^{-1}$; its intensity increases with an increase of monomer concentration during polymerization. The chemical analysis of the cyclopolymers by bromometry makes it possible to evaluate quantitatively the ratio k_c/k_p of the rate constant of vinyl propagation to that of cyclization; at 35°C. this ratio is equal to 0.17. By analysis of the polymers obtained at 25, 45, and 70°C. it has been demonstrated that the cyclization reaction is enhanced by an increase of temperature; the difference between the activation energies of propagation and cyclization is equal to 2.4 kcal.

Crawshaw and Butler[1] have suggested that the polymerization of acrylic anhydride results from alternate propagation and cyclization reactions; consequently the polymer was considered to be mainly a cyclopolymer of α-methylene-glutaric anhydride:

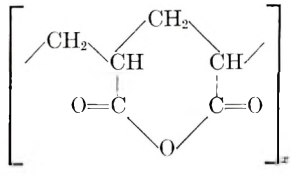

It is the purpose of the present paper to report on the chemical structure of this polymer on the basis of infrared spectrometric data as well as analytical data. Indeed, these polymers contain always some vinyl unsaturation, the importance of which is a function of the monomer concen-

* Paper presented at the IUPAC Symposium on Macromolecules, Montreal, Canada, July 1961. Part II in *J. Polymer Sci.*, **57**, 763 (1962).

tration and of the temperature. Moreover differences in the position as well as in the relative intensities of the carbonyl absorption bands were found in the cases of polymers prepared in different reaction conditions (solvent, temperature). Therefore before describing the kinetics of cyclopolymerization, we will first of all consider the structure of polyacrylic anhydride on the basis of infrared analysis and from chemical determination.

I. INFRARED SPECTROSCOPY

a. Hexaatomic Ring Anhydrides

The existence of two types of hexaatomic anhydrides has been deduced from two pairs of carbonyl absorption bands at 1810 and 1740 cm.$^{-1}$ (isomer A), and 1805 and 1765 cm.$^{-1}$ (isomer B). The relative intensity of the bands is inversed, the band at 1810 cm.$^{-1}$ showing the highest intensity for the first isomer. Isomer A is unstable and can be converted to isomer B by heating at 97°C. for 4 hr. in cyclohexanone solution and reprecipitation (Fig. 1*a* and 1*b*). This transformation is also favored at much lower temperature (35°C.) by traces of acrylic acid or by polymerization in a strong polar solvent as dimethylformamide. This last case is represented by Figure 1*c*, in which bands can be observed at 1740–1765 and 1810 cm.$^{-1}$ and correspond to a partial isomerization A → B.

The structural assignment of both anhydride types has been made possible by comparison of these polymeric anhydrides with the homologous low molecular weight compounds, the α,α'-dimethylglutaric anhydrides. Indeed, the positions of the two carbonyl absorption bands of the *meso*-α,α'-dimethylglutaric anhydride at 1810 and 1765 cm.$^{-1}$ agree remarkably with those of the polymeric anhydride B; the 1765 cm.$^{-1}$ band is also stronger

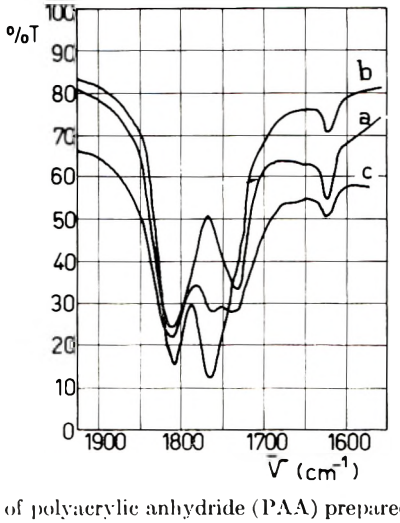

Fig. 1. Infrared spectra of polyacrylic anhydride (PAA) prepared (*a*) at 35°C. in cyclohexanone; (*b*) at 97°C. in cyclohexanone; (*c*) at 35°C. in dimethylformamide.

than the first one. This *meso* anhydride is obtained by reaction of the *meso* acid with acetyl chloride; it is easily soluble in benzene and in chloroform. On the other hand, the synthesis of the racemic variety from the racemic acid is very difficult on account of its unstability and direct transformation into the *meso* form under the normal reaction conditions. As obtained from *l*-α,α'-dimethylglutaric acid, this *l*-anhydride is much less soluble than the *meso* variety; for example, it is insoluble in benzene and in chloroform. This therefore indicates that this anhydride forms a polymeric anhydride by intramolecular dehydration. The absorption bands situated at 1810 and 1755 cm.$^{-1}$ could be explained on this basis; consequently, the spectrum must be and is indeed different from that of the cyclic polymeric anhydride A. This tendency for intermolecular condensation of the optically active variety instead of an intramolecular deshydratation of the *meso*-derivative has been strengthened by measurements of infrared OH absorption bands in the case of the corresponding α,α'-dimethylglutaric acids. By measuring the hydroxyl absorption bands at different dilutions in chloroform, the amounts of the intermolecular and intramolecular hydrogen bonding have been evaluated; it was found that the intramolecular hydrogen bonding (cyclization) is much more important for the *meso* form than for the racemic variety; in the case of the racemic form, practically no appreciable intramolecular hydrogen bonding could have been detected. These data will be reported later.

From this comparison between the infrared spectra of the polyacrylic anhydride and of α,α'-dimethylglutaric anhydrides, it may be concluded that the *meso* form corresponds to the polymer B which is consequently isotactic. The chemical unstability of the racemic anhydride is analogous to that of the polyanhydride A, for which a syndiotactic structure has been proposed.

The greater stability of the *meso*-glutaric anhydride with respect to the racemic can be understood by comparison with the corresponding 1,3-disubstituted cyclohexane derivatives. Indeed, in this series the interaction between no bonded groups is minimum when both substituents are in equatorial position with respect to each other.[2] The preliminary formation of the less stable racemic anhydride (syndiotactic) in the case of the polyacrylic anhydride must likely be attributed to steric effects which enhance the addition of a monomer in trans-position to a glutaric anhydride radical at the end of a growing chain. The easy isomerization from the syndiotactic (racemic) to the isotactic form (*meso*) presumably involves the enolization of the α-hydrogen with respect to the carbonyl groups. Therefore it can be expected that methacrylic derivatives in which no α-hydrogen are available will not undergo this isomerization and therefore behave differently from the acrylic derivatives.

b. Pentaatomic Anhydride

Under the experimental conditions in which the kinetic determinations have been carried out, no five-membered cyclic anhydrides (I) are formed.

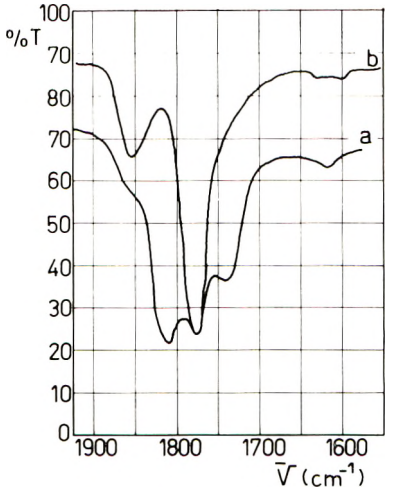

Fig. 2. Infrared spectra of (*a*) PAA prepared at 115°C. in xylene; (*b*) styrene-maleic anhydride copolymer.

Their presence has been detected in the case of a polymer prepared at 60°C. in benzene on the basis of two shoulder bands at 1860 and 1780 cm.$^{-1}$; it is well known indeed that the strain of a five-membered ring induces a shift to higher frequencies for the carbonyl absorption bands.[3]

A polymer with a relatively high content of anhydrosuccinic rings has been obtained by polymerization of acrylic anhydride at 115°C. in xylene as solvent. Figure 2 shows the comparison of this polymer with that of a maleic anhydride-styrene copolymer which absorbs also at 1865 and 1782 cm.$^{-1}$. An increase of temperature of polymerization favors the formation of a less stable pentaatomic ring instead of a hexaatomic anhydride (II) of the glutaric type.

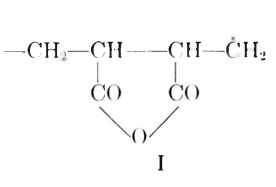

I

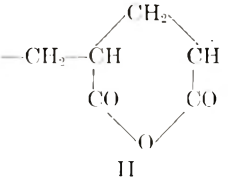

II

c. Vinyl Side Groups

The presence of open anhydride units in the isolated polymers has been easily demonstrated by the stretching vibration absorption band at 1625 cm.$^{-1}$. Its intensity increases strongly with an increase of the monomer concentration and is strongest for bulk polymer. An increase of the reaction temperature increases also the content of vinyl double bonds, as can be seen for polymers prepared at 97 and 0°C. However, at constant reaction temperature and constant monomer concentration, the cyclization is independent of the concentration of initiator over a twentyfold range of

concentration. These infrared unsaturation bands, although determined only qualitatively (paraffin oil suspension), were completely confirmed by quantitative bromometric chemical determinations.

II. KINETICS

a. Influence of the Monomer Concentration

The analysis of the polymers prepared at different monomer concentrations and at different temperatures makes it possible to obtain a deeper insight into the relative importance of the cyclization reaction with respect to the vinyl propagation reaction. Indeed, it is evident that the amount of cyclization in these reactions is determined by the competition between the bimolecular chain propagation by monomer addition and the intramolecular cyclization. Both reactions can be written:

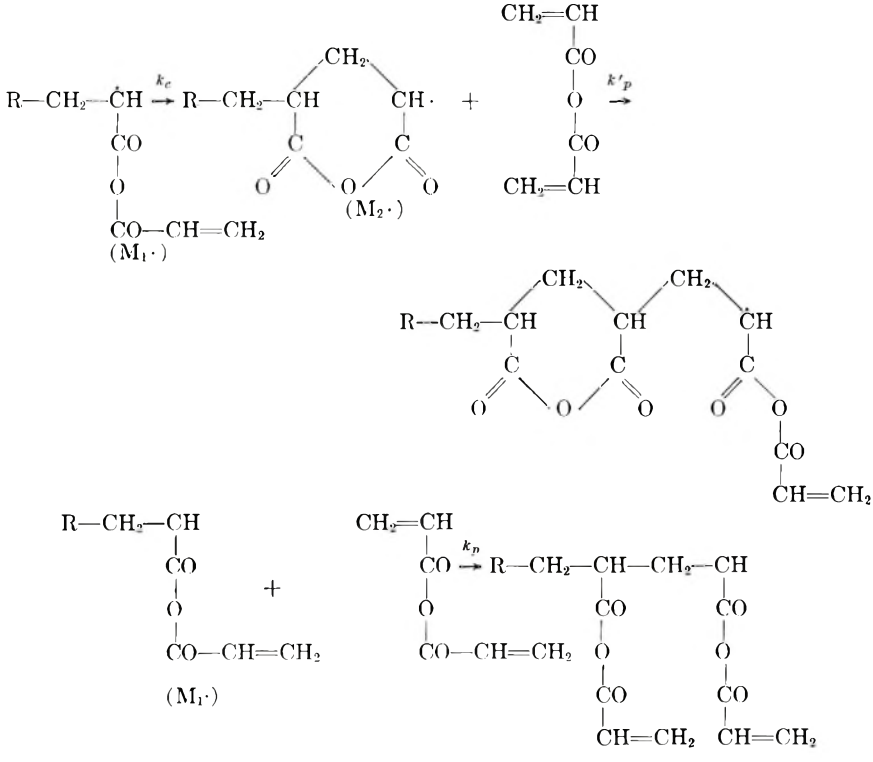

Evidently, on further addition of monomer, the cycloradical $M_2\cdot$ is again transformed into a $M_1\cdot$ radical. If [M] indicates the concentration of monomer, then the initial concentration of vinyl units must be equal to 2[M]. The ratio of the rate of vinyl propagation R_p to the rate of cyclization R_c is therefore equal to

$$R_p/R_c = k_p([M_1\cdot]2[M])/(k_c[M_1\cdot]) = 2K[M] \qquad (1)$$

where $K = k_p/k_c$.

If we define the fraction of cyclized units f_c as $f_c = R_c/(R_v + R_c)$, we obtain

$$1/f_c = 1 + 2K[M] \tag{2}$$

This equation makes it possible to evaluate graphically the ratio of the propagation and cyclization rate constants if the unsaturation of the polymer has been determined; its validity is however limited to low degrees of conversion, for which [M] is equal to the initial monomer concentration and at which chain branching remains negligible, at least from the point of view of the side vinyl groups consumption. In these experiments the per cent conversion was always kept less than 3% (Table I).

TABLE I

Influence of the Monomer Concentration on the Cyclization of Polyacrylic Anhydride [AIBN] = 0.019 mole/l.; Solvent: Cyclohexanone

[M]	f_c	$1/f_c$
8.4	0.25	4
5.9	0.36	2.78
3.4	0.53	1.89
1.8	0.56	1.78
0.7	0.71	1.41
0.6	0.75	1.33
0.3	0.80	1.25

From Figure 3 K was found to be equal to 0.17 l./mole. The cyclization although predominant becomes only complete in extremely diluted solution.

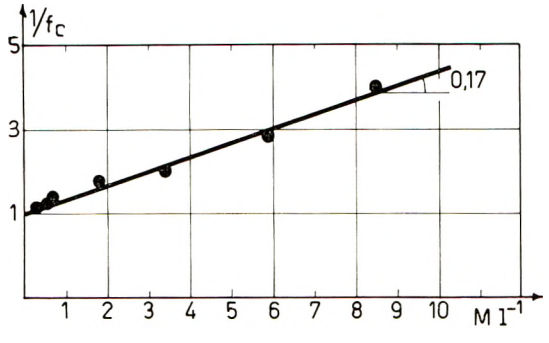

Fig. 3. Determination of the k_p/k_c ratio for acrylic anhydride polymerization.

b. Influence of the Temperature

The temperature also influences the degree of cyclization of polyacrylic anhydride, as can be seen from eq. (1). Indeed, this equation can be rewritten:

$$R_v/R_0 = 2[M](k_{0_v}/k_{0_c}) \exp\{(E_{a_v} - E_{a_c})/RT\} \tag{3}$$

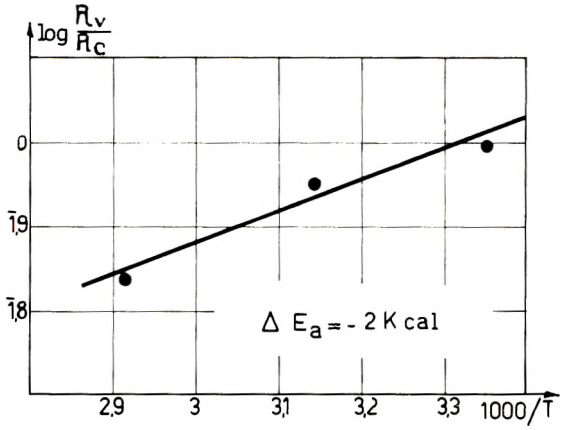

Fig. 4. Difference between the activation energies of propagation and cyclization.

in which k_{0_v} and k_{0_c} indicate the action constants in the Arrhenius equation while E_{a_v} and E_{a_c} are the corresponding activation energies of the propagation and cyclization reactions. An Arrhenius plot of log (R_v/R_c) against the reciprocal of the absolute temperature gives the difference between the activation energies, if [M] is kept constant (Fig. 4). The results are given in Table II.

TABLE II
Dependence of the Degree of Cyclization on the Temperature at [M] = 3.4 mole/l.; Solvent: Cyclohexanone

Temp., °C.	[AIBN], mole/l.	f_c	R_v/R_c
25	0.18	0.50	1
45	0.02	0.53	0.891
70	0.0014	0.59	0.696

As can be seen from these results, the degree of cyclization of the polymer increases markedly with temperature. The difference of the activation energies is 2.4 kcal./mole, while the action constants ratio is 0.006 l./mole; sterically the cyclization reaction is favored with respect to the chain propagation. It must be noticed that these results differ considerably from those of Butler[1] and Jones,[4] who proposed completely cyclized structures for polyacrylic anhydride and polydiacrylmethane, respectively.

III. EXPERIMENTAL

The infrared spectra of the polyanhydrides were recorded in Nujol suspension with a Perkin-Elmer 21 double-beam spectrometer equipped with rock salt prism.

The determination of the unsaturation of the polymer was based on hydrolysis of the polymer followed by bromine addition on the acrylic

present in the aqueous solution. The excess of bromine was titrated iodometrically. The method used was described by Polgar and Jungnickel.[5]

The preparation of acrylic anhydride and its polymers are described in part II of this series.[6]

α,α'-Dimethylglutaric acid was prepared by condensation of methyl methacrylate with the diethyl ester of monomethyl malonate[7] and subsequent hydrolysis of the triester.[8] This acid is an equimolecular mixture of *meso* and racemic forms. The separation of these *meso* and racemic forms was carried out followed the method of Auwers;[9] the resolution of the racemic form in its optically active varieties was obtained with the use of brucine for the formation of salts. The preparation of the anhydrides proceeds by treating with acetyl chloride; the *meso* variety[10] melts at 94–94.5°C., the *l*-form[11] at 42°C.

IV. CONCLUSIONS

The cyclopolymerization of acrylic anhydride produces a polymer of which the content of cyclized units increases with a decrease of the monomer concentration as well as with an increase of the temperature. The influence of the monomer concentration results from competition between the intramolecular cyclization and the bimolecular chain propagation reaction, the cyclization being complete only at infinite dilution. Infrared spectrometry confirms the chemical determinations of the unsaturation; moreover it shows the existence of two types of hexaatomic anhydride rings, of which the isotactic is the most stable. Pentaatomic ring units were formed only under exceptional conditions.

The authors express their thanks to M. V. Hegedus for the preparation of the samples of *meso* and *l*-dimethylglutaric anhydride.

The authors are also indebted to the Fonds National de la Recherche Scientifique for the fellowship of one of them (J. M.) and for financial support to the laboratory.

References

1. Butler, G. B., and A. Crawshaw, *J. Am. Chem. Soc.*, **80,** 5464 (1958).
2. Dauben, W. G., and K. J. Pitzer, *Steric Effects in Organic Chemistry*, M. S. Newman, Ed., Wiley, New York, 1956, p. 13.
3. Bellamy, L. J., *The Infrared Spectra of Complex Molecules*, Methuen, London, 1954, p. 111.
4. Jones, J. F., *J. Polymer Sci.*, **33,** 7, 15 (1958).
5. Polgar, A., and J. L. Jungnickel, in *Organic Analysis*, Vol. III, J. Mitchell, Jr., I. M. Kolthoff, E. S. Proskauer, and A. Weissberger, Eds., Interscience, New York, 1956, p. 240.
6. Smets, G., *J. Polymer Sci.*, **57,** 763 (1962).
7. Ruhl, K., *Z. Naturforschung*, **46,** 199 (1949); H. N. Rydon, *J. Chem. Soc.*, **1936,** 1444.
8. Lim, D., and O. Wichterle, *J. Polymer Sci.*, **29,** 580 (1958).
9. Auwers, K., and J. F. Thorpe, *Ann.*, **285,** 310 (1895).
10. Evans, D. W. S., and J. C. Roberts, *J. Chem. Soc.*, **1957,** 2104.
11. Möller, E., *Lunds Univ. Arsskr., Adv. 2*, **15,** N. 6, 56; *Chem. Zentr.*, **1,** 607 (1919).

Résumé

La cyclopolymérisation de l'anhydride polyacrylique produit un polymère dont la structure a été étudiée par analyse spectrométrique infra-rouge (anhydrides cycliques) et par la méthode bromométrique (insaturation vinylique). L'analyse spectrométrique infra-rouge a été basée sur l'étude des doublets d'absorption carboxylique vers 1750 et 1810 cm.$^{-1}$; elle a permis de mettre en évidence l'existence de deux types de cycles anhydrides hexaatomiques, différents par leur structure stéréochimique. Par comparaison avec les variétés racémiques et méso de l'anhydride α,α'-diméthylglutarique, on attribue la structure syndiotactique (racémique) au polyanhydride obtenu à 35°C. dans la cyclohexanone. Celui-ci se transforme par chauffage ou en présence de trace d'acide acrylique en sa variété isotactique (*méso*). Il ne se forme d'unité cyclique pentaatomique en quantité appréciable que par polymérisation à des températures de 115°C. (1780 et 1860 cm.$^{-1}$). Par contre une insaturation résiduelle est toujours détectable par la bande d'absorption vinylique à 1625 cm.$^{-1}$; elle est d'autant plus prononcée que la concentration en monomère en cours de polymérisation était plus élevée. L'analyse chimique des cyclopolymères par bromométrie a permis d'évaluer quantitativement le rapport des constantes de vitesse de propagation à celle de cyclisation k_p/k_c; à 35°C. ce rapport s'élève à 0.17. Par analyse de polymères obtenus à 25, 45 et 70°C. on a montré que la réaction de cyclisation est favorisée par une élévation de température; la différence entre les énergies d'activation de propagation et de cyclisation s'élève à 2.4 kcal.

Zusammenfassung

Die Struktur der Cyclopolymeren von Acrylsäureanhydrid wurde durch Infrarotspektrometrie (cyclisierte Bausteine) und chemische Analyse (Bromometrie: Vinyldoppelbindungen) untersucht. Die Infrarotuntersuchung basierte auf der Untersuchung der beiden Carbonylabsorptionsbanden bei etwa 1750 und 1810 cm^{-1}; zwei Typen von cyclisierten sechsatomigen Anhydriden mit verschiedener stereochemischer Struktur wurden nachgewiesen. Durch Vergleich mit der meso- und racemischen Form von α,α'-Dimethylglutarsäureanhydrid konnte die syndiotaktische (racemische) Struktur dem bei 35°C in Cyclohexanon erhaltenen Polyanhydrid zugeordnet werden. Durch Erhitzen oder in Gegenwart von Säurespuren isomerisiert sich diese Form zur isotaktischen (*meso*) Form. Funfatomige cyclisierte Einheiten wurden nur durch Polymerisation bei hoher Temperatur, z.B. bei 115°C erhalten (Banden bei 1780 und 1860 cm^{-1}). Dagegen wurde immer ein Restgehalt an Doppelbindungen durch die Vinylabsorptionsbande bei 1625 cm^{-1} nachgewiesen; ihre Intensität steigt mit zunehmender Monomerkonzentration während der Polymerisation. Die chemische Analyse der Copolymeren mittels Bromometrie ermöglicht es, das Verhältnis der Geschwindigkeitskonstanten des Vinylwachstums zu der der Cyclisierung quantitativ zu berechnen; bei 35°C beträgt dieses Verhältnis 0,17. Durch Analyse der bei 25, 45 und 70°C erhaltenen Polymeren wurde gezeigt, das die Cyclisierungsreaktion durch Temperaturerhöhung begünstigt wird; der Unterschied in der Aktivierungsenergie zwischen Wachstum und Cyclisierung beträgt 2,4 Kcal.

Received February 6, 1962

JOURNAL OF POLYMER SCIENCE: PART A VOL. 1, PP. 1501–1508 (1963)

Thermodynamic Properties of Rodlike Polyelectrolyte Solutions in the Presence of Salts

FUMIO OOSAWA, *Institute for Molecular Biology and Department of Physics, Faculty of Science, Nagoya University, Nagoya, Japan*

Synopsis

A theoretical foundation is given to the experimentally established relation called the additivity law, according to which the thermodynamic and transference properties of linear polyelectrolyte solutions with low molecular salts are described as a superposition of the effects of ions from polyelectrolytes and those from low molecular salts. By employing a cylindrical free volume model for a solution of thin and long rodlike polyelectrolytes and analyzing the Poisson-Boltzmann equation it is found that the electrostatic free energy is expressed in a special form as a function of the geometry of the system. On the basis of this expression of the free energy, the additivity law is derived by a thermodynamic treatment without an approximate procedure to solve the Poisson-Boltzmann equation. The additivity is a property not accidental but essential to rodlike polyelectrolytes. The same method is applicable to analysis of the interaction between two parallel rodlike polyions in the presence of low molecular salts.

I. Introduction

Recent experiments on thermodynamic properties of polyelectrolyte solution containing low molecular salts have led to an empirical law, according to which the activity of ions is expressed as a sum of effective ionic concentrations contributed independently by the polyelectrolyte and the salt.[1–3] The osmotic pressure (against the solvent) of the polyelectrolyte solutions containing low molecular salts is also approximately given by a superposition of the pressure of the polyelectrolyte without low molecular salts and that of the added salt. Such an additivity law of contributions of polyelectrolytes and salts has been found in the electric conductivity or transference measurements, too.[4,5] In the electric field the counterions from added salts seem to behave independently of the counterions from the polyelectrolytes.

Theoretical investigations on this phenomenon have been carried out by several authors.[6–8] Laborious analysis of the Poisson-Boltzmann equation showed that the additivity law is approximately numerically satisfied.[7,8] A purely thermodynamic analysis also proved the additivity law under an assumption of the full activity of coions.[6] In this paper we present a new, simple, theoretical analysis which can reveal the essential cause of the additivity law. The law is derived as a characteristic property of the rod-

like polyelectrolytes in the cylindrical coordinate system. The necessary and sufficient conditions for the additivity are shown.

II. Fundamental Equations

Let us consider a solution of polyelectrolytes containing low molecular salts and as usual, employ a free volume model, in which an electrically neutral volume v is assigned to each polymer; where v is equal to the total volume V of the solution divided by the total number of polyions M. (The availability of the free volume model was discussed in a separate paper in which the interaction between polyions was theoretically treated.[9]) The electrostatic potential ψ in each volume v is related to the charge of the polyion and the distribution of mobile ions by the equation:

$$\Delta\psi = (4\pi/D)(\rho_p + \rho) \tag{1}$$

where D is the dielectric constant of the solvent, ρ_p is the charge density of the fixed polyion, and ρ the charge density of mobile ions expressed as $\sum_i c_0 z_i n_i$. On the statistical average, the number density of n_i of ions of the ith type of valency z_i is given by

$$n_i = N_i \exp\{-z_i e_0 \psi/kT\} / \int_v \exp\{-z_i e_0 \psi/kT\} dv \tag{2}$$

where N_i is the total number of the ith ions in v. Combination of eqs. (1) and (2) leads to the Poisson-Boltzmann equation. When the equation is solved under boundary conditions determined by the position of the polyion or $\rho_p(x)$ and the geometry of the free volume v, the potential ψ and the density of mobile ions n_i are obtained as functions of coordinate x.

The electrostatic internal energy u_e due to the average distribution of ions around the fixed polyion is given by[10]

$$u_e = (D/8\pi) \int (\text{grad } \psi)^2 dv = (1/2) \int \psi(\rho_p + \rho) dv \tag{3}$$

and the electrostatic free energy f_e is derived from this internal energy by the charging process as

$$f_e = \int_0^{e_0} 2u_e(de_0/e_0) \tag{4}$$

Each mobile ion has its own ionic atmosphere produced by other mobile ions. The contribution of such an atmosphere to the electrostatic free energy of the solution must be taken into consideration. The statistical mechanical analysis in a previous paper[11] showed that the total electrostatic free energy is approximately expressed as the sum $f_e + f_{0e}$; the latter is due to the ionic atmospheres among mobile ions. In an electroneutral uniform solution of low molecular ions, f_{0e} is calculated by the Debye-Hückel theory. In the present case, the Debye-Hückel theory is not straightforwardly applicable because the average distribution of mobile ions is not uniform around the fixed polyion, and the mobile ions do not satisfy the electroneutrality without the fixed polyion. Nevertheless, we assume that the free energy f_{0e} may be approximated by the electrostatic free energy of a

hypothetical uniform solution of counterions and coions, the average concentrations of which are equal to those of the real solution. Then, f_{0e} is a function of volume v and numbers of mobile ions N_i.

Thus, the total free energy per polyion f is expressed as

$$f = f_{00} + f_{0e} + f_e \tag{5}$$

where the zero point free energy f_{00} is given by the ideal mixing entropy of mobile ions without electric charge. The sum $f_0 = f_{00} + f_{0e}$ is a function of v independent of its shape. The free energy F of the solution is given by Mf.

III. Free Energy of Rodlike Polyelectrolyte Solutions

For a solution of rodlike polyelectrolytes we apply a cylindrical free volume model of radius R at the center of which a cylindrical (rigid rodlike) polyion of radius a is fixed. In this case, the Poisson-Boltzmann equation is expressed as

$$d^2\phi/dx^2 + (1/x)(d\phi/dx) = \sum_i A_i \exp\{-z_i\phi\} \tag{6}$$

$$\text{for } 1 < x < R/a$$

where

$$A_i = (4\pi N_i z_i e_0^2/DkT)\left(\int_1^{R/a} \exp\{-z_i\phi\} 2\pi x dx\right)^{-1}$$

and boundary conditions are given by

$$(xd\phi/dx)_{R/a} = 0 \tag{7}$$

$$(xd\phi/dx)_1 = -(4N_p e_0^2/DkT)$$

where $\phi = e_0\psi/kT$, $x = r/a$ (r being the distance from the center), and N_p is the number of charge per unit length of the fixed polyion, N_i is the total number of the mobile ions of the ith type per unit length of the polyion.

These equations show that the solution ψ is expressed as a function of the ratio $x = r/a$ as the spatial coordinate and contains only the ratio R/a as the quantity designating the geometry of the system. Accordingly, it is found from eqs. (3) and (4) that the electrostatic energy u_e and the electrostatic free energy f_e can be expressed as functions of R/a. They do not contain R or a separately. Thus we have

$$f = f_e(R/a) + f_0(v) \tag{8}$$

where

$$v = \pi(R^2 - a^2)$$

IV. Osmotic Pressure

The osmotic pressure P of the solution against the pure solvent (water) is given by

$$P = -(\partial F/\partial V)_{M,N_i} = -(\partial f/\partial v)_{N_p,N_i,a}$$

$$= -(1/2\pi R^2)(R\partial f/\partial R)_{N_p,N_i,a}$$
$$= -(1/2\pi R^2)(R\partial f_0/\partial R + R\partial f_e/\partial R)_{N_p,N_i,a} \quad (9)$$

By the use of the special expression of the free energy, eq. (8), as a function of the geometry of the system, we can derive a remarkable relation between the pressure of the solution of rodlike polyelectrolytes with low molecular salts and that without salts. Since f_e is a function of R/a, we have

$$R\partial f_e/\partial R + a\partial f_e/\partial a = 0 \quad (10)$$

and since f_0 is a function of v, we have

$$a\partial f_0/\partial a + R\partial f_0/\partial R = 2\pi(R^2 - a^2)(\partial f_0/\partial v) \quad (11)$$

Therefore

$$R\partial f/\partial R = -a\partial f/\partial a + a\partial f_0/\partial a + R\partial f_0/\partial R \quad (12)$$
$$= -a\partial f/\partial a + 2v\partial f_0/\partial v$$

or

$$2\pi R^2 P = 2vP_0 + a\partial f/\partial a \quad (13)$$

where

$$P_0 = -\partial f_0/\partial v \quad (14)$$

P_0 is the osmotic pressure of a hypothetical solution of counterions and coions without polyions and expressed as

$$P_0 v/kT = \gamma \sum_i N_i \quad (15)$$

where γ is the osmotic coefficient of the hypothetical solution.

According to the general expression of the free energy change due to the shape change of the boundary derived by Bell et al.,[12] the last term of eq. (13), $a(\partial f/\partial a)$, is composed of the self-energy change of the rod and the entropy change of mobile ions at the surface of the rod. For a thin rod of a small charge density, the contribution of the self-energy is predominant over the contribution of mobile ions. For a high charge density, however, the excess counterions are condensed at the surface of the rod, and the contribution of these counterions can not be neglected. In the simplest case of rodlike polyelectrolytes with monovalent counterions containing no low molecular salts, where the exact solution of the Poisson-Boltzmann equation was obtained,[13] we have

$$a\partial f/\partial a = -2N_p^* e_0^2/D \quad (16)$$

where

$$N_p^* = N_p \qquad \text{for } N_p e_0^2/DkT \leq 1$$
$$N_p^* = DkT/e_0^2 \qquad \text{for } N_p e_0^2/DkT > 1$$

On the basis of the Donnan approximation employed in a previous paper[14] it is proved that for a very thin rod ($R/a \gg 1$), the amount of the counterion condensation at the surface of the rod is not influenced by the presence of salts if all counterions from polyions and from salts are of the same valency. Therefore, the above expression of $a(\partial f/\partial a)$ is available even when low molecular (monovalent) salts are added. In other words, $a(\partial f/\partial a)$ is not changed by the addition of salts.

V. Additivity Law

The osmotic pressure P_1 of a solution of rodlike polyelectrolytes containing no low molecular salts is written as

$$P_1 = P_{10} + (1/2v)(a\partial f/\partial a)_1 \tag{17}$$

$$P_{10} = \gamma_1 m_p kT \tag{18}$$

Here we put $R_2 \gg a^2$ in eq. (13), and m_p is the average concentration N_p/v of counterions from polyions. When low molecular salts are added, the osmotic pressure P_2 is given by

$$P_2 = P_{20} + (1/2v)(a\partial f/\partial a)_2 \tag{19}$$

$$P_{20} = \gamma_2(m_p + m_s)kT \tag{20}$$

where m_s is the concentration of counterions and coions of added salts ($\Sigma N_i/v$). Then

$$P_2 = P_1 + (P_{20} - P_{10}) + (1/2v)[a(\partial f/\partial a)_2 - a(\partial f/\partial a)_1] \tag{21}$$

As shown in the previous section, for a very thin rod we can put

$$a(\partial f/\partial a)_2 = a(\partial f/\partial a)_1 \tag{22}$$

and have

$$P_2 = P_1 + (P_{20} - P_{10}) \tag{23}$$

$$P_{20} - P_{10} = [\gamma_2 m_s + (\gamma_2 - \gamma_1)m_p]kT \tag{24}$$

In ideal solutions of mobile ions

$$P_{20} - P_{10} = m_s kT$$

and

$$P_2 = P_1 + m_s kT$$

In most cases ${}_2\gamma m_s \gg (\gamma_2 - \gamma_1)m_p$, because when $m_s < m_p$, $(\gamma_2 - \gamma_1) \ll \gamma_2$, and when $m_s > m_p$, $\gamma_2 m_s \gg (\gamma_2 - \gamma_1)m_p$. Hence the approximate relation

$$P_2 = P_1 + P_s \tag{25}$$

is obtained, where $P_s = \gamma_2 m_s kT$ means the osmotic pressure of the solution of added salts. Thus, the osmotic pressure of a polyelectrolyte solution in the presence of salts is given by the sum of the osmotic pressure of the

polyelectrolyte solution without salts and the osmotic pressure of added salts.

In the present model the osmotic pressure is approximately proportional to the total concentration of mobile ions at the boundary of the cylindrical free volume where there is no electric field. Therefore, the above additivity law of the osmotic pressure means the additivy of the ion concentration. At the boundary the concentration of counterions and coions in the polyelectrolyte solution with low molecular salts is nearly equal to the sum of the counterion concentration in the polyelectrolyte solution without added salts and the counterion and coion concentrations of added salts without the polyelectrolytes. Mobile ions of added salts seem to have no correlation with counterions from polyions. If the activity of coions is not influenced by the presence of polyions, the above result means that on the activity of counterions also the additivity law is satisfied.

VII. Interaction between Two Rods in Salts

The interaction between two parallel rodlike polyions in the absence of low molecular salts was calculated by the use of the exact solution of the Poisson-Boltzmann equation.[15] Here we estimate the effect of low molecular salts on the interaction between these rods on the basis of the general treatment of a cylindrical coordinate system developed here and in the previous paper.[9] Let us consider two parallel rods of radius a fixed in a large cylindrical free volume of radius R with distance b. For such a system also it is found that the electrostatic free energy f_e is a function of ratios R/a and b/a because of the logarithmic type of the electric potential in the cylindrical coordinate system. This special form of the electric free energy leads us to the relation

$$b\partial f/\partial b = 2v\,\partial f_0/\partial v - R\partial f/\partial R - a\partial f/\partial a \tag{26}$$

which is comparable to eq. (12) in the previous section. When two rods, each of which has charge N_p, approach closely so that the distance b is much smaller than R, the concentration of mobile ions at the boundary R can be approximated by the concentration of mobile ions at R in the system of one rod having charge $2N_p$. For such a one-rod system of radius A, the same relation as eq. (13) can be applied, and

$$2v\partial f_0/\partial v - R\partial f/\partial R = A\partial f/\partial A \tag{27}$$

$$b\partial f/\partial b = A\partial f/\partial A - a\partial f/\partial a \tag{28}$$

For very thin rods, $a(\partial f/\partial a)$ is equal to twice the right-hand side of eq. (16), and $A(\partial f/\partial A)$ is approximated by the right-hand side of eq. (16), in which N_p is replaced by $2N_p$. Accordingly, both terms are not changed by the addition of low molecular salts. This means that the force $(\partial f/\partial b)$ between two parallel rods is little changed by the addition of low molecular salts if two rods are sufficiently thin and approach closely. This strange

result is valid only when two rods are infinitely long and completely parallel together.

VIII. Discussion

The present theory made it clear that the additivity law is not an accidental but a necessary consequence in rodlike polyelectrolyte solutions to which a cylindrical free volume model can be applied. The law was derived on the assumption of a very thin and long rodlike shape of polyions. Most of linear polyions, however, are not rigid but flexible. Nevertheless, they are in a stretched form to which the rod model is applicable as long as the salt concentration is not too high. As a result, the additivity law was experimentally observed in different kinds of polyelectrolytes and in a wide range of salt concentration. When the salt concentration is very high, the polyions are coiled up so that the rod model becomes inapplicable. For a rod of the finite thickness, the relation (22) becomes invalid if the salt concentration becomes sufficiently high. For a finite concentration of salts, eq. (22) becomes valid if the rod is sufficiently thin. If the valency of counterions of added salts is higher than that of counterions from polyions, the additivity law is not always satisfied, because the counterion condensation strongly depends on the valency. Even in such a case, however, the thermodynamic properties of solution can be expressed in a form of the sum of contributions from two kinds of counterions if an appropriate classification of counterions is defined.

References

1. Mock, R. A., and C. A. Marshall, *J. Polymer Sci.*, **13**, 263 (1954).
2. Nagasawa, M., M. Izumi, and I. Kagawa, *J. Polymer Sci.*, **37**, 375 (1959); also M. Nagasawa, A. Takahashi, M. Izumi, and I. Kagawa, *J. Polymer Sci.*, **38**, 213 (1959).
3. Alexandrowicz, Z., *J. Polymer Sci.*, **43**, 337 (1960).
4. Ikegami, A., and N. Imai, *J. Polymer Sci.*, **56**, 133 (1962).
5. Wall, J. T., and M. J. Eittel, *J. Am. Chem. Soc.*, **79**, 1556 (1957).
6. Katchalsky, A., and Z. Alexandrowicz, private communication.
7. Alexandrowicz, Z., *J. Polymer Sci.*, **56**, 97, 115 (1962).
8. Kotin, L., and M. Nagasawa, *J. Chem. Phys.*, **36**, 873 (1962).
9. Ohnishi, T., N. Imai, and F. Oosawa, *J. Phys. Soc. Japan*, **15**, 896 (1960).
10. Lifson, S., and A. Katchalsky, *J. Polymer Sci.*, **13**, 43 (1954).
11. Oosawa, F., N. Imai, and I. Kagawa, *J. Polymer Sci.*, **13**, 94 (1954).
12. Bell, G. M., and S. Levine, *Trans. Faraday Soc.*, **54**, 785 (1958).
13. Fuoss, R., A. Katchalsky, and S. Lifson, *Proc. Natl. Acad. Sci. (U. S.)*, **37**, 579 (1951).
14. Oosawa, F., *J. Polymer Sci.*, **23**, 421 (1957).
15. Imai, N., *J. Phys. Soc. Japan*, **16**, 746 (1961); also N. Imai, and T. Ohnishi, *J. Chem. Phys.*, **30**, 1115 (1959).

Résumé

On donne une explication théorique de la relation expérimentale dite loi d'additivité suivant laquelle les propriétés thermodynamiques et de transfert d'une solution de polyélectrolyte linéaire en présence de sels de bas poids moléculaire résultent de la superposition des effets d'ions des polyélectrolytes et ceux des sels à poids moléculaire réduit. En

faisant usage d'un modèle de volume libre cylindrique pour une solution de molécules de polyélectrolytes minces et rigides, et en analysant l'équation de Poisson-Boltzmann, on trouve que l'énergie libre électrostatique est exprimée sous une forme spéciale comme fonction de la géométrie du système. Se basant sur cette relation de l'énergie libre, on en déduit la loi de l'additivité par une opération sans faire usage d'une solution approximative de l'equation de Poisson-Boltzmann. L'additivité n'est pas une propriété accidentelle, mais essentielle des polyélectrolytes linéaires. La mème méthode est applicable à l'analyse des interactions entre deux polyions linéaires en présence de sels de bas poids moléculaire.

Zusammenfassung

Eine theoretische Begründung des experimentelle gefundenen, sogenannten Additivitätsgesetzes wird gegeben, nach welchem die thermodynamischen und Beweglichkeitseigenschaften von Lösungen linearer Polyelektrolyte mit neidermolekularen Salzen als Überlagerung der Effekte der Ionen des Polyelektrolyten und des niedermolekularen Salzes beschrieben werden können. Unter Benützung eines Modells mit zylinderförmigem freien Volumen für eine Lösung dünner und langer stäbchenförmiger Polyelektrolyte und durch Analyse der Poisson-Boltzmann-Gleichung kann die elektrostatisch freie Energie in einer speziellen Form als Funktion der Geometrie des Systems ausgedrückt werden. Auf der Grundlage dieses Ausdruckes für die freie Energie wird das Additivitätsgesetz thermodynamisch ohne Näherungsverfahren bei der Lösung der Poisson-Boltzmann-Gleichung abgeleitet. Die Additivität ist eine nicht zufällige, sondern wesentliche Eigenschaft stäbchenförmiger Polyelektrolyte. Die gleiche Methode ist auf die Analyse der Wechselwirkung zweier paralleler stäbchenartiger Polyionen in Gegenwart neidermolekularer Salze anwendbar.

Received March 9, 1962

JOURNAL OF POLYMER SCIENCE: PART A VOL. 1, PP. 1509–1520 (1963)

Stereoregularity in Polyvinyl Alcohols and Esters

W. COOPER, F. R. JOHNSTON, and G. VAUGHAN, *Central Research Division, Dunlop Research Centre, Dunlop Rubber Company Limited, Birmingham, England*

Synopsis

From solution properties and x-ray crystallinities of polyvinyl esters and alcohols derived from several vinyl esters polymerized at different temperatures, it is considered that polyvinyl haloacetates are more regular in structure than polyvinyl acetate, but this regularity has not been proved to result from increased syndiotacticity. It has been found that the crystallinities of polyvinyl trifluoroacetates prepared from vinyl-acetate via polyvinyl alcohols are comparable with those prepared directly from vinyl trifluoroacetate at similar polymerization temperatures. The x-ray diffraction patterns of polyvinyl acetate prepared from the monomer and of acetylated polyvinyl alcohol obtained by hydrolysis of polyvinyl trifluoroacetate are identical. Likewise, those of polyvinyl alcohols derived from several different vinyl esters cannot be distinguished from one another. Polyvinyl acetates prepared at high and low temperatures and prepared from the trifluoroacetate all hydrolyze in alkaline solution at substantially the same rate. The significant finding in this investigation is that whereas polymerization temperature has a marked effect on the crystallinity of polyvinyl trifluoroacetate, it has little influence on the water solubility of the polyvinyl alcohols. Water solubility is determined by the structure of the monomer from which the polyvinyl alcohol was obtained.

INTRODUCTION

The dependence of stereospecificity in vinyl polymers on the structure of the monomer and temperature of polymerization has recently attracted considerable interest. Fordham, McCain, and Alexander[1] reported that polyvinyl alcohols derived from polyvinyl haloacetates were less readily soluble in water than polyvinyl alcohol obtained from polyvinyl acetate, an observation first made by Haas, Emerson, and Schuler[2] on polyvinyl alcohol obtained from polyvinyltrifluoroacetate (PVTFA). This was attributed to greater syndiotacticity in the former, resulting from the polar repulsion of the haloester groupings during polymerization. In support of this it was pointed out that PVTFA is crystalline and that the repeat distance (4.6 ± 0.1 A.) in an orientated sample corresponds to syndiotactic placement. More recently it has been pointed out[3] that the existence of crystallinity in PVTFA is not conclusive of high stereospecificity, since the trifluoroacetate of polyvinyl alcohol obtained by hydrolysis of polyvinyl acetate is also crystalline. In addition, examination of the x-ray diffraction patterns from PVTFA indicated that most of the sharper bands result from lateral

order between the polymer chains. Nevertheless it seems reasonable to assume that any change in the regularity of the polymer molecules will still be reflected to a greater or lesser extent in corresponding changes in the diffraction patterns.

In this report samples of polyvinyl esters prepared at different temperatures have been examined in an attempt to resolve the rather conflicting evidence.

EXPERIMENTAL

Polymer Preparation

Polyvinyl esters were prepared with the use of 0.2% benzoyl peroxide as catalyst or by exposure to γ-radiation from a Co^{60} source at a dose rate of 2×10^4 r/hr. (Table I).

TABLE I
Preparation of Polyvinyl Esters

Monomer	Initiation	Temp., °C.	Time of polymerization, hr.	Conversion, %	$[\eta]_{MEK}$	$\bar{M}_w \times 10^{-6}$
Vinyl acetate	γ	−80	48	80	1.61	—
" "	γ	+20	16	100	1.36	—
" "	Bz_2O_2	+44	24	75	0.53	—
Vinyl monochloroacetate	γ	−15 to −20	15.5	100	0.83	3.2[a]
" "	γ	+20	43	61	0.59	1.8[a]
" "	Bz_2O_2	+44	15	72	0.28	0.2
Vinyl dichloroacetate	γ	−15 to −20	16	—	0.57	—
" "	γ	+20	5	50	0.52	0.4
" "	Bz_2O_2	+44	15	32	0.34	—
Vinyl trichloroacetate	γ	−15 to −20	60	100	0.12	0.04
" "	γ	+20	30	100	0.09	—
" "	Bz_2O_2	+44	80	33	0.07	—
Vinyl trifluoroacetate	γ	−15 to −20	15.5	100	7.32	—
" "	γ	+20	2	100	1.76	—
" "	Bz_2O_2	+44	15	100	1.36	—

[a] Small amount of gel also formed.

The polymers were hydrolyzed by 50% ethanol/0.880 ammonia at 100°C. (acetates and monochloroacetates), 50% ethanol/ethylenediamine hydrate at 100°C. (dichloro and trichloroacetates), or ethylenediamine hydrate at 20°C. (trifluoroacetates).

Acetylation of the isolated polyvinyl alcohols was carried out with acetic

anhydride and sodium acetate at 100°C. for 12 hr. Trifluoroacetylation was carried out in a similar manner with sodium trifluoroacetate as catalyst at a temperature of 40°C.

The purities of the samples were checked by quantitative alkaline hydrolysis and infrared examination, both indicating absence of hydroxyl groups.

Rate of Hydrolysis

Hydrolyses were carried out at 22°C. on the polymer (5 ml. of a 0.75% solution in ethanol) in 50% ethanol (10 ml.) to which was added 0.2*N* alcoholic KOH (5 ml.). Unchanged alkali was determined by back titration at appropriate intervals.

Solubility Measurements

Samples of polyvinyl alcohols (3 mg.) and water (0.5 ml.) were sealed in small glass ampules and heated for periods of 2 hr. at temperatures progressively increased by steps of 10°C. The minimum temperature that resulted in a homogeneous solution was noted.

X-Ray Examination of the Polymers

Polyvinyl Alcohols. A small quantity (ca. 5 mg.) of the finely powdered polyvinyl alcohol was treated with a single drop of a 0.5% solution of gum arabic in acetone/water (60:40, v/v). The moistened sample was placed inside a 1.5 mm. bore veridia tube and carefully compacted by use of two close-fitting steel rods, and dried at 50°C. to give a small cylindrical pellet about 4 mm. long × 1.3 mm. diameter; different samples were reproducible in size. The cylindrical pellets were thoroughly dried before being mounted on the goniometer. Intensities of the diffractions were compared with one from a standard crystalline sample fixed in a Goppel cone[4] and exposed simultaneously. The techniques followed those outlined by Hermans and Weidinger,[5] and corrections were made for variations in incident beam intensity, for air scatter, and for variations in sample dimensions. However, as the agreement between the products of diameters and densities measured in this way and by direct measurement was not good, diffraction patterns were compared after first adjusting their total integrated intensities (over a radius of 40 mm. at a sample-to-film distance of 40 mm.) to the same arbitrary value. Samples of amorphous polyvinyl alcohol are not available, but an estimate was made of the amorphous diffraction pattern by use of polyvinyl alcohol swollen with water or of 1,3-propanediol. This enabled an approximate idea of the relative amounts of crystalline and amorphous polymer to be gained.

Polyvinyl Esters. Powder diagrams of the polyvinyl trifluoroacetates were obtained from samples prepared in the same manner as the alcohols. Polyvinyl acetates were examined as cast films.

RESULTS

The properties of the various polyvinyl esters use dare summarized in Table I.

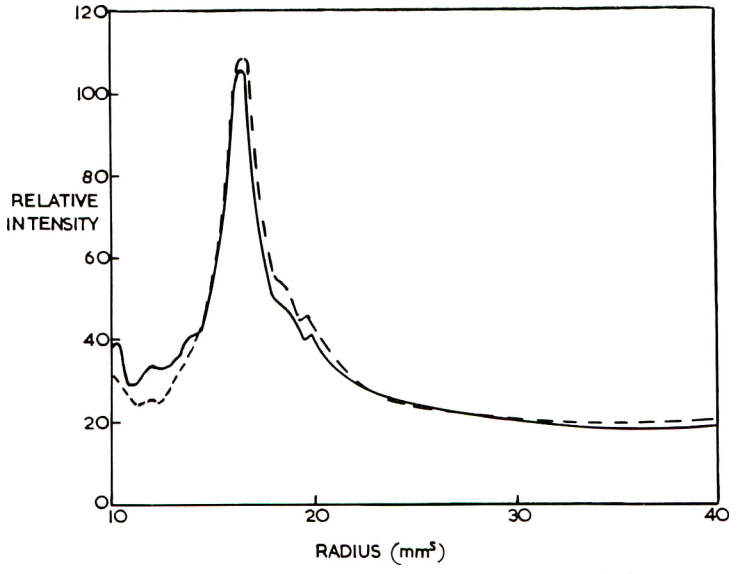

Fig. 1. Polyvinyl alcohol crystallinity: (——) from polyvinyl trichloroacetate; (- -) from polyvinyl trifluoroacetate.

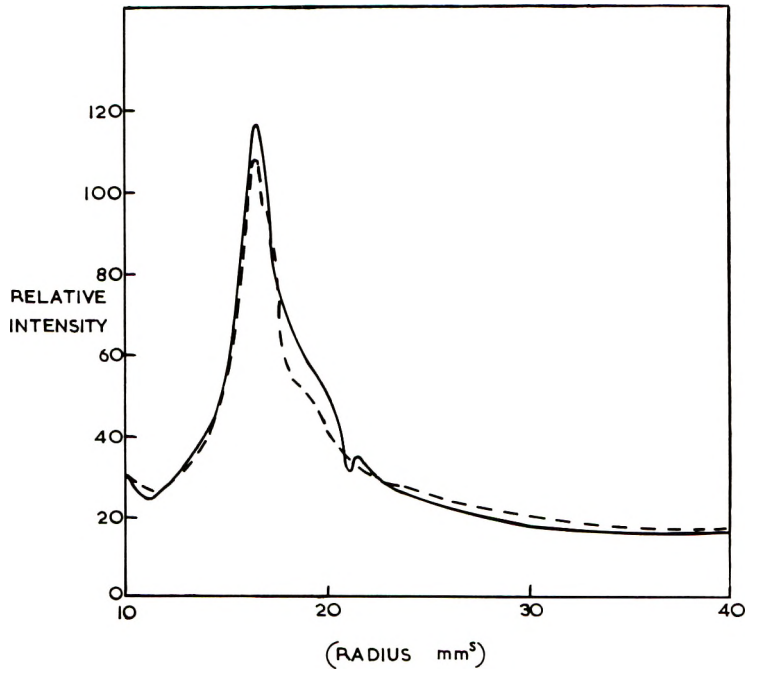

Fig. 2. Polyvinyl alcohol crystallinity: (——) from polyvinyl acetate; (- -) from polyvinyl chloroacetate.

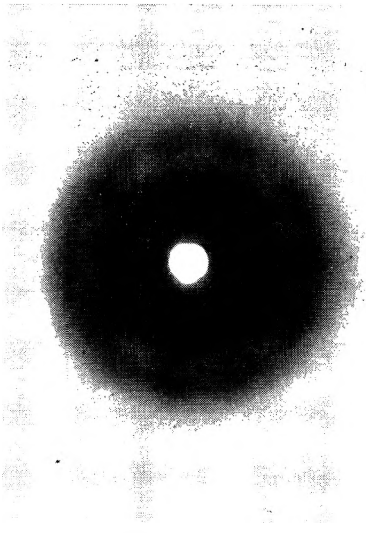

Fig. 3. Polyvinyl acetate (from vinyl acetate 20°C., γ).

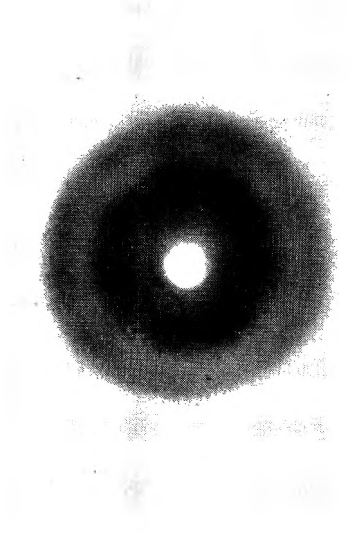

Fig. 4. Polyvinyl acetate (from vinyl trifluoroacetate, 20°C., γ).

The x-ray diffraction data are summarized in Figures 1–9. Table II describes the solubility characteristics of the different polyvinyl alcohol samples used in this study. The data from the quantitative hydrolysis of the acetates are collected in Figure 10.

DISCUSSION

The x-ray crystallinity of polyvinyl alcohol is substantially the same, whether it is prepared from polyvinyl acetate or from polyvinyl trifluoroacetate. No significant differences in structure could be detected in the

TABLE II
Behavior toward Water of Polyvinyl Alcohols from Different Sources

Source of PV alcohol	Temperature of polymerization, °C.	Behavior at various water temperatures[a] 80°C.	90°C.	100°C.	110°C.	120°C.	130°C.
PV acetate	50	D(76)					
	−80	H.Sw.	D				
PV monochloroacetate	44	I	Sw.	D			
	20	I	Sw.	D			
	−20	I	Sw.	D			
PV dichloroacetate	44	I	L.Sw.	Sw.	D(101)		
	20	I	L.Sw.	Sw.	D		
	−20	I	L.Sw.	L.Sw.	Sw.	D	
PV trichloroacetate	44	I	Sw.	Sw.	D		
	20	I	Sw.	Sw.	H.Sw.	D	
	−20	I	Sw.	Sw.	Sw.	D(120)	
PV trifluoroacetate	44	I	Sw.	H.Sw.	H.Sw.	D	
	20	I	Sw.	Sw.	Sw.	D(120)	
	−20	I	Sw.	Sw.	Sw.	H.Sw.	D(126)

[a] D = dissolved; Sw. = swollen; H.Sw. = highly swollen; L.Sw. = lightly swollen; I = insoluble. Figures in parentheses give temperature of dissolution (determined in separate experiments).

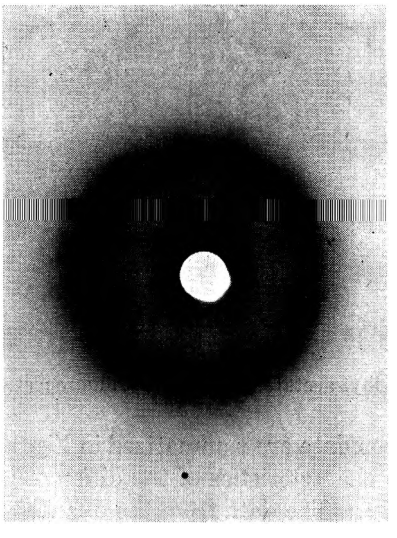

Fig. 5. Polyvinyl trifluoroacetate (from 90°C. polyvinyl acetate).

diffraction patterns of polyvinyl alcohols derived from 14 different esters. The data in Figures 1 and 2 show typical photometer traces corrected to the same total integrated intensities. This may be due, as Bunn has suggested,[6] to the ability of the hydroxyl groups to replace hydrogen isomor-

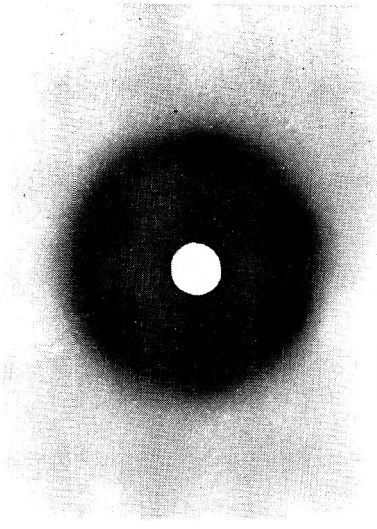

Fig. 6. Polyvinyl trifluoroacetate (50°C.).

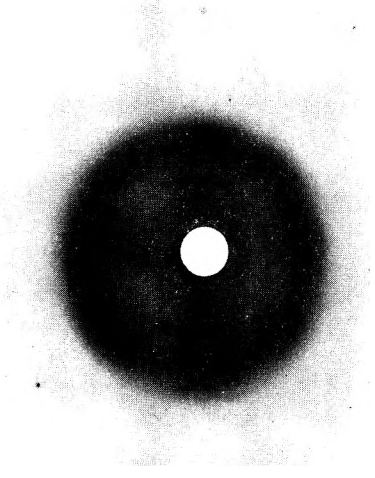

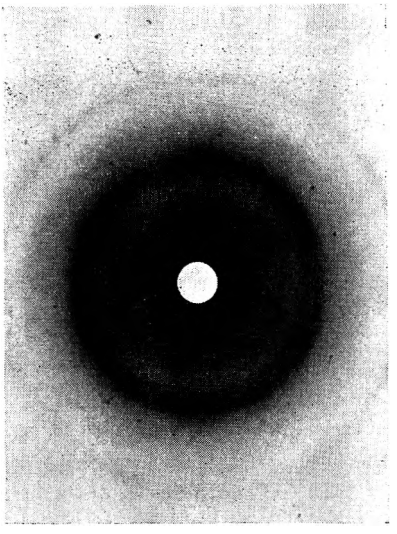

Fig. 8. Polyvinyl trifluoroacetate (−20°C.).

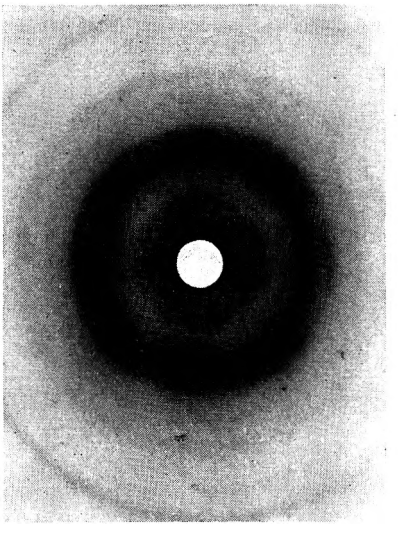

Fig. 9. Polyvinyl trifluoroacetate (from −80°C. polyvinyl acetate).

there was no major difference in tacticity; this might have been expected to be exhibited in the x-ray patterns. Figures 5–9 show that the samples of PVTFA obtained directly from the monomer possess the same order of crystallinity as those prepared via the acetates polymerized at comparable temperatures. In Table III are given the relative crystallinities of the polymers. From the greater crystallinity of the trifluoroacetates prepared from polyvinylacetates produced at lower temperatures it would appear that the latter are more regular in microstructure than are polyvinyl tri-

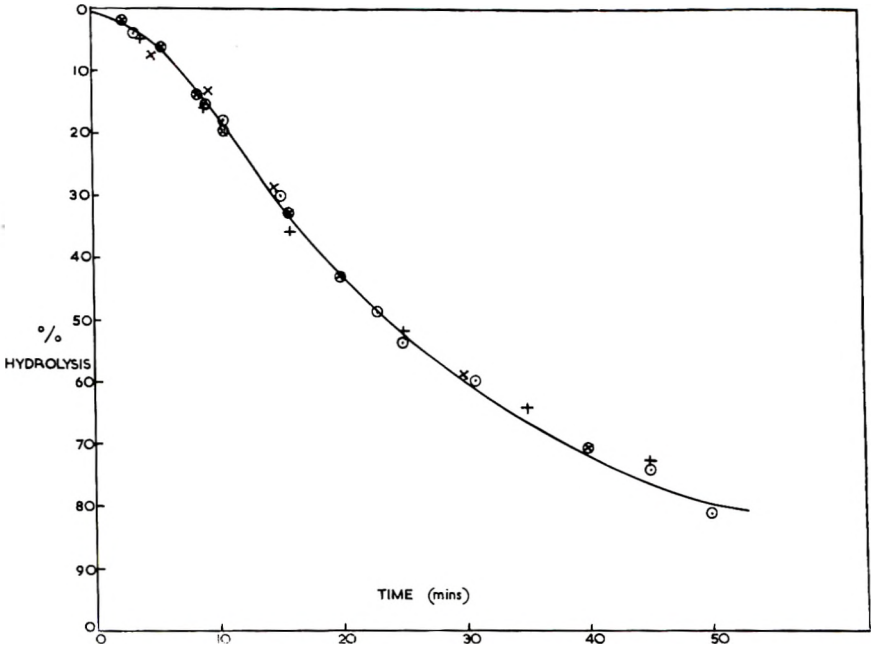

Fig. 10. Hydrolysis of polyvinyl acetates: (⊙) 50°C., from vinyl acetate (Bz_2O_2); (×) 20°C., from vinyl acetate (γ); (+) −80°C., from vinyl acetate (γ); (⊗) from 50°C. PVTFA (Bz_2O_2).

TABLE III
Relative Crystallinities of Polyvinyl Trifluoroacetates

Vinyl ester	Polymerization temperature, °C.	Figure no.	Relative amount of crystallinity
Acetate	+90	5	1
Trifluoroacetate	+55	6	1.2
Trifluoroacetate	+20	7	1.4
Trifluoroacetate	−20	8	1.9
Acetate	−80	9	2.3

fluoroacetates prepared at higher temperatures. These observations lead to contrary findings to those based on the water solubility of the polyvinyl alcohols of the previous workers, which we have fully confirmed (Table II).

It is to be noticed that although polymerization temperature has a marked effect on the crystallinities of PVTFA it has little influence on the water solubility, whereas the latter characteristic is determined largely by the structure of the monomer. This raises the issue as to whether factors other than steric regularity can influence water solubility. The hydrogen-bonded crystallites of polyvinyl alcohol possess some resistance to breakdown by water, which presumably first swells the amorphous regions of the polymer, so the increase in temperature of solubilization can

be attributed to an increase in the size or perfection of these polymer crystallites. Such an increase is, of course, what would be anticipated, as Fordham et al. have suggested,[1] from a corresponding increase in the syndiotacticity of the polymers. However, as it could also result from a decrease in the incidence of the main chain branching or other structural irregularities, the evidence from the water solubility of these polymers is not conclusive. (Branching through the ester groups is not considered here, since this would be eliminated during hydrolysis.) Further, there are known to be several peculiarities in the hydrolysis of haloacetate groups. Polyvinyl trifluoroacetate readily loses trifluoroacetic acid at room temperature and becomes insoluble in all solvents, and heterogeneous hydrolysis in water at room temperature also gives an insoluble polyvinyl alcohol (possibly by the formation of ether crosslinks). Haas, et al.[2] have also reported that the solubility of polyvinyl alcohol obtained from polyvinyl trifluoroacetate depends on the conditions of hydrolysis, but it is not certain whether these polymers were crosslinked. On the other hand, it has been reported that all the polyvinyl alcohols, whether prepared from vinyl acetate or other monomers, are essentially linear.[7] If this is so, branching cannot be considered a likely explanation of the differences.

The rates of hydrolysis of several of the alcohols were measured and, within the limits of reproducibility, were not significantly different (Fig. 10). In the case of polymethyl methacrylates it is known that the rates depend on the configuration of the polymer[8–10] and a similar effect might have been expected in this case. It is possible that the conformation of the alternative forms are not so different as to significantly affect hydrolysis rates, especially since the differences in tacticity may be relatively small.

Attempts to show up differences between the polymers by their ability to coordinate with heavy metal salts, which might also be expected to depend on configuration, also were negative; polyvinyl acetate polymerized as such or converted from polyvinyl trifluoroacetate combined with exactly the same amount of lead compound, both leading to enhancement of a higher order (13 A. x-ray) reflection.

Thus two techniques (staining with iodine[7] and water solubility) are indicative of greater syndiotacticity in PVTFA, x-ray crystallinity leads to the conclusion that the acetates and trifluoroacetates have comparable stereospecificity at the same polymerization temperature, and two techniques (hydrolysis rates and coordination of the acetates with lead salts) do not distinguish between the various polymers.

In conclusion, there seems no doubt that low polymerization temperatures favor increased steric regularity in free radical-initiated polyvinyl esters, and we suggest that, on balance, the evidence favors greater syndiotacticity in the polyvinyl trifluoroacetate, but that the differences are not large. The greater (lateral) order evidenced by x-ray crystallinity in the trifluoroacetates derived from low temperature polyvinyl acetates is to be ascribed to some other effect. No clear indication has been obtained as to what this might be, but the incidence of other steric irregularities, for ex-

ample, head-to-head, tail-to-tail addition, or minor amounts of branching, may vary with temperature and could affect one property (for example, crystallinity) without changing another (e.g., water solubility).

The authors thank the Dunlop Rubber Company Limited for permission to publish this paper.

References

1. Fordham, J. W. L., G. H. McCain, and L. E. Alexander, *J. Polymer Sci.*, **39**, 335 (1959).
2. Haas, H. C., E. S. Emerson, and N. W. Schuler, *J. Polymer Sci.*, **22**, 291 (1956).
3. Bohn, C. R., J. R. Schaefgen, and W. O. Statton, *J. Polymer Sci.*, **55**, 531 (1961).
4. Goppel, J. M., *Appl. Sci. Research*, **A1**, 3 (1947).
5. Hermans, P. H., and W. Weidinger, *J. Appl. Phys.*, **19**, 49 (1948).
6. Bunn, C. W., *Nature*, **161**, 929 (1948).
7. Imai, K., and M. Matsumoto, *J. Polymer Sci.*, **55**, 335 (1961).
8. Glavis, F. J., *J. Polymer Sci.*, **36**, 547 (1959).
9. Smets, G., and W. de Loecker, *J. Polymer Sci.*, **45**, 461 (1960).
10. Chapman, C. B., *J. Polymer Sci.*, **45**, 237 (1960).

Résumé

Se basant sur les propriétés en solution et les cristallinités par rayons-X d'esters polyvinyliques et d'alcools dérivés de plusieurs esters polyvinyliques polymérisés à des températures différentes, on considère que les haloacétates polyvinyliques ont une structure plus régulière que l'acétate polyvinylique. Néanmoins, il n'est pas prouvé que cette régularité résulte d'une syndiotacticité accrue. On a trouvé que les cristallinités des trifluoroacétates polyvinyliques préparés à partir d'acétate de vinyle via les alcools polyvinyliques sont comparables avec ceux préparés directement au départ de trifluoroacétate vinylique à des températures de polymérisation similaires. Les réseaux de diffraction aux rayons-X de l'acétate polyvinylique préparé à partir du monomère et ceux de l'alcool polyvinylique acétylé, obtenu par hydrolyse du trifluoroacétate polyvinylique sont identiques. De même les réseaux des alcools polyvinyliques dérivés de plusieurs esters vinyliques différents ne peuvent être distingués l'un de l'autre. Les acétates de polyvinyle préparés à haute et basse température à partir du trifluoroa cétate subissent tous l'hydrolyse en solution alcaline à une vitesse quasi égale. La découverte importante de cette recherche est la suivante: tandis que la température de polymérisation a un effet marqué sur la cristallinité du trifluoroacétate polyvinylique, elle a une influence minime sur la solubilité dans l'eau des alcools polyvinyliques. La solubilité dans l'eau est déterminée par la structure du monomère qui forme l'alcool polyvinylique.

Zusammenfassung

Aus den Lösungseigenschaften und der Röntgenkristallinität von Polyvinylestenr und von Polyvinylalkoholen, die sich von mehreren, bei verschiedener Temperatru polymerisierten Polyvinylestern ableiten, wird geschlossen, dass Polyvinylhaloacetate eine regelmässigere Struktur besitzen als Polyvinylacetat; es konnte aber nicht nachgewiesen werden, dass diese Regelmässigkeit in einer erhöhten Syndiotaktizität besteht. Die Kristallinität von Polyvinyltrifluoracetat, das aus Vinylacetat über den Polyvinylalkohol dargestellt wurde, ist der direkt aus Vinyltrifluoracetat bei vergleichbarer Polymerisationstemperatur dargestellten Substanz vergleichbar. Die Röntgendiagramme von Polyvinylacetat aus dem Monomeren und aus acetyliertem Polyvinylalkohol, der durch Hydrolyse von Polyvinyltrifluoracetat erhalten wurde, sind identisch. In gleicher Weise können die Diagramme von Polyvinylalkoholen aus mehreren verschiedenen Vinylestern nicht unterschieden werden. Bei hoher und tiefer Temperatur

dargestellte Polyvinylacetate und solche aus dem Trifluoracetat hydrolysieren in alkalischer Lösung alle mit im wesentlichen gleicher Geschwindigkeit. Ein wichtiges Ergebnis der vorliegenden Untersuchung ist der Befund, dass zwar die Polymerisationstemperatur einen merklichen Einfluss auf die Kristallinität von Polyvinyltrifluoroacetat besitzt, die Wasserlöslichkeit der Polyvinylalkohole aber wenig beeinflusst. Die Wasserlöslichkeit wird durch die Struktur des Monomeren bestimmt, aus welchem der Polyvinylalkohol erhalten wurde.

Received February 26, 1962

JOURNAL OF POLYMER SCIENCE: PART A VOL. 1, PP. 1521–1529 (1963)

Electron Spin Resonance Spectra of Aged, γ-Irradiated Polystyrenes*

R. E. FLORIN, L. A. WALL, and D. W. BROWN, *National Bureau of Standards, Washington, D. C.*

Synopsis

The electron spin resonance spectrum of polystyrene that has been γ-irradiated at -196°C. changes gradually with time from a broad three-peaked structure with outer derivative peaks at ± 46 gauss to a much narrower structure with poorly separated outer derivative peaks at ± 21–24 gauss. The deuterated polystyrenes behave likewise in general. The aged radicals of α,β,β-trideuterostyrene and β,β-dideuterostyrene exhibit only a single peak with derivative maxima at ± 7 or 8 gauss from center. The aged spectra are all consistent with the hypothesis of major hyperfine interaction with β hydrogens. During the aging about 80% of the original radicals are lost, but the remainder are very long-lived. Poorly evacuated samples or those with added benzene decay much more rapidly.

INTRODUCTION

When polystyrene is exposed to ionizing radiation, radicals are formed which can be observed by electron spin resonance (ESR) spectroscopy. The hyperfine structure (hfs) consists of three poorly separated peaks. The separation between the outermost derivative peaks was estimated to be near 93 gauss for samples irradiated at -196°C.[1,2] and near 50 gauss for other samples irradiated at about 20°C.[3] Both the insensitivity to isotopic substitution in the chain and at the *para* position in the ring and the relatively large value of the hyperfine splitting led to the tentative proposal that the radical is formed by removal of the α-hydrogen atom and that the hyperfine structure is caused principally by interaction with the two ring hydrogen atoms in the *ortho* position[1] in a strained configuration. After several months the outer peaks disappeared, and the inner peak developed traces of structure and slight differences between the isotopic polystyrenes; these changes were attributed to a gradual relaxation of the ring and chain to a more stable position, at which the *ortho* hydrogen interaction became minor and the smaller interaction with the β chain hydrogen atoms became dominant. These changes have been investigated in detail with high-sensitivity detection.

* Paper presented before the 140th National Meeting of the American Chemical Society, Chicago, September 4, 1961.

EXPERIMENTAL

The general experimental procedure has been described previously, and most of the samples were identical with those previously studied.[1] Samples consisting of cut film (about 0.04 g.) and lumps and plugs (about 0.10 g.) were evacuated in tubes of glass or high-purity silica to a pressure of less than 10^{-4} mm. Hg and at 100–145°C. for upwards of 15 hr., except for a few instances to be discussed later in which the evacuation was of only 1 hr. duration. The samples were irradiated at −196°C., at doses of 1×10^{21}–3×10^{21} e.v./g., in a Co^{60} gamma source having a dose rate of 0.4×10^{6}–0.7×10^{6} r/hr. and were subsequently stored in subdued daylight at about 27°C. ESR spectra were observed at microwave power of about 0.1 mw. with 100 kcycle field modulation. The temperature of observation was usually 27°C., but occasionally it was −196°C. When benzene, to the extent of 30% by weight of sample, was added at a pressure of about 100 mm. to a sample of irradiated poly-α,β,β-trideuterostyrene film, the radicals disappeared in a few days. On the other hand, radicals which had remained two years *in vacuo* disappeared in less than 1 hr. on opening to the atmosphere. In the aged samples, the background from the irradiated high-purity quartz containers proved troublesome; this was eliminated by the usual expedient of heating the tube end for a few minutes while keeping the sample cold with liquid nitrogen.

RESULTS AND DISCUSSION

1. Radical Concentrations

The concentrations of the radicals at various times are shown in Table I. As mentioned earlier, there is only a minor change in concentration upon warming from −196°C. to +27°C. In well-evacuated samples, moderate concentrations of radicals persist for years, after an initial decrease to about 20% within the first few months. With poorly evacuated samples the corresponding decrease occurs in 2 days. Since the admission of oxygen destroys all radicals in an hour, oxygen may be responsible. Some other substances, for example, traces of monomer or solvent, which plasticize the polymer slightly and facilitate diffusion may play a role in the two-day disappearance. With the added benzene vapor the concentration decreases fairly rapidly but without any appreciable change in the ratio of side-peak to central-peak intensity. Apparently there are two different processes: a relaxation allowing disappearance of side peaks, with modification of the central peak structure, which is facilitated by only a few percent of solvent, and a general diffusion permitting disappearance by radical combination. In the presence of benzene the data fit a simple second-order plot with $k = 3.5 \times 10^{-3}$ l./mole-sec. at 27°C. In the well-evacuated sample the kinetics is complicated, and some radicals survive for a long time. Second-order plots from the badly scattered data suggest rate constants near 3×10^{-4} l./mole-sec. in the period from 2 to 20 days and $1 \times$

10^{-4} l./mole-sec. in the whole 550-day period. Simple second-order kinetics seem to be associated with soft media (for example, crystals near the melting point), where diffusion is not too slow. The solvent might have been expected to cause narrowing of lines by rotational motion or oscillation, but narrowing was not observed.

TABLE I
Radical Concentrations in Irradiated Polystyrenes after Storage

Polymer	Radical concentrations after storage, 10^{16} radicals/g.						
	Initial	1 day	2 days	12 days	20 days	76 days	400–550 days
Polystyrene[a]	209	—	—	—	—	45	56
Polystyrene[b]	126	—	27	—	—	—	—
Poly-β,β-d_2-styrene[a]	120	—	—	—	—	—	13
Poly-α,β,β-d_3-styrene[a]	52	—	—	—	—	—	12
Polystyrene[a]	118	97	67	81	91	—	—
Poly-α,β,β-d_3-styrene[a]	75	52	48	38	54	—	—

[a] Evacuated before irradiation at 0.1 μ, 16 hr., 145°C.
[b] Evacuated before irradiation at 0.1 μ, 1 hr., 70°C.

2. Spectra: General

Typical spectra are shown in Figures 1 and 2*c*, and numerical parameters in Table II. Age broadens the central peak of polystyrene and

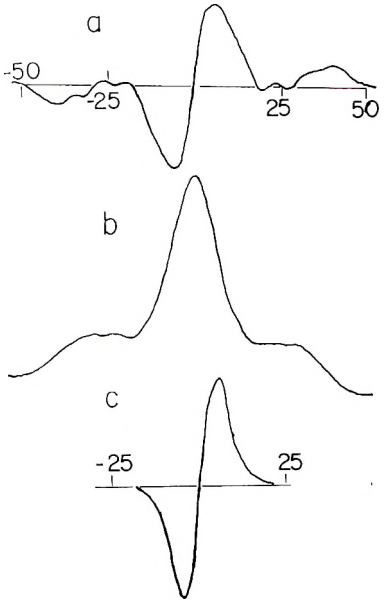

Fig. 1. ESR spectra of poly-α,β,β-trideuterostyrene radicals: (*a*) derivative of absorption curve, freshly irradiated at −196°C.; (*b*) integrated derivative of (*a*); (*c*) derivative curve, aged radicals. Abscissae are magnetic field in gauss.

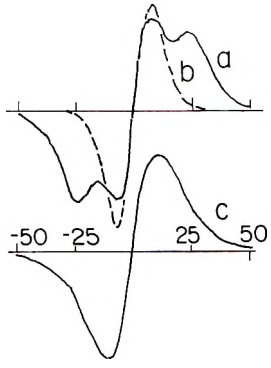

Fig. 2. ESR spectra of aged irradiated deuterium-substituted polystyrenes: (*a*) polystyrene; (*b*) poly-α,β,β-trideuterostyrene; (*c*) poly-β-deuterostyrene. Abscissae are magnetic field in gauss.

narrows that of poly-α,β,β-trideuterostyrene (Table II, last column). The spectrum of freshly irradiated material has complications not evident on casual inspection. The central peak of the derivative curve (Figure 1*a*, other examples in reference 1) is too high for any combination of three simple absorption lines in 1:2:1 ratio, regardless of line width and spacing. Also, the side peaks of Figure 1*a* and of its analogs in reference 1, are actually composite, showing minor derivative peaks at ± 45, ± 37, and ± 26 gauss when examined under sufficient resolution. These minor spacings are the same in normal polystyrene and poly-α,β,β-d_3-styrene. Two general explanations are available for the peak height anomaly. (*1*) The intensity ratio is indeed 1:2:1, but the side components are unusually broad and not symmetrical. This can happen ideally for two geometrically equivalent protons with a large anisotropic hyperfine splitting parameter.[4,5] The minor splittings are neglected in rough approximation. The absorption curve (Fig. 1*b*) obtained by integration of Figure 1*a*, is loosely reminiscent of certain line shapes of this sort.[4] Although the spectra of the somewhat related radicals of irradiated olefins,

$$\mathrm{R\dot{C}HCH{=}CHR} \longleftrightarrow \mathrm{RCH{=}CH\dot{C}HR},$$

did not give evidence of especially large anisotropic hyperfine interaction,[6] it is possible that this was minimized in the reference cited by the occurrence of torsional oscillations, and that the two *ortho* ring hydrogens in the rigid polystyrene are a special case. According to this view, Figure 1 is the spectrum of a pure species. (*2*) The second explanation of the height anomaly is that Figure 1*a* is not the spectrum of a pure species (I) but of a mixture of I with the final species (II). If this is so, the spectrum of pure I is unknown, as many combinations of arbitrary I spectra with varying proportions of the II spectrum might give the observed Figure 1*a*. Reliable isolation of the spectrum of pure I from decay observations would require rather precisely controlled field and intensity measurements. If the

TABLE II
Derivative Curve Spacings in Aged Polystyrene Radicals

Polymer	Spacing, gauss from center		
	Inner peak	Outer peak	0.75 maximum level[a]
Polystyrene			
1-day[b]	9.5	—	19.6
2-day[b]	7.1	24.0	28.7
400-day[c]	8.3	21	27
Poly-*d*-styrene, 500-day	6.6	23	28.6
Poly-α,β,β-d_3-styrene			
3-hr.[b]	7.6	—	15.4
2-day[b]	7.4	—	13.0
400-day[c]	7.8	—	12.0
Poly-β,β-d_2-styrene, 550-day[c]	7.2	—	12.0
Poly-β-*d*-styrene, 550-day[c]	10.4	—	19.9

[a] Arbitrary measure approximating the point of half maximum absorption.
[b] Evacuated before irradiation at 0.1 μ, 1 hr., 70°C.
[c] Evacuated before irradiation at 0.1 μ, 16 hr., 145°C.

spectrum of pure I is approximately a set of 3 lines of intensity ratio 1:2:1, derivative peak width 26 gauss (somewhat greater than experimental for the center line of Fig. 1*a*), and separation 35 gauss, then the samples freshly irradiated at −196°C. contain perhaps 75% of species I and 25% of II. Samples irradiated at 20°C. for long periods contain very much less of species I.

3. Spectra: Poly-β-deuterostyrene

The spectra of aged poly-α-deuterostyrene, poly-*p*-deuterostyrene, and poly-*m*-methylstyrene resemble the spectrum of aged polystyrene (Fig. 2*a*), with derivative peaks at ±7 to 9 and ±21–24 gauss (see also Table II). The spectra of aged poly-α,β,β-trideuterostyrene and poly-β,β-dideuterostyrene differ from them and resemble each other, being merely a single sharp line having derivative peaks at ±7.5 gauss (Figs. 1*c* and 2*b*). These line shapes are consistent with a radical structure formed by removal of α-hydrogen, and hyperfine interaction with two of the four β-hydrogen atoms, as originally proposed by Abraham and Whiffen.[3]

The spectrum of poly-β-deuterostyrene (Fig. 2*c*) is more complicated. If the interaction is with any two β-hydrogens taken at random the spectrum should be obtained by adding 0.25 of the DD spectrum, 0.25 of the HH spectrum, and 0.50 of the HD spectrum.

A rough approximation to the latter can be made as follows. The outer peaks of ordinary polystyrene are isolated by subtracting the single-peak spectrum of poly-α,β,β-trideuterostyrene, normalized to 0.5 integrated intensity (Fig. 3). This assumes that in the trideutero compound the broadening due to all other causes is large compared to that from two D

nuclei. The two peaks are then moved to half the separation, corresponding to the two peaks for interaction with a single H atom. The component peak width may be either left unchanged or reduced proportionally. The former procedure should be valid if the line width is due to unresolved minor hyperfine structure. If the line width is due principally to a large anisotropic hyperfine interaction, then the line widths for two interacting protons are in general much larger than for a single proton,[4,5] but the proportional reduction is taken here as a representative

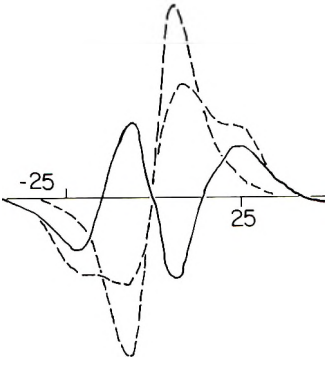

Fig. 3. Outer peaks of aged normal polystyrene by substraction: (*a*) normal polystyrene; (*b*) poly-α,β,β-trideuterostyrene (0.5 intensity); (*c*) the difference of other two spectra.

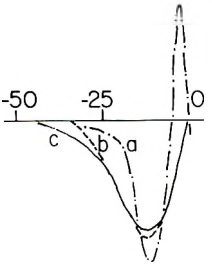

Fig. 4. Calculated and experimental ESR spectra of aged irradiated poly-β-deuterostyrene; (*a*) calculated for anisotropic broadening alone; (*b*) calculated for unresolved hfs broadening alone; (*c*) experimental.

compromise. The spectrum so obtained (HD) is added to those for normal polystyrene (HH) and α,β,β-trideuterostyrene (DD) in the 2:1:1 ratio of probability of occurrence. The results are compared with the observed spectrum in Figure 4c. The assumption of totally anisotropic broadening (Fig. 4*a*) is very unrealistic in the center. The assumption of unresolved minor hyperfine broadening (Fig. 4*b*) gives a much better picture. Constructions by methods recently described,[4,5] while laborious, should give a reasonable fit in both regions.

4. Relation between the Two Radical Spectra

It was hoped that controlled decay experiments would reveal whether the aged radical (II) is formed from the fresh radical (I) or is merely a species present in low concentration but with a long lifetime. The emergence of II in amount equal to the original I would be decisive evidence that I becomes II. However, some interference from I is present after 20 days, when the total radical concentration has fallen to 70% of the initial, and a clear spectrum of II is not obtained until 76 days, when the radical concentration has fallen to about 25% of the initial. If we assume a simple three-line spectrum for I, the concentration of I after 20 days is 25–35% of the initial total, and of II, 37–53%. The rate constant for disappearance of I is about 8×10^{-4} l./mole-sec. if second order, or 3×10^{-7}–6×10^{-7} sec.$^{-1}$ if first order; the second-order constant for this process is about twice that for disappearance of total radicals in this period. The absolute amount of II seems to increase in the 20-day interval; however, the basis of the subtractive estimation is rather uncertain, and the results scatter greatly.

In the benzene addition experiment, I remains the principal species, despite greater overall decay. It was tentatively supposed that II is merely a relaxed configuration of I. Unfortunately, most agents, such as solvent or heat, which could cause relaxation of I into II, would also promote diffusion and recombination. Unstrained II, if initially present and not formed from I, might have slightly superior chemical stability and a higher activation energy for transfer reactions with mobile impurities, if any. Small radicals formed by transfer would diffuse and recombine rapidly. Both diffusion and relaxation, in the absence of impurities, should involve a series of cooperative jumps of chain segments. Diffusion resulting in recombination would presumably require more such jumps. Since most of the chain segments involved are not radical sites, one might expect similar second-order rate constants for combinations of I + I, I + II, and II + II, and a first-order rate constant for the relaxation I → II. Nevertheless, relaxation I → II is experimentally not especially rapid relative to the combination processes, and it is not certain whether it is first-order. The existence of radical sites of widely differing lattice energy would complicate the kinetics. A possible mechanism for termination without long-range diffusion is a sequence of abstractions or additions, as considered by Dole for irradiated polyethylene.[11] It is plausible that both strained and unstrained radicals could be formed as intermediates with relatively little change in the ratio of the two with progress of the reaction.

One cannot altogether exclude the possibility that I is chemically different from II, perhaps a cyclohexadienyl radical formed by addition of H or D to the ring (see note added in proof). By analogy with the allyl and substituted allyl radicals formed in irradiated olefins,[6] this radical would have appreciable spin density distributed in sites *ortho* and *para* to the CH_2 group resulting from addition, and hence hyperfine interactions of about 15 gauss

with two or three hydrogen atoms on double-bonded carbon, and somewhat larger hyperfine interactions, perhaps 21–29 gauss, with the methylene hydrogen atoms. The number of atoms involved seems too large to account for the simple observed spectrum of I; however, if the interactions with the methylene are made especially large and all others diminished (which might happen in molecules with less torsional freedom than aliphatic allyl radicals), this cyclohexadienyl radical structure for I remains a possibility. If this is so, only H atoms and not D atoms must add to the ring to form the radical, even in irradiated α,β,β-trideuterostyrene.

Polystyrene negative ions in solution are reported to have complicated spectra,[8,9] and detailed molecular orbital calculations for these ions predict a distribution of spin density over many positions, none predominant.[8] A widespread distribution of spin density might at first sight be expected for the radicals of irradiated polystyrene also.[10] The spin distribution in a radical of the present type, at least in species II, is probably very different from that of the ion; for example, the spin density is 0.60 or higher at the methyl carbon atom of triphenylmethyl and dimesitylmethyl, which is analogous to the α-carbon atom of the present radical II.[11,12] Two recent experimental anomalies with regard to poly-α-methylstyrene should be mentioned briefly. The spectrum of poly-α-methylstyrene negative ion in solution[8] has a very similar shape to that previously reported,[1] although the spacing parameters are different; and the irradiation of very finely divided poly-α-methylstyrene does not result in the spectrum seen earlier,[1] but in a broad complicated spectrum.[10] We have confirmed the latter observation on several finely divided samples.

Note added in proof: Experiments now in progress on poly 2,3,4,5,6-pentadeuterostyrene eliminate the possibility that *ortho* protons give the outer peaks in the spectra of radical I and demonstrate that radical I has a cyclohexadienyl structure.

This paper is based on work supported by the Aeronautical Research Laboratory, Wright-Patterson Air Force Base, Ohio.

References

1. Florin, R. E., L. A. Wall, and D. W. Brown, *Trans. Faraday Soc.*, **56**, 1304 (1960).
2. Tsvetkov, Yu. D., Yu. H. Molin, and V. V. Voevodskiĭ, *Vysokomolekulyarnye Soedineniya*, **1**, 1807 (1959).
3. Abraham, R., and D. M. Whiffen, *Trans. Faraday Soc.*, **54**, 1291 (1958).
4. Blinder, S. M., *J. Chem. Phys.*, **33**, 748 (1960).
5. Sternlicht, H., *J. Chem. Phys.*, **33**, 1128 (1960).
6. Poole, C. P., and R. S. Anderson, *J. Chem. Phys.*, **31**, 346 (1959).
7. Dole, M., and C. D. Keeling, *J. Am. Chem. Soc.*, **75**, 6082 (1953).
8. Morigagi, K., K. Kuwata, and K. Hirota, *Bull. Chem. Soc. Japan*, **33**, 952, 958 (1960).
9. Szwarc, M., private communication.
10. Fischer, H., K. H. Hellwege, and U. Johnsen, *Kolloid-Z.*, **170**, 62 (1960).
11. Jarrett, H. S., and G. J. Sloan, *J. Chem. Phys.*, **22**, 1783 (1954).
12. Adam, F. C., and S. I. Weissman, *J. Am. Chem. Soc.*, **80**, 2057 (1958).

Résumé

Le spectre de résonance de spin électronique du polystyrène, irradié aux rayons gamma à −196°C, change graduellement en fonction du temps d'une structure large à trois pics à ±46 gauss avec les pics extérieurs dérivés peu séparés à ±21 à 24 gauss. Les polystyrènes deutérés se comportent d'une manière analogue. Les radicaux plus anciens de α,β,β-trideutérostyrène et β,β-dideutérostyrène ne donnent qu'un seul pic avec des maxima dérivés à ±7 à 8 gauss du centre. Les spectres plus vieux sont tous en accord avec l'hypothèse d'une interaction hyperfine majeure avec les hydrogènes β. Pendant le vieillissement environ 80% des radicaux originaux sont perdus mais les restants ont une très longue durée de vie. Des échantillons sous vide insuffisant ou ceux contenant encore du benzène se désaggrègent beaucoup plus vite.

Zusammenfassung

Das Elektronspinresonanzspektrum von bei −196°C γ-bestrahltem Polystyrol geht mit der Zeit von einer breiten Struktur mit drei Maxima und äusseren Derivativmaxima bei ±46 Gauss zu einer viel engeren Struktur mit schlecht aufgelösten äusseren Derivativmaxima bei ±21 bis 24 Gauss über. Die deuterierten Polystyrole verhalten sich im allgemeinen gleich. Die gealterten Radikale von α,β,β-Trideuteropolystyrol und β,β-Dideuteropolystyrol zeigen nur ein Maximum mit Derivativmaxima bei ±7 oder 8 Gauss vom Zentrum. Die gealterten Spektren entsprechen alle der Annahme einer hauptsächlichen Hyperfein-Wechselwirkung mit β-Wasserstoff. Während der Alterung gehen etwa 80% der ursprünglichen Radikale verloren, der Rest ist aber sehr langlebig. Schlecht evakuierte Proben oder solche mit Benzolzusatz zeigen einen viel rascheren Abfall.

Received March 6, 1962

JOURNAL OF POLYMER SCIENCE: PART A VOL. 1, PP. 1531–1541 (1963)

Polybenzimidazoles. II*

HERWARD VOGEL and C. S. MARVEL, *Department of Chemistry, University of Arizona, Tucson, Arizona*

Synopsis

A polybenzimidazole has been prepared from 3,3′-diaminobenzidine and phthalic anhydride which has a high molecular weight and very good heat stability. Replacement of the hydrogen atoms on the nitrogen of the imidazole nuclei in a polybenzimidazole does not improve the heat stability as indicated by the properties of poly-2,6-(*m*-phenylene)-3,5-diphenyldiimidazobenzene. Polybenzimidazoles with aliphatic units have been prepared from 3,3′-diaminobenzidine and the diphenyl ester of succinic and glutaric acids. The diphenyl esters of oxalic and malonic acids did not yield polymers presumably because cyclic amides were formed. Further hydrolytic stability tests on polybenzimidazoles have been reported. Some model compounds have been prepared for comparison of their melting points and absorption spectra with those of the corresponding polymer.

In an earlier publication[1] it has been reported that the melt condensation of suitable aromatic tetraamines with the diphenyl esters of aromatic dicarboxylic acids produced linear, high molecular weight materials which contained benzimidazole nuclei as recurring units. The wide applicability of this polycondensation reaction and the remarkable thermal stabilities of the polybenzimidazoles were also noted. In continuation of this work some new polybenzimidazoles and some model compounds have been synthesized.

A convenient procedure was worked out for laboratory scale production of 3,3′-diaminobenzidine following basically a combination of the methods given by Brunner and Witt,[2] Hodgson,[3] and Hoste.[4] The amine was purified by recrystallization from methanol and melted at 178–179°C. It was obtained in 37% overall yield based on benzidine dihydrochloride. Since this amine is difficult to obtain, a detailed description of its preparation is given in this paper.

It has been found that a polybenzimidazole can be readily prepared from phthalic anhydride and 3,3′-diaminobenzidine and this polymer has as good or better stability at high temperatures (Fig. 1) than that reported for the polymer previously described from isophthalic acid. The *ortho*-isomer is soluble in formic acid but is not soluble in dimethyl sulfoxide.

* Part of this work was carried out at the University of Illinois under the sponsorship of Contract No. AF-33(616)-5486 with the Nonmetallic Materials Laboratory of Wright Air Development Division, Wright-Patterson Air Force Base, Ohio. The other part was supported by an E. I. du Pont de Nemours and Company, Inc. fellowship at the University of Arizona.

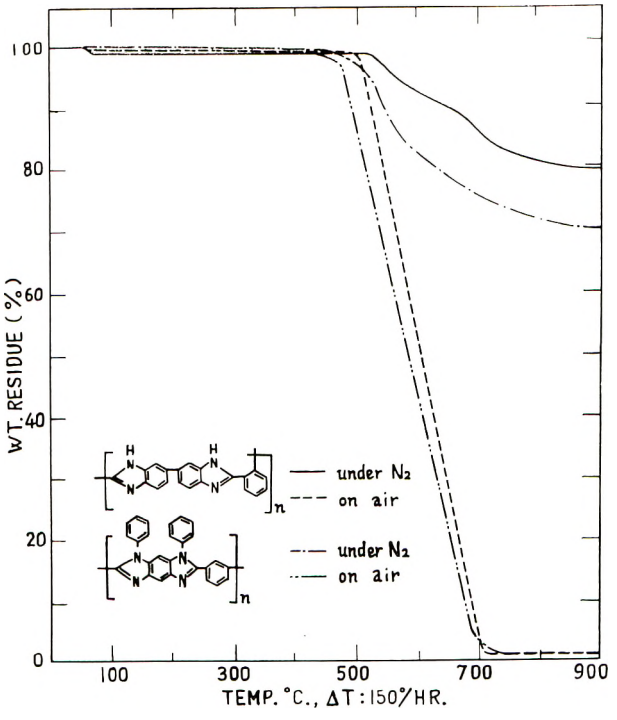

Fig. 1. Thermal gravimetric curves of benzimidazole polymers.

It was thought that perhaps a more stable structure would result if the hydrogens on the nitrogens of the recurring imidazole units were replaced by aryl groups. To test this idea 1,3-dianilino-4,6-diaminobenzene was synthesized and condensed with diphenyl isophthalate to give the phenyl-substituted polymer (II).

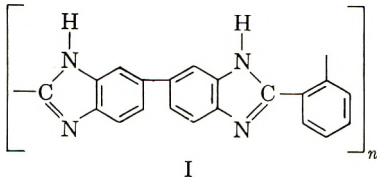

I

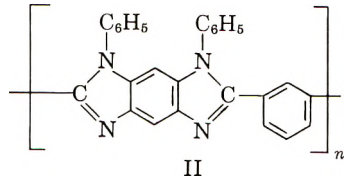

II

A slightly higher molecular weight polymer was prepared by use of the *p*-phenylphenol ester of isophthalic acid in place of the phenyl ester. In thermal gravimetric analyses tests (see Fig. 1) this polymer was actually less stable to heat than the unphenylated product reported earlier.[1]

For comparative tests with the polymers, model compounds were prepared from *o*-phenylenediamine and phthalic, isophthalic, and terephthalic acids.

Attempts were made to prepare polybenzimidazoles from 3,3′-diaminobenzidine and the diphenyl esters of oxalic, malonic, succinic, and glutaric acids. No polymers were obtained from the oxalic and malonic derivatives

apparently because of cyclic amide formation. High molecular weight polymers were obtained from the succinic and glutaric derivatives.

Some further tests on the hydrolytic stability of this class of polymers are reported. A comparison of the infrared spectra of the new polymers and the model compounds are recorded in Figure 2.

EXPERIMENTAL

3,3′-Diaminobenzidine

a. Benzidine. A 257-g. portion (1 mole) of benzidine dihydrochloride was dissolved in 3.5 l. of hot water, and with stirring a solution of 90 g. of sodium hydroxide in 300 ml. of water was added. The mixture was then cooled to 10°C. and the benzidine was collected by suction filtration, washed with cold water, and dried in a vacuum oven. The yield was 182 g. (99%).

b. Diacetylbenzidine. In a 3-l., three-necked flask fitted with a mechanical stirrer and a reflux condenser was placed 182 g. (0.99 mole) of benzidine and 1500 ml. of glacial acetic acid. The mixture was heated until all was dissolved and then 200 ml. of acetic anhydride was added. The slurry thus obtained was stirred at reflux temperature for 2 hr. The reaction mixture was allowed to cool to room temperature and the solid was filtered by suction, washed with alcohol, and dried overnight at about 80°C. in a vacuum oven. The yield of diacetylbenzidine melting at 340–343°C. (dec.) was 246 g. (92%). Direct acetylation of benzidine dihydrochloride did not give a sufficiently pure product.

c. 3,3′-Dinitrobenzidine. In a 2-l., three-necked flask fitted with a thermometer, mechanical stirrer, and a powder funnel was placed 1200 ml. of yellow fuming nitric acid (90%). With the temperature maintained at −10°C. by a Dry Ice–acetone bath and with vigorous stirring, 246 g. (0.91 mole) of diacetylbenzidine was added carefully within about 10 min. The red solution was stirred for an additional ½ hr. with cooling bath removed. The temperature was allowed to rise to 0°C. The solution was then poured with stirring into 6 l. of crushed ice. The precipitated yellow nitro compound was collected on a 12-in. Buchner funnel, sucked and pressed as dry as possible with a large glass stopper. The filter cake was then suspended in 3 l. of water and the filtration was repeated. The crude diacetyl-3,3′-dinitrobenzidine, dried as completely as possible by suction and pressing, was placed in a 5-l. three-necked flask fitted with a mechanical stirrer and reflux condenser, and suspended in 2.5 l. of 95% ethanol. The suspension was stirred and heated to about 60°C. Then 200 g. of potassium hydroxide dissolved in 300 ml. of water was added. If the filter cake was too wet, a larger excess of potassium hydroxide was necessary to effect complete removal of the acetyl groups. The mixture was then brought to boil and refluxed with stirring for 10 min. After cooling, the separated red crystalline powder was filtered, washed with

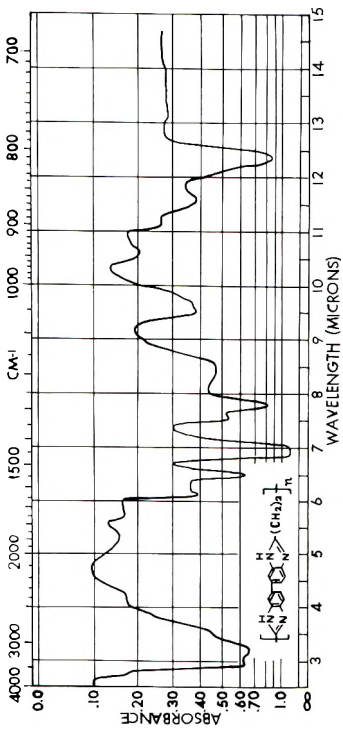
4000 3000 2000 1500 CM-1 1000 800 700
WAVELENGTH (MICRONS)
ABSORBANCE

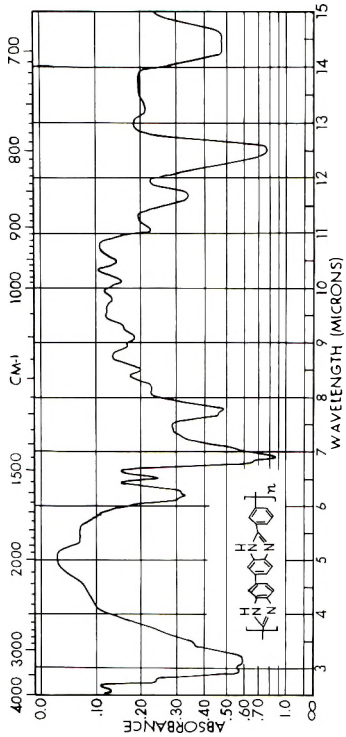
4000 3000 2000 1500 CM-1 1000 900 800 700
WAVELENGTH (MICRONS)
ABSORBANCE

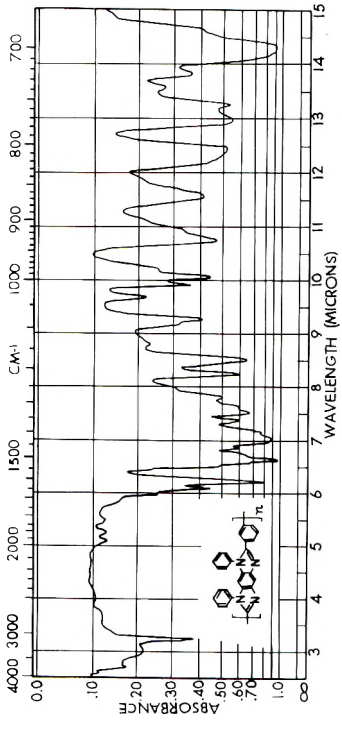
4000 3000 2000 1500 CM-1 1000 900 800 700
WAVELENGTH (MICRONS)
ABSORBANCE

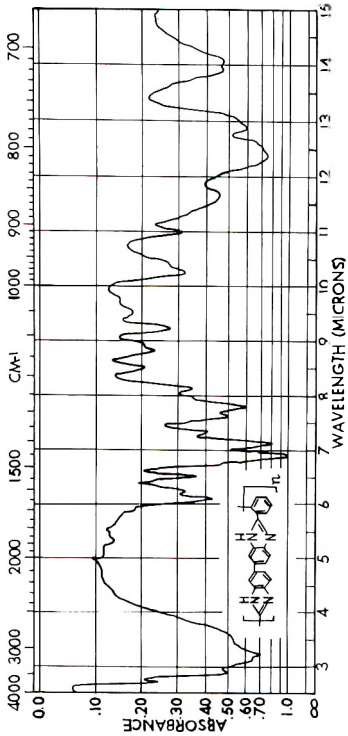
4000 3000 2000 1500 CM-1 1000 900 800 700
WAVELENGTH (MICRONS)
ABSORBANCE

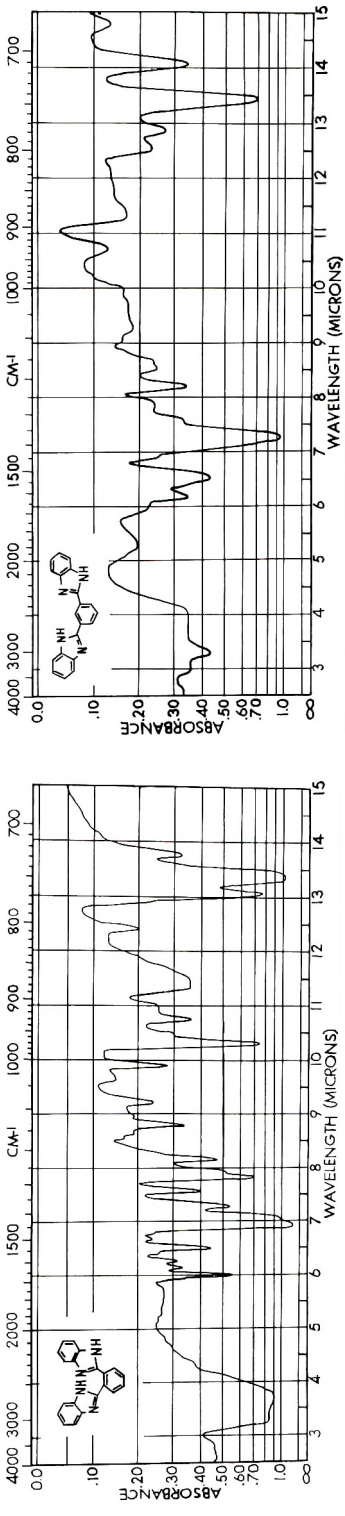

Fig. 2. Infrared patterns of benzimidazole polymers and model compounds.

methanol, and dried in a vacuum oven at 80°C. The yield of 3,3′-dinitrobenzidine melting at 280–283°C. was 216 g. (86%).

d. 3,3′-Diaminobenzidine. In a 5-l. flask were placed 2.5 l. of concentrated hydrochloric acid and 1200 g. of stannous chloride dihydrate. The mixture was stirred and 216 g. (0.79 mole) of 3,3′-dinitrobenzidine was added in small portions over about 15 min. Occasional cooling was required so that the reaction temperature did not rise above 60°C. The thick slurry was then stirred for an additional 2 hr. at about 40°C. in order to complete the reduction. After cooling to 10°C., the solid was filtered by suction and washed with 300 ml. of hydrochloric acid (sp. gr. 1.09). The filter cake was then dissolved in 3 l. of water and treated with about 10 g. of decolorizing Darco. After filtration, the 3,3′-diaminobenzidine tetrahydrochloride was precipitated with 1.5 l. of concentrated hydrochloric acid. The mixture was cooled and filtered. This purification by reprecipitation was repeated with the same quantities of reagents. It was repeated a third time if the product still contained a significant amount of tin salts or was still significantly colored. The recovered white 3,3′-diaminobenzidine tetrahydrochloride was dried as completely as possible by suction and pressing. It was then dissolved in 2 l. of water and added to a stirred solution of 200 g. of sodium hydroxide in 1800 ml. of water, cooled by an ice bath. It was necessary to check that the reaction mixture was still basic. The precipitate was filtered with suction, washed on the filter with 200 ml. of cold water, an l dried as completely as possible by suction and pressing. The yield of the slightly purple 3,3′-diaminobenzidine, dried in a vacuum desiccator over phosphorus pentoxide, was 126 g. (74%), melting at 175–178°C. The product was recrystallized in three portions from about 3 l. of boiling methanol. The hot solutions were filtered, cooled rapidly to −10°C. and allowed to stand for about 6 hr. The rate of crystallization was enhanced by scratching with a glass rod. The separated solid was then filtered. The mother liquors were concentrated on the water bath to $^1/_5$ of their volume and on cooling gave a second batch of crystals. The combined portions gave 80 g. (48%) of slightly pink 3,3′-diaminobenzidine, melting at 178–179°C. The overall yield was 37%.

ANAL. Calcd. for $C_{12}H_{14}N_4$: C, 67.19%; H, 6.54%; N, 26.17%. Found: C, 67.15%; H, 6.50%; N, 25.93%.

Poly-2,2′-(*o*-phenylene)-5,5′-bibenzimidazole

a. From Phthalic Anhydride. Commercial reagent phthalic anhydride was recrystallized from benzene, m.p. 134–135°C. A mixture of 4.28 g. (0.02 mole) of 3,3′-diaminobenzidine and 10 g. of phenol was heated under nitrogen at 200°C. until a melt had formed. After cooling, 2.962 g. (0.02 mole) of phthalic anhydride was added. The reaction mixture was then heated for $^1/_2$ hr. at 170°C. and $^1/_2$ hr. at 250°C. The reaction flask was then evacuated to 0.1 mm. Hg pressure and heated at 270°C. for $^1/_2$ hr.

After this time, the product was powdered and reheated under vacuum for 5 hrs. at temperatures increasing from 270 to 400°C. The polymer had an inherent viscosity of 5.01 (0.2%, formic acid, 25°C.).

ANAL. Calcd. for $(C_{20}H_{12}N_4)_n$: C, 77.92%; H, 3.90%; N, 18.18%. Found: C, 76.35%; H, 3.96%; N, 17.85%.

b. From Phthalic Acid. Phthalic anhydride was converted to the acid in hot sodium hydroxide solution. After precipitation with hydrochloric acid, the phthalic acid was recrystallized from methanol, m.p. 208–210°C. A mixture of 1.661 g. (0.01 mole) of phthalic acid, 2.140 g. (0.01 mole) of 3,3′-diaminobenzidine and 5 g. of phenol was heated under nitrogen at 220°C. The reaction started, and a red-brown melt was formed. After 15 min., when the melt had become very viscous and partially solid, it was heated at 250°C. for 45 min. Then high vacuum was employed and the temperature raised to 270°C. for 1 hr. After powdering and reheating at 0.1 mm. Hg for 4 hr., the temperatures being allowed to rise to 400°C., a polymer was obtained which had an inherent viscosity of 2.35 (0.2%, formic acid, 25°C.).

ANAL. Calcd. for $(C_{20}H_{12}N_4)_n$: C, 77.92%; H, 3.90%; N, 18.18%. Found: C, 76.62%; H, 3.97%; N, 18.17%.

c. From Diphenyl Phthalate. The phenyl ester was prepared by reacting phthaloyl chloride with phenol. The reaction was completed at 130°C. The melting point was 77–78°C. after recrystallization from methanol. A mixture of 3.188 g. (0.01 mole) of diphenyl phthalate and 2.140 g. (0.01 mole) of 3,3′-diaminobenzidine was melted under nitrogen at 250°C. and then heated at 270–280°C. for $^1/_2$ hr. and 300°C. for $1^1/_2$ hr. Vacuum was then applied for $^1/_2$ hr. at 300°C. After powdering and reheating for $3^1/_2$ hr. at 0.1 mm. Hg while the temperature was allowed to rise from 300 to 400°C., a polymer with an inherent viscosity of 1.60 (0.2% formic acid, 25°C.) was obtained.

ANAL. Calcd. for $(C_{20}H_{12}N_4)_n$: C, 77.92%; H, 3.90%; N, 18.18%. Found: C, 76.43%; H, 3.98%; N, 17.96%.

A sample of this polymer when heated in a nitrogen atmosphere consecutively for 1 hr. each at temperatures of 400, 450, 500, and 550°C. lost 0%, 0.4%, 0.4%, and 3.7%, respectively. In air under the same conditions of heating the loss was 0%, 1.5%, 7.0%, and 7.6%, respectively.

Poly-2,6′-(*m*-phenylene)-3,5-diphenyldimidazobenzene

The 1,3-dianilino-4,6-diaminobenzene was synthesized by the procedure of Nietzki and Schedler[5] and Manjunath[6] from *m*-dichlorobenzene.

Preparation of 1,3-Dianilino-4,6-diaminobenzene

a. 1,3-Dichloro-4,6-dinitrobenzene. A mixture of 250 g. of fuming nitric acid (90%) and 500 g. of concentrated sulfuric acid was cooled in an ice bath to 10°C. With stirring, 100 g. of *m*-dichlorobenzene was added

within about 10 min. The reaction mixture was then heated on the water bath for 1 hr. in order to complete the nitration and finally poured onto crushed ice. The pale yellow precipitate was collected and recrystallized from methanol. The yield of 1,3-dichloro-4,6-dinitrobenzene was 140 g. (89%), melting at 102–103°C.

b. 1,3-Dianilino-4,6-dinitrobenzene. A mixture of 71 g. (0.3 mole) of 1,3-dichloro-4,6-dinitrobenzene and 100 g. of aniline was slowly heated to 180°C. and the temperature was then maintained at 180°C. for 15 min. The melt was then poured into 250 ml. of ethanol. After cooling the precipitate was collected in a Buchner funnel, washed with alcohol, and recrystallized from a dimethylformamide/methanol mixture. The product was first dissolved in 300 ml. of hot dimethylformamide and, after addition of 300 ml. of methanol, allowed to crystallize. The reaction yielded 86 g. (82%) of the light red colored 1,3-dianilino-4,6-dinitrobenzene melting at 188.5–189°C.

c. 1,3-Dianilino-4,6-diaminobenzene. A mixture of 30 g. (0.086 mole) of 1,3-dianilino-4,6-dinitrobenzene, 150 g. of sodium sulfide nonahydrate, 450 ml. of ethanol, and 60 ml. of water was heated to reflux with stirring for 8 hr. The major part of the alcohol was then distilled under reduced pressure and the residue diluted with 500 ml. of water, adding small portions at a time. The precipitate was collected by suction filtration, washed with aqueous alcohol, and recrystallized from benzene (decolorizing charcoal). The yield of 1,3-dianilino-4,6-diaminobenzene was 8.1 g. (34%, overall yield 25%), melting at 208–209°C. The melting point rose to 210–211°C. after an additional recrystallization from alcohol.

ANAL. Calcd. for $C_{18}H_{18}N_4$: C, 74.46%; H, 6.25%; N, 19.29%. Found: C, 74.65%; H, 6.41%; N, 19.62%.

Melt Condensation of 1,3-Dianilino-4,6-diaminobenzene with Diphenyl Isophthalate and Di(biphenyl) Isophthalate

a. Condensation with Diphenyl Isophthalate. In a 50-ml. flask, connected to a tubing, receiver, and outlet, was placed 4.355 g. (0.015 mole) of the diphenyltetraaminobenzene and 4.772 g. (0.015 mole) of diphenyl isophthalate. The flask was purged with nitrogen by repeated evacuation and refilling and then placed in a Wood's metal bath preheated to 300°C. The reaction mixture formed a melt and the slowly beginning evolution of bubbles of phenol indicated that the reaction had started. After 1 hr. the pressure was reduced to 0.05 mm. Hg and heating was continued at 300°C. for $\frac{1}{2}$ hr. The dark brown material was then powdered and reheated under reduced pressure for 3 hr. at temperatures gradually rising from 300 to 400°C. The inherent viscosity of the polymer obtained was 0.81 (0.2%, formic acid, 25°C.). The polymer was insoluble in dimethyl sulfoxide but dissolved in sulfuric acid, formic acid, and trifluoroacetic acid. It did not melt below 500°C.

ANAL. Calcd. for $(C_{26}H_{16}N_4)$: C, 81.22%; H, 4.20%; N, 14.56%. Found: C, 80.08%; H, 4.50%; N, 14.50%.

A sample of this polymer when heated in a nitrogen atmosphere for 1 hr. at each of the temperatures 400, 450, 500, and 550°C. consecutively lost 0%, 0.4%, 1.6%, and 6.0% weight, respectively. In air under the same conditions the weight losses were 1.0%, 4.8%, 10.1%, and 12.1%, respectively.

b. Condensation with Di(biphenyl) Isophthalate. The di(biphenyl) isophthalate was prepared from isophthaloyl chloride and *p*-phenylphenol at melt temperatures. The ester was recrystallized from toluene and melted at 238–240°C. For the polymerization a mixture of 2.340 g. (0.00806 mole) of the diphenyltetraaminobenzene and 3.791 g. (0.00806 mole) of di(biphenyl) isophthalate was heated under nitrogen at 300°C. for several minutes until a uniform melt had formed. The temperature of the Wood's metal bath was then raised to 340°C. in order to start the condensation reaction. After $^1/_2$ hr. heating at temperatures of 340–360°C. the pressure was reduced to 0.1 mm. Hg and heating was continued for 2 hr. while the temperature was gradually increased to 400°C. The polymer obtained had an inherent viscosity of 1.08 (0.2%, formic acid, 25°C.).

Melt Condensation of 3,3′-Diaminobenzidine with Diphenyl Glutarate and Diphenyl Succinate

a. Condensation with Diphenyl Glutarate. Diphenyl glutarate was prepared from glutaryl chloride and phenol. The mixture was allowed to stand for $^1/_2$ hr. at room temperature and was then heated to 130°C. for $^1/_2$ hr. The ester was recrystallized from methanol, it melted at 55–56°C. A mixture of 2.843 g. (0.01 mole) of the diphenyl glutarate and 2.141 g. (0.01 mole) of 3,3′-diaminobenzidine was placed in a 100-ml. flask and heated under nitrogen at 240–250°C. for 15 min. The pressure was then carefully reduced to 0.1 mm. Hg and heating was continued for 45 min. at temperatures gradually rising to 300°C. The polymer was a glassy foam. The inherent viscosity was 1.19 (0.2%, formic acid, 25°C.); m.p. 420°C.

ANAL. Calcd. for ($C_{17}H_{14}N_4$): C, 74.45%; H, 5.15%; N, 20.40%. Found: C, 71.51%; H, 5.37%; N, 19.46%.

b. Condensation with Diphenyl Succinate. A charge of 1.802 g. (0.00667 mole) of diphenyl succinate (m.p. 124–125°C.) and 1.427 g. (0.00667 mole) of 3,3′-diaminobenzidine was polymerized under the same conditions. The polymer showed an inherent viscosity of 2.71 (0.2%, formic acid, 25°C.); m.p. 470°C. with decomposition.

ANAL. Calcd. for ($C_{16}H_{12}N_4$): C, 73.80%; H, 4.65%; N, 21.55%. Found: C, 71.10%; H, 4.98%; N, 18.09%.

Both of these polymers were soluble in dimethyl sulfoxide. Both were unstable above 450°C.

Hydrolytic Stability Tests

A freshly prepared, 0.5% concentrated solution of poly-2,2′-(*m*-phenylene)-5,5′-bibenzimidazole in concentrated sulfuric acid (commercial, 95%)

showed an inherent viscosity of 1.00 at 25°C. After 5 hr. heating at 160°C., the inherent viscosity was 1.02. Of the same polymer, which had an inherent viscosity of 0.72 in a 0.5% concentrated solution in dimethyl sulfoxide, 2 g. were dissolved in concentrated sulfuric acid, heated to 100°C., and then reprecipitated by pouring the solution into dilute sodium hydroxide solution. The collected polymer was washed in boiling water, filtered and dried. The inherent viscosity of the recovered material (1.62 g.) was 1.00 (0.5%, dimethyl sulfoxide, 25°C.).

A 0.5% concentrated solution of poly-2,2′-(*o*-phenylene)-bibenzimidazole in concentrated sulfuric acid at 25°C. showed an inherent viscosity of 0.80. After 5 hr. heating at 160°C., the inherent viscosity of the solution was 0.79 at 25°C. The material recovered from this solution by reprecipitation showed an inherent viscosity of 5.10 in a 0.2% concentrated solution in formic acid. Before the treatment with sulfuric acid the inherent viscosity was 5.01 in formic acid.

A 0.5% concentrated solution of poly-2,6-(*m*-phenylene)-3,5-diphenyldiimidazobenzene in concentrated sulfuric acid at 25°C. showed an inherent viscosity of 0.32. After 5 hr. heating at 160°C. the inherent viscosity was 0.30. The solution was then poured into dilute aqueous sodium hydroxide. The precipitated polymer was collected on a Buchner funnel, washed in boiling water, recovered, and dried. The inherent viscosity of the recovered material was 0.82 in a 0.2% concentrated solution in 98% formic acid at 25°C. Before the treatment with sulfuric acid the inherent viscosity was 1.00 in formic acid.

A sample of poly-2,2′-(ethylene)-5,5′-bibenzimidazole which showed an inherent viscosity of 2.71 in formic acid was dissolved in concentrated sulfuric acid at 100°C. and then reprecipitated with water. The inherent viscosity of the recovered polymer was 2.68 in formic acid.

MODEL COMPOUNDS

o-Phenylene Bibenzimidazole

A mixture of 4.32 g. (0.04 mole) of *o*-phenylenediamine and 3 g. (0.02 mole) of phthalic anhydride was heated in a nitrogen atmosphere for 15 min. at 160°C. The temperature was then increased to 300°C. and heating was continued for 15 min. The reaction product was recrystallized from dimethylformamide. The yield of *o*-phenylene bibenzimidazole was 4.2 g., m.p. 445–450°C. Walther and Pulawski[7] have prepared this compound and mentioned that it melted above 310°C.

m-Phenylene Bibenzimidazole

A charge of 4.32 g. (0.04 mole) of *o*-phenylenediamine and 6.36 g. (0.02 mole) of diphenyl isophthalate was heated under nitrogen at 250–300°C. for ½ hr. The reaction product was recrystallized from a benzene/methanol mixture. The *m*-phenylene bibenzimidazole melted at 330–333°C.

p-Phenylene Bibenzimidazole

p-Phenylene bibenzimidazole was prepared in the same way from *o*-phenylene-diamine and diphenyl terephthalate. It was purified by recrystallization from ethanol and melted at 475–480°C.

We are indebted to Micro-Tech Laboratories, Skokie, Illinois for the analyses reported here. The thermogravimetric analysis curves were prepared by Dr. G. Ehlers of Wright Air Development Division, Wright-Patterson Air Force Base, Ohio. One of us (Herward Vogel) is indebted for a travel grant from the International Educational Exchange Service (Fulbright Commission) in cooperation with Exchange Visitors Program. The financial support of the Textile Fibers Department of E. I. du Pont de Nemours and Company is gratefully acknowledged.

References

1. Vogel, H., and C. S. Marvel, *J. Polymer Sci.*, **50,** 511 (1961).
2. Brunner, Ph., and O. Witt, *Ber.*, **20,** 1023 (1897).
3. Hodgson, H. H., *J. Chem. Soc.*, **1926,** 1757.
4. Hoste, J., *Anal. Chim. Acta*, **2,** 402 (1948).
5. Nietzki, R., and A. Schedler, *Ber.*, **30,** 1666 (1897).
6. Manjunath, B. L., *J. Indian Chem. Soc.*, **4,** 276 (1927).
7. Walther, R., and Th. v. Pulawski, *J. prakt. Chem.*, **59,** 255 (1899).

Résumé

On a préparé un polybenzimidazol de haut poids moléculaire et de très bonne stabilité à la chaleur, à partir de 3,3′-diaminobenzidine et de l'anhydride phtalique. Un remplacement de l'atome d'hydrogène fixé à l'azote du noyau imidazolique dans un polybenzimidazol n'augmente pas la stabilité à la chaleur. Comme il a été démontré par les propriétés du poly-2,6-(*m*-phénylène)-3,5-diphényl diimidazobenzène. On a préparé des polybenzimidazols avec des groupes aliphatiques à partir de la 3,3′-diaminobenzidine et l'ester diphénylé des acides succénique et glutarique. Les esters diphénylés des acides oxalique et malonique ne fournissent pas de polymère, probablement parce que des amides cycliques sont formés. On a également effectué des essais de stabilité à l'hydrolyse des polybenzimidazols. Certains composés modèles furent préparés afin de servir de comparaison avec le polymère correspondant quat à leur point de fusion et leurs spectres d'absorption.

Zusammenfassung

Aus 3,3′-Diaminobenzidin und Phthalsäureanhydrid wurde ein Polybenzimidazol mit hohem Molekulargewicht und sehr guter Hitzebeständigkeit dargestellt. Ersatz der Wasserstoffatome am Stickstoff des Imidazolkerns in einem Polybenzimidazol verbessert die Hitzebeständigkeit nicht, wie die Eigenschaften von Poly-2,6-(*m*-phenylen)-3,5-diphenyl-diimidazobenzol zeigen. Polybenzimidazole mit aliphatischen Bausteinen wurden aus 3,3′-Diaminobenzidin und Bernsteinsäure- und Glutarsäurediphenylester dargestellt. Die Diphenylester von Oxal- und Malonsäure lieferten, wahrscheinlich wegen der Bildung cyklischer Amide, keine Polymeren. Weiters wurde die Hydrolysenbeständigkeit der Polybenzimidazole überprüft. Einige Modellverbindungen wurden zum Vergleich ihrer Schmelzpunkte und Absorptionsspektren mit dem entsprechenden Polymeren dargestellt.

Received March 6, 1962

JOURNAL OF POLYMER SCIENCE: PART A VOL. 1, PP. 1543–1552 (1963)

Polymers Derived from Unsaturated Esters of Hydronopoxyalkanols*

TOSHIYUKI SHONO and C. S. MARVEL, *Department of Chemistry, The University of Arizona, Tucson, Arizona*

Synopsis

Homopolymers of the acrylates of a series of hydronopoxyalkanols have been prepared and characterized as soft rubbery materials with some adhesive properties. The polymer from the methacrylate of hydronopoxyethanol was hard, brittle and insoluble. The crotonate of this alcohol did not homopolymerize in a free radical system. All of these esters copolymerized readily with vinyl chloride, styrene, acrylonitrile and butadiene. The vinyl chloride copolymers and styrene copolymers were rigid plastics. The butadiene copolymers were rubbery and easily crosslinked in air. The acrylonitrile copolymers were soluble in dimethylformamide. Terpolymers of these esters with butadiene and acrylonitrile were tough, rubbery compositions.

A number of unsaturated esters of hydronopoxyalkanols (I) have been described recently by Clark, Bieber, and Pettyjohn.[1] These compounds have been made available to us through the Southern Utilization Research

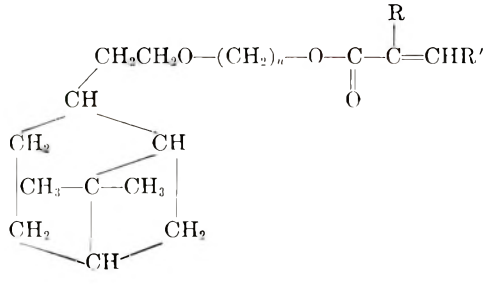

Ia, $n = 2$; R = R′ = H
Ib, $n = 2$; R = CH_3, R′ = H
Ic, $n = 2$; R = H, R′ = CH_3
Id, $n = 3$; R = R′ = H
Ie, $n = 4$; R = R′ = H
If, $n = 5$; R = R′ = H

and Development Division of the Agricultural Research Service. This paper describes some homopolymerization experiments with these monomers and the properties of the new polymers. It also describes some

* This is a partial report of work done under contract with four Utilization Research and Development Divisions, Agricultural Research Service, U. S. Department of Agriculture and Authorized by the Research and Marketing Act. The contract was supervised by Dr. J. C. Cowan of the Northern Division.

copolymers and terpolymers of these esters with vinyl chloride, styrene, butadiene, and acrylonitrile.

Earlier work has demonstrated[2] that hydronopol acrylate gives a variety of interesting polymers, copolymers, and terpolymers. The terpolymer of that ester with butadiene and acrylonitrile was an especially interesting oil-resistant rubber; hence it was felt that some of these new esters with the ether linkage and longer alkyl chain might show characteristics that would render them useful.

In our experiments, all hydronopoxyalkyl acrylates polymerized readily in emulsion systems with standard free-radical initiation to give tough, rubbery polymers which were soluble in chloroform and had inherent viscosities of 0.78–1.07. However hydronopoxyethyl methacrylate polymerized to give an insoluble, brittle solid, and hydronopoxyethyl crotonate did not polymerize in the usual emulsion system. Copolymerization experiments were run with these monomers and styrene, acrylonitrile, butadiene, and vinyl chloride. Fairly homogeneous copolymers were obtained. Although hydronopoxyethyl crotonate did not homopolymerize, it did enter into copolymerization reactions with the above monomers.

Terpolymers have been prepared from the esters of the hydronopoxyalkanols with acrylonitrile and butadiene using an emulsion system. These terpolymers had rubberlike properties. In particular, the terpolymers starting with equal amounts of hydronoproxyamyl acrylate, butadiene and acrylonitrile were very tough, rubberlike materials.

EXPERIMENTAL

The esters were distilled under reduced pressure; the following fractions were used in the polymerization work: Ia, 2-hydronopoxy-1-ethyl acrylate (HNEA), b.p. 143–145°C./3.5 mm.; Ib, 2-hydronopoxy-1-ethyl methacrylate (HNEM), b.p. 101–103°C./0.04 mm.; Ic, 2-hydronopoxy-1-ethyl crotonate (HNEC), b.p. 145–147°C./0.17 mm.; Id, 3-hydronopoxy-1-propyl acrylate (HNPA), b.p. 117–119°C./0.04 mm.; Ie, 4-hydronopoxy-1-butyl acrylate (HNBA), b.p. 119–121°C./0.04 mm.; If, 5-hydronopoxy-1-amyl acrylate (HNAA), b.p. 137–139°C./0.03 mm. These monomers contained 0.001% hydroquinone as an inhibitor, which could not be removed by vacuum distillation, but it was removed by dissolving the ester in ether and washing with 5% caustic soda solution.

Homopolymerization Experiments

The homopolymerization procedure was to charge the monomer, water, emulsifier, and 2.5% aqueous solution of potassium persulfate into a 2-oz. polymerization bottle in the following ratio: monomer, 1 g.; 2.5% aqueous solution of potassium persulfate, 0.4 ml.; emulsifier (Triton X-301, Rohm and Haas Co.), 0.2 g.; water, 2 ml.

The bottle was flushed with nitrogen and tumbled in a 50°C. bath. The resulting polymer latex was coagulated with 5% sulfuric acid solution

saturated with sodium chloride. The polymer was purified by dissolving it in chloroform and precipitating it by pouring this solution into methanol. The polymer was separated and dried under vacuum. Inherent viscosities were determined in an Ostwald viscometer, a solution of 0.125 g. of polymer in 25 ml. of chloroform at 30°C. being used. The results of the homopolymerizations are collected in Table I.

TABLE I
Homopolymerization of Unsaturated Esters of Hydronopoxyalkanols

Monomer	Wt. monomer, g.	Time, hr.	Conversion, %	η_{inh}	C, % Found	C, % Calcd. for monomer	H, % Found, %	H, % Calcd. for monomer, %
Ia	1.0	17	~100	1.07	70.51	72.1	9.70	9.7
Id	2.7	17	~100	[a]	72.47	72.8	10.01	10.0
Ie	1.3	41	94	0.78	73.31	73.4	10.12	10.2
If	1.2	17	89	0.99	73.23	74.0	10.45	10.3
Ib	1.0	17	~100	—	71.95	72.8	9.75	10.0
Ic	1.0	20	0	—	—	72.8	—	10.0

[a] Partially insoluble.

The homopolymers of the acrylates were soft, rubbery, somewhat sticky products which had some adhesive properties.

Copolymerization Experiments

The esters of the hydronopoxyalkanols were copolymerized with vinyl chloride, styrene, butadiene, and acrylonitrile in an emulsion system, Triton X-301 being used as an emulsifier. Fairly homogeneous copolymers were obtained. The polymerization experiments and the properties of the various polymers obtained are described in Tables III–VI. The copolymerization procedure was to charge the monomer mixture, water, emulsifier, and 2.5% aqueous solution of potassium persulfate into a 2-oz. polymerization bottle in the ratio indicated in Table II. The bottle was swept with nitrogen, capped, and tumbled in a 50°C. bath.

In the case of vinyl chloride or butadiene, an excess of liquid vinyl chloride or butadiene was added and the bottle allowed to warm up so that the gaseous monomer distilled out of the bottle until the desired weight

TABLE II
Ratios of Reagents in Copolymerization Experiments

Series No.	Triton X-301, g.	Water, ml.	Initiator solution, ml.	Monomer mixture, g.
No-75	0.4	4	0.8	2
No-50	0.2	2	0.4	1
No-25	0.4	4	0.8	2

TABLE III

Copolymerization Experiments with Hydronopoxyethyl Acrylate (HNEA)

Expt. No.	HNEA, g.	Other monomer	Wt., g.	Time, hr.	Conversion, %	η_{inh}	Solvent	Softening range, °C.	Elementary analyses			Acrylate calcd., %
									Cl, %	C, %	N, %	
EVc-75	1.5	Vinyl chloride	0.5	16	73.5	1.13	Chloroform	30–40	2.01			96.5
EVc-50	0.5	Vinyl chloride	0.5	16	66.0	1.51	Tetrahydrofuran	95–100	14.34			74.8
EVc-25	0.5	Vinyl chloride	1.5	16	68.0	1.58		160–165	36.05			36.6
Est-75	1.5	Styrene	0.5	18	79.5	3.50	Chloroform	60–70		77.88		71.6
Est-50	0.5	Styrene	0.5	18	91.0	3.42	Benzene	80–85		82.62		48.1
Est-25	0.5	Styrene	1.5	18	93.5	5.06		100–105		87.23		25.1
EBd-75	1.5	Butadiene	0.5	17	~100	—	Insoluble; swollen by	Rubbery		76.43		74.5
EBd-50	0.5	Butadiene	0.5	17	95.0	—	benzene, chloroform	material		78.73		60.2
EBd-25	0.5	Butadiene	1.5	17	76.5	—	and tetrahydrofuran			81.43		44.6
EAn-75	1.5	Acrylonitrile	0.5	16	93.0	0.96	Chloroform	65–75			6.47	75.5
EAn-50	0.5	Acrylonitrile	0.5	16	88.0	2.53	Dimethylformamide	115–125			12.18	53.9
EAn-25	0.5	Acrylonitrile	1.5	16	~100	4.13		200–215			19.71	25.4

TABLE IV
Copolymerization Experiments with Hydronopoxyethyl Methacrylate (HNEMA)

Expt. No.	HNEMA, g.	Other monomer	Wt., g.	Time, hr.	Conversion, %	η_{inh}	Solvent	Softening range, °C.	Elementary analyses			Methacrylate calcd., %
									Cl, %	C, %	N, %	
EMVc-75	1.5	Vinyl chloride	0.5	12	83.5	0.33	Tetrahydrofuran	35–40	3.00			94.8
EMVc-50	0.5	Vinyl chloride	0.5	12	59.0	0.40	Tetrahydrofuran	50–55	8.55			85.0
EMVc-25	0.5	Vinyl chloride	1.5	12	55.0	0.87		100–110	37.20			34.51
EMSt-75	1.5	Styrene	0.5	17	90.0	0.28		Rubbery		78.43		71.1
EMSt-50	0.5	Styrene	0.5	17	90.0	0.47	Benzene	40–50		83.01		47.6
EMSt-25	0.5	Styrene	1.5	17	~100	0.91		70–75		87.78		23.1
EMBd-75	1.5	Butadiene	0.5	17	80.0	—	Insoluble; swollen by benzene	Rubbery material		72.92		[a]
EMBd-50	0.5	Butadiene	0.5	17	70.0	—				72.67		[a]
EMBd-25	0.5	Butadiene	1.5	17	17.5	—				73.43		[a]
EMAn-75	1.5	Acrylonitrile	0.5	16.5	89.5	—	Insoluble	70–80			6.34	76.0
EMAn-50	0.5	Acrylonitrile	0.5	16.5	86.0	—		75–85			11.66	55.9
EMAn-25	0.5	Acrylonitrile	1.5	16.5	~100	1.86	Dimethylformamide	140–150			19.40	26.6

[a] Small amounts of ash could not be removed and thus this calculation was therefore not significant.

TABLE V
Copolymerization Experiments with Hydropoxyethyl Crotonate (HNEC)

Expt. no.	HNEC, g.	Other monomer	Wt., g.	Time, hr.	Conversion, %	η_{inh}	Solvent	Softening range, °C.	Elementary analyses Cl, %	C, %	N, %	Crotonate calcd., %
ECVc-75	1.5	Vinyl chloride	0.5	17	2.5	—	Tetrahydrofuran	50–55	13.29			76.6
ECVc-50	0.5	Vinyl chloride	0.5	17	4.0	—		70–75	26.97			52.5
ECVc-25	0.5	Vinyl chloride	1.5	17	41.0	0.37		100–105	45.82			19.3
ECSt-75	1.5	Styrene	0.5	16.5	60.0	0.63	Benzene	100–105		87.91		22.5
ECSt-50	0.5	Styrene	0.5	16.5	~100	1.87		100–105		90.70		8.2
ECSt-25	0.5	Styrene	1.5	16.5	93.5	3.55		100–105		91.94		1.8
ECBd-75	1.5	Butadiene	0.5	15.5	trace	—	Benzene	—		—		—
ECBd-50	0.5	Butadiene	0.5	15.5	trace	—		—		—		—
ECBd-25	0.5	Butadiene	1.5	15.5	11.5	0.62	Rubbery material			78.4		65.3
ECAn-75	1.5	Acrylonitrile	0.5	18	79.0	0.23	Dimethylformamide	50–60			6.03	77.17
ECAn-50	0.5	Acrylonitrile	0.5	18	80.0	0.76		110–115			16.44	38.0
ECAn-25	0.5	Acrylonitrile	1.5	18	79.5	0.76		110–115			22.58	14.5

remained. The resulting polymer latex was coagulated with 5% sulfuric acid solution saturated with sodium chloride. The polymer was purified by reprecipitation and was dried under vacuum. Inherent viscosities were determined in an Ostwald viscometer on a solution of 0.06 g. of polymer in 25 ml. of solvent at 30°C.

The visual softening ranges were determined in a capillary tube. (The softening ranges were measured in an open capillary tube having a copper wire plunger. The low temperature was that at which the polymer became sticky and at the higher temperature the polymer was a transparent, gummy material.) Softening points determined in this way indicate only the general range of softening temperature.

Unsaturated esters of hydronopoxyalkanols were found to copolymerize readily with vinyl chloride to give polymers which ranged from soft, sticky materials to tough, plastic materials, depending on the ratio of ester to vinyl chloride. The polymers were soluble in tetrahydrofuran. The copolymer containing 36.6% hydronopoxyethyl acrylate was cast from tetrahydrofuran solution to give a transparent, flexible film. This result shows some slight plasticization was achieved as a result of the incorporation of hydronopoxyethyl acrylate.

Hydronopoxyamyl acrylate was found to copolymerize readily with vinyl chloride to give polymers which are more flexible than hydronopoxyethyl acrylate copolymers. Figure 1 shows the copolymer composition. These results indicate that the hydronopoxyalkyl acrylates have similar reactivity toward vinyl chloride.

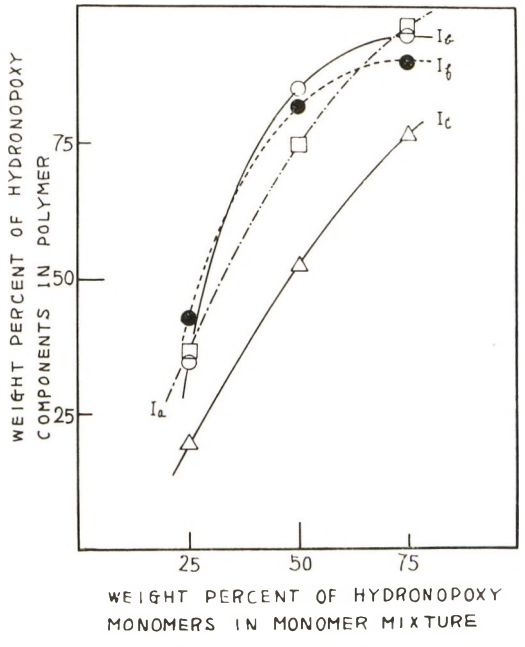

Fig. 1. Copolymer composition curve, (□) Ia, (○) Ib, (●) Ic, and (△) If.

TABLE VI. Copolymerization Experiments with Hydronopoxyamyl Acrylate (HNAA)

Expt. No.	HNAA, g.	Other monomer	Wt., g.	Time, hr.	Conversion, %	η_{inh}	Solvent	Softening range, °C.	Elementary analyses Cl, %	Elementary analyses N, %	Acrylate calcd., %
AAVc-75	1.5	Vinylchloride	0.5	17	50.0	0.98	Tetrahydrofuran	~30	5.84		89.8
AAVc-50	0.5	Vinylchloride	0.5	82	66.0	0.95		40–50	10.47		81.6
AAVc-25	0.5	Vinylchloride	1.5	17	50.0	1.43		80–85	32.65		42.6
AAAn-75	1.5	Acrylonitrile	0.5	18	12.5	0.37	Chloroform	55–65		7.06	73.3
AAAn-50	0.5	Acrylonitrile	0.5	18	64.0	2.95	Dimethylformamide	90–95		13.04	50.7
AAAn-25	0.5	Acrylonitrile	1.5	18	86.0	4.54		160–170		20.69	21.7

TABLE VII. Terpolymerization Experiments with Various Unsaturated Esters of Hydronopoxyalkanols

Expt. no.	Hydronopoxy monomer, g.		Acrylonitrile, g.	Butadiene, g.	Modifier,[a] mg.,	Time, hr.	Conversion, %	η_{inh}	Elementary analyses C, %	Elementary analyses N, %	Composition of polymer: Hydronopoxy monomer, %	Composition of polymer: Butadiene, %	Composition of polymer: Acrylonitrile, %
EA-1	HNEA	1.0	1.0	1.25	—	17	~100	—	76.37	7.94	37.3	32.7	30.0
EA-2	HNEA	1.0	1.0	1.0	15.4	2	95.0	1.58	76.82	7.15	38.3	34.7	27.0
EA-3	HNEA	1.1	1.0	1.15	15.4	17	~100	—	76.27	7.67	39.1	31.9	29.0
AA-1	HNAA	1.0	1.0	1.0	—	3	57.3	0.95	78.48	9.84	17.4	45.3	37.3
AA-2	HNAA	1.0	1.0	—	—	3	55.6	1.36	78.23	9.75	19.3	43.8	36.9
AA-3	HNAA	1.0	1.0	1.0	15.4	3	84.7	2.08	78.15	8.82	25.7	40.9	33.4
BA-1	HNBA	1.0	1.0	1.0	—	18	73.0	—	77.10	9.07	29.8	35.9	34.3
EC-1	HNEC	1.0	1.0	1.0	15.4	2	38.3	0.55	78.44	11.50	8.3	48.2	43.5
EC-2	HNEC	1.0	1.0	1.0	15.4	3.5	74.6	0.57	77.67	8.74	38.3	34.7	27.0
EM-1	HNEM	1.0	1.0	1.0	15.4	3.5	86.3	1.12	71.51	7.39	71.8	0.3	27.9

[a] Technical lauryl mercaptan (Hooker Electrochemical Co.).

The products resulting from the copolymerization of the unsaturated esters of the hydronopoxyalkanols with butadiene were elastic, insoluble materials and were swollen by tetrahybrofuran and benzene.

Styrene, when copolymerized with the unsaturated esters of the hydronopoxyalkanols, was found to yield copolymers which ranged from brittle to tough, plastic materials. The copolymers of the unsaturated esters of the hydronopoxyalkanols with acrylonitrile were usually powdery or hard, brittle materials.

The copolymers of hydronopoxyamyl acrylate with acrylonitrile had softening points which were lower than hydronopoxyethyl acrylate copolymer. The copolymer containing 21.7% hydronopoxyamyl acrylate was cast from dimethylformamide solution to give a flexible film. Little plasticization was noticed as a result of the copolymerization of these esters with acrylonitrile.

Terpolymerization Experiments

The terpolymerization procedure was to charge the monomer mixture, water (6 ml.), emulsifier (1 g.) and 2.5% aqueous solution of potassium persulfate (1.2 ml.) into a 2-oz. polymerization bottle. The bottle was tumbled in a 50°C. bath. The resulting polymer latex was coagulated with a 5% sulfuric acid solution saturated with sodium chloride. The polymer was purified by reprecipitation ($CHCl_3$-CH_3OH) and dried under vacuum. DuPont antioxidant No. 29 (2,6-di-*tert*-butyl-4-methylphenol) was added during the reprecipitation. Inherent viscosities were determined in an Ostwald viscometer using a solution of 0.06 g. of polymer in 25 ml. of chloroform at 30°C. The polymerization experiments and the properties of the various polymers obtained are described in Table VII.

The polymers were soluble in chloroform and benzene, but during the purification process the polymers formed insoluble gels rather easily.

References

1. (a) Pettyjohn, B. M., M. S. Thesis, University of Mississippi, August 1960; (b) T. I. Bieber, S. F. Clark, and B. M. Pettyjohn, paper presented before the Organic Division at the 138th National Meeting, American Chemical Society New York, 1960. Abstracts, page 103; S. F. Clark, T. I. Bieber, and R. E. Bissell, *J. Miss. Acad. Sci.*, in press.

2. Marvel, C. S., R. Schwen, R. W. Hobson, and R. J. Coleman, *J. Polymer Sci.*, **33**, 27 (1958).

Résumé

On a préparé et décrit des homopolymères des acrylates d'une série de hydronopoxyalcanols. Ce sont des matériaux doux et caoutchouteux possédant certaines propriétés adhésives. Le polymère du méthacrylate de l'hydronopoxyéthanol était dur, cassant et insoluble. Le crotonate de cet alcool ne homopolymérise pas dans un système à radicaux libres. Tous ces esters copolymérisaient aisément avec le chlorure de vinyle, le styrène, l'acrylonitrile et le butadiène. Les copolymères de chlorure de vinyle et ceux du styrène étaient des plastiques rigides. Les copolymères de butadiène étaient caoutchouteux et sepontaient aisément àl l'air. Les copolymères d'acrylonitrile étaient solubles dans

le diméthylformamide. Des terpolymères de ces esters avec le butadiène et l'acrylonitrile étaient des compositions caoutchouteuses dures.

Zusammenfassung

Homopolymere der Acrylate einer Reihe von Hydronopoxyalkanolen wurden dargestellt und als weiche, gummiartige Stoffe mit einer gewissen Adhäsionsfähigkeit charakterisiert. Das Polymere des Methacrylsäureester von Hydronopoxyäthanol war hart, spröde und unlöslich. Der Crotonsäureester dieses Alkohols zeigte keine radikalische Homopolymerisation. Alle Ester gaben leicht Copolymerisation mit Vinylchlorid, Styrol, Acrylnitril und Butadien. Die Vinylchlorid- und Styrolcopolymeren bildeten starre Massen. Die Butadiencopolymeren waren kautschukartig und vernetzten unter Luft leicht. Die Acrylnitrilcopolymeren waren in Dimethylformamid löslich. Terpolymere dieser Ester mit Butadien und Acrylnitril bildeten zähe, kautschukartige Massen.

Received April 2, 1962

JOURNAL OF POLYMER SCIENCE: PART A VOL. 1, PP. 1553–1572 (1963)

Reaction of Polymeric Radicals with Organometallic Compounds

T. HUFF and ELI PERRY,* *Plastics Division, Monsanto Chemical Company, Texas City, Texas*

Synopsis

The reactivities of polystyryl, polymethyl methacrylyl and polyacrylonitryl radicals with thirteen organometallic substrates were measured and correlated at 60°C. The organometallics chosen were saturated, aliphatic derivatives of elements from Groups 2b, 3a, 4a, and 5a of the Periodic Table. Correlation was accomplished by the method proposed by Bamford, Jenkins, and Johnston. The correlation based on the above three monomers allowed the prediction of the chain transfer constant C of four of the tested substrates with an untested radical, the polymethyl acrylyl, with an accuracy of better than 10^1. Since the correlation was based on absolute values of C which covered the range of 10^6 and which were accurate to within $10^{0.8}$, it was concluded that the correlation was a valid one and was useful for predictive purposes. Values of C for untested substrates can be predicted with only a low order of accuracy because data are not available on the polarizability of most compounds. The introduction of oxygen into the vicinity of the metal–carbon bond reduces the value of C drastically and confirms that C is very sensitive to polar factors. There appears to be a correlation between α (the polarizability of the substrate) and β (the intrinsic reactivity of the substrate) within a given group of the Periodic Table. The fact that there is not a general correlation between α and β for the whole Periodic Table suggests that the mechanism of the transfer reaction is different from group to group.

INTRODUCTION

Most of the kinetic data in the literature dealing with polymeric radicals are concerned with their reactivity towards monomers. Hence, radical reactivity correlations are limited to the attack on one of the carbon atoms of a vinyl group.[1a] Other than monomers, the most common substrates are hydrocarbons, organic halides, and organic sulfur compounds.[1b] The radical reactivity information available for the few substrates other than monomers and for some monomers has been reviewed by Bamford, Jenkins, and Johnston[2] in their attempt to correlate these reactivities by a new scheme. A recent article[3] reviews the status of chain transfer studies from which radical reactivities with substrates are obtained, the difficulty of obtaining precise values of the chain transfer constant C, and some data available on less common substrates. Additional C values are available for diphenylmethylamine,[4] R_3SiH, and triphenyl silicon hydride.[5]

* Present address: Chemstrand Research Center, Inc., Durham, North Carolina (to which all correspondence should be sent).

The present paper presents data on the reactivity of three polymeric radicals with thirteen substrates, all of which are aliphatic derivatives of metals or metalloids in Groups 2b, 3a, 4a, and 5a of the Periodic Table. Correlation is accomplished by the scheme of Bamford et al.[2] which emphasizes the reactivity of the substrate rather than by the Price-Alfrey Q–e scheme[6] which has been used to emphasize the reactivity of the radical.

PROCEDURE

Polymerization

Styrene. The monomer and organometallic were added to clean tubes dried at 130°C. and cooled under argon. The tubes were cooled further to −76°C., sealed, warmed to room temperature, mixed thoroughly, and suspended in a bath at 100 ± 0.3°C., for a definite time. Tubes were cooled rapidly to 25°C., and the polymer was precipitated by pouring the mixture into 7–10 volumes of methanol. Drying was accomplished at 60°C., and <1 mm. Hg. Repurification procedures of solution, filtration, and precipitation were used to remove solid residues and residual traces of monomer.

Acrylonitrile. The procedure was the same as for styrene, except that dimethylformamide (DMF) and catalyst were included in the charge (10.0 ml. acrylonitrile, 40.0 ml. DMF, 0.0100 g. AIBN, plus substrate). The polymerization temperature was 60 ± 0.3°C.

Methyl Methacrylate. The procedure was the same as for styrene except for the use of catalyst (20.0 ml. monomer, 0.0020 g. AIBN, plus substrate). The polymerization temperature was 60 ± 0.3°C. The precipitating medium was 10 volumes of methanol plus 1 volume of water.

Methyl Acrylate. The procedure was the same as for methyl methacrylate through the polymerization step (10.0 ml. monomer, 10.0 ml. benzene, 0.0200 g. AIBN, plus substrate). The precipitant was petroleum ether at −40°C., and the excess monomer was removed over the temperature range of −40 to 20°C., as the mass was allowed to warm slowly over an 8-hr. period.[7] Final drying was at 60°C. and <1 mm. Hg.

For all polymerization work, the conversion was kept below 10% to minimize changes in the molar ratio of the transfer agent to the monomer.

Degree of Polymerization (DP)

The DP was estimated from viscosity measurements by use of the relationships given in Table I, where C_v is in units of grams per 100 cc., and C'_v is in grams per cubic centimeter. In the case of styrene, when the molecular weights were low, the DP was obtained cryoscopically with diphenyl as a solvent.

Chain Transfer Constant

The chain transfer constant was determined from a Mayo plot of 1/DP as a function of [S]/[M].[13] The Mayo plot holds without restrictions

TABLE I

Polymer	Conversion from relative viscosity η_r or specific viscosity η_{sp} to intrinsic viscosity $[\eta]$	Solvent	$[\eta]$–DP relationship	Reference
Acrylonitrile	$[\eta] = \frac{\eta_{cp}/C_v}{1 + 0.28\,\eta_{sp}}$	Dimethyl-formamide	$[\eta] = 5.74 \times 10^{-4}(53\mathrm{DP})^{0.733}$	8
Methyl methacrylate	$[\eta] = \frac{\ln \eta_r}{C_v} + \frac{1}{4}\left[\frac{\eta_{sp}}{C_v} - \frac{\ln \eta_r}{C_v}\right]$	Benzene	$\mathrm{DP} = 2.22 \times 10^3[\eta]^{1/0.76}$	9
Methyl acrylate	$[\eta] = (\eta_{sp}/C'_v)_{\lim C'_v \to 0}$	Acetone	$\mathrm{DP} = 11.2[\eta]^{1.22}$	7
Styrene	$[\eta] = \frac{\eta_{sp}/C'_v}{1 + 0.28\,\eta_{sp}}$	Benzene	—	3, 10, 11, 12

TABLE II

Chain Transfer with Organometallic Compounds in the Free-Radical Polymerization of Styrene at 100°C.

Chain transfer agent	[S]/[M] $\times 10^3$	Monomer concn. [M], moles/l.	Rate of polymerization, % conversion/hr.	DP	DP_0 (for control runs)	R/R'_0, notes in moles/l. sec.	Chain transfer constant C (±90% confidence limits)	Pr·
$(C_2H_5)_2Zn$	12.1	7.95	2.16	223	4256	0.88	0.366 (±0.009)	0.34
	27.6	7.86	1.79	106		0.74		
	55.2	7.65	1.56	53		0.66		
$(C_4H_9)_2Cd$	11.6	7.02	2.36	569	4672	1.17	0.117 (±0.071)	−0.15
	19.3	6.42	2.71	403		1.49		
$(C_2H_5)_2Hg$	21.2	7.88	2.54	4115	4256	1.05	3.35×10^{-5} ($\pm 24.59 \times 10^{-5}$)	−4.35
	44.0	7.75	2.40	4491		1.01		
	81.4	7.52	2.30	4146		1.00		
	108.7	7.30	2.31	4185		1.03		
$(C_4H_9)_3B$	4.64	7.97	2.42	4009	4117	1.10	3.48×10^{-3} ($\pm 13.17 \times 10^{-3}$)	−1.74
	4.64	7.97	2.44	3748		1.10		
	9.29	7.88	2.58	3567		1.17		
	13.90	7.82	2.72	3158		1.25		
$(C_2H_5)_3Al$	0.93	8.02	2.10	539	4525	0.89		
	1.62	8.01	1.85	131		0.79	8.05 (±3.06)	2.05
	2.31	8.00	1.65	67		0.70		
	3.47	7.98	1.38	37		0.59		
$(i\text{-}C_4H_9)_2AlH$[a]	1.98	—	25.0	18	—	—		
	2.16	—	28.3	15	—	—	26.9 (±0.6)	2.53
	2.50	—	26.7	7	—	—		
	14.00	—	27.9	2.9	—			

$(C_2H_5)_3In$	0.83	8.02	2.59	2386		1.01		
	1.66	8.00	1.99	445	4208	0.78	1.76 (±0.84)	1.35
	3.33	7.97	1.65	173		0.65		
$(C_2H_5)_4Si$	15.4	7.86	2.25	3705	4035	1.01		
	23.0	7.77	2.32	3797	4224	0.99	8.12×10^{-4}	−2.30
	31.0	7.68	2.14	3726	4035	0.98	($\pm 9.00 \times 10^{-4}$)	
$(C_4H_9)_4Sn$	8.8	7.85	2.33	4233	4525	1.01		
	17.7	7.70	2.17	4429	4470	1.03	3.71×10^{-4}	
	26.4	7.50	2.26	4274	4525	1.03	($\pm 5.01 \times 10^{-4}$)	−2.60
	35.5	7.35	2.13	4167	4470	1.06		
$(C_2H_5)_4Pb$	29.5	7.65	2.55	3881		1.08		
	59.0	7.52	2.58	3791	4256	1.15		
	88.5	7.02	2.48	3876		1.15	1.24×10^{-4}	
	89.0	7.02	2.84	2609	4035	1.43	($\pm 4.91 \times 10^{-4}$)	−3.08
	147.5	6.42	2.38	3871	4256	1.20		
	148.0	5.14	2.92	2966	4035	1.64		
$(C_3H_7)_3N$	1.60	8.00	2.28	4226	4518	1.03		
	3.01	7.93	2.07	3547		0.91	2.42×10^{-3}	−1.80
	6.07	7.83	1.77	2891	4426	0.80	($\pm 1.66 \times 10^{-3}$)	
	11.65	7.72	1.59	2880		0.73		
$(C_4H_9)_2P$	3.0	7.97	2.10	4183		0.90		
	14.0	7.79	2.07	3746	4795	0.90	2.44×10^{-3}	−1.80
	73.0	6.95	1.81	2255		0.90	($\pm 0.17 \times 10^{-3}$)	
	230.0	5.38	1.38	1275		0.87		
$(C_4H_9)_3Sb$	7.1	7.93	2.22	3533	4224	0.92		
	12.0	7.86	2.30	3028	4035	1.03	5.80×10^{-3}	−1.40
	17.8	7.77	2.09	3052	4224	0.89	($\pm 3.95 \times 10^{-3}$)	
	24.0	7.68	2.21	2520	4035	1.01		

[a] Chain transfer agent added continuously to keep [S]/[M] constant. [S]/[M]C dominant termination term. DP value determined by cryoscopy.

TABLE III

Chain Transfer with Organometallic Compounds in the Free-Radical Polymerization of Methyl Methacrylate at 60°C.

Chain transfer agent	[S]/[M] $\times 10^3$	[M], moles/l.	Rate of polymerization, % conversion/hr.	DP	DP_0 (for control runs)	R/R'_0	C ($\pm$90% confidence limits)	Pr*
$(C_2H_5)_2Hg$	25.2	8.78	2.81	11,480	12,810	0.94		
	50.5	8.57	2.96	12,010		1.00	8.98×10^{-5}	−3.27
	101.0	8.18	3.06	11,060		1.06	($\pm 6.01 \times 10^{-5}$)	
	151.5	7.82	2.99	10,680		1.06		
$(C_4H_9)_3B$	5.43	8.88	4.98	8,900	13,075	1.57		
	6.60	8.86	4.67	8,850		1.48		
	10.86	8.78	5.91	6,384	12,670	1.93	7.45×10^{-4}	−2.36
	13.20	8.73	7.12	5,000		2.35	($\pm 6.18 \times 10^{-4}$)	
	22.00	8.57	4.51	8,078		1.50		
	44.00	8.18	5.26	5,832		1.80		
$(C_2H_5)_3Al$	10.7	8.78	—	585	12,775	<0.20	0.124	
	16.0	8.67	—	275			($\pm$0.056)	−0.13
	21.4	8.57	—	305				
	42.8	8.18	—	180				
$(i\text{-}C_4H_9)_2AlH$	1.5	8.95	3.14	12,550	13,400	1.03		
	3.0	8.91	3.34	12,100		1.10		
	7.5	8.78	3.48	9,500	12,500	1.11		
	11.2	8.67	3.16	3,000	12,775	1.07	ca. 0.36	0.29
	15.0	8.57	3.48	5,650	12,500	1.08		
	15.0	8.57	3.37	2,450	12,675	1.13		
	22.4	8.37	3.32	1,200		1.13		
	30.0	8.18	2.96	265	12,775	1.03		

$(C_2H_5)_3In$	0.77	8.97	4.21	12,230		1.37		
	1.54	8.95	5.23	9,303	13,470	1.70	0.0332	−0.70
	3.09	8.91	4.67	6,234		1.53	(±0.0046)	
$(C_2H_5)_4Si$	8.54	8.86	2.99	11,250	13,075	0.94		
	11.40	8.82	2.83	11,000	12,775	0.96		
	14.20	8.78	3.08	11,900	13,075	0.98	5.75×10^{-4}	−2.72
	17.10	8.73	2.86	10,800		0.97	($\pm 5.52 \times 10^{-4}$)	
	22.80	8.65	2.92	11,900	12,775	0.99		
	28.40	8.57	2.82	8,600		0.97		
$(C_4H_9)_4Sn$	4.1	8.89	3.01	13,000	12,775	1.01		
	8.1	8.78	3.02	12,850	13,075	0.96	1.32×10^{-4}	−3.12
	12.2	8.67	3.01	12,650	12,775	1.02	($\pm 1.32 \times 10^{-4}$)	
	16.3	8.57	2.98	12,850	13,075	0.95		
$(C_2H_5)_4Pb$	5.5	8.91	3.13	12,620		1.02	3.14×10^{-4}	−2.77
	12.9	8.78	2.87	12,000	12,670	0.94	($\pm 2.30 \times 10^{-4}$)	
	27.4	8.57	2.60	11,630		0.87	>(c)	
	54.8	8.18	2.64	11,100		0.90	$3.14(\pm 2.30) \times 10^{-4}/2$	
$(C_3H_7)_3N$	14.1	8.78	2.81	10,100	13,075	0.89		
	21.2	8.68	2.74	9,000	12,675	0.91	1.46×10^{-3}	−2.04
	28.2	8.57	2.74	8,650	13,075	0.88	($\pm 0.070 \times 10^{-3}$)	
	42.4	8.37	2.41	6,900	12,675	0.82		
$(C_4H_9)_3P$	1.07	8.97	3.04	12,150	12,675	1.00		
	2.14	8.95	3.02	11,900	12,500	0.99	3.06×10^{-3}	−1.74
	10.70	8.78	2.96	8,650	12,675	0.98	($\pm 0.50 \times 10^{-3}$)	
	21.40	8.57	2.86	7,100	12,500	0.99		
$(C_4H_9)_3Sb$	1.52	8.97	3.38	13,050	13,400	1.11		
	3.26	8.93	3.55	13,350		1.16	$<1 \times 10^{-4}$	<−3.00
	10.90	8.78	3.45	12,550		1.14		
	21.80	8.57	3.28	12,100	12,675	1.10		
	32.70	8.37	3.89	10,550		1.32		

TABLE IV
Chain Transfer with Organometallic Compounds in the Free-Radical Polymerization of Acrylonitrile at 60°C.

Chain transfer agent	[S]/[M] × 10^3	[M], moles/l.	Rate of polymerization, % conversion/hr.	DP	DP_0 (for control runs)	R/R'_0	C (±90% confidence limits)	Pr*
$(C_2H_5)_2Zn$	19.1	2.86	10.62	128		3.56	ca. 1.6	−0.28
	38.2	2.84	2.17	11.2	469	0.73		
	63.6	2.82	1.19	9.7		0.40		
$(C_4H_9)_2Cd$	9.2	2.77	2.85	18.7	460	1.00	ca. 5.5	0.22
	23.4	2.62	26.27	27.1		10.30		
$(C_2H_5)_2Hg$	30.6	2.85	3.18	432		1.07		
	62.5	2.82	3.16	376	469	1.07	7.22×10^{-3}	−2.62
	125.0	2.77	2.97	330		1.01	($\pm 0.76 \times 10^{-3}$)	
	187.5	2.72	3.00	287		1.03		
$(C_4H_9)_3B$	13.6	2.85	4.74	104		1.54		
	27.2	2.82	4.62	54	478	1.51	0.647	−0.67
	40.8	2.80	4.50	35		1.48	(±0.090)	
$(C_2H_5)_3Al$	5.3	2.87	2.72	400		0.84		
	10.6	2.86	3.24	421	478	1.01	0.059	−1.74
	15.9	2.84	3.30	390		1.03	(±0.031)	
	29.1	2.82	3.54	225		1.11		
$(i\text{-}C_4H_9)_2AlH$	1.9	2.88	2.46	387	460	0.80		
	5.6	2.86	1.04	134		0.32	0.394	−0.91
	11.2	2.84	1.19	167	478	0.37	(±0.266)	
	18.5	2.82	0.79	99		0.25		

$(C_2H_5)_3In$	0.95	2.88	3.15	380		1.46		
	1.91	2.88	3.22	358	486	1.50	0.222	−1.15
	3.81	2.87	3.84	322		1.79	(±0.167)	
$(C_2H_5)_4Si$	35.0	2.82	2.84	447	478	0.89		
	106.0	2.72	2.38	390		0.76		
	176.0	2.62	2.22	402	462	0.88	2.10×10^{-3}	−3.18
	264.0	2.50	2.22	378	478	0.74	($\pm 0.90 \times 10^{-3}$)	
	352.0	2.40	2.03	325	462	0.84		
$(C_4H_9)_4Sn$	4.0	2.87	2.36	467		1.00		
	10.1	2.85	2.34	443	473	0.98	8.08×10^{-3}	−2.56
	20.2	2.82	2.30	423		0.98	($\pm 2.12 \times 10^{-3}$)	
	60.5	2.72	2.17	382		0.85		
$(C_2H_5)_4Pb$	34.0	2.82	2.66	315		0.90		
	68.0	2.77	2.34	263	469	0.80	24.3×10^{-3}	−2.10
	102.0	2.72	2.13	195		0.74	($\pm 4.8 \times 10^{-3}$)	
	170.0	2.62	1.89	161		0.66		
$(C_3H_7)_3N$	7.0	2.87	2.86	223		0.97		
	17.5	2.85	2.45	132	473	0.83	0.428	−0.89
	35.0	2.82	2.02	75		0.69	(±0.045)	
	35.1	2.82	1.78	60	462	0.69		
	105.0	2.72	1.21	21		0.48		
$(C_4H_9)_3P$	Ionic initiation—no C data possible							
$(C_4H_9)_3Sb$	1.35	2.88	2.39	55	486	0.81		
	2.69	2.88	3.52	35		1.12		
	5.38	2.87	1.66	16		0.56	11.1	0.52
	13.50	2.85	0.97	3	478	0.33	(±1.9)	
	26.90	2.82	0.76	6		0.26		

only if the molecular weight is high, and either (*a*) the rate of polymerization is not affected by the additive or (*b*) the $C([S]/[M])$ term is so large that the other variable terms can be neglected in eq. (1) (which is valid for radical combination):

$$1/DP = C_m + C_s([S]/[M]) + (k_1[R\cdot]/2k_3[M]) + (k_2[S\cdot]/k_3[M]) \quad (1)$$

where DP = degree of polymerization, C_m = chain transfer constant for monomer, C_s = chain transfer constant for additive, $[S]/[M]$ = molar ratio of additive to monomer, $[R\cdot]$ = molar concentration of polymeric radicals, $[S\cdot]$ = molar concentration of the radical derived from the additive as a result of the chain transfer step, k_3 = specific rate constant for propagation, k_1 = rate constant in $+ d[P]/dt = k_1[R\cdot]^2/2$ (reaction of polymeric radicals to yield polymer), k_2 = rate constant in $+ d[P]/dt = k_2[R\cdot][S\cdot]$ (reaction of a polymeric radical with a radical derived from a chain transfer agent to yield polymer), and $[P]$ = molar concentration of polymer chains.

For the present work, no $C_I([I]/[M])$ term is needed for the initiator I, since C_I for AIBN is known to be zero.[1c] It is obvious, also, that $[R\cdot]$, $[M]$, $[S]$, and $[I]$ must be constant for each reaction at a given $[S]/[M]$ for the Mayo plot to hold.

It is clear from Tables II-IV showing R/R'_0 (the ratio of the actual rate to the ideal rate calculated only on the basis of dilution with no retardation or acceleration) that acceleration and retardation are the rule rather than the exception. An analysis of the Mayo equation allowed the following conclusions to be drawn concerning its use.

(*1*) When C_s ($[S]/[M]$) is so large that other terms can be neglected, a plot of 1/DP against $[S]/[M]$ will yield the correct C_s for all values of R/R'_0.

(*2*) When $R/R'_0>1$, the Mayo plot gives the correct values of C_s when $(1/DP) - \{C_m + (k_1[R]/2k_3^2[M]^2)\}$ is used as the ordinate.

(*3*) When $0.08<R/R'_0<1$, a plot of $(1/DP) - \{C_m + (k_1[R]/2k_3^2[M]^2)\}$ against $[S]/[M]$ will yield a value of C_s which might be in error by a factor of two. This variation follows from the possible range of $0<k_4<\infty$ in the reinitiation expression $+ d[R\cdot]/dt = k_4[S\cdot][M]$.

In practice, the variation in k_4 is much smaller, since with k_4 equal to zero, severe retardation, rather than minor retardation, would result. Likewise, k_4 should never exceed k_3 or no retardation would occur, so that the actual uncertainty in C_s may be a factor of 1.3–1.5 rather than of 2.

(*4*) When $0<R/R'_0<0.20$, a plot of $(1/DP) - \{C_m + (k_2/k_3[M])(G/k_5)^{1/2}\}$ against $[S]/[M]$ will yield C_s with no restrictions. Here G is equal to $2k_6[I]$ or the rate of radical formation and k_5 is the constant in the expression $- d[S\cdot]/dt = 2k_5[S\cdot]$.[2]

(*5*) When $0.20<R/R'_0<0.80$, C_s can only be estimated unless the transfer term predominates so that the others can be ignored. If all terms must be included, one can assume values for k_2 and make a plot of $(1/DP) - \{C_m + (k_1[R\cdot]/2k_3[M]) + (k_2[S\cdot]/k_3[M])\}$ against $[S]/[M]$ to obtain a

corrected but uncertain value of C_s. Fortunately, actual experience in measuring chain transfer constants has shown that this uncertain case occurs rarely.

In order to correlate all of the reactivity data at 60°C., the C_s values obtained with styrene at 100°C. were estimated at 60°C. by assuming (*1*) the activation energy was 0.0 when C was greater than 1, (*2*) the activation energy was 5.0 when C was between 1×10^{-4} and 1, and (*3*) the activation energy was 14 when C was less than 1×10^{-4}. This method of estimation was adopted after studying some of the available data about the variation of C with temperature.[1b] In the correlation of the data, this procedure introduces only a relatively minor error as explained below.

In the case of tri-*n*-butylantimony with methyl methacrylate, C appeared to be zero. Since C must be positive, even if very small, its value was recorded as less than the lowest value of C which was measured for that monomer.

The values of the kinetic constants used in making the calculations are given in Table V.

TABLE V

Monomer	k_t (60°C.)	k_p (60°C.)	Reference
Styrene	1.3×10^8 (100°C.)	740 (100°C.) 176	14
Acrylonitrile	9.8×10^8	2458	2
Methyl methacrylate	3.74×10^7	734	15
Methyl acrylate	9.5×10^6	2090	16

Correlation of Radical Reactivities According to Bamford, Jenkins, and Johnston. The procedure suggested by these authors[2] was used with modifications as noted in the text below. The specific rate constants for the reaction of the polymeric radicals with toluene were taken from the reference article.

Accuracy and Reliability. The value of C in Tables II–IV is given along with the 90% confidence limits as obtained from the scatter of points about the Mayo plot. There are other sources of error which increase the uncertainty range of C, and it is estimated that the overall maximum uncertainty in the value C lies in a sixfold ($10^{0.8}$) range if all possible errors occur in the same direction. This result follows from the sources of error which are given in Table VI. The difficulty of measuring absolute values of C precisely has been reviewed.[3] When predicting C for unknown monomers, a further uncertainty is introduced by the choice of σ.

All of the sources of error rarely work in the same direction nor do they have their maximum variability. Most values of C in this report are probably correct to better than a factor of 3 or 4 as indicated by the data obtained using transfer agents for which C values are available in the literature (Table VII).

TABLE VI

Source of error	Estimated resulting maximum uncertainty range in C
1. Use of a minimum number of points to make the Mayo plot	4.0-fold
2. Use of $[\eta]$–DP relationships	0.7
3. Estimation of C for styrene at 60°C. from 100°C. data	0.6
4. Approximation used to correct the DP for rate effects	0.5
5. Change in [S]/[M] during polymerization	0.2
6. Nonreproducibility in measuring the rate and DP	0.1
7. Deviation from constant rate kinetics	<0.1
Overall error	~6.0-fold or $10^{0.8}$

No matter how great the uncertainty range may be, the average value of C is the most probable value and these values were used in collating the data. While it would be desirable to have more accurate values of C, the correlations and trends which are being reported are still real, since a range for C of greater than 10^6 has been covered.

TABLE VII
Comparison of Measured C Values with Literature C Values

Transfer agent	Monomer	Measured chain transfer value, C	Literature C value	Reference
n-Dodecyl mercaptan	Styrene	26 (110°C.) 13 (100°C.)	19 (60°C.)	17
Tri-n-propylamine	Acrylonitrile	0.4 (60°C.)	1.0 (60°C.)	18

The possibility that the transfer agent reacts with chemicals in the mixture other than the polymeric radical must be considered. This reaction would result in a value of C which is too low. Impurities, such as oxygen and water, could be present only in extremely small quantities, but, in some cases, the monomer itself reacts with the organometallic. This reaction causes a curvature on the Mayo plot and is, therefore, detectable. In most cases where reaction was detected, it was still possible to get an approximate value of C by using the data from the experiments containing large quantities of transfer agent. These values of C have been recorded in Tables II–IV as being approximate and are shown without confidence limits. For those cases in which reaction was severe, no transfer constant was calculated (e.g., methyl methacrylate with diethylzinc and dibutylcadmium).

Raw Materials

Monomers. Styrene was of >99.7% purity. The monomer was washed with caustic to remove inhibitor, dried with $CaSO_4$, and fractionated under vacuum.

Acrylonitrile was of >99.5% purity and contained <100 ppm methyl vinyl ketone. The monomer was dried with $CaSO_4$ and CaH_2 and was fractionated under vacuum.

Methyl methacrylate was >99.0% pure and contained <0.10% H_2O, <0.005% methacrylic acid. The monomer was washed with caustic, dried over $CaSO_4$, and fractionated under vacuum.

Methyl acrylate was >98.0% pure, b.p. 79.6–80.3°C./760 mm.; it contained <0.004% acid as acrylic acid and <0.1% H_2O. The monomer was washed with caustic, dried over $CaSO_4$, and fractionated under vacuum.

All of the monomers were handled and stored under argon and only the center cuts of the fractionated materials were used.

AIBN. Azobisisobutyronitrile (AIBN) was recrystallized from methanol to a constant melting point of 101–102°C. and stored at 0°C.

Argon. On analysis the argon used contained <0.002% O_2; <0.002% H_2; <0.0008% H_2O.

Transfer Agents. The following transfer agents were used: *n*-dodecyl mercaptan: sp. gr. (20/20)0.845, n_D^{20} 1.4588, b.p. 146–148/15 mm. Hg; triethylaluminum: >95%, material fractionated at 1 mm. Hg and center cut taken for chain transfer work; tri-*n*-butylphosphine: b.p. 107–108°C./7.5 mm. Hg; tri-*n*-propylamine: b.p. 154–156°C./760 mm. Hg; tetra-*n*-butytin: b.p. 144–147°C./10 mm. Hg; tri-*n*-butylantimony: b.p. 131–131.5°C./12 mm. Hg; tetraethylsilane: b.p. 38–39°C./10 mm. Hg; tetraethyllead: >99.1%; di-*n*-butylcadmium: b.p. 103.5°C./12.5 mm. Hg, density (19.4°C.) 1.3056; diethylzinc (Chemicals Procurement Company): purity unspecified; diethylmercury (Chemicals Procurement Company): purity unspecified; diisobutylaluminum hydride: >99%; triethylindium: b.p. 144°C./760 mm. Hg, n_D^{20} 1.538, d_4^{20} 1.260; tributylboron: >99%.

Solvents. Toluene, methanol, dimethylformamide, benzene, acetone, and petroleum ether were used; AR grade materials were fractionated and the center cuts were dried over either sodium or molecular sieves.

RESULTS

The primary data and the calculated values of C for styrene, methyl methacrylate, and acrylonitrile monomers are shown in Tables II–IV. The 90% confidence limits as obtained from the Mayo plot are included for C. The quantity Pr· was found as described by Bamford et al.,[2] and these values are included in Tables II–IV. Plots of Pr· versus σ were made for each chain transfer agent except tributylboron and the Group 5a elements. For these substances, σ^+ was used instead of σ as will be explained below. Figure 1 is a typical plot of Pr· as a function of σ. The values of σ chosen were:[19] −0.01 for styrene, +0.28 for methyl methacrylate, and +0.66 for

acrylonitrile. The values of σ^+ chosen were:[20] -0.18 for styrene, $+0.17$ for methyl methacrylate, and $+0.66$ for acrylonitrile. The quantity α is the slope of the Pr· versus σ curve. Three values of β were calculated from

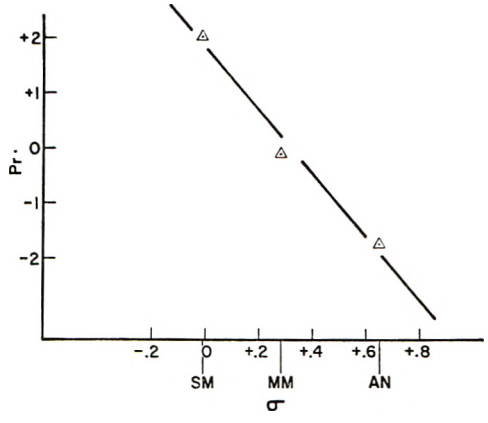

Fig. 1. Plot of Pr· vs. σ for triethylaluminum. The slope α is equal to -5.58.

the α for a given chain transfer agent, for each of the three monomers, and an average β was found. The results, shown in Table VIII, represent the correlation of the data following the suggestion advanced by Bamford et al.[2]

TABLE VIII
Values of α and β Calculated According to the Method of Bamford, Jenkins, and Johnston

Chain transfer agent	α	β			
		From styrene	From methyl methacrylate	From acrylonitrile	Arithmetic mean
Et_2Zn	-0.80	4.29	—	4.29	4.29
Bu_2Cd	$+0.65$	3.88	—	3.88	3.88
Et_2Hg	$+2.54$	-0.33	0.01	-0.32	-0.21
Bu_3B	$+1.67$[a]	2.66	1.36	2.20	2.08
Et_3Al	-5.58	5.97	5.42	5.95	5.78
$(i\text{-}Bu)_2AlH$	-5.03	6.50	5.73	6.41	6.18
Et_3In	-4.98	5.42	4.68	6.13	5.41
Et_4Si	-1.31	1.72	1.64	1.68	1.68
Bu_4Sn	$+0.13$	1.39	0.85	1.32	1.18
Et_4Pb	$+1.48$	0.93	0.85	0.90	0.89
Pr_3N	$+1.38$[a]	2.45	1.70	2.21	2.12
Bu_3P	$+1.00$[a]	2.39	2.09	—	2.24
Bu_3Sb	$+3.57$[a]	3.22	—	2.18	2.70

[a] Due to the uncertainty in the σ^+ value for methyl methacrylate, these α values are obtained by giving extra weight to the points for styrene and acrylonitrile. In all other cases, the line used to obtain α was drawn according to the method of least squares.

DISCUSSION

Test of the Correlation

A severe test of the correlation as well as its predictive value is provided by measuring the C values for a fourth monomer for some of the same substrates from which the correlation was developed and comparing these with C values which are calculated knowing only k_{toluene} and σ or σ^+ for the monomer. The α and β values for the substrates are available from the correlation. The results are shown in Table IX for methyl acrylate at 60°C. ($\sigma = 0.45$, $\sigma^+ = 0.48$).

TABLE IX
Calculated and Experimental C Values for Organometallic Compounds in Methyl Acrylate; Polymerization at 60°C.

Organometallic	Calculated chain transfer constant C	Experimental C (±90% confidence limits)
Et_3Al	0.316	ca. 0.048
Et_4Si	3.31×10^{-3}	1.78×10^{-3} ($\pm 3.80 \times 10^{-3}$)
Pr_3N	0.163	0.047 (±0.047)
Bu_3P	0.141	0.189 (±0.078)

One can conclude that the measured and predicted C agrees to better than an order of magnitude. Since the correlation was based on absolute values of C ranging from 10^1 to 10^{-5} which were individually accurate within the range of $10^{0.8}$, it is seen that the results are as good as the data could allow them to be. More accurate values of C are needed to judge the complete generality of the method of correlation. Bamford, Jenkins, and Johnston found, by using six monomers and eleven substrates, that the predicted and calculated values of C agreed to within a factor of $10^{0.5}$. However, they appeared to reach this conclusion by calculating C for monomers and substrates which were used initially to develop the correlation so that their test was only of that particular correlation and not of its generality or its predictive value. In the calculation of C for methyl acrylate, the α, σ, and β terms are much larger than the k_{toluene} term, so that a reasonable test of the correlation is being provided. One must recall, also, that the choice of the values used for σ and σ^+ can increase the error in the calculation of C.

The method of correlation, like the Q–e scheme, divides the reactivity into two factors: (*a*) a normal reactivity and (*b*) an additional reactivity due to polar factors. There is no attempt to describe the mechanism by which the reaction occurs, nor need that mechanism be the same for all reactions included in the correlation. The approach is pragmatic rather than rigorously theoretical and, as such, is to be judged by its success. That polar factors are probably of great importance can be deduced by comparing C for some organometallics with the C for the same compounds into which an oxygen atom has been introduced in the vicinity of the element (Table X).

TABLE X
Effect of Introducing an Oxygen Atom in the Vicinity of the Element on the Chain Transfer Constant with Styrene at 100°C.

Substrate	Chain transfer constant C
$(C_2H_5)_3Al$	8.1
$(C_2H_5O)_3Al$	$<10^{-5}$
$(n\text{-}C_4H_9)_3B$	3.5×10^{-3}
$(n\text{-}C_4H_9O)_3B$	$<10^{-5}$
$(n\text{-}C_4H_9)_3P$	2.4×10^{-3}
$(n\text{-}C_4H_9)_3P{=}O$	$<10^{-5}$

α and β Values

When β is plotted as a function of α for the organometallics in each group of the Periodic Table, a series of lines is obtained (Fig. 2). The slope of these lines is greatest, negatively for Group 2b and progressively becomes more positive as one goes to Group 5a, the slope of which is close to zero.

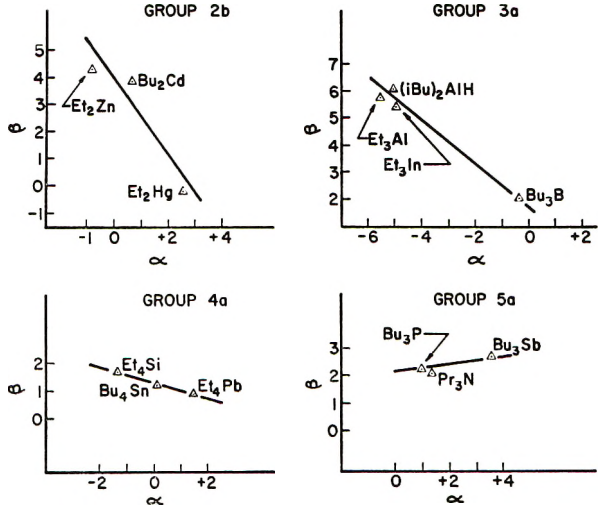

Fig. 2. β vs. α by groups in the Periodic Table for organometallic compounds: Group 2b, slope = -1.39; Group 3a, slope = -0.54; Group 4a, slope = -0.32; Group 5a, slope = $+0.21$.

These trends may be consistent with the changing electronic structure of the elements. α is a measure of the polarizability of the substrate, and β is its intrinsic reactivity. A negative α implies that the substrate can be polarized by the attacking radical so as to accept its electron in the transition state. Such substrates in the absence of polar substituent groups on the radical may still not repel the approaching electron. A positive α implies the reverse. In moving from Group 2b to Group 5a, one goes from a deficiency to an excess of electrons. This fact is reflected in the positive value of α for all Group 5a elements. These substrates tend to repel elec-

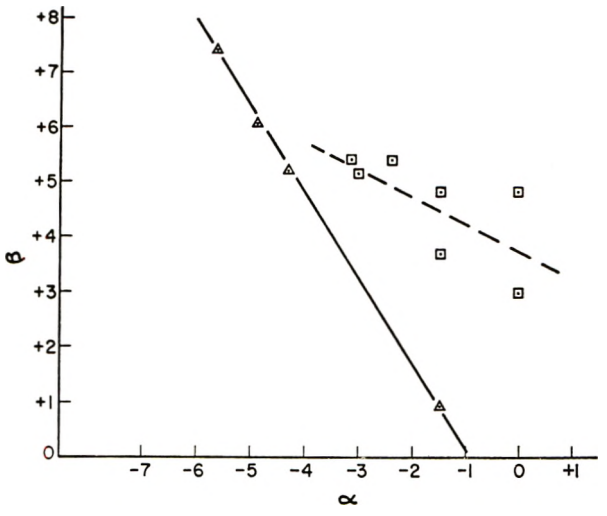

Fig. 3. β vs. α for (⊡) monomeric substrates and (◬) nonmonomeric substrates as reported by Bamford, Jenkins, and Johnston.[2]

trons so that β is generally low and essentially constant. Since a high electron density already exists around the Group 5a elements, the effect of small variation in this density will not be observable.

When the β–α data of Bamford, Jenkins, and Johnston are plotted (Fig. 3), two curves seem to result. The first curve is for those reactions which involve the extraction of an atom from the substrates by the attacking free radical. The second curve is for those reactions in which the attacking free radical adds to the substrates (e.g., monomers) with the disappearance of a double bond. These are two entirely different mechanisms and it is not surprising that two curves are required to represent them. It is suggested that a change in mechanism occurs for the organometallic substrates as one goes from Group 2b to Group 5a. Hence, a different curve is needed to represent the data for each group (see Fig. 2).

The correlation of α and β may be worsened by the indiscriminate use of ethyl, propyl, and butyl groups in the organometallic derivatives. Since a family of curves is required to represent β–α data, one would not expect to be able to predict the values of these constants for unknown substrates. Values of α should be related to the polarizability of the substrates within a group in the Periodic Table. Polarizability values are not available for the elements. The next best quantity to use is the electronegativity(E.N.). However, a plot of α against E.N. shows very little regularity.

When α is plotted as a function of the group for a given period in the Periodic Table, it clusters around zero at Group 4 elements. α increases as one goes from lighter to heavier metals in any given Group. The exception to this latter statement is boron and Group 5a elements. β shows very poor correlation with any parameter except the group in the Periodic Table, Group 4a elements being least reactive. Group 4a elements have, therefore,

the lowest value of C, which follows from their low values of α and β. The lack of reactivity of Group 4a elements may be a consequence of their having a more balanced electron structure (i.e., exactly four outer shell electrons). The most balanced organometallic compounds in the Periodic Table, those containing only C—C bonds, are known to be very unreactive toward radical attack. Thus, it has been reported[21] that degradation of polymers by free-radical attack occurs via hydrogen extraction and not by direct chain transfer with a C—C bond.

Use of σ and σ^+ Values

With one exception, the organometallics of Groups 2b, 3a and 4a gave linear plots when Pr· was plotted against σ. For boron and the Group 5a elements, no correlation resulted when σ values were used, and an approximate but usable line was drawn when σ^+ values were used. In order to obtain completely linear plots, one would have had to use a σ^+ value of -0.7 instead of $+0.17$ as recommended in the literature for methyl methacrylate. The ultimate justification for using σ^+ instead of σ is the same as that for any empirical correlation, i.e., it is successful as shown by the data in Table IX. Bamford, Jenkins, and Johnston found a lack of correlation for triethylamine when using σ constants and suggested that the σ^+ function should be more suitable since it is especially applicable to electrophilic reactions,[22] but they did not feel that sufficient data for σ^+ were available. It may be that lack of precision in the σ^+ values in the present work is the cause of the imperfect correlations. In any case, the theoretical basis for the use of σ^+ as opposed to σ is still not clear.

The fact that derivatives of the electron-rich Group 5a elements can be correlated better with the σ^+ function may not be surprising, but the correlation for boron is unexpected. Benzing[23] has suggested that the use of σ^+ implies a change in the transition state from $R^{\ominus}M^{\oplus}$—CH to $R^{\ominus}H^{\oplus}$—C—M rather than the often suggested change from $R^{\ominus}M^{\oplus}$—CH to $R^{\oplus}M^{\ominus}$—C—H. According to this view, the critical factor is the relative electronegativities[24] of the M and H (E.N. = 2.1) since the carbon (E.N. = 2.5) would not be involved in the competition for the positive charge. When the E.N. exceeds 1.8, σ^+ must be used in place of σ. This suggestion accounts for the behavior of boron as well as the Group 5a elements. Confirmation of this idea would require detailed data on the mechanism of the transfer reaction for a great many reactions.

We wish to express our gratitude to Dr. W. H. Urry, Dr. G. Henrici-Olivé and Dr. S. Olivé for helpful discussions.

References

1. Walling, C., *Free Radicals in Solution*, Wiley, New York, 1957, (a) p. 118, 119; (b) *ibid.*, pp. 152–153; (c) *ibid.*, p. 161.

2. Bamford, C. H., A. D. Jenkins, and R. Johnston, *Trans. Faraday Soc.*, **55**, 418 (1959).

3. Henrici-Olivé, G., and S. Olivé, *Fortschr. Hochpolymer. Forsch.*, **2**, 496 (1961).

4. Imoto, M., T. Otsu, T. Ota, H. Takatsugi, and M. Matsuda, *J. Polymer Sci.*, **22,** 137 (1956).

5. Curtice, J., H. Gilman, and G. S. Hammond, *J. Am. Chem. Soc.*, **79,** 4754 (1957).

6. Alfrey, T., Jr., and C. C. Price, *J. Polymer Sci.*, **2,** 101 (1947).

7. Fuhrman, N., and R. B. Mesrobian, *J. Am. Chem. Soc.*, **76,** 3281 (1954).

8. Bamford, C. H., A. D. Jenkins, R. Johnston, and E. F. T. White, *Trans. Faraday Soc.*, **55,** 168 (1959).

9. O'Brien, J. L., and F. Gornick, *J. Am. Chem. Soc.*, **77,** 4757 (1955).

10. Schulz, G. V., and F. Blaschke, *Z. Physik. Chem.*, **B50,** 305 (1941).

11. Schulz, G. V., G. Henrici-Olivé, and S. Olivé, *Z. Physik. Chem. (Frankfurt)*, **19,** 9 (1959).

12. Meyerhoff, G., *Z. Physik. Chem. (Frankfurt)*, **4,** 335 (1955).

13. Mayo, F. R., *J. Am. Chem. Soc.*, **65,** 2324 (1943).

14. Henrici-Olivé, G., and S. Olivé, *Makromol. Chem.*, **37,** 71 (1960).

15. Matheson, M. S., E. E. Auer, E. B. Bevilacqua, and E. J. Hart, *J. Am. Chem. Soc.*, **71,** 497 (1949); further corrected for disproportionation by C. F. Bamford, W. G. Barb, A. D. Jenkins, and P. F. Onyon, *The Kinetics of Vinyl Polymerization by Radical Mechanisms*, Butterworth, London, 1958, p. 82.

16. Matheson, M. S., E. E. Auer, E. B. Bevilacqua, and E. J. Hart, *J. Am. Chem. Soc.*, **73,** 5395 (1951).

17. Gregg, R. A., D. M. Alderman, and F. R. Mayo, *J. Am. Chem. Soc.*, **70,** 3740 (1958).

18. Bamford, C. H., and E. F. T. White, *Trans. Faraday Soc.*, **52,** 716 (1956).

19. McDaniel, D. H., and H. C. Brown, *J. Org. Chem.*, **23,** 420 (1958). It has been assumed that σ for $—COOCH_3$ is equal to σ for $—COOC_2H_3$.

20. Brown, H. C., and Y. Okamoto, *J. Am. Chem. Soc.*, **80,** 4979 (1958). (See comment under reference 19 which applies to σ^+, also.)

21. Dolgoplosk, B. A., B. L. Erusalimskii, T. N. Kuren'gina, and E. I. Tinyakova, *Bull. Acad. Sci. USSR, Div. Chem. Sci. (Eng. Transl.)*, **1960,** 283.

22. Jaffe, H. H., *J. Chem. Phys.*, **20,** 279 (1952).

23. Benzing, E. P., private communication.

24. Pauling, L., *The Nature of the Chemical Bond*, Cornell Univ. Press, Ithaca, N.Y., 1960, Chapter 3.

Résumé

On a mesuré et comparé à 60°C les réactivités des radicaux polystyryles, polyméthylméthacrylyles et polyacrylonitriles avec des substrats organométalliques. Les organométalliques choisis étaient des dérivés aliphatiques saturés d'éléments des groupes 2b, 3a, 4a, et 5a du tableau périodique. La comparaison fut faite d'après la méthode proposée par Bamford, Jenkins et Johnston. La corrélation basée sur les trois monomères précités permet la prédiction de la constante de transfert, C, de quatre des substrats avec un radical non examiné, le polyméthyl-acrylyle, la précision étant supérieure à 10^1. Puisque la corrélation était basée sur des valeurs absolues de C se trouvant aux environs de 10^0 et exactes à $10^{0.8}$ près, on en conclut que la comparaison est valable et utile à la prédiction. Les valeurs de C ne peuvent être prédites pour des substrats non-examinés qu'avec une précision réduite, parce qu'on ne connait pas les valeurs de polarisabilité de la plupart des composés. L'introduction d'oxygène au voisinage de la liaison métal-carbone réduit fortement la valeur de C, et confirme que C est très sensible aux facteurs polaires. Il semble qu'il n'y ait une relation entre α (la polarisabilité du substrat) et β (la réactivité intrinsèque du substrat) au sein d'un groupe donné du tableau périodique. Le fait qu'il n'y ait pas de relation générale entre α et β pour tout le tableau périodique semble indiquer que le mécanisme de la réaction de transvert diffère d'un groupe à l'autre.

Zusammenfassung

Die Reaktivität von Polystyrol-, Polymethylmethacrylyl- und Polyacrylnitrylradikalen mit dreizehn organometallischen Reaktionspartnern wurde bei 60° gemessen und die bestehenden Gesetzmässigkeiten untersucht. Die untersuchten organometallischen Verbindungen waren gesättigte, aliphatische Derivate von Elementen der Gruppen 2b, 3a, 4a, und 5a des periodischen Systems. Zur Korrelation wurde die Methode von Bamford, Jenkins und Johnston verwendet. Die auf den erwähnten drei Monomeren beruhende Korrelation erlaubte die Bestimmung der Übertragungskonstanten, C, von vier der untersuchten Substanzen mit einem neuen Radikal, dem Polymethylacrylylradikal, mit einer Genauigkeit besser als 10^{1}. Da die Korrelation auf Absolutwerten von C beruhte, die einen Bereich von 10^{6} bedecken und auf $10^{0.8}$ genau sind, erscheint die Korrelation sinnvoll und heuristisch brauchbar zu sein. C-Werte für nicht getestete Substanzen können nur mit geringer Genauigkeit angegeben werden, da für die meisten Verbindungen keine Polarisierbarkeitsangaben verfügbar sind. Die Einführung von Sauerstoff in der Nachbarschaft der Metall-Kohlenstoffbindung setzt den Wert von C stark herab, was bestätigt, dass C gegen polare Faktoren sehr empfindlich ist. Es scheint eine Korrelation zwischen α (der Polarisierbarkeit des Überträgers) und β (der spezifischen Reaktivität des Überträgers) innerhalb einer gegebenen Gruppe des periodischen Systems zu bestehen. Die Tatsache, dass keine allgemeine Korrelation zwischen α und β für das ganze periodische System besteht, spricht für einen unterschiedlichen Mechanismus der Übertragungsreaktion von Gruppe zu Gruppe.

Received January 2, 1962
Revised March 15, 1962

JOURNAL OF POLYMER SCIENCE: PART A VOL. 1, PP. 1573–1583 (1963)

Structure of the Normal Crystal Form of Polyoxymethylene

GIAN ALVISÉ CARAZZOLO, *Montecatini Istituto Ricerche e Applicazioni Resine, Castellanza (Varese), Italy*

Synopsis

The structure of hexagonal polyoxymethylene has been re-examined by means of x-rays. The parameters of the elementary cell, the space groups, and the model of the spiral chain previously described in the literature for this polymer have been discussed. A new elementary cell and a new type of helical chain with a higher periodicity have been proposed. The condition of isomorphism for chains belonging to the same lattice, which had already been found in the case of orthorhombic POM, has also been found valid for hexagonal POM.

1. Introduction

Polyoxymethylene (POM) was one of the first macromolecular substance with a crystalline structure investigated by mean of x-rays.

The groundwork in this field was carried out mainly by the school of Staudinger[1–5] and provided the basis for the formulation of many concepts essential in the field of macromolecular crystallography.

Among these are that of the elementary cell whose parameters are independent of the length of the macromolecule, the concept of spiralization of the chain, etc. In particular, the long periodicity of the helical chains of POM, although composed of very simple monomeric units, helped to explain the concept of the repetition period of a helical chain as the lowest common multiple of the period of the helix and the period of the smallest structural unit whose projection is repeated identically along the axis of the chain.

A number of studies have since been carried out in order better to define the structure of this crystalline polymer: these have involved such methods as infrared spectroscopy,[6,7] dipolar moments,[8] and x-ray diffraction.[9,10]

However, all the above studies have been concerned with the same hexagonal crystalline form of POM (hexagonal POM), to which has been assigned the lattice constants $a = 4.46$ A. and $c = 17.3$ A. and the space groups $P3_1$ and $P3_2$; so far this is the only structure to be dealt with by the literature.

It is only recently that Bezzi, in the Montecatini laboratories at the Organic Chemistry Institute of the University of Padova, obtained a new crystalline form of POM (orthorhombic POM) with an orthorhombic cell, space group $P2_12_12_1$ and lattice constants $a = 4.77$ A., $b = 7.65$ A. and $c = 3.56$ A.

We have solved and described this structure in a previous paper.[12]

As has already been noted in the previous publication,[12] the space group of orthorhombic POM possesses the interesting property of admitting only isomorphous chains in the same lattice.

As far as artificial polymers are concerned, a similar condition of isomorphism of the chains belonging to the same lattice had already been noted by Natta et al.[11] for poly (*tert*-butyl acrylate) and for poly-5-methylhexene. This phenomenon, however, is particularly evident in the case of orthorhombic POM, since this polymer possesses the unusual property of showing a practically 100% crystallinity when examined under x-rays and also a spectrum rich in reflections at very high diffraction angles corresponding to interplanary distances of even less than 0.9A.

These same spectrum properties are also observable in samples of hexagonal POM, for which, on the basis of the space groups $P3_1$ and $P3_2$, the same condition of isomorphism found for orthorhombic POM would hold good.

Nevertheless, the solution of the structure of hexagonal POM had not yet been completed; in fact, although the spiral form of the chain had been defined, the mutual positions of the chains themselves had still to be determined.

The work covered by the present paper was, therefore, undertaken with the initial intention of bringing to a finish the determination of the structure of hexagonal POM and then to ascertain whether the condition of isomorphism for chains belonging to the same lattice also held good in this case.

The results obtained exceeded our original intentions. In fact, apart from finding an inaccuracy in the assignation of the space group of hexagonal POM, even in the 9-monomer and 5-turn chain-model most recently described in the literature,[9,10] it was also possible to ascertain that after nine monomers hexagonal POM does not indeed show an exact structural repetition but that this repetition takes place after a much greater number of monomeric units.

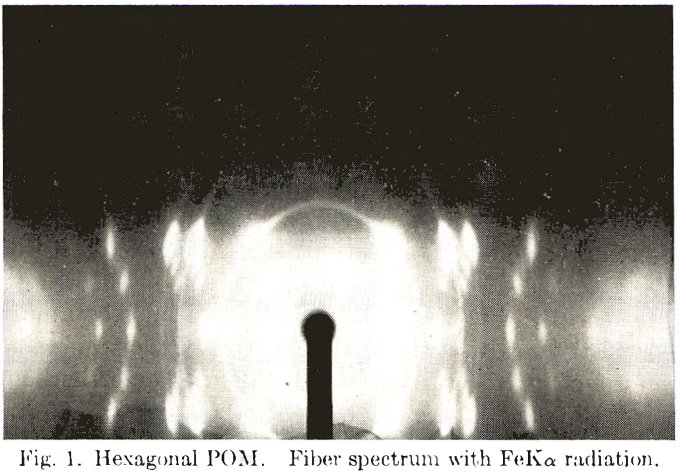

Fig. 1. Hexagonal POM. Fiber spectrum with FeKα radiation.

2. X-Ray Diffraction Patterns

Both fiber (Figs. 1–4) and powder spectra were made, the latter, by preference, on samples of trigonal POM obtained by annealing orthorhombic POM for the sake of the good crystallinity and crystallite size of the substance obtained in this way.

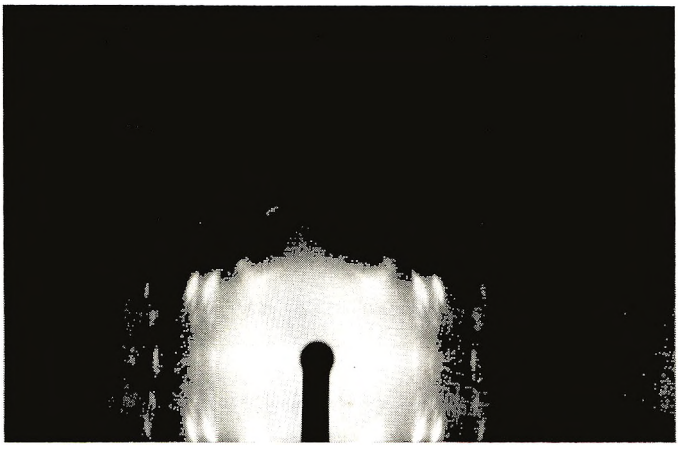

Fig. 2. Hexagonal POM. Fiber spectrum with CuKα radiation.

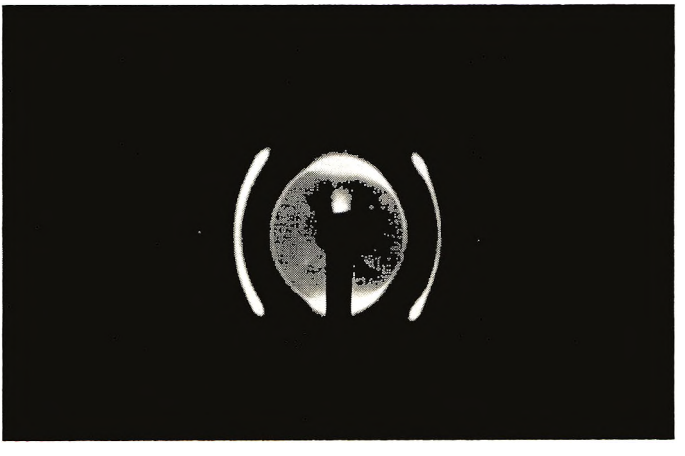

Fig. 3. Hexagonal POM. Spectrum of tilted fiber with FeKα radiation.

The X-ray spectra were obtained with the use of tubes with copper, iron, or chromium anticathodes.

The measurements of intensity were made on the basis of the peak areas on the spectra obtained with a Philips wide-range goniometer; the mean value of those obtained with CuKα and FeKα radiations was taken as the final intensity value for each single peak, after taking the normal angular correction coefficients into account.

Wherever a number of reflections were superimposed in one peak, the total intensity of the latter was divided on the basis of the intensities of the

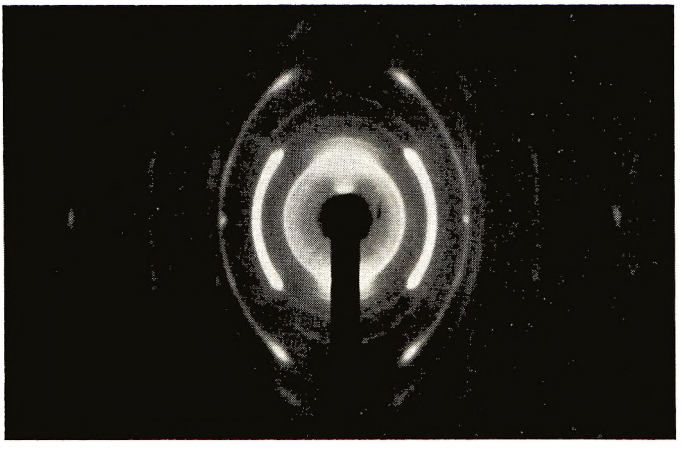

Fig. 4. Hexagonal POM. Spectrum at tilted fiber with CuKα radiation.

single reflections obtainable from the fiber spectra. A total of over fifty reflections was observed with intensity ratios ranging from 1 to 1000.

3. Structure of Hexagonal POM Chain with Identity Period of Nine Monomers

Two different types of helix for hexagonal POM have been described in the literature: both involve an identity period of nine monomers, but differ in the number of turns of the helical chain, which is four according to Sauter[4,5] (9/4 helix) and five according to Huggins[9] (9/5 helix).

The normal POM fiber spectrum shows a layer which is far more intense than all the others and whose periodicity is approximately 3.49 A., whereas the spectrum of the tilted fiber gives only two equatorial spots whose periodicities are approximately 0.97 A. and 1.94 A.; the latter corresponds to the repeat period of the monomeric unit along the axis of the fiber Z, which is contained nine times within the identity period of approximately 17.4 A.

The spots of the strongest layer have therefore the index $l = 5$, since the periodicity of 3.49 A. is contained five times in the identity period.

The hypothesis of a 9/5 helix, i.e. one with a periodicity equal to that of the fifth layer, is confirmed by the latter's particular intensity; in the case of a 9/4 helix the most intense layer should be the fourth, which, however, appears very weak in the photograms.

These observations inclined us to discard Sauter's hypothesis and to take into consideration that of Huggins, which supposes the helical chain of nine monomers and five turns shown diagrammatically in Figure 5.

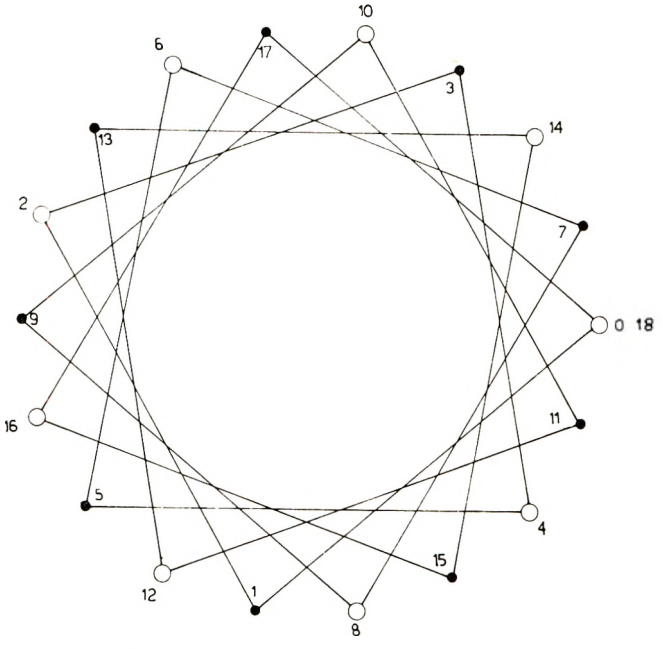

Fig. 5. Hexagonal POM. Projection of the 9/5 helix on the plane normal to the axis of the chain: (●) carbon atoms; (O) oxygen atoms. Internal numbers and external numbers are Z coordinates of the carbon and oxygen atoms, respectively, expressed as eighteenths of C.

4. Elements of Symmetry and Space Group of Hexagonal POM with 9/5 Helices

The POM chain (Fig. 5) involves a triad screw axis coinciding with the axis of the chain, enantiomorphous with respect to the helix; there are also eighteen diad axes normal to the chain, each of which passes through the axis of the helix and one atom of carbon or of oxygen.

The hexagonal elementary cell with $a = 4.46$ A. and $c = 17.3$ A. contains one chain only, so that the molecules may be positioned in two different ways in the same hexagonal lattice.

One of these means that, on the projection onto the plane normal to the chain, six diad axes of the chain coincide with the axes of the hexagonal lattice; these come at the respective levels $1/6C$, $1/3C$, $1/2C$, $2/3C$, $5/6C$, and C. This structure belongs to the space group $P3_121$ if the chain is right-handed and $P3_221$ if it is left-handed.

In the second case, the projections of six diad axes bisect the angles contained between the three axes of the hexagonal lattice; the levels of the six axes of symmetry are the same as in the last case, and the structure belongs to the space group $P3_112$ if the chain is right-handed and $P3_212$ if left-handed.

In order that the conditions imposed by the above four space groups be respected, it is in every case necessary to take as the origin of the axis Z the

TABLE I
Observed and Calculated Intensities I and Structure Factors F According to 9/5 Helical Chain Model for Hexagonal POM

	2θ	I		F	
hkl	(CuKα)	calculated	observed	calculated	observed
100	22.9	12.123	11.591	65.0	63.4
110	40.3	211	197	15.6	15.2
200	46.9	13	12	4.6	4.5
210	63.5	54	55	9.4	9.5
300	73.2	29	19	11.2	9.1
220	87.1	17	21	9.9	11.0
310	91.6	27	33	9.0	9.9
400	105.4	6	6	6.0	6.0
101	23.5	51	—[a]	3.0	—[a]
111	40.6	56		5.8	3.4
201	47.2	46	17	6.2	3.8
211	63.7	26	15	4.6	3.5
202	48.1	8	4[b]	2.6	1.9
212	64.5	26	4[b]	4.7	1.9
302	74.2	14	4[b]	5.6	3.0
222	88.0	14	4[b]	6.3	3.4
312	92.5	28	4[b]	6.4	2.5
402	106.3	13	4[b]	6.2	3.5
103	27.9	20	32	2.3	2.9
113	43.5	68	93	6.8	7.9
203	49.7	77	68	8.5	8.0
213	65.9	137	93	11.0	9.1
303	75.5	53	30	11.0	8.3
223	89.2	35	16	9.9	6.7
313	93.8	62	29	9.5	6.6
403	107.6	20	7	7.7	4.6
104	31.0	281	73	9.6	4.9
114	45.7	97	119	8.7	9.6
204	51.7	55	67	7.4	8.3
214	67.5	9	12	3.0	3.4

(*continued*)

point at which it intersects with one of the binary axes considered; in other words, one of the atoms of the chain must have the coordinate $Z = 0$.

Sauter[4] placed the origin of the lattice half-way between the projections onto the axis Z of two adjacent atoms, and was thus obliged to assign the structure to the space groups $P3_1(C_3^2)$ and $P3_2(C_3^2)$.

5. Observed and Calculated Intensities for the Two Possible Structures of 9/5 Hexagonal POM

In order to be able to decide for one of the two possible structures described above we carried out the calculations of all the structure factors of the two cases under consideration, using an isotrope thermal factor $B = 2.3$ (see Table I).

TABLE I (*continued*)

	2ϑ	I		F	
hkl	(CuKα)	calculated	observed	calculated	observed
105	34.6	2701	3366	33.5	37.5
115	48.3	1005	1166	30.0	32.0
205	54.1	546	589	25.0	25.9
215	69.6	142	147	11.9	12.0
305	79.0	12	7	5.5	4.2
108	48.4	60	116	7.3	10.1
118	59.6	135	162	13.8	15.0
208	64.7	130	150	14.9	16.0
218	79.0	148	121	13.7	12.4
308	88.2	45	43	11.3	11.1
228	101.9	19	13	7.7	6.4
318	106.5	28	10	6.4	3.9
109	53.0	80	88	9.3	9.7
1010	57.8	26	12	5.8	4.0
1110	68.0	72	74	11.7	11.8
2010	72.8	74	75	12.7	12.8
2110	86.6	100	75	12.0	10.4
3010	95.7	34	34	10.2	10.2
2210	109.7	17	17	7.0	7.0
3110	114.6	26	19	5.9	5.1
1013	75.5	89	121	14.3	16.7
1113	84.6	80	96	15.0	16.3
2013	89.2	60	55	13.1	12.6
2113	102.9	30	24	6.6	6.0
3013	112.4	4	6	3.3	3.4
1014	81.0	2	13	2.3	5.8
2115	115.6	18	10	4.9	3.7
1018	110.8	52	75	12.2	14.6
009	47.1	46	51	15.2	15.9
0018	106.2	19	40	18.4	26.6

[a] Not observed because of disturbance by (100) reflection.

[b] Not observed; value given taken as equal to $^2/_3$ the lowest observed intensity.

The structure factors of the reflections corresponding to all possible combinations of the indices $\pm(hki) \pm l$ were practically identical for all the reflections considered; further, contrary to expectations, the two series of factors calculated for the two different structures were also practically identical to each other. For this reason Table I gives only (hkl) with h, k, and l positive, and only one series of calculated values of F has been given, corresponding to both the structures which came into consideration.

Table I does not give the reflexes not observed whose calculated intensities were lower than the lowest observed intensity; on the other hand, an observed intensity equal to two-thirds of the minimum intensity detectable from the photograms has been assigned to the reflections which are not

visible on the photograms themselves and to which correspond calculated intensities stronger than the lowest observed intensity.

An overall comparison of all calculated and observed values of F gives a value $R = 0.18$ which is, of course, the same for both structures considered.

At this stage it might seem legitimate to conclude that the hexagonal POM helix is of the 9/5 type, and x-rays are not able to distinguish between the two structures deriving from the two possible arrangements of the macromolecules in a hexagonal lattice of $a = 4.46$ A. and $c = 17.3$ A.; furthermore, on the basis of the four possible space groups, the results confirm that the lattice of hexagonal POM is made up of isomorphous chains.

6. Evidence of a Hexagonal POM Structure Different from Those Proposed of the 9/5 Type with $c = 17.3$A.

During the course of our work on the structure of hexagonal POM a check on the cell constants was also made, since the figures given in the literature did not always seem completely satisfactory.

The measurement of the 2θ angles was made with the Philips wide-range spectrogoniometer for all peaks where superimposition of reflections of comparable intensity could be excluded; measurement was made on photograms of fiber only in a few cases.

Tubes were used with anticathodes of Cu, Fe and Cr; the d values were taken as the mean of the values obtained with the three different radiations with a slight preference for the FeKα radiation values.

In fact, CrKα gives a very weak spectrum, and in the CuKα spectrum it is more difficult to correct satisfactorily the angular errors which are due to the low absorption of the sample.

Calculating the constant a on the basis of the reflexes 100 e 110, the following values were obtained for CrKα, FeKα, and CuKα, respectively: 4.467 A., 4.470 A., and 4.476 A. We then used the mean value 4.47 A., as against the value of 4.46 A. given in the literature.

C was calculated for groups of reflexes belonging to the same layer, giving the values listed in Table II.

TABLE II

Layer	C, A.				Periodicity of layer along axis Z, A.
	CrKα	FeKα	CuKα	Mean	
3	17.10	16.68	16.91	16.80	5.600
4	17.22	17.22	17.23	17.23	4.308
8	17.25	17.27	17.22		
5	17.50	17.50	17.45		
10	—	17.48	17.50	17.49	3.498
15	—	17.50	17.45		
9	17.38	17.38	17.38	17.38	1.931
18	—	—	17.37		
13	—	17.33	17.33	17.33	1.333

(The layers giving the same values of C have been grouped together.)

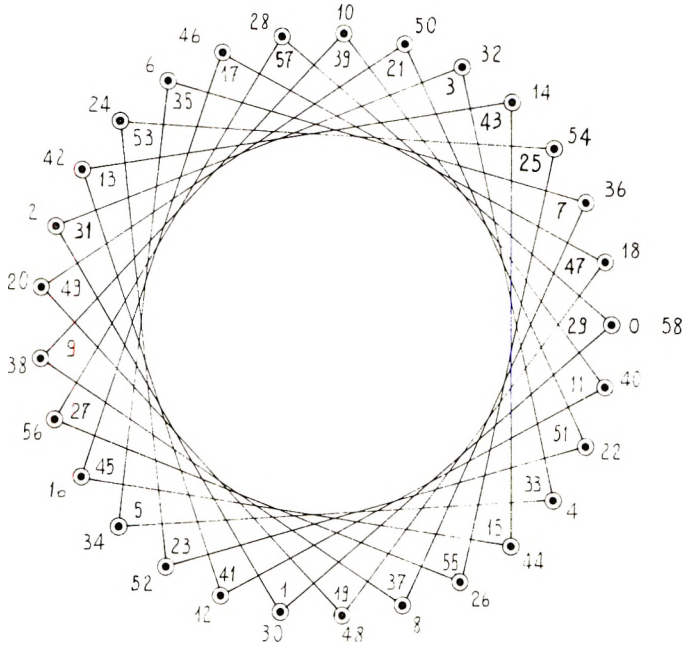

Fig. 6. Hexagonal POM. Projection of the 29/16 helix on the plane normal to the axis of the chain: (●) carbon atoms; (○) oxygen atoms. Internal numbers and external numbers are coordinates of the carbon and oxygen atoms, respectively, expressed as fifty-eights of C.

The calculation was not carried out for the first and fourteenth layer; in fact, the reflections of the first layer are weak and disturbed by those corresponding of the equator, while the only reflection observable for the fourteenth layer (1 0 14) is too weak for exact measurement.

The differences in the mean values of C cannot clearly be explained as experimental errors, and the only conclusion is that after nine monomeric units there is not in fact an exact repetition of the structure. This is contrary to what had been found by all the previous workers.

According to our experimental findings, the identity period of hexagonal POM, calculated as the lowest common multiple of the basic periodicities of the various layers along the axis Z, is 56.00 A., containing 29 monomeric units and 16 turns of the helical chain (Fig. 6). In fact:

$$5.600 \times 10 = 56.00 \text{ A.}$$
$$4.308 \times 13 = 56.00 \text{ A.}$$
$$3.498 \times 16 = 55.97 \text{ A.}$$
$$1.931 \times 29 = 56.00 \text{ A.}$$
$$1.333 \times 42 = 55.99 \text{ A.}$$

The values which have so far been recorded in the literature for the l indices in the observable layers on the spectra are therefore to be corrected as given in Table III.

TABLE III

Old l indices	New l indices
1	3
2	6
3	10
4	13
5	16
8	26
9	29
10	32
13	42
14	45
15	48
18	58

Other figures which must also be slightly modified are the theoretical density of the crystalline polymer, which is 1.492 g./cc. instead of 1.505 g./cc. according to the new lattice constants, and the internal rotation angle, which comes to 76° 21′ instead of 77° 23′.

We also computed all of the structure factors for the structure with a 29/16 helix, using the same isotropic thermal factor $B = 2.3$. Apart from the above-mentioned differences in the l indices, the results obtained were practically identical with those found for the 9/5 helix.

7. Discussion of the Structure

The most remarkable property of the structure of hexagonal POM with the 29/16 helix is undoubtedly the very high figure for the period of identity along the axis of the chain, which cannot be left in doubt by the surprising coincidence of the values of C calculated on the basis of the reflections of the various layers.

After discovering the inaccuracy of the 9/5 model with periodicity of 17.3 A., we considered that it would be difficult to find a higher periodicity whose accuracy could be demonstrated on the basis of the diffractometric findings. In fact, on this argument, it could be expected that hexagonal POM would show a chain of practically infinite periodicity.

On the other hand, at least as far as can be ascertained from the information obtainable from normal x-ray examination of a polymer, a periodicity higher than 100 A. is no longer distinguishable from an infinite periodicity. However, we feel that beyond a certain limit there is no point in speaking of the identity period of a helical chain but that it is more useful to express the degree of spiralization of the chain itself on the basis of the monomer/pitch ratio of the chain; expressing this ratio by means of two whole prime numbers in relation to each other is equivalent to a stretch of the imagination which could lead to the formulation of a model without real physical significance. The same argument is valid for the assignment of the space group, since this is also tied up with the formulation of the model.

In any case, one condition which is also applied to the structure with the 29/16 chain is the isomorphism of the chains belonging to a single lattice, as in the case of orthorhombic POM.

This problem will, however, be dealt with in a later paper.

I am greatly indebted to Prof. Silvio Bezzi, director of the Sezione di Padova del Centro Italiano di Strutturistica Chimica del C.N.R. and of the Istituto di Chimica Organica of the Padova University for his helpful advises and his authoritative survey to my work, and to Dr. Sabino Leghissa of the Società Montecatini IRAR for his continuous assistance and encouragement during the course of this work.

I thank the Centro Elettronico di Calcolo of the Societa Olivetti for its kind cooperation in the structure factors computation.

References

1. Staudinger, H., H. Johner, R. Singer, G. Mie, and J. Hengstenberg, *Z. Physik. Chem.*, **A126**, 425 (1927).
2. Hengstenberg, J., *Z. Physik. Chem.*, **A126**, 435 (1927).
3. Hengstenberg, J., *Ann. Physik.*, **84**, 245 (1927).
4. Sauter, E., *Z. Physik. Chem.*, **B18**, 417 (1932).
5. Sauter, E., *Z. Physik. Chem.*, **B21**, 186 (1933).
6. Novack, A., and E. Whalley, *Trans. Faraday Soc.*, **55**, 1484 (1959).
7. Phillpotts, Evans, and Sheppard, *Trans. Faraday Soc.*, **51**, 1051 (1955).
8. Uchida, T., Y. Kurita, and M. Kubo, *J. Polymer Sci.*, **19**, 365 (1956).
9. Huggins, M. L., *J. Chem. Phys.*, **13**, 37 (1945).
10. Tadokoro, H., T. Yasumoto, S. Murashashi, and I. Nitta, *J. Polymer Sci.*, **44**, 266 (1960).
11. Natta, G., *Makromol. Chem.*, **35**, 109 (1960).
12. Carazzolo, G. A., and M. Mammi, *J. Polymer Sci.*, **A1**, 965 (1963).

Résumé

On a examiné; au moyen des rayons-x, la structure hexagonale du POM. On discute les constantes réticulaires, les groupements spatiaux et le modèle de chaîne en spirale, déjà décrits dans la littérature. On propose de nouvelles constantes réticulaires et un nouveau modèle de chaîne en spirale possédant une plus longue périodicité. Comme dans le cas du POM orthorhombique, les cristaux sont formés par des macromolécules isomorphes.

Zusammenfassung

Eine neue Röntgenstrukturbestimmung des hexagonalen POM wurde durchgeführt. Eine Diskussion der Gitterkonstanten, der Raumgruppe und eines schon in der Literatur beschriebenen Kettenmodells wird gegeben und eine neue Elementarzelle und ein neues spiralförmiges Kettenmodell mit längerer Periodizität wird vorgeschlagen. Wie bei orthorhombischem POM wird das Gitter nur von links- oder rechtsschraubigen Makromolekülen gebildet.

Received March 13, 1962

JOURNAL OF POLYMER SCIENCE: PART A VOL. 1, PP. 1585–1600 (1963)

Apparatus for Measuring the Dynamic Tensile Modulus of Thin Polymeric Films

ORIN C. HANSEN, JR., THOMAS L. FABRY, LEON MARKER, and ORVILLE J. SWEETING, *Packaging Division, Film Operations, Olin Mathieson Chemical Corporation, New Haven, Connecticut*

Synopsis

A method and apparatus have been developed specifically for the determination of the dynamic tensile modulus of thin polymeric films. A weight is attached to a 2 × 60-mm. strip of film, the upper end of which is clamped to a phonograph recording head. The recording head is used to set the system into either longitudinal or transverse vibration. The cross-sectional area of the film is determined in place from the length, the density, and the transverse resonant frequency (the Vibroscope principle). The modulus is found from the dimensions of the specimen and the longitudinal resonant frequency. The apparatus has been used to study the moduli of a series of polymeric packaging films, the dependence of the modulus of polyethylene film on the angle between the long axis of the specimen and the machine direction, the gage dependence of the stiffness of polyolefin films, and the relationship between the modulus and the moisture and glycerol contents of cellophane.

INTRODUCTION

The wide use of polymeric films for packaging and other purposes has brought about an increased interest in the mechanical properties of thin polymeric films. Although many methods are available for the determination of the dynamic elastic modulus of polymeric materials,[1–5] the number of methods which are satisfactory for the determination of the modulus of these materials in the form of a film is relatively small. Because of the strong influence of the thermal and mechanical history on the mechanical properties of polymers, a proper evaluation of the modulus of polymeric films may be made only by carrying out a measurement on the film itself and not on the bulk material.

This paper describes an apparatus which was developed especially for the determination of the dynamic modulus in tension of cellulosic and other polymeric packaging films. The tensile modulus was chosen so that the apparatus may be used to study the effect of orientation on the elastic properties of the film. Such effects are very important in packaging film performance, and they cannot be studied in detail by the use of a torsion pendulum, for example, which can detect directional effects only if the width and thickness of the specimen are similar in magnitude (this cannot be true in film whose thickness is a few mils or even less than a mil). The

vibrating reed method, which can detect directional differences, has been used for packaging film measurements,[6] but this method is subject to serious difficulties if the film tends to curl. Another approach which has been used is the method of determining the speed of propagation of sound in the material.[4] This method requires rather long specimens, however, and it was hoped that a method could be developed which could be used with small pieces of experimental films and which would be easily adaptable to carrying out measurements under a variety of experimental conditions.

METHOD AND APPARATUS

Principle of the Method

In the method considered here the film specimen, which is in the form of a narrow strip, is treated as if it were a simple spring with a spring constant, K. If a mass is suspended from the lower end of such a spring, the resonant frequency of the system in longitudinal vibration, f_l, is given by eq. (1);

$$f_l = (1/2\pi)\ (K/m)^{1/2} \tag{1}$$

$$= (1/2\pi)\ (EA/lm)^{1/2}$$

m is the mass supported by the spring. The spring constant of such a strip of film is given by EA/l where E is Young's modulus of the material in the direction parallel to the long dimension of the specimen, A is the cross-sectional area of the specimen, and l is the length of the specimen. In the apparatus to be described, the strip of film is held at the top in a clamp which is mounted in the needle-holder of a phonograph recording head. This arrangement permits a longitudinal vibration of variable frequency to be impressed on the specimen. The frequency is varied until resonance occurs. The modulus may be calculated from the resonant frequency, the cross-sectional area, the length of the specimen, and the mass supported by the strip.

As is often found in determining the properties of films, one of the most important factors in this measurement is the determination of the cross-sectional area of the specimen. The method used here employs the principle of the Vibroscope[7] which is used in the textile industry for the determination of the linear density of fibers. This method was chosen since it is superior in accuracy to the use of mechanical or gravimetric methods on the small specimens used here, and also because it can be carried out on the specimen itself. The method consists of merely using the phonograph recording head to excite the transverse mode of vibration in the specimen by vibrating its upper end in the direction perpendicular to the plane of the film. Equation (2) relates the transverse resonant frequency of a string,

$$f_{tr} = (1/2l)\ (T/\mu)^{1/2} \tag{2}$$

$$= (1/2l)\ (mg/\rho A)^{1/2}$$

f_{tr}, to the length, l, the tension on the string, T, and the linear density, ρ. In our case the tension is equal to the gravitational force on the specimen, mg, and the linear density is equal to the usual volumetric density, ρ, times the cross-sectional area of the specimen, A.

If the eqs. (1) and (2) are combined we get:

$$E = (4\pi^2/g)\rho l^3(f_l f_{tr})^2 \tag{3}$$

By use of eq. (3), the modulus may be calculated directly from the density, the length of the specimen, and the two resonant frequencies without calculating the cross-sectional area explicitly.

Design and Construction of the Apparatus

The apparatus which was constructed to carry out the measurement has been described cursorily, but not in detail.[8,9] Figure 1 is a scale drawing of the arrangement of parts described below.

Phonograph Recording Head (A). The recording head is an Astatic Model No. M-41-500. This unit has an internal resistance of 500 ohms and is driven by a Hewlett-Packard Audio Oscillator Model 210C. This oscillator has sufficient output to drive the recording head without additional amplification.

Upper Clamp (B). The upper clamp is a steel rod, 1/8 in. in diameter, which has been turned down at one end so that it will fit the needle holder of the recording head. The larger end of the rod contains a slot 0.015 in. wide, which terminates in a No. 52 drill hole through the center of the rod in the plane of the slot. An 0-80 screw through the opposite faces of the slot serve to tighten and loosen the clamp. This arrangement has proved to be quite satisfactory for polyolefin films. For stiffer films, such as cellophane, however, it has been found necessary to slip a small piece of No. 50 cotton thread across the specimen, parallel to the edge of the clamp, in order to obtain a uniform gripping across the entire width of the specimen.

Lower Clamp Assembly. The lower clamp (C) is suspended from the specimen (D) and it in turn supports the weight (E). The lower clamp itself consists of two small aluminum blocks held together by two 0-80 screws. Two eyelets, approximately 3/32 in. in diameter, are mounted, one on either side of the clamp, to receive the hooks which support the weight. These eyelets were located as close as possible to the upper edge of the clamp and hence to the line along which the specimen is held. The weight was pivoted in this way to minimize the nonuniform tension across the width of the specimen which would result from the center of the clamp not coinciding precisely with the center of the specimen. Some degree of misalignment of this type is unavoidable with the 2-mm.-wide specimens employed here.

The weight consists of a 2-in. 1/4-20 bolt provided with a stack of 20 washers, 3/4 in. in diameter. These are held between two nuts, of which the upper one also serves to hold the suspension hooks in place. By removing some or all of the washers, the weight, including the aluminum clamp,

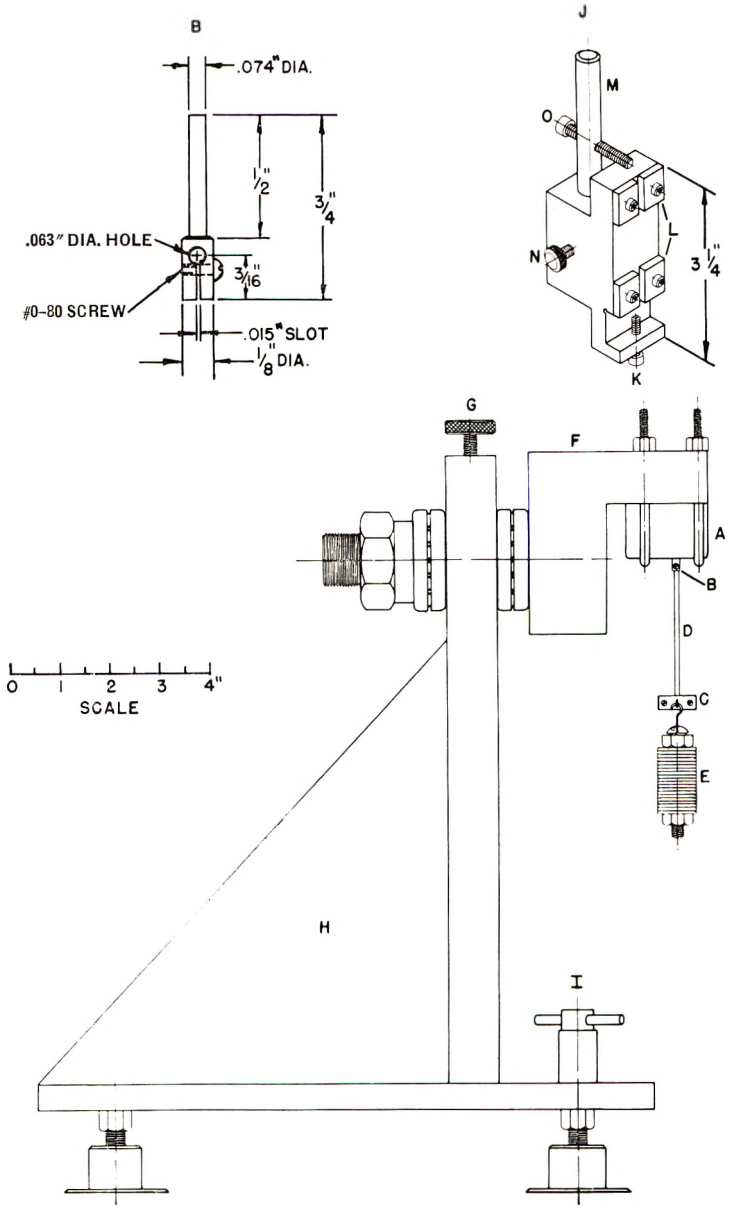

Fig. 1. Dynamic tensile modulus apparatus: (A) phonograph recording head; (B) upper clamp; (C) lower clamp; (D) specimen, 2 × 60 mm.; (E) weight; (F) rotatable steel block; (G) set screw for rotatable block; (H) frame, boiler plate; (I) adjustable machinery mounts; (J) jig; (K) screw for holding lower clamp in jig; (L) guide blocks; (M) keyed guide rod; (N) set screw for jig; (O) support screw for upper clamp.

can be varied from 19 to 90 g. For soft films, such as low density polyethylenes, another weight weighing only 9.7 g. together with the aluminum clamp has been used.

Mounting for the Recording Head. The recording head is mounted on an L-shaped steel block (F), by means of two U-bolts. The block is attached to the frame of the apparatus by means of a 1-in. shaft which is held in place by two thrust bearings and a lock nut. This permits the L-shaped block to rotate about the axis of the shaft, so that it may be positioned with the upper clamp pointed downward, as shown, for the determination of the transverse resonant frequency, or horizontally for the determination of the longitudinal resonant frequency. The block is held in the desired position by means of the set screw (G).

Frame (H). The frame of the apparatus is constructed from boiler plate and weighs approximately 55 lb. so that the apparatus as a whole is not influenced by external vibration. The front plate, to which the rotating block is attached, is $^{15}/_{16}$ in. thick, 12 in. high, and 6 in. wide. The base and the two triangular webs which help support the front plate are made of 0.5-in. plate. The frame is welded together. The base is supported by three adjustable machinery mountings (I) (Vibra-Levlers, obtained from McMaster Carr Supply Co., Chicago) which provide vibration insulation and also permit the apparatus to be levelled. The front shock mount has been modified to permit the adjustment to be carried out more easily. This was done by adding a threaded cylinder which screws onto the mount and which passes through a hole in the base. A flange on the cylinder supports the base of the apparatus and a handle on the upper end of the cylinder permits the operator to change the level of the instrument while the specimen is in place if necessary.

Jig (J). The jig is used to mount the specimen in the apparatus so that it will be properly aligned. The jig consists of a steel block to which one of the two aluminum blocks comprising the lower clamp may be attached by means of a screw (K). The surface on which the aluminum block rests is lower than that of the rest of the jig so that the upper surface of the aluminum block and the surface of the main portion of the jig are flush. This permits the 2- × 60-mm. film specimen to be laid across the surface of the jig between the two pairs of guide blocks (L) and across the aluminum block. The other aluminum block is then placed on top of the first, with the film between them, and the two are screwed together. When the film specimen is placed in the jig a few millimeters are allowed to extend over the opposite end of the jig to permit mounting in the upper clamp.

The jig is then slid onto a keyed guide rod (M) which is permanently mounted on the L-shaped block (F) (this rod was omitted from the diagram of the block so that it would not obscure the specimen). The rod is positioned so that when the jig is slid along it toward the recording head, the protruding end of the specimen slides into the upper clamp. During this operation the L-shaped block is turned so that the guide rod and the jig are horizontal. When the jig is in the proper position for fastening the

specimen in the upper clamp, it is secured by a set screw (N). A screw (O) through the guide rod is then turned up until it touches the upper clamp. This provides support for the upper clamp while the specimen is being fastened in place and prevents the clamp and the recording head from being damaged by the pressure exerted by the screwdriver. After the film specimen has been fastened in the upper clamp, the screw (K) which holds the lower clamp is released, and the L-shaped block is rotated so that the guide rod and the jig are vertical. A slight additional rotation permits the lower clamp and the specimen to swing free of the jig which is then removed from the guide rod after the set screw (N) has been released. The screw (O) which supports the upper clamp is backed away from the clamp and the weight is hung from the lower clamp. The apparatus and the specimen are now ready for the beginning of the measurement.

Operation of the Apparatus

Preparation of the Specimen. The specimen is cut, with the use of a template 2 mm. in width, $^1/_4$ in. thick, and $4^1/_2$ in. long. The template is fastened by screws between two flat steel bars. The bars are of the same length and thickness as the template and are relieved for a distance of 85 mm. in the center to permit a razor blade to pass between each bar and the template. This permits the operator to hold the template more easily and protects the fingers from the razor blade. It is most important that the film be placed on a flat surface and that sufficient pressure be applied to the template to prevent its moving during the cutting of the specimen. The ends of the specimen are cut after the template is removed and the specimen is placed on the jig as described above using tweezers to prevent damage to the film and to prevent moisture and oil from being absorbed from the fingers. If the film shows a tendency to curl, it is advisable to lay a 2-mm.-wide metal bar on top of it as it lies on the jig. The specimen is then mounted in the apparatus as described in the preceding section.

Adjustment of the Apparatus. Before the measurement of the resonant frequencies is begun, the behavior of the specimen in transverse vibration must be examined as a function of frequency. It frequently happens, particularly in the case of stiff films, that there are two resonant frequencies in the transverse mode rather than one. One of these frequencies is associated with a vibration having a larger amplitude on the front edge of the film than on the back. The other is associated primarily with the back edge of the film. Observation of these vibrations under stroboscopic illumination shows that in each case the film appears to be twisting about a vertical axis near the front edge of the film in one case and near the back edge in the other. The vibrations of the opposite edges of the film in each case are seen to be 180° out of phase. The effect is best checked by focussing the microscope used to observe the vibrations first on one edge and then on the other to be sure that the same resonant frequency is observed on both edges. The effect is caused by an uneven tension across the width of the specimen. The edge exhibiting the higher resonant frequency is the edge

with the higher tension. If the effect is observed, therefore, it may be eliminated by releveling the apparatus in the proper direction to lower the side of the upper clamp holding the edge showing the higher resonant frequency.* This reduces the tension on that edge and hence tends to bring the two resonant frequencies closer together. This process is continued until the same resonant frequency is observed on both edges of the specimen.

Measurement of the Resonant Frequencies. When it has been ascertained that the front and back edges both exhibit the same resonant frequency, this value is recorded. The L-shaped block is then rotated so that the upper clamp is horizontal, and the resonant frequency of the specimen in longitudinal vibration is determined. Here the microscope is focussed on some part of the weight supported by the lower clamp and the frequency corresponding to the maximum amplitude is observed as the frequency is varied. This frequency is somewhat more difficult to determine than the transverse frequency; so ten individual determinations are made and their results averaged.

In both cases it is necessary to be sure that the resonant frequency corresponds to the first mode of vibration, especially in the case of new film types. In the case of the transverse frequency, overtones will be observed at twice and at three times the natural frequency. These can be identified as the second and third overtones by moving the microscope along the edge of the film and observing the number of nodes. In the case of the longitudinal vibration, overtones do not exist. Undertones may be observed in both types of vibration, however, which are generally of very small amplitude. It is imperative that in both cases the resonance of largest amplitude be selected which, in the case of the transverse vibration, will have no nodes.

Determination of Length and Density. The length of the specimen between the upper and lower clamps may be determined in a number of ways. The two methods used with the apparatus described here are a direct measurement with a cathetometer, and a method in which the lower clamp and its weight are allowed to swing freely from side to side and the period of oscillation is measured. This is done by determining with a stopwatch the time required for 100 vibrations. The length obtained from the usual equation for the period of a simple pendulum corresponds to the distance between the upper clamp and the center of gravity of the lower clamp assembly. A correction term corresponding to the distance from the center of gravity to the edge of the lower clamp must be subtracted from the length of the pendulum. The length desired is then given by

$$L = 24.831 T_p^2 - L_0$$

where L is the length, T_p is the period of the pendulum in seconds, and L_0

* In more recent work it has been found that the leveling in this step can be carried out more conveniently by altering the angle of just the recording head by using an arrangement of adjusting screws subsequently added to the mounting block (F).

is the correction term. The correction term may be found by using this method on a number of films which have been measured using the cathetometer. A different value of L_0 applies for each different number of washers used as the weight, however. The pendulum method requires only 1 min. per determination and does not involve the difficulty of choosing the exact points at which the clamps hold the specimen as does the cathetometer method. Its principal disadvantage is that it is necessary to calibrate it against the cathetometer method.

The density of the film may be determined by flotation methods or density gradient tubes[10] if necessary. It is often possible, however, in the case of many materials, to obtain sufficiently reliable values from the literature.

EXPERIMENTAL VERIFICATION OF METHOD

Experiments were carried out to determine the self-consistency of the formulas used in this method for determining the modulus. These measurements were made on polyethylene or polypropylene films for various values for the mass of the lower clamp, the length of the specimen, and other parameters. It was found that the resonant frequencies depend somewhat on the amplitude of the vibrations. Consequently measurements are usually carried out with the same voltage applied to the recording head.

An examination of eq. (2) relating the transverse resonant frequency with the mass of the clamp, the density, the length, and the cross-sectional area of the specimen shows that if the square of the product of the transverse resonant frequency and the length is plotted as a function of the mass suspended from the lower clamp, a straight line should be obtained. Figure

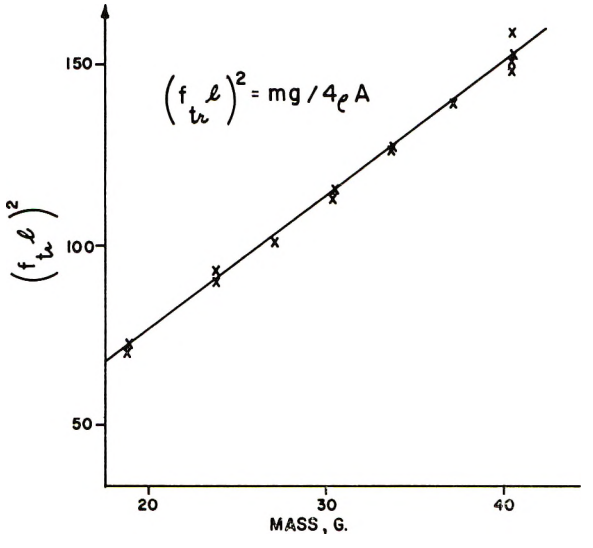

Fig. 2. Square of the product of the transverse resonant frequency and the length of the specimen as a function of the mass of the lower clamp assembly. Pro-fax polypropylene film.

2 shows the line which resulted when such a plot was carried out for a series of determinations made with different weights. The linearity of the resulting plot indicates that the formula holds within experimental error, and that there is no appreciable error in the determination of the transverse frequency or the length. The slope of this curve should be equal to $g/4\rho A$ according to eq. (2). A value for the cross-sectional area A of the film was calculated from its width and a thickness obtained by dividing the unit weight of the film by its density. The slope of the line calculated from this value of A is 3.84×10^5. The actual slope of the line is 3.73×10^5 which is good agreement, considering the method by which the thickness was determined. The line intersects the horizontal axis at a value of -0.6 g., also in good agreement with the predicted value of 0.0 g., if one considers the length of the extrapolation. In later work on the mechanical properties of polyolefin films it was found that the thickness of the specimens as determined by this method agreed within 1.5% with those obtained with a mechanical gage. This comparison included over forty determinations.

A linear plot was also obtained when the square of the period of the pendulum vibration was plotted as a function of the length of the specimen measured with a cathetometer. The result indicates an error in the determination of the length by this method of less than 1%.

It was discovered that with polyolefin films the reproducibility of the measurement depended to some extent on the order in which the various operations were carried out. Six specimens taken from the same sheet of polypropylene (extruded from Avisun resin) were measured using an exactly timed schedule in which each operation was carried out at the same time during the measurement. The standard deviation of the six results was 0.65% compared to 2.5% when no timed procedure was used and the operations were not always carried out in the same order.

A series of measurements carried out with different specimen lengths and lower clamp weights is summarized in Table I. The conclusions to be

TABLE I
Modulus of DGDA (Du Pont) High Density Polyethylene Measured Using Various Weights and Specimen Lengths

Length of specimen, cm.	Modulus with various weights, 10^9 dynes/cm.^{2}					Standard deviation, %
	18.8 g.	23.9 g.	30.5 g.	40.6 g.	$\bar{E}$	
6	12.05	12.10	11.84	11.98	11.99	0.94
7	11.51	11.84	11.83	11.78	11.74	1.3
7.2	11.93		11.84	11.94	11.90	0.46
7.5	12.00	11.86	11.97	11.95	11.95	0.5
Average modulus, $\bar{E}$	11.87	11.93	11.87	11.91	11.90	0.3
Standard deviation, %	2.1	1.2	0.56	0.44	0.92	

drawn from this set of experiments are that neither the mass of the clamp nor the length of the specimen influences the result of the measurement. It may also be concluded that the result is not influenced by the value of the longitudinal resonant frequency used in the 30–45 cycle/sec. region.

In an experiment made on a specimen of polypropylene film, it was found that the length of the specimen may increase slightly when it is vibrated longitudinally. Before the recording head was turned on, the specimen was observed to extend somewhat less than 0.7% from its length prior to the application of the weight. After this initial creep had leveled off, the specimen was vibrated transversely for 2 min. This caused no detectable increase in length. Vibrating the specimen longitudinally, however, caused an additional increase in length of about 0.13%. This amount of additional creep should not affect the measurement significantly and is probably due to the higher average stress on the film during the period of vibration.

APPLICATIONS OF THE DYNAMIC TENSILE MODULUS APPARATUS

The balance of this paper will be devoted to several examples of investigations which have been carried out with the use of this apparatus.

First Results

The first results obtained with the tensile modulus apparatus are shown in Table II. Each of the values shown in the table was obtained on a separate specimen of film. The precision of this apparatus is considerably better than that of a vibrating reed apparatus used previously. In the vibrating reed measurement referred to here, a strip of film about 1 cm.

TABLE II
Dynamic Modulus for Three Films Determined by the Dynamic Tensile Modulus Apparatus

Film	Frequency, cycles/sec.	Temperature, °C.	Modulus, 10^9 dynes/cm.^{2}	Modulus by vibrating reed apparatus at 32° C., 10^9 dynes/cm.^{2}
Low density polyethylene	27.3	24.2	2.71	2.2
	28.2	24.0	2.77	
Olin, 1.8 mil, machine direction	27.4	24.0	2.66	
Spencer Hi-D polyethylene, machine direction	28.3	24.0	7.33	7.4
	29.2	24.0	7.39	
	29.2	24.0	7.81	
Hercules Pro-fax polypropylene, machine direction	36.7	24.1	10.7	11
	37.7	24.1	11.3	
	36.0	24.2	11.1	

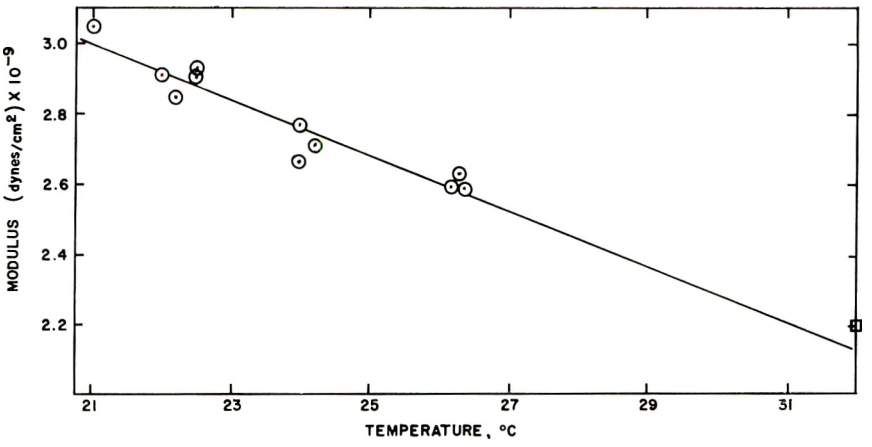

Fig. 3. Modulus as a function of temperature for low density polyethylene film: (⊙) dynamic tensile modulus apparatus; (⊡) vibrating reed value.

long was clamped at one end in a driving mechanism similar in principle to the recording head used in the present apparatus. The resonant frequency was found by varying the driving frequency to obtain the maximum amplitude of the free end of the reed. The motion of the reed was observed by means of an optical projection system which employed stroboscopic illumination to give a sharp image of the edge of the reed and to permit a precise determination of the point of maximum excursion. The modulus was calculated from the resonant frequency, the length, the thickness, and the density of the specimen. The thickness was determined from the length, the width, the weight, and the density of the film.

The results reported in this table were obtained in a room controlled at 75°F. and 15% R.H. A number of determinations were made previously in a room in which the temperature fluctuated somewhat. The results of eleven determinations on a low density polyethylene at temperatures ranging from 21 to 26°C., including those from Table II, are shown in Figure 3. These points are quite well represented by a straight line the slope of which indicates that the modulus of this film decreases at a rate of 2.9%/°C. at 25°C. The magnitude of the variation of the modulus of this film with the temperature serves to emphasize the importance of carrying out such measurements under carefully controlled conditions. According to this graph, the value of the modulus of this film at 32°C. should be 2.14×10^9 dynes/cm.^{2}, which agrees quite well with the value found at this temperature with the use of the vibrating reed apparatus. When the results shown in the graph were least-squared, it was found that the average deviation of the points from the line was 1.5%.

Measurement of the Modulus of Specimens Cut at Various Angles to the Machine Direction

Measurements of the dynamic modulus as a function of the direction in which the specimen is cut were carried out on two different polyethylene

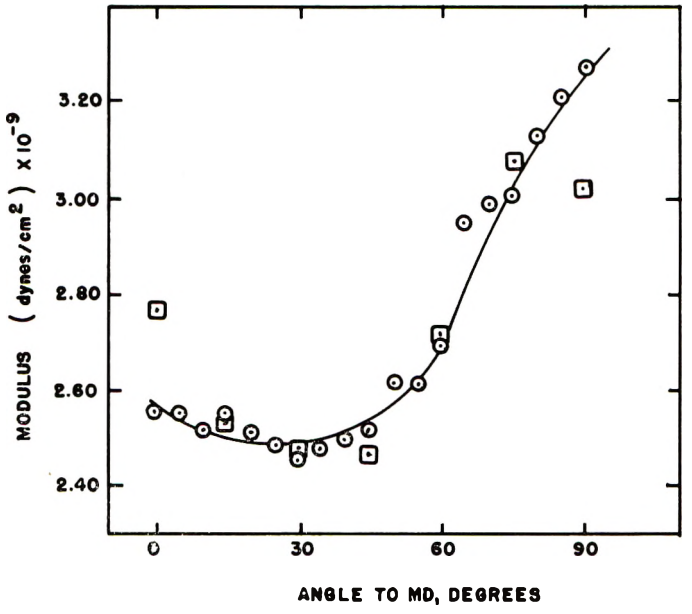

Fig. 4. Modulus as a function of angle to machine direction for low density polyethylene film: (⊡) first set; (⊙) second set.

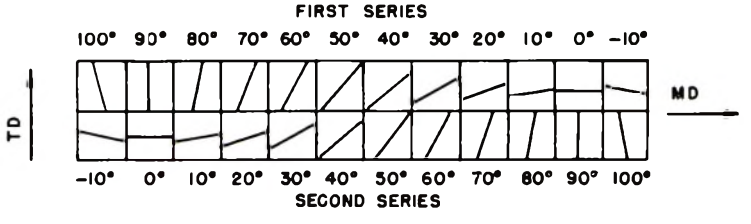

Fig. 5. Pattern used for cutting specimens for measurement of modulus as a function of angle from the machine direction.

films to determine whether or not this method was sufficiently sensitive for use in studying the effect of orientation on the mechanical properties of thin films.

The first series of specimens was cut from a 4 × 6-in. rectangle of low density polyethylene film. The specimens were cut at 15-degree intervals from 0° (the so-called machine direction, MD) to 90° (the so-called transverse direction, TD). The moduli of these films were then measured with the dynamic tensile modulus apparatus in a room controlled at 75°F. and 15% R.H. The results of these measurements are represented by the squares on the graph in Figure 4. The values show that the modulus does not simply increase as the angle increases from 0° to 90° but rather passes through a minimum at about 30° and then increases rather rapidly to the 90° or TD value. The experiment was repeated, specimens being cut at 5° intervals from the same large sheet of film from which the 4 × 6-in.

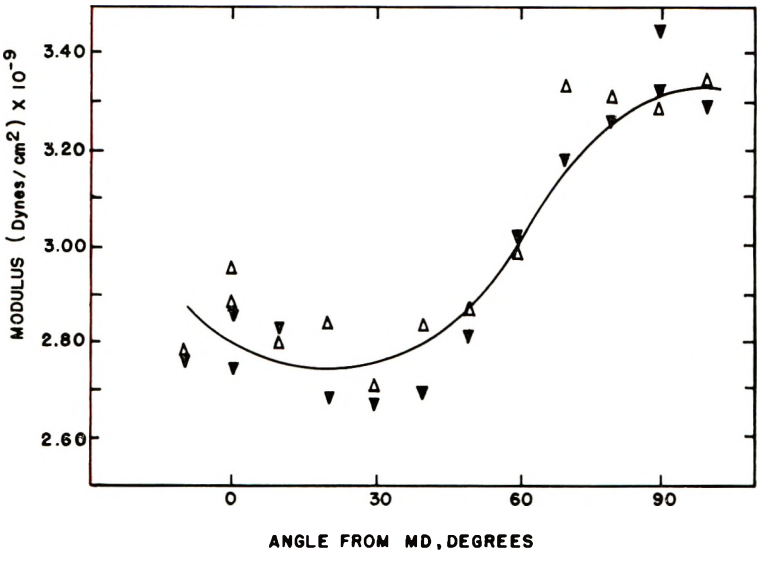

Fig. 6. Modulus as a function of angle from machine direction for Dow polyethylene resin film: (△) first series; (▼) second series.

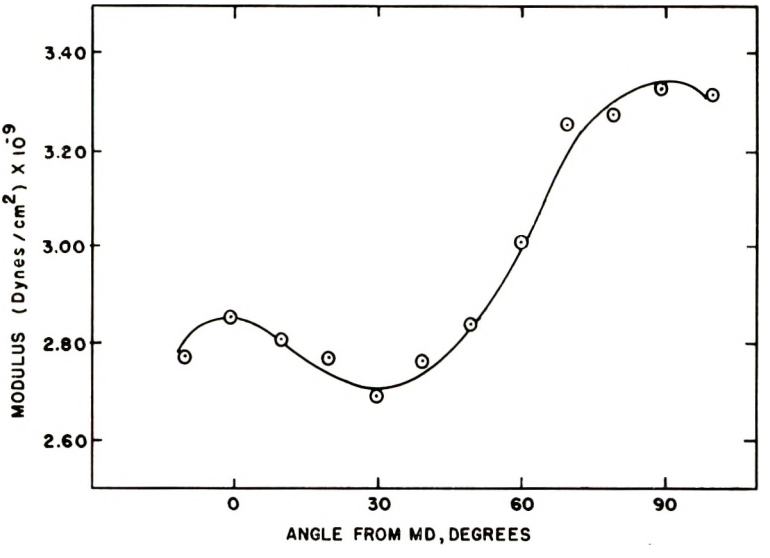

Fig. 7. Modulus as a function of angle from machine direction for Dow polyethylene resin film. Average of two series.

square had been cut. These specimens were all cut within a few inches of a line drawn in the machine direction on the film. The values obtained with these specimens are represented by the circles on the graph of Figure 4. The new results confirm the presence of the minimum at 30° and agree with the previous results everywhere except at 0° and 90°. The same measurement was carried out on two series of specimens cut from a poly-

TABLE III
Dynamic Modulus of Packaging Films

Film	By vibrating reed (32°C.) modulus, 10^{-9} dynes/cm.^{2}	By dynamic tensile modulus apparatus (24°C., 15% R.H.)	
		Modulus, 10^9 dynes/cm.^{2}	Standard deviation, %
Low density polyethylene, M.D.	2.0	2.10	4
Low density polyethylene, M.D.	2.2	2.71	2
DFD-0103 polyethylene,[a] M.D.	3.2	2.96	2
Hi-D polyethylene,[b] M.D.	7.4	7.52	4
DGDA polyethylene,[c] M.D.	9.4	11.0	2
Pro-fax polypropylene,[d] M.D.	11	11.1	3
Cry-O-Vac[e]		11.2	3
Pliofilm[f]	14	16.4	2
Saran[g]		18.9	2
Polystyrene[h]		29	0.5
Mylar[c]		41	3

[a] Union Carbide Corp.
[b] Spencer Chem. Co.
[c] E. I. du Pont de Nemours & Co.
[d] Hercules Powder Co.
[e] W. R. Grace & Co.
[f] Goodyear Tire & Rubber Co., Inc.
[g] Dow Chemical Co.
[h] Plax Corp.

ethylene film made from Dow resin. The two series were cut with the use of the system depicted in Figure 5. The upper series was so cut that the angle varied from 0° to 90° in the direction along the film, and the lower series was so cut that the variation from 0° to 90° was in the opposite direction. This was done in order to cancel out any variation in modulus along the machine direction. Any serious variation in modulus along the transverse direction would be indicated by a general difference in level of the curves obtained from the two series. Specimens were also cut at −10° and at 100° to be sure that a complete curve would be obtained even if the direction of the orientation in the film did not coincide with the machine direction. The results obtained from the two series of specimens are shown in Figure 6. The averages of the two values obtained at each angle (four at 0° and 90°) are plotted against the angle in Figure 7. These curves show that the minimum at 30° is characteristic of polyethylene film and not peculiar to the particular film chosen for the first series of measurements. Whether the rather large differences observed between the upper and lower

series at some angles is caused by some randomly occurring experimental difficulty or whether it indicates a true variation of the modulus has not yet been determined. The measurements indicate that this method is sufficiently sensitive for use in this type of study.

Dynamic Modulus of a Series of Packaging Films

Table III shows the values of the dynamic modulus obtained for a variety of thin films by means of both the vibrating reed apparatus and the dynamic tensile modulus apparatus. The agreement between the values of the modulus obtained by the two methods is quite good. Complete agreement is not to be expected, however, because the two sets of measurements were not made at the same temperature.

Another series of measurements was carried out on a group of samples of both polyethylene and polypropylene films ranging in gage from 0.5 mils to 4 mils.[9]

The applicability of the apparatus to the study of cellophane has also been demonstrated.[8]

Note Added in Proof: Recent work has shown that the modulus of stiff films should be corrected using the equation $E = E_{\text{measured}}\,(1 - f^2m/k)^{-1}$ where k is an instrumental constant which corrects for the compliance the recording head. For our instrument, $k = 9.42 \times 10^6$ dynes/cm. The method for determining k will be discussed in a note at a future date.

The authors are indebted to R. J. Russell of this department for the design of the apparatus.

References

1. Ferry, J. D., in *Rheology*, Vol. 2, F. R. Eirich, Ed., Academic Press, New York, 1958, Chap. 11.
2. Staverman, A. J., and F. Schwarzl, in *Die Physik der Hochpolymeren*, Vol. 4, H. A. Stuart, Ed., Springer-Verlag, Berlin, 1956, Chap. 1.
3. Koppelmann, J., *Kolloid-Z.*, **144**, 12 (1955).
4. Nolle, A. W., *J. Appl. Phys.*, **19**, 753 (1948).
5. Richardson, E. G., *Relaxation Spectrometry*, Interscience, New York, 1957.
6. Horio, M., S. Onogi, C. Nakayama, and K. Yamamoto, *J. Appl. Phys.*, **22**, 966 (1951).
7. Gonsalves, V. E., *Textile Res. J.*, **17**, 369 (1947).
8. Hansen, O. C., Jr., L. Marker, and O. J. Sweeting, *J. Appl. Polymer Sci.*, **5**, 655 (1961).
9. Hansen, O. C., Jr., L. Marker, K. W. Ninnemann, and O. J. Sweeting, *J. Appl. Polymer Sci.*, **7**, 817 (1963).
10. Boyer, R. F., R. S. Spencer, and R. M. Wiley, *J. Polymer Sci.*, **1**, 249 (1946).

Résumé

On a développé une méthode et un appareillage pour la détermination du module de tension dynamique de films minces de polymère. Un poids est appliqué à un ruban de film de 2 × 60 mm., dont l'extrémité supérieure est attachée à une cellule d'enrégistrement phonographique. La cellule d'enrégistrement est employée pour mettre le système dans une vibration longitudinale et transversale. La coupe transversale du film est déterminée par la longueur, la densité et la fréquence de résonance transversale (le principe du Vibroscope). On trouve le module au moyen des dimensions du spécimen

et de la fréquence de résonance longitudinale. L'appareil a été employé pour étudier les modules d'une série de films polymériques d'emballage, la dépendance du module du film de polyéthylène de l'angle entre le grand axe du spécimen et la direction de la machine, la dépendance de la taille suivant la rigidité des films de polyoléfines, et la relation entre le module et l'humidité et le taux en glycérine de la cellophane.

Zusammenfassung

Eine Methode und Apparat wurden speziell für die Bestimmung des dynamischen Zugmoduls dünner Polymerfolien entwickelt. Ein Gewicht wird an einem 2 × 60 mm.-Folienstreifen befestigt, dessen oberes Ende an einem Grammophonrecorder sitzt. Der Recorder wird benützt, um das System entweder in longitudinale oder transversale Schwingung zu versetzen. Die Querschnittsfläche der Folie wird in situ aus Länge, Dichte und transversaler Resonanzfrequenz (Vibroscop-Prinzip) bestimmt. Der Modul ergibt sich aus den Probendimensionen und der longitudinalen Resonanzfrequenz. Der Apparat wurde zur Untersuchung der Moduln einer Reihe von Verpackungsfolien, der Abhängigkeit des Moduls einer Polyäthylenfolie vom Winkel zwischen der langen Achse der Probe und der Maschinenrichtung, der Abhängigkeit der Steifigkeit von Polyolefinfilmen von den Messbedingungen und der Beziehung zwischen Modul und Feuchtigkeits- und Glyceringehalt von Cellophan verwendet.

Received March 13, 1962

JOURNAL OF POLYMER SCIENCE: PART A VOL. 1, PP. 1601–1608 (1963)

Steric Structures in Copolymerization

M. BERGER, *Central Basic Research Laboratory, Esso Research and Engineering Company, Linden, New Jersey*

Synopsis

Using normal copolymerization equations we have developed graphical techniques for predicting the amount of crystallinity in ethylene–propylene copolymers.

Introduction

In the last two or three years a great deal of attention has been given to the steric arrangements of the two components in various copolymer systems. Through these studies it has become increasingly evident that the distribution of the two types of monomer units in the polymer chain is almost as important as the overall ratio of one component to the other in the copolymer. This is especially true if one or both components are capable of crystallization. If the copolymer is an elastomer then, of course, nonoriented crystallization is to be avoided. In order to obtain perfectly amorphous polymers, it appears that two questions must be answered: (*1*) What is the minimum number of monomer units in a row which can cause crystallinity (at a given temperature)? (*2*) How does one go about obtaining polymers with "blocks" less than this minimum? There has been very little experimental work done from which one can deduce an answer to the first question. Unfortunately, we can only offer very speculative ideas on this question. However, we will develop an approach to answering the second question which we hope will provide an incentive for finding the minimum block size required for crystallinity in various copolymers. In the main, we will be concerned with an elastomer which is a copolymer of ethylene and propylene usually called EP rubber. Both monomers are capable of producing highly crystalline polymers. The problem is to incorporate them in a copolymer with a minimum of crystallinity.

Copolymerization Equations

In a copolymerization with two monomers M_1 and M_2, the mole fraction, F_1 of M_1 in the growing chain can be shown to be[1]

$$F_1 = \frac{(M_1/M_2)r_1 + 1}{(M_1/M_2)r_1 + 2 + (M_2/M_1)r_2} \tag{1}$$

where M_1 is the mole fraction of M_1 in feed, M_2 is the mole fraction of M_2 in feed, r_1 is the reactivity ratio for M_1, and r_2 is the reactivity ratio for M_2.

Sakaguchi[2] has derived the following relationships for ascertaining the sequential distribution of syndiotactic and isotactic units in a polymer,

$$F(n) = \frac{{f_{iso}}^n}{(1 + r_1)^2}\left(\frac{r_1}{1 + r_1}\right)^{n-1} \tag{2}$$

$$G(m) = f_{iso}\left(1 + \frac{m - 1}{1 + r_1}\right)\left(\frac{r_1}{1 + r_1}\right)^{m-1} \tag{3}$$

where $F(n)$ is the fraction of polymer chains existing in blocks of isotactic units n long, f_{iso} is the total fraction of isotactic structure in the polymer. $G(m)$ is the fraction of polymer chains existing in blocks of isotactic units m and longer, and r_1 is a pseudoreactivity ratio for the isotactic unit. A similar expression exists for syndiotactic units. By appropriate manipulation we have altered eqs. (2) and (3) so as to apply for copolymers in general and thus be compatible with eq. (1). In their altered form they are:

$$F(n) = \frac{F_1 n}{[1 + (M_1/M_2)r_1]^2}\left[\frac{(M_1/M_2)r_1}{1 + (M_1/M_2)r_1}\right]^{n-1} \tag{4}$$

$$G(m) = F_1\left[1 + \frac{m - 1}{1 + (M_1/M_2)r_1}\right]\left[\frac{(M_1/M_2)r_1}{1 + (M_1/M_2)r_1}\right]^{m-1} \tag{5}$$

where M_1, M_2, and F_1 have the same meaning as in eq. (1). $F(n)$ now means the fraction of polymer existing in blocks of M_1 units n long. $G(m)$ is the fraction of polymer existing in M_1 units of m and longer. There are corresponding equations for M_2.

C_2–C_3 Copolymer

The data used for the calculations on ethylene-propylene copolymers were obtained from three unpublished reports. We shall consider the three cases a, b, and c shown in Table I, where

TABLE I

Case	M_p/M_e	F_p	r_e	r_p
a	2.57	0.238	7.0	0.07
b	10.7	0.508		
c	32.3	0.73		

M_p is the mole fraction of propylene in feed, M_e is the mole fraction of ethylene in feed, and F_p is the fraction of propylene in the polymer.

The pertinent equations for ethylene then become

Case a:

$$F_e(n) = \frac{0.762n}{[1 + (7/2.57)]^2}\left[\frac{(7/2.57)}{1 + (7/2.57)}\right]^{n-1}$$

Case b:

$$F_e(n) = \frac{0.492n}{[1 + (7/10.7)]^2}\left[\frac{(7/10.7)}{1 + (7/10.7)}\right]^{n-1}$$

Case c:

$$F_e(n) = \frac{0.27n}{[1 + (7/32.3)]^2}\left[\frac{(7/32.3)}{1 + (7/32.3)}\right]^{n-1}$$

where $F_e(n)$, again, is the fraction of polymer existing in blocks of ethylene of n or longer. There are corresponding equations for propylene.

Figures 1, 2, and 3 show the distribution of block sizes of ethylene and propylene for cases a, b, and c, respectively. These plots show per cent of ethylene and propylene existing in a block n units long.

If we assume that the kinetics described are the only ones operative, then the distributions shown in Figures 1–3 represent all the species of polymer

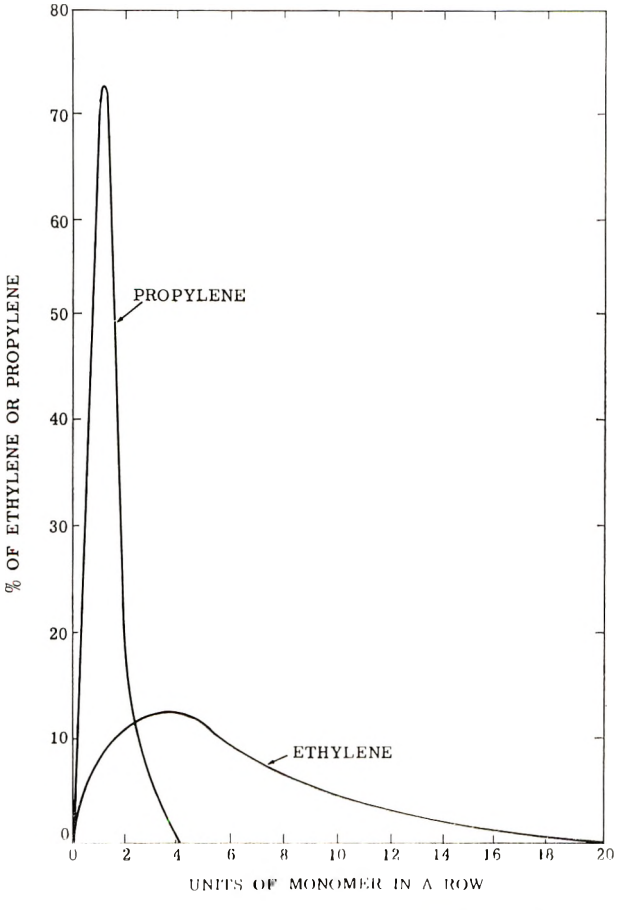

Fig. 1. Ethylene–propylene copolymer. Feed $C_3/C_2 = 2.57$; C_3 in polymer = 23.8 mole-%.

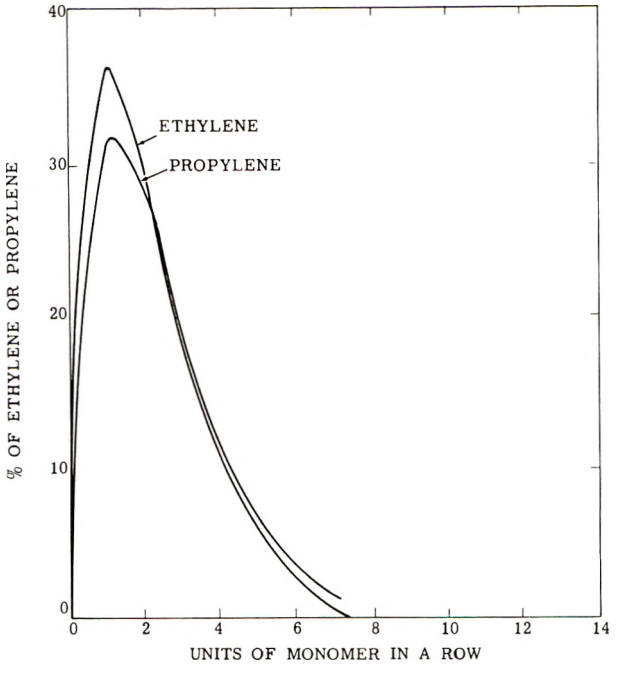

Fig. 2. Ethylene–propylene copolymer. Feed C_3/C_2 = 10.7; C_2 in polymer = 50.8 mole-%.

chains. This being the case, we can proceed to find the minimum block size necessary for crystallization. (This is not strictly true, since account should be taken of packing factors. What we shall actually calculate is a pseudominimum size which depends on packing.)

Experimental work shows that a polymer of 60% ethylene, and made with a feed ratio of M_e/M_p = 0.204, is 8% crystalline. Using eq. (5), setting $G(m)$ = 0.08, and inserting appropriate values for r_e, M_e/M_p, and F_e, we can solve for m by means of successive approximations. Carrying out this operation, we find m = 7. This means that whenever seven successive ethylenes in a row occur, the unit is capable of crystallizing.

In order to make the most use of the above information, there are some preliminary operations to be carried out first. Going back to eq. (1) we have plotted $(M_1/M_2)r_1$ for various values of F_1. These are the straight lines radiating from the x axis in Figure 4. Going to eq. (5), setting $G(m)$ = 0.005, m = 7, and various values for F_1, we solve for $(M_1/M_2)r_1$. This value of $(M_1/M_2)r_1$ is the one which will give a maximum crystallinity of 0.005 or $^1/_2$% due to M_1 in a polymer having a molar fraction F_1 of M_1. In other words, for ethylene–propylene, this value of $(M_e/M_p)r_e$ will give a maximum of 0.5% crystallinity due to ethylene for a polymer having a mole fraction F_e of ethylene. Similar values are found for $G(m)$ = 0.01 (1% crystallinity) and $G(m)$ = 0.05 (5% crystallinity). These values of $(M_1/M_2)r_1$ are then picked off the lines in Figure 4. Values for common

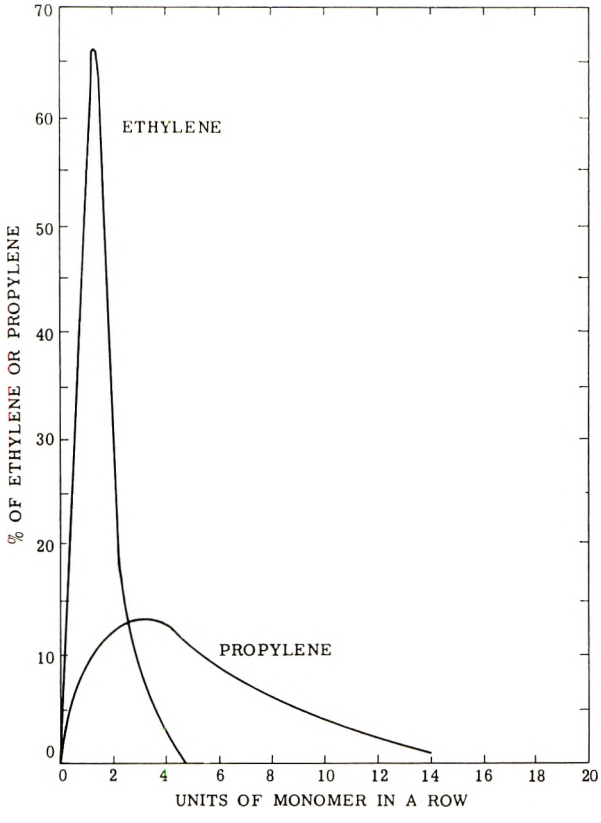

Fig. 3. Ethylene–propylene copolymer. Feed C_3/C_2 = 32.3; C_3 in polymer = 7.3 mole-%.

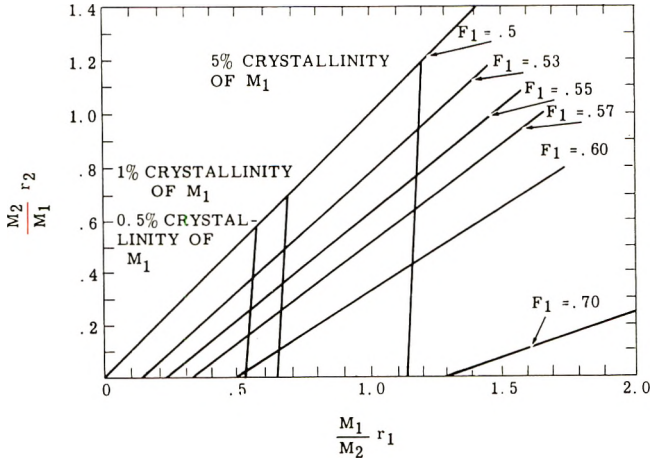

Figure 4.

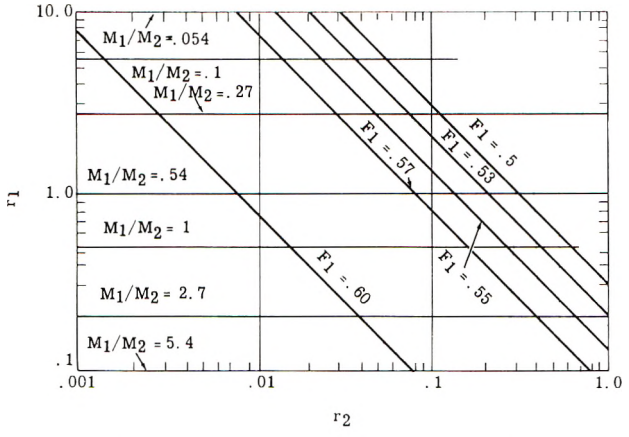

Fig. 5. Reactivity ratio chart for 0.5% crystallinity.

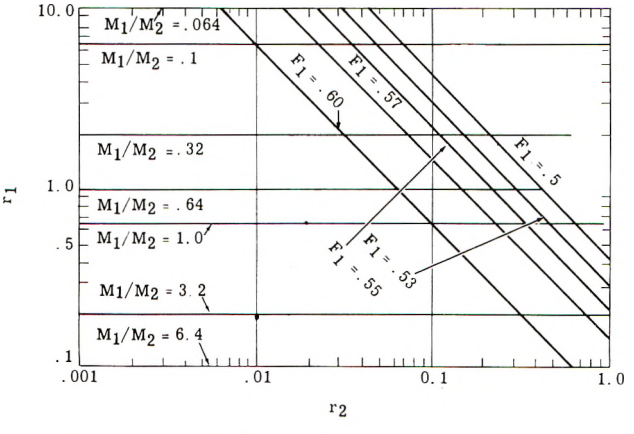

Fig. 6. Reactivity ratio chart for 1.0% crystallinity.

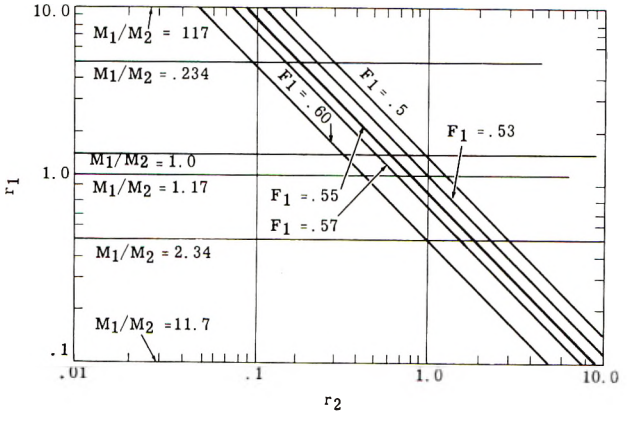

Fig. 7. Reactivity ratio chart for 5.0% crystallinity.

per cent crystallinity are connected. They are the practically vertical lines shown in Figure 4. This plot has some very interesting features. For example, considering r_1 as the reactivity ratio for ethylene, it shows that it is impossible to have a polymer of more than 60% ethylene and have less than $^1/_2$% crystalline polyethylene, for a polymer to have more than about 62% ethylene and less than 1% crystallinity, and for a polymer to have about 68% ethylene and less than 5% crystallinity. Figure 4 quickly shows the limitation of catalysts (in terms of reactivity ratio) and feeds in preparing polymer of specific composition and crystallinity.

By using Figure 4, it is possible to construct reactivity ratio charts such as those of Figures 5–7. Each chart is for a specific per cent crystallinity. These charts must be constructed and used within the limitations of Figure 4, i.e., one cannot use the chart to find conditions to make a 70% ethylene polymer of 0.5% crystallinity, since Figure 4 shows that no such system exists. The best way to demonstrate the use of these charts is by an example. Suppose one wished to make a polymer of 57% ethylene, and could tolerate up to 1% crystallinity. In addition, one was interested in keeping the monomer ratio in the feed close to unity so as to avoid excessive recycling. What should the reactivity ratio of the catalyst be? To answer this we go to Figure 6, which is the 1% crystallinity chart. We find the $M_1/M_2 = 1$ line and proceed along it to the right until the $F_1 = 0.57$ curve is intersected. At the intersection of these two lines, we see, reading the x and y axes, $r_2 = 0.24$, $r_1 = 0.62$. Thus, the objectives can be obtained with a reactivity ratio for the ethylene of 0.62 and for propylene of 0.24.

Actually, these charts are incomplete, since we have not included values of $F_1 < 0.5$. This was done so as to illustrate the principles involved in as simple a manner as possible. However, low values of F_1 can be included by using the same technique as employed for the higher ones. It should also be emphasized that these calculations hold only for low conversions (i.e., where M_1/M_2 equals a constant throughout the run). Extensions of the theory to include high conversion can be made by considering M_1/M_2 an instantaneous value which changes during the run in accordance with the rate equations.

Discussion

Admittedly the above results are based on rather naive assumptions. We are reasonably sure that all the units above a certain critical "block size" do not crystallize. In addition, the reactivity ratios mentioned here probably represent some average ratio and thus are not easily related to the polymer structure. One might attempt this analysis by calculating the reactivity ratios from the melt using Flory's equation

$$[(1/T_m^0) - 1/T_m] = (R/\Delta H) \ln [\gamma_1/(1 + \gamma_1)]$$

A third objection that may be raised is that we have taken no cognizance of penultimate (and other) effects in the determination of the distributions.

Nevertheless, the present approach does agree reasonably well with the experiments. Work by Rogers, Stannett, and Szwarc[3] shows the average "block size" in polyethylene to be 12–15 monomer units long. Thus our number of seven units as a minimum appears reasonable.

References

1. See, for example, P. J. Flory, *Principles of Polymer Chemistry*, Cornell Univ. Press, Ithaca, N. Y., 1953. p. 180.
2. Sakaguchi, Y., *Kobunshi Kagaku*, **17**, 333 (1960).
3. Rogers, C. E., V. Stannett, and M. Szwarc, *J. Phys. Chem.*, **63**, 1406 (1959).

Résumé

Par l'utilisation des équations de copolymérisation, nous avons développé des techniques graphiques pour la prédiction des taux de cristallinité dans les copolymères d'éthylène et de propylène.

Zusammenfassung

Ein graphisches Verfahren zur Angabe des kristallinen Anteils in Äthylen–Propylen. copolymeren mit Hilfe der normalen Copolymerisations-gleichungen wurde entwickelt.

Received March 13, 1962

JOURNAL OF POLYMER SCIENCE: PART A VOL. 1, PP. 1609–1620 (1963)

High Frequency Titrations of Polydicarboxylic Acid Copolymers: Polyitaconic Acid-*Co*-Styrene and Polymaleic Acid-*Co*-Styrene

J. DROUGAS,* A. TIMNICK, and R. L. GUILE,† *Kedzie Chemical Laboratory, Michigan State University, East Lansing, Michigan*

Synopsis

A useful method, more rapid and more accurate than elemental analysis, has been developed to determine the composition of copolymers of itaconic anhydride and maleic anhydride with styrene. The method involves a high frequency titration of the sample. The method can also be used to detect traces of acidic impurities in polymers and in the identification of mixtures of similar acidic copolymers. Titration indicates that the acid segments in the copolymers of itaconic acid–styrene, maleic acid–styrene, and the homopolymer polyitaconic acid act as dibasic acids. The method appears to have a sensitivity that permits identification and approximate resolution of two carboxylate species in the same polymer.

INTRODUCTION

Itaconic anhydride and styrene can be copolymerized under a variety of conditions to give copolymers of varying itaconic anhydride content.[1] Maleic anhydride and styrene can be copolymerized to yield copolymers in which maleic anhydride units usually alternate with styrene units in an approximately 50:50 molar composition.[2]

Compositions of these copolymers usually prepared from the anhydride and styrene have been determined by elemental analysis for carbon and hydrogen and subsequent calculation of the amount of dibasic acid unit, using as references the theoretical percentage of carbon in polystyrene (92.30), polymaleic anhydride (48.98), and polyitaconic anhydride (52.57).

This method of copolymer analysis is tedious and is subject to considerable error when small differences in elemental analyses are involved.

Since the anhydride units in a copolymer readily hydrolyze to diacid groups, a titration method of analysis appeared desirable.

A study of the potentiometric titrations of a maleic acid–styrene copolymer was made by Garrett and Guile.[2] Difficulties were encountered by these workers and later by Bamford[3] in locating with precision the inflection points in the potentiometric curves. These difficulties were partially

* Present address: Textile Research Laboratory, E. I. du Pont de Nemours & Co., Inc., Wilmington, Delaware.

† To whom requests for reprints should be sent.

overcome by using more dilute solutions (0.2 g./180 ml.), and titration values were used with some success in evaluating copolymer composition.

Potentiometric titrations carried out on maleic acid–styrene copolymers which are insoluble in water depend on adding a known amount of standard sodium hydroxide in excess of that necessary to prepare the disodium salt (water-soluble) and back-titrating with standard hydrochloric acid. The reactions involved in the back-titration procedure are illustrated in eq. (1) for a 1 : 1 itaconic anhydride–styrene copolymer unit:

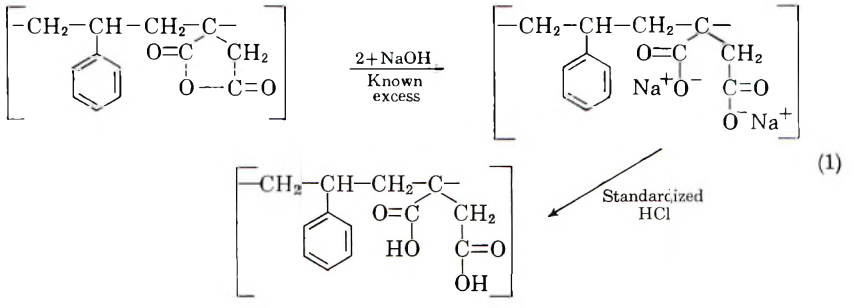

(1)

Precipitation as a faint cloudy solution occurs only at the final endpoint. One of the major difficulties encountered in potentiometric back-titration procedure is the lack of a definite inflection point for the titration of excess sodium hydroxide. Copolymer composition can be calculated based on the difference between the two inflection points related to the two carboxyls of the dibasic acid units, but the inflection point for the weaker carboxyl is often poorly delineated.

With the greater possible range of copolymer composition in copolymers of itaconic anhydride–styrene, the potentiometric method is even less satisfactory.

The high frequency titration technique is a rapid and reproducible method for the determination of the composition of certain polymers containing carboxylic acid segments. It also permits the evaluation of sodium hydroxide excess, gives a more precise location of the inflection points related to the polymer carboxyl groups, and is a sensitive method for the determination of the freedom of the copolymer samples from monobasic acid impurities (comonomer acids), since mixtures of copolymer acids with monobasic and dibasic acids show definite inflection points that can be related to the individual carboxylate species present. The method may also be useful in the detection of slight variations in the structure between very similar copolymer acids in mixtures or in some cases identification of several species of carboxylate groups when attached and repeated in a single type of polymer chain.

EXPERIMENTAL

Equipment

The hydrogen ion concentration was measured by a line-operated Beckman pH meter equipped with glass reference and saturated calomel electrodes.

The high frequency titration apparatus was a capacitative type originally designed by Johnson and Timnick[4] and later modified by Lai, Mortland, and Timnick.[5] The titrations were performed with the titration apparatus operated at 141 Mcycles/sec. Oscillator tube grid current change was followed during the course of the titration. To follow this change a potentiometer set-up had been designed to follow the potential drop change across a resistor which was connected in series with the grid leak resistor. The potential drop across this added measuring resistor was compensated with a potentiometer. Instrument response is expressed throughout this study in terms of arbitrary potentiometer dial units of the compensating potentiometer. A polyethylene cup of about 200 ml. capacity was employed as a cell in the high frequency titrator. The potentiometric electrodes were immersed in the solution in the cup, and the solution was stirred during titration either by an air or electrically driven glass stirrer.

Purity of Samples

High frequency titration is extremely sensitive to very small traces of acid impurities and utmost care must be exercised in the preparation of samples.

Copolymer anhydride samples in a finely divided or powdered form were subjected to Soxhlet extraction with boiling anhydrous benzene for at least 50 hr. to remove all traces of the comonomer anhydride.

Commercial samples of the low molecular weight organic acids are always too impure to give satisfactory high frequency titrations and must be recrystallized as many times as necessary to obtain extremely pure samples. Dibasic acids were converted to the anhydrides and their anhydrides recrystallized for their purification.

Titration Procedure

An accurately weighed sample (approx. 0.2 g.) of the finely divided copolymers, usually the anhydride, since this is the most easily obtained and purified form of the copolymer, was dissolved in purified (alcohol- and acid-free) acetone. To this solution was added a known quantity of standard sodium hydroxide just in excess of the amount to convert the copolymer to the disodium salt. Precipitation occurred on addition of the sodium hydroxide, but final solution of the sample was obtained on removal of the acetone on a steam bath. When the odor of acetone had disappeared and a clear solution was obtained, the sample was transferred quantitatively to the polyethylene cell of the high frequency titration apparatus.

The sample was then diluted to 180 ml. with distilled water; the electrodes of the Beckman pH meter were placed in the solution; mechanical stirring was started and the sample titrated with standardized hydrochloric acid. After each addition of titrant, about 2 min. was allowed for the reaction to reach equilibrium. The compensating potentiometer was adjusted so that the microammeter of the high frequency titrator indicated zero and this new potentiometer dial reading was recorded simultaneously with the corresponding pH reading of the Beckman pH meter.

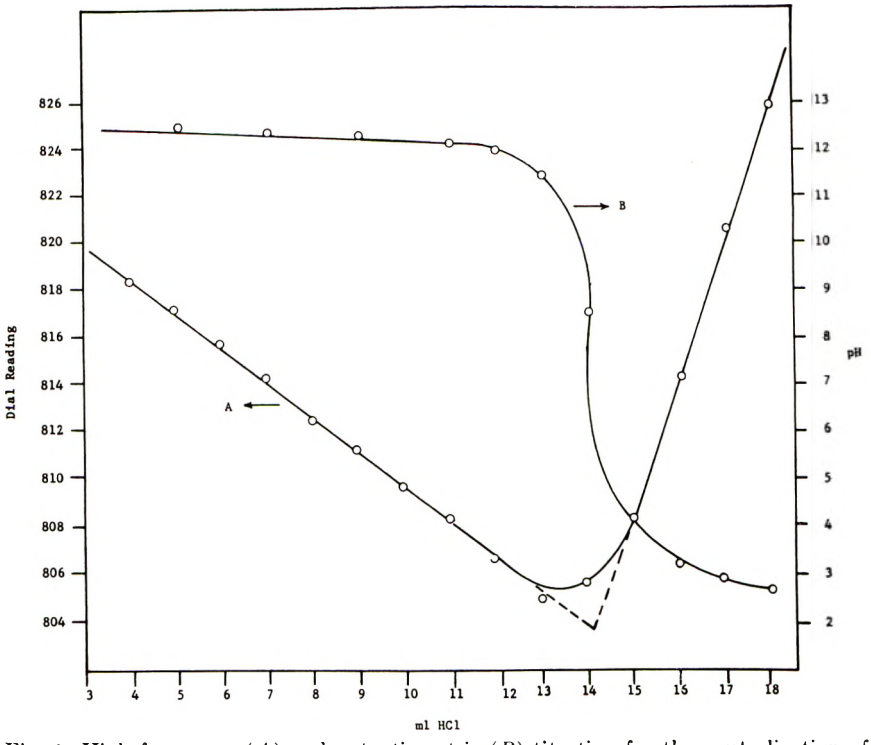

Fig. 1. High frequency (A) and potentiometric (B) titration for the neutralization of 19 ml. NaOH (0.0964N) with HCl (0.1286N).

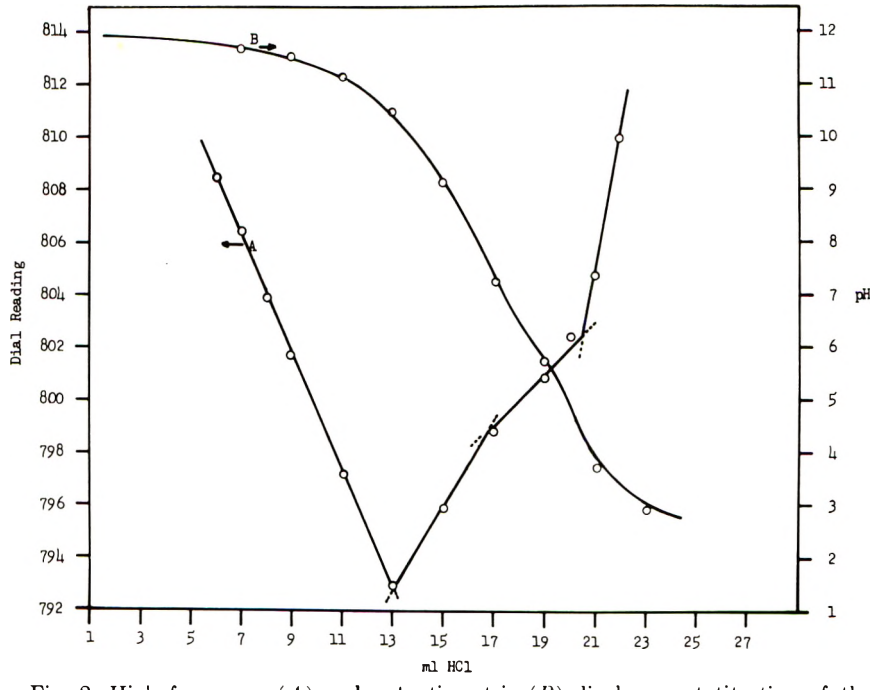

Fig. 2. High frequency (A) and potentiometric (B) displacement titration of the disodium salt of poly(itaconic acid-*co*-styrene). Titration of 0.1018 g. 57:43 anhydride–styrene copolymer + excess NaOH with 0.1286N HCl.

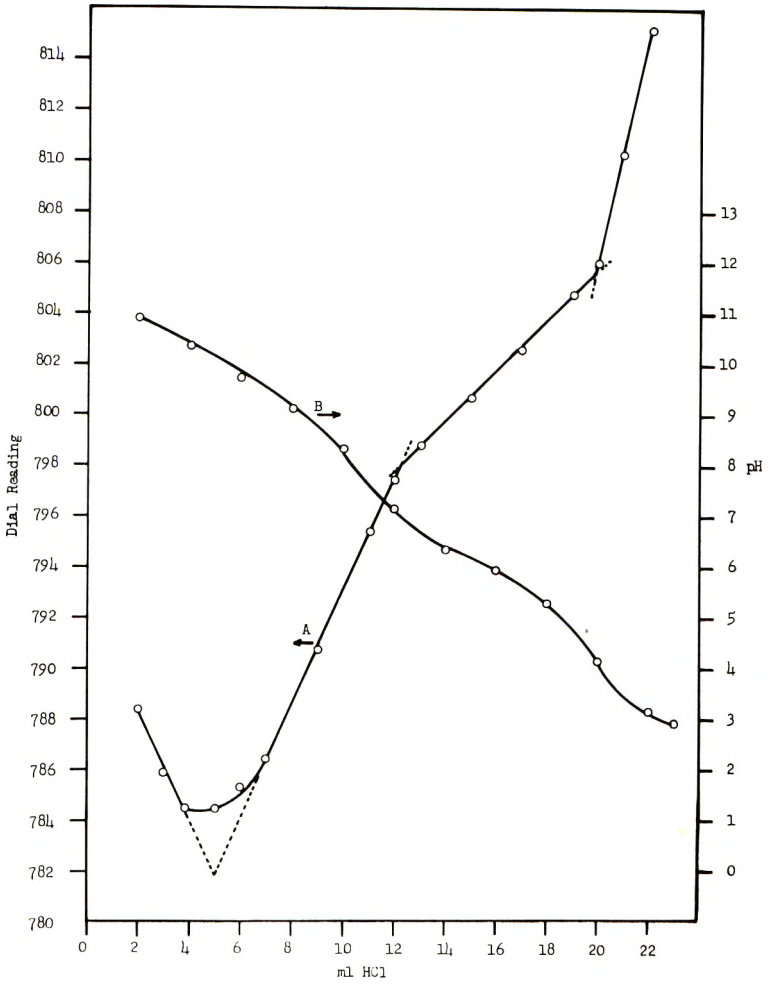

Fig. 3. High frequency (*A*) and potentiometric (*B*) displacement titration of the disodium salt of poly(itaconic acid-*co*-styrene). Titration of 0.2006 g. 55:45 anhydride–styrene copolymer + excess NaOH with 0.1286*N* HCl.

Figure 1 illustrates a plot of the titration results for a simple test case, the titration of 0.1*N* NaOH with 0.1*N* HCl. The break in the high frequency titration curve coincides with the inflection point in the pH titration curve.

A brief summary of the results on the titration of various copolymers is shown in Table I. Graphs in Figures 2–4 illustrate individual titrations. A titration curve, Figure 5, is included for a monomethyl ester of an itaconic acid-styrene copolymer. This sample was prepared by refluxing (6 hr.) a weighed amount of the 57:43 itaconic anhydride–styrene copolymer with absolute methyl alcohol, a reaction which gives quantitative yields[6] of half esters by splitting the anhydride. Titration was carried out as usual after dilution to a desired volume with distilled water.

A similar technique can be employed to prepare and titrate ethyl esters of the itaconic anhydride-*co*-styrene copolymers and also the methyl and ethyl esters of maleic anhydride-*co*-styrene copolymers.

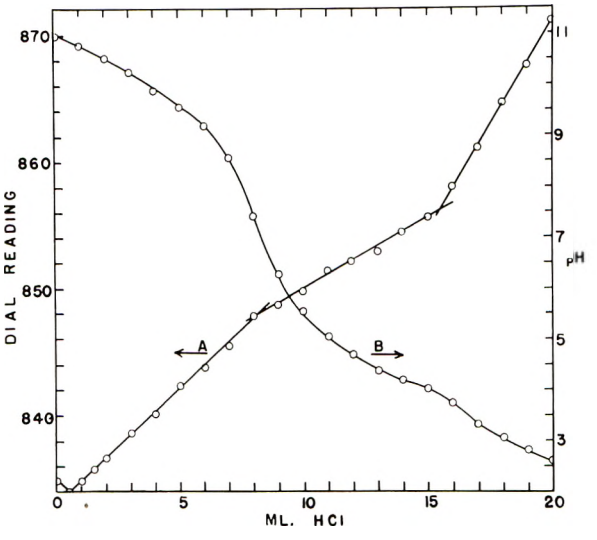

Fig. 4. High frequency (*A*) and potentiometric (*B*) displacement titration of the disodium salt of poly(maleic acid-*co*-styrene). Titration of 0.2 g. 50:50 anhydride–styrene copolymer + excess NaOH with 0.1286*N* HCl.

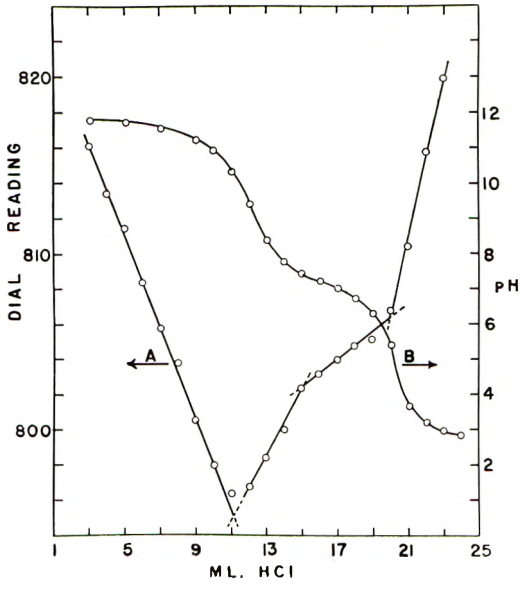

Fig. 5. High frequency (*A*) and potentiometric (*B*) displacement titration of the monosodium salts of the mono methylesters of poly(itaconic acid-*co*-styrene). Titration of 0.2345 g. 57:43 anhydride–styrene copolymer + MeOH (heat) + excess NaOH with 0.1286*N* HCl.

Illustrative formula for the preparation and titration of the monomethyl ester of the itaconic acid–styrene copolymer is given in eq. (2):

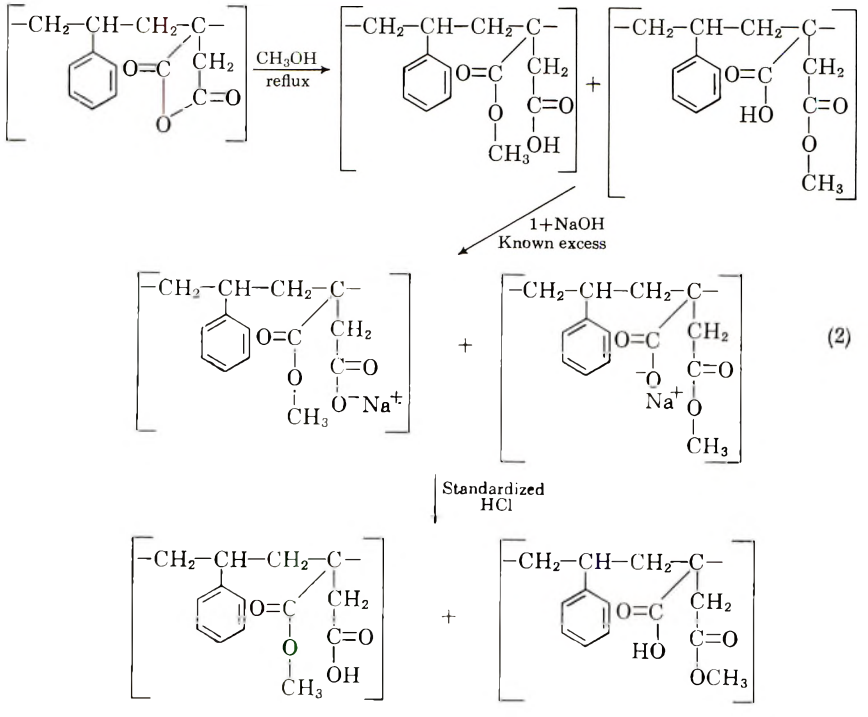

(2)

A titration plot for polyitaconic acid is shown in Figure 6, and the titration data are included in Table I. Methyl and ethyl esters of polyitaconic acid have been prepared.

In the course of these investigations several mixtures of organic acids and copolymers and mixtures of acidic copolymers were titrated. An example of the results obtained in one such titration is shown in Figure 7. It was noted that, while inflection points in the curves correspond in number to titration of excess sodium hydroxide plus the number of carboxylate species present, and total neutralization values are often in agreement, the individual inflection points are not independent of other carboxylate species (Table II). Resolution possible with high frequency titration under the experimental conditions tested becomes more difficult as the number of carboxylate species in the system increases and probably is fairly satisfactory only if the number of species does not exceed two.

DISCUSSION

A titration method to determine the composition of an itaconic acid–styrene copolymer must depend on the determination of the itaconic acid segment of the copolymer. Since both the anhydride and free acid copolymers are insoluble in water but the disodium salts of the acid copolymer are

TABLE I
Titration Data on Copolymers

Copolymer composition[a]	Sample	Type I carboxylate, meq.		Type II carboxylate, meq.		Total carboxylate, meq.	
		Calcd.[b]	Found[c]	Calcd.[b]	Found[c]	Calcd.[b]	Found[c]
57:43 Poly (itaconic anhydride-*co*-styrene)	1(Fig. 2)	0.530	0.489	0.530	0.489	1.060	0.978
	2	1.062	1.093	1.062	1.031	2.124	2.124
	3	1.042	1.019	1.042	1.065	2.084	2.084
Monomethyl ester	1(Fig. 5)	0.530	0.490	0.530	0.630	1.060	1.120
Monoethyl ester	1	0.422	0.451	0.422	0.469	0.850	0.921
	2	0.535	0.572	0.535	0.522	1.070	1.100
55:45 Poly (itaconic anhydride-*co*-styrene	1(Fig. 3)	1.023	0.952	1.023	0.979	2.022	1.931
	2	0.501	0.487	0.501	0.565	1.002	1.002
61:39 Poly (itaconic anhydride-*co*-styrene)	1	0.287	0.287	0.287	0.287	0.574	0.574
	2	0.275	0.285	0.275	0.287	0.563	0.550
Monomethyl ester	1	0.465	0.493	0.465	0.437	0.930	0.930
Monoethyl ester	1	0.103	0.088	0.103	0.112	0.270	0.270
50:50 Poly (maleic anhydride-*co*-styrene)	1(Fig. 4)	0.994	0.976	0.994	0.947	1.988	1.923
monomethyl ester	1	0.500	0.651	0.500	0.496	1.000	1.148
Poly(itaconic anhydride)	1(Fig. 6)	0.890	0.860	0.890	0.985	1.780	1.745

[a] Average mole-% based on C analysis.
[b] Calculated from C analysis.
[c] Found by titration.

soluble, back-titration is the only useful method of titration in an aqueous medium.

Titration of the acid segment depends on the addition of standard base in slight excess of the amount to hydrolyze the anhydride completely and convert the sample to the disodium salt of the polymer acid followed by back-titration with standard mineral acid.

Attempts to titrate the itaconic acid segments with the use of an indicator were unsuccessful. Phenolphthalein, for example, was observed to change from pink to colorless not at the usual range of 8–9 but anywhere in the pH 6–11 range.

Potentiometric back-titration indicated the dibasic nature of the itaconic acid segment but the neutralization of excess sodium hydroxide could not be detected, the inflection points for the liberation of the two types of carboxylate ions were not sharply delineated, and the stoichiometry in many cases was such that satisfactory agreement between composition of polymer calculated by this type of titration and from elemental analysis were not in satisfactory agreement.

Concentration and amount of sample greatly affected the sharpness and presence of an inflection point in the potentiometric titrations for the weaker

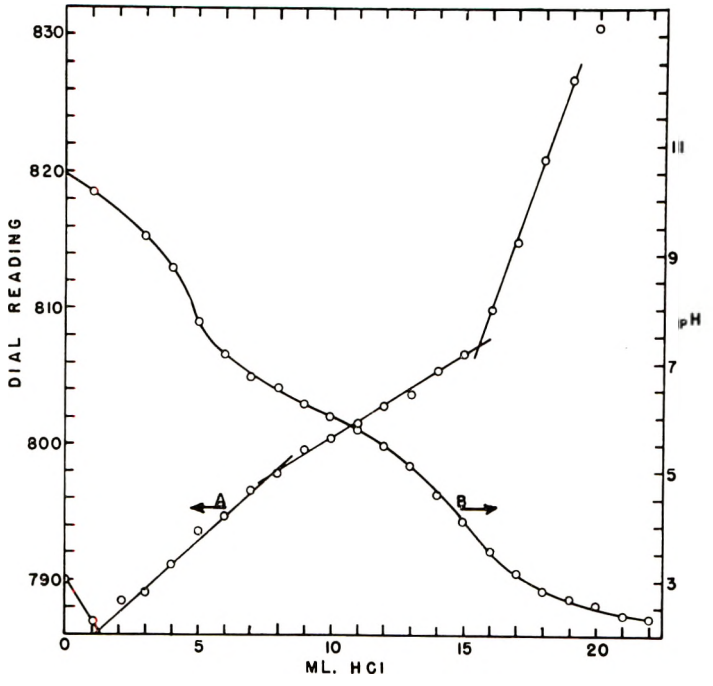

Fig. 6. High frequency (A) and potentiometric (B) displacement titration of the disodium salt of polyitaconic acid. Titration of 0.0997 g. polymer anhydride + excess NaOH with 0.1286N HCl.

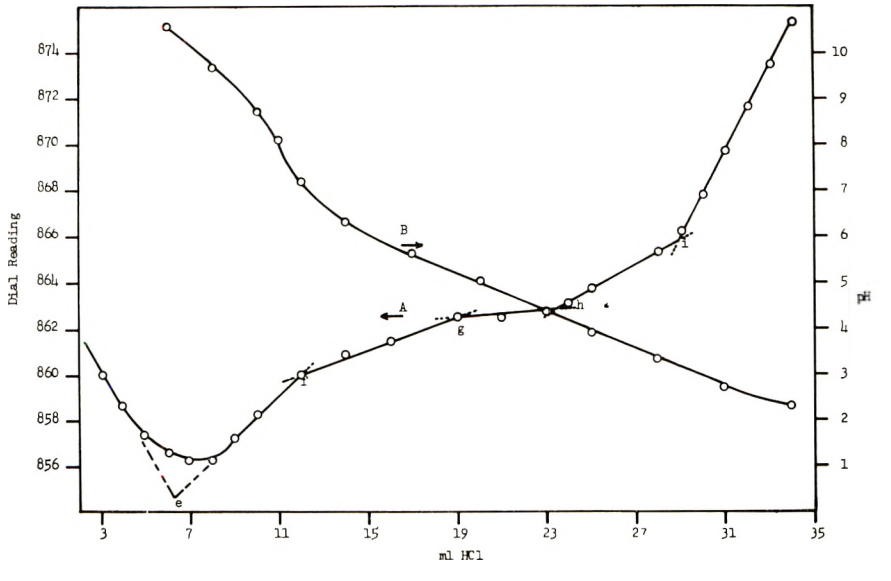

Fig. 7. High frequency (A) and potentiometric (B) displacement titration of a mixture of the sodium salts of poly(itaconic acid-*co*-styrene) and itaconic acid. Titration of 0.0686 g. 61:39 anhydride–styrene copolymer and 0.0606 g. itaconic anhydride + excess NaOH with 0.0966N HCl.

TABLE II
Titration Data on Mixtures

Sample	Substances	Carboxylate, meq.	NaOH added, meq.	Number of inflection points in high frequency titration	HCl (back-titration), meq.
1 (Fig. 7)	61:39 Poly (itaconic anhydride-*co*-styrene	1.042			
	Itaconic anhydride	1.083			
		2.125	2.720	5 (e-i Fig. 7)	2.780(0.579)[a]
2	61:39 Poly (itaconic anhydride-*co*-styrene	0.228			
	Itaconic anhydride	0.373	0.601	4	0.601
		0.601			
3	61:39 Poly (itaconic anhydride-*co*-styrene)	1.296			
	61:39 Poly (itaconic anhydride-*co*-styrene), monoethyl ester	2.250			
		3.546	3.556	4	3.560
4	61:39 Poly (itaconic anhydride-*co*-styrene), monoethyl ester	0.467			
	Itaconic anhydride	1.815			
		2.282	2.282	4	2.223
5	63:37 Poly (itaconic anhydride-*co*-styrene)	0.914			
	Poly(itaconic anhydride)	1.063			
		1.977	2.400	5	2.400(0.13)[a]

[a] Excess NaOH.

carboxylate ion. Sample weights no larger than 0.3 g. and no smaller than 0.1 g. in 180 ml. were found most satisfactory. With 1 g. samples of maleic acid–styrene copolymer, pH titration curves did not show a second inflection point.

High frequency titration, at present a relatively new method, offered the distinct advantage of greater sensitivity and on investigation was found to be adaptable to the titration of acidic copolymers. Titration of these substances in excess sodium hydroxide gave definite inflection points on the high frequency titration plots for the excess sodium hydroxide for the titration or liberation of each carboxylate species and for the total titration or liberation of all polymer carboxylate ions.

In the titrations described there are no problems encountered with desensitization of electrodes due to precipitation of polymeric substances as a coating on the electrode surfaces. The precipitation occurs at the final end point as discrete, nonsticking particles. The electrodes of the pH meter are easily cleaned by washing between samples and the electrodes of the high frequency titrimeter are outside the solution.

The polymers investigated were shown to be free of acidic interfering substances by the absence of inflection points in the high frequency plots other than those corresponding to the titration of polymer carboxylate ions. Nonpolymeric acids always yield inflection points on titration, but they are often less distinct than those from polymeric acids. This may be explained on the basis of the reinforcement of an effect by the repeating nature of the polymer structure, or by a carboxylate function made more easily available to titration when it is part of the polymer structure.

References

1. Drougas, J., and R. L. Guile, *J. Polymer Sci.*, **55**, 297 (1961).
2. Garrett, S. R., and R. L. Guile, *J. Am. Chem. Soc.*, **73**, 4533 (1951).
3. Bamford, C. H., and W. G. Barb, *Discussions Faraday Soc.*, **No. 14**, 208 (1953).
4. Johnson, A. H., and A. Timnick, *Anal. Chem.*, **28**, (1956).
5. Lai, T. M., M. M. Mortland, and A. Timnick, *Soil. Sci.*, **33**, 359 (1957).
6. Moran, M. K., and E. F. Siegel, *J. Am. Chem. Soc.*, **48**, 2318 (1926).
7. Reilley, C. N., and W. H. McCurdy, Jr., *Anal. Chem.*, **25**, 86 (1953).

Résumé

On a mis au point une méthode utile, plus rapide et plus précise que l'analyse élémentaire pour déterminer la composition des copolymères des anhydrides itaconique et maléique avec le styrène. La méthode consiste en une titration à haute fréquence de l'échantillon. Elle peut être employée aussi pour détecter de traces d'impuretés acides dans les polymères, et pour identifier de mélanges de copolymères acides analogues. La titration indique que les segments acides dans les copolymères acide itaconique–styréne, acide maléique–styrène et l'homopolymère de l'acide polyitaconique se comportent comme des acides dibasiques. La méthode semble avoir une sensibilité qui permet l'identification et la résolution approximative de deux groupements carboxylates différents dans le même polymère.

Zusammenfassung

Eine brauchbare Methode, die rascher und genauer als die Elementaranlyse ist, wurde zur Bestimmung der Zusammensetzung von Copolymeren aus Itaconsäure- und Maleinsäureanhydrid mit Styrol entwickelt. Die Methode besteht in einer Hochfrquenztitration der Probe. Sie kann auch zur Auffindung von Spuren saurer Verunreinigungen in Polymeren und zur Identifizierung von Gemischen ähnlicher saurer Copolymerer verwendent werden. Die Titration zeigt, dass die Säuresegmente in Itaconsäure–Styrol- und Maleinsäure–Styrol–Copolymeren und im Polyitaconsäure-Homopolymeren sich wie zweibasische Säuren verhalten. Die Methode scheint eine zur Identifizierung und näherungsweisen Auflösung zweier Carboxylatarten im gleichen Polymeren ausreichende Empfindlichkeit zu besitzen.

Received September 1, 1961
Revised March 20, 1962

JOURNAL OF POLYMER SCIENCE: PART A VOL. 1, PP. 1621–1626 (1963)

Nuclear Radiation Effects in Polytetrafluoroethylene*

D. E. KLINE, *Nuclear Engineering Department*, and J. A. SAUER, *Physics Department, The Pennsylvania State University, University Park, Pennsylvania*

Synopsis

Dynamic mechanical studies of polytetrafluoroethylene, subjected to a total reactor radiation dose of about 10^8 rads, have shown that a decrease occurs in the height of the three damping peaks which are observed in unirradiated samples near 200, 300, and 400°K. Since the 200°K. and 400°K. peaks are associated with configurational changes in the amorphous regions of the material, the experimental observations are compatible with an increased degree of crystallinity. The effects observed in the dynamic modulus–temperature relation upon irradiation are consistent with those found in the internal friction spectrum. The changes that occur in degree of crystallinity upon irradiation have been studied by both infrared and density measurements, and an increase in crystallinity has been found. The changes in the dynamic mechanical properties in the vicinity of room temperature are not well understood, but possible reasons for the observed behavior are given.

I. Introduction

The effects of radiation on the properties of polytetrafluoroethylene (PTFE) have been studied by various means. Bopp and Sisman[1] concluded, on the basis of static measurements of mechanical properties, that severe deterioration occurs in this polymer at low irradiation doses. Charlesby[2] reported that the polymer was reduced to a coarse powder at higher irradiation doses and attributed this to cleavage of the C—C bond.

Many investigations of the chemical nature of the changes occurring upon irradiation of PTFE have been made by electron spin and nuclear spin resonance studies,[3–7] and a summary is given in a recent article by Florin and Wall.[8] It is now believed that the primary radical produced as a result of radiation is $CF_2\dot{C}FCF_2$, that this radical is stable in the absence of other gases such as oxygen, and that crosslinking is a possible occurrence. In the presence of molecular oxygen, new types of radicals appear and the polymer tends to degrade. In the absence of oxygen, Wall[3] has shown that the polymer does not markedly deteriorate and will retain a high percentage of its initial tensile strength up to doses of 10^7–10^8 rads.

No investigations have as yet been reported on the effects of radiation of polytetrafluoroethylene by means of dynamic mechanical methods,

* Supported in part by the U. S. Atomic Energy Commission Contract No. AT(30-1)-1858.

even though many such studies[9–15] have been made on unirradiated samples. It is the purpose of this paper to report and discuss the changes that occur in the dynamic mechanical properties of PTFE subjected to a radiation dose of 10^8 rads.

II. Experimental

Tests were made with an apparatus which is a modification of that described in a previous publication[16] at frequencies ranging from 100 to 2100 cycles/sec. and with samples of 0.25 in. diameter and about 4 in. in length. The resonance frequency of a transverse vibrational mode yields the dynamic modulus of the material if the density is known. Room temperature density values are used in obtaining the modulus; thus the moduli are only nominal and may be a few per cent in error, especially at high temperatures.[17]

The sample irradiation of 18 hr. was carried out at the Penn State University Nuclear Reactor Facility in a sealed container in which some air was present. From measurements made during the course of other experiments, where conditions were similar, the energy deposited by reactor radiation in the PTFE sample was estimated to be 10^{10} ergs/g. or about 10^8 rads. The energy deposited in this case is approximately $^1/_6$ the result of fast neutron collisions and $^5/_6$ the result of gamma-ray interactions. The other contributions, in terms of energy deposited, are rather small.

III. Results

The damping curve for unirradiated PTFE is generally characterized by several dispersion regions from 80 to 600°K. Results for the unirradiated sample tested here are given in Figure 1. Near 200°K., a rather symmetrical damping peak with maximum height of about 0.15 is present, accompanied by a sharp drop in the modulus. This peak has been shown to be evidence of an amorphous transition by Kabin[11] and has been attributed to the onset of mobility of small segments of CF_2 links in the amorphous regions.[9–13] Another dispersion region is noted as the temperature approaches 300°K., and, again, a drop is present in the accompanying modulus graph. This peak is attributed to configurational changes in the crystallites.[9,12,13] The damping peak near 400°K. is reported to be associated with a transition in the amorphous regions involving large segments of polymer molecules.[13] This is accompanied by inflection points in the dynamic modulus graph.

For the PTFE sample irradiated to 10^8 rads, the damping and dynamic modulus values as a function of temperature are also given in Figure 1. In observing the effects of irradiation on PTFE, one notes a severe decrease in the height of the 200°K. peak to less than half the original value. The dispersion region near 300°K. is still present but is reduced in size, and the 400°K. peak has been largely removed. Modulus values of the irradiated sample are higher than that of the unirradiated sample at all temperatures above 160°K. Most of these changes appear to be explainable on the

basis that the average degree of crystallinity of the PTFE samples has increased as a result of the irradiation treatment.

To investigate more directly the effects of radiation on crystallinity, a number of samples of the PTFE material were exposed to reactor radiation and measurements made of density and infrared absorption both before and after irradiation. The data are given in Table I. Density measurements may not be reliable indicators of crystallinity content because of difference in sample structure (voids); nevertheless, the experimental values given in column 2 have been used to provide estimates of crystallinity content (column 3) on the basis of the data of McCrum.[18] Table I also gives (column 4) estimated crystallinity percentages for one unirradiated and one irradiated sample as determined by the infrared

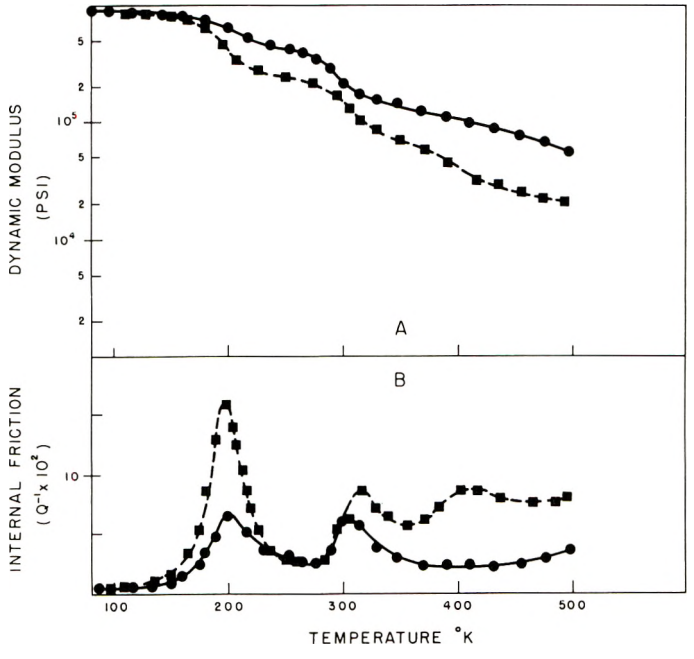

Fig. 1. Plots of (*A*) Dynamic modulus and (*B*) internal friction of (●) irradiated and (■) unirradiated polytetrafluoroethylene.

method. Values of crystallinity obtained by either of these methods show that an increase in crystallinity has taken place as a result of the irradiation treatment. Similar effects on PTFE specimens irradiated to low doses ($<10^7$ rads) have been noted by other investigators[19] by density and x-ray measurements. The density measurements shown in Table I indicate that the maximum degree of crystallinity obtained is about 83%. For example, the density of our samples increased from 2.17 in the unirradiated state to 2.23 g./cc. at 25 Mrads and to 2.24 g./cc. at 50 Mrads and above (Table I). Nishioka et al.[19] reported an increase in density to 2.21 g./cc. at about 10^7 rads, and their values appear to be

TABLE I
Characteristics of Irradiated Samples

Irradiation dose, Mrads	Density, g./cc.	Crystallinity, %	
		Density method	Infrared
0	2.17	59	56
25	2.23	79	—
50	2.24	83	—
75	2.24	83	—
100	2.24	83	83

increasing with increasing dose. The infrared data further substantiate the increase in crystallinity obtained on increasing irradiation dose.

IV. Discussion

The decrease of the internal friction peak near 200°K. with irradiation (Fig. 1) indicates a decrease in the number of short segments of molecular chains in the amorphous regions which are free to undergo configurational changes. Since McCrum[13] has shown this peak height to be approximately proportional to the amount of amorphous material present, the 50% decrease in height would imply a 50% decrease in the amorphous content (from about 40% of the total to about 20% of the total). This would give a crystallinity value of about 80%, which is of the order of that given in Table I.

The data of Figure 1 also show that the relaxation peak at 400°K. has been largely eliminated as a result of the irradiation. This absorption is considered to be a consequence of large segments of polymer chains in the amorphous regions reorienting in response to the applied stress. An increase in crystallinity, resulting in a decreased amorphous volume, would therefore be expected to decrease the magnitude of this relaxation. The observed decrease is, however, larger than can be attributed to this case alone. One reason for this may be that motion of the chains in the remaining amorphous regions are severely hindered by the increased crystallization. If any crosslinking has occurred as a result of the irradiation, such crosslinks might also restrict the movement of the larger segments.

One puzzling feature of our data is the decrease in the height of the room temperature damping peak. If the radiation has caused an increase in crystallinity in the present specimens to a value of 80% or more, it might be expected, on the basis of the earlier work of Illers and Jenckel[12] and of McCrum,[13] that the internal friction peak at 300°K. would increase also. One reason for the observed decrease might be that part of the damping in this region is a result of the "tail" of the 400°K. peak, and this part has been reduced by the radiation. Another possible factor is that although the average degree of crystallinity may have increased, the degree of perfection of the crystallites may be reduced as a result of the radiation-induced defects.

The changes observed in the modulus upon irradiation can be explained in terms of an increased crystallinity. For instance, in McCrum's data,[13] the modulus values for the more crystalline samples are observed to depart from the modulus value for the sample of lowest crystallinity near 160°K. Above this temperature samples of successively higher crystallinity have successively higher modulus values. This same pattern is observed for our irradiated sample as compared to the unirradiated polytetrafluoroethylene sample (Fig. 1). Also, it should be noted that the changes in the degree of inflection in the modulus curve after irradiation are compatible with the changes in internal friction. The inflection in the 200°K. region is greatly reduced corresponding to the observed reduction in damping peak height at this temperature. In the 400°K. region, where the original damping peak has essentially vanished as a result of the irradiation treatment, no noticeable inflection remains.

Infrared measurements were arranged for by Dr. H. W. Starkweather, E. I. du Pont de Nemours and Company.

References

1. Bopp, C. P., and O. Sisman, *Nucleonics*, **13**, No. 7, 28 (1955).
2. Charlesby, A., *Nucleonics*, **12**, No. 6, 18 (1954).
3. Wall, L. A., *ASTM Special Tech. Publ.*, **276**, 208 (1959).
4. Rexroad, H. N., and W. Gordy, *J. Chem. Phys.*, **30**, 399 (1959).
5. Kusumoto, H., *J. Phys. Soc. Japan*, **15**, 867 (1960).
6. Tsvetkov, Yu. D., Ya. S. Lebedev, and V. V. Voevodskii, *Vysokomolekul. Soedin.*, **1**, 1519 (1959).
7. Tsvetkov, Yu. D., Yu. N. Molin, and V. V. Voevodskii, *Vysokomolekul. Soedin.*, **1**, 1805 (1959).
8. Florin, R. E., and L. A. Wall, *J. Res. Natl. Bur. Std.*, **65A**, 375 (1961).
9. Sauer, J. A., and D. E. Kline, *J. Polymer Sci.*, **18**, 491 (1955).
10. Sauer, J. A., and D. E. Kline, *Intern. Congr. Appl. Mech., 9th Congr., University of Brussels*, **5**, 368 (1957).
11. Kabin, S. P., *Zhur. Tekh. Fiz.*, **26**, 2628 (1956).
12. Illers, K. H., and E. Jenckel, *Kolloid-Z.*, **160**, 97 (1958).
13. McCrum, N. G., *J. Polymer Sci.*, **27**, 555 (1958); *ibid.*, **34**, 355 (1959).
14. Sauer, J. A., and A. E. Woodward, *Rev. Modern Phys.*, **32**, 88 (1960).
15. Woodward, A. E., and J. A. Sauer, *Fortschr. Hochpolymer. Forsch.*, **1**, 114 (1958).
16. Kline, D. E., *J. Polymer Sci.*, **22**, 449 (1956).
17. Merrill, L. J., J. A. Sauer, and A. E. Woodward, *Polymer*, **1**, 351 (1960).
18. McCrum, N. G., *ASTM Bull., No.* **242**, 80 (1959).
19. Nishioka, A., K. Matsumae, M. Watanabe, M. Tajima, and M. Owaki, *J. Appl. Polymer Sci.*, **2**, 114 (1959).

Résumé

Des études dynamiques mécaniques du polytétrafluoroéthylène, soumis à une dose de radiation d'un réacteur égale à environ 10^8 rads, ont montré qu'il se présente une diminution de la hauteur des trois pics amortis observés dans des échantillons non-irradiés vers 200, 300, et 400°K. Puisque les pics à 200°K. et 400°K. sont liés à des changements de configuration dans les régions amorphes de la substance, les observations expérimentales sont compatibles avec un degré de cristallinité croissant. Les effets observés dans la relation entre le module dynamique et la température par irradiation sont en concordance avec ceux trouvés dans le spectre de friction interne. On a étudié les modifications du

degré de cristallinité causées par l'irradiation par des examens infrarouges et des mesures de densité. Une augmentation de la cristallinité a été trouvée. Les changements des propriétés dynamiques mécaniques au voisinage de la température de chambre ne s'expliquent pas très bien mais des causes possibles ont été indiquées pour justifier le phénomène observé.

Zusammenfassung

Dynamisch-mechanische Untersuchungen an Polytetrafluoräthylen, das einer Dosis totaler Reaktorstrahlung von 10^8 rad unterworfen wurde, haben gezeigt, dass eine Abnahme der Höhe der drei, bei unbestrahlten Proben bei 200°K, 300°K und 400°K beobachteten Dämpfungsmaxima stattfindet. Da die Maxima bei 200°K und 400°K mit Konfigurationsänderungen in den amorphen Bereichen der Substanz verknüpft sind, sprechen die Versuchsergebnisse für einen erhöhten Kristallinitätsgrad. Die bei Bestrahlung in der Abhängigkeit des dynamischen Moduls von der Temperatur beobachteten Effekte entsprechen den im Spektrum der inneren Reibung gefundenen. Die Änderungen des Kristallinitätsgrades bei der Bestrahlung wurden sowohl infrarotspektroskopisch als auch durch Dichtemessungen untersucht; eine Kristallinitätszunahme wurde festgestellt. Die Änderungen der dynamischmechanischen Eigenschaften in der Nachbarschaft der Raumtemperatur sind noch schwer verständlich, es werden aber mögliche Gründe für das beobachtete Verhalten angeführt.

Received March 19, 1962

JOURNAL OF POLYMER SCIENCE: PART A VOL. 1, PP. 1627–1633 (1963)

Mécanisme réactionnel de la Polymérisation alcaline des Lactames

HIKARU SEKIGUCHI, *Laboratoire de chimie macromoléculaire, Ecole supérieure de Physique et de Chimie industrielles de Paris, Paris, France*

Synopsis

As a consequence of objections raised to our interpretation concerning the reaction mechanism of the alkaline polymerization of lactams, we have re-examined and justified our anionic "lactamolytic" mechanism. The criticism of our opponent is invalidated by mechanisms of analogous reactions, such as the reactions of organometallic compounds and hydrolysis of esters and amides. The opposing mechanism is criticized from a theoretical point of view and disproved by experimental facts which plainly justify our interpretation. The growth mechanism through imide, which consists of a nucleophilic attack of the polarized carbonyl group by the lactam anion, followed by neutralization of the resulting carbinolate ion and opening of the penultimate ring, is thus unequivocally confirmed.

Introduction

Le mécanisme "lactamolytique"[1-3] que nous avons présenté pour la formation des polyamides par polymérisation alcaline des lactames:

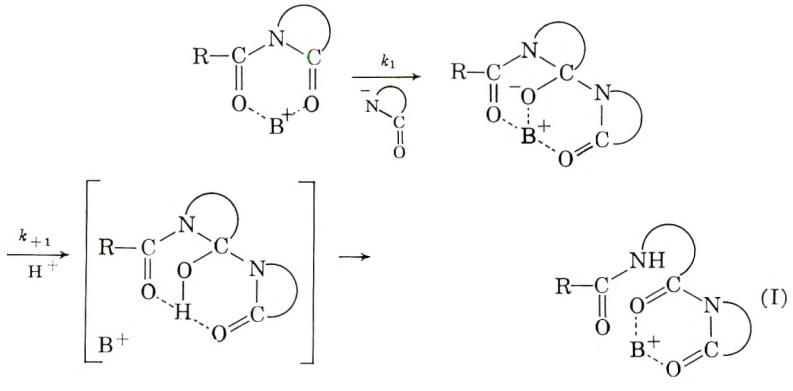

(où R—CO— représente $+NH(CH_2)_xCO+_n$, avec $x = 1, 2, 3, \ldots$, B^+ le cation alcalin provenant du catalyseur et k_1 l'étape déterminant la vitesse de réaction) ayant soulevé quelques objections,[4] nous nous voyons dans l'obligation d'étudier de façon plus détaillée cette réaction et d'indiquer des considérations théoriques et expérimentales justifiant notre interprétation.

En partant de ce mécansime, nous avons proposé pour la dimérisation et la polymérisation des lactames en l'absence d'initiateur (imide), le mode de réaction suivant:[3]

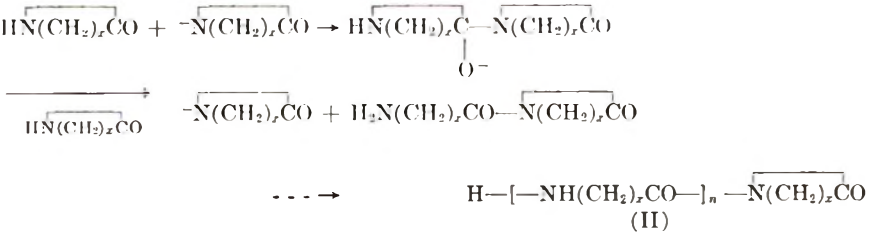

(II)

Shpital'nyĭ[4,5] a constaté que, d'une part, lors de l'action d'un excès de soude avec la lactame, il se forme le sel sodé de l'aminoacide dérivé de la lactame, qui serait capable d'initier la transformation de la lactame en polymère, et que, d'autre part, indépendamment de leurs méthodes d'obtention, tous les polyamides possèdent, lors de l'analyse (après traitement par de l'eau chaude), un nombre égal de groupements acide et basique. Il attribue alors au dimère, en se servant du processus de formation du benzimidazole rapporté par Poraĭ-Koshitz,[6] une formule du type *N*-desoxylactamyl-ω-aminoacide et au polymère celle envisagée par Heikens[7] (III). Il propose donc un schéma[4,5] que nous résumons ainsi:

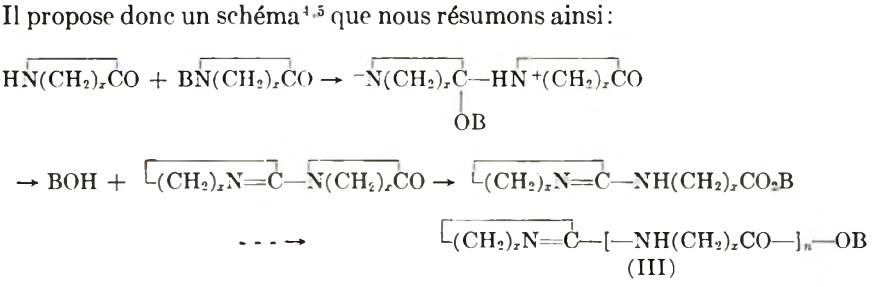

(III)

Il critique[4] notre mécanisme réactionnel en soulignant notamment: (*1*) que le carbonyle de l'imide se trouve polarisé même en l'absence d'un agent alcalin, (*2*) que la coupure de la liaison azote–carbinol par le proton est peu probable dans un milieu basique, (*3*) que son schéma s'applique aux diverses réactions de formation des polyamides alors que le nôtre n'est relatif qu'à la polymérisation anionique.

Discussion

Au cours de cette polymérisation alcaline des lactames deux modes de croissance de la chaîne sont possibles: addition d'un nouveau motif monomère, soit sur l'amine, soit sur le carbonyle. Etant donné que le groupement acyle de l'initiateur imide s'incorpore dans le polymère formé et se fixe sur l'amine terminale de la chaîne,[3,8,9] et que la vitesse initiale de polymérisation est proportionnelle à la quantité de l'initiateur,[8] nous considérons comme peu important le rôle que jouent les groupements amine et amidure (—NHNa)[10] et l'ion amidure (—NH^-),[11] l'existence de ces

deux derniers[12,13] n'étant d'ailleurs pas prouvée. Nous pouvons nous demander, d'autre part, si la formule de Shpital'nyĭ peut impliquer, comme il le pense lui-même,[5] cette croissance par le carbonyle, alors que l'autre extrémité est d'après lui du type amidine, facilement décomposable;[14] ce serait donc celle-ci qui devrait plutôt se transformer dans les conditions de la polymérisation.

Afin d'étudier le pouvoir catalytique des groupements carboxyle et carboxylate, postulé par Shpital'nyĭ,[5] nous avons essayé de polymériser des lactames en présence de sels alcalins d'aminoacides (Tableau I). Il est évident, à partir des résultats de cette étude, que les sels alcalins d'aminoacides ne sont pas des corps intermédiaires dans la polymérisation des lactames, et, par conséquent, que les groupements carboxyle ou carboxylate ne sont pas le centre de croissance de la chaîne. Si une polymérisation se produit à haute température, elle est due à la formation d'un vrai centre de croissance, qui est certainement une imide.

La formule que nous avons adoptée se trouve justifiée plus visiblement par les motifs terminaux du polymère: présence d'un nombre de groupements amine égal à celui des macromolécules lors de la polymérisation sans initiateur imide et absence de groupement carboxyle avant l'hydrolyse du polymère formé,[10,15] fixation sur l'amine terminale du groupement acyle de l'initiateur imide,[3,8,9] formation de la *N*-(*N'*-acyl-ω-aminoacyl)-lactame (dimère *N*-acylé: acyl-NH$(CH_2)_xCO$—$\overline{N(CH_2)_xCO}$) au cours de la préparation de la *N*-acyl-lactame[2,16] (par réaction d'un chlorure d'acyle avec le sel sodé de la lactame); ce dimère acylé, composé intermédiaire de la polymérisation initiée par l'imide, étant d'ailleurs capable d'initier la même polymérisation. Ces faits permettent de justifier la formule (II) pour le polymère, tandis que la formule (III) n'est fondée que sur des preuves chimiques peu décisives aussi bien pour le polymère que pour le dimère ou ses dérivés. (Le dimère du type *N*-desoxylactamyl-ω-aminoacide n'a jamais été isolé, ni sa formule du type (III) jamais prouvée.[4,7]) D'autre part, le fait que l'addition d'un initiateur imide accélère la réaction[17] et permette la polymérisation à froid[3,13,18] (au voisinage du point de fusion du monomère: ε-caprolactame, 70°C; α-pyrrolidone, 24,6°C) met en évidence que seule, la formation du centre de croissance imide, c'est-à-dire l'étape de dimérisation, exige une haute température;[13] ceci justifie le mécanisme de croissance par l'imide que nous avons présenté précédemment.[1–3,19]

Il est très probable que, dans notre schéma, la haute réactivité des groupements imide provient, au fond, de leurs carbonyles polarisés. La coordination du métal alcalin aux carbonyles de l'imide sert alors à compléter la polarisation de ces carbonyles et à faciliter la création de l'anion lactame dans un milieu faiblement polaire tel que la lactame. Ceci est le cas également des réactions du carbonyle avec des organométalliques[20] comme les organolithiens et les organomagnésiens. Nous estimons toutefois que le métal alcalin n'a qu'un rôle auxiliaire dans la polymérisation

TABLEAU I

Monomère	Initiateur imide, % en mole[a]	Catalyseur, % en mole		Température, °C	Temps de réaction h.	Produit de la réaction, %	
		Sel de lactame[b]	Sel d' aminoacide[c]			Polymère[d]	Monomère[e]
α-Pyrrolidone.	0,1	0,1	—	30	0,166	4	96
	2,0	2,0	—	30	1,00	32	68
	—	—	2,0	30	24,00	0	100
ε-Caprolactame.	1,7	1,7	—	100	1,00	20–30	80–70
	1,2	0,6	—	209	24,00	90–93	10–7
	—	—	1,7	100	72,00	0	100
	—	—	1,5	206	24,00	21–25	79–75

[a] *N*-Benzoyl-α-pyrrolidone.
[b] Sel de sodium de la lactame monomère.
[c] Sel de sodium de l'aminoacide dérivé de la lactame monomère.
[d] Partie insoluble dans l'eau.
[e] Partie soluble dans l'eau.

anionique, ainsi que nous l'avons sous-entendu dans la discussion de la cinétique,[3] et que Wichterle nous l'a confirmé ultérieurement.[21]

Nous signalons également que dans le composé intermédiaire (I) de notre schéma il y a neutralisation de l'ion carbinolate par arrachement de l'hydrogène de l'amide (du monomère ou du polymère) et formation d'un anion lactame.[3] Il faut noter que cette neutralisation se produit sur l'ion intermédiaire du motif cyclique dans le corps (I), dont l'ouverture a lieu, ensuite, par réarrangement intramoléculaire du type imidol–amide. Les études sur le mécanisme et le composé intermédiaire de l'hydrolyse alcaline des esters et des amides, rapportées par Bender et d'autres auteurs,[22] justifient cette interprétation.

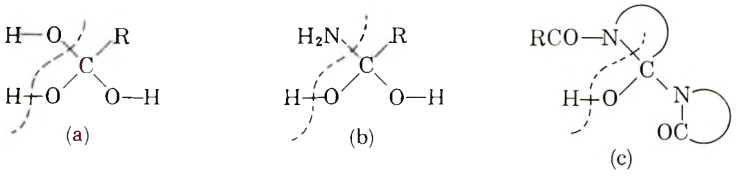

Corps intermédiaires dans (a) l'hydrolyse de l'ester, (b) l'hydrolyse de l'amide, et (c) la "lactamolyse" de l'imide.

Enfin, comme Shpital'nyĭ[4,5] l'a signalé, l'action d'un excès de soude sur l'ε-caprolactame anhydre aboutit à la formation du sel de sodium de l'acide ε-aminocaproïque, ce qui est aisément explicable au moyen de notre mécanisme. En effet, si dans notre schéma nous remplaçons l'anion lactame par un anion hydroxyle, et la *N*-acyl-lactame par la lactame, nous réalisons l'hydrolyse alcaline de l'amide, dont le mécanisme est bien connu:[22]

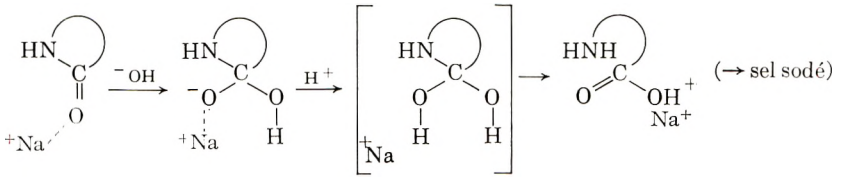

Conclusion

Les considérations exposées ci-dessus, nous permettent de conclure que la polymérisation alcaline des lactames obéit, comme notre schéma le représente, à un mécanisme anionique (dit "lactamolytique" par analogie avec le mécanisme hydrolytique), dont l'étape déterminant la vitesse de réaction est l'attaque nucléophile du carbonyle polarisé de l'imide du motif terminal cyclique de la chaîne par l'anion lactame (étape exprimée par k_1), suivie de la neutralisation de l'ion intermédiaire carbinolate formé et de l'ouverture de l'avant-dernier cycle. Ainsi étant donné: (*1*) que les critiques de notre schéma présentées par Shpital'nyĭ se trouvent infirmées par les mécanismes bien connus de réactions analogues; (*2*) que notre formule est justifiée théoriquement et expérimentalement sans pouvoir être contredite; (*3*) que le schéma de Shpital'nyĭ n'explique pas de façon satis-

faisante les faits expérimentaux expliqués par le nôtre; (*4*) que les formules du dimere et du polymere de Shpital'nyĭ reposent uniquement sur des preuves expérimentales peu décisives; (*5*) que les sels alcalins d'aminoacides (corps intermédiaires suggérés par le schéma de Shpital'nyĭ) n'ont pas de pouvoir catalytique dans la croissance de la chaîne dans les conditions qui permettent la catalyse par les imides; nous estimons que le schéma de Shpital'nyĭ ne peut pas représenter le mécanisme réactionnel de la polymérisation alcaline des lactames.

Références

1. Champetier, G., et H. Sekiguchi, *Compt. Rend.*, **249**, 108 (1959).
2. Sekiguchi, H., *Bull. Soc. Chim. France*, **1960**, 1835.
3. Champetier, G., et H. Sekiguchi, *J. Polymer Sci.*, **48**, 309 (1960).
4. Shpital'nyĭ, A. S., *Zhur. Obshcheĭ Khim.*, **31**, 1037 (1961).
5. Shpital'nyĭ, A. S., et. M. A. Shpital'nyĭ, *Zhur. Obshcheĭ Khim.*, **29**, 1285 (1959); A. S. Shpital'nyĭ, M. A. Shpital'nyĭ et N. S. Yablotchnik, *Zhur. Priklad. Khim.*, **32**, 617 (1959).
6. Porat-Koshitz, B. A., O. F. Guinzburg, et L. S. Efors, *Zhur. Obshcheĭ Khim.*, **17**, 1768 (1947).
7. Heikens, H., *Makromol. Chem.*, **18/19**, 62 (1956).
8. Sekiguchi, H., *Bull. Soc. Chim. France*, **1960**, 1831.
9. Sekiguchi, H., *Bull. Soc. Chim. France*, **1960**, 1839.
10. Griehl, W., *Faserforsch. Textiltech.*, **7**, 207 (1956).
11. Yumoto, H., et N. Ogata, *Bull. Chem. Soc. Japan*, **31**, 907 (1958); S. Chrzczonowicz et M. Włodarczyk, Symposium International sur les macromolécules (1959), Wiesbaden, Allemagne; S. Chrzczonowicz, M., Włodarczyk, et B. Ostaszewski, *Makromol. Chem.*, **38**, 159 (1960).
12. Hall, H. K., Jr., *J. Am. Chem. Soc.*, **80**, 6404 (1958).
13. Šebenda, J., et J. Králíček, *Chem. Listy*, **52**, 758 (1958); *Collection Czech. Chem. Communs.*, **23**, 766 (1958).
14. Pinner, A., *Ber.*, **16**, 1643 (1883); *ibid.*, **17**, 171, 179 (1884).
15. Chrzczonowicz, S., et M. Włodarczyk, *Makromol. Chem.*, **48**, 135 (1961); N. Yoda et A. Miyake, *J. Polymer Sci.*, **43**, 117 (1960).
16. Murahashi, S., H. Sekiguchi, R. Suzuki, et H. Yuki, 10ème Congrès annuel de la Soc. Chim. du Japon (1957), Tokyo, Japon.
17. Matthes, A., K. Zimmermann, et R. Gläsmann, D.D.R.P. 19.839 (1960); O. Wichterle, *Makromol. Chem.*, **35**, 174 (1960).
18. Ney, W. O., Jr., W. R. Nummy, et C. E. Barnes, U.S. Pat. 2,638,463 (1953); W. O. Ney, Jr., et M. Crowther, U.S. Pat. 2,739,959 (1956); C. E. Barnes, W. O. Ney, Jr., et W. R. Nummy, U.S. Pat. 2,891,031 (1959).
19. Murahashi, S., H. Yuki, et H. Sekiguchi, *Sen'i-Kagaku Kenkyûsho Nempô (Osaka)*, **10**, 88, 93 (1957); Symposium des Fibres Synthétiques, 1956, Osaka, Japon, *Communications* p. 11.
20. Gilman, H. et al., *Organic Chemistry, An Advanced Treatise*, 2ème Ed., Vol. 1, Wiley, New York, 1949, p. 515; *ibid.*, Vol. 2, p. 1880; H. Gilman, *Organic Reactions*, Ed. par R. Adams et al, 1re Ed. Vol. 8, Wiley, New York, 1954, p. 261.
21. Wichterle, O., correspondance privée.
22. Bender, M. L., *J. Am. Chem. Soc.*, **73**, 1626 (1951); O. Mumm, Ber., **72**, 1874 (1939); H. K. Hall, Jr., M. K. Brandt, et R. M. Mason, *J. Am. Chem. Soc.*, **80**, 6420 (1958); E. Müller, *Neuere Anschauungen der Organischen Chemie*, 1re Ed., Springer, Berlin, 1940, p. 149; C. K. Ingold, *Structure and Mechanism in Organic Chemistry*, 1re Ed. Cornell Univ. Press, Ithaca, N. Y., 1953, p. 775.

Résumé

Notre interprétation du mécanisme réactionnel de la polymérisation alcaline des lactames ayant soulevé des objections, nous avons repris et justifié notre mécanisme "lactamolytique" anionique. Les critiques de notre schéma, présentées par l'adversaire, sont infirmées par les mécanismes de réactions analogues: réactions des organométalliques et hydrolyse des esters et des amides. Le schéma adverse est critiqué au point de vue théorique et réfuté à partir de faits expérimentaux qui justifient manifestement notre interprétation. Le mécanisme de croissance par l'imide, dû à l'attaque nucléophile par l'anion lactame du carbonyle polarisé, suivie de la neutralisation de l'ion carbinolate formé et de l'ouverture de l'avant-dernier cycle, est ainsi confirmé de façon certaine.

Zusammenfassung

Auf Grund des Einwandes, der gegen unsere Deutung des Reaktionsmechanismus der alkalischen Lactampolymerisation erhoben worden ist, haben wir unseren anionischen "lactamolytischen" Mechanismus erneut überprüft und als richtig befunden. Die Einwände werden durch Mechanismen analoger Reaktionen entkräftet, wie zum Beispiel die Reaktionen metallorganischer Verbindungen und die Hydrolysen von Estern und Amiden. Der von der Gegenseite vorgeschlagene Mechanismus wird durch theoretische Überlegungen und experimentelle Tatsachen widerlegt, welche eindeutig unsere Ansicht unterstreichen. Der Wachstumsmechanismus über Imide, welcher durch einen nucleophilen Angriff des Lactamanions auf die polarisierte Carbonylgruppe eingeleitet wird, worauf Neutralisation und schliesslich Öffnung des vorletzten Ringes erfolgt, wird somit eindeutig bestätigt.

Received March 19, 1962

JOURNAL OF POLYMER SCIENCE: PART A VOL. 1, PP. 1635–1643 (1963)

Polymerization and Copolymerization of 1- and 9-Vinylanthracenes and 9-Vinylphenanthrene

DOV KATZ,* *Scientific Department, Israel Ministry of Defence, Tel Aviv, Israel*

Synopsis

The free radical polymerization and copolymerization with styrene of 1- and 9-vinylanthracenes and 9-vinylphenanthrene was studied. The highest reactivity was shown by 9-vinylphenanthrene and the lowest by 9-vinylanthracene. From the experimental data on the copolymerization reactions the reactivity ratios r_1 and r_2 were calculated and for the two vinylanthracenes the values of Q_2 (general reactivity) were obtained after application of the Price-Alfrey scheme for correlating reactivities of vinyl compounds in copolymerization. The scheme was not used for 9-vinylphenanthrene as the product of $r_1 \times r_2$ was in this case greater than unity. It appears that the rates of polymerization (and copolymerization) of the three monomers are influenced by two factors: the steric hindrance to conjugation between the anthracene or phenanthrene system and the exocyclic double bond, and the nonaromatic character of the 9,10 double bond in phenanthrene. In 9-vinylanthracene the conjugation between the anthracene system and the vinyl group is sterically more hindered that in the 1-isomer, the resonance stabilization of the radical adduct of 1-vinylanthracene is greater than in the case of the 9-isomer and the latter is less reactive. In 9-vinylphenanthrene and 1-vinylanthracene the steric hindrance is the same and the higher reactivity of the first monomer as compared with the second seems to be due to the non-aromatic character of the 9, 10 double bond in phenanthrene, which makes the 9-vinylphenanthrene and almost aliphatic diene.

While the polymerization and copolymerization of the vinylnaphthalenes has been studied systematically,[1–4] only very few vinyl derivatives of more complex polycyclic systems have been investigated.[5–8] The easy availability[9] of 1-vinylanthracene, 9-vinylanthracene, and 9-vinylphenanthrene made it desirable to study quantitatively their polymerization and copolymerization with styrene. 2-Vinylanthracene is so high melting and difficultly soluble in most organic solvents, including styrene, that it was not included in this study.

In the free-radical polymerization of the three vinyl compounds, the reaction rates observed were as given in Table I.

The same order of decreasing activity (9-vinylphenanthrene > 1-vinylanthracene > 9-vinylanthracene) is observed also in the copolymerization of the three hydrocarbons with styrene. The reactivities of the monomers were: styrene–9-vinylphenanthrene, $r_1 = 0.58$, $r_2 = 2.36$ (60°C., 0.5

* Present address: Department of Chemistry, Princeton University, Princeton, N. J.

TABLE I

Monomer	Catalyst	Temp., °C.	Rate, %/sec.
9-Vinylphenanthrene	Benzoyl peroxide (1 mole-%)	65	4.7×10^{-3}
1-Vinylanthracene	Benzoyl peroxide (1 mole-%)	65	1.5×10^{-3}
9-Vinylanthracene	Di-*tert*-butyl peroxide (2 mole-%)	100	5.8×10^{-5}

mole-% benzoyl peroxide); styrene–1-vinylanthracene, $r_1 = 0.81$, $r_2 = 0.57$ (65°C., 1 mole-% benzoyl peroxide); styrene–9-vinylanthracene, $r_1 = 2.12$, $r_2 = 0.25$ (100°C., 2 mole-% di-*tert*-butyl peroxide).

From the experimental data, the values of Q_2 (general reactivity) in the Price-Alfrey scheme of treatment of copolymerization kinetics[10,11] have been calculated. They are for 9-vinylanthracene 0.89, for the 1-isomer 3.50. As the product $r_1 r_2$ for 9-vinylphenanthrene is greater than unity, Q_2 becomes unfortunately meaningless in this scheme. There are other cases known, which for the same reason defy their inclusion into the Price-Alfrey scheme; for some of them calculations have been carried out which, however, do not seem to us justified.[12–14]

It appears that two factors influence the rates of polymerization (and copolymerization) of the substances studied. In 9-vinylanthracene, the conjugation between the anthracene system and the exocyclic double bond is sterically more hindered than in the 1-isomer, as two hydrogen atoms (1,8) interfere with coplanarity in the former compound, the resonance stabilization of the radical adduct of 1-vinylanthracene is greater than in the case of the 9-isomer, and the latter is less reactive.

A similar effect has been observed in the spectra of the phenylanthracenes[15] and has been ascribed to analogous causes.[16] It is, therefore, of interest to recall the spectra of the vinylanthracenes.[9] The 252 mμ maximum of anthracene ascribed to longitudinal polarization[9] remains practically unchanged on the transition to 1- and 9-vinylanthracene (255, 256 mμ), while in 2-vinylanthracene, in which there is no interference with coplanarity, it is shifted to 277 mμ. The 375 mμ maximum of anthracene which should thus be ascribed to a 2,7-polarized form[17] remains practically unchanged by vinylation in either of the two positions 1 and 9.

On the other hand, the high reactivity of 9-vinylphenanthrene, as compared with 1-vinylanthracene must be due to an additional factor, since the steric hindrance is the same as in 1-vinyl-anthracene. One might think of the nonaromatic character of the 9,10 double bond in phenanthrene which makes 9-vinylphenanthrene a rather aliphatic diene.[18] In any event, the decisive factor in determining the reactivity of the monomers must be their affinity to radicals. This conclusion is supported by the fact that the same sequence of affinities has been found by Carrock and Szwarc,[19] for the reaction with methyl radicals, as the figures in Table II show.

In conclusion, the data compiled in Table III tend to show that the same effect of steric interference with radical affinity in polymerization is evident

TABLE II

Monomer	Methyl affinity K_2/K_1	General reactivity Q_2
1-Vinylanthracene	1350 ± 30	3.55
Styrene	792 ± 26	1.00
9-Vinylanthracene	440 ± 10	0.89

also in the naphthalene system, in which 1-vinylnaphthalenes have been shown to be less reactive than the 2-isomers.

In Table III, $1/r_1$, the relative reactivity of the monomers with the styrene radical, has been calculated.

TABLE III
Copolymerization of Styrene (M_1) with Polycyclic Vinyl Compounds (M_2)

Monomer M_2	r_1	r_2	$1/r_1$
1-Vinylnaphthalene[a]	0.67	1.35	1.50
2-Vinylnaphthalene[b]	0.50	1.40	2.00
4-Chloro-1-vinylnaphthalene[b]	0.85	0.80	1.18
6-Chloro-2-vinylnaphthalene[b]	0.40	1.50	2.50
1-Vinylanthracene	0.81	0.57	1.23
9-Vinylanthracene	2.12	0.25	0.47
9-Vinylphenanthrene	0.58	2.36	1.72

[a] Data of Loschak et al.[4]
[b] Data of Price et al.[8]

EXPERIMENTAL

The synthesis of the monomers has been described previously.[9]

Polymerization of the Monomers

The bulk polymerizations were carried out, at least in quintuplicate, in test tubes sealed under pressure of 1 mm. of nitrogen. The monomers and catalysts were weighed to the nearest milligram. After different periods, the test tubes were opened, and the polymers were precipitated several times with methanol from benzene solutions until the weight of the precipitate did no longer change in two successive operations. From the initial straight portion of the plot of per cent of conversion versus time the rate of polymerization was calculated.

Copolymerization of the Monomers with Styrene

The technique of copolymerization was similar to that of polymerization. Series of five or six test tubes, containing solutions of monomer, styrene, and catalyst (with amounts of the monomer ranging from 10 to 80 mole-%) were sealed under pressure. The test tubes were kept in constant temperature baths (for 9-vinylphenanthrene 60 ± 0.5°C., 1-vinylanthracene 65 ± 0.5°C., 9-vinylanthracene 100 ± 0.5°C.) for different times. The

test tubes were opened, and the copolymer was precipitated several times with methanol from benzene solution. In most experiments the copolymerization was stopped before the conversion reached 10%, and in no case the conversion exceeded 15%. The composition of the copolymer was calculated from extinction coefficients of the copolymers and the individual polymers, measured at 261 mμ in chloroform.

The formula used was:

$$X = (E^* - E_B^*)/(E_A^* - E_B^*)$$

where X is the per cent of monomer A in the copolymer, and E_A^*, E_B^*, and E^* are extinction coefficients of polymer A, polymer B, and the copolymer, respectively. This method was first used by Mechan for the determination of the composition of G.R-S rubbers.[20]

From the data on the initial composition of the monomer mixture (M_1, M_2) and the amount of the monomers in the copolymer (m_1, m_2) in each experiment in the three series, the relative reactivity of styrene and of the other monomer was calculated according to the method of Mayo and Lewis,[21] but with a slight modification which we believe to be an improvement. In the graphic representation of the copolymerization equation

$$r_2 = \frac{M_1}{M_2}\left[\frac{m_2}{m_1}\left(1 + \frac{M_1}{M_2}\,r_1\right) - 1\right]$$

and for each series of copolymerization reactions, a family of straight lines was obtained in the r_1, r_2 coordinates, each one representing one experiment. No one family of lines does intersect in one point, and the mean values of r_1 and r_2 are usually calculated from coordinates of all the intersections between the lines composing the same family. As, however, the weight of the intersecting points is different (those obtained from two lines intersecting in flat angles are less important than those obtained from lines intersecting at nearly 90°), we used for the calculation of the mean values r_1 and r_2 the following formulas:

$$r_2 = (m_1x_1 + m_2x_2 + \ldots + m_mx_m)/\Sigma m_n$$

$$r_1 = (m_1y_1 + m_2y_2 + \ldots + m_ny_n)/\Sigma m_n$$

where x_n and y_n are the coordinates of the nth intersection and m_n is the sinus of the angle between the two lines intersecting at this point.

RESULTS

A. Polymerization

In Tables IV–VI the conversion rates are listed for the three isomers.

TABLE IV
Polymerization of 1-Vinylanthracene (65°C., 1 mole-% Benzoyl Peroxide)

Polymerization time, hr.	Conversion, %
1	5.3
2	9.8
3	13.5
5	16.0
10	19.5

TABLE V
Polymerization of 9-Vinylanthracene (100°C., 2 mole-% Di-*tert*-butyl Peroxide)

Polymerization time, days	Conversion, %
1	3.0
2	4.5
3	6.7
5	11.5
6	13.4
7	15.4
8	16.5

TABLE VI
Polymerization of 9-Vinylphenanthrene (65°C., 2 mole-% Benzoyl Peroxide)

Polymerization time, hr.	Conversion, %
1	16.8
2	32.5
3	44.0
4	55.6
5	66.0

B. Copolymerization

The data representing the copolymerizations are summarized in Tables VII–IX.

The temperature at which a change in the consistency of the copolymer in a capillary tube occurs was considered as softening temperature of the polymer.

The molecular weight of the copolymer was calculated from the Staudinger equation $\eta_{sp}/c = K_m M_n$, and the value of K_m for styrene depending on the polymerization temperature was used.[22] The extinction coefficient of polystyrene measured at 261 mμ was 2.17.

TABLE VII
Copolymerization of Styrene (M_1) and 1-Vinylanthracene (M_2) (65°C., 1 mole-% Benzoyl Peroxide)

M_2 mole-% in initial monomer mixture	Polymerization time, hr.	Conversion, %	Softening point, °C.	Molecular weight[a]	E^* at 261 mμ[b]	m_2, mole-% in the copolymer
10	14	5.9	156	26,100	65.3	14.20
20	15	5.0	190	24,000	115.8	28.82
30	14	6.0	212	24,000	147.4	39.91
40	12	8.1	Decomposition[c]	22,200	158.7	44.36
50	8	7.3	Decomposition[c]	23,700	173.0	50.31
60	8	9.8	Decomposition[c]	25,500	200.0	63.04
70	8	10.8	Decomposition[c]	24,800	214.0	70.63

[a] $K_m = 0.47 \times 10^{-4}$.
[b] The extinction coefficient of poly-1-vinylanthracene at 261 mμ was 259.0.
[c] The decomposition begins at 215°C.

TABLE VIII
Copolymerization of Styrene (M_1) and 9-Vinylanthracene (M_2) (100°C., 2 mole-% Di-*tert*-butyl Peroxide)

M_2, mole-% in initial monomer mixture	Polymerization time, hr.	Conversion, %	Softening point, °C.	Molecular weight[a]	E^* at 261 mμ[b]	m_2, mole-% in the copolymer
10	24	10.2	128	42,000	11.2	5.12
20	48	10.7	142	17,000	18.5	9.53
30	72	10.3	151	14,500	27.5	15.53
40	72	9.1	167	13,400	37.7	23.16
50	72	7.8	177	16,400	42.9	27.46
60	72	7.5	182	21,100	53.4	37.09
70	72	7.2	189	25,800	63.2	47.20
80	72	6.8	197	26,000	70.5	56.16

[a] $K_m = 0.57 \times 10^{-4}$.
[b] The extinction coefficient of poly-9-vinylanthracene at 261 mμ was 98.0.

TABLE IX
Copolymerization of Styrene (M_1) and 1-Vinylphenanthrene (M_2) (65°C., 0.5 mole-% Benzoyl Peroxide)

M_2, mole-% in initial monomer mixture	Polymerization time, hr.	Conversion, %	Softening point, °C.	Molecular weight[a]	E^* at 261 mμ[b]	m_2, mole-% in the copolymer
10	4½	15.7	157	84,900	40.5	16.09
20	4	13.5	168	59,700	70.4	32.56
30	4	9.8	173	58,900	92.2	47.93
40	4½	11.4	180	31.600	104.7	57.92
50	5	13.2	190	37,700	114.3	66.84
70	4	10.7	201	37,000	130.7	84.56

[a] $K_m = 0.47 \times 10^{-4}$.
[b] The extinction coefficient of poly-9-vinylphenanthrene at 261 mμ was 142.6.

The author wishes to thank Prof. E. D. Bergmann for his valuable advice and encouragement during the course of this work and for reading the manuscript.

References

1. Koton, M. M., *J. Polymer Sci.*, **30**, 331 (1958).
2. L. Palfray, S. Sabetay, and D. Sontag, *Compt. Rend.*, **194**, 2065 (1932); *ibid.*, **196**, 622 (1933).
3. Sontag, D., *Ann. Chim.*, [11], **1**, 399 (1937).
4. Loschack, S., E. Broderick, and Ph. Bernstein, *J. Polymer Sci.*, **39**, 227, 241 (1959).
5. Flowers, R. G., and F. S. Nichols, *J. Am. Chem. Soc.*, **71**, 3104 (1949).
6. Mowry, D. T., M. Ranoll, and W. F. Auber, *J. Am. Chem. Soc.*, **68**, 1105 (1946).
7. Price, C. C., and B. D. Halpern, *J. Am. Chem. Soc.*, **73**, 818 (1951).
8. Price, C. C., B. Halpern, and S.-T., Voong, *J. Polymer Sci.*, **11**, 575 (1953).
9. Bergmann, E. D., and D. Katz, *J. Chem. Soc.*, **1958**, 3226.
10. Alfrey, T., Jr., and C. C. Price, *J. Polymer Sci.*, **2**, 101 (1947).
11. Alfrey, T., J. J. Bohrer, and H. Mark, *Copolymerization*, Interscience, New York, 1952, p. 79 ff.
12. Lewis, R. M., F. R. Mayo, and W. F. Hulse, *J. Am. Chem. Soc.*, **67**, 1701 (1945).
13. Price, C. C., *J. Polymer Sci.*, **3**, 772 (1948).
14. Mayo, F. R., and C. Walling, *Chem. Revs.*, **46**, 191 (1950).
15. Hirshberg, Y., *Trans. Faraday Soc.*, **44**, 285 (1941); cf. E. de Barry Barnett, J. W. Cook, and Th. E. Ellison, *J. Chem. Soc.*, **1928**, 885.
16. Jones, R. N., *Chem. Revs.* **32**, 1 (1943); *J. Am. Chem. Soc.*, **63**, 1658 (1941); *ibid.*, **67**, 2127 (1945); cf. Y. Hirshberg, ref. 15.
17. Jones, R. N., *J. Am. Chem. Soc.*, **67**, 2127 (1945); cf. Y. Hirshberg, ref. 15.
18. Bergman, E., and F. Bergmann, *J. Am. Chem. Soc.*, **59**, 1443 (1937); *ibid.*, **62**, 1699 (1940); F. Bergmann, *ibid.*, **64**, 69 (1942); F. Bergmann, and S. Israelashwili, *ibid.*, **67**, 1951 (1945).
19. Carrock, F., and M. Szwarc, *J. Am. Chem. Soc.*, **81**, 4138 (1959).
20. Mechan, E. J., *J. Polymer Sci.*, **1**, 175 (1946).
21. Mayo, F. R., and F. M. Lewis, *J. Am. Chem. Soc.*, **66**, 1954 (1944).
22. Boundy, R. H., and R. F. Boyer, *Styrene, its Polymers, Copolymers and Derivatives*, Reinhold, New York, 1952, p. 329.

Résumé

La polymérisation et la copolymérisation radicalaire du 1-vinylanthracène du 9-vinylanthracène et du 9-vinylphénanthrène avec le styrène ont été étudiées. Le 9-vinylphenanthrène présente la réactivité la plus élevée tandis que le 9-vinylanthracène est le moins réactif. Les rapports de réactivités r_1 et r_2 ont été calculés aux dépens des données expérimentales obtenues au cours des réactions de copolymérisation. Les valeurs de Q_2 (réactivité générale) pour les deux vinylanthracènes ont été obtenues après application du schéma d'Alfrey-Price reliant les réactivités des dérivés vinyliques en copolymérisation. Ce schéma n'a pas été utilisé pour le 9-vinylphénanthrène, le produit $r_1 \times r_2$ étant, dans ce cas, supérieur à l'unité. Il apparaît que les vitesses de polymérisation (et de copolymérisation) de trois monomères sont influencées par deux facteurs: l'empêchement stérique à la conjugaison entre les systèmes aromatiques (anthracène ou phénanthrène) et la double liaison exocyclique d'une part, et le caractère non-aromatique de la double liaison en 9–10 du phénanthrène d'autre part. Dans le 9-vinylanthracène l'empêchement stérique à la conjugaison entre le système anthracénique et le groupe vinylique est plus prononcé que pour l'isomère 1. La stabilisation par résonance du radical issu du 1-vinylanthracène est supérieure à la stabilisation du radical issu de l'isomère 9 et ce dernier est plus réactif. Dans le 9-vinylphénanthrène et le 1-vinylanthracène l'empêchement stérique est identique et la réactivité supérieure du premier

monomère est due au caractère non-aromatique de la double liaison 9–10 du phénanthrène, rendant le 9-vinylphénanthrène pratiquement semblable à un diène aliphatique.

Zusammenfassung

Die radikalische Polymerisation und Copolymerisation mit Styrol von 1- und 9-Vinylanthracen und 9-Vinylphenanthren wurde untersucht. Die höchste Reaktivität zeigte 9-Vinylphenanthren, die niedrigste 9-Vinylanthracen. Aus den Versuchsdaten über die Copolymerisation wurden die Reaktivitätsverhältnisse r_1 und r_2 berechnet und für die beiden Vinylanthracene wurden die Q_2 Werte (allgemeine Reaktivität) nach Anwendung der Price-Alfrey-Beziehung für die Copolymerisationsreaktivität von Vinylverbindungen erhalten. Diese Beziehung wurde nicht für 9-Vinylphenanthren verwendet, da das Produkt $r_1 \times r_2$ in diesem Fall grösser als eins war. Es scheint, dass die Polymerisations-(und Copolymerisations-)-geschwindigkeit der drei Monomeren durch zwei Faktoren beeinflusst wird: die sterische Hinderung der Konjugation zwischen dem Anthracen- oder Phenanthrensystem und der exocyclischen Doppelbindung und den nichtaromatischen Charakter der 9,10-Doppelbindung in Phenanthren. Im 9-Vinylanthracen wird die Konjugation zwischen dem Anthracensystem und der Vinylgruppe sterisch mehr gehindert als im 1-Isomeren, die Resonanzstabilisierung des Radikaladdukts von 1-Vinylanthracen ist grösser als im Falle des 9-Isomeren und das letztere ist weniger reaktiv. Im 9-Vinylphenanthren und 1-Vinylanthracen ist die sterische Hinderung die gleiche und die höhere Reaktivität des ersteren im Vergleich zum letzteren scheint durch den nichtaromatischen Charakter der 9,10-Doppelbindung im Phenanthren bedingt zu sein, durch welchen das 9-Vinylphenanthren nahezu zum aliphatischen Dien wird.

Received March 19, 1962

JOURNAL OF POLYMER SCIENCE: PART A VOL. 1, PP. 1645–1650 (1963)

Isomorphism in Polycarbonates. Copolymers of Hydroquinone and Substituted Hydroquinones

ISAAC D. RUBIN,* *Chemical Materials Department, General Electric Company, Pittsfield, Massachusetts*

Synopsis

Copolycarbonates were synthesized by phosgenating various proportions of chlorohydroquinone with hydroquinone, toluhydroquinone, and 4,4′-dihydroxydiphenylmethane. It was found, by means of x-ray diffraction diagrams and melting point–composition data, that the copolymers prepared from hydroquinone–chlorohydroquinone and toluhydroquinone–chlorohydroquinone mixtures were isomorphous over their entire composition range. The copolymerizations of 4,4′-dihydroxydiphenyl with chlorohydroquinone resulted in products characterized by reduced crystallinity. The effect of the monomer structure on changes in the lattice constants of the crystalline copolymers was investigated briefly.

Introduction

Isomorphous replacements are relatively common among low molecular weight compounds; they occur, however, only rarely in polymeric systems. In polymers, isomorphism consists of the introduction of repeat units having different structures into a single crystalline lattice. This may happen either when polymers having different structures cocrystallize in the same lattice (isomorphism of chains) or when different repeat units are incorporated into the chain of a crystallizable polymer without breaking up the crystalline lattice of the resulting copolymer (isomorphism of monomeric units). Several instances of isomorphism have been reported for copolyamides[1–3] and for stereoregular copolymers of styrene and substituted styrenes.[4] We have investigated the possibility of isomorphous replacements in crystalline polycarbonate copolymers of hydroquinone and substituted hydroquinones and have found two systems in which the different monomeric units can replace each other in the crystalline lattice of the copolymer without disrupting it.

Results and Discussion

In an effort to determine the effects of the monomer structure on isomorphism in polycarbonates, we investigated the phosgenation products of the monomer pairs hydroquinone–chlorohydroquinone and toluhydroquinone–chlorohydroquinone over the entire composition range and 4,4′-

* Present address: Texaco Research Center, Beacon, N. Y.

dihydroxydiphenylmethane–chlorohydroquinone over a limited composition range. The compositions of the polycarbonates made by phosgenating various amounts of chlorohydroquinone with hydroquinone and with toluhydroquinone are given in Tables I and II. As may be seen from the chlorine analyses, they were the same, within experimental error, as those of the monomeric mixtures they were prepared from.

TABLE I
Hydroquinone–Chlorohydroquinone Polycarbonates

Chlorohydroquinone, mole-%	Copolymer melting point, °C.	Cl, %	
		Calculated	Found
100	316	20.8	20.9
88.3	328	18.8	19.3
82.0	336	17.7	17.7
75.3	344	16.5	15.8
65.5	>360	14.8	14.9
50.0	>360	11.7	11.6
20.0	>360	5.0	5.1
0	>360	—	—

TABLE II
Toluhydroquinone–Chlorohydroquinone Polycarbonates

Chlorohydroquinone, mole-%	Copolymer melting point, °C.	Cl, %	
		Calculated	Found
85.3	300–305 (dec.)	18.1	18.3
68.3	290–295 (dec.)	14.8	15.0
50.2	290–295 (dec.)	11.1	11.1
30.0	295–300 (dec.)	6.8	7.2
14.8	285–290 (dec.)	3.4	3.7
0	285–290 (dec.)	—	—

Isomorphism in polymers is characterized by the retention of an orderly packing of chains in the crystalline lattice. Since, however, it involves the replacement of one of the repeat units in the chain by another one of a different type, it can be accompanied by changes in lattice dimensions. We have found that the polycarbonates shown in Tables I and II were crystalline over the entire composition range. No broadening of the sharp x-ray diffraction peaks was observed at any of the intermediate compositions. This indicates that in each of the copolymers both of the repeat units could be accommodated within the same lattice structure without disrupting it to any appreciable extent; i.e., the copolymers were isomorphous over the entire composition range. The dependence of the d values for the two systems on copolymer composition for 2θ values of up to about 45° is shown in Figures 1 and 2. The diffraction lines corresponding to larger 2θ values were too diffuse to be measured with any

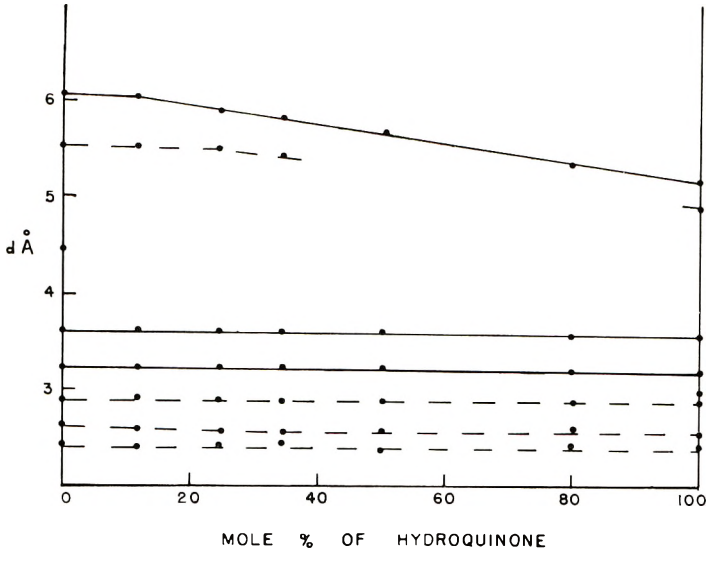

Fig. 1. X-ray diffraction data for hydroquinone–chlorohydroquinone polycarbonate copolymers (broken lines indicate either very weak or diffuse reflections).

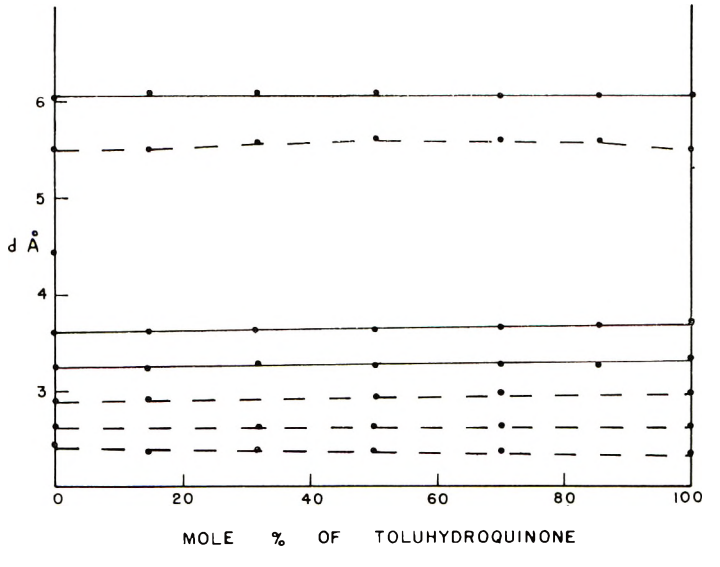

Fig. 2. X-ray diffraction data for chlorohydroquinone–toluhydroquinone polycarbonate copolymers (broken lines indicate either very weak or diffuse reflections). Differences in number of weak reflections may be due to differences in x-ray intensities.

degree of accuracy. It may be seen that the introduction of increasing amounts of chlorohydroquinone into the hydroquinone polymer lattice caused a continuous change in the lattice dimensions. It is, however, noteworthy that only two of the reflections changed appreciably with

composition, while all the others remained almost constant (Fig. 1). This could mean that the unit cell was changing in size predominantly along one direction. Chlorohydroquinone and toluhydroquinone, on the other hand, were able to replace each other in the copolymer crystalline lattice without greatly modifying any of the lattice constants (Fig. 2). This is not surprising in view of the fact that the van der Waals radii of the methyl group and chlorine are, respectively, 2.0 and 1.8 A., while the radius of the hydrogen they replaced is only 1.0 A.[7]

The crystalline melting points of copolymers exhibiting isomorphism are generally higher than the melting point of the lower melting homopolymer.[1,4] We have found this to be true of the copolymers of hydroquinone and chlorohydroquinone. The melting points reported in Table I were obtained on untreated polymer samples. Even though treating the polymers with various nonsolvents changed their melting points appreciably, the same general relationship was maintained. The copolymers containing more than 25 mole-% of hydroquinone were birefringent up to 360°C., the highest temperature which could be obtained with the available equipment. No melting temperatures could be obtained for the copolymers of chlorohydroquinone and toluhydroquinone since the disappearance of their birefringence was due not to melting but to decomposition. The approximate temperatures at which their birefringence disappeared are shown in Table II.

It should be noted that in the absence of isomorphism the melting points of copolymers decrease in accordance with Flory's theory and their composition–melting point curves are characterized by V-shaped depressions.[5] From Flory's expression for melting point lowering and a value of 2100 cal./repeat unit for the melting enthalpy of chlorohydroquinone polycarbonate,[6] it may be seen, for example, that the addition of 30 mole-% of a comonomer should depress the copolymer melting temperature to below 250°C. No such drastic depressions were obtained with any of the samples.

In addition to the polymer systems discussed above, in which similar monomers were used, we have also studied the products obtained by phosgenating solutions of chlorohydroquinone containing, respectively, 15 and 31 mole-% of 4,4′-dihydroxydiphenylmethane. The x-ray diffraction picture of the copolymer containing 15% of 4,4′-dihydroxydiphenylmethane indicated that the material was crystalline; the reflections, however, were less sharp than those of chlorohydroquinone polycarbonate. The two strong peaks had d spacings of 5.50 and 3.58 A.; weaker peaks were located at 3.21 and 2.89 A. The corresponding peaks in the x-ray diagram of the chlorohydroquinone polycarbonate homopolymer appeared at 6.05, 3.61, 3.23, and 2.87 A. The retention of crystallinity combined with this deformation of the unit cell seems to indicate that, despite the large difference in the sizes of the two monomers, small amounts of 4,4′-dihydroxydiphenylmethane could be incorporated into the chlorohydroquinone polycarbonate lattice. One cannot exclude, however, the pos-

sibility that the change in structure was due not to the incorporation of the 4,4′-dihydroxydiphenylmethane into the lattice but merely to the stresses imposed upon it by the presence of the comonomer. Melting point data could not be used to distinguish between these alternatives since the copolymer decomposed at about 265°C. In contrast to this copolymer in which crystallinity was retained, the copolymer containing 31% of 4,4′-dihydroxydiphenylmethane was completely amorphous. It is thus apparent that the addition of larger amounts of the comonomer inhibited the orderly packing of the molecules in a three-dimensional lattice.

The insolubility of the crystalline polycarbonates of hydroquinone and substituted hydroquinones investigated in this work precluded the possibility of separating from the copolymers any homopolymers that may have been formed during the phosgenation reactions. The fact that no reflections of the polycarbonates of hydroquinone and chlorohydroquinone were observed in the x-ray diagrams of the copolymers prepared from those compounds indicates that either only very small amounts of crystalline homopolymers were formed or that any homopolymers that were formed were incorporated into the copolymer crystalline lattice. It is thus possible that in these systems one is dealing not only with isomorphism of monomeric units but also with isomorphism of chains.

Experimental

The starting materials were all commercially available chemicals. The solids were purified by recrystallizations; their melting points agreed well with those reported in the literature. The liquids were fractionally distilled.

The monomers (7.0 g.) were dissolved in 50 cc. methylene chloride containing 10.7 g. pyridine in a 100 cc. resin flask equipped with a gas inlet tube, reflux condenser, thermometer, and an efficient stirrer. Phosgene was then added to the rapidly stirred reaction mixture at the rate of 0.1 g./min. for 50–70 min. During that time the temperature in the flask rose from about 27°C. (room temperature) to 37–38°C. The polymer precipitated out of solution as it formed. Phosgene addition was terminated when no further thickening of the reaction mixture was observed; this coincided with a slight temperature drop. The mixture was stirred for an additional 30 min. and then precipitated into an excess of methanol in a Waring Blendor. The filtered polymer was washed several times with methanol, dilute HCl, water, and again methanol to remove the solvents and any unreacted monomer. It was dried at 80°C.

The composition of the products was obtained by determining their chlorine content. Polymer samples weighing 40–70 mg. were ignited in a 250 cc. Schoniger flask containing 10 cc. of 0.1*N* NaCl and about 0.2 cc. of a 30% solution of H_2O_2. Prior to ignition the flask was flushed out with oxygen. The samples were then agitated vigorously for 15 min., diluted with 150 cc. of methanol containing 3.0 cc. of concentrated HNO_3, and titrated potentiometrically with a silver nitrate solution. The polymer melt-

ing points were determined by placing polymer particles between the crossed polaroids of a microscope equipped with a Kofler hot stage and observing the temperature at which the last traces of birefringence disappeared. CuKα radiation was used to obtain the x-ray diffraction diagrams of the powdered polymers.

The author would like to thank Mr. R. Hirst for obtaining the X-ray diffraction diagrams.

References

1. Cramer, F. B., and R. G. Beaman, *J. Polymer Sci.*, **21**, 237 (1956).
2. Yu, A. J , and R. D. Evans, *J. Am. Chem. Soc.*, **81**, 5361 (1959).
3. Levine, M., and S. C. Temin, *J. Polymer Sci.*, **49**, 241 (1961).
4. Natta, G., P. Corradini, D. Sianesi, and D. Morero, *J. Polymer Sci.*, **51**, 527 (1961).
5. Flory, P. J., *J. Chem. Phys.*, **17**, 233 (1949).
6. Rubin, I. D., unpublished results.
7. Pauling, L., *The Nature of the Chemical Bond*, 3rd Ed., Cornell Univ. Press, Ithaca, N. Y., 1960, Chap. 7.

Résumé

On a synthétisé des copolycarbonates par traitement par le phosgène de proportions différentes de chlorohydroquinone avec l'hydroquinone, toluhydroquinone, et 4–4′–dihydroxydiphénylméthane. Au moyen de diagrammes de diffraction aux rayons-X et des relations entre le point de fusion et la composition, on a trouvé que les copolymères préparés à partir de mélanges de hydroquinone–chlorohydroquinone et de toluhydroquinone–chlorohydroquinone étaient isomorphes quelques soient leurs compositions. Des copolymérisations de 4–4′–dihydroxydiphényle avec le chlorohydroquinone donnaient des produits caractérisés par une cristallinité réduite. On a examiné brièvement l'effet de la structure du monomère sur les modifications des constantes du réseau des coploymères cristallins.

Zusammenfassung

Copolykarbonate wurden durch Phosgenisierung von Gemischen von Chlorhydrochinon mit Hydrochinon, Toluhydrochinon, und 4,4′–Dihydroxydiphenylmethan in verschiedenem Verhältnis synthetisiert. Durch Röntgenbeugungsdiagramme und Schmelzpunkts–Zusammensetzungsdaten wurde festgestellt, dass die aus Hydrochinon-Chlorhydrochinonmischungen und Toluhydrochinon–Chlorhydrochinonmischungen hergestellten Copolymeren über den ganzen Zusammensetzungsbereich isomorph waren. Die Copolymerisation von 4,4′–Dihydroxydiphenylmethan und Chlorhydrochinon führte zu Produkten mit geringerer Kristallinität. Der Einfluss der Monomerstruktur auf die Gitterkonstanten der kristallinen Copolymeren wurde kurz untersucht.

Received March 21, 1962

JOURNAL OF POLYMER SCIENCE: PART A VOL. 1, PP. 1651–1669 (1963)

Radiation Degradation of Polymethacrylates. Dose Rate and Medium Effects*

A. R. SHULTZ, P. I. ROTH, and J. M. BERGE, *Central Research Department, Minnesota Mining and Manufacturing Company, St. Paul, Minnesota*

Synopsis

γ-Irradiations of polymethyl methacrylate (PMMA) powders confirm observations in literature that air retards the radiation-induced molecular weight lowering of this polymer. The energy absorptions per scission E_d are 91 e.v. in air at 0.117 Mreps/hr., 76 e.v. in air at 0.70 Mrep/hr., and 56 e.v. in vacuum at 0.117 Mrep/hr. γ-Radiation degradation of PMMA solutions (5 gm. PMMA/100 ml. solvent) in butanone and in ethyl acetate gave apparent energies per scission of 63 e.v. and 26–30 e.v., respectively. The latter low value is not understood. Poly-*n*-butyl methacrylate (PNBMA) displays considerable sensitivity to air and dose-rate effects during γ-irradiation. Apparent energy absorptions per main-chain scission observed for γ-irradiated PNBMA powder are: E_d = 454 e.v. in air at 0.117 Mrep/hr. and E_d = 226 e.v. in vacuum at 0.117 Mrep/hr. The latter value is far above the E_d (146 e.v.) observed for electron-irradiated PNBMA film. To decrease possible chain recombination and/or polymer–polymer crosslinking reactions degassed solutions of 4.5, 10.0, and 55 wt.-% PNBMA in ethyl acetate were γ-irradiated. Apparent E_d values of 74 e.v., 74 e.v., and 226 e.v., respectively were found. Thus, the more dilute solutions give PNBMA scission energies near that of bulk PMMA. The 55 wt.-% PNBMA solution gives a scission energy indistinguishable from that of bulk PNBMA under the same irradiation conditions. Competitive crosslinking and main-chain scission are postulated for electron-irradiated poly-*n*-alkyl methacrylates. The energy per main-chain scission is assumed constant for all the homologs. The ratio of crosslinked units to chain scissions, α/β, is then found to increase linearly with $(n-1)$, where n is the number of carbon atoms in *n*-alkyl groups of the side chain. This scheme yields a consistent explanation of the radiation response of the lower members of the poly-*n*-alkyl methacrylate homologous series. A comparison of light-scattering $\bar{M}_w$ and solution viscosity $(\bar{M}_w)_\eta$ molecular weight changes did not reveal the concurrent crosslinking in PNBMA films undergoing chain scission by 1 m.e.v.-peak electron irradiation. Some inquiry is made into the theoretical sensitivity of this comparison method.

INTRODUCTION

A previous publication reviewed studies prior to 1957 concerning ionizing radiation effects on polyacrylates and polymethacrylates.[1] Polymethacrylic esters of lower alkyl alcohols were found to undergo predominantly random main-chain scission reactions. Polymethacrylic esters of higher

* Presented in part at the 135th National Meeting of the American Chemical Society, Boston, Massachusetts, April 1959.

normal alkyl alcohols exhibited crosslinking reactions which overshadowed the main-chain scissions and yielded infinite networks. The present study investigates further the relative importance of main-chain scission and crosslinking reactions in polyalkylmethacrylates. It also inspects the effects of air and of low molecular weight diluents on these reactions. Dose rate dependence of the reactions and the cooperative influence of dose rate and medium variations are noted.

The main purpose of this study is to present and interpret new data pertinent to understanding ionizing radiation effects in some specific polyalkylmethacrylate systems.

EXPERIMENTAL

Materials

Two polymethyl methacrylate preparations were used in this study. PMMA I, thermally polymerized in bulk at 93°C. to 10.2% conversion, has been previously described.[2] PMMA IV was formed by the bulk polymerization at 37°C. of 300 ml. distilled monomer containing 1.098 g. azobisisobutyronitrile. One-third of the polymerizate was dissolved in 2150 ml. butanone and precipitated in 90:10 (by volume) methanol–water solutions. The polymer precipitate, after being allowed to stand 24 hr. in a fresh methanol–water mixture and the liquid decanted off, was dried under vacuum for 24 hr. at approximately 65°C.

A 300 ml. portion of *n*-butyl methacrylate (Monomer-Polymer Corp.) was further inhibited with phenyl-β-naphthylamine and distilled at 30 mm. Hg pressure and 72–74°C. through a Vigreaux column. Following a 30 ml. forerun takeoff, 250 ml. of monomer was collected, $n_D^{25} = 1.4215$; C = 67.5%, H = 9.6%; saponification number 142. Two Pyrex ampules, each containing 40 ml. monomer plus 0.080 g. azobisisobutyronitrile were degassed by freeze-thaw operations under vacuum. Polymerization was effected in 1.5 hr. under a G. E. sunlamp with air cooling. A thermal buildup must have occurred, yielding high conversion polymerization in this short period. The solid polymer was dissolved in acetone and precipitated in 90:10 methanol–water solution, steeped in methanol–water, dried under vacuum at room temperature for several hours, then dried under vacuum at 50°C. for 60 hr. The total yield was 69.2 g. This polymer is designated PNBMA-I.

The acetone, butanone, and benzene used were reagent grade, commercial solvents which were not subjected to further purification. Isopropanol was distilled through a glass helices-packed column and possessed a resultant refractive index n_D^{25} of 1.3747.

Irradiation

Two irradiation sources were used in this work. A G. E. resonant-transformer electron-beam generator[3,4] operating at 1000 kv. peak energy was employed to give high dose rate energy delivery to polymethacrylate

films in air. Films of PMMA-I and PNBMA-I were cast from butanone solution into steel ointment tins and air-dried. The films were transported through the beam by means of a horizontally traversing aluminum tray. The tray was cooled by internal water circulation. Maximum dose rate at the center of the beam in high current runs was 31 Mreps/min. (The term megarep is here used to represent the absorption of 5.24×10^{19} e.v. of beam energy/g. of irradiated polymer. A more consistent unit, 1 Mrad = 6.2×10^{19} e.v./g., is now becoming generally accepted.) A rather broad spectrum of electron energies is present in the beam. The dose rate varied as the polymer passed through the beam. The major fraction of the energy, however, was delivered at a dose rate exceeding 5 Mreps/min.

A Co^{60} pipe positioned in an irradiation facility very similar to one described in literature[5] was the γ-radiation source. Powdery or fibrous polymer samples in Pyrex glass ampoules or in glass screw-top vials were irradiated while spinning and orbiting around the pipe. The dose rate in the spinning positions was 0.117 Mrep/hr. as determined by ferrous–ferric ion dosimetry assuming $G = 15.3$ for the oxidation reaction. A dose rate of 0.70 Mrep/hr. was attained for samples in small-diameter ampules positioned inside the Co^{60} pipe at the center of the facility.

The polymer powder samples for γ-irradiation *in vacuo* were loaded into Pyrex ampules, held at 60°C. under oil-pump vacuum for 2 hr. after evacuation and flushing with prepurified nitrogen, and then sealed. This procedure reduces the oxygen concentration to a low value, but obviously does not entirely remove all air. The polymer solutions in butanone or ethyl acetate were deaerated by three successive freeze-thaw cycles under vacuum before sealing.

Solution Viscosity and Light-Scattering Measurements

Solution viscosities were measured in Cannon-Fenske capillary viscometers. Benzene at 25°C. was the viscosity solvent for PMMA-I and PMMA-IV. Butanone at 25°C. and isopropanol at 23°C. were viscosity solvents for PNBMA-I. The solutions were filtered through medium frit, sintered-glass filters. Polymer concentrations were chosen such that the relative flow times of solution to solvent lay in the range 1.1–1.5, except in a few high dose samples in which the η_{rel} were less than 1.1. No kinetic energy or shear corrections were applied to the data. When single concentration viscosity measurements were used the intrinsic viscosities, $[\eta]$, were calculated from the inherent viscosities, $\langle\eta\rangle = (\ln \eta_{rel})/c$, by the relations:

PMMA in benzene:

$$[\eta] = \langle\eta\rangle + 0.13\langle\eta\rangle^2 c \tag{1}$$

PNBMA in butanone:

$$[\eta] = \langle\eta\rangle + 0.10\langle\eta\rangle^2 c \tag{2}$$

PNBMA in isopropanol:

$$[\eta] = \langle\eta\rangle - 0.60\langle\eta\rangle^2 c \tag{3}$$

where $[\eta]$ is expressed in units of deciliters/gram.

The weight-average molecular weights of PMMA samples were calculated from the intrinsic viscosities in benzene by the equation[6]

$$\log \bar{M}_w = (4.102 + \log[\eta])/0.73 \tag{4}$$

Viscosity-average molecular weights, $\bar{M}_v$, for PNBMA samples were calculated from the relations:[7]

$$[\eta] = 1.56 \times 10^{-5} \bar{M}_v^{0.81} \tag{5}$$

$$[\eta] = 2.95 \times 10^{-4} \bar{M}_v^{0.50} \tag{6}$$

for butanone at 25°C. and isopropanol at 23°C., respectively.

To the approximation that these relations were established on monodisperse fractions and the PNBMA samples under present study are linear polymers possessing most probable distributions in molecular weight, the weight-average molecular weights are calculated for PNBMA by

$$(\bar{M}_w)_v = 1.047\ \bar{M}_v \tag{7}$$

$$(\bar{M}_w)_v = 1.137\ \bar{M}_v \tag{8}$$

for butanone at 25°C. and isopropanol at 23°C., respectively.

Isopropanol was the light-scattering solvent. The solutions were filtered through ultrafine sintered-glass filters using nitrogen pressure. Light-scattering measurements were made with a modified Debye instrument.[8] Nonpolarized 4358 A. light was employed. A solid glass cylinder was used as an operating turbidity standard. The primary reference standards were solutions of Cornell polystyrene (0.75% in butanone and 0.50% in toluene) for which the absolute turbidity values of Carr and Zimm were accepted.[9] A refractive index increment $dn/dc = 0.102$ cm.^{3}/g. was used for the PNBMA-I solutions in isopropanol.[7] Scattering was observed at eight angles in the range 40° to 135° off the direction of the incident beam. Three to six concentrations of each polymer sample were studied.

RESULTS AND DISCUSSION

I. Polymethyl Methacrylate

Table I lists the doses, intrinsic viscosities in benzene, and calculated weight-average molecular weights of the PMMA-I powder γ-irradiated in air and under vacuum. Figure 1 presents the data as plots of $10^6/\bar{M}_w$ versus dose R. Each set of points is satisfactorily approximated by a straight line representing direct proportionality of random main-chain scissions to the radiation dose. The total energy absorptions per chain scission, E_d, are calculated from the slopes of the lines in Figure 1 by eq. (9):

$$10^6/\bar{M}_w = 10^6/\bar{M}_{w_0} + 10^6(5.24 \times 10^{19}/2 \times 6.02 \times 10^{23})(R/E_d) \tag{9}$$

TABLE I
γ-Irradiated Polymethyl Methacrylate, PMMA-I Powder

	Dose rate, Mrep/hr.	Dose, Mrep	$[\eta]$, dl./g.	$\bar{M}_w \times 10^{-6}$
In vacuum	0.117	0	4.42	31.9
		0.97	1.66	8.3
		2.61	0.955	3.91
		5.35	0.611	2.11
		8.25	0.451	1.40
In air	0.117	0.66	2.52	14.7
		1.21	2.00	10.8
		1.87	1.61	8.0
		2.40	1.34	6.2
		3.87	1.04	4.39
		4.62	0.95	3.91
		5.57	0.84	3.25
		8.78	0.622	2.17
		9.18	0.545	1.81
		10.4	0.507	1.64
		12.6	0.436	1.33
In air	0.70	1.65	1.59	7.85
		2.80	1.12	4.85
		11.3	0.438	1.34
		30.5	0.202	0.465
		48.8	0.132	0.260

The calculated E_d are 91 e.v. in air at 0.117 Mrep/hr. dose rate, 76 e.v. in air at 0.70 Mrep/hr. dose rate, and 56 e.v. in vacuum at 0.117 Mrep/hr. dose rate. The latter value is comparable to the values 59 e.v. found for electron-irradiated film in air,[2] and 60–61 e.v. found for γ-irradiated solid rods in air.[10] Thus, in the absence of readily accessible oxygen, the efficiency of degrading PMMA by ionizing radiations appears independent of dose rate. The electron irradiations were so rapid that air replenishment in the moderately thick films was negligible. Similarly, in the massive polymer rods undergoing γ-irradiation in a pile, air accessibility appears to have been negligible. However, irradiation of the PMMA powder in air at different dose rates does reveal a dose-rate dependence. The energy absorbed per stabilized main-chain scission is greater at the lower dose rate than it is at the higher dose rate. The presence of air decreases the apparent scission efficiency. This "protection" has been tentatively ascribed to the bridging of incipient break points by oxygen to form moderately stable peroxide links within the chain backbone.[11] An equally plausible explanation is a crosslinking reaction involving oxygen. This crosslinking would not need to be associated with the scission sites. The difficulty of explaining rapid diffusion of oxygen to incipient break points would then not arise.

Previous studies have shown that no crosslinking of polymethyl methacrylate by ionizing radiation is detectable. This should therefore mean that the chain scission efficiency as measured by solution viscosity molecular

weights is valid. If the main-chain scissions result from the primary interaction of ionization tracks or spurs with the polymer chains, the effect of a surrounding solvent should be the same ast hat of contiguous polymer

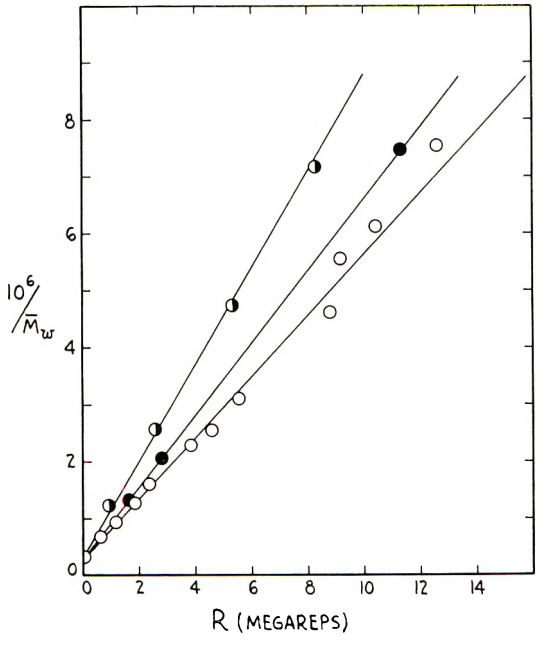

Fig. 1. Reciprocal weight-average molecular weights of γ-irradiated polymethyl methacrylate powder (PMMA-I): (◑) in vacuum, 0.117 Mrep/hr.; (○) in air, 0.117 Mrep/hr.; (●) in air, 0.70 Mrep/hr.

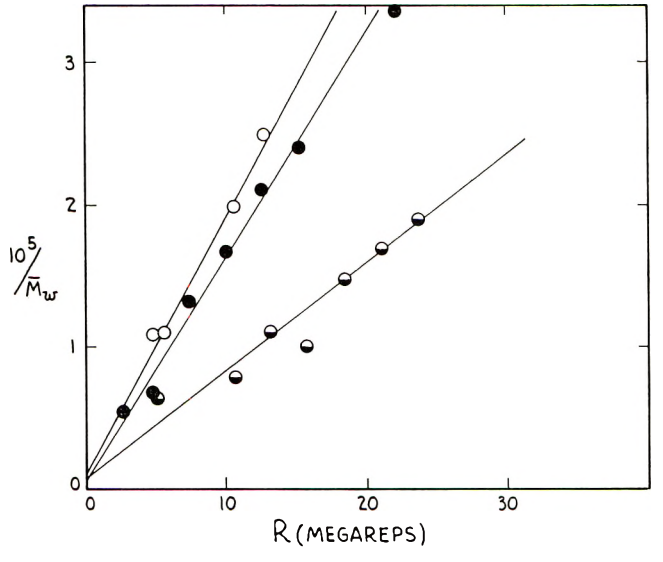

Fig. 2. Reciprocal weight-average molecular weights of PMMA-IV γ-irradiated in (○, ●) ethyl acetate solution and (◒) butanone solution.

TABLE II
Intrinsic Viscosities in Benzene at 25°C. of PMMA-IV γ-Irradiated in Solutions

Butanone solutions		Ethyl acetate solutions	
Dose, Mrep	$[\eta]$, dl./g.	Dose, Mrep	$[\eta]$, dl./g.
0	1.83	0	1.83
5.1	0.485	2.6	0.556
10.6	0.420	4.7	0.470
13.1	0.326	7.3	0.288
15.7	0.353	10.0	0.243
18.4	0.265	12.5	0.205
21.0	0.240	15.1	0.186
23.6	0.221	22.0	0.146
		0	1.83
		4.7	0.336
		5.6	0.330
		10.5	0.214
		12.6	0.181
		20.2	0.143
		28.1	0.108

chains. Deaerated polymethyl methacrylate solutions (5.00 g. PMMA-IV/100 ml. solvent) in butanone and in ethyl acetate were γ-irradiated (0.117 Mrep/hr.) to determine the chain scission efficiency in solvents having free radical yields comparable to PMMA. The results are given in Table II. Calculation of $\bar{M}_w$ for the irradiated polymer samples by eq. (4) leads to the plot (Fig. 2) of $10^6/\bar{M}_w$ versus R for the butanone solution series and the two ethyl acetate solution series.

The data for PMMA-IV γ-irradiated in butanone solution (Fig. 2) are satisfactorily represented by a straight line having a slope corresponding to $E_d = 63$ e.v. [cf. eq. (9)]. The experimental scatter may be due partly to differing efficiencies in air removal from the individual ampules. The observed value of E_d for PMMA-IV in butanone is comparable to the $E_d = 56$ e.v. found for *in vacuo* γ-irradiated solid PMMA-I and to the earlier values for solid PMMA under ionizing radiation. It would therefore appear to substantiate the belief that crosslinking is nonexistent in the solid polymer undergoing irradiation. Also, the essential radiation response equivalence of butanone to PMMA as a surrounding medium is suggested.

The data for the two series of γ-irradiated PMMA-IV in ethyl acetate solution (Fig. 2) yield apparent scission energies $E_d = 26$ e.v. and 30 e.v. These runs are experimentally identical except for a separation of a few months between their study. The low E_d values are surprising in the light of the butanone solution results. Ethyl acetate, being an alkyl ester of an aliphatic acid, was expected to resemble PMMA in radiation response. An earlier study involving γ-irradiation of PMMA solutions in oxygen-free ethyl acetate yielded $E_d = 83$ e.v./scission based on the energy absorbed

by the polymer molecules.[12] The presence of oxygen in the PMMA–ethyl acetate solutions increased E_d (apparent) to 100 e.v./scission. The cause of the low value we observe is not understood at present.

The complexity of reaction possibilities in polymer–solvent systems under irradiation should not be underestimated. Direct and indirect action of the radiation upon the polymer must be recognized and analyzed if possible. Early work of Wall and Magat[13,14] indicated the importance of solvent and additives to the gamma and neutron radiation response of polymers. Extensive experimental studies of γ-irradiation of polymethyl methacrylate in several solvents have been reported.[12,15] Apparent E_d values were calculated on the basis of energy absorbed directly by the PMMA. In oxygen-free solutions (15 g. PMMA/l.) at 1.5×10^5 rad/hr. dose rate benzene provided the highest apparent E_d medium and carbon tetrachloride the lowest. These also held the extreme positions in the presence of oxygen where in benzene E_d (apparent) rose from 210 e.v. to 770 e.v. while in carbon tetrachloride E_d (apparent) dropped from 16 e.v. to 5 e.v. The latter solvent yields chlorine atoms which readily attack the PMMA. In the presence of oxygen an oxidative chain reaction is also possible in this solvent.

Considering energy transfer from polymer to solvent as a degradation-deactivating mechanism an attempt was made to correlate PMMA protection with the long wavelength ultraviolet light absorption edge character of the solvent.[12] This correlation appears weak due to specific interactions of solvent decomposition fragments with the PMMA. Attachments of iodine and of diphenylpicrylhydrazyl to PMMA during radiation in solution occurred in numbers 10 times and 70 times, respectively, the number of chain breaks observed.[15] These numerous free radical sites on the polymer chains would provide many potential locations for competitive crosslinking reactions. Elevated apparent E_d values under certain conditions could then be expected.

II. Poly-*n*-butyl Methacrylate

Poly-*n*-butyl methacrylate was chosen for study as a polymer predominantly degraded by ionizing radiations, but suspected of some concurrent crosslinking.

Table III presents data for PNBMA γ-irradiated at 0.117 megarep/hour as powder in vacuum, as powder in air, and as 55, 10, and 4.5 wt.-% polymer solutions in deaerated ethyl acetate. The intrinsic viscosities of the original and irradiated polymer samples were measured in butanone at 25°C. The weight-average molecular weights, $(\bar{M}_w)_v$, were calculated from these viscosities by use of eqs. (5) and (7) applicable to linear PNBMA samples having the most probable molecular weight distribution. Plots of the reciprocal of $(\bar{M}_w)_v$ thus obtained versus the radiation doses for the five PNBMA systems listed in Table III are shown in Figure 3. Table IV presents the apparent energy absorptions per main-chain scission, E_d

TABLE III
Intrinsic Viscosities in Butanone at 25°C. of γ-Irradiated Poly-*n*-butyl Methacrylate, PNBMA-I; Dose rate 0.117 Mrep/hr.

	Dose, Mrep	$[\eta]$, dl./g.	$(M_w)_v \times 10^{-5}$
Powder in vacuum	0	0.64	5.2
	0.47	0.594	4.7
	1.31	0.564	4.4
	2.19	0.529	4.1
	3.16	0.494	3.8
	4.03	0.476	3.6
	5.00	0.445	3.3
	5.34	0.439	3.3
	5.96	0.421	3.1
	6.84	0.412	3.0
	8.15	0.386	2.8
Powder in air	2.79	0.551	4.3
	4.67	0.514	4.0
	7.48	0.487	3.7
	10.7	0.426	3.1
	13.5	0.425	3.1
	14.6	0.410	3.0
55 wt.-% in EtOAc	0.47	0.585	4.7
	1.31	0.570	4.5
	2.66	0.533	4.2
	4.87	0.446	3.3
10.0 wt.-% in EtOAc	0.44	0.565	4.8
	0.79	0.525	4.1
	1.27	0.472	3.6
	1.99	0.417	3.1
	2.34	0.394	2.9
	2.82	0.369	2.6
4.5 wt.-% in EtOAc	0.78	0.510	3.9
	1.58	0.449	3.4
	2.35	0.397	2.9
	3.86	0.334	2.3

(apparent), calculated from the slopes of these lines [cf. eq. (9)]. The E_d (apparent) values for PMMA are also listed.

The high E_d (apparent) = 454 e.v./scission found for the γ-irradiated PNBMA powder in air shows here, as in PMMA, that the presence of air decreases the net scission efficiency. E_d (apparent) for the PNBMA powder in vacuum is 226 e.v./scission. If the total "protection" of polymethacrylates by air is due to oxygen bridging of incipient chain breaks, the bridging is more efficient in PNBMA than in PMMA. Otherwise oxygen-assisted crosslinking is greater in PNBMA. One is also forced to conclude that the presence of air in the PNBMA does not diminish the postulated crosslinking reaction of the pure polymer (cf. seq.).

At present the only obvious explanation available for the difference in E_d (apparent) of the *in vacuo* γ-irradiated PNBMA powder (226 e.v./

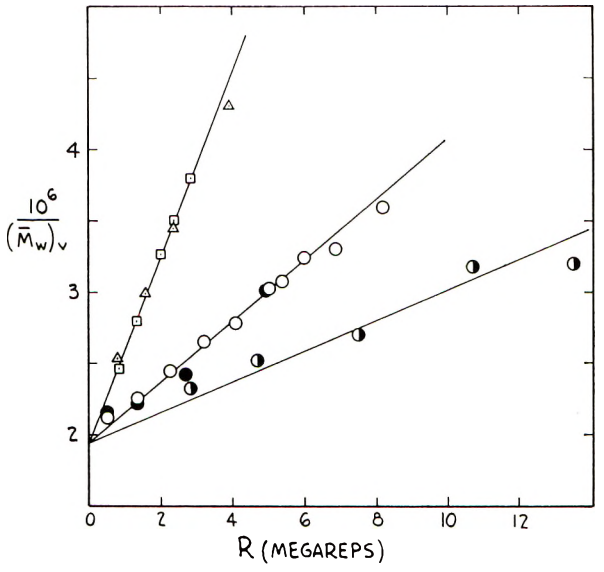

Fig. 3. Reciprocal weight-average molecular weights (by solution viscosity) of γ-irradiated poly-*n*-butyl methacrylate PNBMA: (◑) powder in air; (○) powder in vacuum; (●) 55% in ethyl acetate; (□) 10% in ethyl acetate; (△) 4.5% in ethyl acetate.

scission) and electron-irradiated film (146 e.v./scission)[1] is invocation of dose rate dependence of the scission and/or crosslinking reactions in the solid polymer. We cannot exclude the possibility that slight residual air is preventing the further lowering of the PNBMA E_d (apparent) from 226 e.v./scission to 146 e.v./scission. The air effect on E_d (apparent) in PMMA was only a matter of 91 − 56 = 35 e.v. The air effect under similar conditions

TABLE IV

Apparent Energy Absorptions per Chain Scission in Polymethyl Methacrylate and Poly-*n*-butyl Methacrylate. Radiation Type, Dose Rate, and Environment Effects

Polymer	Radiation type	Dose rate, Mrep/hr.	Environment	E_d (apparent), e.v./scission
PMMA	Co^{60}, γ	0.117	Powder in air	91
	Co^{60}, γ	0.70	Powder in air	76
	Co^{60}, γ	0.117	5 g./100 ml. butanone	63
	1000kvp.electrons	~1800	Film in vacuum	59
	Co^{60}, γ	0.117	Powder in vacuum	56
	Co^{60}, γ	0.117	5 g./100 ml. EtOAc	26–30
PNBMA	Co^{60}, γ	0.117	Powder in air	454
	Co^{60}, γ	0.117	Powder in vacuum	226
	Co^{60}, γ	0.117	55:45 PNBMA–EtOAc	226
	1000kvp.electrons	~1800	Film in air	146
	Co^{60}, γ	0.117	10:90 PNBMA–EtOAc	74
	Co^{60}, γ	0.117	4.5:95.5 PNBMA–EtOAc	74

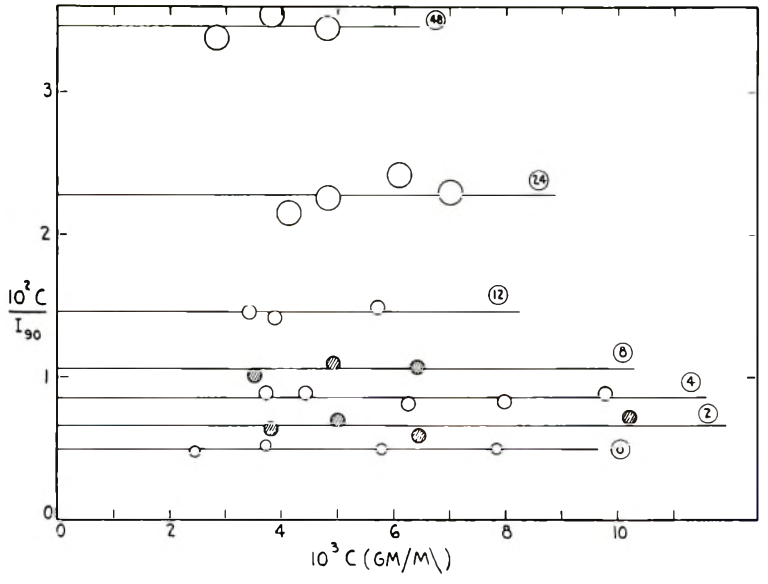

Fig. 4. Light-scattering in isopropanol at 90° angle of γ-irradiated PNBMA at 23°C., 4358A wavelength. Concentration-to-scattered intensity ratio (arbitrary units) vs. concentration.

for PNBMA has already amounted to 454 − 226 = 228 e.v. at the degree of experimental refinement employed. A further 226 − 146 = 80 e.v. lowering upon rigorous outgassing of the PNBMA powder is conceivable.

The possibility of suppressing polymer-to-polymer crosslinking by the addition of a chemically similar diluent prompted the γ-irradiation of the three PNBMA–ethyl acetate solutions. The 55:45 (by weight) PNBMA–ethyl acetate solution exhibited an E_d (apparent) of 226 e.v./scission, which is identical to that of the PNBMA powder under similar conditions. Both the 10 and 4.5 wt.-% PNBMA solutions had E_d (apparent) = 74 e.v./scission. This approaches the PMMA E_d = 56–61 e.v./scission and strengthened our belief that the true main-chain scission efficiencies of PNBMA and PMMA are equal.

An interesting sidelight on the concentration dependence of E_d (apparent) in the PNBMA–ethyl acetate solutions is provided by proton magnetic resonance measurements on PNBMA–chloroform solutions.[16] An abrupt line-width broadening is observed for the —O—CH_2— proton resonance as the PNBMA concentration is increased in the region of about 33 vol.-% polymer. Upon admittedly tenuous evidence we ascribe this broadening to the onset of pronounced polymer side-chain mobility hindrance with increasing polymer concentration. The transition from E_d (apparent) = 74 e.v./scission at 4.5 and 10 wt.-% PNBMA in ethyl acetate solution to E_d (apparent) = 226 e.v./scission at 55 wt.-% PNBMA may well be associated with this change in side-chain mobility. Another explanation for the E_d (apparent) increase with increasing polymer concen-

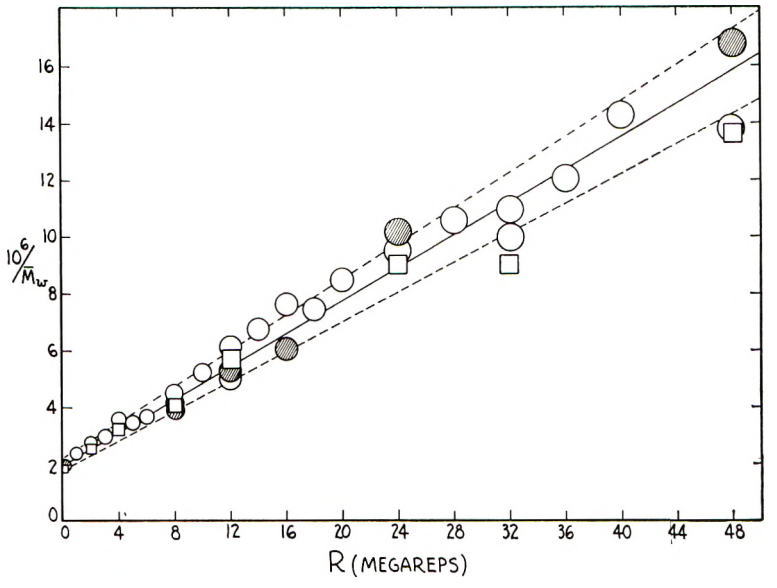

Fig. 5. Reciprocal weight-average molecular weight vs. radiation dose for γ-irradiated PNBMA: (○) butanone viscosity data; (●) isopropanol viscosity data; (□) light-scattering data.

tration is the collisional probability favoring polymer–polymer linking reactions relative to polymer–solvent combination reactions. Normally, the suppression of interpolymer crosslinking and encouragement (relatively) of intrapolymer chain crosslinking has been found to become important only at polymer concentrations considerably lower than those employed in this series.[17]

Detection of crosslinking in electron-irradiated PNBMA was attempted by comparing weight-average molecular weights, $\bar{M}_w$, calculated from light-scattering data with weight-average molecular weights, $(\bar{M}_w)_v$, calculated from solution viscosity data. The light-scattering measurements were made in the theta-solvent isopropanol at 23°C. Figure 4 shows the ratio of concentration to scattered light intensity at 90° angle plotted against concentration for the original and six electron-irradiated PNBMA samples. The independence of c/I_{90} on concentration and the low angular dissymmetry of scatter in the theta-solvent both aided in data extrapolations to zero angle and zero concentration for $\bar{M}_w$ calculation. Solution viscosities on these and several other irradiated samples were run in isopropanol and in butanone. $(\bar{M}_w)_v$ values were calculated from these viscosities by eqs. (2), (3), (5), (6), (7), and (8) as applicable.

The corrections from inherent viscosity $\langle\eta\rangle = (\ln \eta_{rel})/c$ to intrinsic viscosity $[\eta]$ were not large in the concentration range employed. The relations of $(\bar{M}_w)_v$ to $\bar{M}_v$ here assume that the viscosity-molecular weight relations were established on sharp fractions, and that the original and irradiated PNBMA in the present study are linear polymers having most

TABLE V
Light-Scattering and Viscosity Data on Electron-Irradiated Poly-*n*-butyl Methacrylate, PNBMA-I

Dose, Mrep	Light scattering $\bar{M}_w \times 10^{-5}$	In butanone, 25°C.		In isopropanol, 23°C.	
		$[\eta]$, dl./g.	$(M_w)_v \times 10^{-5}$	$[\eta]$, dl./g.	$(M_w)_v \times 10^{-5}$
0	5.5	0.64(0.61)	5.2(4.9)	0.202	5.3
1		0.544	4.3		
2	4.0	0.493	3.8		
3		0.457	3.4		
4	3.1	0.416	3.05		
5		0.403	2.93		
6		0.378	2.7		
8	2.44	0.316(0.324)	2.2(2.24)	0.138(0.140)	2.5(2.6)
10		0.286	1.92		
12	1.76	0.264(0.252)	1.47(1.64)	0.120	1.89
14		0.231	1.49		
16		0.209	1.31	0.113	1.67
18		0.214	1.34		
20		0.193	1.18		
24	1.11	0.188	1.14	0.087	0.99
28		0.162	0.95		
32	1.11	0.170(0.157)	1.01(0.92)		
36		0.145	0.83		
40		0.127	0.71		
48	0.735	0.131	0.73	0.068	0.60
72		0.104	0.55		

probable molecular weight distributions. The failure of the linear chain and fixed molecular weight distribution assumptions for the irradiated polymer was the basis upon which crosslinking detection was attempted.

Table V presents the results of the light-scattering and viscosity studies of electron-irradiated PNBMA. Figure 5 is a plot of these $1/\bar{M}_w$, and $1/(\bar{M}_w)_v$ versus radiation dose. A fair amount of experimental scatter is observed. No distinct progressive divergence of the $1/(\bar{M}_w)_v$ from the $1/\bar{M}_w$ values with increasing radiation dose is detectable. Crosslinking should cause the $1/(\bar{M}_w)_v$ values to increase more with increasing R than the $1/\bar{M}_w$ values. Here, as in the earlier study of PMMA,[2] this divergence of $1/(\bar{M}_w)_v$ and $1/\bar{M}_w$ is not evident. Crosslinking concurrent with chain scission in PNBMA under ionizing radiation is not proven by these results. The expected sensitivity of the light-scattering plus solution viscosity comparison test for PNBMA crosslinking will be mentioned in the concluding section of this paper.

III. Crosslinking in Poly-*n*-Alkyl Methacrylates

It is appropriate that we now examine the reasons for our belief that the lower *n*-alkyl methacrylate polymers are undergoing crosslinking reactions under ionizing radiation treatment.

If main chain scissions and polymer–polymer crosslinks are both propor-

tional to absorbed radiant energy R, an irradiated polymer should exhibit the following reciprocal weight-average molecular weight relation:

$$1/\bar{M}_w = (1/\bar{M}_{w0}) + [(1/2E_d) - (1/E_c)](R/\tilde{N})$$
$$= (1/\bar{M}_{w0}) + R/2\tilde{N}E_d \text{ (apparent)} \quad (10)$$

$$1/E_d \text{ (apparent)} = (1/E_d)(1 - 2\alpha/\beta) \quad (11)$$

where R is expressed in electron volts per gram, $\tilde{N}$ is Avogadro's number, $\bar{M}_w$ is the weight-average gram molecular weight, E_c is the energy absorption in electron volts per crosslinked unit (one-half crosslink) formation, and $\alpha/\beta = E_d/E_c$ is the ratio of radiation-induced crosslinked units to radiation-induced main-chain scissions in the polymer. The equations assume a most probable distribution of molecular weights in the original, nonirradiated polymer. Light-scattering molecular weight measurements will therefore yield an E_d (apparent) value which will differ from the true E_d value for an irradiated polymer by the factor $(1 - 2\alpha/\beta)^{-1}$.

E_d (apparent) values have been calculated as 59 e.v./scission for PMMA (light scattering and viscosity data),[2] 75 e.v./scission for polyethyl methacrylate (PEMA) (viscosity data),[1] and 146 e.v./scission for PNBMA (light scattering and viscosity data) for electron-irradiated films. Let us assume that all poly-*n*-alkyl methacrylates have the same total energy absorption, $E_d = 59$ e.v., per main-chain scission. From the above E_d (apparent) values and eq. (11) we calculate $\alpha/\beta = 0$, 0.107, and 0.298 for PMMA, PEMA, and PNBMA, respectively. A plot of these α/β against the number of carbon atoms in the sidechain alkyl group is shown in Figure 6. The three points lie approximately on a straight line which we arbitrarily extrapolate into the higher *n*-alkyl group region. The linearity suggests that the probability of crosslinking is directly proportional to the number of methylene groups in the sidechain alkyl group. We postulate that these are crosslinking sites. This proportionality must eventually fail. As the side chain becomes longer, the average composition of the polymethacrylate approaches that of polymethylene, and E_c must approach the constant value characteristic of polymethylene.

Interesting predictions may be made on the basis of Figure 6. E_d (apparent) for electron-irradiated poly-*n*-propyl methacrylate and poly-*n*-pentyl methacrylate should be 98 e.v./scission and 295 e.v./scission, respectively, when measured by light-scattering molecular weight change. $\alpha/\beta = 0.5$ is the critical ratio for crossover from predominant main-chain scission to predominant crosslinking. Poly-*n*-hexyl methacrylate lies so close to this crossover (Fig. 6) that it is not possible to say with assurance whether or not infinite network formation (partial insolubilization) should occur in it. This polymer should exhibit nearly constant $\bar{M}_w$ under electron bombardment and exhibit a slowly decreasing intrinsic viscosity. Poly-*n*-heptyl methacrylate should be the lowest member of this homologous series to yield an infinite network under electron irradiation. Previous to the construction of Figure 6 it was found that electron-irradiated poly-

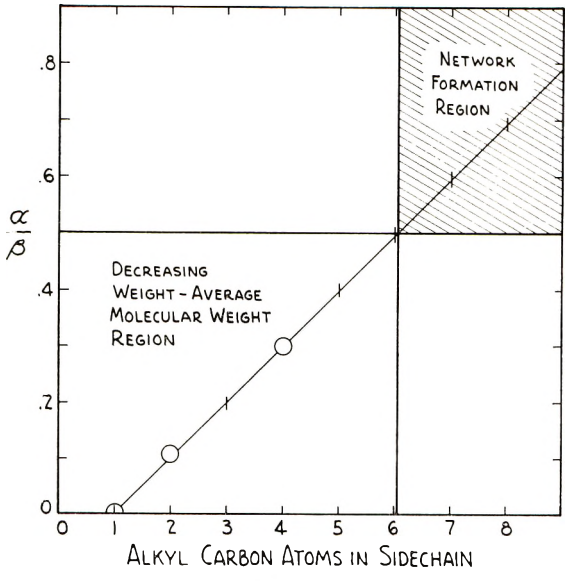

Fig. 6. Ratio of crosslinked units to chain scissions, α/β, of lower n-alkyl methacrylates vs. the number of alkyl carbon atoms. Electron-irradiated films.

dodecyl methacrylate and polyoctadecyl methacrylate formed infinite networks.[1] Subsequent to the construction of Figure 6, Graham[18] reported that poly-n-heptyl methacrylate ($[\eta]_0$ = 1.52 in benzene) was partially insolubilized by 15 Mreps of γ-irradiation at 23°C. No insoluble polymer was found in poly-n-hexyl methacrylate ($[\eta]_0$ = 1.2 in benzene) when γ-irradiated to 30 Mreps at 23°C. Our assumption of constant E_d and decreasing E_c with increasing n-alkyl chain length in the poly-n-alkyl methacrylates is experimentally supported, but not proven.

The observation that *sec*-heptyl, *sec*-octyl and *sec*-nonyl methacrylate polymers and also poly-2-ethylhexyl methacrylate fail to gel under fairly high γ-radiation doses is instructive.[18] In polyalkyl acrylates both the backbone α-hydrogens and the sidechain carbinol carbon hydrogens appear to contribute (possibly independently) to crosslinking. In the polyalkyl methacrylates the latter only of these two types is available and their obstruction takes on a much greater importance in crosslinking probability. This importance was further demonstrated in the aryl and alkaryl methacrylate and acrylate polymer irradiation studies.[19]

The correlation of the crosslinkability of a polymer under irradiation with its graftability under radiation in the presence of a monomer is evident in the experiments of Graham, Gluckman, and Kampf,[20] although they fail to register complete comprehension of the interplay. The confusing element was the ready graftability of *sec*-alkyl methacrylate polymers to monomers although they exhibit greatly impeded crosslinkability relative to their n-alkyl counterparts. This remains an observation requiring further clarification. It is conceivable that the steric hindrance to crosslink-

ing caused by the branch is more pronounced than steric hindrance to polymerization initiation by the same radical. The combination of two tertiary radicals to form the structure

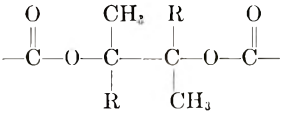

would seem to involve some difficulty. The failure of polymethyl methacrylate and poly-*tert*-butyl methacrylate to serve as graft substrates is an important observation.[20] We suggest that the grafting of monomer occurs at sites which are potential crosslinking sites and not at chain-rupture sites. The grafts thus formed should be of the trifunctional branch type

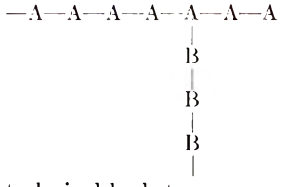

rather than of the straight-chain block type

If our suggestion has merit, an extremely short lifetime of radicals created by main-chain scission is indicated. This supports an instantaneous, "concerted" mechanism or molecular disproportionation mechanism of chain cleavage.[1]

Finally let us inspect briefly the degree of sensitivity which one should expect in detecting crosslinking by molecular weight and solution viscosity comparisons. An approximate combination of existing radiation, branching, and solution viscosity theories to predict viscosity behavior of polymers undergoing concurrent crosslinking and scission was made several years ago.[2] It correctly indicated some of the gross features to be expected and anticipated the possibility of solution viscosity decrease during the approach to gelation of a polymer. By joining existing theories in a nonrigorous fashion it overestimated the viscosity depression due to branched chain structures at high extents of branching. A more thorough and self-consistent development of branched-polymer solution viscosity theory has recently appeared.[21,22] Its application to irradiated polymer systems[23] offers a framework which should more nearly approximate reality than have previous theoretical constructions.

A polymer undergoing random crosslinking and main-chain scission during irradiation exhibits diminishing primary chainlength, branched molecule buildup and a broadening of the molecular weight distribution. The number of crosslinked units per instantaneous primary weight-average molecule, δ''(called γ' by Kilb[23]), is given by

$$\begin{aligned} \delta'' &= (R/R^*)/\{1 - (\beta/2\alpha)[1 - (R/R^*)]\}, \quad \delta'' < 1 \\ &= R/[(\bar{N}E_c/\bar{M}_{w_0}) + (\beta/2\alpha)R], \qquad \delta'' < 1 \end{aligned} \tag{12}$$

If α/β is less than 0.5, it is seen that δ'' will approach the limiting value $2\alpha/\beta$ as R approaches infinity. The number of crosslinked units per primary weight-average molecule is then restricted to $0 \leq \delta'' \leq 2\alpha/\beta$. The two above-mentioned treatments of the intrinsic viscosities of irradiated polymers allow calculation of a ratio $[\eta]$ (branched)/$[\eta]$(linear) for each R and corresponding $\bar{M}_w = \bar{M}_{w_0}[1 - (R/R^*)]^{-1}$. An apparent weight-average molecular weight is calculated from the observed intrinsic viscosity $(\bar{M}_w)_v = K^{-1/a}[\eta]^{1/a}$. From δ'' and the derived relations, a theoretical ratio of $\bar{M}_w/(\bar{M}_w)_v$ is calculated for each dose R.

Let us assume for poly-*n*-butyl methacrylate that $\alpha/\beta = 0.298$, $E_c = (\beta/\alpha)E_d = 59/0.298 = 198$ e.v./crosslinked unit. The equations for $10^6/\bar{M}_w$ and δ'' then become

$$10^6/\bar{M}_w = 1.83 + 0.298R \tag{13}$$

$$\delta'' = R/(4.16 + 1.68\,R) \tag{14}$$

R is here expressed in megarep units. Table VI lists calculated $10^6/\bar{M}_w$ and δ'' for the poly-*n*-butyl methacrylate PNBMA-I samples studied. The theoretical ratios of true weight-average molecular weights to weight-average molecular weights calculated from solution viscosities by the earlier (SRR) and more recent (K) treatments are given in the last two columns. Although the SRR calculation overestimates the influence of branching on the solution viscosity at high δ'', the Kilb (K) calculation predicts a greater depression of $(\bar{M}_w)_v$ below $\bar{M}_w$ in the δ'' region covered. This presumably results from inclusion of the molecular weight distribution broadening effect in the K treatment. Table VI predicts a spread between $1/\bar{M}_w$ and $1/(\bar{M}_w)_v$ of 23.4% (SRR) or 35.4% (K) at 48 Mreps for this PNBMA.

TABLE VI

R, Mrep	$10^6/\bar{M}_w$	δ''	$\bar{M}_w/(\bar{M}_w)_v$ SRR	$\bar{M}_w/(\bar{M}_w)_v$ K[a]
0	1.83	0	1.000	1.000
4	3.02	0.368	1.101	1.171
8	4.21	0.455	1.143	1.236
16	6.6	0.515	1.187	1.292
32	11.4	0.552	1.222	1.337
48	16.1	0.566	1.234	1.354
(∞)	—	0.596	1.264	1.395

[a] We assume $\langle[\eta]_{br}\rangle/\langle[\eta]_l\rangle$ for $a = 0.81$ is equal to that for $a = 0.68$ when $\delta'' = 0.596$; cf. ref. 22, Table III.

These predicted deviations should be sufficient for experimental observation, Failure to observe these deviations leaves our interpretation of the lower poly-*n*-alkyl methacrylate radiation response, which assumes constant E_d and decreasing E_c with increasing sidechain length, still open to criticism.

References

1. Shultz, A. R., *J. Polymer Sci.*, **35**, 369 (1959).
2. Shultz, A. R., P. I. Roth, and G. B. Rathmann, *J. Polymer Sci.*, **22**, 495 (1956).
3. Charlton, E. E., and W. F. Westendorp, *G. E. Rev.*, **44**, 652 (1941).
4. Lawton, E. J., W. D. Bellamy, R. E. Hungate, M. P. Bryant, and E. Hall, *Tappi*, **34**, 113A (Dec. 1951).
5. Blomgren, R. A., E. J. Hart, and L. S. Markheim, *Rev. Sci. Instr.*, **24**, 298 (1953).
6. Hecht, C. E., and R. L. Cleland, Massachusetts Institute of Technology, unpublished data.
7. Chinai, S. N., and R. A. Guzzi, *J. Polymer Sci.*, **21**, 417 (1956).
8. Debye, P. J., *J. Appl. Phys.*, **17**, 392 (1946).
9. Carr, C. I., Jr., and B. H. Zimm, *J. Chem. Phys.*, **18**, 1616 (1950).
10. Alexander, P., A. Charlesby, and M. Ross, *Proc. Roy. Soc.* (*London*), **A223**, 393 (1954).
11. Wall, L. A., and D. W. Brown, *J. Phys. Chem.*, **61**, 129 (1957).
12. Henglein, A., C. Schneider, and W. Schnabel, *Z. Physik. Chem.* (*Frankfurt*), **12**, 339 (1957).
13. Wall, L. A., and M. Magat, *Mod. Plastics*, **30**, 111 (July 1953).
14. Wall, L. A., and M. Magat, *J. Chim. Phys.*, **50**, 308 (1953).
15. Henglein, A., M. Boysen, and W. Schnabel, *Z. Physik. Chem.* (*Frankfurt*), **10**, 137 (1957).
16. Unpublished data, This Laboratory.
17. Charlesy, A., *Atomic Radiation and Polymers*, International Series on Radiation Effects in Materials, Pergamon, New York, 1960, Chap. 25.
18. Graham, R. K., *J. Polymer Sci.*, **38**, 209 (1959).
19. Graham, R. K., *J. Polymer Sci.*, **37**, 441 (1959).
20. Graham, R. K., M. S. Gluckman, and M. J. Kampf, *J. Polymer Sci.*, **38**, 417 (1959).
21. Zimm, B. H., and R. W. Kilb, *J. Polymer Sci.*, **37**, 19 (1959).
22. Kilb, R. W., *J. Polymer Sci.*, **38**, 403 (1959).
23. Kilb, R. W., *J. Phys. Chem.*, **63**, 1838 (1959).

Résumé

Des irradiations γ de poudres de polymethacrylate de méthyle (PMMA) confirment les observations de la littérature admettant que l'air retarde l'abaissement de poids moléculaire de ce polymère induit par radiation. Les absorptions d'énergie par scission, E_d, sont de 91 e.v. dans l'air, à 0.117 megareps par heure, 76 e.v. dans l'air à 0.70 mégareps par heure et de 56 e. v. sous vide à 0.117 mégareps par heure. La dégradation par radiation γ de solutions de PMMA (50 g. PMMA/100 ml. de solvant) dans la butanone et dans l'acétate d'éthyle donnent des energies apparentes par scission de 63 e. v. et 26–30 e.v. respectivement. Cette dernière basse valeur n'est pas interpretée. Le polyméthacrylate de *n*-butyle (PNBMA) manifeste une sensibilité considérable à l'air et aux effets d'intensité et de vitesse durant l'irradiation γ. Les absorptions apparentes d'énergie pour une scission de chaîne principale observées pour des poudres de PNBMA obtenues par irradiation γ sont de: E_d = 454 e.v. dans l'air à 0.117 mégarep par heure et de E_d = 226 e.v. sous vide à 0.117 mégarep par heure. Cette dernière valeur est de loin supérieure à celle (146 e.v.) observée pour un film de PNBMA irradié électroniquement. Pour diminuer la recombinaison possible de chaîne et/ou les réactions de pontage polymère–polymère, des solutions dégazées do 4,5, 10 et 55% en poids de PNBMA dans l'acétate d'éthyle ont été soumises à l'irradiation γ. On a respectivement trouvé des valeurs apparentes E_d de 74 e.v., 74 e.v., et 226 e.v. Ainsi donc, les solutions plus diluées donnent des énergies de scissions pour le PNBMA proches de celles du PMMA en bloc. La solution à 55% en poids de PNBMA donne une énergie de scission indéterminable à

partir de celle du PNBMA dans les mêmes conditions d'irradiation. Il a été envisagé une compétition entre le pontage et la scission de la chaîne principale pour les polyméthacrylates de *n*–alcoyle. L'énergie de scission de la chaîne principale est considéré comme constante pour tous les homologues. On a trouvé en outre que le rapport des unités pontées aux scissions de chaîne α/β augmente linéairement avec $(n-1)$ ou n est le nombre d'atomes de carbone dans les groupes alcoyles normaux de la chaîne latérale. Ce schéma donne une explication valable de la réaction des plus bas éléments des séries homologues de polyméthacrylate de *n*-alcoyle. Une comparison des changements de poids moléculaire obtenu par diffusion lumineuse $\bar{M}_w$ et par viscosimétrie $(\bar{M}_w)_v$ ne met pas en évidence de pontage simultané dans des films de PNBMA subissant une scission de chaîne par irradiation électronique de maximum 1 m.e.v. Certains travaux ont été fait, sur la sensibilité théorique de cette méthode comparative.

Zusammenfassung

γ–Bestrahlung von Polymethylmethacrylat–(PMMA)–pulver bestätigt die Literaturangaben, dass Luft die strahlungsinduzierte Molekulargewichtserniedrigung dieses Polymeren verzögert. Die Energieabsorption pro Spaltung, E_d, beträgt 91 e.v. in Luft bei 0,117 megarep pro Stunde, 76 e.v. in Luft bei 0,70 megarep pro Stunde und 56 e.v. im Vakuum bei 0,117 megarep pro Stunde. γ–Strahlenabbau von PMMA–Lösungen (5 g. PMMA/100 ml. Lösungsmittel) in Butanon und in Äthylacetat lieferte scheinbare Spaltungsenergien von 63 e.v. bzw. 26–30 e.v. Der letztgenannte niedrige Wert kann noch nicht erklärt werden. Poly–*n*–butylmethacrylat (PNBMA) zeigt eine beträchtliche Empfindlichkeit gegen Luft und Dosisleistungseffekte während der γ–Bestrahlung. Die scheinbare Energieabsorption pro Hauptkettenspaltung beträgt für γ–bestrahltes PNBMA–Pulver: E_d = 454 e.v. in Luft bei 0,117 megarep pro Stunde und E_d = 226 e.v. im Vakuum bei 0,117 megarep pro Stunde. Der letztere Wert liegt weit oberhalb des an elektronen–bestrahlten PNBMA–Folien beobachteten Wertes. Zur Herabsetzung einer möglichen Kettenrekombination und Polymer–Polymervernetzung wurden entgaste Lösungen mit 4,5, 10,0 und 55 Gew.% PNBMA in Äthylacetate γ-bestrahlt. Scheinbare E_d–Werte von 74 e.v., 74 e.v. bzw. 226 e.v. wurden gefunden. Die verdünnteren Lösungen liefern also PNBMA-Spaltungsenergien, die mit der von PMMA in Substanz vergleichbar sind. Die Lösung mit 55 Gew.% PNBMA ergibt eine mit der von PNBMA in Substanz unter den gleichen Bestrahlungsbedingungen identische Spaltungsenergie. Kompetitive Vernetzung und Haauptkettenspaltung werden für elektronenbestrahlte Poly–*n*–alkylmethacrylate postuliert. Die Energie pro Hauptkettenspaltung wird bei allen Homologen als konstant angenommen. Das Verhältnis von Vernetzung zu Kettenspaltung, α/β, nimmt dann mit $(n-1)$, wo n die Zahl der Kohlenstoffatome in den *n*–Alkylgruppen der Seitenkette ist, linear zu. Dieses Schema erlaubt zugleich eine Erklärung des Strahlungsverhaltens der niedrigeren Glieder der homologen Reihe der Poly–*n*–alkylmethacrylate. Ein Vergleich der Änderung des Lichtstreuungsmolekulargewichts $\bar{M}_w$ und des Viskositätsmolekulargewichts $(\bar{M}_w)_v$ liess in PNBMA–Folien bei Kettenspaltung durch 1 m.e.v.–Elektronenbestrahlung keine konkurrierende Vernetzung erkennen. Die theoretische Empfindlichkeit dieser Vergleichsmethode wird untersucht.

Received March 23, 1962

JOURNAL OF POLYMER SCIENCE: PART A VOL. 1, PP. 1671–1686 (1963)

Degradation of a Polycarbonate by Ionizing Radiation*

J. H. GOLDEN and E. A. HAZELL, *Materials Research Laboratory, Explosives Research and Development Establishment, Ministry of Aviation, Waltham Abbey, Essex, England*

Synopsis

The degradation of a polycarbonate by electron irradiation in oxygen and in vacuum has been examined. It was found that the polymer undergoes chain scission and that crosslinking apparently did not occur, the molecular weights of irradiated specimens were therefore determined from the intrinsic viscosity of methylene chloride solutions. From the relationship of molecular weight to radiation dose the value of G (scissions per 100 e.v. of energy absorbed) was found to be 0.14 in oxygen and 0.09 in vacuum. The effect of both molecular weight and radiation dose on the mechanical properties of polycarbonate irradiated in vacuum was studied. Conventional tensile properties were examined, and fracture energies were also obtained by use of a tensile impact apparatus based on the flywheel principle which was used to strain the specimens at 340 in./sec. With increase in radiation dose the maximum yield strength and extension fall slowly at first and then rapidly at a dose of approximately 100 Mrad. The elastic modulus is, however, virtually unaffected by irradiation and the attendant changes in molecular weight. The fracture energy falls steadily with radiation dose, and from the results a linear relationship, $F = 0.0044\ \bar{M}_n - 59$, between fracture energy F and molecular weight $\bar{M}_n$ has been obtained over the range examined, the energy becoming immeasurably small at molecular weights below 13,500. The results suggested that in this case fracture energy was a better measure of residual strength after irradiation than other tensile properties. The chemical changes caused by radiation lead to greatly enhanced ultraviolet light absorption with a maximum at 305 mμ and a shoulder at 320 mμ. The absorption (E; 1%, 1 cm.), in oxygen and in vacuum was shown to be a linear function, $E = 0.020\ R + 0.32$ of the radiation dose R. The changes in the infrared spectrum, in particular the carbonyl absorption, of irradiated specimens have been discussed. Mass spectrographic measurements showed that degradation proceeded with evolution of H_2, CO, and CO_2, both in oxygen and in vacuum.

INTRODUCTION

Despite the increasing importance of polycarbonates, little information has so far been reported on the degradation of these polymers and, in particular, on the effects of high energy radiation. Harrington and Giberson[1] examined the effects of radiation doses up to 3 Mrad, both in air and vacuum, on polycarbonate film and reported that the mechanical properties deteriorated similarly in the two cases, suggesting that the

* Presented at the Second International Congress of Radiation Research, Harrogate, August, 1962.

presence of oxygen did not greatly affect the degradation. Evidence was, however, found from infrared spectra for the formation of carbonyl and hydroxyl groups during irradiation in air. The optical changes in irradiated polycarbonate have also been studied by Barker and Moulton.[2] Finally, Krasnansky, Achhammer, and Parker[3] found that Co^{60} irradiation of polycarbonate film caused evolution of carbon monoxide, carbon dioxide, and hydrogen which they attributed to main chain cleavage.

In the present investigation an attempt has been made to elucidate the effects of ionizing radiation on the mechanical properties of the polymer and to relate these to concurrent changes in molecular weight determined viscometrically. The resultant chemical changes have also been studied by infrared, ultraviolet, and mass spectroscopy.

EXPERIMENTAL

A. Preparation of Specimens

Lexan natural polycarbonate (a product of the General Electric Company of America), poly[2,2-propanebis(4-phenyl carbonate)] was employed throughout.

Granules dried at 60°C./12 mm. for 8 weeks were placed in glass ampules and, after rigorous degassing (100°C./10^{-6} mm.) for 6 hr. the ampules were sealed, either immediately, or after the introduction of air or oxygen at atmospheric pressure. After irradiation these specimens were used for molecular weight and ultraviolet light absorption measurements. Polycarbonate films (0.001 in.) were cast from chloroform, dried thoroughly, and sealed in ampules. After irradiation the films were used for infrared light absorption measurements. Injection-molded dumbbells (see Fig. 1)

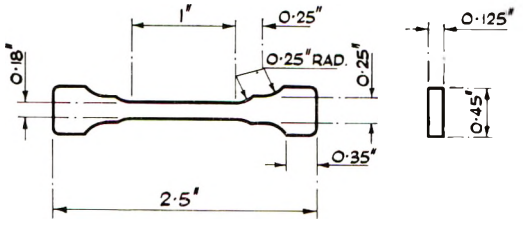

Fig. 1. Dimensions of dumbbell specimen used for tensile testing.

were used either unconditioned (moisture content 0.2%) or after drying at 60°C./12 mm. for 8 weeks. After irradiation such specimens were used for measurement of tensile properties and molecular weight.

B. Irradiation

Ampules, cooled externally by a water spray, were exposed to a linear accelerator electron beam (4 m.e.v.) at a dose rate of 5 Mrad/min. Dumbbell specimens held flat on an aluminum tray were placed in a water-cooled

aluminum chamber. The face of the chamber, immediately in front of the specimens and exposed to the beam, was a thin aluminum window ($^1/_{32}$ in. thick). The chamber could be sealed and then evacuated continuously throughout the irradiation if required. Irradiation of the dumbbells was carried out at a dose rate of 1 Mrad/min.

C. Test Methods

Specimens were tested after a period of not less than two weeks after irradiation. Dumbbells were kept in vacuum during this period, and ampules were not opened.

Viscosity Measurements. The specimens were dissolved in methylene chloride, and the intrinsic viscosities of the solutions were determined from measurements obtained in a dilution viscometer modified according to Harding.[4] Molecular weights ($\bar{M}_v$) were calculated from the relationship $[\eta] = 1.23 \times 10^{-5} M^{0.83}$ derived by Schnell[5] for methylene chloride solutions.

Ultraviolet Absorption Spectra. Specimens were dissolved in methylene chloride and the absorption spectra measured with a Unicam S.P.500 spectrophotometer.

Conventional Tensile Measurements. Tensile properties were obtained with a Baldwin P.T.E. 60 machine at a crosshead speed of 0.1 in./min. Load/crosshead records were obtained autographically, and, from these, estimates of changes in modulus at different dose rates were determined. For specimens which yielded, the strength was recorded as maximum yield load divided by the original cross-sectional area of the specimen; for specimens which broke without yielding the strength was recorded as the breaking load divided by the original cross-sectional area. For convenience all these results are plotted as maximum yield strength in Figures 4 and 8. Extension is reported as the distance moved by the crosshead in breaking the specimen (test length approximately 1 in.). Thus strength and extension values correspond only when the specimen breaks before yield; this condition was fulfilled at higher radiation doses.

High-Speed Tensile Impact Measurements. Fracture energy measurements were made with a tensile impact apparatus, based on the fly-wheel principle, capable of straining the dumbbell specimens (Fig. 1) in tension at rates in the range 100–500 in./sec. The apparatus was based on the method described by Maxwell and Harrington[6] and has been described elsewhere.[7] It consisted essentially of an inertia bar which could be rotated at various speeds in a horizontal plane about a central spindle. Different speeds of rotation were obtained from a variable-speed motor with a friction drive which was disconnected when the required speed was obtained. The dumbbell-grip assembly was attached to the inertia bar by the leading grip while the trailing grip was lightly supported on an adjustable frame which kept the specimen in a horizontal plane with just sufficient tension to make the assembly rigid. When the inertia bar was rotating at the required speed a claw was thrust into the path of a pin

which projected through the trailing grip. On impact the specimen was stretched to failure, the broken portion fell away, and the inertia bar continued to rotate. An aluminum recording drum fitted to the spindle of the apparatus revolved with the inertia bar and was fitted with a strip of Teledeltos paper. A stylus when energized sparked through the paper at intervals of $^1/_{200}$ sec. The spacing between sparks on the Teledeltos paper, when used in conjunction with known constants of the apparatus and the inertia of the system, was used as the basis for calculation of the energy dissipated in breaking a specimen. Fracture energy was measured at a velocity of impact of 340 in./sec. which corresponded to a maximum straining rate of 34,000%/sec. on the specimen.

The specimen grip assembly used for both conventional tensile and high-speed tensile impact testing was similar to that used by Maxwell and Harrington.[6] The grips consisted of two steel plates which, when screwed together, clamped the lugs of the dumbbell. Annular washers, slightly thinner than the specimen, were mounted on pins through the grips and part of their outer circumference was in contact with the additional shoulders on the specimen (Fig. 1). These washers prevented the specimen from being drawn through the grips and, being free to rotate, assisted in reducing stress concentrations at the shoulders.

RESULTS AND DISCUSSION

Molecular Weight

Irradiated polycarbonate was soluble in chloroform and in methylene chloride at all doses employed, the ease of solution increasing with the dose. The complete absence of gel formation indicated that cross-linking does not occur and that main-chain scission was the predominant effect of irradiation. This conclusion was borne out by determination of the molecular weight of irradiated specimens. Figure 2 illustrates the progressive decrease in viscosity-average molecular weight ($\bar{M}_v$) with increasing dose both in vacuum and in oxygen. The breakdown is slightly accelerated by the presence of oxygen, a result which has been observed for other polymers which undergo chain scission, e.g., polytetrafluoroethylene[8] and polymethyl isopropenyl ketone;[9] polyisobutylene, however, showed identical rates.[10]

In Figure 3 the data are presented as reciprocal viscosity-average molecular weight versus radiation dose R. Pure random chain scission requires that the relationships shall be linear according to the equation.[9,11,12]

$$(10^6/\bar{M}_n) = (10^6/\bar{M}_{n_0}) + 10^6(NE_d)^{-1}R \qquad (1)$$

where $\bar{M}_{n_0}$ is the initial number-average molecular weight, E_d is the total energy absorbed per chain scission produced, and N is Avogadro's number. As expected, Figure 3 shows that the initial molecular weight distribution is not random in character but that the distribution rapidly becomes

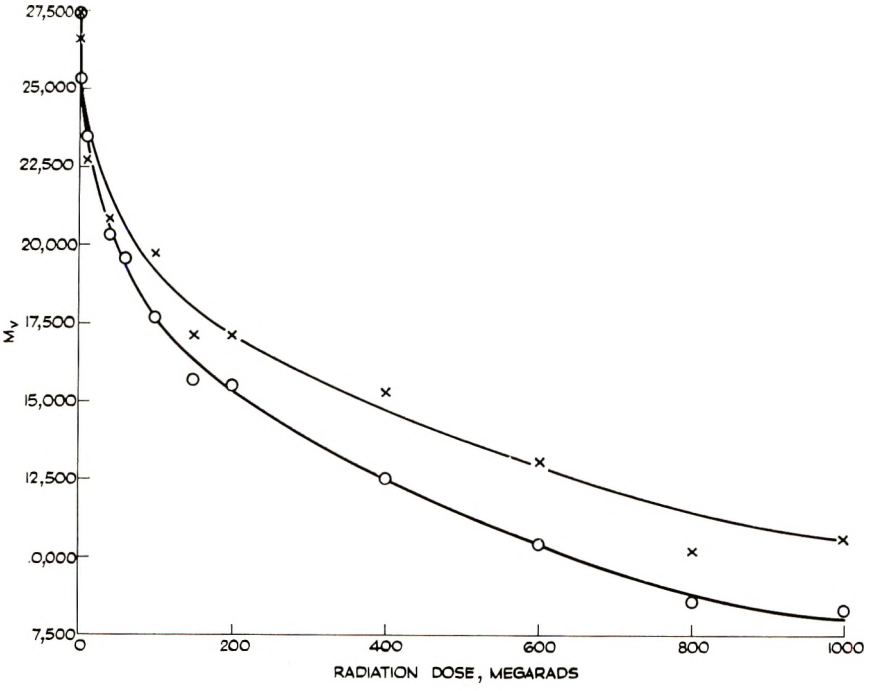

Fig. 2. Viscometric-average molecular weight $\bar{M}_v$ vs. radiation dose R for polycarbonate granules irradiated (×) in vacuum and (○) in oxygen.

random as a result of radiation-induced fracture (compare polyisobutylene[10]), so that at doses above 50 Mrad a linear relationship is obtained.

For the application of eq. (1) the measured values of $\bar{M}_v$ can be related to values of $\bar{M}_n$ by the equation derived for a random distribution:[10,11]

$$\bar{M}_v = \bar{M}_n[(\alpha + 1)\Gamma(\alpha + 1)]^{1/\alpha} \tag{2}$$

where Γ is a gamma-function. In the case of polycarbonates, where $\alpha = 0.83$ (Schnell[5]), this leads to

$$\bar{M}_v = 1.92\bar{M}_n \tag{3}$$

Hence from the slope of the lines obtained in Figure 3 and by applying eqs. (1) and (3), the total energy absorbed per chain scission, E_d, is 1100 e.v. for polycarbonate irradiated in vacuum and 700 e.v. for polycarbonate irradiated in oxygen. The corresponding G values (number of scissions per 100 e.v. energy absorbed) are 0.09 in vacuum and 0.14 in oxygen. The low G values obtained illustrate the considerable resistance to degradation by ionizing radiation afforded by the predominantly aromatic system.

Effect of Radiation on Tensile Properties

In this study two methods were employed to investigate the deterioration of tensile properties of polycarbonate irradiated in vacuum. Conventional

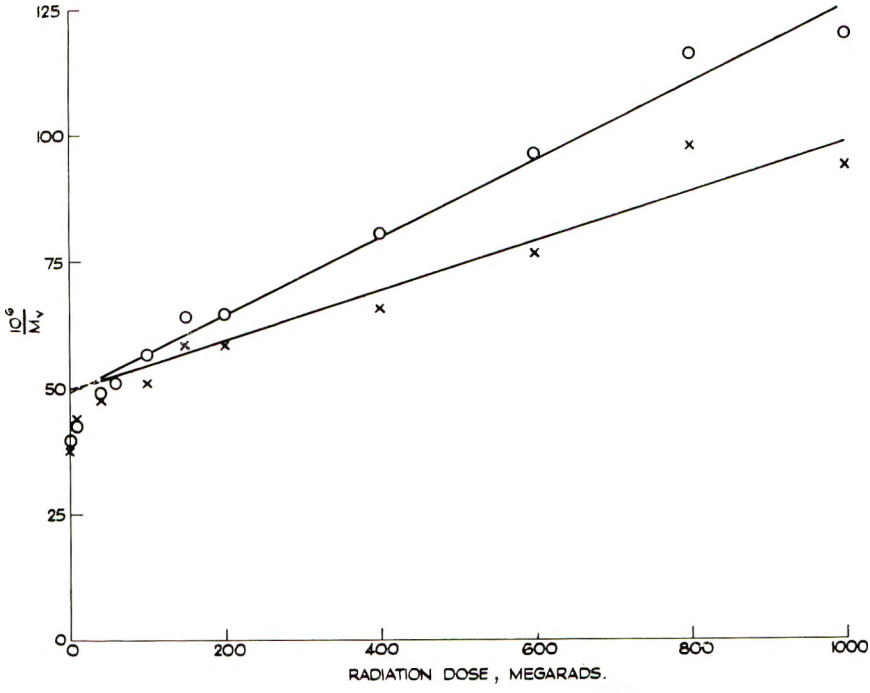

Fig. 3. Reciprocal viscometric-average molecular weight, $1/\bar{M}_v$, vs. radiation dose R for polycarbonate granules irradiated (×) in vacuum and (○) in oxygen.

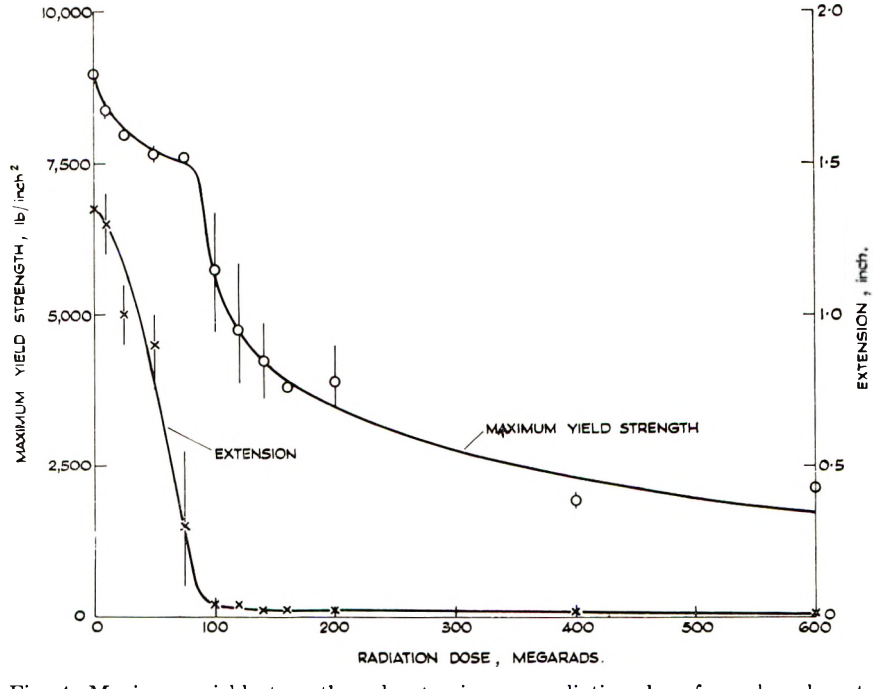

Fig. 4. Maximum yield strength and extension vs. radiation dose for polycarbonate dumbbells (dried), irradiated in vacuum.

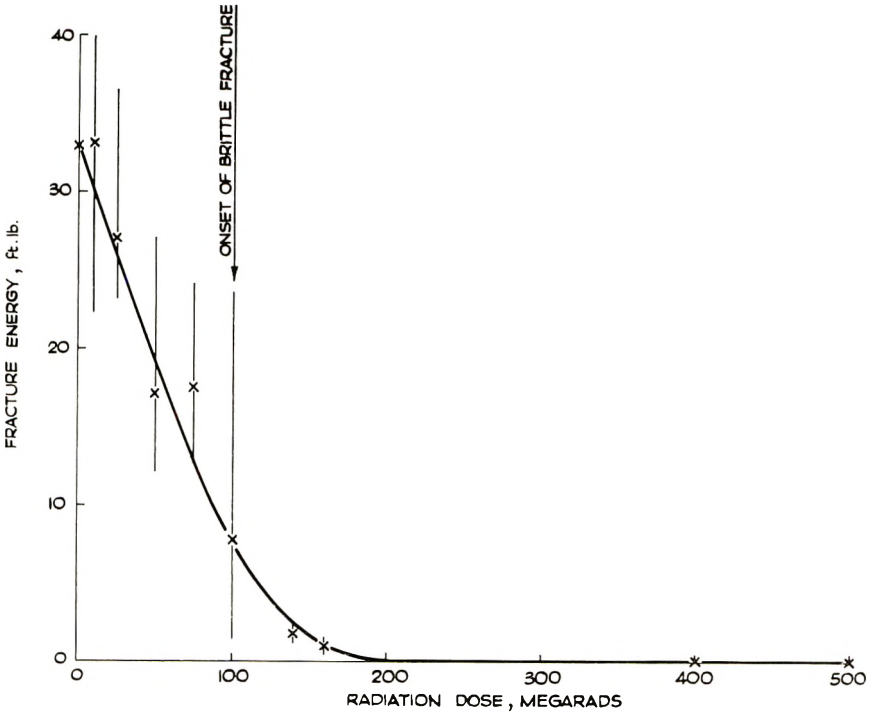

Fig. 5. Fracture energy vs. radiation dose for unconditioned polycarbonate dumbbells irradiated in vacuum.

tensile testing was used to determine the maximum yield strength and extension of the specimen, and high-speed tensile impact testing[7] to determine the fracture energy; the effect of radiation on these properties is illustrated in Figures 4 and 5.

The maximum yield strength and extension both decrease slowly until, at a dose of approximately 100 Mrad, the maximum yield strength falls rapidly and the extension becomes extremely small.

A measure of the modulus of the specimen can be obtained from the slope of the tangent modulus at the origin of the load–time curve. As all specimens had the same gage length, positive gripping, and constant strain rate was applied, the slope of this tangent will vary with the modulus. However, it was found thus, that over the range studied the change in modulus with dose was negligible; this is noteworthy when the concurrent drastic changes in yield strength and elongation are considered.

Figure 6 shows the appearance of typical specimens after tensile impact testing and illustrates the extreme brittleness of highly irradiated material. The fracture energy (Fig. 5) shows a steady fall with increasing dose and, soon after the onset of brittle fractures, becomes negligible.

From the results obtained here it would appear that fracture energy is a more sensitive measure of the residual strength of the irradiated material than other tensile properties such as maximum yield strength and extension.

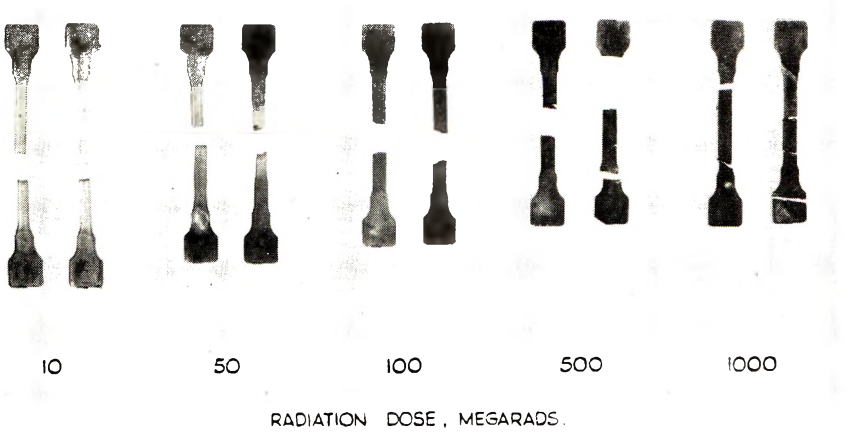

Fig. 6. Appearance of typical high-speed tensile impact specimens, unirradiated and irradiated, after testing.

Effect of Molecular Weight on Tensile Properties

The overall effects of molecular weight on the mechanical properties of polymers have been reviewed by Mark,[13] and more recent work has been carried out on, e.g., polyethylene[14] and polypropylene.[15] Earlier

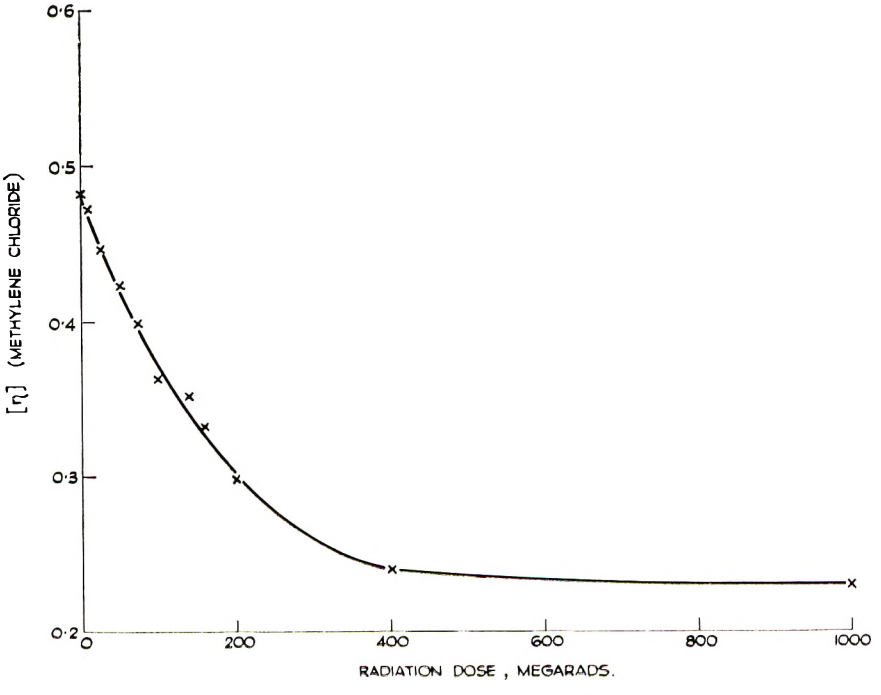

Fig. 7. Intrinsic viscosity $[\eta]$ in methylene chloride vs. radiation dose for unconditioned polycarbonate dumbbells irradiated in vacuum.

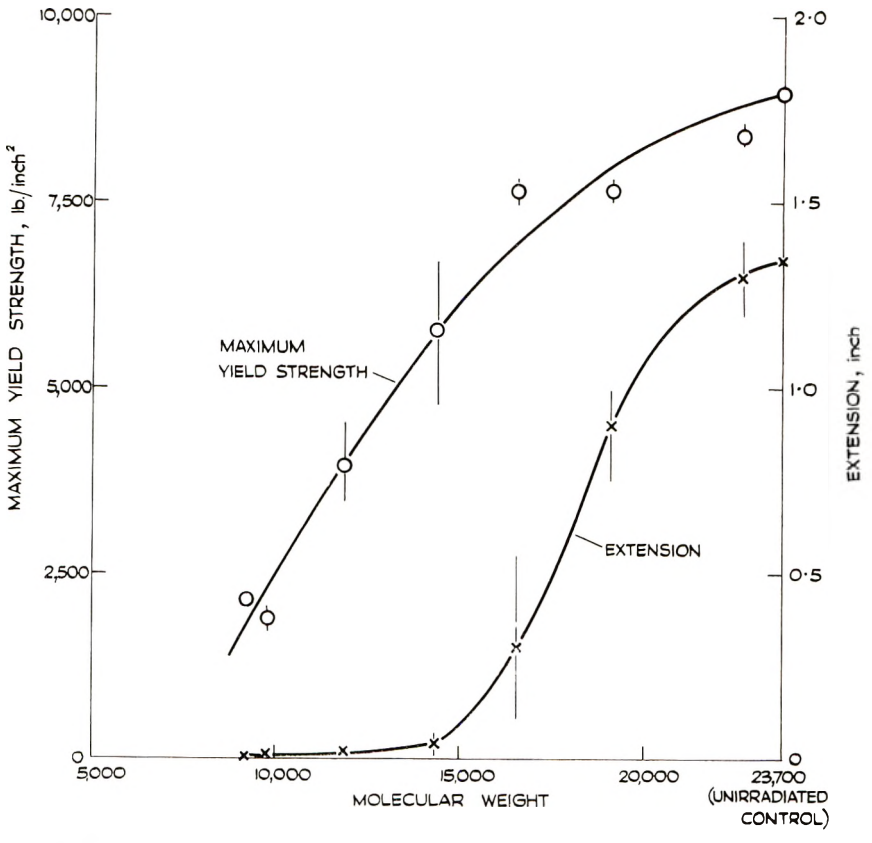

Fig. 8. Maximum yield strength and extension vs. viscometric-average molecular weight for polycarbonate dumbbells (dried), irradiated in vacuum.

work has utilized polymer preparations of differing molecular weights or fractionated polymers, etc.; however, irradiation of a polymer which undergoes chain scission and does not crosslink provides a very convenient method of determining the progressive effect of changes of average molecular weight on mechanical properties. As polycarbonates apparently fulfill these conditions, determination of the viscosities of solutions of the dumbbell specimens used for mechanical testing made it possible to investigate the effect of molecular weight (the average of a random distribution) on the tensile properties. Figure 7 shows the relationship of intrinsic viscosity to radiation dose for specimens used for conventional tensile testing, and Figures 8 and 9 illustrate the effect of molecular weight on the tensile properties of dumbbells.

It is apparent (Fig. 8) that the extension of the irradiated specimens drops fairly rapidly with reduction of molecular weight following a sigmoid curve to a negligible value at a molecular weight of approximately 15,000. In contrast, although the maximum yield strength also drops steadily the material still retains over 50% of its initial value at this molecular weight.

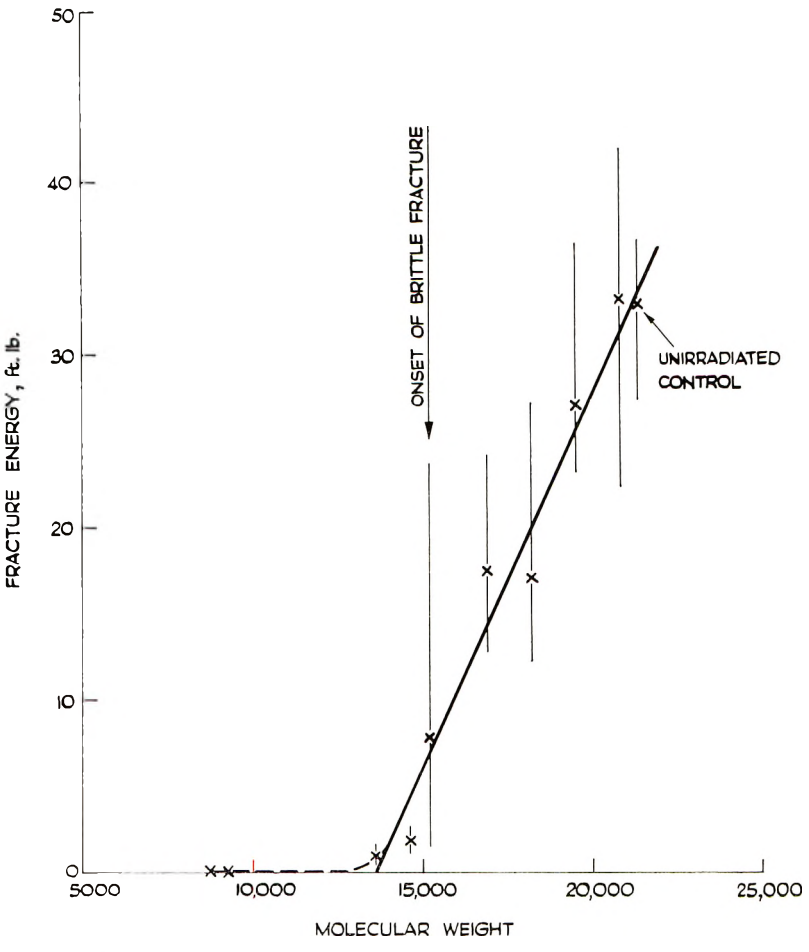

Fig. 9. Fracture energy vs. viscometric-average molecular weight for unconditioned polycarbonate dumbbells irradiated in vacuum.

Similar rapid loss of extensibility with much slower loss of maximum yield strength on degradation has been observed for other materials, e.g., polytetrafluoroethylene.[16]

The effect of molecular weight on fracture energy in tensile impact is illustrated in Figure 9, which shows that decrease in molecular weight causes a steady reduction in fracture energy through the ductile–brittle transition which occurs at a molecular weight of approximately 15,000. The onset of brittle fracture is characterized by the occurrence of high energy ductile fractures (average energy 17.2 ft.lb.) and low energy brittle fractures (average energy 2.1 ft.lb.) at the same radiation dose (100 Mrad). Irrespective of the kind of fracture, the average of the results at this dose has been used in Figure 9 (and also in Figure 5 where a similar transition occurs), since continuity in the change of fracture energy with molecular weight is to be expected in view of the continuous nature of the scission

process. Over the range of measurable fracture energy, the fracture energy F can conveniently be expressed as a linear function of the molecular weight ($\bar{M}_v$), i.e.,

$$F = 0.0044\ \bar{M}_v - 59 \tag{4}$$

Extrapolation of this linear plot indicates that the fracture energy becomes zero at a molecular weight of 13,500; however, as the polycarbonate did not completely disintegrate below this value, the dotted line in Figure 9 indicates the probable form of the relationship. It is also likely that, at molecular weights higher than those studied here, the rate of increase of fracture energy with molecular weight would decrease, leading to an overall sigmoid relationship of fracture energy to molecular weight.

Ultraviolet Light Absorption

The final color[2] of polycarbonate specimens irradiated in oxygen or in vacuum changes progressively from transparent light amber through amber-brown to brownish-black with increase in dose (compare Fig. 6). This darkening in color is paralleled by the increased light absorption of solutions of the irradiated polymer, typical curves of which are illustrated

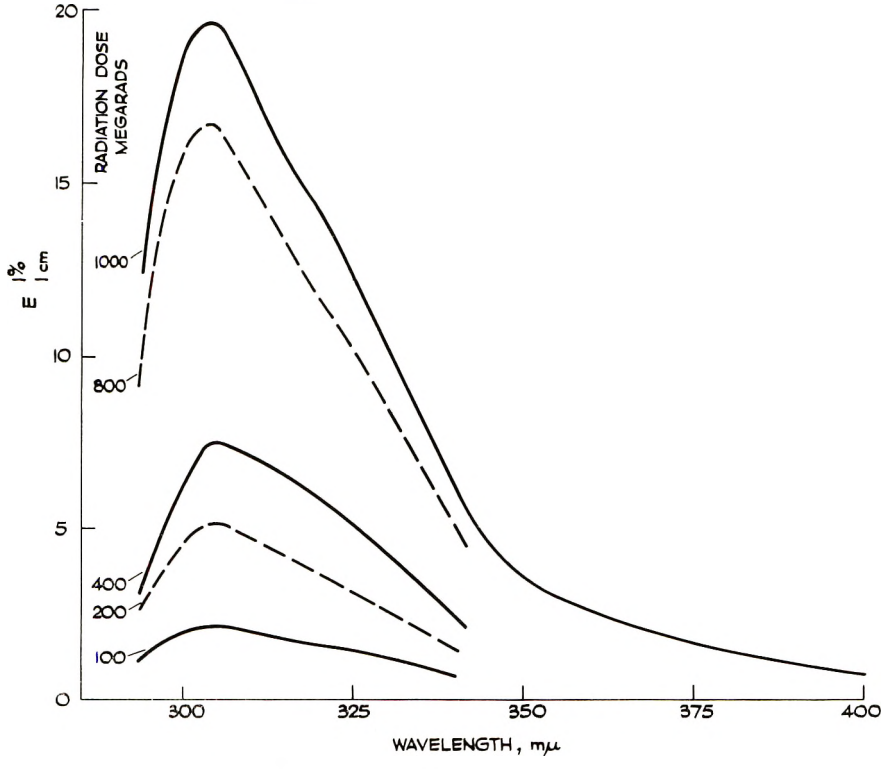

Fig. 10. Absorption (E, 1%, 1 cm.) vs. wavelength of methylene chloride solutions of polycarbonate specimens irradiated (—) in oxygen and (- -) in vacuum to various doses.

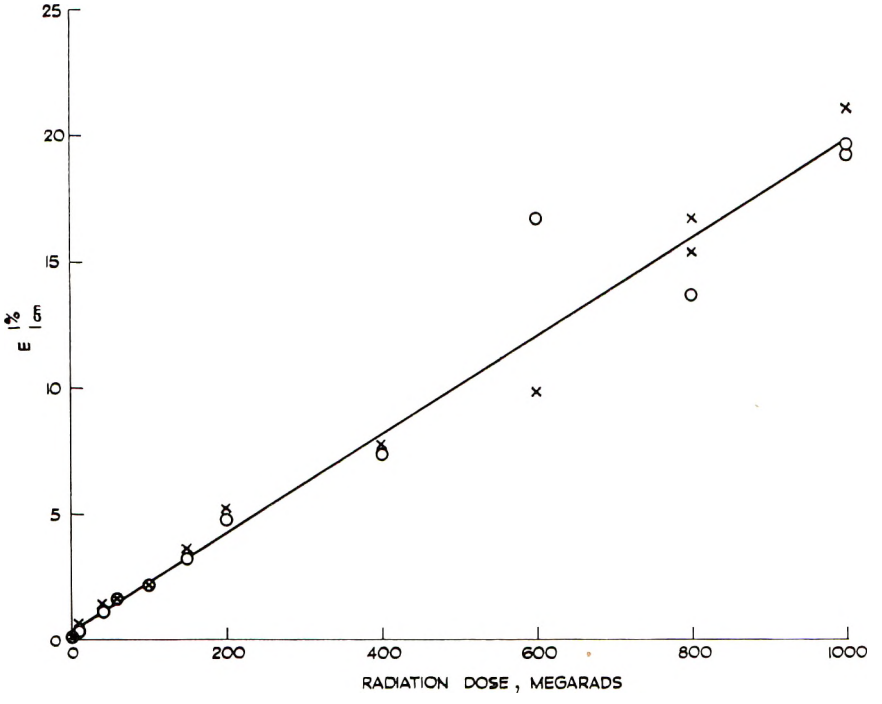

Fig. 11. Absorption (E, 1%, 1 cm.) in methylene chloride vs. radiation dose for polycarbonate specimens irradiated (O) in oxygen and (×) in vacuum.

in Figure 10, where absorption (E, 1%, 1 cm.) is plotted against wavelength for methylene chloride solutions. The intensity of the absorption maximum (305 mμ) and the associated shoulder (approx. 320 mμ) increase steadily with dose, similar curves being obtained in oxygen to those in vacuum.

Figure 11 illustrates the relationship between the absorption intensity (E, 1%, 1 cm.) at 305 mμ and radiation dose R. The results obtained in oxygen and in vacuum gave coincident straight lines represented (from least squares) by the equation

$$E = 0.020R + 0.32 \tag{5}$$

A slight discrepancy exists in this result, in that the actual absorption of unirradiated polymer (0.09) at this wavelength is less than the value (0.32) obtained by extrapolation; the reason for this is not obvious.

Barker and Moulton[2] studied the ultraviolet light absorption of solid Lexan irradiated to moderate doses and found absorption maxima at 340 and 400 mμ for freshly irradiated specimens. After an aging period of 14 days or after a short period of heating at 120°C., the longer wavelength absorption band disappeared due to destruction of the active centers responsible by oxygen diffusion, the shorter wavelength absorption being left virtually unaffected. As the specimens irradiated in the present work

were aged for at least two weeks and then examined in solution, transient species should be absent. The results obtained therefore indicate that the permanent chemical change or changes induced by radiation and responsible for the absorption maximum at 305 mμ is independent of the presence of oxygen. In addition the degree of this chemical change is linearly dependent on the radiation dose.

Infrared Light Absorption

Examination of the infrared spectra (2–15 μ) of polycarbonate film (0.001 in.) before and after irradiation to 1000 Mrad in vacuum or in oxygen revealed differences in three regions of the spectrum; those absorption bands which were altered by or formed by irradiation are given in Table I.

TABLE I
Absorption Bands in Polycarbonate Film Altered by or Formed by Irradiation

Absorption bands in unirradiated film, cm.$^{-1}$	Absorption bands in irradiated film, cm.$^{-1}$	
	In vacuum	In oxygen
1340	1340[a]	1340[a]
—	1533	1533
1594	1594	1594
1601	1599	1599
(1635)[b]	1633	1635
1656	1663	1659
—	1695	1695
—	(1735)[b]	(1732)[b]
1766	1762	1762
(1776)[b]	(1776)[b]	1776
—	3369	3359
—	3458	3454
—	3638	3632
3662	—	—

[a] Enhanced absorption.
[b] Shoulder.

Little difference is observable between the results obtained in oxygen and those in vacuum; in both cases the major effect appears to be complex changes in the carbonyl bands associated with the carbonate linkage. The C=O frequency in the polycarbonate occurs at 1766 cm.$^{-1}$ with an associated shoulder at 1776 cm.$^{-1}$ and is comparable to that of diphenyl carbonate[17] (1775 cm.$^{-1}$).

The changes noted by Harrington[1] in the 875–1000 cm.$^{-1}$ region of specimens irradiated in air were not found in the present study after irradiation either in air or oxygen.

Gas Evolution

Mass spectrographic analyses of the gas contents of ampules containing polycarbonate granules initially either evacuated or filled with oxygen at atmospheric pressure, after irradiation to a dose of 1000 Mrad are given in Table II.

TABLE II
Partial Pressure of Gases Present in Ampules after Irradiation of Polycarbonate

Gas	Partial pressure of gases, %	
	Irradiation in vacuum	Irradiation in oxygen[a]
CO	81.2	27.5 (59.1)
CO_2	16.7	18.3 (39.4)
H_2	2.0	0.7 (1.5)
O_2	0.1	53.5 (nil)

[a] Values in parentheses denote actual partial pressure assuming no oxygen evolved.

No evidence of hydrocarbon or other products was found. The pattern of products is thus closely similar for irradiation both in vacuum (compare Krasnansky[3]) and in oxygen, although in the latter case the ratio of carbon dioxide to carbon monoxide is greatly increased. Both carbon monoxide and carbon dioxide apparently arise from destruction of the carbonate linkage.

Effect of Radiation on Structure

The predominance of main-chain scission and the absence of crosslinking as radiation effects are indicated by the complete solubility of irradiated specimens (up to doses of 1000 Mrad) and the lack of any evidence for crosslinking. This conclusion is supported by the relationship between viscometric molecular weight and radiation dose (Fig. 3), which indicates degradation by random chain scission.

As the benzene ring is very resistant to radiation the most likely points of scission in the chain are the carbonate and isopropylidene linkages. Considerable degradation of carbonate groups is apparent from the mass-spectrographic results, although no products apart from a trace of hydrogen are formed which could be directly attributed to breakdown of the isopropylidene grouping. The complexity of the carbonyl absorption of irradiated specimens in the infrared is further evidence of the destruction of carbonate linkages. The ultraviolet absorption after irradiation suggests the development of conjugated unsaturation, which may be due to the interaction of carbonyl groupings adjacent to the benzene rings.

The accelerated degradation which occurs in oxygen as distinct from vacuum may be due to the combination of oxygen with free radicals preventing the recombination of adjacent radicals which might otherwise occur. It is evident from the results of Barker and Moulton[2] that active species are formed which are long-lived in the absence of oxygen.

The reactions accompanying degradation are at present uncertain, and investigations of the detailed mechanism of these are at present being carried out.

The authors thank Messrs. J. McCann and F. Hazell (Technological Irradiation Group, Wantage) for assistance in the irradiation of samples, Dr. G. A. Heath (R.P.E., Ministry of Aviation) for mass spectrographic results, Mr. R. W. Tobias (E.R.D.E.) for viscosity determinations, and Mr. R. J. Pace (E.R.D.E.) for infrared measurements.

References

1. Harrington, R., and R. Giberson, *Modern Plastics*, **36**, No. 3, 199 (1958).
2. Barker, R. E., and W. G. Moulton, *J. Polymer Sci.*, **47**, 175 (1960).
3. Krasnansky, V. J., B. G. Achhammer, and M. S. Parker, *S.P.E. Trans.*, **1**, 133 (July 1961).
4. Harding, G. W., *J. Polymer Sci.*, **55**, S27 (1961).
5. Schnell, H., *Angew. Chem.*, **68**, 633 (1956).
6. Maxwell, B., and J. P. Harrington, *Trans. Am. Soc. Mech. Engrs.*, **74**, 5 (1952).
7. Hazell, E. A., unpublished Ministry of Aviation reports.
8. Golden, J. H., *J. Polymer Sci.*, **45**, 534 (1960).
9. Schultz, A. R., *J. Polymer Sci.*, **47**, 267 (1960).
10. Alexander, P., R. M. Black, and A. Charlesby, *Proc. Roy. Soc. (London)*, **A232**, 31 (1955).
11. Alexander, P., A. Charlesby, and M. Ross, *Proc. Roy. Soc. (London)*, **A223**, 392 (1954).
12. Alexander, P., and A. Charlesby, *Proc. Roy. Soc. (London)*, **A230**, 136 (1955).
13. Mark, H., *Ind. Eng. Chem.*, **34**, 1343 (1942).
14. Sandiford, D. J. H., and A. H. Willbourn, in *Polythene*, A. Renfrew and P. Morgan, Eds., Iliffe and Sons, London, 1960, p. 167.
15. Van Schooten, J., H. Van Hoorn, and J. Boerma, *Polymer*, **2**, 161 (1961).
16. Golden, J. H., and E. A. Hazell, unpublished Ministry of Aviation report.
17. Hales, J. L., J. Idris Jones, and W. Kynaston, *J. Chem. Soc.*, **1957**, 618.

Résumé

La dégradation d'un polycarbonate par irradiation électronique a été examinée en présence d'oxygène et sous vide. On a trouvé que le polymère subissait une scission de chaîne et que le pontage ne se produisait apparemment pas. Les poids moléculaires des échantillons irradiés ont été déterminés à partir de leur viscosité intrinsèque au départ de solutions avec le chlorure de méthylène. A partir de la relation liant le poids moléculaire à la dose de radiation, on a trouvé que la valeur de G (scission par 100 e.v. d'énergie absorbée) était de 0.14 en présence d'oxygène et de 0.09 sous vide. On a étudié l'effet simultané du poids moléculaire et de la dose de radiation sur les propriétés mécaniques du polycarbonate irradié sous vide. Les propriétés habituelles de traction ont été examinées et les énergies de rupture ont également été obtenues en utilisant un appareil à impact au choc, basé sur le principe du volant d'inertie qui a été employé pour étirer des échantillons à 340 ins./sec. En augmentant la dose de radiation, la force de tension maximum et l'extension diminuent d'abord lentement et puis rapidement pour une dose de 100 mégarads approximativement. Toutefois le module d'élasticité est virtuellement inaffecté par l'irradiation et par les changements attendus du poids moléculaire. L'énergie de rupture diminue proportionnellement avec la dose de radiation et à partir des résultats trouvés, on a obtenu une relation linéaire $F = 0.0044\ \bar{M}_v - 59$ entre l'énergie de rupture F, et le poids moléculaire $\bar{M}_v$ sur tout le domaine étudié. À des poids moléculaires inférieurs à 13,500, l'énergie trop faible n'est plus mesurable. Les résultats suggèrent que dans ce cas l'énergie de rupture est une meilleure mesure de la force résiduelle après irradiation que les autres propriétés élastiques. Les changements

chimiques provoqués par irradiation conduisent à une augmentation importante de l'absorption dans l'ultraviolet avec un maximum à 305 mμ et un épaulement à 320 mμ. On a montré que l'absorption (E; 1%, 1 cm) en présence d'oxygène et sous vide est une fonction linéaire, $E = 0.020\,R + 0.32$ de la dose de radiation R. On a également discuté les changements dans le spectre infrarouge en particulier l'absorption du carbonyle des échantillons irradiés. Les mesures de spectrographie de masse ont montré que la dégradation se produit avec dégagement de H_2, CO et CO_2 à la fois en présence d'oxygène et sous vide.

Zusammenfassung

Der Abbau eines Polykarbonates durch Elektronenbestrahlung unter Sauerstoff und im Vakuum wurde untersucht. Es zeigte sich, dass Kettensspaltung des Polymeren eintritt, offenbar aber keine Vernetzung stattfindet; das Molekulagewicht der bestrahlten Proben konnte daher aus der Viskositätszahl in Methylenchloridlösung bestimmt werden. Aus der Beziehung zwischen Molekulargewicht und Bestrahlungsdosis ergab sich der G-Wert (Spaltungen auf 100 e.v. absorbierter Energie) unter Sauerstoff zu 0,14 und im Vakuum zu 0,09. Der Einfluss von Molekulargewicht und Bestrahlungsdosis auf die mechanischen Eigenschaften von bestrahltem Polykarbonat wurde untersucht. Konventionelle Zugeigenschaften wurden geprüft und unter Benützung eines auf dem Schwungradprinzip beruhenden Stosszugapparates, der zur Verformung der Proben mit 340 ins./sec. verwendet wurde, konnten auch Bruchenergien erhalten werden. Mit Zunahme der Bestrahlungsdosis fallen die Fliessgrenze und -dehnung zuerst langsam und dann, bei einer Dosis von etwa 100 megarad, rasch ab. Der Elastizitätsmodul bleibt jedoch von der Bestrahlung und den entsprechenden Molekulargewichtsänderungen praktisch unbeeinflusst. Die Bruchenergie fällt stetig mit der Bestrahlungsdosis ab und aus den Ergebnissen wurde im untersuchten Bereich eine lineare Beziehung, $F = 0{,}0044\ \bar{M}_v - 59$, zwischen Bruchenergie F und Molekulargewicht $\bar{M}_v$ erhalten. Bei Molekulargewichten unterhalb 13500 wird die Energie unmessbar klein. Die Ergebnisse lassen erkennen, dass in diesem Fall die Bruchenergie ein besseres Mass für die nach der Bestrahlung verbleibende Festigkeit bildet, als andere Zugeigenschaften. Die durch Strahlung verursachten chemischen Veränderungen führen zu stark erhöhter Lichtabsorption mit einem Maximum bei 305 mμ und einer Schulter bei 320 mμ. Die Absorption (E; 1%, 1 cm) unter Sauerstoff und im Vakuum ergab sich als lineare Funktion, $E = 0{,}020\ R + 0{,}32$ der Strahlungsdosis R. Die Veränderungen im Infrarotspektrum, besonders die Carbonylabsorption, von bestrahlten Proben wurde diskutiert. Massenspektrographische Messungen zeigten, dass der Abbau sowohl unter Sauerstoff als auch im Vakuum unter Entwicklung von H_2, CO und CO_2 verläuft.

Received March 28, 1962

JOURNAL OF POLYMER SCIENCE: PART A VOL. 1, PP. 1687–1692 (1963)

The Infrared Spectrum of Crystalline Polysaccharides. IX. The Near Infrared Spectrum of Cellulose

K. H. BASSETT,* C. Y. LIANG, and R. H. MARCHESSAULT,†
Research and Development Division, American Viscose Corporation, Marcus Hook, Pennsylvania

Synopsis

The near infrared region of the spectra of cellulose from about 4000 to 8000 cm.$^{-1}$ was investigated and assignments made to the absorption bands in this region. Assignments were made on the basis of combinations and overtones of fundamental frequencies and were checked where possible by various chemical and physical sample modifications. The dichroism of all absorption bands in this region was very slight.

I. Introduction

The near infrared spectrum, 4000–8000 cm.$^{-1}$, is receiving increased attention from analytical spectroscopists. Several good reviews have appeared recently,[1,2] including one directed specifically toward polymer applications.[3] The near infrared spectrum has a special attraction for polymer chemists who must deal with fibrous specimens, most of which have proved to be too thick for transmission spectra in the fundamental region of the infrared spectrum. By the use of special techniques, e.g., the infrared microscope or single-layer fiber mounting,[4] it has been possible to record spectra for fibrous samples, but by and large workers have not found these approaches convenient. These sampling difficulties disappear in the near infrared portion of the spectrum because one is dealing then with overtone and combination bands which because of their low optical densities allow the use of relatively thick fiber bundles.

The recent study by Fraser and MacRae[5] of the near infrared spectrum of wool is a good example of what information is available in this spectral region. Their work showed that the contribution of the crystalline and noncrystalline regions to the dichroism of a given band could be differentiated by means of the deuteration technique. The object of this study was similar, viz., to study the dichroism of the fiber as a whole and to separate the contributions of the crystalline and noncrystalline regions.

* Present address: Research Division, Weyerhaeuser Technical Center, Longview, Wash.

† Present address: State University of New York, College of Forestry, Syracuse, N. Y.

The near infrared spectrum of cellulose has received only brief attention so far. Ellis and Bath[6] observed absorption bands at 6940 and 4740 cm.$^{-1}$ in the spectrum of ramie which they associated with OH oscillators. The present study was initially directed, therefore, to the problem of band assignment.

II. Experimental Procedure

In this study four cellulosic materials were used: cellophane, tire cord rayon, bacterial cellulose, and ramie. All were used in their natural, air-dry state for the basic spectra. It was found that cellophane produced severe interference fringes if used in its usual form. However, this was overcome by drying gel cellophane on frosted glass to give it a frosted light-scattering surface.

To obtain a spectrum, a bundle of fibers or number of layers of film were placed in a suitable holder. The thickness of the sample was approximately 0.5 mm. To reduce scattering losses it was necessary to wet all samples (cellophane excepted) in a suitable medium of about the same refractive index as cellulose. Initially, Nujol was used for this purpose, but after it became apparent that the Nujol showed some absorption bands in this region, a mixture of CS_2 and CCl_4 was used. All spectra were recorded on a Perkin-Elmer model 112 single-beam and double-pass spectrometer equipped with lithium fluoride prism. For the polarized spectra, a silver chloride plate polarizer was used. In all cases an attempt was made to adjust the background to a constant level, but as shown in the figures this was not always achieved.

To assist in identifying certain of the absorption bands a number of special samples were prepared. A sample of the tire cord rayon was par-

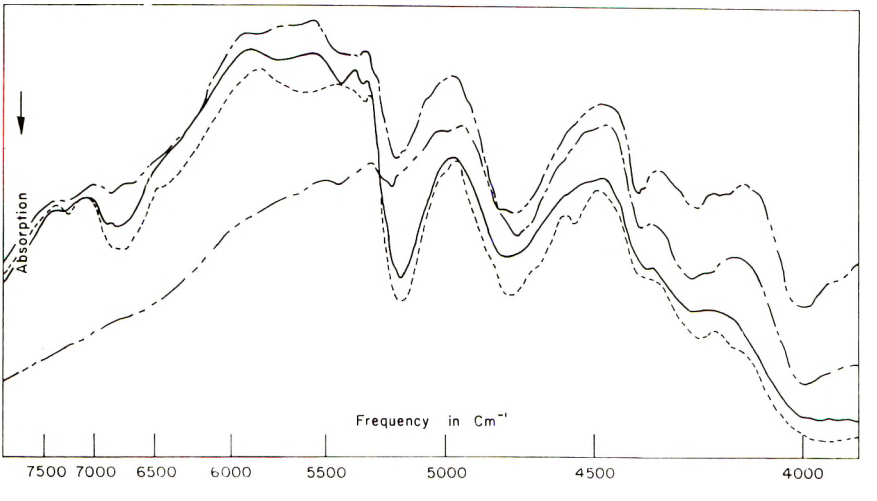

Fig. 1. Near infrared spectra of four cellulosic materials: (——) tire cord rayon; (- -) cellophane; (— - —) ramie; (— - - —) bacterial cellulose.

tially deuterated by soaking in D_2O for several days and then drying in a stream of dry nitrogen in a closed cell. Another tire cord sample was hydrolyzed by boiling for three minutes in 2.5*N* HCl.

A sample of completely deuterated bacterial cellulose was produced by first acetylating and then saponifying according to the following schedule. For acetylation, the sample was first treated in 15% perchloric acid for 30 min. at room temperature, followed by treatment with 10 parts acetic anhydride to 20 parts toluene for 15 min. at room temperature; the sample was then washed in H_2O.

The saponification procedure was to treat in 1% NaOD and 10% NaOAc in D_2O for 16 hr. on steam bath, followed by a wash in D_2O.

Finally, a sample of skin cellophane was prepared by taking cellulose acetate film and deacetylating it by treating with 0.5% solution of sodium methoxide in dry methanol for 16 hr. at room temperature followed by 1.5 hr. at a boil. The sample was then washed in methanol.[7] A standard staining procedure[8] verified that better than 80% of this sample was skin.

III. Results and Discussion

Figure 1 shows spectra of the four materials used in this study. Since the absorption bands in the near infrared region of the spectrum are overtones and combinations of fundamental frequencies, assignments were made by finding the proper combinations of the fundamentals. Where possible the assignments were checked by other means. By these methods the assignments have been made as shown in Table I.

TABLE I
Near Infrared Spectrum of Cellulose

Frequency, cm.$^{-1}$	Assignment
3970 3990	CO stretching + CH and CH_2 stretching
4235	OH and CH deformational modes + CH and CH_2 stretching
4365	CO stretching + OH stretching CH_2 bending + CH_2 stretching
4560	Cellophane only
4780	OH and CH deformation modes + OH stretching
5190	Absorbed H_2O
5310–5480	Background
6770	2× OH stretching from cellulose and absorbed H_2O
7265	Background

The fundamental absorption bands found in cellulose have been investigated in some detail by Liang and Marchessault.[9,10] By drawing on their work, it was possible in most cases to make assignments from binary combinations of strong fundamental bands. In a few cases, it was apparent that more than one assignment was possible to give the observed band.

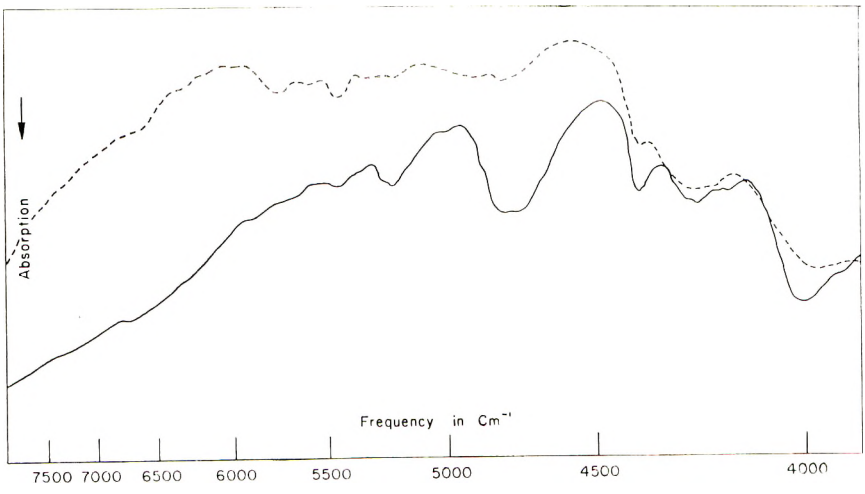

Fig. 2. Deuterated and basic spectra of bacterial cellulose: (——) untreated; (- -) deuterated.

The band occurring at 3970 cm.$^{-1}$ has been assigned to combination of CO-stretching bands occurring at 985–1058 cm.$^{-1}$ plus CH- and CH_2-stretching bands occurring at 2870–2970 cm.$^{-1}$. In the native celluloses this band is sharper and occurs at 3990 cm.$^{-1}$. The fundamentals involved here are strong ones and, since no other direct combinations occur at this frequency, the assignment is believed to be correct. Deuteration (Fig. 2) does not affect this band to any significant degree.

Similarly, assignments were made on the bands occurring at 4235 and 4365 cm.$^{-1}$. The first of these was assigned to a combination of OH and CH deformational modes at 1235–1430 cm.$^{-1}$ plus CH- and CH_2-stretching frequencies occurring at 2853–2940 cm.$^{-1}$. The band at 4365 cm.$^{-1}$ was assigned to CO stretching at 985–1058 cm.$^{-1}$ plus OH stretching at 3305–3405 cm.$^{-1}$. If this assignment were completely correct, the band should disappear in the deuterated sample where the OH is replaced by OD. As seen in Figure 2, this is not the case, although the band is reduced in intensity. Also occurring at this point is a combination of CH_2 bending at 1430 cm.$^{-1}$ and CH_2 stretching at 2945 cm.$^{-1}$ which could be contributing toward this band. In the polarized spectra that were obtained on tire cord both of these bands showed a very slight polarization, with the band at 4235 cm.$^{-1}$ appearing to be perpendicular, while that at 4365 cm.$^{-1}$ was parallel. Considering the fundamental combinations, the 4365 cm.$^{-1}$ band would be predicted as parallel, since both fundamental bands are essentially parallel and two parallel bands will give a parallel combination band. No prediction for the 4235 cm.$^{-1}$ band could be made because combinations gave both parallel and perpendicular bands in the overtone region.

There is a small band at 4560 cm.$^{-1}$ that occurs only in the cellophane. Since this is its only occurrence and there are no obvious combinations of

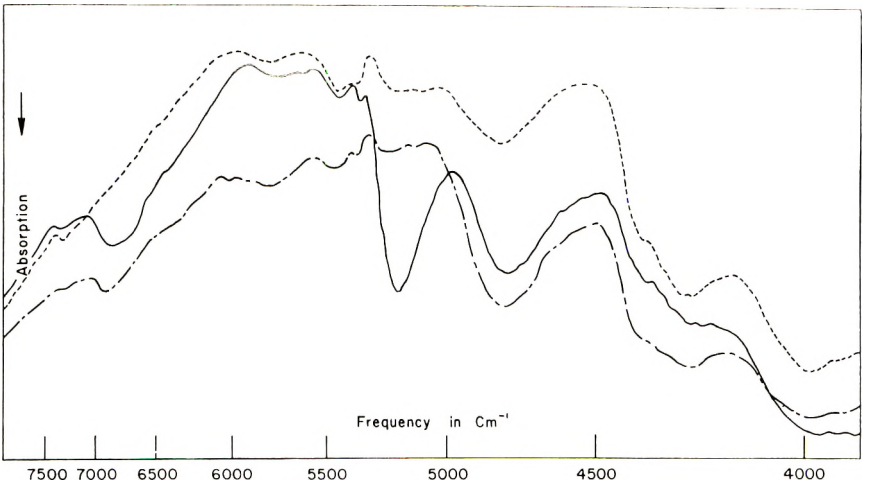

Fig. 3. Deuterated, oven dried, and basic spectra of tire cord rayon: (——) untreated; (- -) deuterated; (— - —) oven dried.

fundamentals at this point, it was not possible to make an assignment. It was felt that this band might be characteristic of the core structure of regular cellophane; however, the skin cellophane showed an indication of a band at this point although the resolution was poor.

The broad strong absorption band at 4780 cm.$^{-1}$ has been assigned to OH- and CH-deformational modes occurring at 1282–1455 cm.$^{-1}$ plus OH stretching at 3275–3405 cm.$^{-1}$. In addition to this combination of strong fundamentals, evidence for this assignment is obtained from the deuterated samples. Upon partial deuteration, the tire cord sample seen in Figure 3 showed a small decrease in the intensity of this band. The sample of bacterial cellulose which was more highly deuterated showed very little absorption at this wave number. As this latter sample was exposed to air and the OD groups returned to OH, the band again became strong. It did not, however, return to its original intensity, since the OD groups in the more crystalline material could not be exchanged, even when the sample was soaked in water. The presence of remaining OD groups was confirmed by observation of a portion of the sample in the fundamental region.

The absorption band occurring at 5190 cm.$^{-1}$ seems to be due exclusively to absorbed water. The band is weakest in the native celluloses which are known to have lower regain than the regenerated samples. It was possible in the case of the tire cord rayon to weaken the band by hydrolyzing the sample to a more crystalline form. It was also possible to eliminate the band completely by either deuteration or oven drying of the sample (Figs. 2 and 3). Conversely, the band could be strengthened by increasing the moisture content of the sample.

There are a number of small bands in the region of 5310–5480 cm.$^{-1}$ which are characteristic of the background and are not all a part of the cellulose structure. A similar small band occurs at 7265 cm.$^{-1}$.

The absorption band at 6770 cm.$^{-1}$ has been assigned to cellulosic OH and OH contributed by absorbed water. The absorption frequency corresponds to the first of the fundamental OH-stretching bands at 3245–3405 cm.$^{-1}$. Upon deuteration, the band disappears, substantiating the OH assignment. Oven drying causes the band to become less intense, but it is still present; conversely, an increase in the moisture content of the sample causes a strengthening of the band, both facts indicating that absorbed water is also a contributor. The bacterial cellulose does not show any distinct band at this point but has a very broad absorption region. There is no explanation at present for this, but it is evident that the broad band is due to OH overtones, since the deuterated sample seen in Figure 2 shows a return to the normal background.

The lack of pronounced dichroism in any of the absorption bands in this region is disappointing with respect to the usual structural applications of this property. It would appear to result from the combinatory nature of most of the bands, involving fundamentals with opposite polarizations. Oriented polyvinyl alcohol fibers showed very pronounced dichroism in this region under the same experimental conditions as used for cellulose.

References

1. Kaye, W., *Spectrochim. Acta*, **6**, 257 (1954).
2. Goddu, R. F., in *Advances in Analytical Chemistry and Instrumentation*, Vol. I, Interscience, New York, 1960.
3. Miller, R. G. J., and H. A. Willis, *J. Appl. Chem. (London)*, **6**, 385 (1956).
4. Holliday, P., *Nature*, **163**, 602 (1949).
5. Fraser, R. D. B., and T. P. MacRae, *J. Chem. Phys.*, **28**, 1120 (1958).
6. Ellis, J. W., and J. Bath, *J. Am. Chem. Soc.*, **62**, 2859 (1940).
7. Haskell, V. C., and D. K. Owens, *Textile Res., J.*, **30**, 993 (1960).
8. Morehead, F. F., and W. A. Sisson, *Textile Res. J.*, **15**, 443 (1945).
9. Liang, C. Y., and R. H. Marchessault, *J. Polymer Sci.*, **37**, 385 (1959).
10. Liang, C. Y., and R. H. Marchessault, *J. Polymer Sci.*, **39**, 269 (1959).

Résumé

On a étudié le spectre de la cellulose dans la région du proche infrarouge de 4000 à 8000 cm.$^{-1}$ environ, et on a conféré des attributions aux bandes d'absorption dans cette région. Les attributions ont été faites sur la base de combinaisons et recouvrements de fréquences fondamentales. Elles ont été contrôlées, quand c'était possible, par diverses modifications chimiques et physiques de l'échantillon. Le dichroïsme de toutes les bandes d'absorption de cette région était très faible.

Zusammenfassung

Das Absorptionsspektrum der Cellulose im nahen Infrarot von etwa 4000 bis 8000 cm.$^{-1}$ wurde untersucht und eine Bandenzuordnung vorgenommen. Die Zuordnung beruhte auf Kombinations- und Obertönen der Grundfrequenzen und wurde, wenn möglich, durch verschiedene chemische und physikalische Modifizierungen der Probe überprüft. Der Dichroismus aller Banden in diesem Bereich war sehr schwach.

Received April 2, 1962

JOURNAL OF POLYMER SCIENCE: PART A VOL. 1, PP. 1693–1700 (1963)

Transient Analysis of a Vibrating Reed

R. D. GLAUZ, *Aerojet-General Corporation, Sacramento, California*

Synopsis

A new simplified test for obtaining the physical properties of a viscoelastic material is described and analyzed. A reed, clamped at one end, is displaced at the free end and the damped oscillations measured. From measurements of the damping factor and frequency the complex modulus is computed. Tables of eigenvalues have been calculated for various masses and moments of inertia attached to the free end of the reed. Many experimental tests have shown the simplicity and usefulness of the method.

Introduction

The analysis of the transient behavior of a vibrating reed is considered from the standpoint of decaying oscillations. Previous authors, such as Glauz[1] and Bland and Lee[2] have considered the steady-state oscillations with driving force applied to the clamped end of the reeds. This has the disadvantage of involving instrumentation difficulties in obtaining a purely sinusoidal vibration with no change in slope of the driven end. The present analysis with a nonoscillating clamped end removes this difficulty.

An apparatus for testing based on this analysis might consist of a container for the vibrating reed (evacuted to remove the drag of air friction), an optical or electrical means of measuring the amplitude of oscillation of the free end, and a solenoid to initiate the oscillation. As stresses, strains, and displacements all satisfy the same relation with respect to time, any of these could be measured at any point on the reed.

Analysis

This analysis studies the free vibration of a clamped reed as a means of obtaining the physical properties of a viscoelastic material. The reed is considered to be thin and sufficiently long that motion may be represented by the differential equation

$$Q(\partial^4 w/\partial x^4) + (\gamma a_1/Ig)P(\partial^2 w/\partial t^2) = 0 \tag{1}$$

in which P and Q represent the differential operators in the linear time-dependent stress strain law

$$P(\sigma) = Q(\epsilon) \tag{2}$$

The boundary conditions at the clamped end are zero displacement and

zero slope. The free end has a mass attached with a moment of inertia. Thus

$$\begin{aligned} w(0) &= w'(0) = 0 \\ [-(QI/P)(\partial^2 w/\partial x^2) &= J(\partial^3 w/\partial t^2 \partial x)]_{x=l} \\ [(Q/P)I(\partial^3 w/\partial x^3) &= W(\partial^2 w/\partial t^2)]_{x=l} \end{aligned} \tag{3}$$

The special case of a perfectly elastic reed would vibrate continuously with zero change of amplitude

$$w = H(x)e^{i\omega t} \tag{4}$$

The effect of internal viscosity as exhibited by viscoelastic materials is a damping which causes a decrease in amplitude with time. This may be represented by the addition of an exponential damping factor $e^{-\lambda t}$ to eq. (4) resulting in

$$w(x,t) = H(x)e^{i\omega t}e^{-\lambda t} \tag{5}$$

Substitution of eq. (5) into the differential equation (1) and boundary conditions (3) yields the determining equations for $H(x)$ as

$$\begin{aligned} H^{IV}(x) - (\psi^4/l^4)H(x) &= 0 \\ H(0) = H'(0) &= 0 \\ H''(l) - B(\psi^4/l)H'(l) &= 0 \\ H'''(l) + A(\psi^4/l^3)H(l) &= 0 \end{aligned} \tag{6}$$

where we have defined

$$\begin{aligned} (\psi/l)^4 &= -\frac{m(i\omega - \lambda)^2 P(i\omega - \lambda)}{IQ(i\omega - \lambda)} \\ A &= W/ml \\ B &= J/ml^3 \end{aligned} \tag{7}$$

The solution of eq. (6) is given by

$$H = C_1 \sin(\psi/l)x + C_2 \cos(\psi/l)x + C_3 \sinh(\psi/l)x + C_4 \cosh(\psi/l)x \tag{8}$$

The boundary conditions become relations determining the C_1, C_2, C_3, C_4.

$$\begin{aligned} C_2 + C_4 &= 0 \\ C_1 + C_3 &= 0 \\ C_1(-\sin\psi - B\psi^3 \cos\psi) + C_2(-\cos\psi + B\psi^3 \sin\psi) & \\ + C_3(\sinh\psi - B\psi^3 \cosh\psi) + C_4(\cosh\psi - B\psi^3 \sinh\psi) &= 0 \\ C_1(-\cos\psi + A\psi \sin\psi) + C_2(\sin\psi + A\psi \cos\psi) & \\ + C_3(\cosh\psi + A\psi \sinh\psi) + C_4(\sinh\psi + A\psi \cosh\psi) &= 0 \end{aligned} \tag{9}$$

In order for this set of homogeneous equations to have nontrivial solutions for C_1, C_2, C_3, C_4, the determinant of their coefficients must vanish:

$$\begin{vmatrix} 0 & 1 & & \\ 1 & 0 & & \\ -\sin\psi - B\psi^3\cos\psi & -\cos\psi + B\psi^3\sin\psi & & \\ -\cos\psi + A\psi\sin\psi & \sin\psi + A\psi\cos\psi & & \\ & & 0 & 1 \\ & & 1 & 0 \\ & & \sinh\psi - B\psi^3\cosh\psi & \cosh\psi - B\psi^3\sinh\psi\, i \\ & & \cosh\psi + A\psi\sinh\psi & \sinh\psi + A\psi\cosh\psi \end{vmatrix} = 0 \tag{10}$$

Expanding yields eq. (11):

$$1 + \cos\psi\cosh\psi + A\psi(\cos\psi\sinh\psi - \sin\psi\cosh\psi)$$
$$-B\psi^3(\sin\psi\cosh\psi + \cos\psi\sinh\psi) + AB\psi^4(1 - \cos\psi\cosh\psi) = 0 \tag{11}$$

In the case of no mass or moment of inertia at the free end of the reed eq. (11) reduces to

$$1 + \cos\psi\cosh\psi = 0 \tag{12}$$

It is proven in Appendix I that eq. (12) has only solutions

$$\psi = \pm 1.87510,\ \pm 1.87510i \tag{13}$$

in the region $-\pi < Re\{\psi\} < \pi$, $-\pi < Im\{\psi\} < \pi$. All four values of eq. (13) yield the same value for ψ^4.

In the general case of eq. (11) for nonzero A and B, one would conjecture that the same situation would occur, that is, the value of ψ^4 would be a real positive number with ψ satisfying eq. (11). In fact, one could pick sufficiently small A, B to make the only values of ψ satisfying eq. (11) to be in the neighborhood of $\psi = \pm 1.87510,\ \pm 1.87510i$ and to have zero complex part. This is easily seen by expanding eq. (11) into real and imaginary parts and for small b finding that there is no solution near $\psi = 1.87510$ for $b \neq 0$.

Equation (11) has been solved for various values of A, B and the results tabulated in Tables I and II.

Separating eq. (7) defining $(\psi/l)^4$ into real and imaginary parts yields the two equations

$$E_1 = (ml^4/I\psi^4)(\omega^2 - \lambda^2) \tag{14}$$

$$E_2 = (ml^4/I\psi^4)(2\omega\lambda) \tag{15}$$

where we have defined the complex modulus as

$$E_1 + iE_2 = Q(i\omega - \lambda)/P(i\omega - \lambda) \tag{16}$$

For the perfectly elastic case, $\lambda = 0$, note that eqs. (14) and (15) reduce to

$$E_1 = (ml^4/I\psi^4)\omega^2 \tag{17}$$
$$E_2 = 0$$

TABLE I
Solution of Eq. (11) for Various Values of A and B

	ψ										
B	$A=0.0$	$A=0.01$	$A=0.02$	$A=0.03$	$A=0.04$	$A=0.05$	$A=0.06$	$A=0.07$	$A=0.08$	$A=0.09$	$A=0.10$
0	1.875	1.857	1.839	1.823	1.807	1.791	1.776	1.762	1.749	1.735	1.723
0.01	1.840	1.823	1.807	1.791	1.776	1.762	1.748	1.735	1.722	1.710	1.698
0.02	1.805	1.789	1.774	1.760	1.746	1.733	1.720	1.708	1.696	1.685	1.674
0.03	1.771	1.757	1.743	1.730	1.717	1.705	1.694	1.682	1.671	1.660	1.650
0.04	1.738	1.726	1.713	1.701	1.690	1.678	1.667	1.657	1.647	1.637	1.627
0.05	1.707	1.696	1.684	1.673	1.663	1.653	1.642	1.633	1.623	1.614	1.605
0.06	1.678	1.668	1.657	1.647	1.637	1.628	1.619	1.610	1.601	1.592	1.584
0.07	1.651	1.641	1.631	1.622	1.613	1.604	1.596	1.587	1.579	1.571	1.564
0.08	1.625	1.616	1.607	1.598	1.590	1.582	1.574	1.566	1.559	1.551	1.544
0.09	1.600	1.592	1.584	1.576	1.568	1.561	1.553	1.546	1.539	1.532	1.526
0.10	1.577	1.569	1.562	1.555	1.548	1.541	1.534	1.527	1.521	1.514	1.508

TABLE II
Solution of Eq. (11) for Various Values of A and B

	ψ										
B	$A=0.0$	$A=0.1$	$A=0.2$	$A=0.3$	$A=0.4$	$A=0.5$	$A=0.6$	$A=0.7$	$A=0.8$	$A=0.9$	$A=1.0$
0.0	1.875	1.723	1.616	1.536	1.472	1.420	1.376	1.338	1.304	1.274	1.248
0.1	1.577	1.508	1.451	1.403	1.361	1.326	1.294	1.265	1.240	1.217	1.196
0.2	1.405	1.367	1.333	1.302	1.274	1.249	1.226	1.204	1.185	1.166	1.149
0.3	1.296	1.271	1.248	1.226	1.206	1.187	1.169	1.153	1.137	1.123	1.109
0.4	1.219	1.201	1.183	1.167	1.152	1.137	1.123	1.110	1.097	1.085	1.074
0.5	1.160	1.146	1.132	1.120	1.107	1.095	1.084	1.073	1.063	1.052	1.043
0.6	1.113	1.101	1.091	1.080	1.070	1.060	1.050	1.041	1.032	1.024	1.015
0.7	1.074	1.064	1.055	1.047	1.038	1.030	1.021	1.014	1.006	0.998	0.991
0.8	1.041	1.033	1.025	1.018	1.010	1.003	0.996	0.989	0.982	0.976	0.969
0.9	1.012	1.006	0.999	0.992	0.986	0.979	0.973	0.967	0.961	0.955	0.950
1.0	0.988	0.981	0.976	0.970	0.964	0.958	0.953	0.947	0.942	0.937	0.932

In the special case of a Voigt model,

$$\sigma = \eta(d\epsilon/dt) + E\epsilon \tag{18}$$

$$E_1 = E - \lambda\eta$$

$$E_2 = \eta\omega \tag{19}$$

$$E = E_1 + \lambda\eta = (ml^4/I\psi^4)(\omega^2 + \lambda^2)$$

$$\eta = E_2/\omega = (ml^4/I\psi^4)(2\lambda)$$

Hence, from eqs. (14), (15), and (19)

$$\lambda = (E/\eta) - (E/\eta)[1 - (\omega^2\eta^2/E^2)]^{1/2} \tag{20}$$

For the case of a Maxwell model:

$$(1/E)(d\sigma/dt) + (\sigma/\eta) = d\epsilon/dt \tag{21}$$

$$E_1 = [\omega^2\eta^2 E - \lambda\eta\, E(E - \lambda\eta)]/[(E - \eta\lambda)^2 + \eta^2\omega^2] \tag{22}$$

$$E_2 = [\omega\eta E(E - \lambda\eta) + \omega\lambda\eta^2 E]/[(E - \eta\lambda)^2 + \eta^2\omega^2]$$

From eqs. (14), (15), and (22) one obtains

$$2\eta\lambda^3 - E\lambda^2 + 2\omega^2\eta\lambda - \omega^2 E = 0$$

with solution

$$\lambda = E/2\eta \tag{23}$$

The values of E_1, E_2 may be written for any linear, time-dependent stress–strain law. The above two are interesting because of the eqs. (20), (23) which give the decay constant λ in terms of the model constants and frequency.

Test Data Analysis

A test apparatus which has been used with good results consists of a steel beam supporting the viscoelastic reed. A strain gage attached to the beam measures the decaying oscillation of the reed. In the analysis it is assumed that the reed is rigidly attached. In actuality, the attached end of the reed oscillates a small amount. It is felt that this effect could be included in the analysis with little change in the answers and it has been therefore neglected.

The resulting trace of a representative test of a highly damped material is shown in Figure 1.

In analyzing this trace it is necessary to obtain the frequency of vibration and the damping factor. The frequency is readily obtained from the time between successive crossings of the reference axis. Several crossings of the axis are measured, and the data fitted with a least-squares straight line. A computer program which analyzes the data will handle measurements of

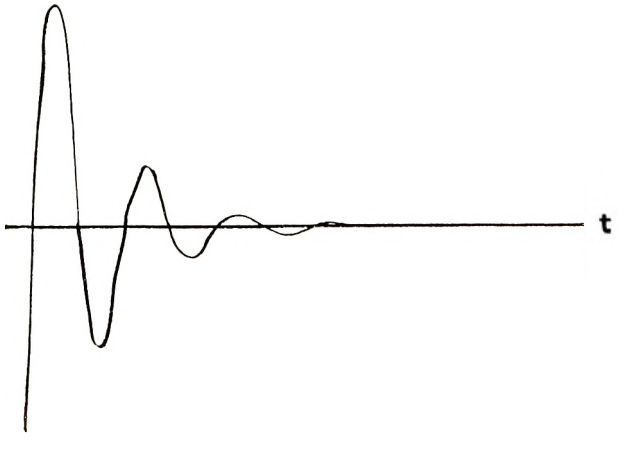

Figure 1.

every crossing or every nth crossing. For the decay constant the peaks are measured from the axis in arbitrary units and the log of the amplitude fitted with a least-squares straight line. The slopes of the two least-squares straight lines yield the frequency and damping, respectively.

Physical Considerations

Testing has been performed on some highly damped materials. These materials yield a test trace which has only three or four measurable peaks and crossings. Analysis of the data has indicated that the resulting values of damping ratio

$$\text{damping ratio} = \lambda/\omega$$

are in the neighborhood of $^1/_3$ to $^1/_4$. These high values of damping give values for the complex modulus which are definitely located in the middle of the complex plane. The complex modulus as measured in these tests gives both the real and imaginary parts of E as functions of a complex variable. Thus we have essentially generalized the concept of the complex modulus. This more generalized complex modulus is necessary in analyzing the damped dynamic stresses in a given stress field. The assumption that the complex modulus is a function of only $i\omega$, is a restriction which is here removed.

The complex modulus on the purely imaginary axis is obtainable by extrapolation. By increasing the loading on the end of the reed it is possible to reduce the damping. Thus, values of damping ratio much smaller than the above indicated values are obtainable. By extrapolation of the data obtained for different damping ratios the values on the imaginary axis are obtained. Confirmation of the above procedures is possible using the steady state forced vibration testing as indicated by other authors.

APPENDIX I

In eq. (12) let

$$\psi = a + ib \tag{A1}$$

Then expanding eq. (12) and separating into real and imaginary parts yields the two equations

$$1 + \cos a \cosh b \cosh a \cos b + \sin a \sinh b \sinh a \sin b = 0 \tag{A2}$$

$$\cos a \cosh b \sinh a \sin b = \sin a \sinh b \cosh a \cos b \tag{A3}$$

We note that for $b = 0$ eq. (A2), (A3) reduce to

$$1 + \cos a \cosh a = 0 \tag{A4}$$

with roots $a = \pm 1.8751, \pm 1.8751i$ for the fundamental mode.

If we multiply eq. (A2) by the factor

$$\sinh a \sin b \sin a \sinh b \tag{A5}$$

which yields

$$\sinh a \sin b \sin a \sinh b + \cos a \cosh b \sinh a \sin b \cosh a \cos b \sin a \sinh b + \sin^2 a \sinh^2 b \sin^2 a \sin^2 b = 0 \tag{A6}$$

and substitute eq. (A3) in the second term of eq. (A6), we have

$$\sinh a \sin b \sin a \sinh b + \sin^2 a \sinh^2 b \cosh^2 a \cos^2 b + \sin^2 a \sinh^2 b \sinh^2 a \sin^2 b = 0 \tag{A7}$$

Now we note that the second and third terms of eq. (A7) are positive. If it can be shown that the first term is also positive for $a, b \neq 0$, then the proof is complete.

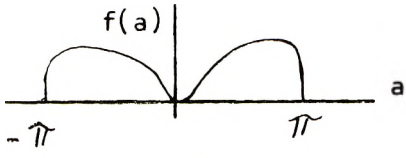

Figure 2.

The first term has factors $\sin a \sinh a$, $\sin b \sinh b$.

Investigation of the function $\sin a \sinh a$ (Fig. 2) shows that it is positive in the range $-\pi < a < \pi$ and zero only at $a = 0$; thus eq. (A7) > 0 except at $a = 0$ or $b = 0$.

APPENDIX II

Nomenclature

a, b	=	complex representation of ψ
a_1	=	cross-sectional area, in.^{2}
A, B	=	constants
E	=	Young's modulus, lb./in.^{2}
E_1, E_2	=	complex modulus components, lb./in.^{2}
g	=	acceleration of gravity, in./sec.^{2}
H	=	displacement distribution, in.
I	=	moment of inertia of cross section, in.^{4}
J	=	moment of inertia of mass, lb.-sec.^{2}in.^{2}/in.
l	=	length of reed, in.
m	=	mass per unit length of reed, lb. sec.^{2}/in.^{2}
Q, P	=	operators in stress–strain law
t	=	time, sec.
w	=	transverse displacement, in.
W	=	end loading, lb.-sec.^{2}/in.

ϵ = strain
γ = density, lb./in.^{3}
η = viscous damping, lb.-sec./in.^{2}
λ = damping factor, 1/sec.
σ = stress, lb./in.^{2}
ω = frequency of vibration, rad/sec.
ψ = eigenvalue

References

1. Glauz, R. D., *The Viscoelastic Vibrating Reed*, Technical Report, Brown University, Providence, R. I., 1952.

2. Bland, D. R., and E. H. Lee, *The Calculation of the Complex Modulus of Linear Visco-Elastic Materials from Vibrating Reed Measurements*, Brown University Technical Report No. 9, January 1955.

Résumé

On décrit et analyse un nouveau test simplifié pour obtenir les propriétés physiques d'un matériel viscoélastique. Un peigne, fixé à ces extrèmités, est déplacé à l'extrémité libre et les oscillations amorties sont mesurées. À partir de mesures du facteur d'amortissement et de fréquence on détermine le module du complexe. On a calculé des tables de valeurs propres pour diverses masses et moments d'inertie attachés à l'extrémité libre du peigne. De nombreux tests expérimentaux ont montré la simplicité et la possibilité d'utilisation de la méthode.

Zusammenfassung

Ein neuer vereinfachter Test zur Bestimmung der physikalischen Eigenschaften eines viskoelastischen Stoffes wird beschrieben und einer Analyse unterzogen. Ein an einem Ende eingespanntes Stäbchen wird am freien Ende abgebogen und die gedämpften Schwingungen gemessen. Aus dem gemessenen Dämpfungsfaktor und der Frequenz wird der komplexe Modul berechnet. Tabellen der Eigenwerte wurden für verschiedene, am freien Stäbchenende angebrachte Massen und Trägheitsmomente berechnet. Viele Versuchstests bewiesen die Einfachheit und Brauchbarkeit der Methode.

Received March 26, 1962

JOURNAL OF POLYMER SCIENCE: PART A VOL. 1, PP. 1701–1708 (1963)

Thermodynamic Properties of Polymethyl Methacrylate and Methyl Methacrylate

R. W. WARFIELD and M. C. PETREE, *U. S. Naval Ordnance Laboratory, White Oak, Silver Spring, Maryland*

Synopsis

From published data the entropy, enthalpy, and Gibbs free energy of polymethyl methacrylate (PMMA) have been calculated over the temperature range 0–260°K. These functions have also been calculated for methyl methacrylate over the range 0–210°K. The entropy of polymerization at 210°K. was found to be 9.63 cal./mole°K. and the free energy of polymerization was found to be −11.8 kcal./mole. The thermodynamic function C_p/T versus T as calculated for PMMA exhibits a maximum at 70–100°K. The number of classically vibrating units per repeating unit of PMMA at 260°K. is 6.38, and the difference C_p–C_v is found to be 0.014 cal./g.°K.

Introduction

A fundamental approach toward an understanding of the structure and internal motions of a polymer is to investigate the temperature dependence and magnitude of the specific heat, C_p, and of the related thermodynamic functions over a temperature range extending down to absolute zero. Changes in C_p and in the related functions, entropy, enthalpy, and free energy, are indicative of changes in the structure and internal motions of a polymer due to crystallization, glass transitions, and melting. In addition, C_p measurements at low temperatures are useful in testing the validity of the various theoretical equations for the heat capacity of linear polymers, such as those advanced by Tarassov[1] and by Stockmayer and Hecht.[2]

Additional thermodynamic data on bulk polymers are needed to elucidate the nature of the glassy and crystalline states and to explain the magnitude of the energy changes which occur when polymers are heated or cooled, crystallized or melted. This paper, which is the fourth in a series[3–5] presents the calculated values of the entropy, enthalpy, and Gibbs free energy for polymethyl methacrylate (PMMA) over the temperature range 0–260°K. and for methyl methacrylate (MMA) monomer over the range 0–210°K. The thermodynamic function C_p/T versus T is calculated for PMMA, as is the difference $C_p - C_v$ and the number of classically vibrating units per repeating unit.

Specific Heats of Polymethyl Methacrylate and Methyl Methacrylate

Specific heat of polymethyl methacrylate is of particular interest because of the presence of pendent —CH_3 and —CO—OCH_3 groups along the

main chain. It would be expected that both the ester methyl group and the main chain methyl group in PMMA would contribute to the specific heat. Thus, while the molecular weights per repeating unit of PMMA and polystyrene (PS) are very similar, it would be expected that the differences in the vibrational spectrum produced by the different pendent groups would be reflected by differences in the temperature dependence of the specific heats.

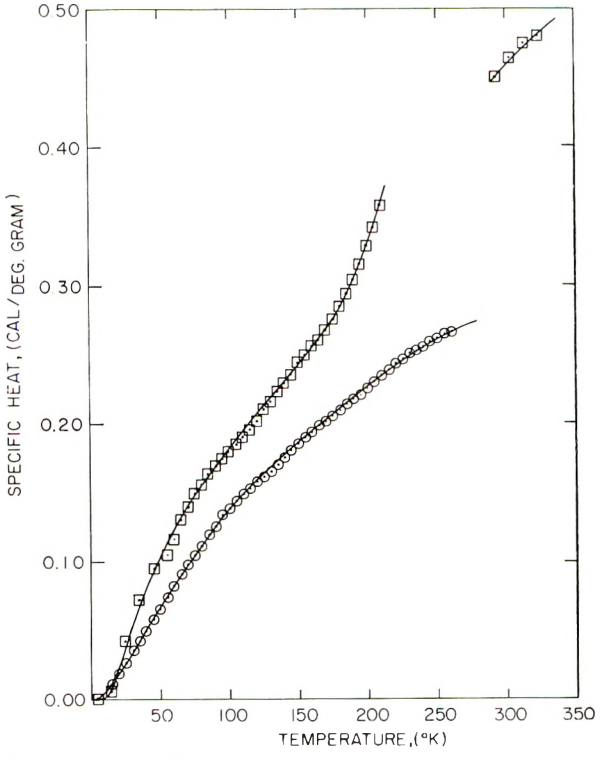

Fig. 1. Specific heat of methyl methacrylate and polymethyl methacrylate: (⊡) methyl methacrylate, data of Sochava (60–210°K.) and Erdos (293–323°K.); (⊙) polymethyl methacrylate, data of Sochava (16–260°K.).

The specific heat of PMMA has been determined by Sochava[6] between 16 and 60°K. and by Sochava and Trapeznikova[7] between 60 and 260°K. These investigators have also determined the C_p of MMA between 60 and 210°K., and Erdos and co-workers[8] have reported data between 293 and 323°K.

The specific heat of PMMA between 0 and 16°K. was obtained by extrapolating a plot of C_p/T versus T^2 of the experimental data between 16 and 30°K. to absolute zero. The specific heat of MMA between 0 and 60°K. was estimated by means of a Debye function with 8 degrees of freedom and a θ_D value of 151°K.[9] C_p of PMMA and MMA are shown in Figure 1 and in Tables I and II.

TABLE I
Specific Heat, Entropy, Enthalpy, and Gibbs Free Energy of Methyl Methacrylate

Temperature, °K.	Specific heat C_p, cal./g.°K.[a]	$S_T - S_{0°K.}$, cal./g.°K.	$H_T - H_{0°K.}$, cal./g.	$-(F_T - F_{0°K.})$, cal./g.
10	(0.004)[b]	0.0021	0.013	0.002
20	(0.027)[b]	0.0153	0.133	0.097
30	(0.059)[b]	0.0372	0.562	0.368
40	(0.084)[b]	0.0616	1.288	0.868
50	(0.103)[b]	0.0856	2.242	1.610
60	0.118	0.1079	3.352	2.582
70	0.142	0.1298	4.662	3.775
80	0.157	0.1512	6.162	5.178
90	0.170	0.1717	7.802	6.792
100	0.181	0.1912	9.552	8.612
110	0.191	0.2097	11.40	10.62
120	0.204	0.2276	13.37	12.80
130	0.217	0.2452	15.48	15.17
140	0.230	0.2624	17.71	17.71
150	0.244	0.2793	20.08	20.42
160	0.256	0.2960	22.58	23.30
170	0.269	0.3124	25.20	26.34
180	0.285	0.3287	27.97	29.55
190	0.305	0.3451	30.92	32.92
200	0.328	0.3617	34.08	36.45
210	0.358	0.3788	37.50	40.15

[a] Data of Sochava (60–210°K.).
[b] Calculated by a Debye function.

Between 16° and 60°K., PMMA and PS[6] exhibit similar magnitudes of C_p. However, the C_p of PMMA increases linearly with temperature, while that of PS exhibits a nonlinear temperature dependence. This suggests that PS has an additional heat capacity which is superimposed upon a linear one. Trapeznikova and Feofanova[10] have concluded that this additional C_p is due to the rotation of the phenyl group in PS.

Warfield and Petree[11] have recently shown that the model of Stockmayer and Hecht[2] and the analytical procedure of Starkweather[12] can be applied to the low temperature heat capacity data of PMMA and PS. Several structural parameters can be calculated by this procedure.

Entropy, Enthalpy, and Gibbs Free Energy Calculations

From C_p data, values of entropy, enthalpy, and Gibbs free energy of PMMA and MMA have been calculated at ten degree increments by numerical integration; results are presented in Tables I and II and in Figure 2. The values were obtained by evaluating the thermodynamic relations

$$S_T - S_{0°K.} = \int_0^T \frac{C_p dT}{T} \tag{1}$$

TABLE II
Specific Heat, Entropy, Enthalpy, and Gibbs Free Energy of Polymethyl Methacrylate

Temperature, °K.	Specific heat C_p, cal./g.°K.[a]	$S_T - S_{0°K.}$, cal./g.°K.	$H_T - H_{0°K.}$, cal./g.	$-(F_T - F_{0°K.})$, cal./g.
10	(0.010)[b]	0.0112	0.070	0.010
20	0.019	0.0246	0.190	0.179
30	0.035	0.0384	0.460	0.500
40	0.051	0.0529	0.890	0.962
50	0.066	0.0675	1.470	1.568
60	0.083	0.0823	2.210	2.316
70	0.098	0.0977	3.130	3.220
80	0.112	0.1127	4.180	4.272
90	0.126	0.1277	5.380	5.474
100	0.139	0.1425	6.710	6.828
110	0.149	0.1569	8.150	8.324
120	0.158	0.1708	9.680	9.962
130	0.166	0.1843	11.30	11.74
140	0.176	0.1975	13.02	13.64
150	0.186	0.2104	14.83	15.68
160	0.194	0.2231	16.73	17.85
170	0.202	0.2356	18.72	20.15
180	0.210	0.2478	20.79	22.58
190	0.218	0.2597	22.93	25.11
200	0.226	0.2709	25.15	27.68
210	0.235	0.2825	27.47	30.44
220	0.244	0.2939	29.86	33.33
230	0.250	0.3051	32.34	36.31
240	0.255	0.3161	34.87	39.41
250	0.262	0.3269	37.46	42.63
260	0.267	0.3375	40.11	45.95

[a] Data of Sochava (16–260°K.).
[b] Calculated by extrapolation.

$$H_T - H_{0°K.} = \int_0^T C_p dT \tag{2}$$

$$F_T - F_{0°K.} = (H_T - H_{0°K.}) - T(S_T - S_{0°K.}) \tag{3}$$

where $(S_T - S_{0°K.})$, $(H_T - H_{0°K.})$, and $(F_T - F_{0°K.})$ are the entropy, enthalpy, and Gibbs free energy relative to absolute zero.

At 260°K., the entropy of PMMA was found to be 0.3375 cal./g.°K. or 33.75 cal./mole°K. Entropy of MMA at 210°K. was found to be 0.3788 cal./g.°K. or 37.88 cal./mole°K. The entropy of polymerization at 210°K. was found by difference to be 9.63 cal./mole°K. At 260°K. the enthalpy of PMMA was found to be 40.11 cal./g., and that of MMA at 210°K. was 37.50 cal./g. Gibbs free energy of PMMA at 260°K. was found to be −45.95 cal./g. and for MMA at 210°K., −40.15 cal./g.

The free energy of polymerization, ΔF, is calculated at 210°K. by means of eq. (4):

$$\Delta F = \Delta H - T\,\Delta S \tag{4}$$

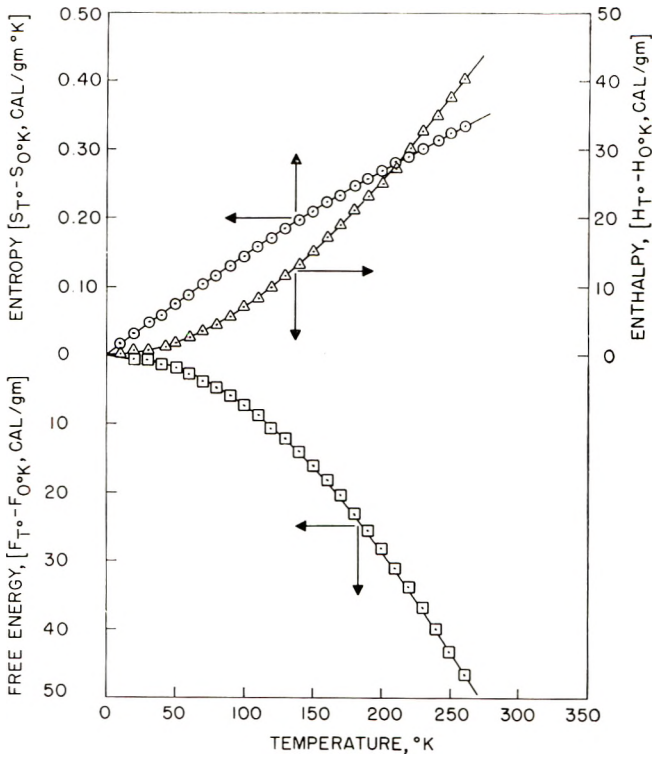

Fig. 2. Thermodynamic functions of polymethyl methacrylate: (⊙) entropy; (△) enthalpy; (⊡) Gibbs free energy.

where ΔH is the heat of polymerization of MMA (13.8 kcal./mole),[13] and ΔS is the entropy of polymerization (9.6 cal./mole°K.). The free energy of polymerization is thus found to be −11.8 kcal./mole at 210°K. This ΔF value may be slightly high, since the ΔH was determined at 300°K. The corresponding (ΔF) value for the polymerization of styrene at 300°K. is −9.4 kcal./mole. These values can be compared with the ΔF value of −14.3 kcal./mole which has been calculated by Dainton et al.[14] for the polymerization of 3,3-bis(chloromethyl)oxyacyclobutane.

Plots of the thermodynamic functions versus temperature for PMMA are shown in Figure 2. These functions change with temperature in a manner very similar to those of PS and polyethylene. Since PMMA is an amorphous polymer, it must be assumed that there will be residual entropy at absolute zero.

The Function C_p/T versus T for Polymethyl Methacrylate

Smith and Dole[15] have pointed out that the function C_p/T versus T is a constant if the specific heat rises linearly with T from a zero value at absolute zero. The function C_p/T measures the rate at which the entropy increases with temperature:

$$(dS/dT)_P = C_p/T \tag{5}$$

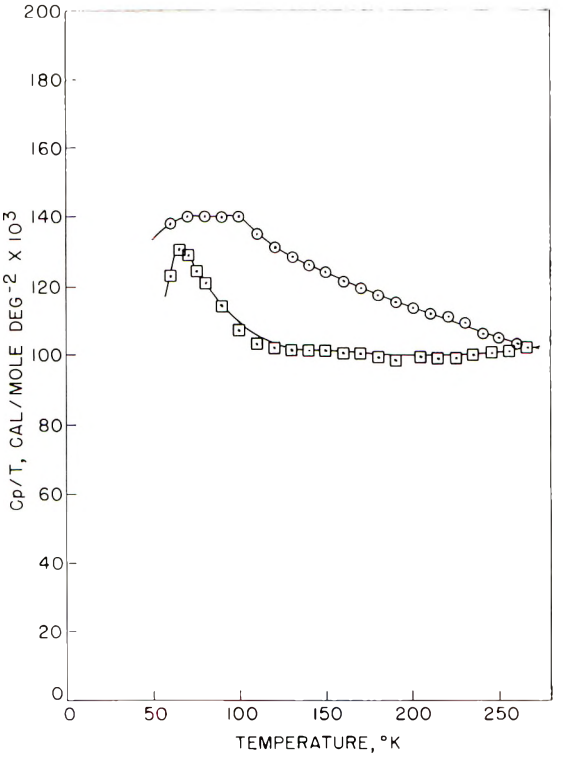

Fig. 3. Specific heat function C_p/T vs. T for polymethyl methacrylate and polystyrene: (⊙) polymethyl methacrylate; (⊡) polystyrene.

Dole and Wunderlich[16] have presented data for the magnitude and temperature dependence of this function for a number of polymers and long chain hydrocarbons. For many of the hydrocarbons, a maximum value of the function is observed at 60–70°K. which, according to Dole and Wunderlich,[16] is due to one or more modes of vibration having the same frequency dominating at this temperature range. Warfield and Petree have found that polystyrene,[3] polyethylene,[4] polyvinyl alcohol,[5] and polytetrafluoroethylene[4] exhibit maxima at temperatures below 100°K.

A plot of C_p/T versus T for PMMA is shown in Figure 3. Data for PS are included for purposes of comparison. It will be noted that PMMA exhibits a maximum value of this function at 70–100°K. and that at higher temperatures the magnitude of the function decreases. These maximum values are probably due to interactions between chains which can best be described by a three-dimensional Debye continuum of acoustic frequencies.[3]

Vibrating Units per Repeating Unit of Polymethyl Methacrylate

Based upon a number of assumptions, Dole[17] was able to calculate the heat capacity per vibrating unit of polyethylene. Employing the same assumptions it is possible to estimate the number of classically vibrating

units at 260°K. in the PMMA repeating unit $—C(CH_3)(COOCH_3)CH_2—$. Three assumptions are employed. The first is that the force constant of the C—H bond is so great that the methyl and methylene groups will vibrate as a single unit; the second is that every group in the chain can vibrate harmonically with two degrees of freedom along mutually perpendicular axes transverse to the chain direction; and the third, that longitudinal or stretching vibrations are negligible at 260°K. If each vibrating unit vibrates with two degrees of freedom, the expected specific heat would be $2R$ or 3.97 cal./mole°K. per vibrating unit. However, these considerations apply to C_v, not C_p.

The number of vibrating units per repeating unit is found by dividing C_v, the heat capacity at constant volume, by $2R$. C_v can be calculated by means of eq. (6):

$$C_v = C_p \left[\frac{1}{1 + (TV^2d^2/C_pJ)} \right] \tag{6}$$

where C_p is the observed heat capacity of PMMA at 260°K. (0.267 cal./g.°K.); V is the sound velocity (2320 m./sec.);[18] d is the cubic coefficient of expansion (2.06×10^{-4});[19] and J is the mechanical equivalent of heat (4.184×10^7 erg/cal.). C_v is found to be 0.253 cal./g.°K. or 25.3 cal./mole°K., and $(C_p - C_v)$ is 0.014 cal./g.°K.) Based upon these values the number of vibrating units per repeating unit of PMMA at 260°K. is 6.38.

References

1. Tarassov, V. V., *Dokl. Akad. Nauk, SSSR*, **100**, 307 (1955); *J. Am. Chem. Soc.*, **80**, 5052 (1958).
2. Stockmayer, W. H., and C. E. Hecht, *J. Chem. Phys.*, **21**, 1954 (1953).
3. Warfield, R. W., and M. C. Petree, *J. Polymer Sci.*, **55**, 497 (1961).
4. Warfield, R. W., and M. C. Petree, *Makromol. Chem.*, **51**, 113 (1962).
5. Warfield, R. W., and R. Brown, *Kolloid-Z.*, **185**, 63 (1962).
6. Sochava, I. V., *Vestn. Leningr. Univ., Ser. Fiz. i Khim.*, **16**, No. 10, 2, 70 (1961).
7. Sochava, I. V., and O. N. Trapeznikova, *Vestn. Leningr.* Univ., *Ser. Fiz. i Khim.*, **13**, No. 16, 65 (1958).
8. Erdos, E., L. Jager, and J. Pouchly, *Chem. Listy*, **46**, 770 (1952).
9. Debye, P., *Ann. Physik.*, **39**, 789 (1912).
10. Trapeznikova, O. N., and E. I. Feofanova, *Zhur. Fiz. Khim.*, **35**, 1114 (1961).
11. Warfield, R. W., and M. C. Petree, *Nature*, **193**, 1280 (1962).
12. Starkweather, H. W., *J. Polymer Sci.*, **45**, 525 (1960).
13. Dainton, F. S., K. J. Ivin, and A. G. Walmsley, *Trans. Faraday Soc.*, **56**, 1784 (1960).
14. Dainton, F. S., D. M. Evans, F. E. Hoarr, and T. P. Melia, *Polymer*, **3**, 263 (1962)
15. Smith, C. W., and M. Dole, *J. Polymer Sci.*, **20**, 37 (1956).
16. Dole, M., and B. Wunderlich, *Makromol. Chem.*, **34**, 29 (1959).
17. Dole, M., *Kolloid-Z.*, **165**, 40 (1959).
18. Butta, E., *Ann. Chim. (Rome)*, **48**, 802 (1958).
19. Clash, R. F., and L. M. Rynkiewicz, *Ind. Eng. Chem.*, **36**, 279 (1944).

Résumé

On a calculé d'après des résultats publiés, l'entropie, l'enthalpie et l'énergie libre de Gibbs du polyméthacrylate de méthyle (PMMA) dans un domaine de température allant de 0–260°K. Ces fonctions ont également été calculées pour le méthacrylate de méthyle entre 0–210°K. L'entropie de polymérisation à 210°K. est 9.63 cal./mole°K. et l'énergie libre de polymérisation est −11.8 kcal./mole. La fonction thermodynamique C_p/T en fonction de T calculée pour le PMMA présente un maximum entre 70–100°K. Le nombre d'unités vibrant d'une façon classique par unité de PMMA à 260°K. est 6.38, et la différence $C_p - C_v$ est 0.014 cal./g.°K.

Zusammenfassung

Aus Literaturangaben wurden Entropie, Enthalpie und Gibbssche freie Energie von Polymethylmethacrylat (PMMA) in Temperaturbereich von 0–260°K berechnet. Die gleichen Funktionen wurden auch für Methylmethacrylat im Bereich von 0–210°K berechnet. Die Polymerisationsentropie bei 210°K ergab sich zu 9,63 cal./Mol.°K und die freie Polymerisationsenergie zu −11,8 kcal./mole. Die für PMMA berechnete thermodynamische Funktion C_p/T zeigt in Abhängigkeit von T ein Maximum zwischen 70–100°K. Die Zahl der klassischen Oszillatoren pro Grundeinheit von PMMA beträgt bei 260°K 6,38 und die Differenz $C_p - C_v$ ergibt sich zu 0,014 cal./g.°K.

Received April 9, 1962

JOURNAL OF POLYMER SCIENCE: PART A VOL. 1, PP. 1709–1720 (1963)

Self-Diffusion and Nuclear Relaxation in Polyisobutylene

DAVID W. McCALL, DEAN C. DOUGLASS, and ERNEST W. ANDERSON, *Bell Telephone Laboratories, Incorporated, Murray Hill, New Jersey*

Synopsis

Various self-diffusion and nuclear relaxation experiments are reported for a polyisobutylene of rather low molecular weight, in bulk and in solution. In the bulk, the self-diffusion coefficient obeys the Arrhenius relation, yielding an activation energy of 5.5 kcal./mole. In solution the activation energies are lower, approaching the value for the solvent at low concentration. The self-diffusion coefficient of the polymer at infinite dilution is 1.2×10^{-5} cm.^{2}/sec. in CS_2 and 0.44×10^{-5} cm.^{2}/sec. in CCl_4. The ratio is close to the inverse ratio of the solvent viscosities. Measurements of self-diffusion of the solvent have been made for cyclohexane in polyisobutylene. A simple interpretation of the data in terms of Stokes-Einstein models yields molecular dimensions which are too small by a factor of two or three.

I. INTRODUCTION

The study of self-diffusion in polymer systems is of fundamental importance. Theories for viscoelastic and dielectric behavior are often presented in terms of parameters called friction factors, and a direct measure of these parameters can be obtained from self-diffusion measurements. This paper presents the results of a series of measurements of self-diffusion for a polyisobutylene of low molecular weight in bulk and in solution. In addition, nuclear magnetic relaxation has been studied in the same systems.

Both self-diffusion and nuclear relaxation measurements provide information on time dependent behavior but the experiments do not require the existence of appreciable gradients (e.g., concentration, velocity, or temperature gradients) in the system. The interpretation of nuclear relaxation times is more complicated than the interpretation of self-diffusion owing to the fact that both rotational and translational motions affect the former, whereas self-diffusion is a measure of translational effects only.

II. EXPERIMENTAL

The proton magnetic resonance spin-echo technique for measuring self-diffusion has been fully described previously.[1,2] No changes have been made in the method, but a slight extension of the analysis is necessary to include the measurement of self-diffusion coefficients for the components of

a mixture. The echo amplitude for an n-component solution can be written as:

$$h(2\tau) = \sum_{i=1}^{n} x_i h_i(2\tau) \tag{1}$$

when the sample is contained in a very homogeneous field (i.e., when diffusion is negligible). τ is the separation in time between the 90° pulse and the 180° pulse and x_i is the fraction of protons contained in the ith component. When a linear field gradient is applied, the echo amplitude is given by

$$g(2\tau) = \sum_{i=1}^{n} x_i h_i(2\tau) \exp\left\{-2(\gamma G)^2 D_i (2\tau)^3/3\right\} \tag{2}$$

where D_i is the self-diffusion coefficient of the ith component, γ is the nuclear gyromagnetic ratio, and G is the field gradient. It will be possible to separate these unknown factors, namely D_i and h_i, only when conditions are favorable. The h_i's contain information regarding the spin-spin relaxation times (i.e., T_2-effects) and the internuclear J-coupling.[3] When the latter factors are missing, it is usually found that

$$h_i(2\tau) = \exp\left\{-2\tau/T_{2i}\right\} \tag{3}$$

Consider now the case of a polymer dissolved in a solvent, such as cyclohexane or benzene. In these solvents (denoted by subscript 1) the protons are all equivalent and eq. (3) applies. Thus

$$h(2\tau) = x_2 h_2(2\tau) + x_1 \exp\left\{-2\tau/T_{21}\right\} \tag{4}$$

and

$$g(2\tau) = x_2 h_2(2\tau) \exp\left\{-2(\gamma G)^2 D_2 (2\tau)^3/3\right\} + x_1 \exp\left\{-2\tau/T_{21}\right\} \exp\left\{-2(\gamma G)^2 D_1 (2\tau)^3/3\right\} \tag{5}$$

The function $h_2(2\tau)$ usually decays much more rapidly than $\exp\left\{-2\tau/T_{21}\right\}$ in a system such as we are considering. Thus a plot of ln $h(2\tau)$ versus (2τ) will approach a straight line at large (2τ), and this line can be extrapolated back to the intercept x_1. It is assumed here that the echo decay function has been normalized such that $h(2\tau) = 1$ at $(2\tau) = 0$. The slope of the line is $-1/T_{21}$. $h_2(2\tau)$ can be obtained by a simple subtraction of the extrapolated line from the experimental curve, $h(2\tau)$.

Usually polymers do not exhibit simple exponential decays, even in solution, and thus one is not justified in defining a parameter T_{22}, eq. (3). In terms of the steady-state resonance experiment, this amounts to saying that the polymer resonance shape is not Lorentzian.

Having obtained the $h_i(2\tau)$'s and x_i's one may analyze the decay function $g(2\tau)$. Since the polymer diffuses more slowly than the solvent, the two terms of eq. (5) decay at approximately the same rate; that is, although $h_2(2\tau)$ decays much facter than $h_1(2\tau)$, the effect is compensated by

the fact that $\exp\{-2(\gamma G)^2 D_2(2\tau)^3/3\}$ decays much more slowly than $\exp\{-2(\gamma G)^2 D_1(2\tau)^3/3\}$. Equation (5) may be written as

$$\ln\left([g(2\tau) - x_2 h_2(2\tau)\exp\{2(\gamma G)^2 D_2(2\tau)^3/3\}]/x_1 h_1(2\tau)\right) \equiv \ln[j(2\tau)] = -2(\gamma G)^2 D_1(2\tau)^3/3 \quad (6)$$

The procedure that has been adopted is to assume a value for D_2 and make a plot of $\ln j(2\tau)$ versus $(2\tau)^3$. If the plot is curved, a different value is assumed for D_2, and a new plot is made. A straight line is obtained when the correct value for D_2 is used. The slope of the line is $-2(\gamma G)^2 D_1/3$, from which D_1 can be computed.[1]

Longitudinal relaxation times have been measured by means of a 180–190° pulse sequence. The "null" procedure has been adopted, i.e., $T_1 = t_{null}/\ln 2$, even when the relaxation behavior is not exponential. Similarly, transverse relaxation times have been measured by means of a 90°–180° pulse sequence, $T_2 = t_{1/2}/\ln 2$, where $t_{1/2}$ is the time between the 90° pulse and the echo when $h = 1/2$. Again, the nuclear magnetization may not decay exponentially.

III. MATERIALS

Solutions of polyisobutylene in cyclohexane, carbon tetrachloride, and carbon disulfide have been studied. The polyisobutylene is a commercial product designated Indopol H-35 (Indoil Chemical Company, Chicago, Illinois). The material is rather low in molecular weight and has a fairly broad distribution; the molecular weight is 1660 from dilute solution viscosity and 700 from melt viscosity.[4] At 25.0°C., the bulk viscosity is 39.64 g./cm.-sec. and the density is 0.8643 g./cm.^{3}. At 39.9°C. the bulk viscosity is 11.38 g./cm.-sec. and the density is 0.8555 g./cm.^{3}.

Reagent grade solvents were used in each case.

IV. RESULTS AND DISCUSSION

A. Self-Diffusion of Polymer in the Melt

Self-diffusion of Indopol H-35 has been studied in the undiluted form at 110–180°C. Figure 1 shows an Arrhenius plot of the data, i.e., log D versus reciprocal temperature. Figure 1 also includes points for lower temperatures which were obtained by extrapolating data for the CCl_4 solution to the pure polymer side (see below). The points are seen to fall on the same line, within the rather generous error involved, and the activation energy, $E_D = -R[\partial \ln D/\partial(1/T)]_p$, is 5.5 kcal./mole. The activation energy for viscosity of the polymer melt, $E_\eta = R[\partial \ln \eta/\partial(1/T)]_p$, is 15.5 kcal./mole.[18] In earlier studies[1,5–7] of low molecular weight liquids, E_D has always been found to be comparable with E_η. On the other hand, E_η was found to be larger than E_D in some fractions of linear polyethylene.[1] Thus it may be that it is characteristic of polymeric materials to have E_η two or three times as large as E_D.

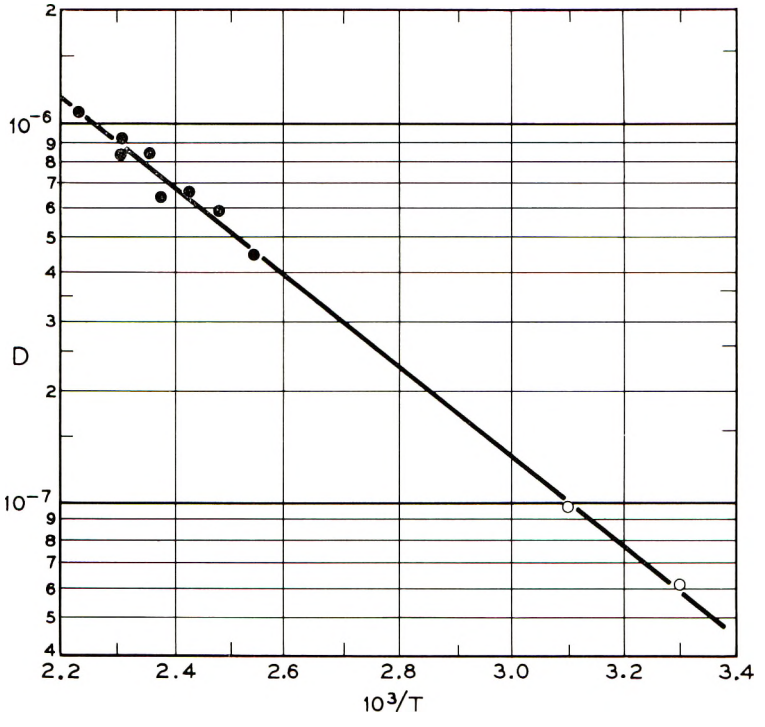

Fig. 1. Arrhenius plot of the self-diffusion coefficient D (cm.²/sec.) for a polyisobutylene melt: (●) direct melt data; (○) obtained by extrapolating the results of solution measurements.

B. Self-Diffusion of the Polymer in Solution

Figure 2 illustrates the concentration dependence of the self-diffusion coefficient for solutions of Indopol H-35 in CCl_4. As the concentration is reduced, the resonance signal strength is reduced proportionately, which reduces the accuracy of the measurements. At higher concentrations the diffusion coefficients are so small that the measurements are also of limited accuracy. Even so, one can say that the concentration dependence of the diffusion is exponential, i.e.,

$$D = D_0 \exp\{-bc\} \tag{7}$$

and b is (approximately) independent of temperature. The plots of Figure 2 were extrapolated to $c = 1$ to obtain the low temperature points of Figure 1, where c is weight fraction of polymer. The fact that the extrapolated points of Figure 1 are consistent with the data for the high temperature melt suggests that the concentration dependence of eq. (7) is valid over the entire range of concentration, except perhaps at very low concentrations.

Arrhenius plots for the 6.6% and 46.5% solutions (in CCl_4) are shown in Figure 3. Activation energies are 3.0 ± 0.4 kcal./mole for the 6.6% solution, 3.6 ± 0.2 kcal./mole for the 46.5% solution, and 5.5 ± 0.1

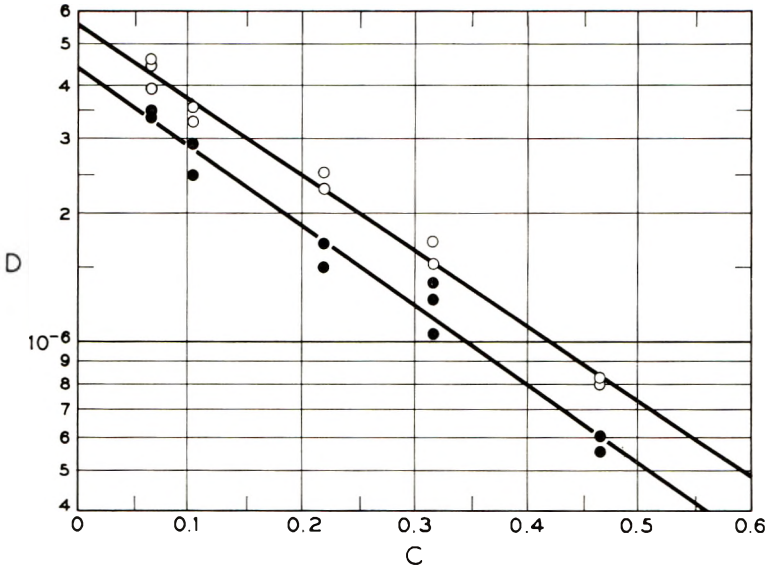

Fig. 2. Concentration C (weight fraction polyisobutylene) dependence of the self-diffusion coefficient D (cm.²/sec.) of polyisobutylene in CCl_4 at (O) 50°C. and (●) 30°C.

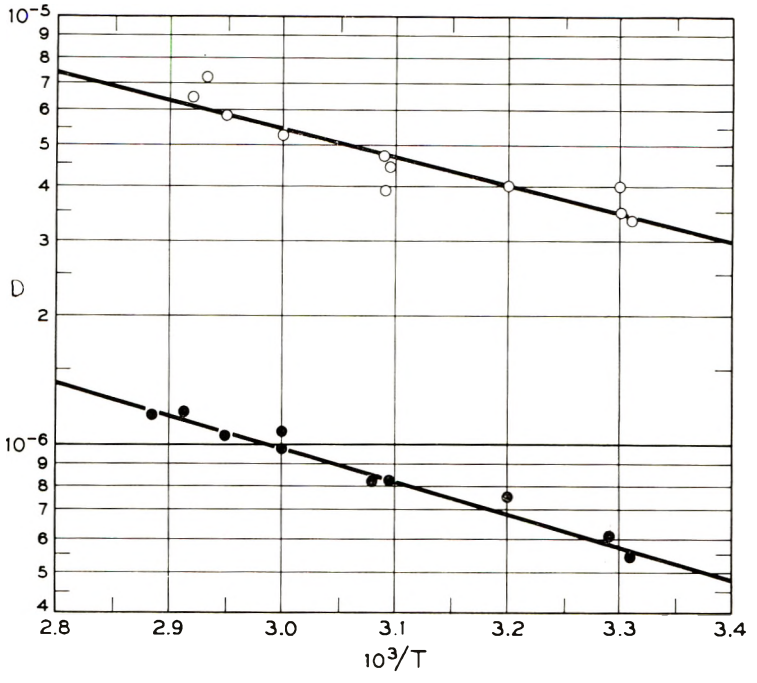

Fig. 3. Arrhenius plots of the self-diffusion coefficient D (cm.²/sec.) for polyisobutylene in solution in CCl_4 at concentrations of (O) 6.6 wt.-% and (●) 46.5 wt.-% polyisobutylene.

kcal./mole for the melt (100%). In the dilute solution (6.6%), the activation energy is near that of the solvent.[8]

C. Self-Diffusion of Solvent

The concentration dependence of the self-diffusion coefficient of cyclohexane in cyclohexane–Indopol H-35 solutions is shown in Figure 4. It is seen that the semilogarithmic plot is linear, and thus eq. (7) holds also when D refers to the solvent. The activation energy varies from 4.1

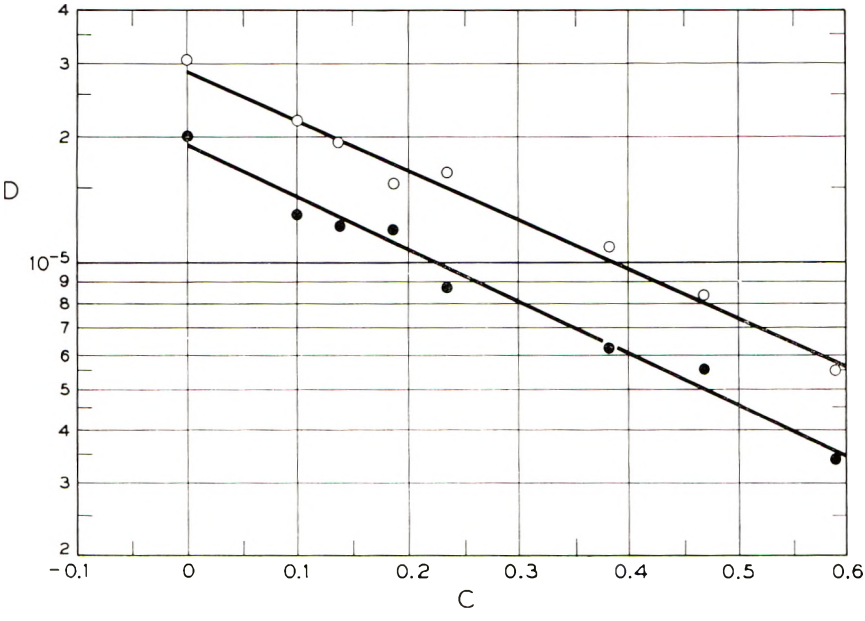

Fig. 4. Concentration C (weight fraction polyisobutylene) dependence of the self-diffusion coefficient D (cm.²/sec.) of cyclohexane at (○) 50°C. and (●) 30°C.

kcal./mole in the pure cyclohexane to 4.8 kcal./mole in 58.7% wt.-% polymer solution. The activation energy for cyclohexane diffusion extrapolated to the pure polymer side is 5.3 kcal./mole. These results and those listed above suggest that the activation energy for self-diffusion is determined by the solvent host rather than by the diffusing molecule, that is, the concentrated substance determines the temperature dependence of the diffusion coefficient of either the low or the high molecular weight component.

D. The Effect of Solvent on Polymer Self-Diffusion

Figure 5 shows the concentration dependence of the self-diffusion coefficient for Indopol H-35 in solution in CS_2. Note that in this case the semilogarithmic plot is not strictly linear. The points at higher concentration exhibit positive deviations from a linear connection of the low concentration points and the melt value extrapolated from the CCl_4 solution plot.

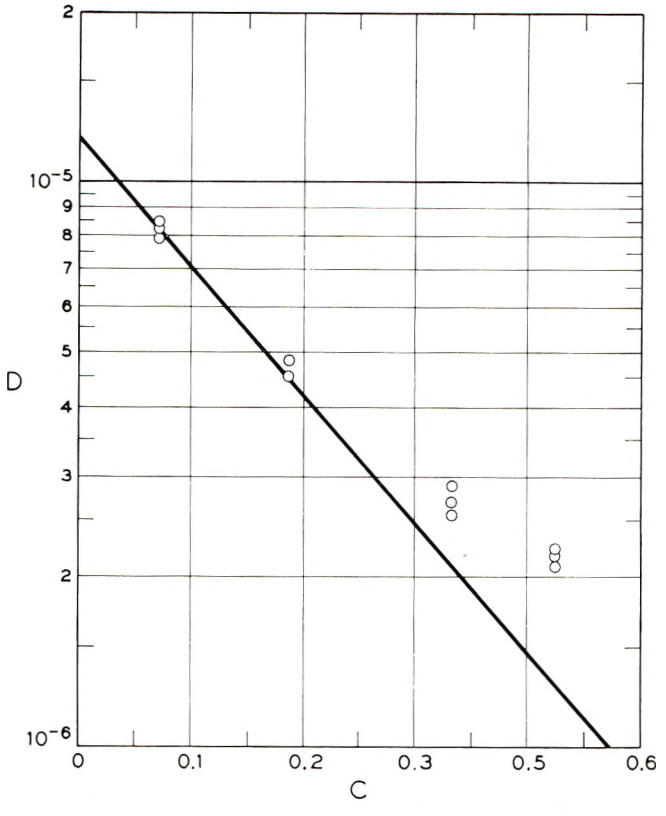

Fig. 5. Concentration C (weight fraction polyisobutylene) dependence of the self-diffusion coefficient D (cm.^{2}/sec.) of polyisobutylene in CS_2 at 30°C.

It is of interest to compare the values of the diffusion coefficient at zero concentration (extrapolated) for the two solvents CS_2 and CCl_4. At 30°C., $D_0(CS_2) = 1.2 \times 10^{-5}$ cm.^{2}/sec. and $D_0(CCl_4) = 0.44 \times 10^{-5}$ cm.^{2}/sec. The ratio is 2.7, whereas the viscosity ratio $\eta(CCl_4)/\eta(CS_2)$ is 2.4. The similarity of these ratios is in agreement with the behavior expected on the basis of the Stokes-Einstein relation. It is apparent that a stronger overall dependence on concentration is to be expected in a solvent of lower viscosity; that is to say, since the polymer diffuses more rapidly in a less viscous solvent and the diffusion rate in the melt is identical, there must be a larger total change in D over the entire concentration range in the less viscous solvent. However, this does not imply that the slope at any particular point will be greater in the less viscous solvent.

E. Nuclear Magnetic Relaxation of the Polymer in Solution

The concentration dependence of the spin-lattice relaxation time T_1 is shown in Figure 6. The data are for Indopol H-35 in CCl_4 and CS_2. The semilogarithmic plot is approximately linear, and the slope is not strongly dependent on temperature. The activation energies obtained from plots

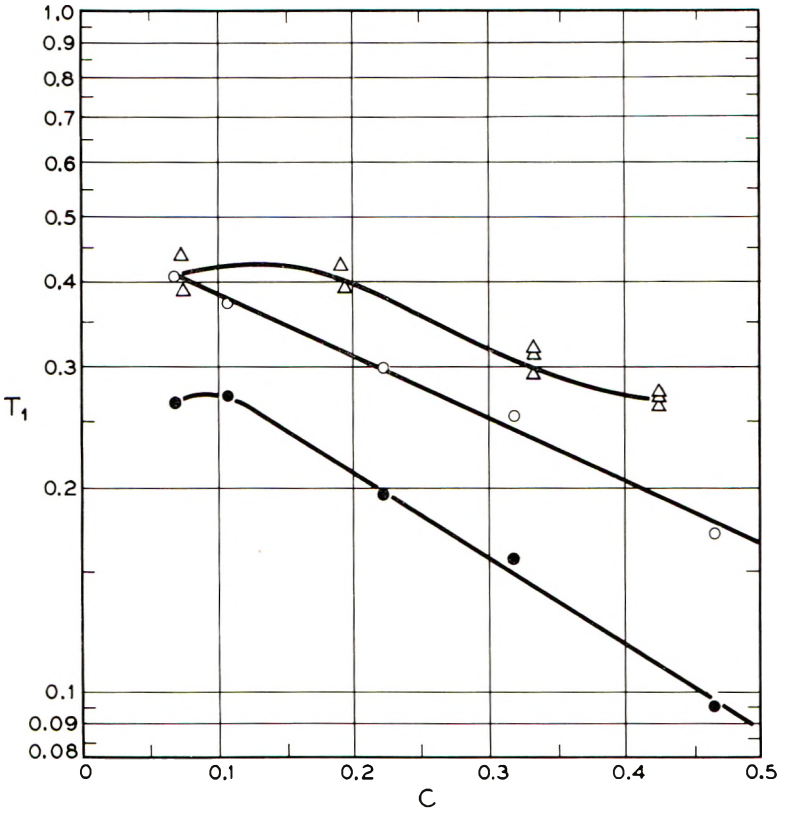

Fig. 6. Concentration C (weight fraction polyisobutylene) dependences of T_1 (sec.): (○) in CCl_4 at 50°C.; (●) in CCl_4 at 30°C.; (△) in CS_2 at 30° C.

of ln T_1 versus $1/T$ (Fig. 7) are 3.9 kcal./mole for the 6.6% solution in CCl_4 and roughly 5 kcal./mole for the 46.5% solution in CCl_4. These activation energies are larger than the corresponding quantities for self-diffusion. The absolute values of T_1 are one order of magnitude lower than those exhibited by low molecular weight hydrocarbons.

Figures 8 and 9 display the T_2 data for Indopol H-35 in solution in CCl_4 and CS_2. The activation energy computed from the slope of Figure 8 is about 3.4 kcal. for the 46.5% solution. In Figure 9 the scatter precludes any quantitative interpretation, but it is evident that $T_2(CS_2) > T_2(CCl_4)$, in accord with the expected viscosity dependence.

V. DISCUSSION AND INTERPRETATION

The experimental results that lend themselves most readily to interpretation in terms of molecular characteristics are those for polymer diffusion and relaxation in solution. It is important to realize, however, that even the most dilute solutions investigated in this study are relatively concentrated, in terms of polymer solution theory. Even so, we have

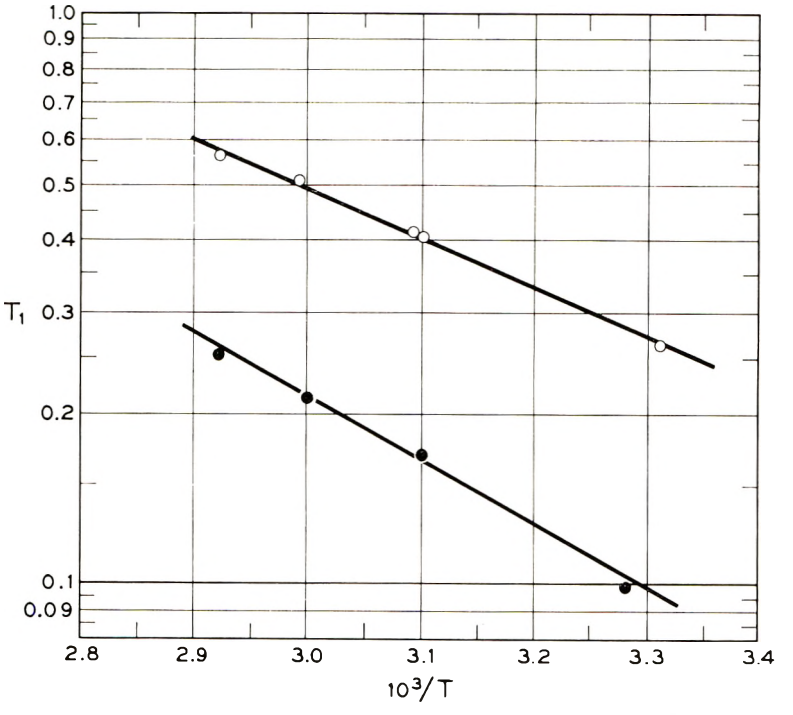

Fig. 7. Arrhenius plots of T_1 (sec.) for polyisobutylene in CCl_4 at concentrations of (O) 6.6 wt.-% and (●) 46.5 wt.-% polyisobutylene.

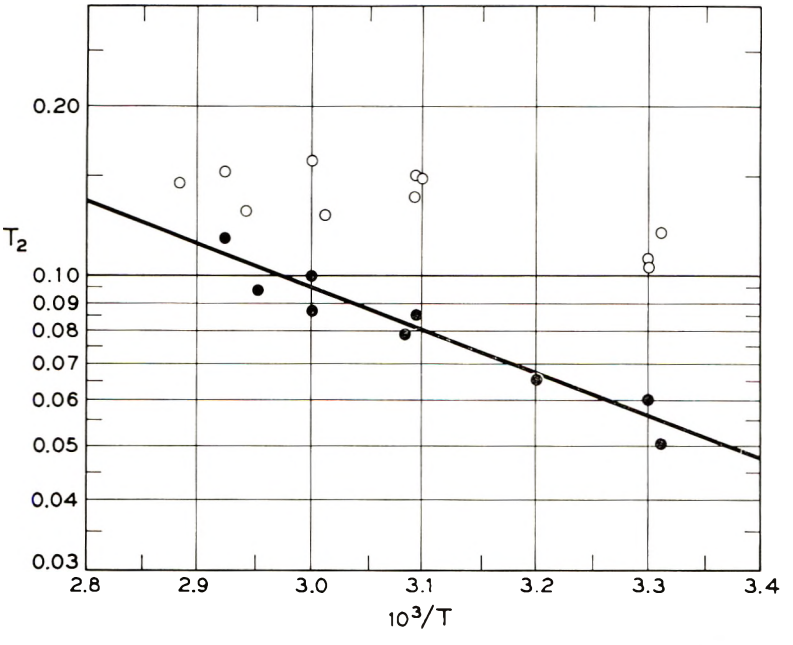

Fig. 8. Arrhenius plots of T_2 (sec.) for polyisobutylene in CCl_4 at concentrations of (O) 6.6 wt.-% and (●) 46.5 wt.-% polyisobutylene.

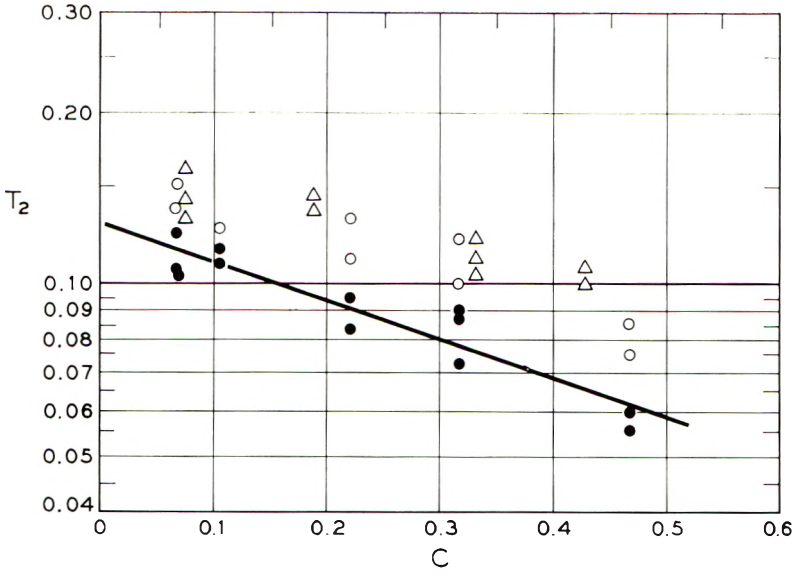

Fig. 9. Concentration C (weight fraction polyisobutylene) dependences for T_2 (sec.): (○) in CCl_4 at 50°C.; (●) in CCl_4 at 30°C.; (△) in CS_2 at 30°C.

simply extrapolated Figures 2, 6, and 9 (for CCl_4) to $c = 0$ and we find $T_{1(c=0)} = 0.37$ sec. at 30°C. and 0.46 sec. at 50°C.; $D_{(c=0)} = 4.41 \times 10^{-6}$ cm.^{2}/sec. at 30°C. and 5.52×10^{-6} cm.^{2}/sec. at 50°C.; and $T_{2(c=0)} = 0.12$ sec. at 30°C. and 0.15 sec. at 50°C. If the relaxation arises from molecular rotation, the correlation time may be written as[4,10]

$$\tau'_c = 3T''_2{}^2/10T_1 \tag{8}$$

when $\tau'_c \ll T_2$ and $\tau'_c \ll 1/\omega$. T''_2 is the value T_2 would possess if the molecules were motionless. A rough estimate of T''_2 is $(\gamma\Delta H_2)^{-1}$, where ΔH_2 is the root second moment of the low temperature proton resonance for polyisobutylene. Using 6.3 gauss[12] for ΔH_2 we find $T''_2 \cong 6 \times 10^{-6}$ sec. and

$$\tau'_c = 1.0 \times 10^{-11}/T_1 \tag{9}$$

These values are to be compared with the Bloembergen, Purcell, and Pound result[10] or (based on a Stokes-Einstein model),

$$\tau'_c = 4\pi\eta a^3/3kT \tag{10}$$

where η is the viscosity and a is the molecular radius. By combining eqs. (9) and (10) we can deduce a, which for Indopol H-35 at 30°C. turns out to be 3.2 A. in CCl_4 and 3.7 A. in CS_2. The difference is insignificant.

A similar estimate of the molecular radius can be calculated from Stokes-Einstein self-diffusion relation,

$$a = kT/6\pi\eta D \tag{11}$$

This relation yields 5.2 A. in CS_2 and 5.8 A. in CCl_4, from the Indopol H-35 diffusion data at 30°C. Again, the difference is not significant.

For a bulk density of 0.86 g./cm.,[3] a molecule of molecular weight 1,000 would be expected to have a radius of about 8 A. Thus the radii determined for Indopol H-35 are too low. This is not surprising, as Stokes-Einstein radii usually turn out to be too small. However, the result is somewhat disappointing, in that there are reasons for expecting the Stokes-Einstein treatment to improve as the size of the diffusing molecule (relative to the size of a solvent molecule) is increased. When eq. (11) is applied directly to the data obtained for bulk polyisobutylene, one obtains a radius of 10 A. at 140°C. and 0.1 A. at 25°C. This result merely reflects the fact that the activation energies for viscosity and self-diffusion are greatly different, which is inconsistent with eq. (11).

It should be noted that the deduction of the radius a from the T_1 data was based on the simplest model available in the limit of motional narrowing. This same theory[10] predicts that $T_1 \cong T_2$ in this limit, although we find that these quantities differ by a factor of about two in dilute solution. There are several aspects of nuclear relaxation that are poorly understood, and a more reliable interpretation may be expected in time. For the present, experiment and theory can be said to be in remarkably good agreement.

Nolle[13] has reported that at low concentrations polyisobutylene in carbon tetrachloride T_2 becomes independent of concentration and molecular weight. This indicates that segmental motions dominate the relaxation behavior at low concentration. However, the limiting T_2 found by Nolle was about 0.07 sec., whereas we observe T_2's of 0.2 sec. at even higher concentrations. The resolution of this apparent discrepancy probably lies in differences of molecular weight. The Indopol H-35 studied herein has a lower molecular weight than any material described by Nolle.

The authors are indebted to Dr. W. P. Slichter and Mr. J. H. Heiss for valuable information and comments.

References

1. Douglass, D. C., and D. W. McCall, *J. Phys. Chem.*, **62**, 1102 (1958).
2. Carr, H. Y., and E. M. Purcell, *Phys. Rev.*, **94**, 630 (1954).
3. Hahn, E. L., and D. E. Maxwell, *Phys. Rev.*, **88**, 1070 (1952).
4. Heiss, J. H., Bell Telephone Laboratories, Murray Hill, N. J., private communication.
5. McCall, D. W., D. C. Douglass, and E. W. Anderson, *J. Chem. Phys.*, **30**, 771 (1959).
6. McCall, D. W., D. C. Douglass, and R. W. Anderson, *Phys. Fluids*, **2**, 87 (1959).
7. McCall, D. W., D. C. Douglass, and R. W. Anderson, *J. Chem. Phys.*, **31**, 1555 (1959).
8. Watts, H., B. J. Alder, and J. H. Hildebrand, *J. Chem. Phys.*, **23**, 659 (1955).
9. Lange, N., Ed., *Handbook of Chemistry*, Handbook Publishers, Sandusky, Ohio, 1946.
10. Bloembergen, N., E. M. Purcell, and R. V. Pound, *Phys. Rev.*, **73**, 679 (1948).

11. Kubo, R., and K. Tomita, *J. Phys. Soc. Japan*, **9**, 888 (1954).
12. Powles, J. G., and K. Luszczynski, *Physica*, **25**, 455 (1959).
13. Nolle, A. W., *Bull. Am. Phys. Soc.*, **1**, 109 (1956).

Résumé

On a effectué différentes expériences de diffusion et de rélaxation nucléaire pour le polyisobutylène de faible poids moléculaire préparé en bloc et en solution. En bloc le coefficient de diffusion obéit à la loi d'Arrhénisu avec une énergie d'activation de 5,5 kcal./mole. En solution les énergies d'activation sont plus faibles, approchant la valeur pour le solvant à faible concentration. Le coefficient de diffusion du polymère à dilution infinie est de $1{,}2 \times 10^{-5}$ cm.²/sec. dans le CS_2 et 0.44×10^{-5} cm.²/sec. dans le CCl_4. Le rapport est voisin de l'inverse du rapport des viscosités des solvants. Les mesures de diffusion du solvant ont été faites pour le cyclohexane dans le polyisobutylène. Une interprétation simple des données sur la base de modèles de Stokes–Einstein fournit des dimensions molèculaires qui sont trop petites d'un facteur de 2 à 3.

Zusammenfassung

Es wird über Versuche zur Selbstdiffusion und Kernrelaxation von ziemlich niedermolekularem Polyisobutylen in Substanz und in Lösung berichtet. In Substanz gehorcht der Selbstdiffusionskoeffizient einer Arrheniusbeziehung und liefert eine Aktivierungsenergie von 5,5 kcal./Mol. In Lösung sind die Aktivierungsenergien niedriger und nähern sich bei niedriger Konzentration dem Wert für das Lösungsmittel. Cer Selbstdiffusionskoeffizient beträgt bei unendlicher Verdünnung in CS_2 $1{,}2 \times 10^{-5}$ cm.²/sec. und in CCl_4 $0{,}44 \times 10^{-5}$ cm.²/sec. Das Verhältnis beider Werte entspricht zeimlich gut dem umgekehrten Verhältnis der Viskosität der Lösungsmittel. Messungen der Selbstdiffusion des Lösungsmittels wurden für Cyclohexan in Polyisobutylen ausgeführt. Eine einfache Interpretation der Ergebnisse nach dem Stokes–Einstein–Modell liefert Moleküldimensionen, die um einen Faktor zwei oder drie zu klein sind.

Received April 5, 1962

JOURNAL OF POLYMER SCIENCE: PART A VOL. 1, PP. 1721–1734 (1963)

The Molecular Structure of Polyethylene. XII. Intrinsic Viscosities of Polyethylene Solutions*

M. O. DE LA CUESTA† and F. W. BILLMEYER, JR.,† *Department of Chemistry, University of Delaware, Newark, Delaware*

Synopsis

While the intrinsic viscosity of polyethylene solutions is reported in the literature for at least 6 different solvents and 14 different temperatures in 23 combinations, few relations exist for converting from one set of conditions to another. Likewise, intrinsic viscosity–molecular weight relations are reported for several sets of conditions and polymer types, in some cases leading to inappropriate comparisons. The following relations are established between the intrinsic viscosities of branched polyethylene in different solvents:

$$[\eta]_d = 1.50[\eta]_\alpha^{1.10}$$

$$[\eta]_t = 1.26[\eta]_\alpha^{1.07}$$

$$[\eta]_x = 1.28[\eta]_\alpha^{1.04}$$

$$[\eta]_d = 1.19[\eta]_t^{1.03}$$

$$[\eta]_x = 1.03[\eta]_t^{0.97}$$

$$[\eta]_d = 1.15[\eta]_x^{1.06}$$

where α denotes α-chloronaphthalene at 125°C.; d, decahydronaphthalene at 70°C.; t, tetrahydronaphthalene at 125°C.; and x, *p*-xylene at 85°C. The relations for linear polyethylene are significantly different from those for branched polyethylene, but have not been established in detail. The literature is examined for the appropriateness and reliability of intrinsic viscosity–molecular weight relationships for polyethylene. Analysis of the experimental data leads to the following relations for linear polyethylene which are proposed as the most consistent, reliable, and appropriate currently obtainable (intrinsic viscosities are expressed in deciliters/gram for measurement conditions of decahydronaphthalene at 135°C., within experimental error of those specified in ASTM D 1601-58T). For the number-averge molecular weight of fractions of linear polyethylene, $[\eta] = 2.3 \times 10^{-4}\bar{M}_n^{0.82}$; for the weight-average molecular weight of whole polymer samples of linear polyethylene, $[\eta] = 2.55 \times 10^{-4}\bar{M}_w^{0.74}$; for the weight-average molecular weight of fractions of linear polyethylene, $[\eta] = 3.9 \times 10^{-4}\bar{M}_w^{0.74}$.

* Presented at the Fourth Delaware Valley Regional Meeting of the American Chemical Society, Philadelphia, Pa., January 25–26, 1962. Portions of this research were performed by (Mrs.) M. O. de la Cuesta in partial fulfillment of the requirements for the degree of Master of Science, University of Delaware. Previous papers in this series were published in *J. Am. Chem. Soc.*, **75,** 6110 (1953); *ibid.*, **79,** 5079 (1957); *ibid.*, **81,** 3129 (1959); *J. Polymer Sci.*, **62,** 251 (1962).

† Mailing addresses: Textile Fibers Department and Plastics Department, respectively, E. I. du Pont de Nemours and Co., Du Pont Experimental Station, Wilmington, Delaware.

INTRODUCTION

Since the first preparation of polyethylene 25 years ago,[1] the dilute solution viscosity of this polymer has been reported in the literature for an unusually wide range of experimental conditions, including at least 6 different solvents and 14 different temperatures in a total of 23 combinations (Table I). However, only a few workers report the viscosity of the same samples measured under different conditions; results of this nature are often approximate or fragmentary. Thus it is difficult to compare measurements made with one set of conditions to those carried out with a different solvent, temperature, or both.

The comparison of the intrinsic viscosity of polyethylene with absolute values of molecular weight has likewise been made for a variety of conditions (Table II). (Here, the more common terminology of Cragg[43] is used rather than that recommended by the International Union of Pure and Applied Chemistry.[44]) All possible comparisons have been made

TABLE I
Experimental Conditions Published for Measurement of the Solution Viscosity of Polyethylene[a]

Temperature, °C.	Solvent					
	α-Chloronaphthalene	Decahydronaphthalene	Bis-2-(ethylhexyl)-adipate	Tetrahydronaphthalene	Toluene	p-Xylene
70		5,6,30, *38*		*38*		
75				2,20,22		4,11,30
80				23,29,30	15	
81.0						24,28,35, 36
81.5				41		
85						6
90						*9*
100		**35**		11,**34**,39		*24*,**35**
105				19,*36*		*13*,*28*,*36*, 41
120		*38*		*3*,**10**,*12*, *27*,*38*		
125	6,*14*,16,*17*, 21,**42**			6,*36*		
129.2	*40*					
130				*7*,*18*,*25*, *37*		
135		*8*,*14*,*26*, *31*,*32*, *33*,*37*				
145			**34**			

[a] Table entries are reference numbers: Roman type indicate measurement of branched polyethylene; italics, linear polyethylene; boldface, both kinds.

between the intrinsic viscosity of both linear and branched polyethylene, fractionated and unfractionated, with both weight-average and number-average molecular weight. The inappropriateness of the comparison or its limited applicability has often passed unrecognized.

TABLE II
Types of Published Comparisons of Intrinsic Viscosity and Molecular Weight for Polyethylene[a]

Type of polymer	Type of molecular weight	
	Number-average	Weight-average
Branched		
Whole polymer	4, 11, 16, 20, 24, 29, 35	6, 10, 11, 19, 21, 24, 35, 36, 42
Fraction	5, 15, 24, 28, 30, 39	23, 24, 41
Linear		
Whole polymer	4, 12, 27, 35	3, 10, 11, 14, 17, 26, 32, 35
Fraction	9, 18, 24, 25, 28 40	14, 31, 32, 33, 36, 37, 40

[a] Table entries are reference numbers.

The purpose of this paper is twofold: (*1*) to present data relating the intrinsic viscosities of polyethylene measured on the same sample with different solvents and temperatures (most results refer to branched polyethylene, but some comments are made with respect to linear polymers); (*2*) to examine for appropriateness and reliability the published intrinsic viscosity–molecular weight relations for polyethylene.

EXPERIMENTAL

Samples

Polyethylene samples 14, 76, 77, and 78 are Fawcett-type[1] (branched, high pressure, free radical) polyethylenes. Sample 84 is an essentially linear polyethylene made in a low pressure synthesis with the use of a transition metal halide-type catalyst.

Viscosity Measurement

The solvents α-chloronaphthalene, decahydronaphthalene, and 1,2,3,4-tetrahydronaphthalene were redistilled before use, while *p*-xylene (Merck and Company, reagent grade) was used as received.

Viscosity measurements for the four branched polyethylenes were made in α-chloronaphthalene at 125°C., tetrahydronaphthalene at 125°C., *p*-xylene at 85°C., and decahydronaphthalene at 70°C. The viscosity of sample 76 was also measured in tetrahydronaphthalene at 80°C., and in decahydronaphthalene at 135°C. The viscosity of sample 84 was measured

in α-chloronaphthalene at 125°C., tetrahydronaphthalene at 125°C., and decahydronaphthalene at 135°C.

The viscosity measurements were made in Cannon-Ubbelohde suspended-level dilution viscometers (Cannon Instrument Co., State College, Pa.). The capillary size of the viscometers was so chosen that the efflux time for the solvent exceeded 150 sec., making kinetic energy corrections negligible. The viscometers were used at shear rates between 1000 and 2000 sec.$^{-1}$, in the range where Wesslau[14] states that shear rate corrections are negligible for intrinsic viscosities below 3.8 dl./g. Since the highest intrinsic viscosity measured in this work was 2.0 dl./g., no shear rate correction was made.

Reduced and inherent viscosities were calculated on a Bendix G-15 computer. The data for duplicate samples were then combined, and reduced viscosity–concentration and inherent viscosity–concentration relations were established by use of a least-squares program on an IBM 650 computer. Results were expressed as the intrinsic viscosities and their 95% confidence limits.

Relations of the type:

$$[\eta]_{\text{solvent A}} = K[\eta]^{a}_{\text{solvent B}} \tag{1}$$

were computed for each pair of solvents for the data obtained with the branched polymers. The computer program used here did not take into account the individual variances of the intrinsic viscosities, but used only the average values. For this reason, no confidence limits have been computed for K and a in eq. (1).

RESULTS

Intrinsic viscosities and their 95% confidence limits are listed in Table III, and the Huggins[45] and Kraemer[46] constants, k' and k'', calculated from the equations

$$\eta_{sp}/c = [\eta] + k'[\eta]^2 c \tag{2}$$

and

$$\ln \eta_r/c = [\eta] - k''[\eta]^2 c \tag{3}$$

respectively, are listed in Table IV. The relations of the form of eq. (1), comparing intrinsic viscosities in different solvents, are summarized in Table V. These relations refer to the branched polymers only. The data points of Table III for both branched and linear polyethylenes are plotted in Figure 1, where the solid lines represent some of the relations of Table V.

From the data of Table III, the temperature coefficient of the intrinsic viscosity is approximately −0.001 dl./g.°C. for solutions of branched polyethylene in decahydronaphthalene and −0.0002 dl./g.°C. for similar solutions in tetrahydronaphthalene.

TABLE III

Intrinsic Viscosity of Polyethylenes as a Function of Solvent and Temperature

Sample No.	Intrinsic viscosity, dl./g.[a]			
	α-Chloronaphthalene (125°C.)	Decahydronaphthalene (70°C.)	Tetrahydronaphthalene (125°C.)	*p*-Xylene (85°C.)
14	0.335 ± 0.005	0.450 ± 0.007	0.389 ± 0.003	0.412 ± 0.002
	0.335 ± 0.004	0.450 ± 0.007	0.389 ± 0.003	0.412 ± 0.004
76	0.746 ± 0.007	1.112 ± 0.015	0.926 ± 0.007	0.954 ± 0.013
	0.750 ± 0.008	1.116 ± 0.012	0.928 ± 0.006	0.957 ± 0.010
	—	1.039 ± 0.007[b]	0.935 ± 0.011[c]	—
	—	1.042 ± 0.005[b]	0.937 ± 0.010[c]	—
77	0.985 ± 0.006	1.460 ± 0.011	1.225 ± 0.016	1.259 ± 0.009
	0.992 ± 0.004	1.470 ± 0.008	1.237 ± 0.012	1.267 ± 0.008
78	0.618 ± 0.008	0.882 ± 0.011	0.753 ± 0.010	0.777 ± 0.014
	0.619 ± 0.007	0.888 ± 0.009	0.754 ± 0.009	0.779 ± 0.011
84	1.525 ± 0.047	2.064 ± 0.048[b]	1.808 ± 0.044	—
	1.537 ± 0.032	2.079 ± 0.030[b]	1.823 ± 0.031	—

[a] The first value in each set is intrinsic viscosity calculated from reduced viscosity; the second value is intrinsic viscosity calculated from inherent viscosity.

[b] Measurements made at 135°C.

[c] Measurements made at 80°C.

TABLE IV

Huggins Constants k' and Kraemer Constants k'' for Polyethylene as a Function of Solvent and Temperature

Sample No.	Huggins constants k' and Kraemer constants k''[a]			
	α-Chloronaphthalene (125°C.)	Decahydronaphthalene (70°C.)	Tetrahydronaphthalene (125°C.)	*p*-Xylene (85°C.)
14	0.443	0.370	0.452	0.295
	0.077	0.140	0.077	0.200
76	0.531	0.433	0.447	0.463
	0.028	0.101	0.089	0.078
	—	0.421[b]	0.425[c]	—
	—	0.107[b]	0.099[c]	—
77	0.490	0.485	0.558	0.496
	0.071	0.078	0.034	0.068
78	0.508	0.490	0.451	0.453
	0.034	0.073	0.075	0.081
84	0.481	0.439[b]	0.469	—
	0.082	0.111[b]	0.092	—

[a] The first value in each set is k'; the second value is k''.

[b] Measurements made at 135°C.

[c] Measurements made at 80°C.

TABLE V
Relations between Intrinsic Viscosities of Branched Polyethylene in Different Solvents[a]

$$[\eta]_d = 1.50[\eta]_\alpha^{1.10}$$
$$[\eta]_t = 1.26[\eta]_\alpha^{1.07}$$
$$[\eta]_x = 1.28[\eta]_\alpha^{1.04}$$
$$[\eta]_d = 1.19[\eta]_t^{1.03}$$
$$[\eta]_x = 1.03[\eta]_t^{0.97}$$
$$[\eta]_d = 1.15[\eta]_x^{1.06}$$

[a] Subscripts α, d, t, and x refer to measurements in α-chloronaphthalene at 125°C., decahydronaphthalene at 70°C., tetrahydronaphthalene at 125°C., and *p*-xylene at 85°C., respectively.

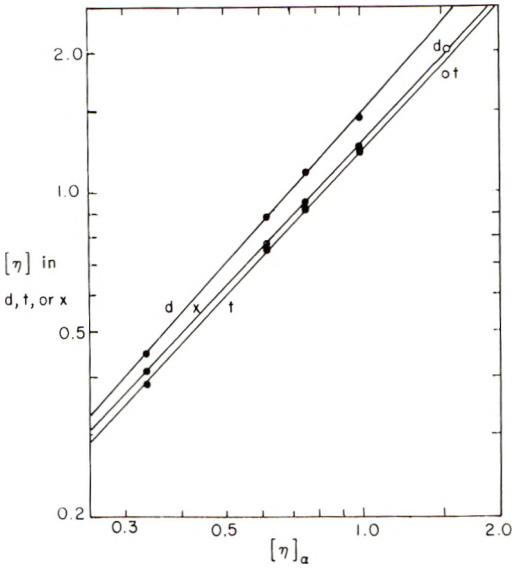

Fig. 1. Logarithmic plot of intrinsic viscosity in α-chloronaphthalene at 125°C. vs. that in other solvents (●) for branched polyethylene (letters d, x, and t indicate results for decahydronaphthalene at 70°C., *p*-xylene at 85°C., and tetrahydronaphthalene at 125°C.) and (○) for linear polyethylene (letters d and t indicate results for decahydronaphthalene at 135°C. and tetrahydronaphthalene at 125°C.).

DISCUSSION

Intrinsic Viscosity as a Function of Solvent

Branched Polyethylene

In Paper III of this series[6] it was stated that the intrinsic viscosity of branched polyethylene is the same in tetrahydronaphthalene at 125°C. and xylene at 85°C. The present work indicates that the intrinsic viscosity is slightly higher in xylene, the difference being within the experimental error of the work reported earlier.

Mendelson[41] states that for branched polyethylene

$$[\eta]_{p\text{-xylene, }105°C.} = 1.04\ [\eta]_{\text{tetrahydronaphthalene, }81.5°C.} \quad (4)$$

This is in fairly good agreement with the present data for sample 76, for which the ratio is 1.03 after correcting to Mendelson's temperatures.

Nicholas' relation,[30]

$$[\eta]_{\text{decahydronaphthalene, }70°C.} = 1.18\ [\eta]^{1.06}_{\text{tetrahydronaphthalene, }80°C.} \quad (5)$$

is in fair agreement with the relation in Table V, but cannot be compared directly because of the difference in temperatures.

Linear Polyethylene

Wesslau[14] reports that intrinsic viscosities in decahydronaphthalene at 135°C. and α-chloronaphthalene at 125°C. are related by the equation

$$\log [\eta]_d = 1.09 \log [\eta]_\alpha - 0.11. \quad (6)$$

If this relation is used to calculate the intrinsic viscosity in decahydronaphthalene of sample 84 from the experimental value in α-chloronaphthalene, the calculated value for decahydronaphthalene differs by 0.02 from the experimental value. This is within the 95% confidence limits of the intrinsic viscosity of sample 84. However, if the above relation is used to calculate the intrinsic viscosity of sample 76, the calculated value is 0.1 dl./g. higher than the experimental value. This indicates that the intrinsic viscosity relation is different for linear and branched polyethylene.

The relation reported by Tung[37] for linear polyethylene,

$$[\eta]_{\text{decahydronaphthalene, }135°C.} = 1.16\ [\eta]_{\text{tetrahydronaphthalene, }130°C.} \quad (7)$$

is in fairly good agreement with the ratio obtained for Sample 84 (1.14). Wisseroth[38] obtains values ranging from 1.12 to 1.16 for the same ratio.

Trementozzi[36] reports that the intrinsic viscosity of linear polyethylene in xylene at 105°C. is 1.02 times that in tetrahydronaphthalene at 105°C. There is no value for sample 84 in xylene in the present investigation, and the ratios of xylene to tetrahydronaphthalene viscosities vary between 1.03 and 1.05 for the branched polyethylenes. These values are not in good agreement with Trementozzi's data for linear polyethylene. (In comparing our data with Trementozzi's, a temperature correction of -0.0002 dl./g.°C. was applied.)

From the foregoing discussion and results, it seems likely but not certain that the relations between intrinsic viscosities are not the same for linear and branched polyethylene. Because only one sample of linear polyethylene was investigated in this work, it is impossible to say whether the ratios are smaller or larger for linear polyethylene than for branched polyethylene. This investigation clearly demonstrates, however, that the intrinsic viscosities in two solvents are not simply linearly related, but that a much better approximation can be established through an exponential relation.

Viscosity–Molecular Weight Relationships

Branched Polyethylene: Number-Average Molecular Weight

As discussed in Paper IX,[17] the comparison of intrinsic viscosity to number-average molecular weight for branched polyethylene is considered inappropriate. The fact that relations of the modified Staudinger type

$$[\eta] = KM^a \tag{8}$$

are obtained is believed to result from fortuitous cancellation of the effects of long-chain branching and molecular weight distribution on the intrinsic viscosity. The relations published for these conditions would not necessarily be expected to agree with one another, since each might be expected

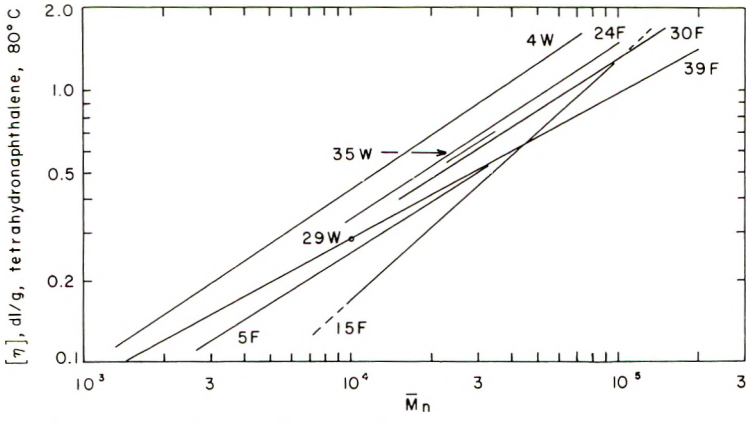

Fig. 2. Viscosity–molecular weight relationships reported for the number-average molecular weight of branched polyethylene. Numbers refer to references and letters F and W indicate relations for fractions and whole polymers, respectively. The lines extend over the range of molecular weight covered. (For the relation of Aggarwal,[15] no range was stated. To obtain this relation, it was assumed that intrinsic viscosities in xylene and toluene were the same.)

to hold only for the specific samples for which it was established. This is confirmed by the lack of agreement indicated in Figure 2, where the various relations are plotted after being converted to the viscosity measurement conditions of tetrahydronaphthalene at 80°C.

Branched Polyethylene: Weight-Average Molecular Weight

The effect of long-chain branching is well established as lowering the intrinsic viscosity below that of a linear polymer of the same molecular weight. No author has considered it appropriate to formulate a viscosity–molecular weight relation for this case.

Linear Polyethylene: Number-Average Molecular Weight

Results for Fractionated Samples. While no viscosity–molecular weight relations have been proposed for the number-average molecular weight of

unfractionated samples of linear polyethylene, several workers have reported such relations for fractionated samples. Examination of the data of Kaufman and Walsh,[18] Tung,[25] and Krigbaum and Trementozzi,[28] after recalculating to a common solvent and temperature, suggests (Fig. 3) that they can be represented by a single relation. Least-squares analysis gives the equation

$$[\eta] = 2.0 \times 10^{-4} \bar{M}_n^{0.82} \text{ dl./g.} \quad (9)$$

for xylene at 105°C. On converting[36,37] to measurement conditions of decahydronaphthalene at 135°C., corresponding within experimental error to those specified[47] in ASTM D1601-58T, eq. 9 becomes for decahydronaphthalene at 135°C.

$$[\eta] = 2.3 \times 10^{-4} \bar{M}_n^{0.82} \text{ dl./g.} \quad (10)$$

The data of Aries and Sachs,[9] also shown in Figure 3, differ widely from those discussed above; their brief note gives no clue to explain the discrepancy. Kotera et al.[40] give no experimental points; after conversion[14,36,37] to measurement conditions of xylene at 105°C., their relation is indicated approximately in Figure 3.

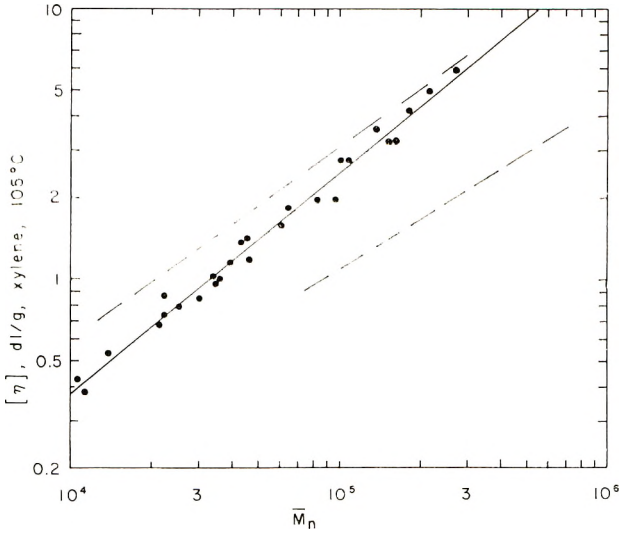

Fig. 3. Intrinsic viscosities and number-average molecular weights for fractions of linear polyethylene: solid line, suggested relation of eq. (9), fitting data points of Kaufman,[18] Tung,[25] and Krigbaum;[29] upper dashed line, relation of Kotera;[40] lower dashed line, relation of Aries.[9]

Linear Polyethylene: Weight-Average Molecular Weight

Results for Unfractionated Samples. Despite indications of unusually broad distributions of molecular weight in some linear polyethylenes (but see Paper XI of this series[42]), it is appropriate to consider intrinsic viscosity–

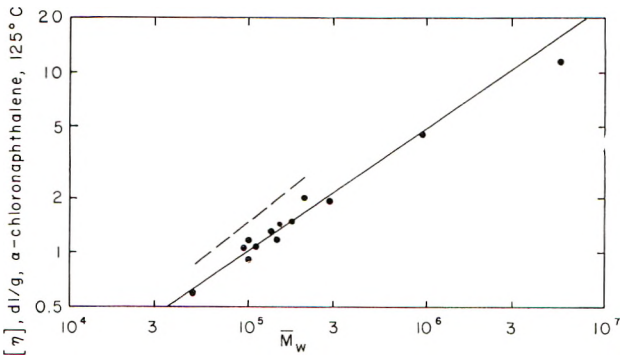

Fig. 4. Intrinsic viscosities and weight-average molecular weights for unfractionated linear polyethylenes: solid line, suggested relation of eq. (11), fitting the data points of Atkins,[17] Chiang,[32] and Kokle;[42] dashed line, relation of Duch.[10]

molecular weight relations for the weight-average molecular weight of unfractionated linear polyethylenes. Experimental data of high reliability were published in Papers IX[17] and XI[42] and by Chiang,[32] who discusses this and the following case in detail. The least-squares relation for α-chloronaphthalene at 125°C. based on these points (Fig. 4) is

$$[\eta] = 4.0 \times 10^{-4} \bar{M}_u^{0.68} \text{ dl./g.} \tag{11}$$

(Following Atkins,[17] we omit the point of highest molecular weight, since the intrinsic viscosity is believed low due to neglect of shear rate correction.) On converting[14] to measurement conditions of decahydronaphthalene at 135°C., eq. (11) becomes

$$[\eta] = 2.55 \times 10^{-4} \bar{M}_w^{0.74} \text{ dl./g.} \tag{12}$$

Other data, including those of Duch and Küchler[10] (whose relation is approximately indicated in Figure 4) were omitted from the calculation since, in our opinion, they are derived from less reliable light scattering measurements.[49]

Results for Fractionated Samples. Of all sets of conditions discussed, the comparison of the weight-average molecular weight of relatively sharp fractions of linear polyethylene to their intrinsic viscosity is the most soundly based. The data of Chiang,[32] Henry,[33] and Tung[37] appear to be the most reliable in the literature. In each case, weight-average molecular weight was measured by light scattering with α-chloronaphthalene as solvent, and linear Zimm plots were obtained (a requirement for unambiguous results; see Paper X[48]).

These data were adjusted by converting to measurement conditions of decahydronaphthalene at 135°C., by use of a factor of 1.15 (an average of Tung's result[37] and that of this paper) to correct Tung's intrinsic viscosities to these conditions. The light-scattering molecular weights reported by Henry and by Tung were raised 1.055% and 3.15%, respectively, to achieve consistency in the value of the specific refractive increment used,

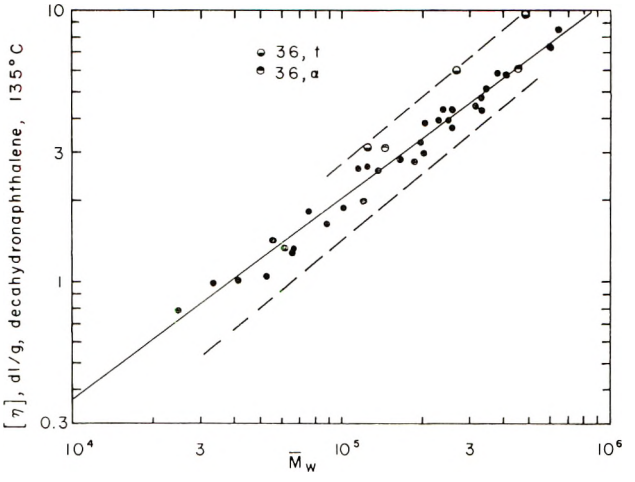

Fig. 5. Intrinsic viscosities and weight-average molecular weights for relatively sharp fractions of linear polyethylene: solid line, suggested relation of eq. (13), fitting the data points of Chiang,[32] Henry,[33] and Tung;[37] upper dashed line, relation of Trementozzi;[36] lower dashed line, relation of Kotera.[40]

as discussed in Paper XI.[42] The three data points assumed by Tung to reflect long-chain branching were omitted.

A least-squares analysis was made for the remaining 33 data points, which were shown statistically to belong to a single population. The resulting intrinsic viscosity-molecular weight relation for decahydronaphthalene at 135°C. is

$$[\eta] = 3.9 \times 10^{-4} \bar{M}_w^{0.74} \text{ dl./g.} \tag{13}$$

The data are plotted in Figure 5. Also shown are the relation of Trementozzi[36] and that of Kotera et al.,[40] who gave no data points. It can be seen that each of these lines is outside the limits of error of the relation proposed in eq. (13).

It is not known whether the specimens of Chiang, Henry, and Tung were examined for "association" in α-chloronaphthalene solution.[36,42] Its existence in these samples seems unlikely, in view of the consistency of the data. It must be pointed out, however, that Trementozzi's relation, plotted in Figure 5, is based on light-scattering measurement in tetrahydronaphthalene, for which association is stated to be absent. His molecular weights obtained with α-chloronaphthalene as solvent, also indicated in Figure 5, lie closer to the main body of the data.

Self-Consistency of Relationships

Equations (10) and (13) may be compared, since they yield values of $\bar{M}_w$ and $\bar{M}_n$ for fractionated samples of linear polyethylene. Over the range of molecular weights found in commercial linear polyethylenes, they yield ratios of $\bar{M}_w/\bar{M}_n$ between 1.3 and 1.9, significantly larger than that

anticipated for sharp fractions (1.0–1.1). The difference in exponents (0.82 versus 0.74), also seems too large, even though the interrelations between viscosities in different solvents, which were involved in deriving the equations, are not thoroughly established.

Equations (12) and (13) may be compared, yielding $\bar{M}_w$ for whole polymers and fractions of linear polyethylene. If it is assumed that the fractions are sharp, the equations may be interpreted as yielding the ratio $\bar{M}_w/\bar{M}_v$, the latter being the viscosity-average molecular weight. The value 1.53 predicted for this ratio seems abnormally large, especially in view of the observed breadths of the molecular weight distributions for some linear polyethylenes.[42]

In each case, we conclude that the equations are not entirely self-consistent and should not be intercompared indiscriminately.

The authors wish to thank P. W. Mullen and N. W. Seitz of the Carothers Research Laboratory, Textile Fibers Department, E. I. du Pont de Nemours and Company, Inc., for assistance in using the Bendix computer; and D. F. Akeley, Pioneering Research Laboratory of the same Department, for supplying the computer pgoram.

The authors wish to thank M. T. Dunleavy of the Plastics Department, E. I. du Pont de Nemours and Company, Inc., for assistance in using the IBM 650 computer, for supplying the program, and for general assistance in the calculations.

References

1. Fawcett, E. W., R. O. Gibson, and M. W. Perrin, U. S. Pat. 2,153,553 (1939); E. W. Fawcett, R. O. Gibson, M. W. Perrin, J. G. Paton, and E. G. Williams, Brit. Pat. 471,590 (1936); see also note by E. W. Fawcett, p. 119, in H. Staudinger, *Trans. Faraday Soc.*, **32**, 97 (1936).

2. Hunter, E., and W. G. Oakes, *Brit. Plastics*, **17**, 94 (1945).

3. Schulz, G. V., and K. Mehnert, *Kunststoffe*, **45**, 110 (1945).

4. Harris, I., *J. Polymer Sci.*, **8**, 353 (1952).

5. Ueberreiter, K., H.-J. Orthmann, and G. Sorge, *Makromol. Chem.*, **8**, 21 (1952); see also K. Ueberreiter and H.-J. Orthmann, *Kolloid-Z.*, **126**, 140 (1952).

6. Billmeyer, F. W., Jr., *J. Am. Chem. Soc.* **75**, 6118 (1953).

7. Rugg, F. M., J. J. Smith, and L. H. Wartman, *J. Polymer Sci.*, **11**, 1 (1953).

8. Ziegler, K., Belg. Pats. 527,736 (1954); 533,362 (1955); 534,792 (1955); 534,888 (1955).

9. Aries, R. S., and A. P. Sachs, *J. Polymer Sci.*, **21**, 551 (1956).

10. Duch, E., and L. Küchler, *Z. Electrochem.*, **60**, 218 (1956).

11. Moore, L. D., *J. Polymer Sci.*, **20**, 137 (1956).

12. Smith, H., *J. Polymer Sci.*, **21**, 563 (1956).

13. Trementozzi, Q. A., *J. Polymer Sci.*, **22**, 187 (1956).

14. Wesslau, H., *Makromol. Chem.*, **20**, 111 (1956).

15. Aggarwal, S. L., and O. J. Sweeting, *Chem. Revs.*, **57**, 665 (1957).

16. Ashby, C. E., J. S. Reitenour, and C. F. Hammer, *J. Am. Chem. Soc.*, **79**, 5086 (1957).

17. Atkins, J. T., L. T. Muus, C. W. Smith, and E. T. Pieski, *J. Am. Chem. Soc.*, **79** 5089 (1957).

18. Kaufman, H. S., and E. K. Walsh, *J. Polymer Sci.*, **26**, 124 (1957).

19. Kobayashi, T., A. Chitale, and H. P. Frank, *J. Polymer Sci.*, **24**, 156 (1957).

20. Mussa, C., *J. Polymer Sci.*, **23**, 877 (1957).

21. Muus, L. T., and F. W. Billmeyer, Jr., *J. Am. Chem. Soc.*, **79**, 5079 (1957).

22. Nasini, A., and C. Mussa, *Makromol. Chem.*, **22**, 59 (1957).

23. Nicolas, L., *Compt. Rend.*, **244**, 80 (1957); *Makromol. Chem.*, **24**, 173 (1957).
24. Trementozzi, Q. A., *J. Polymer Sci.*, **23**, 887 (1957).
25. Tung, L. H., *J. Polymer Sci.*, **24**, 333 (1957).
26. Francis, P. S., R. C. Cooke, Jr., and J. H. Elliott, *J. Polymer Sci.*, **31**, 453 (1958).
27. Hawkins, S. W., and H. Smith, *J. Polymer Sci.*, **28**, 341 (1958).
28. Krigbaum, W. R., and Q. A. Trementozzi, *J. Polymer Sci.*, 28, 295 (1958).
29. Mussa, C., *J. Polymer Sci.*, **28**, 587 (1958).
30. Nicolas, L., *J. Polymer Sci.*, **29**, 191 (1958).
31. Wesslau, H., *Makromol. Chem.*, **26**, 96 (1958); *Kunststoffe*, **49**, 230 (1959).
32. Chiang, R., *J. Polymer Sci.*, **36**, 91 (1959).
33. Henry, P. M., *J. Polymer Sci.*, **36**, 3 (1959).
34. Moore, L. D., Jr., *J. Polymer Sci.*, **36**, 155 (1959).
35. Raman, N. K., and J. J. Hermans, *J. Polymer Sci.*, **35**, 71 (1959); see also L. T. Muus and F. W. Billmeyer, Jr., *ibid.*, **39**, 531 (1959); J. J. Hermans, *ibid.*, **39**, 532 (1959).
36. Trementozzi, Q. A., *J. Polymer Sci.*, **36**, 113 (1959).
37. Tung, L. H., *J. Polymer Sci.*, **36**, 287 (1959).
38. Wisseroth, K., *Kunststoffe*, **49**, 684 (1959).
39. Guillet, J. E., R. L. Combs, D. F. Slonaker, and H. W. Coover, Jr., *J. Polymer Sci.*, **47**, 307 (1960).
40. Kotera, A., and co-workers, *Rept. Progr. Polymer Phys. Japan*, **3**, 58 (1960).
41. Mendelson, R. A., *J. Polymer Sci.*, **46**, 493 (1960).
42. Kokle, V., F. W. Billmeyer, Jr., L. T. Muus, and E. J. Newitt, *J. Polymer Sci.*, **62**, 251 (1962).
43. Cragg, L. H., *J. Colloid Sci.*, **1**, 261 (1946).
44. International Union of Pure and Applied Chemistry, *J. Polymer Sci.*, **8**, 257 (1952).
45. Huggins, M. L., *J. Am. Chem. Soc.*, **64**, 2716 (1942).
46. Kraemer, E. O., *Ind. Eng. Chem.*, **30**, 1200 (1938).
47. American Society for Testing Materials, ASTM Designation: D1601-58T.
48. Bryant, W. M. D., F. W. Billmeyer, Jr., L. T. Muus, J. T. Atkins, and J. E. Eldridge, *J. Am. Chem. Soc.*, **81**, 3219 (1959).
49. (Added in proof) the results of M. Gubler, C. Reiss, and H. Benoit, *J. Chim. Phys.*, **59**, 42 (1962), for the weight-average molecular weight of fractions of linear polyethylene are in excellent agreement with eq. (13). However, their results for whole polymers are not in good agreement with eq. (12), falling closer to the points of Duch and Küchler.[10]

Résumé

Alors qu'on trouve dans la littérature la viscosité intrinsèque de solutions de polyéthylène pour 6 solvants différents au moins at à 14 températures différentes dans 23 combinaisons, il existe peu de relations permettant de passer d'une série de conditions à une autre. De même, on donne des relations entre la viscosité intrinsèque et le poids moléculaire pour plusieurs séries de conditions et types de polymère, ce qui conduit dans certains cas à faire des comparaisons peu appropriées. Les relations ont été établies dans diflérents solvants entre les viscosités intrinsèques du polyéthylène ramifié. (Voyez synopsis ou α désign l'α-chloronaphthalène à 125°C.; d, le décahydronaphthalène à 70°C., t, le tétrahydronaphthalène à 125°C.; et x, le *p*-xylène à 85°C.) Les relations obtenues pour les polyéthylènes linéaires sont assez différentes de celles obtenues pour le polyéthylène ramifié, mais n'ont pas été établies en détail. On a examiné la littérature pour connaître l'exactitude des relations entre la viscosité intrinsèque et le poids moléculaire pour le polyéthylène. L'analyse des résultats expérimentaux conduit aux relations suivantes pour le polyéthylène linéaire. Ces relations sont les plus cohérentes, dignes de confiance et peuvent généralement s'obtenir facilement. (Les viscosités intrinsèques sont exprimées en décilitre/gramme pour le décahydronaphthalène á 135°C., dans les limites des erreurs expérimentales spécifiées par ASTM D 1601-58T.) Pour le poids

moléculaire moyen en nombre des fractions de polyéthylène linéaire, $[\eta] = 2.3 \times 10^{-4} \bar{M}_n^{0.82}$; pour le poids moléculaire moyen en poids de l'ensemble des échantillons de polyéthylène linéaire, $[\eta] = 2.55 \times 10^{-4} \bar{M}_w^{0.74}$; pour le poids moléculaire moyen en poids des fractions de polyéthylène linéaire, $[\eta] = 3.9 \times 10^{-4} \bar{M}_w^{0.74}$.

Zusammenfassung

Während in der Literatur Angaben über die Viskositätszahl von Polyäthylenlösungen für mindestens 6 verschiedene Lösungsmittel und 14 verschiedene Temperaturen in 23 Kombinationen gemacht werden, gibt es nur wenige Beziehungen zur gegenseitigen Umwandlung der Angaben. Ebenso werden Viskositätszahl-Molekulargewichtsbeziehungen für verschiedene Bedingungen und Polymertypen angegeben, die in manchen Fällen zu nicht vergleichbaren Werten führen. Beziehungen werden zwischen den Viskositätszahlen von verzweigtem Polyäthylen in verschiedenen Lösungsmitteln aufgestellt (Sehen synopsis). Hier bezeichnet α, α-Chloronaphthalin bei 125°C.; d, Dekahydronaphthalin bei 70°C.; t, Tetrahydronaphthalin bei 125°C.; x, *p*-Xylol bei 85°C. Die Beziehungen für lineares Polyäthylen unterschieden sich merklich von denen für verzweigtes Polyäthylen, wurden aber nicht näher bestimmt. Eine Überprüfung der Literatur in bezug auf geeignete und verlässliche Viskositätszahl-Molekulargewichtsbeziehungen für Polyäthylen wird durchgeführt. Eine Analyse der Versuchsdaten führt zu folgenden Beziehungen für lineares Polyäthylen, die als die am besten konsistenten, verlässlichsten und geeignetsten unter den gegenwärtig vorhandenen betrachtet werden (Viskositätszahlen werden in Deciliter/Gramm für Messung in Dekahydronaphthalin bei 135°C. mit Versuchsfehler spezifiziert nach ASTM D 1601-58T) angegeben). Für den Zahlenmittelwert des Molekulargewichts von Fraktionen von linearem Polyäthylen, $[\eta] = 2{,}3 \times 10^{-4} \bar{M}_n^{0{,}82}$; für den Gewichtsmittelwert von unfraktionierten Polymerproben von linearem Polyäthylen, $[\eta] = 2{,}55 \times 10^{-4} \bar{M}_w^{0{,}71}$; für den Gewichtsmittelwert von Fraktionen von linearem Polyäthylen, $[\eta] = 3{,}9 \times 10^{-4} \bar{M}_w^{0{,}74}$.

Received April 11, 1962

JOURNAL OF POLYMER SCIENCE: PART A VOL. 1, PP. 1735–1747 (1963)

Homogeneous Anionic Polymerization. IV. Kinetics of Butadiene and Isoprene Polymerization with Butyllithium*

MAURICE MORTON, E. E. BOSTICK,† R. A. LIVIGNI,‡ and L. J. FETTERS, *Institute of Rubber Research University of Akron, Akron, Ohio*

Synopsis

The kinetics of polymerization of butadiene and isoprene with butyllithium initiator have been studied both in *n*-hexane and tetrahydrofuran solution. The overall polymerization rates were much faster in the THF solutions than in *n*-hexane, and the latter also exhibited relatively slow initiation rates compared to propagation. By use of a preinitiation technique, where necessary, it was possible to study the propagation kinetics without any interference by initiation. The propagation reaction was found to be first-order with respect to monomer in both solvents, but much faster in THF. Furthermore, it was first-order with respect to growing chain concentration in the THF system, but only half-order in the *n*-hexane system. This was taken to indicate the existence, in *n*-hexane solution, of an association equilibrium between active single chains and inactive chain pairs. The activation energy for propagation was found to be 6–7 kg. cal. in THF and about 22 kg. cal. in *n*-hexane for both monomers, but the latter value obviously includes the heat of dissociation of the associated chain pairs. The Arrhenius expression for the propagation rate in THF contains a very low frequency factor ($\sim 10^4$) and leads to a propagation rate constant at least two orders of magnitude less than the corresponding value for free radical propagation.

In previous papers[1,2] of this series, it had been shown that the polymerization of styrene and isoprene by organolithium initiators is characterized by the absence of any termination reaction, if suitable precautions are taken. Under those conditions, each molecule of organolithium gives rise to one polymer chain, as indicated by the stoichiometry between the number of polymer chains and concentration of initiator. Furthermore, the same stoichiometry was found to apply regardless of the solvent used, i.e., benzene, *n*-hexane, or tetrahydrofuran solvent.

It was considered of special interest to elucidate the kinetics of these polymerizations with special reference to the effect of solvents, in view of the known effect of these solvents on the chain structure of polyisoprene.[3,4] Thus it is known that, in hydrocarbon solvents, the polyisoprene obtained

* Presented in part at the Second International Synthetic Rubber Symposium, London, October, 1961.

† Present address: Research Laboratory, General Electric Co., Schenectady, N. Y.

‡ Present address: General Tire and Rubber Co., Akron, Ohio.

has a very high content of *cis*-1,4 structure, whereas, in presence of ethers, the chain structure consists of a mixture of isomeric forms. Hence a study of the kinetics of these systems should help to throw some light on the different mechanisms operating in these cases. Butadiene was included in this study as a diene which is known not to show any stereospecificity in these polymerizations, regardless of solvent used.[5] Styrene was not included in these studies, since its rate of polymerization in solvents such as tetrahydrofuran is too fast to be easily measured, so that solvent effects are difficult to compare.

EXPERIMENTAL TECHNIQUES

The general apparatus[6] and the techniques used in the purification of the solvents and isoprene and in the preparation of butyllithium have already been previously described.[1,2]

Butadiene Purification

Butadiene (Phillips high purity; 0.02 wt.-% *tert*-butyl pyrocatechol) was collected over sodium lumps in Flask (R) (Fig. 1). This section of the manifold was fitted with a mercury column pressure release sealed to side-arm (P). Flash distillation from (R) removed the inhibitor. Subsequently, three sodium-coated flasks (F) were used to dry the butadiene and

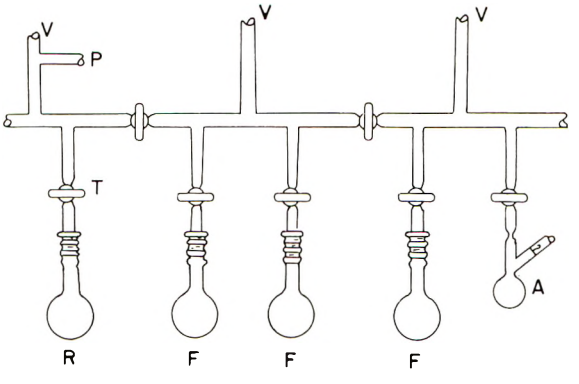

Fig. 1. Butadiene purification apparatus.

to remove dimers. Finally, the distillate was collected in weighed, evacuated ampules at (A). Here, degassing was continued by freezing and pumping several times to 10^{-6} mm. Hg pressure. Thawing was accomplished by isolating the manifold from the vacuum line. Thawing cycles were found to be necessary for removal of occluded air. The thoroughly dried and degassed distillate was removed by sealing off in the usual manner.

Polymerization Procedure and Rate Measurements

For these kinetic studies, a high vacuum polymerization apparatus was constructed similar to the one previously described,[1] except for the inclu-

sion of a dilatometer to enable rate measurements, as illustrated in Figure 2.

A reaction flask (R) was fitted with a cross tube containing monomer (M), solvent (S), lithium alkyl (C), vacuum connection (V), terminator (T), and dilatometer (D).

Sampling tubes (A) were attached directly to the bulb. When assembled, the apparatus was attached to a vacuum line and pumped to 10^{-6} mm. Hg pressure. The entire apparatus was then flamed with a gas/oxygen torch. By continuously moving a large, bushy flame over the glass surface, heating was increased until the orange color associated with sodium emission spectra was noticed. After cooling, the apparatus was sealed off from the vacuum line and placed on a magnetic stirrer. Solvent, catalyst, and monomer were completely transferred to (R) and thoroughly mixed.

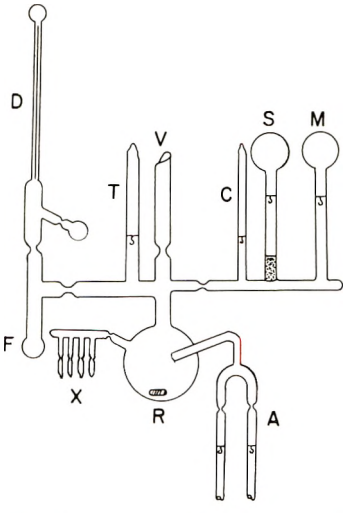

Fig. 2. Polymerization apparatus.

(F), the dilatometer reservoir bulb was filled by tipping, and the dilatometer was removed at the construction. Sample tubes (A) were removed for double titration according to the method of Gilman and Haubein,[7] with modifications for vacuum technique. The capillary and bulb of the dilatometer (D) were filled by inverting so that (F) drained completely. The dilatometer was then immersed in a constant-temperature bath until thermal equilibrium was attained. Excess reaction solution was sealed off in a side bulb. Reaction progress was observed by measuring the height of the meniscus in the capillary. Starkweather and Taylor[8] have shown that the contraction of a polymerizing system is directly proportional to degree of conversion. Therefore, if the extent of reaction is known for the initial dilatometer reading, an accurate record of the entire reaction may be obtained. Further, several dilatometers may be attached to a single reactor, providing an opportunity to determine the effect of temperature on the reaction rate.

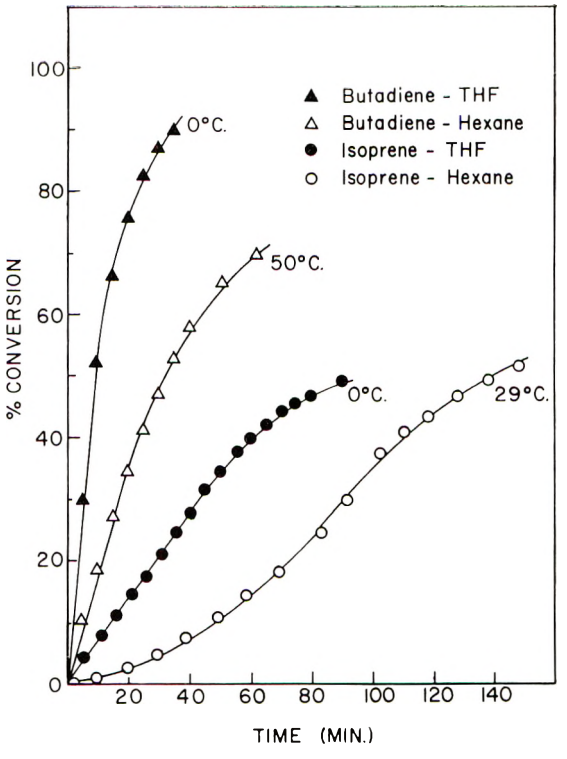

Fig. 3. Polymerization rates.

As previously found in the case of styrene, it was also noted that neither ethyllithium nor *n*-butyllithium reacted instantaneously with isoprene in hydrocarbon solvents. Instead, there was a relatively slow reaction at 29°C. which caused a relatively slow rate of initiation compared to the propagation rate. The net result of this combination is a polymerization curve which is sigmoidal with time, as shown for isoprene in Figure 3. The kinetic treatment of such a process becomes rather complex,[9] but there is an experimental approach which simplifies the system. This approach involves the use of a "seeded" polymerization similar to the type described previously.[1] In this case, seeding was accomplished by mixing alkyllithium and a portion of the monomer in hydrocarbon solvents and allowing polymerization to proceed. A polymer with $\bar{M}_n$ of 6,000–10,000 was generally designed. This active polymer solution was then divided *in vacuo* and used to polymerize additional monomer. A true propagation rate, first-order, was thereby measured. This seeding technique was used for the polymerization of isoprene in *n*-hexane, but was unnecessary for all the other systems, since initiation was sufficiently rapid.

Since a time interval of 5–10 min. usually elapsed between the time of mixing the reaction ingredients and the first reading of the dilatometer, some runs were carried out in which the actual per cent conversion at various times was determined by total solids. In this way, the extent of poly-

merization at the start of the dilatometer readings could be obtained. This was accomplished by attaching a manifold, X, containing 5 or 6 sampling ampules, directly to flask R. An ampule was then removed at specified times after the initial mixing of ingredients, and the total polymer content determined by coagulation in alcohol.

RESULTS AND DISCUSSION

The dilatometric data for the polymerization of butadiene and isoprene are shown as first-order plots in Figures 4–9, where ΔH_m represents the

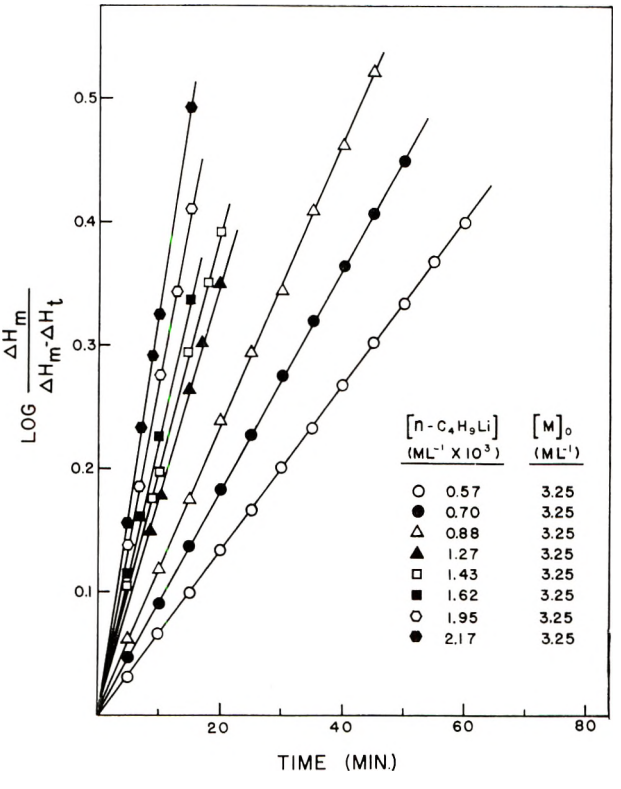

Fig. 4. First-order plots for butadiene in THF (0.°C.)

maximum change in capillary height and ΔH_t refers to the change in height at the given time. It can be seen that all the rates are first-order with respect to monomer concentration and that these kinetics are obeyed over the temperature range shown, regardless of the solvent used. This fact was also confirmed, as will be shown later, by experiments in which the initial concentration of the monomer was varied. These kinetics are, of course, to be expected since the number of growing chains should remain constant and only the monomer concentration is decreasing.

The observed first-order rate constants are listed in Table I. From the constants at the different temperatures (and the same initiator concentration) it is possible to calculate an apparent activation energy for the propagation reaction in each case, and the values are shown in Table II. It can

TABLE I
First-Order Propagation Rate Constants (k_1)

System	Temp., ° C.	[n-C_4H_9Li], mole $l.^{-1}$ $\times 10^3$	[Monomer], mole $l.^{-1}$	k_1, $sec.^{-1}$ $\times 10^4$
Butadiene–THF	0	0.57	3.25	2.53
	30	0.57	3.25	7.67
	0	0.70	3.25	3.45
	30	0.70	3.25	10.69
	0	0.88	3.25	4.60
	0	1.27	3.25	7.13
	0	1.43	3.25	7.18
	0	1.62	3.25	8.62
	0	1.95	3.25	10.58
	0	2.17	3.25	12.25
Isoprene–THF	0	2.85	2.50	0.89
	29	2.85	2.50	3.03
	0	3.00	2.50	1.53
	0	3.00	5.00	1.19
	0	3.45	7.50	1.25
	0	4.00	2.50	1.30
	29	4.00	2.50	4.17
	0	4.25	2.50	2.54
	0	5.10	2.50	1.92
	0	8.00	2.50	3.42
	0	17.75	2.50	7.50
	0	23.00	2.50	8.94
Butadiene–hexane	50	0.90	3.25	1.60
	50	1.60	3.25	2.59
	50	2.50	1.63	3.17
	30	3.60	3.25	0.36
	40	3.60	3.25	1.00
	50	3.60	3.25	3.45
	30	6.40	3.25	0.52
	50	6.40	3.25	4.29
	50	9.30	6.50	5.95
	50	11.00	4.88	5.58
	50	12.00	6.50	6.36
Isoprene–hexane	29	0.24	2.50	0.16
	29	0.96	2.50	0.83
	29	1.65	2.50	0.96
	29	1.97	2.50	1.05
	39.6	1.97	2.50	3.42
	50	1.97	2.50	12.00
	29	2.35	1.60	1.17
	29	3.03	2.50	1.28
	29	4.25	2.50	1.53
	29	5.68	2.50	1.73

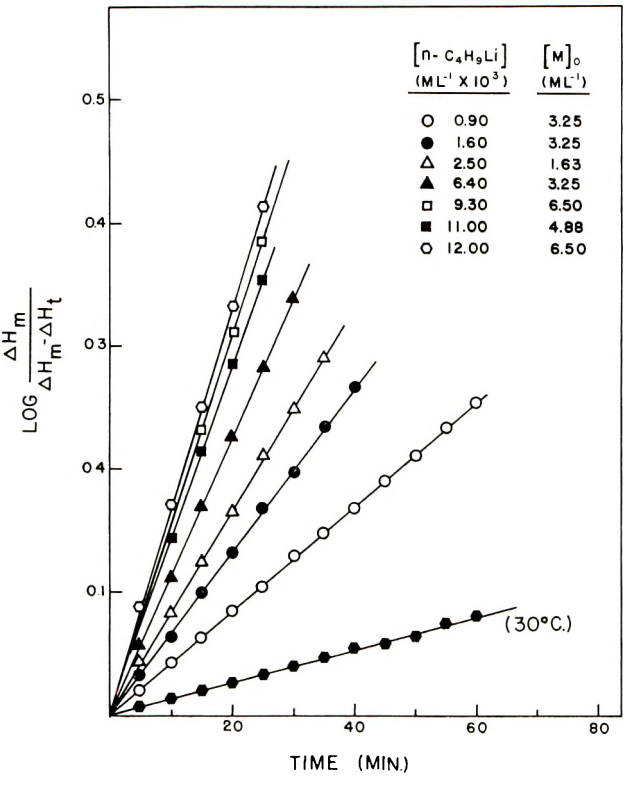

Fig. 5. First-order plots for butadiene in *n*-hexane (0°C.).

be seen at once that there is a very marked effect of the solvent on these apparent activation energies. Thus the observed values are extremely high for both monomers in *n*-hexane but are much more reasonable in the case of the THF. This is a strong indication that the propagation mechanism in the hydrocarbon solvent involves something more than a simple attack of the anion on the monomer double bond. It is also interesting to note the similarity of these activation energies for the two monomers in the same solvent. The values obtained in *n*-hexane are somewhat higher than the 14.3 kg. cal. recently published by Worsfold and Bywater[10] for the propagation step in the butyllithium polymerization of styrene in benzene, but all of these values indicate a complex propagation mechanism.

TABLE II
Apparent Activation Energies for Propagation

Monomer	Solvent	Activation energy, kg. cal. mole^{-1}
Butadiene	*n*-Hexane	21.5 ± 0.3
"	THF	6.1 ± 0.05
Isoprene	*b*-Hexane	22.6 ± 0.3
"	THF	6.8 ± 0.1

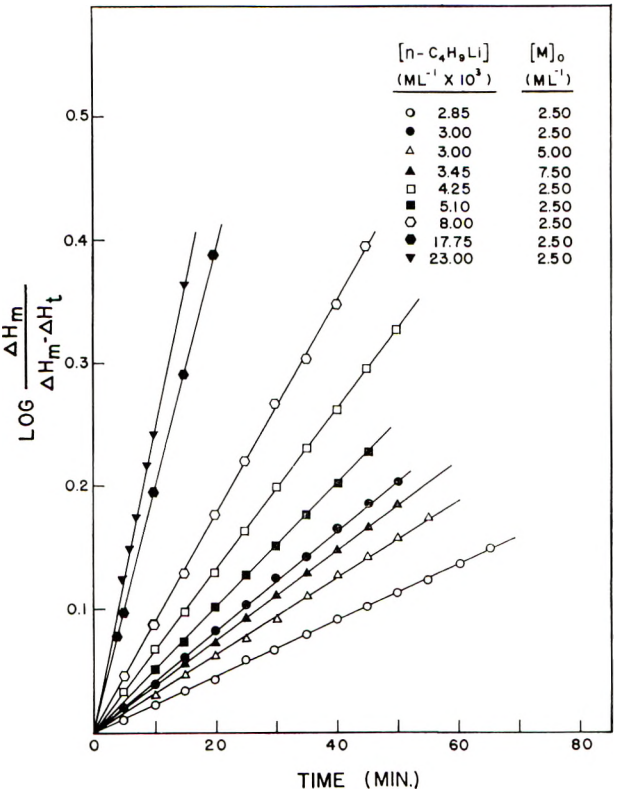

Fig. 6. Isoprene in THF (0°C.).

The dependency of the propagation rate on the concentration of growing chains is illustrated in Figures 10 and 11. Here are plotted the first-order rate constants (k_1) listed in Table I as a function of the initiator concentration. Figure 10 shows that both butadiene and isoprene propagation rates in THF are first-order with respect to the active chain concentration, as would normally be expected. This is consistent with the usual bimolecular mechanism between single polymer chains and monomer molecules.

In the case of the *n*-hexane, however, it can be seen from Figure 11 that the propagation rate for both monomers is only half-order with respect to the concentration of growing chains. This behavior is similar to that found for styrene in benzene[10,11] and therefore seems to represent the general behavior of organo-lithium polymerizations in hydrocarbon solvents. The simplest explanation for this phenomenon would be the assumption of an association–dissociation equilibrium in which the dissociated species represent the active growing chains. Such equilibria may be written in two forms as follows, where RLi represents the polymer–lithium growing chain:

$$RLi \rightleftarrows R^- + Li^+ \quad (1)$$

$$(RLi)_2 \rightleftarrows 2R^-Li^+ \quad (2)$$

Equation (1) above represents a simple dissociation of the organo-lithium bond into free anions and cations, whereas eq. (2) is based on an association of the organolithium in pairs, with the active anion actually being part of an ion pair.

The possibility of a true ionization of the type indicated in eq. (1) above has been minimized, from energetic considerations, by Worsfold and Bywater.[10] In addition, the ion-pair concept shown in eq. (2) is further supported by evidence available from microstructure of polymers and viscosity of polymerizing solutions.

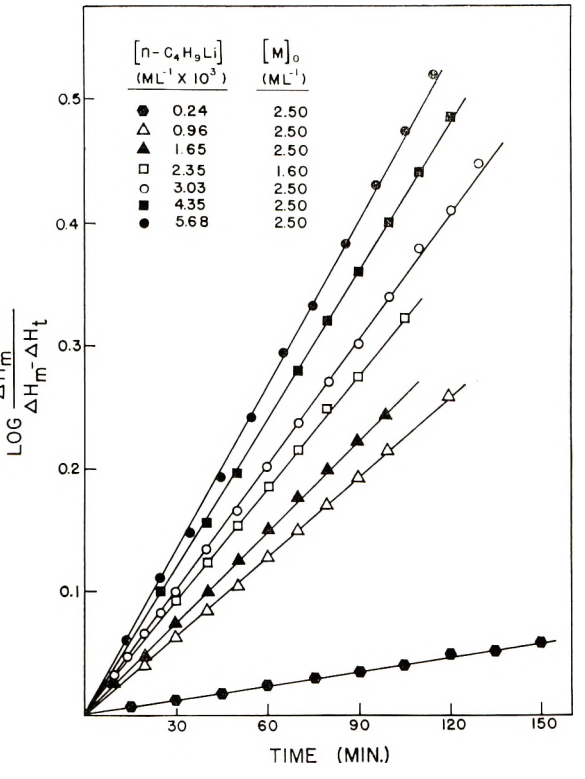

Fig. 7. Isoprene in *n*-hexane (29°C.).

Since it is well known that the nature of the counterion has a very pronounced effect on the microstructure of the dienes polymerized by the alkali metals, such polymerizations are more likely to involve ion pairs rather than free anions. Furthermore, this is corroborated by the fact that even the type of solvent used may affect this microstructure.[4,5] More direct evidence for the existence of an association equilibrium of the type shown in eq. (2) is available from recent studies in this laboratory on the viscosity of the polymerizing solutions.[11] These will be described in detail in the following paper in this series. However, it is sufficient at this point to state that such viscosity studies have indicated that the active

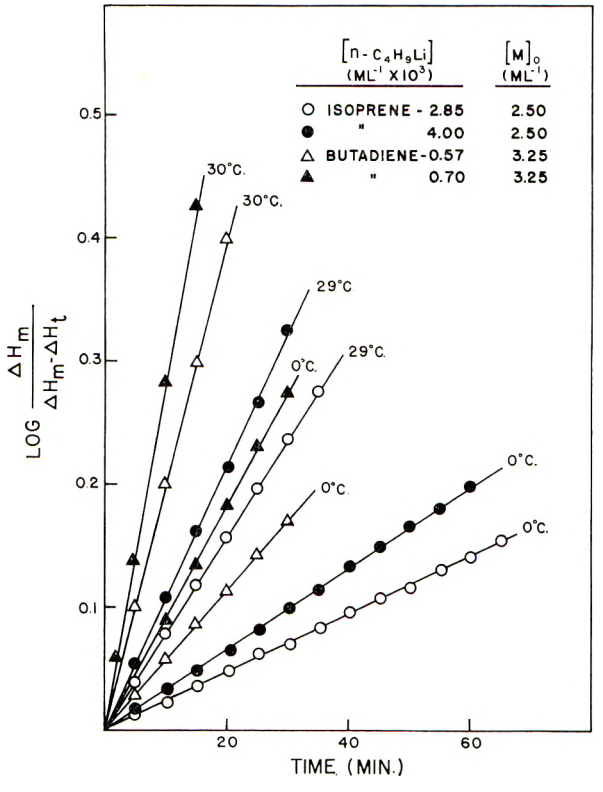

Fig. 8. Polymerizations in THF.

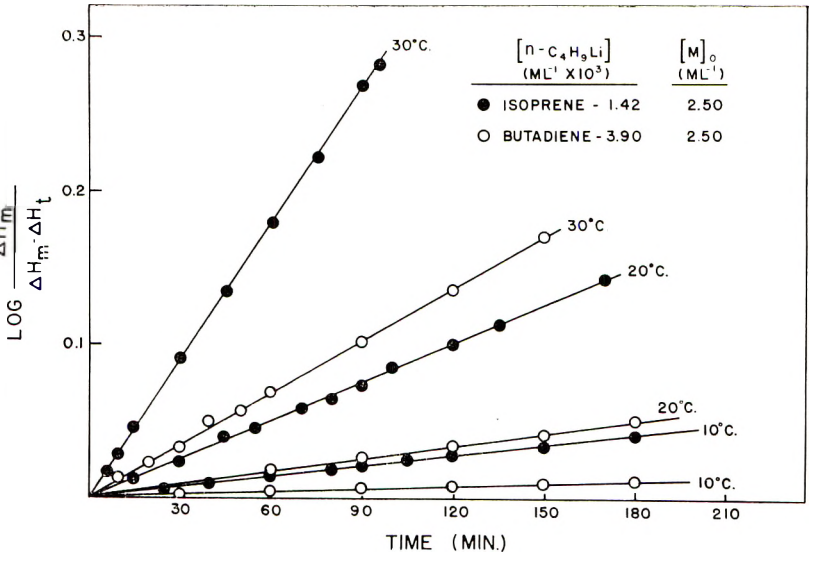

Fig. 9. Polymerizations in *n*-hexane.

polyisoprenyllithium is associated in pairs in *n*-hexane, but no such association is observed in THF. Hence the conclusion is that an equilibrium of the type shown in eq. (2) does exist, with the overwhelming majority of the chains being in the associated (inactive) state.

On this basis, then, the surprisingly high activation energy found for the

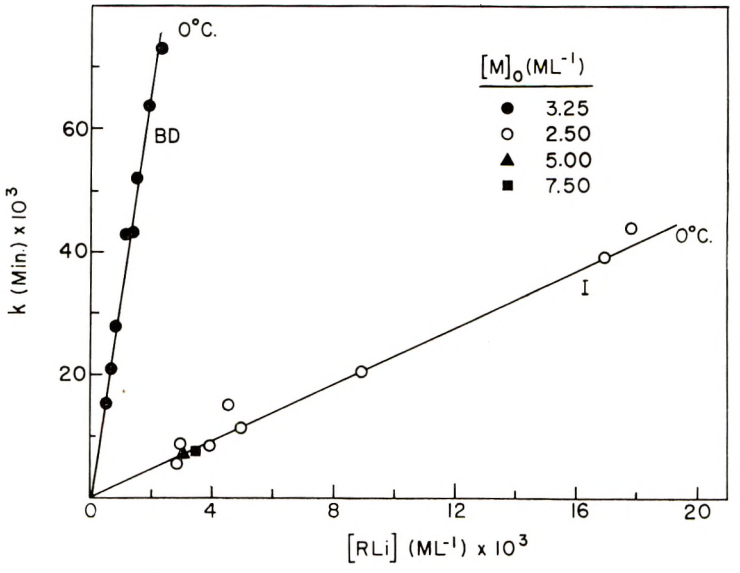

Fig. 10. Dependence of butadiene and isoprene rates on initiator concentration (THF).

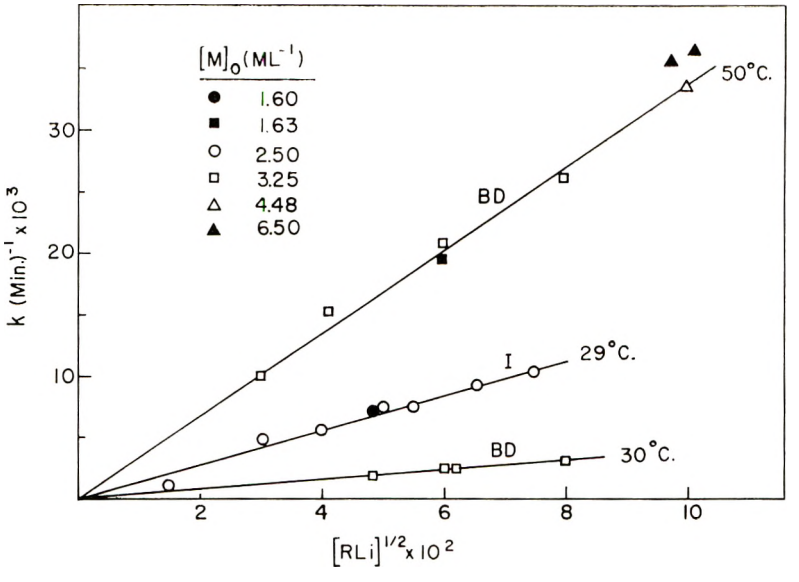

Fig. 11. Dependence of butadiene and isoprene rates on initiator concentration (*n*-hexane).

propagation reactions in *n*-hexane includes, of course, the heat of dissociation of the associated ion pairs. Therefore, in the absence of any precise knowledge concerning this equilibrium, it is impossible to determine the actual propagation rate constant for these systems. No such restriction, however, applies in the case of the THF polymerizations, where all the polymer chain species are presumably active. From the available data it is therefore possible to calculate the following Arrhenius expressions for the propagation rates in THF.

Butadiene: $k_p = 4.3 \times 10^4 \exp\{6100/RT\}$

Isoprene: $k_p = 1.0 \times 10^4 \exp\{6800/RT\}$

It is at once obvious that these reactions have an unusually low frequency factor, with the isoprene being, as expected, even more sterically hindered. In this connection, it is interesting to make a comparison with the free radical propagation reactions for these monomers,[12] where the activation energy is 2–3 kcal. higher but the frequency factor is also several orders of magnitude greater. The net result is that the anionic propagation rate constant at ambient temperatures is much lower than in free radical polymerization. Thus the anionic rate constants calculated for 60°C. are 4.45 and 0.36 l.mole^{-1} sec.$^{-1}$ for butadiene and isoprene respectively, whereas the corresponding free radical propagation rate constants[12] are 100 and 50 l.mole^{-1} sec.$^{-1}$. This can presumably be ascribed to the high steric requirements of the ion-pair species.

This work was supported by National Science Foundation Grant G-5919, and by a research grant from the General Tire and Rubber Co.

References

1. Morton, M., A. A. Rembaum, and J. L. Hall, *J. Polymer Sci.*, **A1,** 461 (1963).
2. Morton, M., E. E. Bostick, and R. G. Clarke, *J. Polymer Sci.*, **A1,** 475 (1963).
3. Diem, H. E., H. Tucker, and C. F. Gibbs, paper presented at 132nd Meeting, American Chemical Society, New York, September 1957.
4. Morita, H., and A. V. Tobolsky, *J. Am. Chem. Soc.*, **79,** 5853 (1957).
5. Kuntz, I., and A. Gerber, *J. Polymer Sci.*, **42,** 299 (1960).
6. Morton, M., R. Milkovich, D. B. McIntyre, and J. L. Bradley, *J. Polymer Sci.*, **A1,** 443 (1963).
7. Gilman, H., and A. Haubein, *J. Am. Chem. Soc.*, **66,** 1515 (1944).
8. Starkweather, H., and G. B. Taylor, *J. Am. Chem. Soc.*, **52,** 4708 (1930).
9. Bauer, E., and M. Magat, *J. Chim. Phys.*, **47,** 841 (1950).
10. Worsfold, D. J., and S. Bywater, *Can. J. Chem.*, **38,** 1891 (1960).
11. Morton, M., E. E. Bostick, and R. Livigni, *Rubber Plastics Age*, **42,** 397 (1961).
12. Morton, M., P. P. Salatiello, and H. Landfield, *J. Polymer Sci.*, **8,** 215, 279 (1952).

Résumé

On étudie la cinétique de la polymérisation du butadiène et de l'isoprène au moyen d'initiateur butyllithium en solution à la fois dans l'hexane et le tétrahydrofuranne. Les vitesses totales de polymérisation sont beaucoup plus rapides dans les solutions de tétrahydrofuranne que dans l'hexane-*n*, et dans ce dernier on constate des vitesses relativement lentes d'initiation comparées à la propagation. En employant une technique de

préinitiation, lorsque cela est nécessaire, il est possible d'étudier la cinétique de propagation, sans aucune interférence due à l'initiation. On trouve que la réaction de propagation est du premier ordre vis-à-vis du monomère dans les deux solvants, mais beaucoup plus rapide dans le tétrahydrofuranne. De plus, elle est du premier ordre vis-à-vis de la concentration en chaînes croissantes dans le système THF, mais seulement d'ordre undemi dans le système hexane. Ceci montre l'existence, en solution dans l'hexane-*n*, d'un équilibre d'association entre les simples chîanes actives et les paires de chaîne inactives. On trouve pour l'énergie d'activation de propagation dans le THF 6–7 kcal. et environ 22 kcal. dans l'hexane-*n*, pour les deux monomères, mais cette dernière valeur inclut évidemment la chaleur de dissociation des paires de chaînes associées. L'expression d'Arrhénius pour la vitesse de propagation dans le THF comprend un facteur de fréquence très faible ($\sim 10^4$) et conduit à une constante de vitesse de propagation de deux ordres de grandeurs plus faible que la valeur correspondante pour la propagation radicalaire libre.

Zusammenfassung

Die Kinetik der Polymerisation von Butadien und Isopren mit Butyllithium als Starter wurde in *n*-Hexan- und Tetrahydrofuranlösung untersucht. Die Bruttopolymerisationsgeschwindigkeit war in THF-Lösung viel grösser als in *n*-Hexan und in letzterem trat auch, im Vergleich zum Wachstum, eine relativ geringe Startgeschwindigkeit auf. Es war möglich, wenn nötig unter Anwendung eines Vorstartverfahrens, die Wachstumskinetik ohne Störung durch den Start zu untersuchen. Die Wachstumsreaktion war in beiden Lösungsmitteln von erster Ordnung in bezug auf das Monomere, in THF aber viel rascher. Ausserdem war sie in THF von erster Ordnung in bezug auf die Konzentration der wachsenden Ketten, in *n*-Hexan aber nur von der Ordnung ein halb. Dies wurde als Hinweis auf das Bestehen eines Assoziationsgleichgewichtes zwischen aktiven Einzelketten und inaktiven Kettenpaaren in *n*-Hexanlösung aufgefasst. Die Aktivierungsenergie des Wachstums betrug für beide Monomere in THF 6–7 kcal. und in *n*-Hexan etwa 22 kcal.; der letztere Wert beinhaltet offenbar die Dissoziationswärme der assozierten Kettenpaare. Die Arrheniusbeziehung für die Wachstumsgeschwindigkeit in THF enthält einen sehr niedrigen Frequenzfaktor ($\sim 10^4$) und führt zu einer Wachstumsgeschwindigkeitskonstanten, die mindestens um zwei Grössenordnungen kleiner ist als der entsprechende Wert für das radikalische Wachstum.

Received March 29, 1962

JOURNAL OF POLYMER SCIENCE: PART A VOL. 1, PP. 1749–1763 (1963)

Narrow Molecular Weight Distribution Polystyrenes

F. M. BROWER and H. W. McCORMICK, *Physical Research Laboratory, The Dow Chemical Company, Midland, Michigan*

Synopsis

A study of the scope and limitations of the anionic polymerization of styrene and substituted styrenes under conditions in which a chain termination reaction is lacking was made. Under these conditions polymers of very narrow molecular weight distributions were obtained. Ultracentrifuge data are presented as evidence confirming the formation of narrow distributions. All reagents used were carefully purified and subsequently were not exposed to the atmosphere. Standard procedure was to conduct the polymerizations by adding monomer solution slowly to initiator solution. Deviations from this procedure were designed to study various reaction conditions. Monomers used were styrene, α-methylstyrene and *m*- and *p*-vinyltoluene. Solvents used were tetrahydrofuran, tetrahydropyran, 2-methyl-tetrahydrofuran, dioxane, ethylene glycol dimethyl ether, and diethylene glycol dimethyl ether. Initiators used were sodium–naphthalene, sodium–biphenyl, sodium–α-methylstyrene, sodium–phenanthrene, and lithium–naphthalene. The choice of solvent had a great effect on the course of the polymerization and the temperature at which narrow distribution polymers could be produced. Solvents promoting rapid initiation and relatively slow propagation were best, and those promoting the reverse situation tended to give side reactions leading to termination and abroad distribution polymer. The order of promotion of rapid initiation and slow propagation for these solvents is dioxan > tetrahydrofuran > ethylene glycol dimethyl ether > diethylene glycol dimethyl ether. In dioxane solutions monodisperse polymer was prepared under a wide range of conditions. Monodisperse polymer could not be prepared under the most favorable conditions in diethylene glycol dimethyl ether. These effects were interpreted in terms of ion pair separation. Other factors which might lead to broad distribution polymers were examined. The age of the initiator was found to be very important, older initiator solutions giving broad distribution polymers. Aged initiator solutions were found to evolve hydrogen when allowed to react with water; freshly prepared initiator solutions evolved no hydrogen. In the presence of toluene there was chain transfer to the methyl group giving a broad distribution polymer. Similar transfer to benzene at the ring gave termination before polymerization was complete. Rusty iron, Fe_2O_3, and Fe_3O_4 adversely effected the course of polymerizations giving broad distribution polymers. Hydrogen-reduced iron in the reaction mixture resulted in only minor deviation from narrow distribution.

INTRODUCTION

Vinyl polymerizations initiated by electron transfer to monomer have been shown by Szwarc and co-workers[1,2] to give polymer molecules with perpetually active ends under conditions where a termination reaction is lacking. Under carefully controlled conditions, where effects of impurities and side reactions are minimized, it has been shown[3,4] that polymers of

narrow molecular weight distribution can be prepared. This paper describes some of the results obtained during an investigation of the scope and limitations of such polymerizations of styrene and substituted styrenes with the use of alkali metal–aromatic hydrocarbon complexes as initiators. The physical and rheological properties of some of the polymers produced are described in previous publications.[5,6] The data were obtained during 1956–1958 but were not released for publication until the present time.

The method involved usually requires the slow addition of monomer solution to initiator solution. There is immediate electron transfer from the initiator to monomer,[1] followed by dimerization or tetramerization of the ion-radicals thus formed to give dimers or tetramers with active terminal ionic sites. Slow addition of monomer leads to propagation which continues until equilibrium between the monomer and polymer is achieved.[7] Following this, the polymer ends are rendered inactive by addition of a proton donor, usually water, or other suitable reagent. Narrow distribution of molecular weights results because initiation is essentially simultaneous for all polymer molecules and each experiences an equal opportunity to grow.

EXPERIMENTAL

A. Reagents

Monomers were purified to impurity concentrations of less than 100 ppm determined as sodium by titration with a standardized sodium–aromatic hydrocarbon complex in tetrahydrofuran or similar solvent. The titration method is an extension[8] of a literature procedure[9] in which all impurities which react readily with sodium complexes are titrated.

Styrene monomer was obtained directly from The Dow Chemical Company stills with impurity levels usually in the range of 50–100 ppm. The impurity level in this and other monomers was often reduced simply by blowing pure nitrogen through the monomer for several hours. Where necessary, monomers were further purified by reduced pressure distillation from calcium hydride or by passage through a column of activated silica gel followed by reduced pressure distillation.

The various ether solvents were purified by distillation from a sodium–aromatic hydrocarbon complex. Usually, the complex was prepared directly in the ether to be distilled, but, where complexing was slow, a previously prepared complex solution in any of several high boiling, end-capped polyethylene oxide solvents was added. Distillation gave ether solutions which contained, by sodium complex titration with an α-methylstyrene indicator, not more than 10 ppm of impurities calculated as sodium. Typical analysis showed 2–5 ppm impurities.

The alkali metal–hydrocarbon complexes used as initiators were prepared by adding to the purified ether under nitrogen or argon atmosphere, equimolar amounts of alkali metal and aromatic hydrocarbon in an amount

sufficient to give a 0.5–1.0 N solution. The rate of complex formation varied tremendously with the different solvents used. In some cases, especially with 1,4-dioxane, the complex formed appeared to have a limited solubility, decreasing and/or reversing to release free sodium as the temperature was raised. The color of the complex also varied with variation of ether and aromatic hydrocarbon; colors ranged from yellow-green through green and blue-green to blue and purple. The exact normality of complexes used as initiators was determined by titration with *n*-propanol as a primary standard.

The nitrogen used as an inert atmosphere was obtained from a direct line to The Dow Chemical Company's air distillation plant. This nitrogen usually analyzed less than 10 ppm oxygen. It was further purified by bubbling through a solution of sodium–biphenyl complex in nonvolatile polyethylene oxide. Nitrogen thus purified contained virtually no measurable quantity of oxygen.

B. Polymerizations

Polymerizations were generally carried out by the slow addition of monomer solution to initiator solution and subsequently to the "living" polymer. A standardized procedure using a Pyrex glass apparatus diagrammed in Figure 1 is outlined below.

1. The apparatus was swept with a slow stream of nitrogen for 16 hr., the gas entering and exiting through appropriate ports. Exit ports were protected from back-diffusion of air in this and subsequent operations by small mineral oil traps.

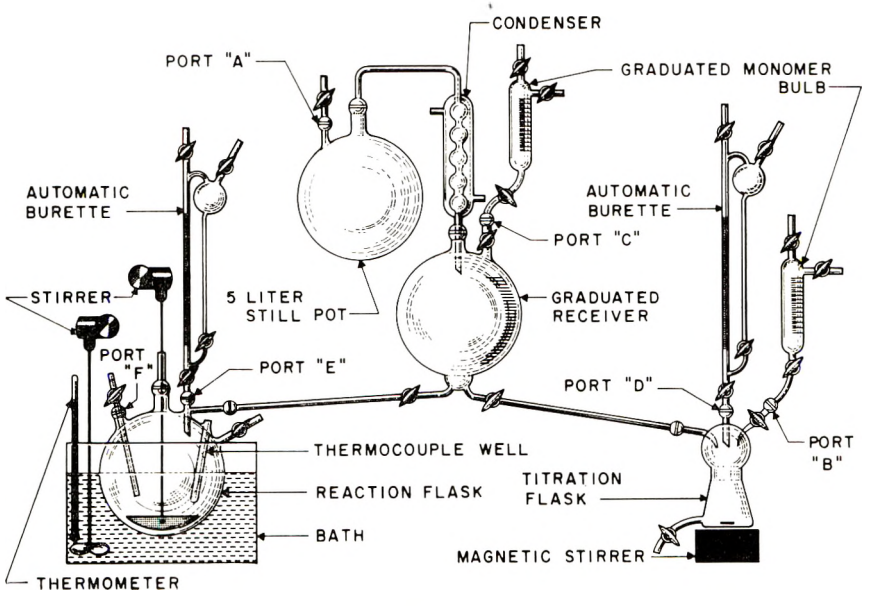

Fig. 1. Polymerization apparatus.

TABLE I
Molecular Weights of Polymers Prepared from Styrene Monomers under Various Conditions

Sample No.	Initiator[a]		Solvent[b]	Reaction temp., °C.	M_n		$\bar{M}_w/\bar{M}_n$	$[\eta]$
	Hydrocarbon	Solvent			Theor.	Measured		
S3	Naphthalene	THF	THF	0–10	40,000	40,000	1.35	0.276
S4	Naphthalene	THF	THF	0–10	60,000	66,300	1.18	0.358
S5	Naphthalene	THF	THF	0–12	80,000	95,700	1.16	0.439
S6	Naphthalene	THF	THF	0–12	100,000	116,000	1.08	0.515
S7	Naphthalene	THF	THF	0–10	120,000	131,000	1.08	0.578
S8	Naphthalene	THF	THF	0–10	140,000	159,000	1.07	0.640
S9	Naphthalene	THF	THF	0–10	160,000	189,000	1.11	0.727
S10	Naphthalene	THF	THF	0–12	200,000	240,000	1.04	0.840
S40	Naphthalene[c]	THF	THF	−70 to −76	59,500	75,000	1.24	0.357
S41	α-Methyl styrene[c]	THF	DME	−45 to −60	52,000	63,000	1.38	
S42	Naphthalene[d]	THF	THF	−70	59,000	100,000	1.25	
S43	Naphthalene	THF	THF	−70 to −78	100,000	148,000	1.99	
S44	α-Methyl styrene	THF	THF	−78	104,000	138,000	1.16	
S45	Naphthalene	THF	THF	25 (initiation), then −70 to −78	52,000	73,500	1.26	
S46	Naphthalene	THF	THF	25 (initiation), then −70 to −78	100,000	137,000	1.15	

S47	Naphthalene	DME	DME	0	52,000	73,000	1.19
S48	Biphenyl	DME	DME	−50 to −78	52,000	51,000	2.14
S49	Naphthalene	THF	Dioxane	17	105,000	145,000	1.39
S50[e]	Naphthalene	THF	Dioxane	15–45	104,000	114,000	1.29
S51[f]	Naphthalene	THF	Dioxane	≥5	52,000	64,000	1.31
S52[g]	Naphthalene	THF	THF	≥0	52,000	69,000	2.41
S53[h]	Naphthalene	THMF	THMF	0–10	52,000	87,000	1.36
S54	Biphenyl	THF	THF	0–10	104,000	79,000	1.13
S55	Phenanthrene	THF	THF	0–10	52,000	67,500	1.30
S56	Naphthalene	THP	THP	0–10	52,000	55,000	1.29
S57	α-Methyl styrene	THF	Toluene	0–10	52,000	6,600	2.41
S58[i]	Naphthalene	THF	THF	0–10	86,000	108,000	1.85
S59[j]	Naphthalene	THF	THF	0–10	105,000	105,000	2.24
S60[k]	Naphthalene	THF	THF	0–10	105,000	238,000	1.13
S61	Naphthalene[a]	THF	THF	5–10	52,000	110,000	1.10

[a] Metal component of initiator was sodium, except in sample S61, where metal was lithium.
[b] DME = dimethoxyethane; THMF = tetrahydro-2-methylfuran; THP = tetrahydropyran.
[c] Monomer was α-methylstyrene.
[d] Monomer was vinyltoluene.
[e] Two peaks; rapid addition of monomer.
[f] Two peaks; initiator added to monomer.
[g] Initiator added to monomer.
[h] Two peaks.
[i] Two peaks; aged initiator.
[j] Rusty iron reactor.
[k] Clean iron.

2. Sodium complex and solvent were charged to the still through port A, and ether was distilled into the graduated receiver.

3. Complex (initiator) solution in the automatic buret was standardized with a measured amount of *n*-propanol in the titration flask.

4. Impurities in the ether and monomer were determined by titration in the titration flask with standard complex solution.

5. The graduated monomer bulb was removed from port B on the titration flask and connected to port C on the graduated receiver.

6. The automatic buret containing standardized complex (initiator) solution was removed from port D on the titration flask and connected to port E on the reaction flask.

7. The desired amount of initiator solution was added to the reaction flask. This was further diluted by pure solvent from the receiver. This solution was then allowed to come to bath temperature.

8. A measured amount of monomer was added to a measured amount of pure ether in the graduated receiver. This monomer solution was mixed by bubbling with nitrogen gas from the titration flask, after which it was added dropwise or in a very small stream to the reaction flask. The internal temperature of the solution was continuously recorded.

9. After addition of all monomer a few milliliters of freshly boiled, distilled water was added to the reaction flask. The solutions were often slightly turbid at this point. If a clear polymer was desired, addition of carbon dioxide as Dry Ice led to formation of a precipitate of sodium carbonate which was filtered off.

10. The reaction flask was removed from the apparatus. The polymer solution was roughly devolatized by allowing solvent to evaporate from it in trays in a hood, or by precipitation with methanol followed by filtration. Final devolatilization was attained by placing the polymer in a tray in a vacuum over at 150°C. for 4–16 hr.

In carrying out the above operations, every effort was made to develop precise techniques and to eliminate impurities. This was found to be essential if meaningful results were to be obtained.

Deviations from the procedure were sometimes necessary in order to study varying conditions; appropriate changes in such cases are obvious.

C. Molecular Weight Distributions

Molecular weight distributions were determined by sedimentation velocity analysis of ultracentrifuge data. Sedimentation velocity data were obtained on a Spinco Model E ultracentrifuge at 59,780 rpm in cyclohexane solution at 35°C. Analysis of the sedimentation data to give a sedimentation constant–molecular weight relationship to obtain a molecular weight distribution have been reported in a previous paper.[10] The weight-average and number-average molecular weights have been calculated from the molecular weight distribution curves by the proper summation processes. Molecular weights are shown in Table I and some representative distribution curves in Figure 2.

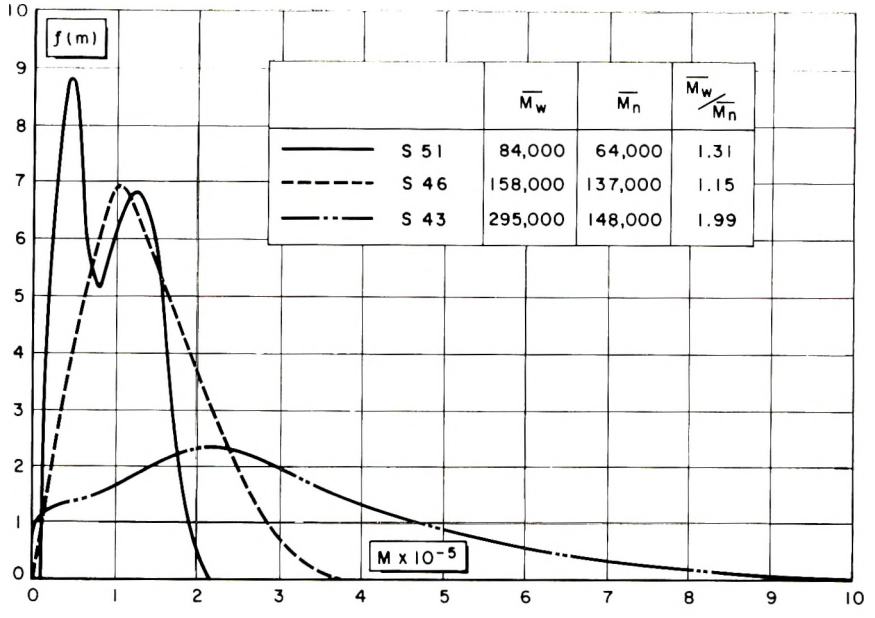

Fig. 2. Molecular weight distributions of polystyrenes.

RESULTS AND DISCUSSION

The molecular weight distributions of the various polymers prepared are best explained by the mechanism proposed by Szwarc. This mechanism is illustrated for styrene polymerization as follows.

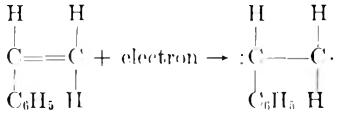

Dimerization or tetramerization through radical interaction leads to either of the following anions:

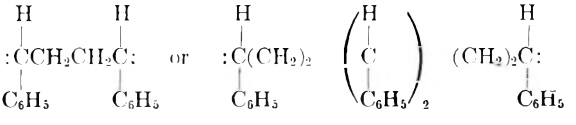

The species thus produced have active anionic sites at both ends and, if given equal opportunity to propagate, a polymer of narrow distribution results. Termination is brought about by addition of a proton donor from which the active anionic sites each abstract a proton. Perhaps the best evidence for this mechanism is the relatively precise control of the intrinsic viscosity of narrow molecular weight distribution polymers which was reproducibly achieved. These data are shown graphically in Figure 3, where molecular weight calculated from initiator concentration is plotted against intrinsic viscosity. The various polymer sample numbers reported

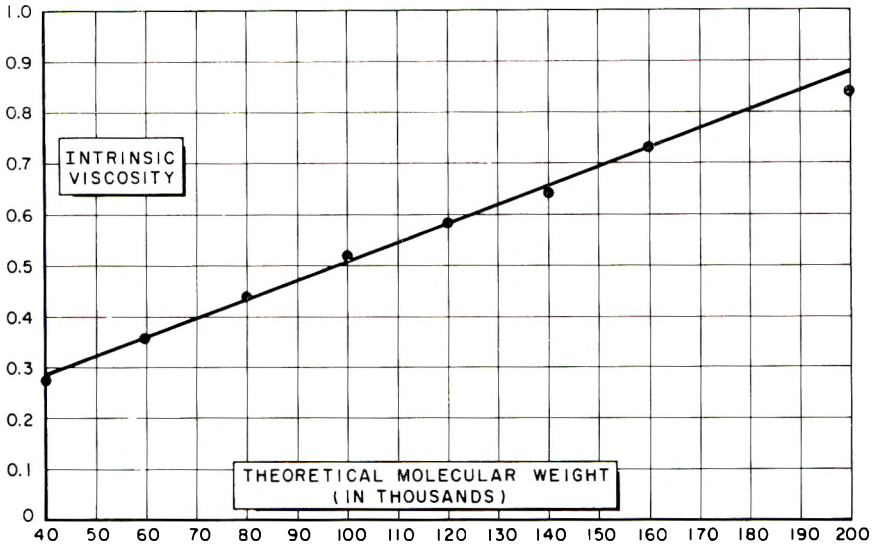

Fig. 3. Relationship of intrinsic viscosity to theoretical molecular weight calculated from initiator concentration.

on the graphs and throughout this discussion are given so that reference may be made to the molecular weight distributions of the samples reported in the experimental section. Preparative data and molecular weights are also given in Table I. Under some conditions, deviation from the assumed mechanism is apparent. The conditions will be described in the discussions of the scope and limitations of the polymerization method which follows.

A. Monomers

Polymerization conditions for styrene monomer giving narrow distribution polymers were intensively investigated. Narrow molecular weight distribution polymers have also been prepared from α-methylstyrene (S40, S41) and a mixture of *m*- and *p*-vinyltoluenes (S42).

B. Initiator and Solvent Systems

Successful polymerizations (i.e., rapid initiation followed by relatively slow propagation with no termination before addition of a protonating substance) are very dependent upon the choice of initiator–solvent system. Behavior of the several systems studied can be rationalized in terms of ion-charge separation; discussion of the results is presented in the interpretation of temperature effects since all of the systems studied are very temperature sensitive. Initiator-solvent systems studied are given in Table I. Ether solvents used were tetrahydrofuran, tetrahydro-2-methylfuran (S53), tetrahydropyran (S56), dioxane, ethylene glycol dimethyl ether, and diethylene glycol dimethyl ether. Lithium and sodium were used to form complexes with naphthalene, biphenyl (S54),[11] phenanthrene (S55), and α-methylstyrene.[12]

It should be pointed out that the α-methylstyrene–sodium initiator is not a true initiator but a dimer or very low molecular weight polymer which is prepared by adding sodium to α-methylstyrene monomer in dilute solvent solution. The solution is prepared at a temperature far above the ceiling temperature for α-methyl-styrene polymerization,[7] and, in the presence of excess sodium, the molecular weight remains low. These low molecular weight α-methylstyrene polymers have active anionic sites on either end and propagation takes place immediately when styrene monomer is added.

C. Temperature Effects

The temperatures at which narrow molecular weight polymer can be produced vary markedly with the catalyst–solvent system used. A catalyst–solvent system which functions in the expected manner at one temperature will not always behave the same at another temperature. Using sodium–naphthalene in tetrahydrofuran produced narrow distribution polymer (S6, S5) at temperatures between 0 and 12°C., but at −70 to −78°C., results were inconsistent, a high molecular weight, broad distribution polymer usually being produced. This effect was shown to be due to slow initiation by carrying out a polymerization using α-methylstyrene–sodium and polymerizing at −70 to − 78°C. The polymer produced had a narrow distribution (S44). Since α-methylstyrene-sodium is really a preinitiated tetramer, there was no initiation step, and propagation proceeded smoothly in the expected manner. In other experiments (S46, S45), narrow distribution polystyrene was produced by initiating polymerization with enough monomer to start all chains at room temperature, after which the solution was cooled to Dry Ice temperature and the remaining major portion of monomer was slowly added.

In satisfactory solvents like dioxane and tetrahydrofuran at 0–25°C., the original initiator solution is green or blue-green, depending upon the hydrocarbon. As one slowly adds dilute monomer solution to the initiator solution, an orange-red or brown-red solution is rapidly formed, and, if the experiment is properly conducted, a narrow distribution polymer is (S49, S5) produced. When ethylene glycol dimethyl ether was used as solvent, the color change was a little slower and the color formed was not quite so brilliant; nevertheless, a fairly narrow distribution polymer was obtained (S47). When ethylene glycol dimethyl ether was used at Dry Ice temperature (S48) or diethylene glycol dimethyl ether was used at room temperature, initiation was obviously very slow; a 10% monomer solution was added at a rate of a few milliliters per second for an hour before the color change was complete. In the case of the diglycol ether, the red color, once formed, slowly faded. Distributions in cases where initiation was obviously slow, were broad.

It should also be noted that these same ethers caused extremely rapid formation of the original sodium complex, and that they promoted extremely rapid styrene polymerization rates. Dioxane, on the other hand, formed sodium complexes very slowly and gave a bright red color rapidly

when styrene monomer was added to complex. Propagation in this case suffered little interference from side reactions and gave polymers of narrow molecular weight distribution. A general interpretation of this and other results will be presented following a discussion of the effect of rate and order of monomer addition during the polymerization.

D. Effect of Rate and Order of Monomer Addition

The general method of preparation of narrow distribution polymers calls for the slow addition of monomer first to initiator solution, and then to polymer with active anionic sites. This is supposed to be necessary in order that all active sites may be initiated before much propagation occurs and in order that all polymer chains experience equal growth opportunity. It has been found that for most conditions this is indeed necessary, but in initiator–solvent systems giving very rapid initiation and relatively slow propagation the rate, and even order, of addition may be varied and narrow distribution polymers still obtained. Sodium–naphthalene–dioxane is such a system. When monomer was added rapidly to this initiator at 5°C., the mixture stirred for 1–2 min. before the heat of reaction caused the temperature to increase. Once propagation began, the temperature rose rapidly to about 25°C. and leveled off. After 10 min. reaction time water was added and the polymer was devolatized in the usual manner. The ultracentrifuge measurement of this polymer indicated two very sharp peaks (S50). This rather peculiar distribution may be interpreted as follows. The initiation step is very rapid and occurs almost instantaneously, giving the active dimer or low molecular weight polymer, which is free to add monomer or to react with any impurities present. Since propagation is relatively slow in dioxane, the impurities present in the system react to kill one or both ends of various dimer molecules. The dimers killed on both ends do not contribute to the polymer, but those killed on only one end do. We now have two propagating species, dimer which is reactive on only one end, and dimer which is reactive on both ends. Propagation ensues, and two different narrow molecular weight polymers are formed, one having a degree of polymerization twice that of the other. This gives a polymer with a distribution curve consisting of two very sharp peaks. It should be noted, however, that these peaks are so close together that they still constitute a fairly narrow molecular weight distribution polymer.

Because there seemed to be an induction period before polymerization began in dioxane, it was thought that in this one case initiator could be added rapidly to monomer to give a narrow distribution polymer. When this was tried, a polymer with a distribution showing two sharp peaks (S51) was again produced. Adding initiator to monomer in tetrahydrofuran gave a broad distribution polymer (S52).

The data presented in this and earlier sections indicate that certain catalyst–solvent systems are more reactive than others when considered from the view point of metal complex formation and of polymerization

propagation. Systems promoting rapid propagation are the slowest to initiate and the most prone to "kill out" during polymerization. These facts are best explained in terms of ion pair separation.

If we use the same metal–hydrocarbon complex in different solvents, then that solvent which can coordinate with the sodium to the highest degree will cause the most rapid formation of complex when the complexing reagents are brought together. This strongly coordinated solvent produces a complex with a relatively great ion pair separation and the aromatic hydrocarbon anion is reluctant to release its electron to monomer during initiation. This may be visualized as follows:

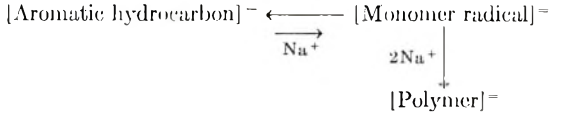

The aromatic hydrocarbon is presumed to have a much greater affinity for the electron than the monomer radical, but the equilibrium is driven in the direction of the monomer radical by the dimerization and subsequent polymerization of the monomer. In cases where the electron is tightly held by the aromatic hydrocarbon, initiation is slower and the rate of initiation compared to that of propagation is very slow. Under these conditions narrow distribution polymer cannot be produced because fresh chains are initiating throughout the polymerization.

The systems which are difficult to initiate and fast to propagate have a greater tendency to "kill out" during polymerization. This too can be interpreted in terms of ion pair separation. Normal alkyl sodium compounds cleave ethers readily even in the cold,[13] and a polymerizing chain may be thought of as an alkyl sodium compound in which the carbanion is moderated by an electron releasing group such as the phenyl group. Any solvent which promotes ion pair separation will also promote cleavage and other side reactions.

An interesting deduction concerning the base strengths of ethers may be drawn from this work. The indicated order of increasing basicity is dioxane < tetrahydrofuran < ethylene glycol dimethyl ether < diethylene glycol dimethyl ether.

Substituents on the carbanion other than phenyl will also alter the ion pair separation; thus the electron-releasing methyl group lessens the ion pair separation, and α-methylstyrene should be converted to monodisperse polymer under a far greater range of conditions than styrene. Ethylene polymerization, on the other hand, if it could be initiated, would probably "kill out" rapidly.

The alkali metal ion also helps determine the ion pair separation and it has been observed that lithium complex polymerization propagation (S61) is generally slower than sodium. Potassium has not been investigated but potassium systems might be expected to be faster than sodium.

E. Side Reactions

It seems probable that ether cleavage could occur during anionic polymerization, and experimental indications of such side reactions were observed in certain cases. It could not be directly determined, however, whether termination was caused by ether cleavage or by reaction with impurities. Ether cleavage should give rise to definite products which could be identified if present in significant quantities. The cleavage reaction is not a simple one, but often proceeds predominantly according to the equation:[13,14]

$$RNa + R'CH_2CH_2OCH_3 \rightarrow R'CH{=}CH_2 + NaOCH_3 + RH$$

In order to test for ether cleavage a sodium–α-methylstyrene–ethylene glycol dimethyl ether complex was prepared and stored under nitrogen at room temperature for about three weeks. This material is comparable to a polymerizing α-methylstyrene polymer in glycol ether solvent. After three weeks the active chains were "killed" with a little water and a portion of the solvent distilled off. An odor was noted coming from the distillate and a gas sample was taken. Analysis by mass spectrometry showed the gas to be almost entirely the expected methyl vinyl ether. The liquid distillate was also analyzed and was expected to contain traces of methanol. None was found, but in the presence of ethylene glycol dimethyl ether, traces of methanol would be difficult to identify. The presence of methyl vinyl ether in the reaction mixture is strong evidence for a cleavage reaction.

A second side reaction giving rise to broad molecular weight distribution polymers was encountered in polymerizations initiated by sodium–naphthalene in tetrahydrofuran. The difficulty was traced to the age of the initiator solutions used. In order to demonstrate the importance of age of initiator, two polymerizations using initiator solutions of approximately equal concentration were conducted. One initiator solution was twelve days old, having been stored under nitrogen at room temperature. The other was used the day it was prepared. The aged initiator gave a polymer shown by ultracentrifuge measurements (S58) to have a broad distribution and two peaks. The fresh initiator gave a narrow molecular weight distribution polymer (S6).

The mechanism of initiator solution deterioration is not known, but an interesting correlation with hydrogen evolution in water was observed. The fresh catalyst solution did not give off gas when dropped into water, but the same solution after standing overnight evolved gas when mixed with water. Portions of the solution were reacted with water each day for several days. The amount of gas evolved increased daily over a period of a week, showing a continuing deterioration of the initiator solution.

F. Effect of Additives

Some interesting effects were noted when polymerizations were carried out in the presence of extraneous materials. With sodium–naphthalene–tetrahydrofuran as initiator and redistilled toluene as solvent in the polymerization of styrene at 0°C., the typical red polymerization color endured

throughout the run. After "killing" with water and devolatilization of the polymer it was found to have an unexpectedly low 10% toluene viscosity of 1.62 cpoise; the molecular weight distribution determined by ultracentrifuge was broad (S57). Polymerizations carried out under similar conditions with tetrahydrofuran as a solvent have a 10% viscosity of about 5–7 cpoise and a narrow distribution. Since the polymer yield was 94% of theoretical, the unexpectedly low viscosity suggests that a transfer was occurring during polymerization.

A similar run made in redistilled benzene "killed out" to form a pale yellow solution before all of the monomer was added. The run was repeated with the use of thiophene-free benzene which was distilled from high boiling sodium complex, but again the run "killed out." The yield from the first benzene run was not taken; that from the second run was 24% of theoretical. Keeping in mind the fact that benzyl sodium is a red compound while pure phenyl sodium is a white solid, the results of the benzene runs can also be interpreted as resulting from chain transfer. The transfer to toluene apparently occurred at the methyl groups while that to benzene was to the rings. Benzyl sodium is red and a polymerization initiator, but phenyl sodium is colorless and, perhaps, due to reduced ion pair separation, does not initiate polymerization to any appreciable extent; thus the ultimate effect of transfer to benzene is to "kill" the chain. A run in cyclohexane was unsuccessful because the red polymer precipitated out as the styrene monomer was added.

Polymerizations in a rusty mild steel reaction vessel gave polystyrene of broad molecular weight distribution (S59), although active sites appeared to endure throughout the polymerizations. In a glass reactor, polymerizations in the presence of a few grams of Fe_3O_4 or Fe_2O_3 gave polymers with unexpectedly high molecular weights, indicating that the normal mechanism had not prevailed. When a few grams of hydrogen-reduced iron was present in a glass reactor, a narrow distribution polymer having a slight low molecular weight tail (S60) was produced.

References

1. Szwarc, M., M. Levy, and R. Milkovich, *J. Am. Chem. Soc.*, **78**, 2656 (1956).
2. Szwarc, M., *Nature*, **178**, 1168 (1956).
3. Waack, R., A. Rembaum, J. D. Coombes, and M. Szwarc, *J. Am. Chem. Soc.*, **79**, 2026 (1957).
4. Brown, W. B., and M. Szwarc, *Trans. Faraday Soc.*, **54**, 416 (1958).
5. McCormick, H. W., F. M. Brower, and L. Kin, *J. Polymer Sci.*, **39**, 87 (1959).
6. Rudd, J. F., *J. Polymer Sci.*, **44**, 459 (1960).
7. McCormick, H. W., *J. Polymer Sci.*, **25**, 488 (1957).
8. Zimmerman, R. L., The Dow Chemical Company, unpublished work.
9. Leggett, L. M., *Anal. Chem.*, **26**, 748 (1954).
10. McCormick, H. W., *J. Polymer Sci.*, **36**, 341 (1959).
11. Wenger, F., *Makromlo. Chem.*, **36**, 200 (1960).
12. Zimmerman, R. L., U. S. Pat. 2,985,594 (1961).
13. Letzinger, R. L., A. W. Schnizer, and E. Bobko, *J. Am. Chem. Soc.*, **73**, 5708 (1951).
14. Letzinger, R. L., and D. F. Pollart, *J. Am. Chem. Soc.*, **78**, 6080 (1956).

Résumé

On a effectué une étude de l'importance et des limites de la polymérisation anionique du styrène et des styrènes substitués dans des conditions où une réaction de terminaison de chaîn n'a pas lieu. Dans ces conditions, on a obtenu des homopolymères possédant une distribution très resserrée de leurs poids moléculaires. Les résultats fournis par ultracentrifugation confirment la formation de cette distribution serrée. Tous les réactifs utilisés ont été soigneusement purifiés et gardés ensuite à l'abri de l'air. La façon habituelle de procéder consiste à effectuer les polymérisations en ajoutant lentement une solution de monomère à la solution d'initiateur. On s'est proposé d'apporter des modifications à ce processus afin d'étudier différentes conditions de réaction. On a utilisé comme monomère: le styrène, l'α–methyl–styrène, le m– et le p–vinyltoluène, et comme solvant: le tétrahydrofuranne, le tétrahydropyranne, le 2–méthyltétrahydrofuranne, le dioxanne, l'éther diméthylique de l'éthylène-glycol et l'éther diméthylique du diéthylène-glycol. Les initiateurs étaient le sodium–naphtalène, le sodium–biphényl, le sodium α–méthyl–styrène, le sodium–phénanthrène et le lithium–naphtalène. Le choix des solvants a un grand effet sur l'allure de la polymérisation et la température à laquelle on peut produire des polymères à distribution resserrée. Les solvants qui provoquent une rapide initiation et une propagation relativement lente sont meilleurs et ceux qui font l'inverse ont tendance à donner des réactions latérales menant à une réaction de terminaison et à un polymère largement distribué. En ce qui concerne la rapidité d'initiation et la lenteur de propagation, ces solvants sont dans l'ordre suivant: dioxane > tétrahydrofuranne > éther diméthylique de l'éthylène glycol > éther diméthylique du diéthylène glycol. En solution dioxannique, on a préparé du polymère monodispersé dans diverses conditions. Dans l'éther diméthylique du diéthylène glycol, on ne peut préparer de polymère monodispersé même dans les conditions les plus favorables. Ces faits s'interprètent en termes de séparation de paire d'ions. On a examiné d'autres facteurs qui peuvent conduire à des polymères à large distribution des poids moléculaires. On a trouvé que l'âge de l'initiateur jouait un rôle important car les solutions plus anciennes d'initiateur fournissent des polymères largement distribués. Des solutions d'initiateur vieilli dégagent de l'hydrogène quand il y a possibilité de réaction avec l'eau, tandis que des solutions fraichement préparées d'initiateur ne dégagent pas d'hydrogène. En présence de toluène il y a transfert de chaîne vers le groupe méthylique et cela provoque une large distribution du polymère. Un transfert semblable au cycle du benzène donne lieu à une terminaison avant que la polymérisation ne soit complète. Du fer rouillé, Fe_2O_3 et Fe_3O_4 affectent défavorablement l'allure de la polymérisation et fournissent des polymères largement distribués. La réduction du fer par l'hydrogène dans le mélange réactionnel cause seulement un écart minime à la distribution serrée des poids moléculaires.

Zusammenfassung

Eine Untersuchung des Umfanges und der Begrenzungen der anionischen Polymerisation von Styrol und substituierten Styrolen bei fehlendem Kettenabbruch wurde durchgeführt. Unter diesen Bedingungen wurden Polymere mit sehr enger Molekulargewichtsverteilung erhalten. Ultrazentrifugenergebnisse beweisen die Bildung enger Verteilungen. Alle verwendeten Reagenzien wurden sorgfältig gereinigt und ohne Berührung mit der Atmosphäre verwendet. Das Standardverfahren bestand in der Durchführung der Polymerisation durch langsamen Zusatz der Monomerlösung zur Starterlösung. Zur Untersuchung verschiedener Reaktionsbedingungen wurde dieses Verfahren variiert. Als Monomere wurden Styrol, α–Methylstyrol sowie m– und p–Vinyltoluol verwendet, als Lösungsmittel Tetrahydrofuran, Tetrahydropyran, 2–Methyltetrahydrofuran, Dioxan, Äthylenglykoldimethyläther und Diäthylenglykoldimethyläther. Die verwendeten Starter waren Naphthalinnatrium, Biphenylnatrium, α–Methylstyrolnatrium, Phenanthrennatrium und Naphthalinlithium. Die Wahl des Lösungsmittels hatte einen grossen Einfluss auf den Verlauf der Polymerisation und auf die Temperatur, bei welcher es zur Bildung von Polymeren mit enger Verteilung kommt. Lösungsmittel, die einen raschen

Start und eine verhältnismässig langsames Wachstum begünstigten, waren am besten geeignet, im umgekehrten Falle traten Nebenreaktionen auf, die zur Abbruch und einem Polymeren mit breiter Verteilung führten. Die Reihenfolge für die Bewirkung von raschem Start und langsamen Wachstum ist bei den genannten Lösungsmitteln die folgende: Dioxan > Tetrahydrofuran > Äthylenglykoldimethyläther > Diäthylenglykoldimethyläther. In Dioxanlösung wurde in einem weiten Bereich an Versuchsbedingungen monodisperses Polymeres hergestellt. In Diäthylenglykoldimethyläther konnte auch unter den günstigsten Bedingungen kein monodisperses Polymeres erhalten werden. Dieses Verhalten wurde als Effekt der Ionenpaartrennung gedeutet. Auch andere Faktoren, die für die Bildung von Polymeren mit breiter Verteilung verantwortlich sind, wurden untersucht. Das Alter des Starters erwies sich als sehr wichtig, wobei ältere Starterlösungen Polymere mit breiter Verteilung lieferten. Gealterte Starterlösungen entwickelten bei der Reaktion mit Wasser Wasserstoff; frisch bereitete Starterlösungen entwickelten keinen Wasserstoff. In Gegenwart von Toluol fand Kettenübertragung zur Methylgruppe statt, was zur Bildung eines Polymeren mit breiter Verteilung führte. Eine ähnliche Übertragung mit Benzol am Ring ergab Abbruch bevor die Polymerisation vollständig war. Rostiges Eisen, Fe_2O_3 und Fe_3O_4 hatten einen ungünstigen Einfluss und lieferten Polymere mit breiter Verteilung. Wasserstoff-reduziertes Eisen im Reaktions gemisch ergab nur eine geringfügige Abweichung von der engen Verteilung.

Received April 9, 1962

JOURNAL OF POLYMER SCIENCE: PART A VOL. 1, PP. 1765–1778 (1963)

Anisotropic Properties of Strained Viscoelastic Fluids. III. Birefringence of Polystyrene Solutions

ROBERT TOGGENBURGER* and STANLEY J. GILL, *Department of Chemistry, University of Colorado, Boulder, Colorado*

Synopsis

Birefringence relaxation has been studied in concentrated polystyrene solutions. The birefringent state is induced by a sudden application of strains and the subsequent relaxation effect is observed by photoelectric monitoring. The effect of temperature concentration on the decay of induced birefringence follows the general patterns observed for stress relaxation. Samples of different molecular weights and different molecular weight distributions have been studied. A particularly simple empirical result was found to express the relaxation behavior of highly fractionated materials. In such instances the birefringence decays with exponential dependence upon the square root of time. The results for samples with broad distributions show curvature when plotted in a similar fashion. This simple relaxation behavior has a simple LaPlace transform, so that a comparison of the exact relaxation distribution function with approximate methods can be made. The general behavior of birefringence relaxation distribution functions is similar to that noted for stress relaxation functions. The method of reduced variables likewise is applicable to bring the birefringence relaxation results into correspondence at different temperatures.

I. INTRODUCTION

The viscoelastic properties of moderately concentrated polymer solutions are complicated by the diversity of molecular contacts and interactions.[1a] Nevertheless, the study of such materials provides an important bridge between the dilute and solid state of polymers. A number of such studies are reviewed by Ferry.[1b] For the most part, these studies have relied upon oscillatory measurements of stress and strain over a range of frequencies. The relaxation spectrum is then derived by approximate techniques from such measurements.[1c]

In a previous paper a technique was described for studying the relaxation of a suddenly induced anisotropic state by the measurement of the associated birefringence.[2] According to theories of rubber elasticity the induced birefringence of long chain networks should be proportional to the stress.[3] This has also been confirmed for several fluid materials.[4,5] The measurement of birefringence relaxation should then provide a parallel to

* Present address: Research Laboratories, Plastic Division, Monsanto Chemical Company, Springfield, Mass.

stress relaxation following a sudden deformation. Neither the birefringence relaxation nor the stress relaxation for rapidly relaxing materials has previously been measured. Some practical advantages may result from a simple relaxation measurement since the general formulation of the measured relaxation is a Laplace integral.

There are presently several theoretical interpretations of the viscoelastic behavior of random coil polymers contained in a medium where the frictional forces can be approximated by macroscopic constants.[6-10] These theories are reasonable for the dilute or solid state where the environment of relaxing segments is approximately uniform but there may be complications where significant molecular interaction is due both to solvent and polymer. These difficulties, or lack of them, might be further revealed by birefringence relaxation experiments on materials of narrow molecular weight distributions.

In this initial study we have been concerned with the relaxation properties of concentrated polystyrene solutions. The principal parameter under investigation has been the effect of molecular weight distribution.

II. EXPERIMENTAL METHODS

A. Apparatus

The strain-birefringence apparatus and method was similar to that described before.[2]

In this method an isotropic viscoelastic medium is suddenly strained through a sudden distortion of the outer confines of the medium. The internal structure of the solution is then no longer random, and the solution becomes birefringent. A suitable optical apparatus measures the induced birefringence and its subsequent decay.

The apparatus consisted of a filtered light source (546 mμ), a light-collimating system, a polarizing Nicol prism, a straining cell, a crossed analyzing Nicol prism, and photomultiplier tube arranged on an optical bench. The quarter wave plate utilized in the previous apparatus was not needed to measure the intensity of the transmitted light and hence it was omitted. When the solution was strained and made birefringent, the resulting elliptically polarized light was transmitted through the analyzing prism and its intensity was read by a photomultiplier tube. This signal was displayed on an oscilloscope and the trace photographed. The induced retardation δ (proportional to the birefringence) was calculated by means of the relation $I/I_0 = \sin^2(\delta/2)$ where I is the intensity of the transmitted light. The proportionality constant I_0 is determined by uncrossing the Nicols to a known angle β. The optical calibration of the apparatus was checked periodically by measuring the ratio I_β/I_0 for different settings β. Alignment was always maintained so that I_β/I_0 was within 1.5% of $\sin^2\beta$.

The temperature of straining cell was held constant to ± 0.05°C. by enclosing the cell in a compartment through which was circulated water

from a thermostatted bath. The dimensions of the straining ellipse were $a = 0.52$ cm., $b = 0.45$ cm., and $l = 9.2$ cm., where $2a$, $2b$, and l are the major axis, the minor axis, and the effective length, respectively. The internal Teflon tube had a double wall thickness of 0.14 cm.

Each relaxation curve is a combination of two relaxation photographs. One photograph recorded the short time portion of the relaxation spectrum and the other measurement recorded the long time portion. This was effected by suitable selections of the signal amplification and of the oscilloscope time sweep. Combination of these two traces resulted in a more complete relaxation curve than if it had been based upon a single measurement.

B. Materials

Polystyrene was prepared from Eastman Kodak purified grade styrene monomer by the method of Outer, Carr, and Zimm.[6] The inhibitor, *tert*-butyl pyrocatechol, was removed by several washings with an aqueous sodium hydroxide solution followed by vacuum distillation at less than 30°C. The monomer was polymerized in a sealed tube with 0.05% Eastman Kodak reagent grade benzoyl peroxide at 60°C. for four days. This sample was labeled P-0.

Seven fractions (P-1 to P-7) were obtained by a fractional precipitation of a portion of polystyrene P-0 by means of a 2-butanone solvent–methanol precipitant system.[11] These samples were dried at 25°C. and 10 mm. Hg for 48 hr. and then weighed.

The fractionated polystyrene (samples P-1 to P-7) and the unfractionated polystyrene (sample P-0) were characterized by viscometry.[12] A differential molecular weight distribution curve for sample P-0 was constructed by use of the viscosity molecular weight data for fractions P-1 to P-7.[13] The differential molecular weight distribution for P-0 is broad and conforms approximately to a most probably type.[13]

Relaxation studies were performed on Szwarc type polystyrene (S-1159). This polystyrene sample was graciously supplied by H. M. McCormick of

TABLE I
Molecular Weights of Polystyrene Samples

Polymer sample	M.W. $\times 10^{-6}$	M.W. distribution
Polystyrene P-0	$M_v = 0.88$	Most probable
Polystyrene P-2	$M_v = 1.4$	Fractionated from
Polystyrene P-3	$M_v = 1.15$	P-0
Polystyrene P-4	$M_v = 0.78$	
Polystyrene S-1159	$M_v = 0.54$[a]	$M_w/M_n = 1.08$[b]
	$M_n = 0.53$[b]	
	$M_w = 0.57$[b]	
	$M_z = 0.495$[b]	

[a] Data of Coure et al.[15]
[b] Data of McCormick.[16]

the Dow Chemical Company. The weight-average and number-average molecular weights as determined by McCormick were 570,000 and 530,000 respectively.[14] As the ratio of the weight-average molecular weight to the number-average molecular weight is near one, the molecular weight distribution is narrow.

Table I lists the molecular weights of the unfractionated and fractionated polystyrenes and of the Szwarc type polystyrene.

C. Procedures

Care was taken to make the solutions used in the straining cell optically clear. Dust was removed by pressure filtration through a medium sintered glass frit. Air bubbles had to be removed from solution in the cell before an examination of the material could be made.

Relaxation measurements were made on two polymer-solvent systems. Polystyrene samples P-0, P-2, P-3, and P-4 were dissolved in thiophene-free reagent grade benzene. The Szwarc type polymer, however, was dissolved in reagent grade 1,4-dioxane, as concentrated solutions in benzene were not optically clear. A sample of P-0 was run in 1,4-dioxane as well as in benzene in order to compare solvent effects.

Table II lists the various experimental conditions under which relaxation studies were conducted. Note that for practical reasons in preparing the solutions the concentrations were expressed as grams of solute per cubic centimeter of solvent and multiplied by one hundred.

TABLE II
Summary of Experimental Conditions

Polymer–solvent system	Concentration, g. polymer/cc. solvent × 100	Temperature, °C.
Polystyrene P-0 in benzene	14	25
Polystyrene P-0 in benzene	16	0, 10, 15, 25, 35
Polystyrene P-0 in benzene	25	0, 25, 35
Polystyrene P-0 in 1,4-dioxane	14	25
Polystyrene P-2 in benzene	12	25
Polystyrene P-3 in benzene	14	10, 15, 25, 35
Polystyrene P-3 in benzene	16	15, 25, 35
Polystyrene P-4 in benzene	14	10
Polystyrene S-1159 in 1,4-dioxane	20	10, 15, 20, 25
Polystyrene S-1159 in 1,4-dioxane	25	10, 15, 20, 25, 35

III. EXPERIMENTAL RESULTS

A. Effect of Temperature on Birefringence Relaxation

In order to extend the relaxation data over as broad a time range as possible, data were taken over a range of temperatures for a particular solution and then reduced into a single reduced relaxation curve.[1d] The

reduced retardation is given by $\delta T_r/T$. A reference temperature of 25°C. was arbitrarily selected. Figure 1 shows a graph of δ_r, versus log (at) for a 25% polystyrene solution in a range of temperatures of 10–35°C.

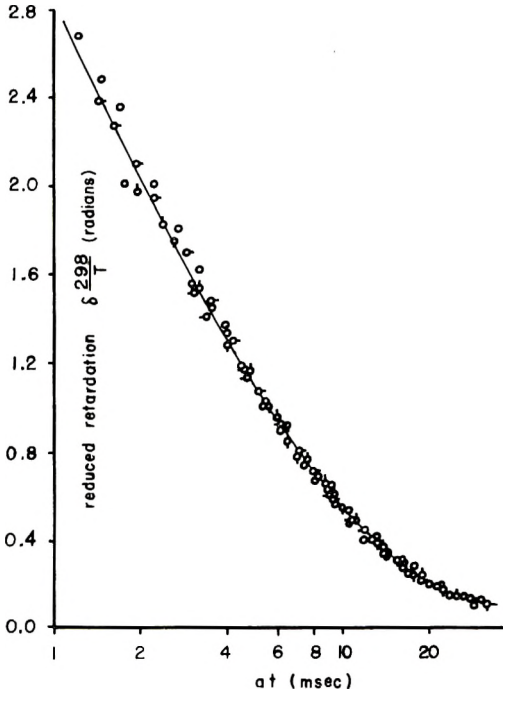

Fig. 1. Temperature-dependent relaxation data reduced to 25°C. for 25% polystyrene S-1159 in 1,4-dioxane: (O) 10°C.; (O-) 15°C.; (O) 20°C.; (O) 25°C.; (-O) 35°C.

B. Form of the Relaxation Function

Since the long-time portion of the relaxation spectrum of viscous solution is emphasized in the method of measurement, the relaxation process might be dominated by a single relaxation mode. If this were the case, one would predict retardation δ to be exponentially dependent on the time. Plots of log δ versus time for the concentrated polystyrene solutions resulted in curved relaxation functions which indicated contributions of several relaxation modes to the relaxation distribution function. As an example of this behavior, a graph of log δ against the time is shown in Figure 2 for a 25% Szwarc polystyrene solution at 25°C.

The shapes of the relaxation functions, however, suggested that a plot of log retardation against some root of time may result in linearity. Empirically, it was found that when the logarithm of the retardation or the normalized retardation was plotted against the square root of time a linear decay curve resulted for the Szwarc polystyrene in 1,4-dioxane (see Fig. 2) and for the fractionated polystyrene samples in benzene (see

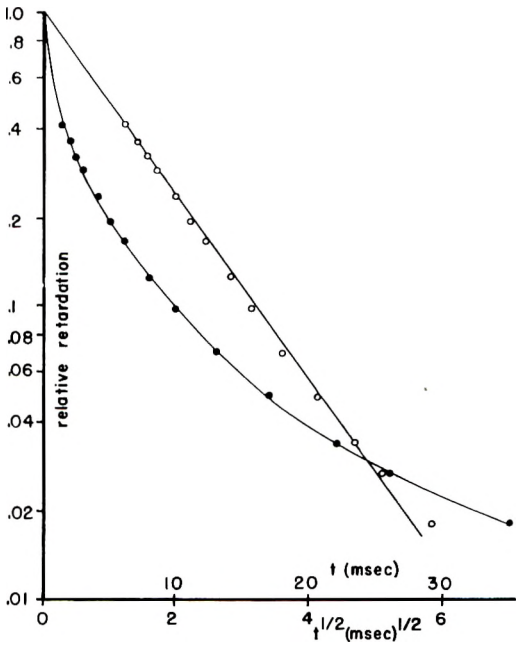

Fig. 2. Log of the relative retardation for 25% S-1159 in 1,4-dioxane plotted against (O) t and (●) against $t^{1/2}$. Reduced temperature data (25°C) used.

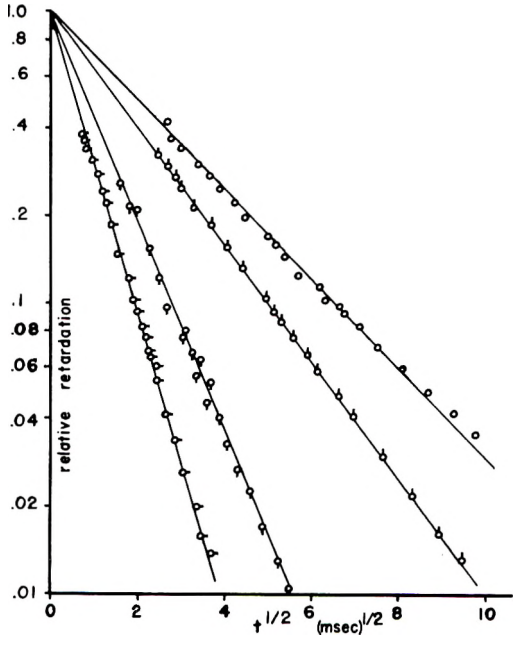

Fig. 3. Log of the relative retardation vs. $t^{1/2}$ for narrow molecular weight distribution polystyrene samples with various molecular weights: (O) 12% P-2; (O) 16% P-3; (O) 14% P-4; (O-) 20% S-1159.

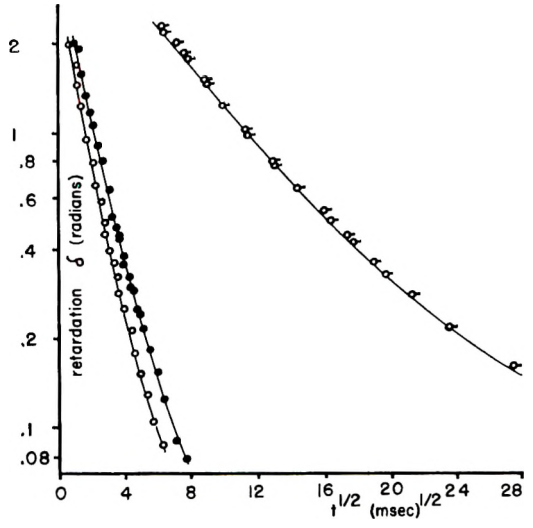

Fig. 4. Log of the retardation vs. $t^{1/2}$ for various concentrations in benzene of broad molecular weight polystyrene sample P-0 at 25°C.: (O-) 25%; (●) 16%; (O) 14%.

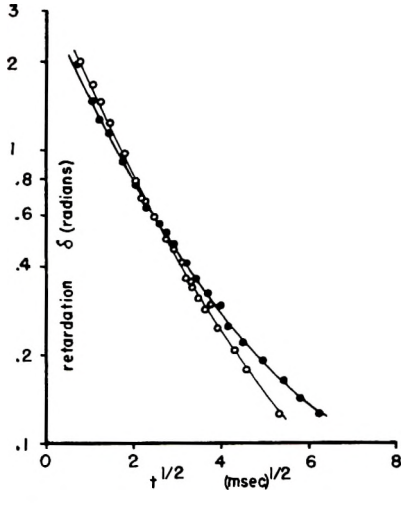

Fig. 5. Log of the retardation vs. $t^{1/2}$ 14% polystyrene sample P-0 (O) in benzene and (●) in 1,4-dioxane at 25°C.

Fig. 3). In most of these cases linearity persisted over the entire range of the relaxation measurements.

The relaxation curves for unfractionated polystyrene solutions deviated from the linear relation log δ versus $t^{1/2}$ (Fig. 4). The observed curvature is attributed to the broad molecular weight distribution.

In order to determine the effect of solvent difference between the Szwarc polystyrene samples and the other polystyrene samples, a comparison of relaxation data of 14% solutions for the unfractionated polystyrene

sample in benzene and 1,4-dioxane was made. These data, plotted in Figure 5, indicate that the general character of the relaxation function is uneffected by the solvent difference. This behavior is supported by intrinsic viscosity measurements made on polystyrene sample P-0, the intrinsic viscosity being about 10% greater in benzene than 1,4-dioxane. Dimensional changes due to solvent are therefore small, and thus it seems unlikely that changes in the parameters controlling the relaxation process are significantly altered.

Variations in temperature from 10 to 35°C., in concentration from 14% to 25%, and in molecular weight from 5000,000 to 1,400,000 did not perceptably alter the linear form noted above for the relaxation behavior of narrowly distributed samples.

C. Distribution Function

The linear dependence between the log of δ and $t^{1/2}$ may be expressed by the equation:

$$\delta = \delta_0 e^{-2.38 t^{1/2}} \tag{1}$$

where δ_0 is the intercept and s is the slope of the log δ versus $t^{1/2}$ curve. We shall find it convenient to use a relative retardation defined by $\delta' = \delta/\delta_0$ for cases where relation (1) is found to hold.

One use of this empirical relation is that it enables us to compare various approximation procedures with an exact Laplace transform in finding the distribution of relaxation times or distribution function. The comparison relies first of all upon assuming that this exponential dependence on the square root of time holds over all ranges of time, although it has been confirmed experimentally only over a limited time scale.

Two approximation methods often used for deriving distribution functions of relaxation have been developed by Ferry and Williams[17] and by Andrews.[18] We shall use these to evaluate an approximate distribution function for this type of exponential decay with $t^{1/2}$.

The general form[19] of decay of relative retardation can be presented by

$$\delta' = \int H(\ln \tau) e^{-t/\tau} \, d\ln \tau \tag{2}$$

where H ($\ln \tau$) is the normalized distribution function in terms of the natural logarithm of the distribution of relaxation times.

In terms of relaxation rates, γ, where we define a distribution function of rates

$$\varphi(\gamma) = H(\ln \tau)/\gamma \tag{3}$$

and

$$\gamma = 1/\tau$$

and

$$\delta' = \int_0^\infty \varphi(\gamma) e^{-t\gamma} \, d\gamma \tag{4}$$

We can evaluate this for $\delta' = e^{-2.38 t^{1/2}}$ by approximate techniques or exactly by use of the Laplace transform.

a. Andrews Approximation.[18] This approximation is given by

$$H(\ln \tau) = -(d\delta'/d\ln \tau) + (0.251 \times 2.3)\ [d^2\delta'/d(\ln \tau)^2] \tag{5}$$

For the case under consideration we find

$$H(\ln \tau) = (2.3/2)\, s\sqrt{\tau}\, e^{-2.3s\sqrt{\tau}} + (0.251 \times 2.3/4)s\sqrt{\tau}(1 - 2.3s\sqrt{\tau}]e^{-2.3s\sqrt{\tau}} \tag{6}$$

b. Ferry and Williams Approximation.[17] We have

$$H(\ln \tau) = -M(m)\delta'(d \log \delta'/d \log t)_{t=\tau} \tag{7}$$

where

$$M(m) = 1/\Gamma(m + 1) \tag{8}$$

and

$$m = -(d \log \delta'/d \log t) = -d \ln \delta'/d \ln t \tag{9}$$

For our empirical decay relation, then,

$$m = -(2.3/2)s\sqrt{\tau} \tag{10}$$

$$H(\ln \tau) = M(m)\ (2.3/2)s\sqrt{\tau}\, e^{-2.3s\sqrt{\tau}} \tag{11}$$

c. Laplace Transform. Here we have

$$\delta' = e^{-2.3s\sqrt{t}} = \int_0^\infty \varphi(\gamma)e^{-t\gamma} \tag{12}$$

The solution of $\varphi(\gamma)$ for this expression has been tabulated by Erdelyi[20] and is given by

$$\varphi(\gamma) = -(2.3/2)\sqrt{\pi}\gamma^{-3/2}s\, e^{-(2.3s)^2/(4\gamma)} \tag{13}$$

or

$$\mathrm{H}(\ln \tau) = -(2.3/2)\sqrt{\pi}s\sqrt{\tau}\, e^{-(2\cdot 3s)^2\tau/4} \tag{14}$$

Since the form of the approximate expressions for $H(\ln \tau)$ for this special case does not appear to conform to that of the exact expression one might suspect some difference to arise in actual computation.

A graph of the three methods of calculating the relaxation distribution function as applies to the 25% Szware polystyrene in 1,4-dioxane at 25°C. is shown in Figure 6.

The Ferry-Williams approximation method corresponds most closely to the exact form at long relaxation times. Both the Ferry-Williams and Andrews approximations have a low distribution maximum than given by the Laplace transform. The Ferry-Williams approximation appears to be the most valid of these two approximate methods.

The effect of temperature on the distribution function $H(\ln \tau)$ as calculated by the exact expressions for the same material is shown in Figure 7.

The displacement of the relaxation distributions to higher times at lower temperatures follows the general findings of viscoelastic behavior. The

distribution can be superimposed by suitable translation with respect to log T. This conforms to general observation in the use of reduced variables.

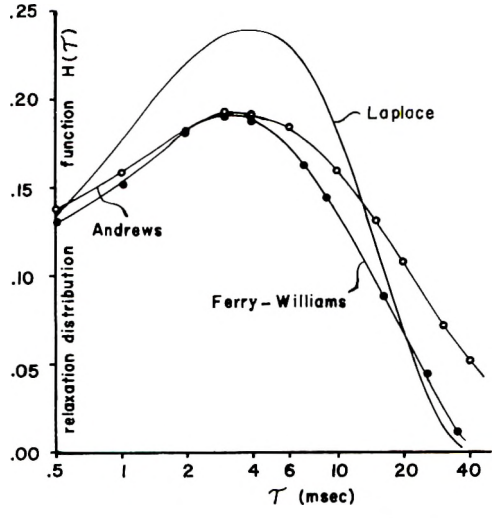

Fig. 6. Relaxation distribution functions vs. log t for 25% S-1159 in 1,4-dioxane at 25°C. as obtained by Ferry-Williams and Andrews approximation methods and by Laplace transform.

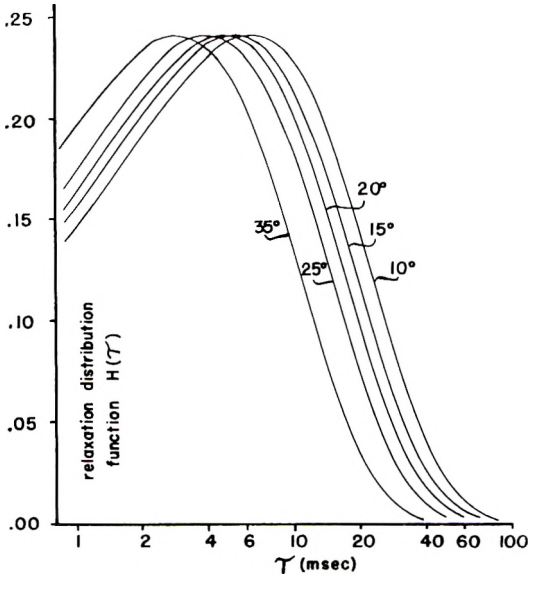

Fig. 7. Relaxation distribution functions vs. log t as obtained by Laplace transform for 25% S-1159 in 1,4-dioxane at various temperatures.

IV. DISCUSSION

One feature of the log δ versus $t^{1/2}$ plot is that it tends to point out the difference in the stress decay between the most probable and the narrower molecular distribution polystyrene samples. Although this difference is not as large as might be expected, it is definite.

In principle one might use the observed curvature to estimate the distribution of molecular weights. However, such a procedure at present would be strictly empirical without a theory which would indicate how the various molecular weights contribute to the observed relaxation behavior. We shall therefore draw only some qualitative conclusions.

In order to explain the relatively small effect molecular weight distribution has on these solution concentrations, one is compelled to say that the effect of molecular weight distribution is almost overwhelmed by multiple interactions in the concentrated solution.

The nature of such interactions in concentrated solutions is not well understood. There is no theory of stress relaxation which would explicitly indicate the simple relation of the exponential decay with $t^{1/2}$ for homogeneous materials.

The effect of concentration would be one of increasing the density of interactions and retarding the relaxation process. The relaxation curves for difference concentrations (of unfractionated material) can not be simply superimposed by simple translation for the solutions we have studied. This lack of superposition may be due to several factors including changes of interaction point density and mobilities of the chain segments.

Ferry[21] has established by mechanical experiments the general shape of the relaxation distribution function for concentrated polystyrene solutions over a broad range of time. A typical transition plateau–terminal zone pattern is evident. The measurements made in this investigation emphasize the terminal portion up to the plateau region of the relaxation

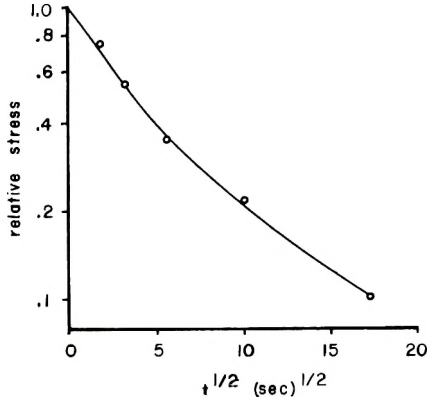

Fig. 8. Log relative retardation plotted against $t^{1/2}$ for 16.5% polyisobutylene in decalin at 25°C. (data of Schremp, Ferry and Evans[22]).

distribution function. Our experiment cannot give the shorter time behavior.

In order to investigate the possible generality of the exponential dependency of the stress on $t^{1/2}$, the stress relaxation data of a 16.5% polyisobutylene solution of Schremp, Ferry, and Evans[22] was plotted in this manner. The polyisobutylene was unfractionated with a molecular weight of 2.5×10^6. The plot for this solution is shown in Figure 8. The shape of the relaxation curve is very similar to our curves on the unfractionated polystyrene and points out the possible generality of the exponential $t^{1/2}$ dependency of the stress to concentrated solutions of other polymeric systems.

The Rouse theory predicts for dilute solution that when the number of relaxation modes is large, the relaxation distribution function is dependent upon $\tau^{-1/2}$. If we assume this applied to concentrated solution, as examination of the log plot of the distribution function against the log of δ for the monodisperse polystyrene system shows a slope much steeper than $-1/2$ dominates the distribution function. This behavior suggests that only a small number of relaxation modes are controlling the relaxation process in this time region. A more complete numerical examination of the molecular theory of relaxation is needed to see if one can find a better correlation between existing theory and experiment.

The results obtained in this work on relaxation of induced birefringence conform to the general behavior of stress relaxation. Similar application of reduced variables illustrates the superimposition of relaxation curves of retardation at various temperatures. Distribution functions have been derived for the relaxation spectrum which follow general stress relaxation behavior. The observed exponential dependence of the retardation upon the square root of time is a significant feature found with the fractionated materials investigated. This relation allows one to extrapolate with some certainty to a condition of instantaneous strain to evaluate the retardation under such conditions.

This work was supported by the Directorate of Chemical Sciences of the Air Force Office of Scientific Research. We are indebted to Dr. McCormick of the Dow Chemical Company for providing samples of Szware polystyrene.

References

1. (a) Ferry, J. D., *Viscoelastic Properties of Polymers*, Wiley, New York, 1961, Chap. 10, p. 161; (b) *ibid.*, Chap. 16; (c) *ibid.*, Chap 4.; (d) *ibid.*, Chap. 11.

2. Gill, S. J., *J. Appl. Polymer Sci.*, **1**, 17 (1959).

3. Treloar, L. R. G., *Physics of Rubber Elasticity*, 2nd Ed., Clarendon Press, Oxford, 1958.

4. Brodnyan, J. G., F. H. Gaskins, and W. Philippoff, *Trans. Soc. Rheol.*, **1**, 109 (1957).

5. Philippoff, W., *Trans. Soc. Rheol.*, **4**, 159 (1960).

6. Outer, P., C. I. Carr, and B. H. Zimm., *J. Chem. Phys.*, **18**, 830 (1950).

7. Rouse, P. E., Jr., *J. Chem. Phys.*, **21**, 1272 (1953).

8. Bueche, F., *J. Chem. Phys.*, **22**, 603 (1954).
9. Zimm, B. H., *J. Chem. Phys.*, **24**, 269 (1956).
10. Mooney, M., *J. Polymer Sci.*, **34**, 599 (1959).
11. Merz, E. H., and R. W. Raetz, *J. Polymer Sci.*, **5**, 587 (1950).
12. Krigbaum, W. R., and P. J. Flory, *J. Polymer Sci.*, **11**, 37 (1953).
13. Flory, P. J., *Principles of Polymer Chemistry*, Cornell Univ. Press, Ithaca, N. Y., 1953.
14. McCormick, H. M., *J. Polymer Sci.*, **36**, 341 (1959).
15. Coure, R. M. G., D. J. Warsfeld, and S. Bywater, *Trans. Faraday Soc.*, **57**, 705 (1961).
16. McCormick, H. M., private communication.
17. Ferry, J. D., and H. L. Williams, *J. Colloid Sci.*, **7**, 347 (1952).
18. Andrews, R. D., *Ind. Eng. Chem.*, **44**, 707 (1952).
19. Gross, B., *Mathematical Structure of the Theories of Viscoelasticity*, Herman, Paris, 1953.
20. Erdelyi, A., Ed., *Tables of Integral Transforms*, Vol. 1, McGraw-Hill, New York, 1954.
21. Ferry, J. D., E. R. Fitzgerald, H. F. Johnson, and L. D. Grandine, *J. Appl. Phys.*, **22**, 716 (1951).
22. Schremp, F. W., J. D. Ferry, and W. W. Evans, *J. Appl. Phys.*, **22**, 711 (1951).

Résumé

On a étudié la rélaxation de la biréfringence de solutions concentrées de polystyrène. L'état biréfringent est provoqué par l'application brusque d'une tension et l'effet de rélaxation qui s'en suit est observé par signal photoélectrique. L'effet de la température locale sur la chute de la biréfringence induite suit l'allure généralement observé pour la rélaxation de tension. On a étudié des échantillons de poids moléculaires différents et des distributions différentes de poids moléculaires. Un résultat empirique particuliérement simple a été trouvé pour exprimer le comportement rélaxationnel de produits fractionnés à des trés élevés. Dans de tels cas la biréfringence décroit d'une manière exponentielle par rapport à la racine carrée du temps. Les résultats pour les échantillons avec de larges distributions montrent en diagramme uue inflexion. Ce comportement de rélaxation a un simple transformateur Laplacien, de telle sorte qu'une comparaison de la distribution de la fonction de rélaxation au moyen de méthodes approximatives peut être faite. Le comportement général des fonctions de distribution de la rélaxation de la biréfringence est semblable à celle notée pour les fonctions de rélaxation de tension. Par analogie, la méthode des variables réduites est applicable aux résultats de rélaxation de biréfringence à différentes températures.

Zusammenfassung

Die Doppelbrechungsrelaxation in konzentrierten Polystyrollösungen wurde untersucht. Die Doppelbrechung wird durch plötzliche Verformung hervorgerufen und der darauffolgende Relaxationseffekt photoektrisch beobachtet. Der Einfluss von Temperatur und Konzentration auf den Avfall der induzierten Doppelbrechung entspricht dem allgemeinen, bei der Spannungsrelaxation beobachteten Verhalten. Proben mit verschiedenem Molekulargewicht und verschiedener Molekulargewichtsverteilung wurden untersucht. Ein besonders einfaches empirisches Ergebnis konnte für das Relaxationsverhalten von gut fraktionierten Substanzen erhalten werden. In diesem Fall fällt die Doppelbrechung exponentiell mit der Wurzel aus der Dauer ab. Die Ergebnisse an Proben mit brieter Verteilung zeigen bei einer solchen Auftragung eine Krümmung. Dieses einfache Relaxtionsverhalten liefert eine einfache Laplace-Transformation und

ermöglicht den Vergleich der exakten Relaxationsverteilungsfunktion mit Näherungsmethoden. Das allgemeine Verhalten der Doppelbrechungsrelaxations-Verteilungsfunktionen ist dem bei den Spannungsrelaxationsfunktionen angetroffenen ähnlich. Die Methode der reduzierten Variablen kann in gleicher Weise zum Vergleich der bei verschiedenen Temperaturen erhaltenen Doppelbrechungsrelaxationsdaten angewendet werden.

Received March 19, 1962

JOURNAL OF POLYMER SCIENCE: PART A VOL. 1, PP. 1779–1787 (1963)

Theoretical Calculations of Stress Relaxation in Concentrated Solutions

R. TOGGENBURGER,* K. BECK, and S. J. GILL, *Department of Chemistry, University of Colorado, Boulder, Colorado*

Synopsis

The Mooney theory for stress relaxation of polymer materials has been numerically evaluated in unmodified and modified forms. The modified expressions include such effects as molecular weight distributions and entanglement or polymer interaction distributions. The relaxation behavior was found to be highly dependent upon the number of interaction points per chain molecule particularly for small numbers. The distributions in molecular sizes and in the number of interaction points have a much smaller effect on the shapes of the relaxation curves. A comparison of the theoretical stress relaxation behavior is made with birefringence relaxation data. The region of correlation indicates a number of five interaction points per molecule of polystyrene at 10 wt. % in benzene.

Introduction

The relaxation properties of concentrated polystyrene solutions have been reported for different molecular weight values and distributions.[1] These measurements were obtained by following the decay of a suddenly induced birefringence. In the case of fractionated materials, the relaxation followed a particularly simple form, an exponential decay depending upon the square root of time. In order to explore some of the theoretical implications of this result, the molecular theory of Mooney[2] for viscoelastic properties of concentrated materials was numerically evaluated for different molecular size distributions and for a Poisson distribution of network junction points.

The applicability of present molecular theories of polymer relaxation to concentrated solutions is somewhat uncertain. However, the general validity of molecular theories of Rouse[3] and Zimm[4] to dilute solution properties of polymers is confirmed by numerous experiments,[5] with a preference towards the theory by Zimm.[6] For highly concentrated polymer solutions or melts, Bueche[7] has also proposed a simplified molecular approach. Mooney[2] has extended the basic technique of Rouse to concentrated materials under conditions of large deformations.

The primary problem in going from dilute solution to highly concentrated solution behavior of a polymer appears to lie in the change in the frictional

* Present address: Research Laboratories, Plastic Division, Monsanto Chemical Company, Springfield, Mass.

coefficients affecting the relaxation process. In either dilute or very concentrated polymer liquids, the frictional coefficient can be assumed to depend upon the bulk properties of the solvent or melt, but in the intermediate case, with few entanglements and with large solvent regions, the frictional coefficient depends upon whether the immediate surroundings of the relaxing segment is primarily solvent or an entanglement. The Mooney theory is suitable to account for some of these effects by a parameter which indicates the number of network junction points within the system. Strictly, the Mooney theory is suitable for stress time effects, but in view of the close relation between stress and birefringence,[8,9] it would seem that the theoretical results could be used as a first step in the molecular interpretation of the birefringence measurements.[1]

Theoretical

Mooney described the relaxation of stress $\Delta\sigma$, which arises from instantaneous elongations α_x, α_y in the x, y directions, by

$$\Delta\sigma = \sigma_x - \sigma_y = NkT(\alpha_x^2 - \alpha_y^2)_3 \sum_{i=1}^{\nu} \exp\left\{-\frac{3kT\mu}{2\nu_s l^2} t \sin^2\left[\frac{i\pi}{2(\nu + 1)}\right]\right\} \tag{1}$$

where there are N chains per unit volume, characterized by ν submolecules, each of which has ν_s freely jointed links of link length l. We shall consider the submolecules defined by entanglement joints. A mobility factor μ can be considered to express the motion of each network junction and is considered as constant under fixed conditions. The thermal energy is determined by Boltzmann's constant k and the temperature T. The summation is taken over the various normal modes of relaxation with the integer values of i running from 1 to ν. The time from the instant of strain is signified by t. At time $t = 0$ the stress is determined by the product of the thermal energy, the difference of the squares of the elongations, and $N\nu$, the number of submolecules per unit volume. This is the same result as one has from rubber elasticity.[8]

For computational purposes it is convenient to write a relative stress $\Delta\sigma_r$, which is referred to the instantaneous stress $\Delta\sigma_0$. The number of freely jointed links per chain ($\nu\nu_s$) is determined by dividing the number of monomers per chain n by the number of monomers ξ per free link. With these terms eq. (1) may be written as:

$$\Delta\sigma_r = \frac{\Delta\sigma}{\Delta\sigma_0} = \frac{1}{\nu} \sum_{i=1}^{\nu} \exp\left\{-\nu\tau \sin^2\left[\frac{i\pi}{2(\nu + 1)}\right]\right\} \tag{2}$$

where τ is defined by:

$$\tau = (3kT\xi/2l^2n)t = t_r/n$$

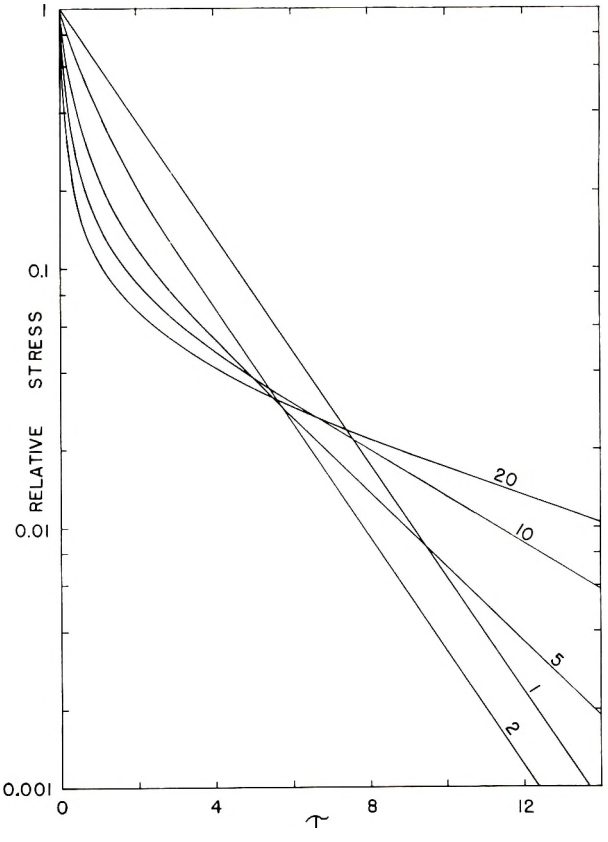

Fig. 1. Logarithm of relative stress vs. the relaxation time factor τ for different numbers of interaction points per molecule.

The relaxation curves for given values of ν versus the dimensionless factor τ are shown in Figures 1 and 2. (The computations were run on a Control Data Corporation 1604 digital computer at the National Bureau of Standards Laboratory, Boulder, Colorado. The sine squared functions and exponentials were approximated to better than six significant figures.)

Distribution of Molecular Sizes

The influence of a distribution of molecular sizes on the relaxation properties is given by weighting the relative stress values in proportion to the fraction of appropriate molecular species and summing over all sizes:

$$\Delta\sigma_r = \frac{1}{\Delta\sigma_0} \sum_n \varphi(n) \sum_{i=1}^{\nu} \exp\left\{ -\frac{\nu}{n} t_r \sin^2\left[\frac{i\pi}{2(\nu+1)}\right]\right\} \tag{3}$$

where ν is now a function of n, and $\varphi(n)$ is the size distribution function. On the average, one would expect the number of interaction junctions to

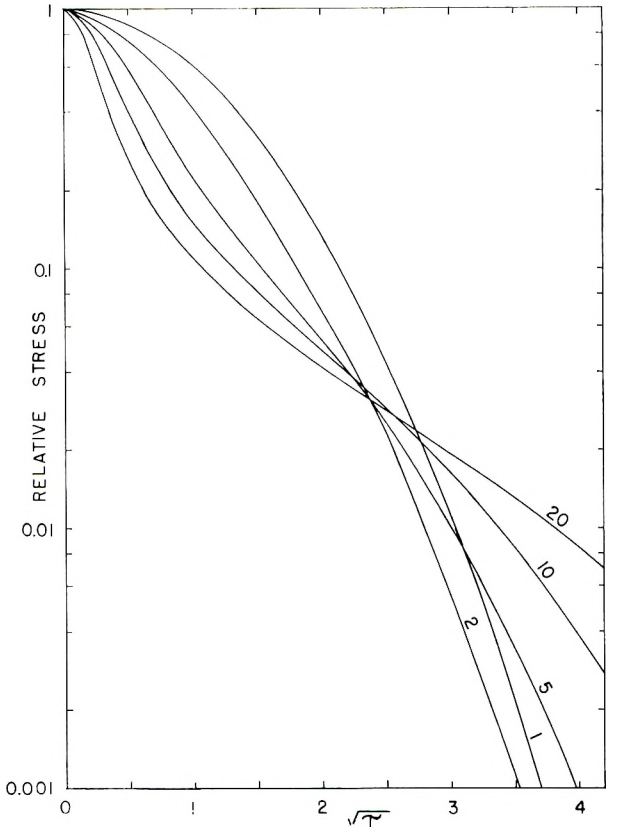

Fig. 2. Logarithm relative stress vs. square root of τ for different numbers of interaction points per molecule.

be directly proportional to n, determined by $\nu = (n/\bar{n})\bar{\nu}$, where $\bar{\nu}$ and $\bar{n}$ are average ν and n, respectively. With this assumption

$$\Delta\sigma_r = \frac{1}{\Delta\sigma_0} \sum_n \varphi(n) \sum_{i=1}^{(n/\bar{n})\bar{\nu}} \exp\left\{-(\bar{\nu}/\bar{n})t_r \sin^2\left[\frac{i\pi}{2(\bar{\nu}n/\bar{n}+1)}\right]\right\} \quad (4)$$

For plotting purposes it is convenient to use the parameter $\tau = t_r/\bar{n}$.

Two distribution functions were used to indicate the importance of these effects, the "most probable" and the Poisson. The most probable distribution is characterized by the fraction of monomeric units condensed p which is given in terms of $\bar{n}$:

$$p = (\bar{n} - 1)/\bar{n} \quad (5)$$

The most probable distribution can then be written as

$$\varphi(n) = p^{n-1}(1 - p) = [(\bar{n} - 1)/\bar{n}]^n 1/(\bar{n} - 1) \quad (6)$$

A Poisson distribution in molecular sizes is given by

$$\varphi(n) = (\bar{n}^n/n!)e^{-\bar{n}} \quad (7)$$

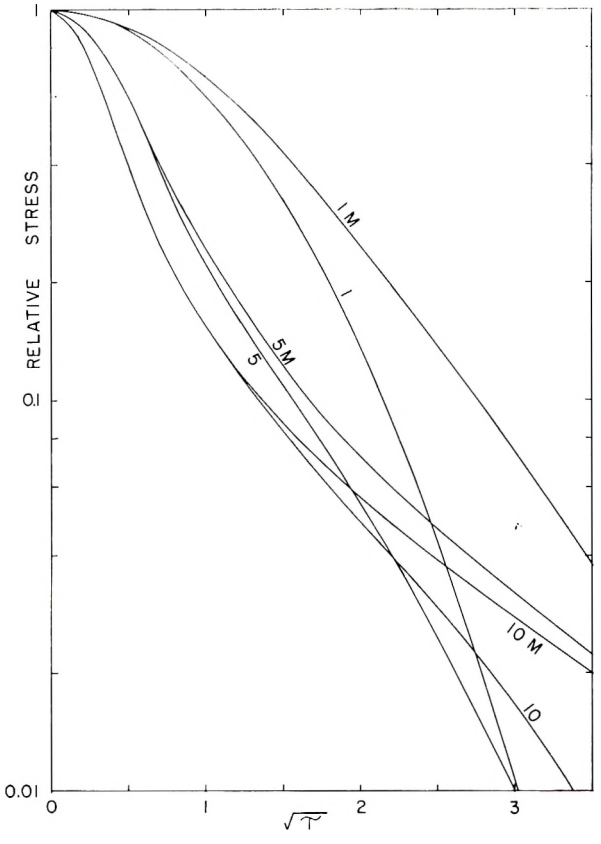

Fig. 3. Relaxation effects with a most probable distribution of molecular sizes for different numbers of interaction points per molecule.

The effect of the most probable distribution function on the relaxation behavior is shown in Figure 3 for different n values. The calculations with the Poisson distribution virtually coincided with the unweighted curves of Figure 1.

Distribution of Interaction Points per Polymer Molecule

In order to evaluate the importance of the assumption of uniform submolecule size we have considered the effect of a distribution of submolecule sizes according to the Poisson rule. For a monodisperse solution of molecules there will be an average number $\bar{\nu}$ submolecules per chain as determined by the network interactions. The Poisson distribution of submolecules $\varphi(\nu)$ is then

$$\varphi(\nu) = (\bar{\nu}/\nu!)e^{-\bar{\nu}} \tag{8}$$

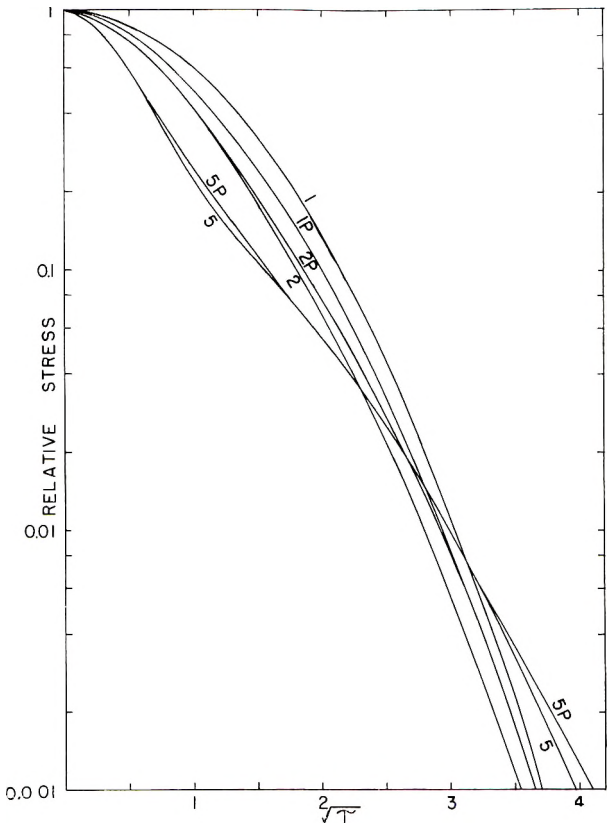

Fig. 4. Effect of Poisson distribution of number of interaction points for different average numbers of interaction points per molecule upon the relative stress relaxation.

The relative stress is then evaluated for given n and $\bar{\nu}$ from

$$\Delta\sigma_r = \frac{1}{\Delta\sigma_0} \sum \varphi(\nu) \sum_{i=1}^{\nu} \exp\left\{-\nu\tau \sin^2\left[\frac{i\pi}{2(\nu+1)}\right]\right\} \tag{9}$$

The results are shown in Figure 4.

RESULTS AND DISCUSSION

In the formulation of Mooney as given by eq. (2), the chain mobility, and consequently the relaxation behavior, is considered to be controlled by the interaction points between polymer chains. In this case the effect of solvent interaction on the intermediate regions of polymer chain is neglected. In highly dilute or molten polymer liquids the mobility of the chain will be determined primarily by the viscosity of the medium. Our calculations have been directed towards the effects of intermolecular interactions on the relaxation behavior of concentrated polymer solutions.

First of all it should be noted that the chain length n in eq. (2) affects

only the relative time scale of relaxation for a fixed number of interaction points per chain. The most significant effects on the shape of the relaxation curve are determined by the number of interaction points ν. An increase in the concentration undoubtedly increases the number ν, though it is difficult to formulate the dependence upon concentration. Likewise for a given concentration (say, weight per cent) an increase in molecular size would increase the number of interaction points per chain.

The effect of interaction points is shown for the unmodified form of the Mooney stress relaxation equation in Figure 1 in which the log of the stress is plotted against time. The relative stress decay varies from a simple exponential, when $\nu = 1$, to rather complex decays for ν values other than one. When ν is greater than 10, the general characteristics of the relaxation curve are similar. This characteristic shape consists of a rather sharp initial drop in the stress, followed by a broadening region in which the longer time decays become dominant.

The evaluated relaxation functions were also plotted as the log of the relative stress versus the square root of time, a plot suggested by some birefringence relaxation data. As may be seen in Figure 2, a near linear dependence for this type of plot occurs in the neighborhood of $\nu = 5$. This near linearity persists over three decades of the stress relaxation. For smaller values of ν the curves are convex; for large values, concave. No significant departure from these trends is observed when the curves are extended to very long times.

The effect of a wide distribution of chain lengths on the relaxation curves is indicated by the calculations shown in Figure 3. The wide distribution, represented by the most probable distribution, causes a pronounced increase in the convexity of the curves, compared to the monodispersed chain length curves. The effect becomes less noticeable with the increasing values of ν. This means that in concentrated polymer solutions, the influence of chain length on the shape of the relaxation curves, and hence the distributions of chain lengths, decrease, due to the large number on interaction points. Of course the time scale is still strongly affected by the chain length.

A Poisson distribution of chain lengths results in an insignificant change from the monodispersed relaxation curves. This signifies that only broadly dispersed materials will affect the shape of the relaxation curves of concentrated solutions.

The effect of a Poisson distribution on ν is shown in Figure 4. The shapes of the curves are, for the most part, only slightly different from those of the monodisperse curves. The smaller values for the $\nu = 1$ curves with the Poisson distribution can be attributed to the fact that a certain fraction of the chains will have a value of $\nu = 0$ and will not contribute to the relaxation process. When $\bar{\nu} = 1$, the fraction will be large, and when $\bar{\nu}$ is large, the fraction will be insignificant.

A comparison of these results with some experimental findings supports several of these theoretical predictions and allows an estimate of the number

of interactions per chain for a moderately concentrated polystyrene solution. As already noted, stress relaxation measurements are unavailable on rapidly relaxing materials, but the analogous data on birefringence relaxation have been taken. For moderately concentrated solutions, with relaxation controlled by interaction points, stress relaxation and birefringence relaxation can be properly assumed to be proportional. This has been verified by the theoretical and experimental treatments of rubber elasticity[8] and by combined measurements on normal stresses and flow birefringence.[10]

Birefringence relaxation of concentrated fractionated polystyrene solutions followed a linear relation of logarithm birefringence versus the square root of time in the region of 15–20 wt.-% for molecular weights near 10^6.[1] From the theoretical evaluations of the Mooney theory for a monodisperse material this straight line behaviour indicates the number of interaction points per chain should be in the neighborhood of five. This number is in essential agreement with estimates of three found by use of the theory of birefringence for a rubberlike material.[11] The theoretically expected curvature that should occur at either higher or lower concentrations was not found in the experiments. This is probably due to the limited range covered as restricted by certain experimental requirements.

Unfractionated samples of similar weight-average molecular weights prepared at similar concentrations showed relaxation curves with a slight upward curvature when compared to the fractionated material. This effect is borne out by the calculations of the Mooney theory for the most probable distribution.

It may be concluded that the number of interactions between molecules is small, perhaps less than one would expect in highly concentrated solutions. The decreasing effect of size distributions with increasing interactions suggests a reasonable hypothesis: chain length is unimportant, when there are many interactions along the chain, in determining the shape of the relaxation curve.

This work was supported by the Directorate of Chemical Sciences of the Air Force Office of Scientific Research.

References

1. Toggenburger, R., and S. J. Gill, *J. Polymer Sci.*, **A1,** 1765 (1963).
2. Mooney, M., *J. Polymer Sci.*, **34,** 599 (1959).
3. Rouse, P. E., Jr., *J. Chem. Phys.*, **21,** 1272 (1953).
4. Zimm, B. H., *J. Chem. Phys.*, **24,** 269 (1956).
5. A comprehensive discussion is given by J. D. Ferry, *Viscoelastic Properties of Polymers*, Wiley, New York, 1961.
6. DeMallie, R. B., Jr., M. H. Birnboim, J. E. Frederick, N. W. Tschoegl, and J. D. Ferry, *Rheol. Bull.*, **30,** No. 2, 3 (1961).
7. Bueche, F., *J. Chem. Phys.*, **22,** 603 (1954).
8. Treloar, L. R. G., *The Physics of Rubber Elasticity*, 2nd Ed., Oxford Press, London, 1958, p. 205.
9. Lodge, A. J., *Trans. Faraday Soc.*, **52,** 120 (1956).

10. Philiphoff, W., *Trans. Soc. Rheol.*, **1**, 109 (1957).
11. Gill, S. J., and R. Toggenburger, *J. Polymer Sci.*, **60**, 869 (1962).

Résumé

La théorie de Money pour la rélaxation de tension de produits polymériques a été évaluée numériquement dans des formes modifiées et non-modifiées. Les expression modifiées incluent des effets tels que les distributions de poids moléculaire, l'intreprétation et les interactions des polymères. Le comportement de rélaxation a été trouvé fort dépendant du nombre de points d'interaction par chaîne de molécules, particulièrement pour des petits nombres. Les distributions dans les grandeurs moléculaires et dans le mombre de points d'interaction ont un effet beaucoup plus faible sur les formes des courbes de rélaxation. Une comparaison du comportement du rélaxation de tension au point de vue théorque est fait avec des données de rélaxation de biréfringence. La région de corrélation indique un nombre de 5 points d'interaction par molécule de polystyrène en solution benzénique à 10% en poids.

Zusammenfassung

Die Theorie der Spannungsrelaxation von polymeren Stoffen von Mooney wurde in nicht modifizierter und modifizierter Form numerisch ausgewertet. Die modifizierten Ausdrücke umfassen Einflüsse, wie Molekulargewichtsverteilung und Verschlingungs- oder Polymerwechselwirkungsverteilung. Das Relaxationsverhalten war in hohem Grade von der Zahl der Wechselwirkungspunkte pro Kettenmolekül, besonders bei kleinen Zahlen, abhängig. Die Molekülgrössenverteilung und die Verteilung der Zahl der Wechselwirkungspunkte besitzen einen viel kleineren Einfluss auf die Gestalt der Relaxationskurve. Ein Vergleich des theoretischen Spannungsrelaxationsverhaltens mit Doppelbrechungs relaxationsdaten wird durchgeführt. Der Korrelationsbereich spricht für eine Zahl von fünf Wechselwirkungspunkten pro Molekül Polystyrol in Benzol bei 10 Gew. %.

Received March 19, 1962

JOURNAL OF POLYMER SCIENCE: PART A VOL. 1, PP. 1789–1797 (1963)

Orientation and Strength of Branched Polymer Systems

C. C. HSIAO and T. S. WU,* *Institute of Technology, University of Minnesota, Minneapolis, Minnesota*

Synopsis

A previous theory is simplified and extended to analyze the effect of macromolecular orientation on the tensile strength of a branched polymer solid. The analytical result is then compared with some known experimental data for oriented polymethyl methacrylate.

Introduction

The branching and crosslinking phenomena of polymeric solids have been noticed as very common variations of polymer growth. However, the mechanical behavior as a result of branching, is not fully understood. This is especially true as far as the strength problem is concerned. Many scientists have done significant work on this very difficult problem.† However, the effect of macromolecular orientation on strength of branched polymer solids has not yet been treated. In view of some previous successes with the theory[1] in this report, it is simplified and extended to analyze the effect of branching and macromolecular orientation on the strength of a polymeric solid. The physical idea underlying the subsequent analysis is that in a given specific stress field, an assembly of linear polymeric macromolecular elements, including their branches, can withstand a total breaking stress which is intimately tied in with their orientations as well as the molecular configurations of the system. Comparable to the so-called flaws in the well-known Griffith theory of failure, we have what we may call perhaps openings or vacant spaces in the natural molecular configurations and from the packing of the polymeric molecular chains. If we assume that for a particular polymer system there exists a critical breaking stress for which the inception and growth of the complicated fracture mechanism will result, eventually, complete failure of the polymeric solid will occur. It is the interest of this report to evaluate, under a simple state of stress, the critical breaking stress by obtaining the total contributions from all the oriented macromolecules including branches.

According to the earlier theory, only elastic stresses are calculated. Any flow will result in the orientation of the macromolecules. In order to get

* Present address: Columbia University, New York, N.Y.

† See references given by Hsiao.[1]

the elastic contribution, a known elastic deformation of the molecules is required, but this is not easily determined in view of the variation of the complicated macromolecular configuration under stress. However, if we assume that the total maximum obtainable elastic strains under stress are the same before failure as has been found to be for polystyrene,[2] then we can evaluate the critical breaking stress ratio so that the quantity of elastic strain will not be involved in the expression. Furthermore, the geometry of the openings or vacant spaces is likely to affect the general result. For simplicity, we neglect this factor for the present analysis. The result thus obtained is compared with some experimental data for oriented polymethyl methacrylate.

Now, let us consider a system of polymeric molecules. By taking into consideration the effect of macromolecular orientation and the contribution from all the molecules, the stress tensor $\sigma_{ij}(i,j = 1,2,3)$ in the vicinity of a point in the polymer as referred to an orthogonal set of the coordinate system O,X_i may be expressed in the following form:

$$\sigma_{ij} = \int El^2\epsilon_{mn}s_m s_n s_i s_j \lambda \rho f d\omega \tag{1}$$

where E = spring modulus of macromolecular chains, l = length of linear molecular element, $\epsilon_{mn}s_m s_n$ = scalar strain of the spring molecule in an instantaneous direction designated by a unit vector s_i, λ = number of molecular elements per unit volume, ρ = the density of probability distribution function of orientation of the molecular chains, f = the fraction of unbroken molecular elements, and $d\omega$ = the solid angle.

If E, l, λ, f are assumed constants throughout the process of orientation, eq. (1) may be written as follows:

$$\sigma_{ij} = El^2\lambda f \int \epsilon_{mn}s_m s_n s_i s_j \rho d\omega \tag{2}$$

For tensile strength along the X_3 direction, we have $\epsilon_{11} = \epsilon_{22}$ and all σ_{ij} will vanish except σ_{33}, which may be expressed as:[3]

$$\sigma_{33} = \lambda f \epsilon_{33}\left[\frac{2I_{12}I_{13}I_{23} - I_{22}(I_{13})^2 - I_{11}(I_{23})^2}{I_{11}I_{22} - (I_{12})^2} + I_{33}\right] \tag{3}$$

where

$$I_{ij} = \int El^2(s_i)^2(s_j)^2\rho d\omega \tag{4}$$

for $i,j = 1,2,3$ and $I_{ij} = I_{ji}$.

On the basis of the general framework of the present theory, it seems possible to develop the theory further. The following section is an account of the development when branches or side groups of an essentially linear polymer molecules are taken into consideration. The assumptions and limitations as well as the general procedures and final results are exhibited and explained in the process of the development of the analysis.

Analysis for Uniaxial Orientation

In the following analysis, it is considered that the short-range molecular forces in a polymeric solid are randomly distributed as individual units,

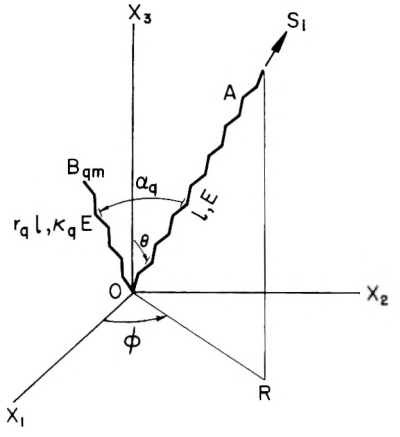

Fig. 1. Geometric configuration of a branched polymer molecule.

and may be represented by a system of linear spring elements. Assuming that the configuration of such an ordered unit be consisted of a principal chain A which has a length l and spring moleduls E as shown in Figure 1, and Q groups of branches or side chains with each group formed by M_q identical branches which are uniformly distributed around the principal chain A. A typical branch B_{qm} ($q = 1,2,\ldots, Q$, $m = 1,2,\ldots, M_q$) of the qth group has length $r_q l$ and spring constant $\kappa_q E$ and makes an angle α_q with A.

Consider that a system consisting of a large number of such units is oriented along the X_3 direction. During the process of orientation, we assume that the final direction of the principal chain A will eventually be in phase with the direction of orientation. Each individual unit will have the same configuration before and after orientation, i.e., the relative positions between A and B_{qm} are not altered.

If the degree of orientation is indicated by a homogeneous finite deformation strain ϵ in the X_3 direction, then a point $P_0(x_{01},x_{02},x_{03})$ will displace to $P(x_1,x_2,x_3)$ on the assumption that the volume of the solid is maintained constant. Then the relation between the original and new coordinates will be:

$$\begin{aligned} x_1 &= x_{01}(1 + \epsilon)^{-1/2} \\ x_2 &= x_{02}(1 + \epsilon)^{-1/2} \\ x_3 &= x_{03}\,(1 + \epsilon) \end{aligned} \tag{5}$$

If the spherical coordinates θ and ϕ are employed, then the density of the probability distribution function ρ of orientation is found to be:[1]

$$\rho = \rho_0(1 + \epsilon)^3[\cos^2\theta + (1 + \epsilon)^3 \sin^2\theta]^{-3/2} \tag{6}$$

where ρ_0 is the probability density function for random orientation.

The problem now is to evaluate the quantities ΣI_{ij} for the branched polymeric solid. This can be achieved by summing up the contributions of all elements, i.e., eq. (4) will become

$$\sum I_{ij} = (I_{ij})_{\mathrm{A}} + \sum_{q=1}^{Q} \sum_{m=1}^{M_q} (I_{ij})_{\mathrm{B}_{qm}} \tag{7}$$

The unit vectors involved in I_{ij} may be obtained by referring to Figure 1. If ψ is the angle between the plane AOB_{qm} and plane ARO, then the unit vectors $\boldsymbol{u}$ of the principal chain A and $\boldsymbol{v}_{qm}$ of the branch B_{qm} will be:[3]

$$\boldsymbol{u} = u_1\boldsymbol{i} + u_2\boldsymbol{j} + u_3\boldsymbol{k}$$

$$\boldsymbol{v}_{qm} = v_{qm1}\boldsymbol{i} + v_{qm2}\boldsymbol{j} + v_{qm3}\boldsymbol{k} \qquad \begin{pmatrix} q = 1,2,\ldots, \mathrm{Q} \\ m = 1,2,\ldots, M_q \end{pmatrix}$$

where

$$\begin{aligned} u_1 &= \sin\theta\cos\phi \\ u_2 &= \sin\theta\sin\phi \\ u_3 &= \cos\theta \end{aligned} \tag{8}$$

$$\begin{aligned} v_{qm1} &= \{\cos\alpha_q \sin\theta + \cos[\psi + (m-1)(2\pi/M_q)]\cos\theta\sin\alpha_q\}\cos\phi \\ &\quad - \sin\alpha_q \sin[\psi + (m-1)(2\pi/M_q)]\sin\phi \\ v_{qm2} &= \{\cos\alpha_q \sin\theta + \cos[\psi + (m-1)(2\pi/M_q)]\cos\theta\sin\alpha_q\}\sin\phi \\ &\quad + \sin\alpha_q \sin[\psi + (m-1)(2\pi/M_q)]\cos\phi \\ v_{qm3} &= \cos\theta\cos\alpha_q - \cos[\psi + (m-1)(2\pi/M_q)]\sin\theta\sin\alpha_q \end{aligned} \tag{9}$$

Since eqs. (8) and (9) are in terms of trigonometric functions and the limits of integration are taken as: ψ: 0 to 2π, ϕ: 0 to 2π, θ: 0 to π,

$$\sum I_{11} = El^2\left\{\int_0^{2\pi} d\psi \int_\omega \rho(u_1)^4 d\omega + \sum_{q=1}^{Q} M_q\kappa_q(r_q)^2 \int_0^{2\pi} d\psi \int_\omega \rho(v_{q1})^4 d\omega\right\} \tag{10}$$

and with similar expressions for others. In eq. (10) the index m is dropped, and the variable $[\psi + (\mathrm{m}-1)(2\pi/M_q)]$ is simply replaced by ψ.

Substituting eqs. (6), (8), and (9) in eq. (10) and integrating, we obtain:

$$\begin{aligned} I_1 &= \sum I_{11} = \sum I_{22} = \sum I_{12} \\ &= El^2\rho_0\pi^2\left\{{}^3/_2(2 - 2F_1 + F_2) + \sum_{q=1}^{Q} M_q\kappa_q(r_q)^2[{}^3/_2(2 - 2F_1 + F_2)\cos^4\alpha_q\right. \\ &\quad \left. + {}^3/_2(2 + 2F_1 - 3F_2)\cos^2\alpha_q \sin^2\alpha_q + {}^3/_{16}(6 + 2F_1 + 3F_2)\sin^4\alpha_q]\right\} \end{aligned} \tag{11}$$

$$I_2 = \sum I_{13} = \sum I_{23}$$

$$= El^2\rho_0\pi^2\Big\{2(F_1 - F_2) + \sum_{q=1}^{Q} M_q\kappa_q(r_q)^2[2(F_1 - F_2)\cos^4\alpha_q$$

$$+ (2 - 5F_1 + 6F_2)\cos^2\alpha_q\sin^2\alpha_q + {}^1/_4\,(2 + 2F_1 - 3F_2)\sin^4\alpha_q]\Big\} \quad (12)$$

$$I_3 = \sum I_{33} = El^2\rho_0\pi^2\Big\{4F_2 + \sum_{q=1}^{Q} M_q\kappa_q(r_q)^2[4F_2\cos^4\alpha_q$$

$$+ 12\,(F_1 - F_2)\cos^2\alpha_q\sin^2\alpha_q + {}^3/_2\,(2 - 2F_1 + F_2)\sin^4\alpha_q]\Big\} \quad (13)$$

where

$$F_1 = [2/(1 - a^6)] - [2a^3/(1 - a^6)^{3/2}]\cos^{-1}a^3$$

$$F_2 = [(a^6 + 2)/(1 - a^6)^2] - [3a^3/(1 - a^6)^{5/2}]\cos^{-1}a^3 \quad (14)$$

with

$$a = [1/(1 + \epsilon)^{-1/2}]$$

In eqs. (11)–(13), all sine and cosine terms are in even powers. Therefore, the negative α_q will give the same value for I_1, I_2, I_3 as the positive ones.

By use of eqs. (11)–(13), eq. (3) may be simplified as:

$$\sigma_{33}(\epsilon) = \lambda f\epsilon_{33}[I_3 - 3(I_2)^2/2I_1] \quad (15)$$

To examine how the orientation will affect the strength, we must know the strength for the random system.

Since the limiting values for F_1, F_2 are: $F_1 = 2/3$, $F_2 = 2/5$ when $\epsilon = 0$ or $a = 1$; $F_1 = F_2 = 2$ when $\epsilon \to \infty$ or $a \to 0$; thus for the random system, eqs. (11)–(13) become

$$I_1(0) = I_3(0) = {}^8/_5\,\pi^2El^2\rho_0[1 + \sum_{q=1}^{Q} M_q\kappa_q(r_q)^2]$$

$$I_2(0) = {}^8/_{15}\pi^2El^2\rho_0\,[1 + \sum_{q=1}^{Q} M_q\kappa_q(r_q)^2]$$

Substituting these values in eq. (15), we obtain:

$$\sigma_{33}(0) = {}^4/_3\,\lambda f\rho_0\pi^2El^2\epsilon_{33}[1 + \sum_{q=1}^{Q} M_q\kappa_q(r_q)^2] \quad (16)$$

and a corresponding equation governing the ratio $\sigma^{33}(\epsilon)/\sigma_{33}(0)$ can be found.

Usually the ranges of r_q, α_q are $0 < r_q < 1$ and $0 < \alpha_q < \pi/2$. In the case if all $\alpha_q = 0$, from Figure 1 it is obvious that there will be no branches, only the principal chain will exist. Then the stress ratio reduces to:[4]

$$\left.\frac{\sigma_{33}(\epsilon)}{\sigma_{33}(0)}\right|_{\alpha_q = 0} = 3F_2 - \left[\frac{(F_1 - F_2)^2}{2 - 2F_1 + F_2}\right] \quad (17)$$

Another special case is that when all α_q are the same and equal to $\pi/2$, then the strength ratio is:

$$\frac{\sigma_{33}(\epsilon)}{\sigma_{33}(0)} = \frac{4F_2 + {}^3/_2(2 - 2F_1 + F_2)\sum_{q=1}^{Q} M_q\kappa_q(r_q)^2}{{}^4/_3[1 + \sum_{q=1}^{Q} M_q\kappa_q(r_q)^2]} - \frac{[2(f_1 - F_2) + {}^1/_4(2 + 2F_1 - 3F_2)\sum_{q=1}^{Q} M_q\kappa_q(r_q)^2]^2}{(2 - 2F_1 + G_2) + {}^1/_8(6 + 2F_1 + 3F_2)\sum_{q=1}^{Q} M_q\kappa_q(r_q)^2} \Big/ {}^4/_3[1 + \sum_{q=1}^{Q} M_q\kappa_q(r_q)^2] \tag{18}$$

and

$$\left.\frac{\sigma_{33}(\epsilon)}{\sigma_{33}(0)}\right|_{\alpha_q = \pi/2} = \frac{6}{1 + \sum_{q=1}^{Q} M_q\kappa_q(r_q)^2} \tag{19}$$

Equation (19) shows that when the branches are perpendicular to the main chain, the ratio of ultimate strength is inversely proportional to the number of branches, the spring constants, and also to the square of the length of branches.

When the values of α_q are between 0 and $\pi/2$, the limits of I_1, I_2, I_3 as ϵ approaches infinity, i.e., for complete orientation, are:

$$I_1(\infty) = 3\pi^2 El^2\rho_0 \sum_{q=1}^{Q} M_q\kappa_q(r_q)^2 \sin^4 \alpha_q$$

$$I_2(\infty) = 4\pi^2 El^2\rho_0 \sum_{q=1}^{Q} M_q\kappa_q(r_q)^2 \sin^2 \alpha_q \cos^2 \alpha_q$$

$$I_3(\infty) = 8\pi^2 El^2\rho_0[1 + \sum_{q=1}^{Q} M_q\kappa_q(r_q)^2 \cos^4 \alpha_q]$$

Hence, for any values of α_q aside from all being zero or all $\pi/2$, the ratio of $\sigma_{33}(\infty)/\sigma_{33}(0)$ will be

$$\frac{\sigma_{33}(\infty)}{\sigma_{33}(0)} = \frac{6}{1 + \sum_{q=1}^{Q} M_q\kappa_q(r_q)^2} \times \left[1 + \sum_{q=1}^{Q} M_q\kappa_q(r_q)^2 \cos^4 \alpha_q - \frac{\left[\sum_{q=1}^{Q} M_q\kappa_q(r_q)^2 \sin^2 \alpha_q \cos^2 \alpha_q\right]^2}{\sum_{q=1}^{Q} M_q\kappa_q(r_q)^2 \sin^4 \alpha_q}\right] \tag{20}$$

Since each of the values of r_q, sin α_q, cos α_q is less than one, and usually M_q, κ_q are not very large, eq. (19) will then give a good approximation for eq. (20). Therefore, the ratio of ultimate strength after orientation will be relatively small if there are branches. The maximum value of $\sigma_{33}(\infty)/\sigma_{33}(0)$ occurs when there is no branch.

Numerical Results for Polymethyl Methacrylate

In order to illustrate the application of the theoretical method and to see how satisfactory the analytical predictions are, an idealized molecular system based upon the macromolecular structure of polymethyl methacrylate was constructed and analyzed. The various constants were assigned according to the known geometry and characteristics of the polymeric molecular configuration. Neglecting the carbon-hydrogen bonds and considering the methyl group as group 1 and the $COOCH_3$ group as group 2, the various quantities are respectively:

$$Q = 1$$

$M_1 = 1$	$M_2 = 1$
$\kappa_1 = 2$	$\kappa_2 = 6$
$\alpha_1 = 70°$	$\alpha_2 = 70°$
$r_1 = {}^1/_2$	$r_2 = {}^9/_{16}$

The assignment of some of these quantities is based upon the molar cohesion forces for the different groups[5,6] given in calories per mole. Referring to Figure 2, the molar cohesion for the $-CH_2-$ group is 900 kg.-cal./mole, for the $-CH_3-$ group is 1800 kg.cal./mole, and for the $-COO-CH_2$ group is 5600 kg. cal./mole. For simplicity, we consider that the

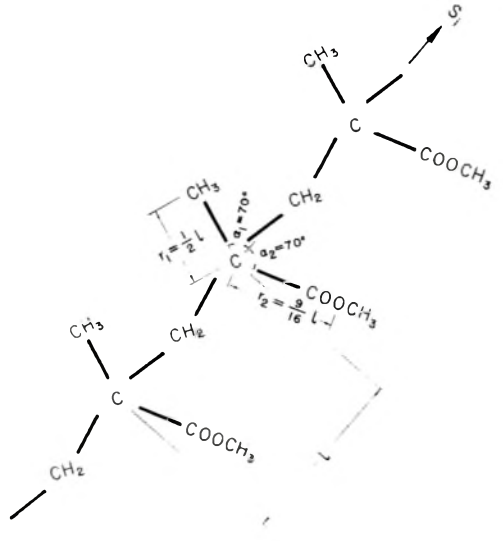

Fig. 2. Schematic diagram of the geometry of the linear chain of polymethyl methacrylate.

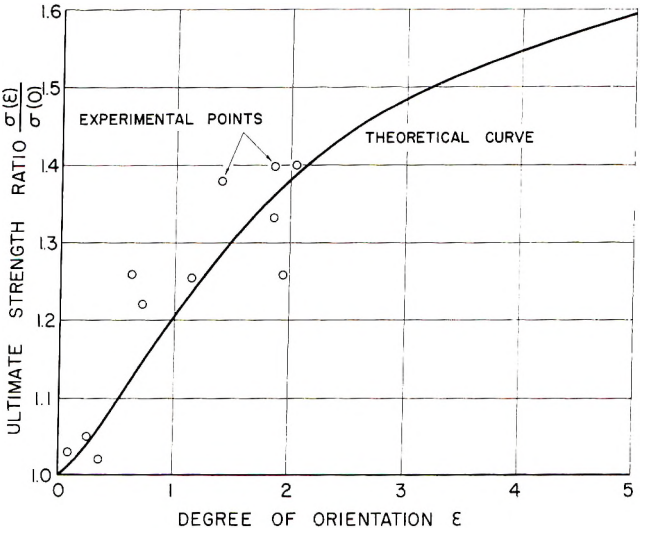

Fig. 3. Effect of orientation on ultimate strength of polymethyl methacrylate.

molar cohesion of the CH_3 group is approximately twice that of the —CH_2— group; thus we assign κ_1 as 2. Similarly the molar cohesion of the —COO-CH_3 group is approximately six times that of —CH_2— group; therefore, we assign κ_2 as 6. The geometry of the linear chain of polymethyl methacrylate is also drawn approximately as shown with $\alpha_1 = 70°$ and $\alpha_2 = 70°$, as the C—C—C type of bond has a bond angle of about 111°30′, which we approximate to 110°, and 70° is the complimentary angle that we use. The distances between the various C—C bonds are also assigned as shown. If we let the distance C—CH_2—C be l, then we assign $r_1 = l/2$ which is approximately the distance for the bond C—CH_3. Similarly, we assign $r_2 = 9l/16$, which represents approximately the average distance for the bond C—$COOCH_3$.

Most polymers have strength values much smaller than the primary valence forces. It is most improbable that in cases of rupture of polymeric materials, primary bonds are broken. However, through the use of the primary bond information, we only hope to deduce some related information on fracture as the fracture mechanism is highly complicated. Thus, the critical breaking stress was estimated. From the present analysis, the variation of the ultimate strength ratio as affected by the orientation of the macromolecular chains is reported in Figure 3. In order to compare the theoretical predictions with the actual results, some experimental data of breaking stress for oriented polymethyl methacrylate specimens were also obtained. The orientation of the specimens was induced at an elevated temperature by homogeneous stretching on a specially designed orientation machine. By cooling under stress, the orientation of the macromolecules was frozen in at room temperature. The corresponding degree of orientation of the macromolecules was recorded in terms of homogeneous

strain ϵ. The specimens were then tested at a constant strain rate for simple tension until rupture of the specimens occurred. The experimental points of the ultimate strength thus obtained were divided by an average random strength of the same solid. Figure 3 shows the comparison of the experimental ultimate strength ratio and the theoretical result.

Supported in part by the U.S. Atomic Energy Commission.

References

1. Hsiao, C. C., *J. Appl. Phys.*, **30**, 1492 (1959).
2. Hsiao, C. C., and J. A. Sauer, *J. Appl. Phys.*, **21**, 1071 (1950).
3. Osborn, J. E., T. S. Wu, and C. C. Hsiao, AEC AT(11–1)-532 T. R. 12, University of Minnesota, 1960.
4. Robinson, A., J. E. Osborn, and C. C. Hsiao, *J. Appl. Phys.*, **31**, 1602 (1960).
5. Dunkel, M., *Z. Physik. Chem.*, **A138**, 42 (1928).
6. Dunkel, M., and K. L. Wolf, *Muller-Pouillets Lehrbuch der Physik*, **4**, 579 (1933).

Résumé

On a simplifié et étendu une théorie antérieure à l'analyse de l'effet de l'orientation macromoléculaire sur la force de tension d'un polymère solide ramifié. Le résultat analytique est alors comparé avec des données expérimentales bien connues du polyméthacrylate de méthyle orienté.

Zusammenfassung

Eine früher mitgeteilte Theorie wird vereinfacht und auf die Analyse des Einflusses der Orientierung der Makromoleküle auf die Zugfestigkeit eines Festkörpers aus verzweigten Polymeren ausgedehnt. Das Ergebnis der Analyse wird mit Versuchsdaten an orientiertem Polymethylmethacrylat verglichen.

Received March 21, 1962

JOURNAL OF POLYMER SCIENCE: PART A VOL. 1, PP. 1799–1811 (1963)

Diffusion of Benzene in Polyacrylates

A. KISHIMOTO and Y. ENDA, *Physical Chemistry Laboratory, Department of Fisheries, University of Kyoto, Maizuru, Japan*

Synopsis

An investigation has been made of the sorption and permeation of benzene vapor in polymethyl acrylate and polyethyl acrylate over relatively wide ranges of temperature and concentration. The mutual diffusion coefficients were estimated from the rates of absorption and desorption, and the steady-state permeability. The diffusion coefficients determined by the different methods agreed within experimental error, suggesting that the sorption processes for these systems are controlled by truly Fickian diffusion mechanism. By using the equations of Frisch, the time lags for permeation have been calculated as a function of concentration from the diffusion coefficient data, and compared with the observed values. The calculated values agreed with the observed ones, indicating that the nonstationary state of permeation is controlled by a purely Fickian diffusion mechanism. Experimental data for the thermodynamic diffusion coefficients D_T of benzene in PMA and PEA have been analyzed in terms of a simple free volume theory previously developed. It is found that, in all cases examined, the derived relation fits well experimental data. Three temperature-dependent parameters involved in the theory are evaluated, and their variation with temperature are discussed.

INTRODUCTION

Absorption and desorption processes of organic vapors in amorphous polymers are of the Fickian type, with a diffusion coefficient which depends appreciably on penetrant concentration, when the systems are well above the glass transition temperatures T_g of the respective polymers.[1-4] If these processes are governed by a purely Fickian diffusion mechanism, the diffusion coefficients derived from sorption experiments should agree with those determined from the steady-state permeation method. At temperatures slightly above T_g, no definite information has been obtained about the sorption behavior. Meares[5] has demonstrated that the integral diffusion coefficient, $\bar{D}$, for the system polyvinyl acetate–allyl chloride at 40°C. determined from steady-state permeation data increased more rapidly with allyl chloride concentration than did the diffusion coefficient from sorption experiments.[6] Both diffusion coefficients, however, converged to the same limit at zero penetrant concentration. A similar discrepancy between steady-state diffusion coefficient and transient diffusion coefficient has recently been reported for the system natural rubber–benzene at 50°C.[7] It should be noted that in this case the measurements were carried out at a temperature far above the glass transition point of the polymer. The main purpose of the present paper is to examine whether the diffusion coefficients

derived from measurements of sorption kinetics and of nonstationary state of permeation agree with the ones determined from steady-state permeation at temperatures well above the glass transition point of a given polymer.

The polymers studied were unfractionated polymethyl acetylate and polyethyl acrylate. Benzene was used as penetrant for both polymers. These materials were chosen because their T_g are relatively low so that they are rubbery at room temperature.

EXPERIMENTAL

The polymethyl acrylate (PMA) used was the same as that employed previously.[4] Its number-average molecular weight, determined osmotically in acetone at 25°C., was 3.1×10^5. The films for sorption and permeation experiments were prepared in a manner similar to that described previously.[8] Their thicknesses varied in the range from 3.2×10^{-3} to 1.22×10^{-2} cm., depending upon the conditions of the particular experiment.

The polyethyl acerylate (PEA) used was furnished by the Department of Polymer Chemistry, University of Kyoto, through the courtesy of Professor H. Kawai. It was purified by precipitation from a 2% acetone solution by the addition of water. The intrinsic viscosity in acetone at 30°C. was 3.21 dl./g. Films of this polymer were prepared following a procedure similar to that used for PMA. The films used for sorption measurements varied from 7.95×10^{-3} to 1.93×10^{-2} cm. in thickness. A value of 1.086 g./ml. was used for the density of PEA in calculating these film thicknesses. This density value was determined in a usual Gay-Lussac type pycnometer at 20°C., *n*-hexane being used as the confining liquid.

The benzene used as organic penetrant was purified by shaking a sample of technical grade successively with concentrated sulfuric acid and water and then was dried over calcium chloride and distilled.

The sorption apparatus described previously[8] was used throughout this investigation. Integral absorption from and integral desorption to zero pressure were measured for several external pressures of benzene vapor at a number of temperatures in the range 30–60°C. for PMA and in the range 5-60°C. for PEA.

The permeation measurements were performed by using an apparatus essentially similar to that described by Rouse.[9] The permeability cell was similar to that employed by Stannett and Szwarc.[10] The film was supported on a stainless steel screen and clamped between the two halves of the cell. In the present permeation experiment, a piece of filter paper was inserted between the film and the screen. Measurements were carried out for several ingoing pressures of benzene vapor at temperatures of 30°C. and 50°C. for PMA. In sorption and permeation experiments the temperature of the system was controlled to within ±0.1°C. According to the literature,[11,12] the glass transition temperatures T_g of dry PMA and PEA are

about 3°C. and −22°C., respectively. Thus all of the present measurements were performed well above the glass transition temperatures of the polymers.

RESULTS AND DISCUSSION

Sorption

It was found that for both PMA and PEA the equilibrium benzene concentrations C_0 (grams of vapor at absorption equilibrium per gram of dry polymer) at given relative pressures are independent of temperature over the ranges studied. For a given relative pressure the equilibrium concentration for polyethyl acrylate is about two times as large as that for polymethyl acrylate. Formal application of the Flory-Huggins thermodynamic equation of polymer solutions, assuming no volume change on mixing, shows that for both systems the interaction parameter χ_1 is nearly independent of equilibrium concentration, giving 0.46 for PMA and zero for PEA.

For all the cases studied both absorption and desorption curves had shapes expected of the normal Fick diffusion mechanism;[13] they are linear in the region of small values of $t^{1/2}$ and concave against the abscissa in the region of large $t^{1/2}$. The absorption is always faster than the corresponding desorption curve. It was found that for a given polymer this difference in initial slope between absorption and desorption at a given temperature increased systematically with increasing equilibrium concentration. This suggests that the mutual diffusion coefficient D for the system increases with penetrant concentration C_0, provided the sorption processes are controlled by purely Fickian diffusion mechanism.

The apparent diffusion coefficients, $\bar{D}_a$ and $\bar{D}_d$, for absorption and desorption may be calculated from the initial slopes of the respective plots, I_a and I_d, by

$$\bar{D}_a = (\pi/16)I_a^2X^2 \qquad (1)$$

$$\bar{D}_d = (\pi/16)I_d^2X^2$$

where X is the thickness of film. The values of $\bar{D}_a$ and $\bar{D}_d$ obtained for the system PMA–benzene at 30°C. are plotted semilogarithmically against vapor concentration C_0 in Figure 1. It is seen that both $\bar{D}_a$ and $\bar{D}_d$ increase with C_0, and the difference between them also becomes larger as C_0 increases. Similar data were obtained for benzene–PMA and benzene–PEA systems at other temperatures. These results indicate that at high temperatures log $\bar{D}_a$ and log $\bar{D}_d$ are approximatey linear against C_0, but as the temperature is lowered, the plots tend to show downward curvature at low values of C_0. This similar behavior has been reported for the systems PMA–*n*-alkyl acetates,[4] PVAc–allyl chloride at 40°C.,[6] and polyethylene–benzene.[14]

The data for $\bar{D}_a$ and $\bar{D}_d$ shown in Figure 1 may be used to evaluate the mutual diffusion coefficient D for the system as a function of benzene

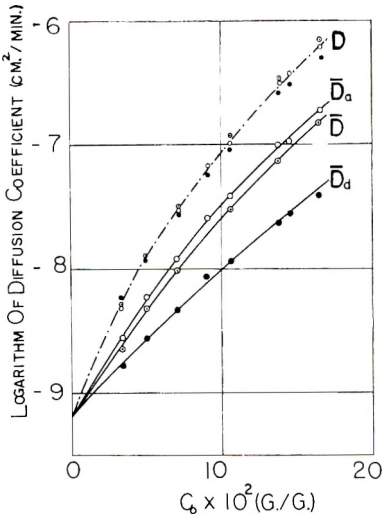

Fig. 1. Plots of various diffusion coefficients against penetrant concentration for the system PMA–benzene at 30°C.: (○) D from $\bar{D}_a$; (●) D from $\bar{D}_d$; (⊙) D from $\bar{D}$.

concentration. Crank[15] had demonstrated that $\bar{D}_a$ is approximated very accurately by the equation:

$$\bar{D}_a(C_0) = (5/3)C_0^{-5/3}\int_0^{C_0} C^{2/3}\, D(C)\, dC \tag{2}$$

provided D is an increasing function of C. He also has shown that for desorption the following equation holds accurately:

$$\bar{D}_d(C_0) = 1.85\,(C_0)^{-1.85}\int_0^{C_0}(C_0 - C)^{0.85}\, D(C)\, dC \tag{3}$$

Equation (2) permits evaluation of $D(C)$ by simple graphical differentiation when the values of $\bar{D}_a$ are given as a function of C_0. To solve eq. (3) for D a more elaborate numerical calculation is necessary. Here we propose an approximate method of solving eq. (3). We assume a polynomial representation for $D(C)$:

$$D(C) = D_0 + k_1C + k_2C^2 + k_3C^3 + \ldots \tag{4}$$

where D_0 is the value of D at the limit of zero concentration and k_1, k_2, k_3, . . . , are unknown coefficients. Introducing eq. (4) into eq. (3) and integrating we obtain an expression for $\bar{D}_d$:

$$\bar{D}_d = D_0 + (k_1/2.85)C + (2!k_2/3.85 \times 2.85)C^2 + (3!k_3/4.85 \times 3.85 \times 2.85)\,C^3 + \ldots \tag{5}$$

In general, $\bar{D}_d$ may be written

$$\bar{D}_d = D_0 + k_1'C + k_2'C^2 + k_3'C^3 + \ldots \tag{6}$$

Comparison of eqs. (5) and (6) gives the following relations:

$$k_1 = 2.85k_1'$$

$$k_2 = (3.85 \times 2.85/2!)\, k_2' = 5.486 k_2', \tag{7}$$

$$k_3 = (4.85 \times 3.85 \times 2.85/3!)\, k_3' = 8.871 k_3'$$

The coefficients of higher order may be readily calculated. If the plot of $\bar{D}_d$ experimentally determined are fitted with eq. (6), we can immediately obtain the $D(C)$ plot by using eqs. (4) and (7) without any tedious numerical calculation. To determine the unknown coefficients D_0 and k_1', k_2', etc., fitting of eq. (6) to experimental data must be made at suitably selected values of C_0. The number of points must be equal to the number of coefficients to be determined. In most cases, it is sufficient to use a cubic equation to fit the desorption data, since the change in $\bar{D}_d$ with C is not so steep, even when the change in D in the corresponding concentration range amounts to several hundredfold.

Figure 1 includes corresponding D values calculated by eqs. (2) and (3). It is seen that the D values derived from both sets of data agree quite well. Such agreements have been observed for two polyacrylates studied at other temperatures. We may thus conclude safely that all the absorption and desorption processes measured in this study were truly Fickian.

Permeation

It was found that for PMA systems at 30°C. and 50°C. the permeation curves (the plots for outgoing pressures versus time) were convex toward the time axis and approached asymptotically a straight line. This is the expected feature when the concentration at the ingoing surface remains constant or increased monotonically with increasing time, provided that the diffusion is a main controlling factor in permeation process.[13] Since the present permeation measurements are concerned with the polymer well above its glass transition, the poymer solid probably contains no microvoids, and so the difficulty arising from a convective flow through a capillary system formed by such voids may be avoided.

If q_s is the steady-state rate of permeation through a film of unit area and thickness X in the unswollen state when the ingoing surface is maintained at concentration C_0 and the outgoing surface at zero concentration, the integral diffusion coefficient $\bar{D}$ is related to q_s by the equation

$$\bar{D}(C_0) = q_s X/C_0 = (1/C_0) \int_0^{C_0} D\, dC \tag{8}$$

The solubility coefficient of the penetrant is given by

$$S(C_0) = C_0/p_0 \tag{9}$$

where p_0 is the pressure at the ingoing surface.

Combination of eqs. (8) and (9) yields

$$\bar{D}(C_0) = P(C_0)/S(C_0) \tag{10}$$

where $P(C_0)$ is called steady-state permeability and is defined by

$$P(C_0) = q_s X/p_0 \tag{11}$$

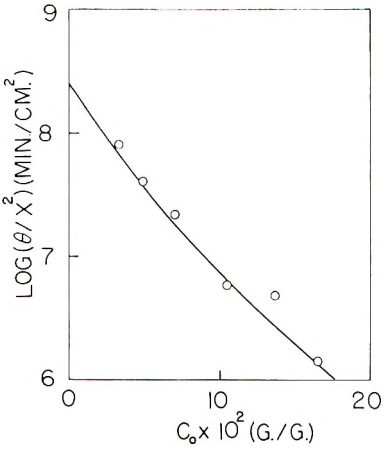

Fig. 2. Reduced time lags for benzene diffusing through PMA at 30°C. as functions of benzene concentration: (O) experimental data; (——) curve calculated by eq. (12).

The steady-state permeability and the equilibrium sorption isotherm enable direct evaluation of $\bar{D}$ as a function of concentration, which in turns allows ready determination of D as a function of concentration. Plots of log $\bar{D}$ and log D versus benzene concentration for the system pMA–benzene at 30°C. are shown in Figure 1. It is seen from the figure that the D values determined from the steady-state permeation rates agree with those deduced from absorption and desorption rates. Similar agreements of the three sets of D values have also been observed for the same system at 50°C. These results indicate that all the measured sorption processes of benzene in PMA at temperatures above 30°C. are truly Fickian and the sorption values of D are correct.

The intercept on the time axis of the steady-state portion of a permeation curve defines the time lag θ for permeation. Figure 2 plots semilogarithmically the reduced time lag θ/X^2 against penetrant concentration for the system PMA–benzene at 30°C. It is seen that the reduced time lag decreases with increase of concentration. This indicates that the mutual diffusion coefficient D increases with concentration, provided the transient permeation processes are controlled by truly Fickian diffusion mechanism.

Frisch[16] has recently shown that θ is related to D by the equation:

$$\theta(C_0) = X^2 \{\int_0^{C_0} w\, D(w) [\int_w^{C_0} D(u)du]dw\} / [\int_0^{C_0} D(v)du]^3 \qquad (12)$$

In his derivation of this equation Frisch assumed the condition of constant surface concentration. In principle, eq. (12) can be converted to find D as a function of concentration from the experimentally determined values of $\theta(C_0)$. In practice, this requires a detailed and accurate knowledge of $\theta(C_0)$, and, in addition, there is little possibility to carry out this conversion in the analytical way. In most cases, the time lag may be obtained as a by-product of steady-state permeation measurements. Therefore, we have to be satisfied with finding θ from the known data for $D(C)$ determined

from steady-state permeability measurements. Data for $D(C)$ shown in Figure 1 are substituted into the right-hand side of eq. (12) to predict θ as a function of concentration, and the result is shown in Figure 2 as a solid line. The time lag values so calculated are in reasonable agreement with those determined experimentally. A similar agreement has been found for the same system at 50°C. Rogers, Stannett, and Szwarc[14] have reported results of a similar nature for the system polyethylene–benzene at 0°C.

Diffusion Coefficient

The thermodynamic diffusion coefficient of the penetrant, D_T, is given by[13]

$$D_T = D(d \ln v_1/d \ln a_1)/(1 - v_1) \tag{13}$$

where v_1 is the volume fraction of penetrant and a_1 the activity of the penetrant in the given polymer–penetrant mixture. Equation (13) shows that the value of D_T may be calculated as a function of v_1 when the data for D and a_1 as functions of v_1 are experimentally determined. The data for $D(C)$ may then be converted to the data for D_T against v_1, provided the densities of the given polymer and penetrant are known and the additivity of the volumes of the two components is assumed. This assumption is almost valid as the present experiment is conducted at temperatures well above the glass transition of the polymers. By way of example, the values of D_T so computed for the system PEA–benzene are plotted semilogarithmically against v_1 in Figure 3; in converting D to D_T the values of the thermodynamic term $d \ln v_1/d \ln a_1$ have been calculated not from the observed isotherm but from the Flory-Huggins thermodynamic equation with an

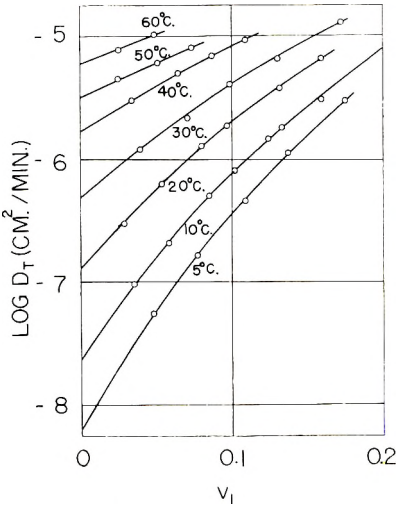

Fig. 3. Thermodynamic diffusion coefficient D_T for the system PEA–benzene at different temperatures.

interaction parameter $\chi_1 = 0$. This family of curves has several important features which are analogous to the systems PMA–*n*-alkyl acetates recently studied.[4] At high temperatures, log D_T varies approximately linearly with v_1 and its dependence on concentration is less appreciable, but as the temperature is lowered, the plots show downward curvature at low values of v_1. This curvature becomes more noticeable as the temperature approaches the glass transition temperature of PEA. These trends were also observed for the system PMA–benzene. On the basis of the free volume concept Fujita, Kishimoto, and Matsumoto[4] have derived the following equation for the concentration dependence of D_T at a fixed temperature T:

$$\frac{1}{\log (D_T/D_0)} = \frac{2.303\, f(0,T)}{B_d} + \frac{2.303[f(0,T)]^2}{B_d \beta(T)} \frac{1}{v_1} \tag{14}$$

Here $f(0,T)$ is the average fractional free volume in the pure polymer at temperature T, B_d is a constant characteristic of the system, and $\beta(T)$ stands for

$$\beta(T) = \gamma(T) - f(0,T) \tag{15}$$

where $\gamma(T)$ is the proportionality factor appearing when we assume a linear relation between the increase in free volumes and the volume of diluent added and is assumed to be a function of T only. Equation (14) indicates that a plot for $1/\log(D_T/D_0)$ against $1/v_1$ at a given temperature should be linear and that the intercept at $1/v_1 = 0$ and the slope of the resulting straight line are $2.303 f(0,T)/B_d$ and $2.303\,[f(0,T)]^2/B_d\,\beta(T)$, respectively. Therefore, provided B_d can be evaluated from other data, both $f(0,T)$ and $\beta(T)$ and hence $\gamma(T)$ may be determined.

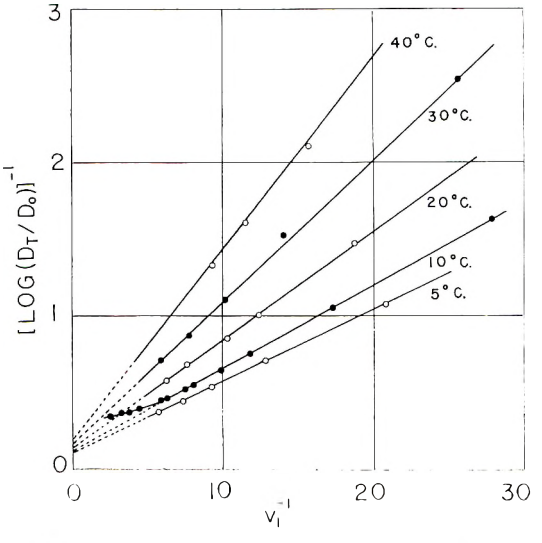

Fig. 4. $[\log(D_T/D_0)]^{-1}$ as a function of reciprocal volume fraction of benzene in PEA.

Tests of eq. (14) with the PEA data are shown in Figure 4. It is seen that the data, except for those at 10°C., follow reasonably a straight line in agreement with the theoretical prediction from eq. (14), but at 10°C. the plot deviates slightly from the straight line in the region of small values of v_1^{-1}. This deviation suggests a limitation of the free volume theory in the region of high concentration of penetrant, which will be discussed later. The data for the system PMA–benzene also give similar results.

Theory[13] shows that the parameter B_d in eq. (14) may be determined by means of either of the following two procedures, when appropriate data are available for both diffusion coefficient and steady flow viscosity of a given polymer–diluent system. One procedure refers to the case in which both the diffusion coefficient and the viscosity are given as functions of diluent concentration at a fixed temperature, while the other is applicable when these quantities at zero diluent concentration are known as functions of temperature. Here we use the second procedure, which resorts to the relation:

$$\ln (D_0/RT) = K - B_d \ln \eta(0,T) \tag{16}$$

where R is the gas constant, T is the absolute temperature of the system, K is a constant independent of T, and $\eta(0,T)$ is the steady flow viscosity of undiluted polymer at a fixed temperature T. The desired value for B_d may be determined from the slope of a plot for $\ln(D_0/RT)$ against $\ln \eta\ (0,T)$. It is a simple matter to show that eq. (16) may be written

$$\ln(D_0/RT) = K' - B_d \ln a_T \tag{17}$$

where K' is a new constant and a_T denotes the value of $\eta(0,T)$ relative to its value at a suitably chosen reference temperature T^*, i.e.,

$$a_T = \eta(0,T)/\eta(0,T^*) \tag{18}$$

The a_T is called the shift factor, which may be derived from transient or dynamic viscoelastic measurements.[17] Equation (17) indicates that the

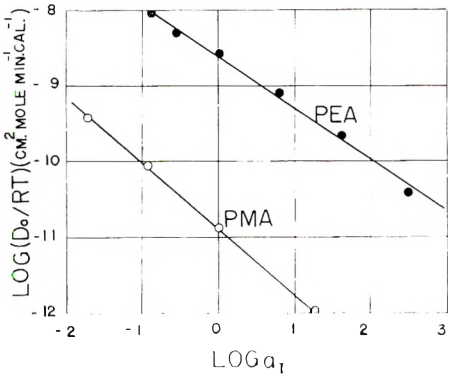

Fig. 5. Correlation between D_0 and a_T.

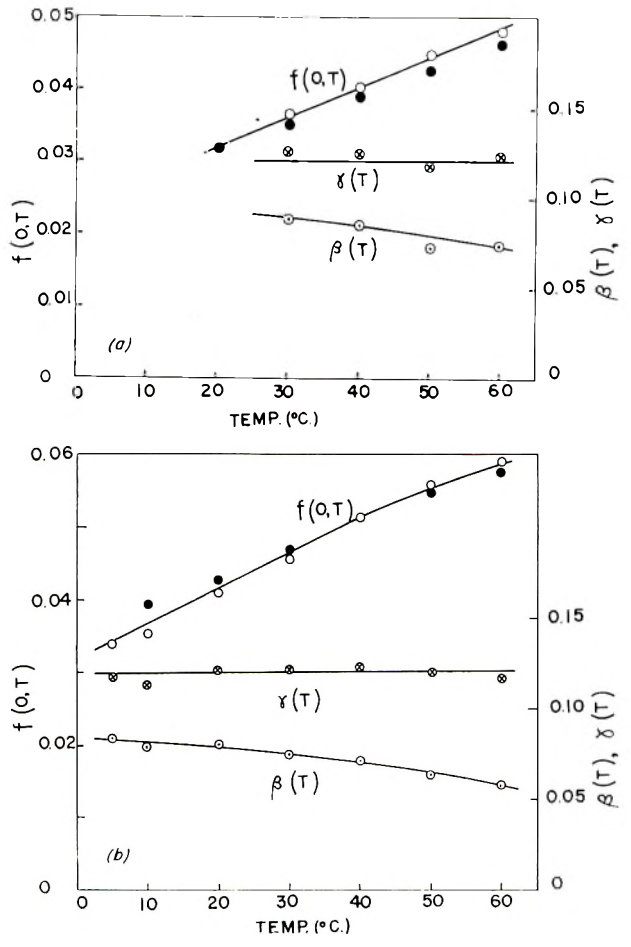

Fig. 6. Values of $f(0,T')$, $\beta(T')$, and $\gamma(T')$ for (*a*) the system PMA–benzene and (*b*) the system PEA–benzene: (●) values of $f(0,T')$ derived from viscosity data on pure PMA and PEA, respectively.

value of B_d may be determined from the slope of a plot for $\ln(D_0/RT)$ against $\ln a_T$.

Data for a_T as a function of temperature are available for PMA from recent viscosity measurements on PMA-diethyl phthalate by Fujita and Maekawa.[18] Since for PEA no a_T data are yet available, we carried out tensile creep measurements over the range of temperature of 10–70°C. By shifting the individual creep curves along the log t axis to construct a master creep curve, the desired shift factor a_T has been determined as a function of temperature. Fits of eq. (16) to the present data are illustrated in Figure 5, where the reference temperature T'^* is chosen as 40°C. for both PMA and PEA. The plots are linear over the range of temperature, giving values of B_d of 0.89 for PMA and 0.68 for PEA. It is noted that, in both cases, the values of B_d are smaller than unity. With these B_d values the

values of $f(O,T)$ (open circles) and $\beta(T)$ have been calculated as functions of temperature from the intercepts and slopes of the plots for $1/\log(D_T/D_0)$ against v_1^{-1}, and are shown in Figures 6*a* and 6*b*. These figures also include the values of $\gamma(T)$ determined.

According to the definition of $f(O,T)$, this function must be characteristic of the species of the polymer concerned; it must be independent of the penetrant with which the diffusion data were taken. Analysis of our previous data[4] for diffusion of *n*-alkyl acetates in PMA gives the values of $f(O,T)$ which fall closely on the $f(O,T)$ curve shown in Figure 6*a*. It is noted that this $f(O,T)$ curve is approximately linear over the range of temperature from 30 to 60°C., and, in this region is represented by $f(O,T) = 0.025 + 4.1 \times 10^{-4}(T - 3)$, where T is expressed in degrees Centrigrade. This is identical in form with the equation derived by Williams, Landel, and Ferry,[17] and the values 0.025 and 4.1×10^{-4} deg.$^{-1}$ may be compared favorably with the universal values $f(O,T_g) = 0.025$ and $\alpha_f = 4.8 \times 10^{-4}$ deg.$^{-1}$, respectively, if the glass transition temperature T_g of PMA be set equal to 3°C. The same conclusion can be drawn from the data for the system PEA + benzene shown in Figure 6*b*. The slope of the line for $f(O,T)$ is about 4.8×10^{-4} deg.$^{-1}$, which is incidentally identical with the α_f value deduced from WLF equation. It is reported that the glass transition temperature of pure PEA is −22°C.[12] If we accept this value, extrapolation of Figure 6*b* gives a value of 0.022 for $f(O,T_g)$, which may also be compared with the universal value 0.025.

According to Williams, Landel, and Ferry,[17] the shift factor a_T is represented by the equation

$$\ln a_T = [1/f(O,T)] - [1/f(O,T^*)] \tag{19}$$

where a_T is defined by eq. (18). If data for a_T are available and if the value of $f(O,T)$ for $T = T^*$ is known, the values of $f(O,T)$ at temperatures other than T^* may be calculated from eq. (19). Fujita and Maekawa[18] analyzed viscosity data for the system PMA–diethyl phthalate and derived a $f(O,T)$ value at 20°C. With this value of f taken as $f(O,T^*)$ they calculated the values of $f(O,T)$ at other temperatures which are shown in Figure 6*a* by solid circles. The two sets of $f(O,T)$ indicated are seen to agree reasonably with one another over a range of T. The corresponding comparison for PEA is indicated in Figure 6*b*. The $f(O,T)$ from creep data stand in good agreement with those derived above from diffusion data. These agreements suggest the internal consistency of the free volume theory of diffusion and viscosity set forth by Fujita and collaborators.

From Figure 6, one may point out some features about the magnitudes as well as the temperature dependence of the parameters $\beta(T)$ and $\gamma(T)$. The values of $\beta(T)$ gradually decrease as T increases, but $\gamma(T)$ remains almost constant in the corresponding region of T. These trends have been reported in our recent analysis of viscosity data on polystyrene and polymethyl methacrylate in the region of T higher than the glass transition point.[19] It is of interest that the value of $\gamma(T)$ shown in Figure 6, is not

only independent of temperature but also of polymer species and equals to about 0.12. As will be expected from its definition, the quantity $\gamma(T)$, to a first approximation, depends upon the diluent species only and may be compared with the fractional free volume of the diluent. A similar conclusion has been deduced by Ferry and Stratton.[20]

A limitation of the free volume theory of diffusion can be seen in Fig. 4. The plot for 10°C. shows some upward deviation from linearity in the region of small values of $1/v_1$ (about 0.2 by volume fraction). This deviation is contrasted to that which we encountered in treating viscosity data in which the plots showed some downward deviation from linearity. Recent data[18] of viscosity for the system PMA–diethyl phthalate have shown that at low temperatures the free volume theory is applicable over a fairly wide range of diluent concentrations, but, as temperature increases, the maximum concentration for which the theory holds shifts toward the low concentration region. It has been suggested from these results that the applicability of the free volume theory of viscosity is limited roughly to values of $f \leqslant 0.06$. Because of the analogy between diffusion and viscosity processes we may expect that eq. (14) should be applicable only for sufficiently low diluent concentrations (probably less than 0.2 by volume fraction).

The authors wish to thank Professor H. Fujita, Department of Polymer Science, Osaka University, Osaka, for his encouragement and his helpful advice in the course of this investigation. Part of this work was supported by a grant-in-aid of research from the Ministry of Education.

References

1. Prager, S., and F. A. Long, *J. Am. Chem. Soc.*, **73,** 4072 (1951).
2. Prager, S., E. Bagley, and F. A. Long, *J. Am. Chem. Soc.*, **75,** 1255 (1953).
3. Hayes, M. J., and G. S. Park, *Trans. Faraday Soc.*, **51,** 1134 (1955).
4. Fujita, H., A. Kishimoto, and K. Matsumoto, *Trans. Faraday Soc.*, **56,** 424 (1960)
5. Meares, P., *J. Polymer Sci.*, **27,** 391 (1958).
6. Kishimoto, A., and K. Matsumoto, *J. Phys. Chem.*, **63,** 1529 (1959).
7. Barrer, R. M., and R. R. Fergusson, *Trans. Faraday Soc.*, **54,** 989 (1958).
8. Fujita, H., and A. Kishimoto, *J. Polymer Sci.*, **28,** 547 (1958).
9. Rouse, P. E., *J. Am. Chem. Soc.*, **69,** 1068 (1947).
10. Rogers, C. E., J. A. Meyer, V. Stannett, and M. Szwarc, *Tappi*, **39,** 737 (1956).
11. Jenckel, E., *Z. Physik. Chem.*, **A190,** 24 (1941).
12. Wood, L. A., *J. Polymer Sci.*, **28,** 319 (1958).
13. Fujita, H., *Fortschr. Hochpolymer. Forsch.*, **3,** 1 (1961).
14. Rogers, C. E., V. Stannett, and M. Szwarc, *J. Polymer Sci.*, **45,** 61 (1960).
15. Crank, J., *Trans. Faraday Soc.*, **51,** 1632 (1955).
16. Frisch, H. L., *J. Phys. Chem.*, **61,** 93 (1957).
17. Williams, M. L., R. F. Landel, and J. D. Ferry, *J. Am. Chem. Soc.*, **77,** 3701 (1955).
18. Fujita, H., and E. Maekawa, *J. Phys. Chem.*, **66,** 1053 (1962).
19. Fujita, H., and A. Kishimoto, *J. Chem. Phys.*, **34,** 393 (1951).
20. Ferry, J. D., and R. A. Stratton, *Kolloid-Z.*, **171,** 107 (1960).

Résumé

On a examiné, dans des intervalles de température et de concentration relativement larges, la sorption et la pénétration de vapeurs benzéniques dans le polyacrylate de

méthyle et le polyacrylate d'éthyle. Les coefficients de diffusion sont déduits des vitesses d'absorption et de désorption, et de la perméabilité à l'état stationnaire. La différence entre les coefficients déterminés par ces méthodes différentes ne dépasse pas l'erreur expérimentale, supposant que les processus de sorption por ces systèmes sont contrôles par un mécanisme de diffusion selon Fick. En employant l'équation de Frisch, et en partant de données sur les coefficients de diffusion, les délais de pénétration sont calculés comme une fonction de la concentration et ces résultats sont comparés avec les valeurs observées. Les deux valeurs s'accordent, ce qui indique que l'état de pénétration non-stationnaire est contrôlé par un mécanisme de diffusion purement Fickien. Les données expérimentales pour les coefficients de diffusion thermodynamiques D_T de benzène dans les polyacrylates de méthyle et d'éthyle, sont analysées en termes simples d'une théorie développée précédement, celle du volume libre. On a trouvé dans tous les cas observés que la relation déduite s'accorde très bien avec les données expérimentales. Trois paramètres dépendant de la température et inclus dans la théorie, sont évalués et leurs variations avec la température sont discutées.

Zusammenfassung

Eine Untersuchung der Sorption und Permeation von Benzoldampf in Polymethylacrylat und Polyäthylacrylat wurde in einem verhältnissmässig grossen Temperatur- und Konzentrationsbereich durchgeführt. Die gegenseitigen Diffusionskoeffizienten wurden aus der Absorptions- und Desorptionsgeschwindigkeit sowie der Permeabilität im stationären Zustand bestimmt. Die nach den verschiedenen Methoden bestimmten Diffusionskoefficienten stimmten innerhalb der Versuchsfehler überein, was zeigt, dass die Sorptionsprozesse bei diesen Systemen durch einen echten Fickschen Diffusionsmechanismus kontrolliert werden. Mit den Gleichungen von Frisch wurde die Permeationsdurchbruchszeit als Konzentrationsfunktion aus den Diffusionskoeffizienten berechnet und mit beobachteten Werten verglichen. Die berechneten Werte stimmten mit den beobachteten überein und lassen erkennen, dass der nichtstationäre Zustand der Permeation durch einen rein Fickschen Diffusionsmechanismus kontrolliert wird. Versuchsergebnisse für den thermodynamischen Diffusionskoeffizienten D_T von Benzol in PMA und PEA wurden mit einer früher entwickelten einfachen Freien-Volums-Theorie behandelt. In allen untersuchten Fällen gibt die abgeleitete Beziehung die experimentallen Daten gut wieder. Drei in der Theorie auftretende temperaturabhängige Parameter werden ermittelt und ihre Temperaturabhängigkeit diskutiert.

Received March 26, 1962

JOURNAL OF POLYMER SCIENCE: PART A VOL. 1, PP. 1813–1837 (1963)

Effect of Solvents on the Anionic Polymerization of Styrene by Phenyllithium

ALBERT ZILKHA, SAMUEL BARZAKAY,* and ARIEL OTTOLENGHI, *Department of Organic Chemistry, The Hebrew University, Jerusalem, Israel*

Synopsis

The anionic polymerization of styrene by phenyllithium was studied in various solvents The order of the decreasing molecular weights obtained depending on the solvent, was: tetrahydrofuran ≫ toluene > benzene > petroleum ether > diethyl ether. The molecular weight, due to absence of termination, is governed by the ratio of the rate propagation to the rate of initiation (R_p/R_i). Both these rates are influenced by the dielectric constant and the solvating power of the solvent for the phenyllithium and for the growing end, solvation of the growing end being greater due to the resonance of the propagating styryl anions. This leads to the fact that on passing from petroleum ether (low dielectric constant) to tetrahydrofuran (relatively high dielectric constant and high solvating power), R_p increases much more than R_i, leading to higher molecular weight. The polymerization of styrene in mixtures of petroleum ether and tetrahydrofuran was studied by the addition of increasing amounts of tetrahydrofuran while keeping the catalyst and monomer concentrations constant. Initially (up to 2 vol.-% tetrahydrofuran) there was a sharp decrease in molecular weight due to a greater dissociation of the phenyllithium, with a corresponding increase in R_i. On further addition of tetrahydrofuran (up to about 25 vol.-%), the molecular weignt increased and approached the order of that obtained in petroleum ether. This is due to a greater increase in R_p over R_i due to greater solvation of the propagating end. At this relatively high tetrahydrofuran concentration we have maximum solvation both of the catalyst and of the growing end. With further addition of tetrahydrofuran there is a linear dependence of the molecular weight both on the concentration of the tetrahydrofuran and on the dielectric constant of the system. Ether gave the lowest molecular weights, in spite of its relatively high dielectric constant, due to greater dissociation of the catalyst associates $(C_6H_5Li)_x$ leading to an increased efficiency of the catalyst (greater R_i). Toluene and benzene led to higher molecular weights than petroleum ether, although the dielectric constants are of approximately the same order, due to the homogeneous nature of the polymerization in these solvents as compared with the heterogeneous polymerization in petroleum ether. The molecular weight increased with decrease in temperature in various solvents due to the increase in the dielectric constant and the lowering in R_i.

INTRODUCTION

The polymerization of styrene by *n*-butyllithium has recently been extensively studied. O'Driscoll and Tobolsky[1] and Welch[2,3] studied the kinetics of the polymerization of styrene in benzene solution and found

* Present address: Polymer Department, the Weizmann Institute of Science, Rehovoth.

that the rate of polymerization is accelerated by small quantities of Lewis bases. The homogeneous polymerization of styrene by *n*-butyllithium in hydrocarbon solvents at low temperatures led to the formation of isotactic polymers, while in the presence of ethers only atactic polymers were formed.[4] It was also found that stereospecific polymerization occurs with linear lithium alkyls and not with branched alkyls.[5] Recently it was reported that there is a great difference in the rates of initiation of styrene polymerization depending on the lithium alkyl derivative.[6]

Now, we have studied the polymerization of styrene by phenyllithium in various solvents, especially in petroleum ether, tetrahydrofuran, and mixtures of both, in order to find the effect of the dielectric constant and that of solvation on the rates of polymerization.

EXPERIMENTAL

Materials

Styrene (B.D.H.) was dried over anhydrous calcium chloride and distilled from sulfur under nitrogen. Before use it was fractionally distilled *in vacuo* under nitrogen, the middle fraction only, about 70% was used. Dry, oxygen-free nitrogen was used. Tetrahydrofuran was dried over potassium hydroxide pellets and then refluxed over sodium wire for several hours. Benzophenone (about 10 g./l.) was added and the reflux continued until the tetrahydrofuran became deeply blue or violet from the sodium benzophenone formed, and then distilled under nitrogen before use. Diethyl ether was refluxed over sodium wire, benzophenone added as in the case of tetrahydrofuran, and distilled. Analar grade petroleum ether (b.p. 60–80°C.), toluene, and benzene were refluxed over sodium wire and distilled under nitrogen. Dimethylformamide (B.D.H.) was dried by azeotropic distillation with benzene and then was fractionally distilled under nitrogen. Acrylonitrile was purified according to Bamford and Jenkins.[7] Methyl methacrylate was dried over sodium sulfate; before use it was fractionally distilled under nitrogen at atmospheric pressure and then *in vacuo;* the middle fraction (about 70%) was used.

Preparation of Phenyllithium

A modified procedure after Gilman and Miller[8] was used. Into a three-necked flask fitted with an adapter for introducing nitrogen, a dropping funnel and a mechanical stirrer, 350 ml. dry ether and 10 g. (1.43 g. atom) lithium wire were introduced. The flask was cooled to 0°C. and 102 g. (0.65 mole) bromobenzene previously dried over calcium chloride and distilled under nitrogen, dissolved in 100 ml. dry ether were added dropwise during 1 hr. The reaction was continued for 2 hr. more. The phenyllithium solution was centrifuged and kept in the cold. Acid-base and Volhard titrations of the catalyst solution showed that the molar ratio of bromide ion (lithium bromide) to phenyllithium in solution was 1:1.

Phenyllithium in petroleum ether (b.p. 60–80°C.) was prepared by adding the ethereal solution of phenyllithium to petroleum ether and removing the ether by distillation under nitrogen. To insure the complete removal of free ether, a part of the higher boiling petroleum ether was also distilled. The catalyst solution was centrifuged from precipitated lithium bromide, and the resulting catalyst solution in petroleum ether was found to contain phenyllithium and lithium bromide in the ratio 4:1, respectively. This ratio was obtained in different preparations and was constant. Due to the low solubility of phenyllithium in petroleum ether, it partially precipitated from solution at room temperature or lower; the supernatant catalyst solutions showed the same ratio of phenyllithium to lithium bromide. The crystals of phenyllithium that separated in the cold were found to contain ether, as shown from the infrared spectrum, so that the catalyst is probably in complex with diethyl ether and with lithium bromide. In this connection it may be mentioned that a recent work,[9] has already shown that the phenyllithium in its crystalline form, obtained from partial evaporation of the ethereal solution, is composed of $2C_6H_5Li \cdot LiBr \cdot 2(C_2H_5)_2O$.

Polymerization of Styrene

The addition of reagents and the polymerization were carried out under nitrogen. Into a three-necked flask fitted with a high-speed stirrer, a gas adapter for introducing nitrogen, a thermometer, and an outlet fitted with a seal-sealing rubber cap, freshly distilled monomer and solvent were transferred with syringes; the flask was brought to and kept at the required temperature of polymerization. The required amount of catalyst solution was then added from a syringe with fine graduations. The polymerization mixture became colored orange-brown, of variable intensity, due to the styryl carbanions formed. The polymerization was stopped after the required time by adding 2% methanolic hydrochloric acid. More methanol was added to insure complete precipitation of the polymer. The polymer was usually precipitated in a sticky condition and was kept under methanol until it completely solidified. It was then filtered off, washed with water and methanol, and then was ground to a fine powder, triturated with water and methanol, and dried to constant weight.

Molecular Weight Determinations

Polymer samples were further purified and dried for molecular weight determinations. Viscosities of polymer solutions in benzene were measured in an Ubbelohde viscosimeter. Average molecular weights of the polymers were calculated from intrinsic viscosities by use of the equation of Pepper:[10] $[\eta] = 4.37 \times 10^{-4} M^{0.66}$. This equation was found to apply to unfractionated polystyrenes having molecular weights in the range of 1×10^3–2×10^6.

Measurements of Dielectric Constants

The heterodyne beat method was used for the measurement of the dielectric constants at the required temperatures.[11] Description of the apparatus has been given elsewhere.[12]

X-Ray Diffraction Diagrams

Debye-Scherrer X-ray diffraction diagrams were taken on a Unicam Rotating Crystal Goniometer (cylindrical film, radius 30 mm.). The sample was placed with its plane approximately normal to the incoming beam, and remained stationary during exposure. CuKα radiation (λ = 1.541 A.) (Ni-filtered) was employed. The exposure time was 3 hr.

Preparation of Block Polymer of Styrene–Acrylonitrile

Styrene was polymerized in petroleum ether according to the conditions of Runs 82, 83 (Table II). The orange-brown polymer having "living" styryl carbanions precipitated from solution. After complete polymerization of the styrene, acrylonitrile (4 g.) was added in one portion, and yellowish polyacrylonitrile started to precipitate. After 30 min. the polymerization was stopped; 6.5 g. polymer was obtained, showing that 2 g. acrylonitrile was polymerized. The polymer was extracted several times with boiling benzene to remove homopolystyrene, until evaporation of the solvent left no residue. Infrared spectra of the insoluble polymer showed absorptions at 4.45 μ (cyano groups) and 14.3 μ (monosubstituted benzene) showing the presence of block polymer of polyacrylonitrile–polystyrene, possibly in admixture with homopolyacrylonitrile.

Duplicate experiments gave similar results.

Preparation of Block Polymer of Styrene–Methyl Methacrylate

Essentially the above procedure was followed. After complete polymerization of the styrene, methyl methacrylate (5 ml.) was added. After 30 min. the polymerization was stopped; 4.9 g. polymer was obtained, showing that 0.4 g. methyl methacrylate was polymerized. The polymer was extracted with boiling acetonitrile in which homopolymethyl methacrylate is soluble.[13] Infrared spectra of the residual polymer showed absorptions at 5.8 μ (ester group) and 14.3 μ (monosubstituted benzene) showing the presence of block polymer of styrene–methyl methacrylate together with homopolystyrene.

Methyl methacrylate differs from acrylonitrile in that it is not polymerized by phenyllithium,[14] so that it could have been polymerized only by the "living" polystyrene.

RESULTS

Dependence of Molecular Weight on Monomer Concentration

This was investigated with the use of tetrahydrofuran and petroleum ether as polymerization solvents. The polymerizations in tetrahydrofuran

TABLE I

Polymerization in Tetrahydrofuran. Dependence of Molecular Weight on Monomer Concentration Catalyst in Ether[a]

Run No.[b]	[Styrene], mole/l.	$[\eta]$, dl./g.	$10^{-3}M$	$\overline{DP}$	[M]/[C]	Catalyst consumed, 10^{-4} mole/l.	Catalyst consumed, %
49	0.523	0.592	55.6	534	5.81	9.8	1.1
50	0.523	0.689	70.0	672	5.81	7.8	0.9
88	0.523	0.645	63.3	608	5.81	8.6	1.0
43	0.871[c]	0.878	101.0	969	9.67	9.0	1.0
44	0.871	0.819	90.9	873	9.67	10.0	1.1
45	1.743	0.818	90.8	872	19.36	20.0	2.2
47	2.614[d]	0.913	107.3	1030	29.04	25.4	2.8

[a] Experimental conditions: catalyst used 4.5 mmole (0.09 mole/l.) in 3 ml. ether, polymerization temp. 0°C.; time 15 min.

[b] The yield in all cases is quantitative.

[c] Dielectric constant at 20°C., of the polymerization mixture = 6.80.

[d] Dielectric constant at 20°C., of the polymerization mixture = 5.67.

TABLE II

Polymerization in Petroleum Ether. Dependence of Molecular Weight on Monomer Concentration. Catalyst in Ether

Run No.[a]	[Styrene] mole/l.	$[\eta]$, dl./g.	$10^{-3}M$	$\overline{DP}$	[M]/[C]	Catalyst consumed, 10^{-2} mole/l.	Catalyst consumed, %
Series A[b]							
82	0.871	0.111	4.4	42	9.67	2.1	23.3
83	0.871	0.111	4.4	42	9.67	2.1	23.3
84	1.743	0.145	6.6	63	19.36	2.8	31.1
85	1.743	0.145	6.6	63	19.36	2.8	31.1
98	2.614	0.228	13.1	126	29.04	2.1	23.3
Series B[c]							
95	0.523	0.118	4.85	47	11.62	1.1	24.4
96	0.523	0.136	6.0	58	11.62	0.9	20.0
86	0.871	0.145	6.6	63	19.35	1.4	31.1
87	0.871	0.145	6.6	63	19.35	1.4	31.1
93	2.614	0.195	10.35	99	58.09	2.6	57.7
94	2.614	0.219	12.3	118	58.09	2.2	48.8

[a] The yield in all cases is quantitative.

[b] Experimental conditions: catalyst used 4.5 mmole (0.09 mole/l.) in 3 ml. ether; polymerization temp. 45°C.; time 30 min.

[c] Experimental conditions: As in series A except that catalyst used was 2.25 mmole (0.045 mole/l.) in 3 ml. ether.

were carried out at 0°C., while those in petroleum ether were carried out at 45°C. (No significant polymerization occurred at 0°C. in petroleum ether.) Monomer concentration was varied between 0.523 and 2.614 mole/l. It was found that in tetrahydrofuran (Table I), the molecular

TABLE III

Polymerization in Petroleum Ether. Dependence of Molecular Weight on Monomer Concentration. Catalyst in Petroleum Ether

Run No.[a]	[Styrene], mole/l.	$[\eta]$ dl./g.	$10^{-3}M$	$\overline{DP}$	[M]/[C]	Catalyst consumed, 10^{-2} mole/l.	Catalyst consumed, %
Series A[b]							
147	0.871	0.106	4.1	39	9.67	2.2	24.4
131	1.743	0.145	6.6	63	19.36	2.8	31.1
133	2.614	0.240	14.2	136	29.04	1.9	21.1
134	2.614	0.212	11.75	113	29.04	2.3	25.5
Series B[c]							
135	0.871	0.138	6.1	59	19.35	1.5	33.3
136	0.871	0.135	5.9	57	19.35	1.5	33.3
149	2.614	0.233	13.5	130	58.09	2.0	44.4
150	2.614	0.215	12.0	115	58.09	2.3	51.1

[a] The yield in all cases is quantitative.

[b] Experimental conditions: catalyst used 4.5 mmole (0.09 mole/l.) in petroleum ether; polymerization temp. 45°C.; time 30 min.

[c] Experimental conditions: as in b series A except that catalyst used was 2.25 mmole (0.045 mole/l.).

weights increased with increasing monomer concentration, at relatively low monomer concentration, and remained approximately constant with increasing monomer concentration within the range investigated. With petroleum ether the molecular weight increased continuously with increasing monomer concentration. This was investigated at two different catalyst concentrations (Table II). Similar results were obtained when catalyst dissolved in ether (Table II) or in petroleum ether (Table III) was used. In both cases approximately the same order of molecular weights was obtained, showing that the presence of a small concentration of ether and different concentrations of lithium bromide in the polymerization mixture had no appreciable effect on the molecular weights.

The molecular weights obtained in tetrahydrofuran were much higher than those in petroleum ether, and also higher than those theoretically calculated from the ratio [M]/[C].

Dependence of Molecular Weight on Catalyst Concentration

It was found that in tetrahydrofuran (Table IV), the molecular weight was independent of catalyst concentration in the catalyst range (0.04–0.18 mole/l.) investigated. In petroleum ether, with catalyst dissolved in ether (Table V) or in petroleum ether (Table VI), there was a similar increase in molecular weight, on decreasing catalyst concentration when monomer concentration was 0.871 mole/l., while on decreasing catalyst concentration, when the monomer concentration was 2.614 mole/l., the molecular weights remained approximately constant in the catalyst range investigated.

TABLE IV
Polymerization in Tetrahydrofuran. Dependence of Molecular Weight on Catalyst Concentration. Catalyst in Ether[a]

Run No.[b]	[Catalyst], mole/l.	$[\eta]$ dl./g.	$10^{-3}M$	$\overline{DP}$	[M]/[C]	Catalyst consumed, 10^{-4} mole/l.	Catalyst consumed, %
55	0.18	0.853	96.7	928	4.84	9.4	0.5
56	0.18	0.947	113.3	1089	4.84	8.0	0.45
43	0.09	0.878	101.0	969	9.67	9.0	1.0
44	0.09	0.819	90.9	873	9.67	10.0	1.1
54	0.06	0.942	112.4	1079	14.5	8.1	1.35
57	0.04	0.942	112.4	1079	21.78	8.1	2.0

[a] Experimental conditions: monomer concentration 0.871 mole/l.; catalyst was dissolved in 3 ml. ether; polymerization temp. 0°C.; time 15 min.

[b] The yield in all cases is quantitative.

TABLE V
Polymerization in Petroleum Ether. Dependence of Molecular Weight on Catalyst Concentration. Catalyst in Ether.

Run No.[a]	[Catalyst], mole/l.	$[\eta]$, dl./g.	$10^{-3}M$	$\overline{DP}$	[M]/[C]	Catalyst consumed, 10^{-2} mole/l.	Catalyst consumed, %
Series A[b]							
86	0.045	0.145	6.6	63	19.35	1.4	31.1
87	0.045	0.145	6.6	63	19.35	1.4	31.1
82	0.09	0.111	4.4	42	9.67	2.1	23.3
83	0.09	0.111	4.4	42	9.67	2.1	23.3
Series B[c]							
93	0.045	0.195	10.35	99	58.09	2.6	57.7
94	0.045	0.219	12.3	118	58.09	2.2	48.8
97	0.09	0.195	10.35	99	29.04	2.6	28.9
98	0.09	0.228	13.1	126	29.04	2.1	23.3

[a] The yield in all cases is quantitative.

[b] Experimental conditions: monomer concentration 0.871 mole/l.; polymerization temp. 45°C.; time 30 min., catalyst dissolved in 3 ml. ether.

[c] Experimental conditions: as in Series A except that monomer concentration was 2.614 mole/l.

Polymerization in Mixtures of Petroleum Ether and Tetrahydrofuran. Dependence of Molecular Weight on Added Tetrahydrofuran

a. Catalyst in Ether, Temperature of Polymerization 20°C. The effect of solvation and the dielectric constant of the solvent on the molecular weight was studied by carrying out polymerizations in mixtures of tetrahydrofuran and petroleum ether while keeping the monomer/solvent ratio constant. It was found that on changing the concentration of tetrahydrofuran in the polymerization mixture, the molecular weights were differently affected, depending on the content of tetrahydrofuran (Table VII, Fig. 1). At low tetrahydrofuran concentrations (up to 2 vol.-%) there is a con-

TABLE VI

Polymerization in Petroleum Ether. Dependence of Molecular Weight on Catalyst Concentration. Catalyst in Petroleum Ether[a]

Run No.[b]	[Catalyst], mole/l.	$[\eta]$, dl./g.	$10^{-3}M$	$\overline{DP}$	[M]/[C]	Catalyst consumed, 10^{-2} mole/l.	Catalyst consumed, %
135	0.045	0.138	6.1	59	19.35	1.5	33.3
136	0.045	0.135	5.9	57	19.35	1.5	33.3
147	0.09	0.106	4.1	39	9.67	2.2	24.4
137	0.196	0.088	3.1	30	4.44	2.9	14.8
138	0.196	0.088	3.1	30	4.44	2.9	14.8

[a] Experimental conditions: monomer concentration 0.871 mole/l.; polymerization temp. 45°C.; time 30 min.

[b] The yield in all cases is quantitative.

TABLE VII

Polymerization in Mixtures of Petroleum Ether and Tetrahydrofuran. Dependence of Molecular Weight on Added Tetrahydrofuran. Catalyst in Ether[a]

Run No.[b]	Tetrahydrofuran, vol.-%[c]	Dielectric constant at 20°C.	$[\eta]$, dl./g.	$10^{-3}M$	$\overline{DP}$	Catalyst consumed, 10^{-2} mole/l.	Catalyst consumed, %
107	—	1.96	0.138	6.1	59	1.5	16.7
108	—	1.96	0.148	6.8	65	1.3	14.4
152	0.5	2.08	0.096	3.55	34	2.6	28.9
153	1	2.11	0.085	2.95	28	3.1	34.4
109	2	2.16	0.053	1.45	14	6.2	68.9
110	2	2.16	0.053	1.45	14	6.2	68.9
154	3	2.20	0.076	2.5	24	3.6	40.0
155	4	2.24	0.092	3.3	32	2.7	30.0
111	6	2.33	0.108	4.2	40	2.2	24.4
112	6	2.33	0.120	4.95	47	1.9	21.1
113	12	2.79	0.121	5.0	48	1.8	20.0
114	12	2.79	0.125	5.25	50	1.7	18.9
115	24	3.24	0.123	5.2	50	1.7	18.9
116	24	3.24	0.135	5.9	57	1.5	16.7
117	50	4.66	0.332	23.15	222	0.4	4.4
118	50	4.66	0.304	20.25	194	0.45	5.0
199	50	4.66	0.348	24.85	239	0.36	4.0
200[d]	50	5.73	0.459	37.8	363	0.24	2.7
201[d]	50	5.73	0.420	33.1	318	0.27	3.0
119	72	5.80	0.456	37.45	360	0.24	2.7
120	72	5.80	0.466	38.7	372	0.23	2.6
102[e]	84	6.80	0.543	48.9	470	0.19	2.1

[a] Experimental conditions: catalyst used 0.09 mole/l. in 3 ml. ether; polymerization temp. 20°C.; time 60 min.; monomer concentration 0.871 mole/l.; [M]/[C] = 9.67.

[b] The yield in all cases is quantitative.

[c] Calculated as part of the total volume of the polymerization mixture (50 ml.).

[d] All the petroleum ether was replaced by diethyl ether.

[e] Polymerization time 15 min.

tinuous decrease of molecular weights with increasing tetrahydrofuran concentrations as compared with petroleum ether. At higher concentrations (2–6 vol.-%) there is a continuous sharp increase of molecular weight. A further increase of the tetrahydrofuran concentration (6–25 vol.-%) caused only a slight increase in molecular weight, until the molecular weights approached the order of those in petroleum ether. At tetrahydrofuran concentrations of 25 vol.-% and above, there is a sharp linear increase in molecular weight (Fig. 1).

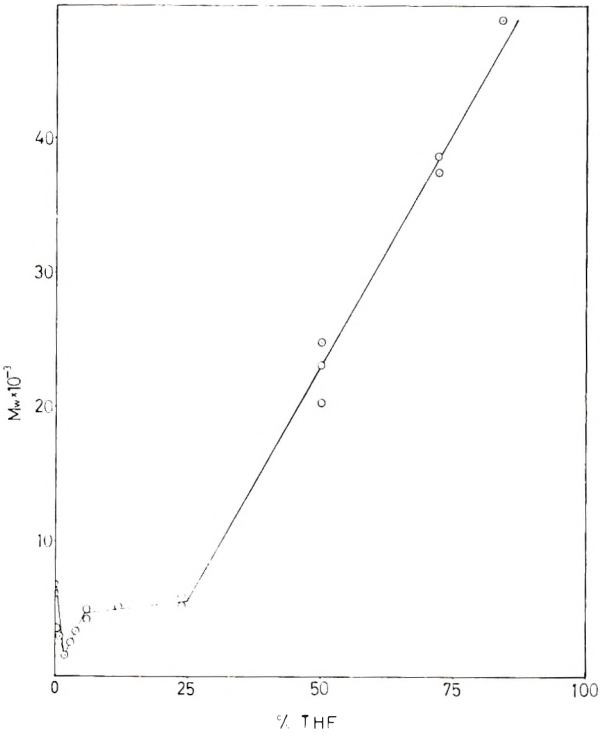

Fig. 1. Polymerization in mixtures of petroleum ether and tetrahydrofuran (catalyst in ether, temperature of polymerization 20°C.). Dependence of molecular weight on tetrahydrofuran content.

The dielectric constants of the polymerization mixtures including monomer, solvent mixture and the catalyst solvent, but without catalyst, were measured. It was found that the molecular weight varied with the dielectric constant in the same way as with tetrahydrofuran content (Fig. 2).

b. Catalyst in Petroleum Ether, Temperature of Polymerization 45°C. The same general effect obtained with change in tetrahydrofuran concentration was also obtained in these experiments (Table VIII, Fig. 3) where only petroleum ether and tetrahydrofuran were present in the polymerization solvent mixture. The lowering and increase in molecular weight over

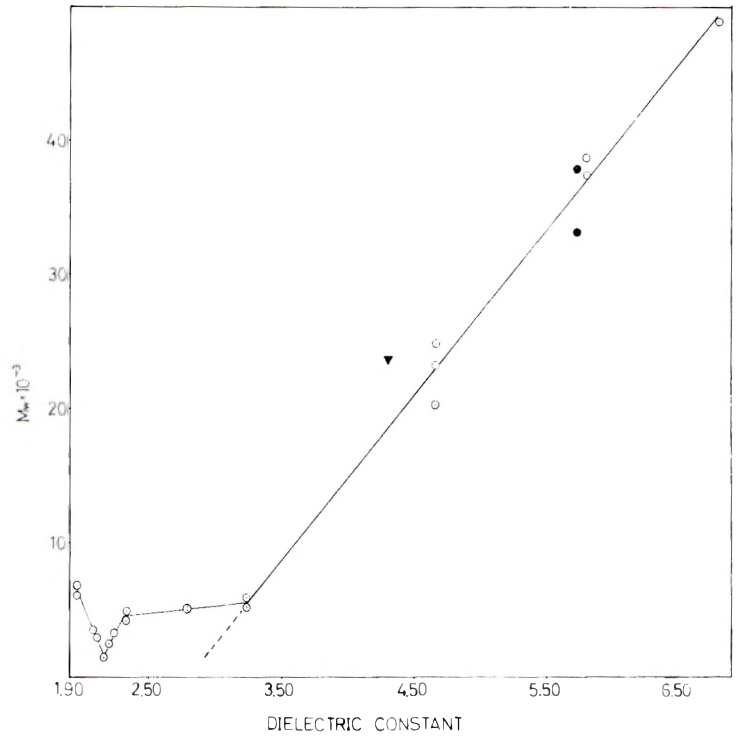

Fig. 2. Polymerization in mixtures of petroleum ether and tetrahydrofuran (catalyst in ether, temperature of polymerization 20°C.). Dependence of molecular weight on the dielectric constant of the polymerization mixture: (⊙) Polymerization in petroleum ether–tetrahydrofuran mixtures; (●) polymerization in ether–tetrahydrofuran mixtures; (▼) polymerization in ether–tetrahydrofuran (run no. 319, Table X).

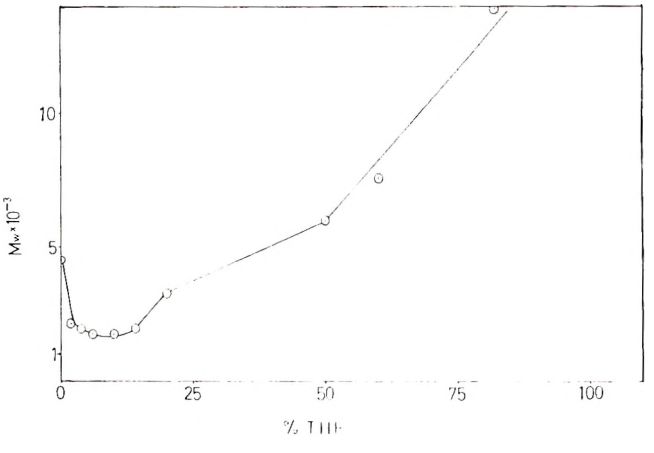

Fig. 3. Polymerization in mixtures of petroleum ether and tetrahydrofuran (catalyst in petroleum ether, temperature of polymerization 45°C.). Dependence of molecular weight on tetrahydrofuran content.

TABLE VIII

Polymerization in Mixtures of Petroleum Ether and Tetrahydrofuran. Dependence of Molecular Weight on Added Tetrahydrofuran. Catalyst in Petroleum Ether[a]

Run No.[b]	Tetrahydrofuran, vol.-%[c]	Dielectric constant at 45°C.	$[\eta]$, dl./g.	$10^{-5}M$	$\overline{DP}$	Catalyst consumed, 10^{-2} mole/l.	Catalyst consumed, %
157	—	1.94	0.113	4.5	43	2.0	22.2
158	2	2.08	0.069	2.15	21	4.1	45.6
159	4	2.16	0.065	1.95	19	4.6	51.1
160	6	2.21	0.06	1.75	17	5.1	56.7
161	10	2.44	0.06	1.75	17	5.1	56.7
162	14	2.57	0.065	1.95	19	4.6	51.1
163	20	2.91	0.092	3.3	32	2.7	30.0
164	50	4.17	0.136	6.0	58	1.5	16.7
165	60	4.78	0.159	7.6	73	1.2	13.3
166	82	5.93	0.237	13.9	133	0.7	7.8

[a] Experimental conditions: catalyst used 0.09 mole/l. in 3 ml. petroleum ether; monomer concentration 0.871 mole/l.; [M]/[C] = 9.67; polymerization temp. 45°C.; time 30 min.

[b] The yield in all cases is quantitative.

[c] Calculated as part of the total volume of the polymerization mixture (50 ml.).

the range of tetrahydrofuran concentrations (0–20 vol.-%) was continuous.

The dependence of molecular weight on the dielectric constant showed similar behavior (Fig. 4).

Polymerization in Ether, Benzene, and Toluene

Experiments carried out under the same general conditions (Table IX) with diethyl ether, benzene, and toluene as solvents showed that the

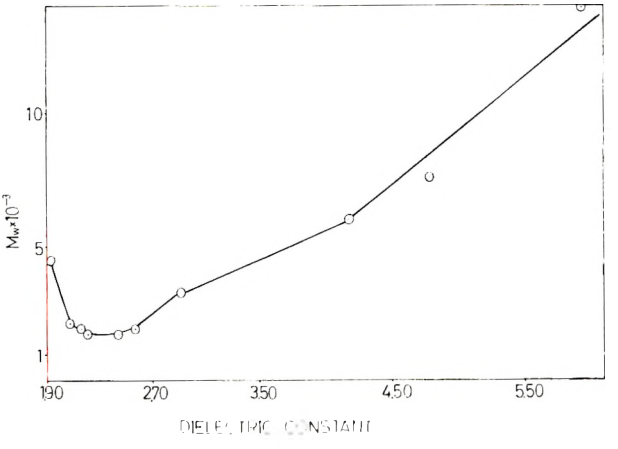

Fig. 4. Polymerization in mixtures of petroleum ether and tetrahydrofuran (catalyst in petroleum ether, temperature of polymerization 45°C.). Dependence of molecular weight on the dielectric constant of the polymerization mixture.

molecular weights obtained as compared with tetrahydrofuran and petroleum ether, were in the order: tetrahydrofuran ≫ toluene > benzene > petroleum ether > diethyl ether. Polymerization in mixtures of ether and tetrahydrofuran showed that there is an initial very large increase in molecular weight with added tetrahydrofuran, followed by a relative decrease. At high tetrahydrofuran concentrations the molecular weight increased (Table X, Fig. 5).

TABLE IX
Polymerization in Various Solvents[a]

Run No.[b]	Solvent	Solvent for catalyst[c]	Time, hr.	$[\eta]$, dl./g.	$10^{-3}M$	$\overline{DP}$	Catalyst consumed, 10^{-2} mole/l.	Catalyst consumed, %
175	Pet. eth.	Pet. eth.	1	0.145	6.6	63	1.4	15.5
107	Pet. eth.	Ether	1	0.138	6.1	59	1.5	16.7
108	Pet. eth.	Ether	1	0.148	6.8	65	1.3	14.4
180	Benzene	Pet. eth.	2	0.207	11.3	109	0.8	8.9
181	Benzene	Pet. eth.	2	0.207	11.3	109	0.8	8.9
305	Benzene	Ether	2	0.138	6.1	59	1.5	16.7
178	Toluene	Pet. eth.	2	0.263	16.3	157	0.55	6.1
182	Toluene	Pet. eth.	2	0.272	17.1	164	0.53	5.9
169	Toluene	Ether	2	0.191	10.0	96	0.91	10.1
170	Toluene	Ether	2	0.191	10.0	96	0.91	10.1
176	Ether	Pet. eth.	18	0.069	2.15	21	4.1	45.5
177	Ether	Pet. eth.	18	0.069	2.15	21	4.1	45.5
312[d]	Ether	Ether	1.5	0.071	2.25	22	4.0	44.4
313[d]	Ether	Ether	1.5	0.067	2.05	20	4.4	48.9
102	T.H.F.	Ether	0.25	0.543	48.9	470	0.19	2.1
193[e]	Pet. eth.	Pet. eth.	1.5 min.	—	—	—	—	—

[a] Experimental conditions: catalyst used 0.09 mole/l.; monomer concentration 0.871 mole/l.; [M]/[C] = 9.67; polymerization temp. 20°C.

[b] The yield in all cases is quantitative.

[c] Catalyst dissolved in 3 ml. solvent.

[d] The same polymerization (run 308) stopped after 2 min. gave 5% conversion.

[e] Polymerization temp. 45°C.; conversion 8%.

Dependence of Molecular Weight on Temperature of Polymerization

It was found that the molecular weight increased with decrease in temperature in tetrahydrofuran (Table XI), in petroleum ether (Table XII) in ether (Table XIII) and in benzene (Table XIV).

Dependence of Molecular Weight on Per Cent Conversion

It was found (Table XV) that the molecular weight increased with per cent conversion. The polymerization in tetrahydrofuran is very fast as seen from the fact that about 80% conversion was obtained after 30 sec.

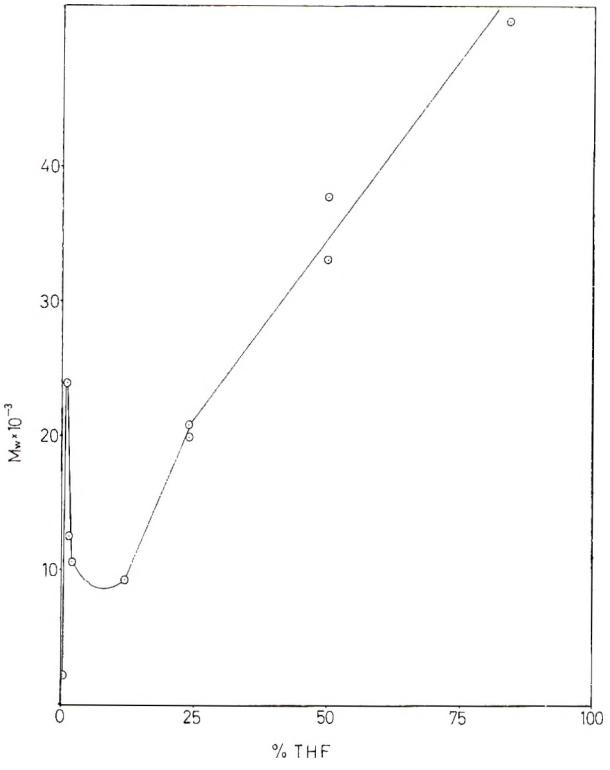

Fig. 5. Polymerization in mixtures of ether and tetrahydrofuran. Dependence of molecular weight on tetrahydrofuran content.

X-Ray Diffraction

Several samples of polystyrene prepared under different conditions were examined. The polymer obtained in petroleum ether with catalyst in the same solvent (molecular weight = 4100) (Run 147, Table III) showed two broad reflections having d values of 4.6 ± 0.4 A. (very strong) and 2.3 ± 0.2 A. (very weak), indicating some partial crystallinity. The polymer obtained in Run 82 (Table II) had similar intensities of reflection, while the very high molecular weight polymer obtained at low temperature (Run 105, Table XI) showed these two reflections a little more intensely. No other reflections were found.

DISCUSSION

In the anionic polymerization of styrene carried out in aprotic solvents, termination is negligible when the polymerizations are carried out at relatively low temperature, and living polymers are obtained. Their molecular weights are given by the ratio of the concentrations of the monomer to catalyst ([M]/[C]), and in case that only a part of the catalyst (C*) has initiated polymerization, they are given by [M]/[C*]. In the

TABLE X

Polymerization in Mixtures of Ether and Tetrahydrofuran. Dependence of Molecular Weight on Added Tetrahydrofuran. Catalyst in Ether[a]

Run No.[b]	Tetrahydrofuran, vol.-%[c]	$[\eta]$, dl./g.	$10^{-3}M$	$\overline{DP}$	Catalyst consumed, 10^{-2} mole/l.	Catalyst consumed, %
312	—	0.071	2.25	22	4.0	44.4
313	—	0.067	2.05	20	4.4	48.9
319	1[d]	0.339	23.9	229	0.38	4.2
321	1.48[e]	0.221	12.5	120	0.73	8.1
320	2	0.198	10.6	102	0.85	9.4
309	12	0.182	9.3	89	0.98	10.9
310	12	0.182	9.3	89	0.98	10.9
315	24	0.309	20.8	200	0.44	4.9
316	24	0.300	19.9	191	0.46	5.1
200[f]	50	0.459	37.8	363	0.24	2.7
201[f]	50	0.420	33.1	318	0.27	3.0
102[g]	84	0.543	48.9	470	0.19	2.1

[a] Experimental conditions: catalyst used 0.09 mole/l. in 3 ml. ether, monomer concentration 0.871 mole/l.; [M]/[C] = 9.67; polymerization temp. 20°C.; time 90 min.

[b] The yield in all cases is quantitative.

[c] Calculated as part of the total volume of the polymerization mixture (50 ml.).

[d] Tetrahydrofuran concentration 0.122 mole/l.

[e] Tetrahydrofuran concentration 0.180 mole/l.

[f] Polymerization time 60 min.

[g] Polymerization time 15 min.

TABLE XI

Effect of Temperature on the Polymerization of Styrene in Tetrahydrofuran. Catalyst in Ether[a]

Run No.[b]	Polymerization temp., °C.	Dielectric constant[c]	$[\eta]$, dl./g.	$10^{-3}M$	$\overline{DP}$	Catalyst consumed, 10^{-4} mole/l.	Catalyst consumed, %
102	20	6.80	0.543	48.9	470	19.0	2.1
43	0	7.20	0.878	101.0	969	9.0	1.0
44	0	7.20	0.819	90.9	873	10.0	1.1
103	−20	7.73	1.487	224.5	2156	4.0	0.45
105	−50	—	3.820	937.4	9001	1.0	0.1
106	−50	—	3.888	962.9	9246	0.9	0.1

[a] Experimental conditions: catalyst used 4.5 mmole (0.09 mole/l.) in 3 ml. ether; monomer concentration 0.871 mole/l.; polymerization time 15 min.; [M]/[C] = 9.67.

[b] The yield in all cases was quantitative.

[c] The dielectric constant of the system at 45°C. is 6.50, and at −33°C. is 8.49.

polymerization of styrene by sodium naphthalene all the catalyst was found to initiate polymerization at relatively high ([M]/[C]) values,[15] but at low values, the molecular weights were much higher than those required if all the catalyst had initiated polymerization.[16] This was ex-

TABLE XII

Effect of Temperature on the Polymerization of Styrene in Petroleum Ether. Catalyst in Ether[a]

Run No.[b]	Polymerization temp., °C.	$[\eta]$, dl./g.	$10^{-3}M$	$\overline{DP}$	Catalyst consumed, 10^{-2} mole/l.	Catalyst consumed, %
82	45	0.111	4.4	42	2.1	23.3
83	45	0.111	4.4	42	2.1	23.3
147[c]	45	0.106	4.1	39	2.2	24.4
157[c]	45	0.113	4.5	43	2.0	22.2
107[d]	20	0.138	6.1	59	1.48	16.7
108[d]	20	0.148	6.8	65	1.3	14.4
140[c,e]	0	—	—	—	—	—

[a] Experimental conditions: catalyst used 4.5 mmole (0.09 mole/l.) in 3 ml. ether; monomer concentration 0.871 mole/l.; [M]/[C] = 9.67; polymerization time 30 min.

[b] The yield in all cases was quantitative.

[c] Catalyst in petroleum ether.

[d] Polymerization time 60 min.

[e] Only traces of polymer were obtained.

TABLE XIII

Effect of Temperature on the Polymerization of Styrene in Ether. Catalyst in Petroleum Ether[a]

Run No.[b]	Polymerization temp., °C.	$[\eta]$, dl./g.	$10^{-3}M$	$\overline{DP}$	Catalyst consumed, 10^{-2} mole/l.	Catalyst consumed, %
188	35	0.060	1.75	17	5.1	56.7
176	20	0.069	2.15	21	4.1	45.5
177	20	0.069	2.15	21	4.1	45.5
189	0	0.124	5.2	50	1.7	18.9
190	−15	0.135	5.9	57	1.5	16.7

[a] Experimental conditions: catalyst used 4.5 mmole (0.09 mole/l.) in 3 ml. petroleum ether; monomer concentration 0.871 mole/l.; polymerization time 18 hr.; [M]/[C] = 9.67.

[b] The yield in all cases was quantitative.

TABLE XIV

Effect of Temperature on the Polymerization of Styrene in Benzene. Catalyst in Ether[a]

Run No.[b]	Polymerization temp., °C.	$[\eta]$, dl./g.	$10^{-3}M$	$\overline{DP}$	Catalyst consumed, 10^{-2} mole/l.	Catayst consumed, %
317	60	0.092	3.3	32	2.7	30.0
304	40	0.097	3.6	35	2.5	27.8
305	20	0.138	6.1	59	1.5	16.7
306	2	0.170	8.4	81	1.1	12.2

[a] Experimental conditions: catalyst used 4.5 mmole (0.09 mole/l.) in 3 ml. ether; monomer concentration 0.871 mole/l.; polymerization time 120 min.; [M]/[C] = 9.67.

[b] The yield in all cases was quantitative.

TABLE XV
Polymerization in Tetrahydrofuran. Dependence of Molecular Weight on Per Cent Conversion. Catalyst in Ether[a]

Run No.	Polymerization time, sec.	Conversion, %	$[\eta]$, dl./g.	$10^{-3}M$	$\overline{DP}$
187	3	17	0.260	16.0	154
186	6	45	0.341	24.1	231
184	15	73	0.459	37.8	363
183	30	84	0.500	43.0	413
102	900	100	0.543	48.9	470

[a] Experimental conditions: monomer concentration 0.871 mole/l.; catalyst concentration 0.09 mole/l.; reaction temp. 20°C.; catalyst dissolved in 3 ml. ether.

plained[16] by the fact that not all the catalyst molecules start polymerization, and that the monomer adds more readily to a growing anion than to catalyst. Recently,[6] the polymerization by different lithium alkyls of styrene in tetrahydrofuran at room temperature was investigated. A low monomer/catalyst ratio ([M]/[C] = 12) was used, so that the initiation will compete with the propagation for monomer throughout the polymerization. It was found that butyllithium initiated polymerization much faster than phenyllithium. This was indicated by the fact that much lower molecular weights were obtained with butyllithium, showing that more catalyst had initiated polymerization.

Polymerization in Tetrahydrofuran and Petroleum Ether

Effect of Solvent on the Degree of Polymerization. In the present work, it is seen that the molecular weights obtained in the polymerization in tetrahydrofuran are much higher than those obtained in petroleum ether. Since the average degree of polymerization (in case that the rate of initiation is relatively low and catalyst is slowly consumed) can be given by $\overline{DP} = R_p/R_i$, due to lack of termination, it follows that the ratio of the rate of propagation to the rate of initiation (R_p/R_i) in tetrahydrofuran is much greater than that in petroleum ether.

In the phenyllithium polymerization, we have the propagating end composed of the ion-pair $P{\sim}CH_2\overline{C}H(C_6H_5)Li^+$. In solvents of low dielectric constant such as petroleum ether (b.p. 60–80°C.) (dielectric constant = 1.915 as measured at 20°C.), there is a smaller separation of the ions in the ion-pair than in solvents of higher dielectric constant such as tetrahydrofuran (dielectric constant = 7.58 at 20°C.),[17] due to the need for energy to overcome the electrostatic interaction between the ions. Now, increasing the charge separation of the ion-pair increases the effective negative charge of the propagating anion and therefore can cause an increase in the rate of propagation.[18–20] Solvation of the cation by solvents that are Lewis bases such as ethers will also increase the effective charge of

the anion. It was also suggested that, in solvents of high dielectric constant and high solvating capacity, "free polymer anions"[21] (whose positive counterions have been separated) and not ion-pairs exist in the polymerization mixture. Also it is reasonable that the macroscopic dielectric constant of mixed solvents would only be of considerable importance after charge separation was made possible by solvation, as will be seen later.

The effect of solvation and dielectric constant in increasing the rate of propagation is also true for the initiation step, which is similarly an interaction of a carbanion with monomer. However, the fact that $\overline{DP}$ increases shows that the effect in increasing R_p is greater. This may be possibly due to differences in ionization and solvation of the phenyllithium and of the propagating ion-pair. It is known[22] that the C—Li bond in lithium alkyls or in phenyllithium has a low ionic character (about 40%). Much greater ionic character is shown by such lithium alkyls as benzyllithium (or styryllithium) where the anion is highly stabilized by four resonance structures.[22] It follows that the propagating ion-pair is more ionizable than the phenyllithium, and consequently, solvation of the lithium in the propagating ion-pair by tetrahydrofuran would be more than in the case of the lithium of the phenyllithium, due to its greater partial positive charge.[23]

From all this it follows that the propagating ion-pair is more ionized and solvated by tetrahydrofuran than phenyllithium. That is why R_p increased much more than R_i on passing from petroleum ether to tetrahydrofuran. It may be mentioned that the polymerization in tetrahydrofuran is much faster than in petroleum ether as indicated by the fact that conversion in tetrahydrofuran is about 80% complete after 30 sec. at 0°C. as compared with petroleum ether where the conversion was only about 8% after 90 sec. at 45°C. (Table IX). Since most of the monomer is consumed by the propagation step, further evidence for the fact that R_p in tetrahydrofuran is much greater than in petroleum ether is obtained.

Effect of Catalyst Concentration. Since in such a polymerization $\overline{DP} = [M]/[C^*]$, where C* is the concentration of catalyst which initiated polymerization, it is possible in each case to calculate the amount of consumed catalyst.[6] Comparison of Tables I and II shows that the percentage of consumed catalyst in tetrahydrofuran is much less than in petroleum ether. Thus, for polymerizations with 0.871 mole/l. monomer and 0.09 mole/l. catalyst, the amount of consumed catalyst in tetrahydrofuran at 0°C. was about 1% and in petroleum ether at 45°C. was about 23%. From this it is seen that the initiation reaction competes with the propagation for monomer much more in petroleum ether than in tetrahydrofuran. That is why the molecular weights decrease in petroleum ether with increasing catalyst concentration and are not affected in tetrahydrofuran in the catalyst range investigated. This is plausible, since only about 1% of the catalyst is consumed in tetrahydrofuran, so that catalyst is always present in very large excess, unlike the case of petroleum ether where about 25% of the catalyst or more initiates polymerization. At high monomer concentration, the influence of catalyst concentration is smaller also in petroleum ether, as

seen from Table II, where a twofold change of catalyst concentration was not found to change the molecular weights.

Polymerization in Mixtures of Petroleum Ether and Tetrahydrofuran

To explain the variations in molecular weight found in different petroleum ether–tetrahydrofuran mixtures (Fig. 1), it is necessary to deal with the following general considerations.

Phenyllithium is present as an etherate complex with lithium bromide. Also there exists the possibility of the presence of associated phenyllithium $(C_6H_5Li)_x$ in petroleum ether. These associated catalyst molecules are in equilibrium with monomeric molecules:

$$(C_6H_5Li)_x \rightleftharpoons nC_6H_5Li + (C_6H_5Li)_{x-n}$$

The monomeric or "free" phenyllithium can initiate polymerization easily. Addition of a solvent which has a greater solvating power than petroleum ether, drives the equilibrium to the right leading to increase in the concentration of free catalyst.

The polymerization steps are as follows:

Initiation:

$$C_6H_5^-Li^+ + M \xrightarrow{k_i} C_6H_5M_1^-Li^+$$

where the rate of initiation is:

$$R_i = k_i[C_6H_5^-Li^+][M]$$

Propagation:

$$C_6H_5M_1^-Li^+ + M \xrightarrow{k_p} C_6H_5M_2^-Li^+$$

$$C_6H_5M_2^-Li^+ + M \xrightarrow{k_p} C_6H_5M_n^-Li^+$$

where the rate of propagation is:

$$R_p = k_p[C_6H_5M^-Li^+][M]$$

The values of k_i and k_p, the initiation and propagation rate constants, depend on the solvation of the catalyst and the growing end, respectively, increasing with greater solvation as was explained before. These values also increase with the dielectric constant of the polymerization medium. Increase of k_i or k_p will increase R_i or R_p, respectively.

As was mentioned before, solvation of the growing end is easier than that of the phenyllithium, and this means that on increasing the solvation capability or the dielectric constant of the polymerization medium, k_p will be increased more than k_i.

These general considerations permit us to explain the dependence of molecular weight on the concentration of tetrahydrofuran. From Figure 1, the following points are observed: (*a*) at low tetrahydrofuran concentrations (up to 2 vol.-%) there is a sharp lowering of molecular weight

with added tetrahydrofuran; (*b*) the molecular weight increases with further addition of tetrahydrofuran (2–6 vol.-%); (*c*) at 6–24 vol.-% tetrahydrofuran there is a slight increase in molecular weight; (*d*) at 24 vol.-% tetrahydrofuran and above there is a linear increase in molecular weight with added tetrahydrofuran.

The initial effect of the addition of tetrahydrofuran (point *a*) is to increase the concentration of phenyllithium that participates in the initiation, by solvating the associated phenyllithium, and hence increasing R_i.

It may be mentioned that experiments carried out in the presence of 6 vol.-% of ether in the polymerization mixture (Tables II and V) led to the same molecular weights as in pure petroleum ether (the catalyst being in the form of an ethereal complex). This shows that ether is a poor solvating agent for phenyllithium as compared with tetrahydrofuran and at these relatively low concentrations it seems that it does not cause appreciable solvation of the catalyst.

Point (*b*) can be explained as follows. With more tetrahydrofuran, competitive reactions are possible. In the first place, it increases the concentration of "free" phenyllithium, and there is a consequent increase in R_i. In the second place, solvation of the growing end occurs, which increases R_p. At the relatively low range of molecular weights which exists in this range of tetrahydrofuran concentrations, the solvation has a relatively greater effect on R_p, and that is why there is increase in the molecular weights. Since the change in the dielectric constant of the system is small at these small concentrations of tetrahydrofuran (Table VII and Figure 2), the sole effect of the addition of tetrahydrofuran in this range is concerned with solvation of the catalyst (i.e., the Li cation), the lithium bromide present, the Li^+ of the growing end, and also breaking the molecular association of the phenyllithium.

It seems that solvation of the phenyllithium–lithium bromide catalyst complex with tetrahydrofuran is different from that of butyllithium, where 2 moles tetrahydrofuran were found to be sufficient to cause total solvation of the catalyst.[1–3]

Point (*c*) can be explained in that in this range of tetrahydrofuran concentration we are approaching maximum solvation of the catalyst, i.e., R_i is being increased to a maximum. The changes in R_p can be connected with the dielectric constant as seen from the next point.

Point (*d*) can be explained as follows. It is seen that the linear dependence of molecular weight on the tetrahydrofuran content starts after about 25 vol.-% of tetrahydrofuran is already present. It is quite plausible that solvation both of the catalyst or of the growing anion is already complete, and the increase in molecular weight is due to increase in the dielectric constant of the polymerization mixture. This is in accordance with the linear dependence found of the molecular weight (or R_p/R_i) with the dielectric constant at this range of tetrahydrofuran concentrations. Increase of the dielectric constant increases both R_p and R_i, only that the increase in R_p is greater, as was explained before.

If the linear curve (Fig. 2) is extrapolated, we see that in the (c) region the molecular weights obtained are higher than those that should have been given by the dielectric constant of the polymerization mixture. This seems to be due to the solvation effect which in turn increases R_p, so that the molecular weights are not much affected. These two effects on the molecular weight, namely, low dielectric constant and high solvation, seem to cancel each other. Also in this region (c) it might be that a localized concentration of the tetrahydrofuran around the polar species such as the growing end may cause the local effective dielectric constant to be higher than the average value given by the tetrahydrofuran and petroleum ether of the polymerization mixture.[24]

Proof for the fact that the linear increase of molecular weight with the dielectric constant is due only to the increase in the dielectric constant was obtained from Runs 200 and 201 (Table VII). Here petroleum ether was replaced by diethyl ether in the polymerization mixture containing 50 vol.-% tetrahydrofuran (Table VII). At such high concentration of tetrahydrofuran (which has much greater solvating power than diethyl ether), the added amount of diethyl ether cannot increase the solvation of either the catalyst or the propagating ion-pair. Its sole effect can be in increasing the dielectric constant of the polymerization mixture, as ether has a dielectric constant[25] of 4.5 at 20°C., compared to 1.915 for the petroleum ether. Actually this addition of ether increased the dielectric constant from 4.74 to 5.72. The molecular weights obtained in these experiments fall nicely on the linear curve (Fig. 1) as required by the value of the dielectric constant of the polymerization mixture. Ether alone was found to give very low molecular weights.

We tried the use of other solvents, such as ethylene dichloride, *o*-dichlorobenzene, dimethylformamide, or dimethylsulfoxide, for increasing the dielectric constants of the polymerization medium to investigate further this interesting linear dependence of molecular weight on the dielectric constant, but in all cases these solvents reacted with the catalyst.

Essentially the same results can be arrived at from consideration of the polymerization of styrene in petroleum ether–tetrahydrofuran mixtures at 45°C. using catalyst in petroleum ether (Table VIII and Figs. 3 and 4).

Reason for the Relatively High Molecular Weights in Petroleum Ether. In petroleum ether we cannot only consider the dielectric constant as being the sole or most important factor in determining the molecular weight as there is also the association of the catalyst $(C_6H_5Li)_x$ and of $(C_6H_5Li \cdot LiBr)$ complexes to be taken into consideration, so that, although for its low dielectric constant we should have obtained lower molecular weights, the small effective catalyst concentration causes lowering in R_i so that higher molecular weights are obtained.

Effect of Monomer Concentration. In petroleum ether the molecular weight increases continuously with monomer concentration at constant catalyst concentration (Tables II and III). This is in accordance with $\overline{DP} = [M]/[C^*]$. The increase is not directly proportional to the monomer

concentration, and for a fivefold increase in monomer concentration the molecular weight was only doubled.

As in the case of petroleum ether, the molecular weights in tetrahydrofuran should have increased with increasing monomer concentration. However, the polymerizations were carried out under conditions whereby the volume of the polymerization mixture was kept constant. Considerable increase of the concentration of the styrene leads to a corresponding decrease in the concentration of tetrahydrofuran present in the polymerization mixture. Since styrene has a lower dielectric constant than tetrahydrofuran (2.4 as compared to 7.58 for tetrahydrofuran at 20°C.), it follows that increasing the styrene concentration is accompanied by a decrease in the dielectric constant of the polymerization mixture (Table I). This decrease causes a lowering in molecular weight. The overall effect is that we have two opposing effects one of increasing and the other of decreasing the molecular weight. Both these effects seem to cancel each other, and that is why we have no appreciable variation of molecular weight in tetrahydrofuran with increase in monomer concentration (0.871–2.164 mole/l.) (Table I).

On the other hand, the molecular weights were found to increase with monomer concentration at low monomer concentrations (0.523–0.871 mole/l.). This is due to the fact that increasing the monomer concentration causes increase in molecular weights, while the very small change in dielectric constant at such low monomer concentrations is not enough to cancel the greater effect of increasing the molecular weight due to increase of the monomer concentration.

Effect of Temperature. It is seen that the molecular weight increased with decrease of temperature. As was mentioned before, the molecular weight is given by the ratio R_p/R_i. The increase in molecular weight shows therefore that R_i is probably decreased. This is especially seen in petroleum ether, where lowering of the temperature alone, prevents initiation of the polymerization (Run 140, Table XII). The initiation step needs a certain activation energy, and on lowering the temperature R_i will therefore decrease. The increase of molecular weight with lowering in temperature is also due to the appreciable changes in the dielectric constant of the polymerization mixture. The dielectric constant increases on lowering the temperature (Table XII), and hence it is also responsible for the increase in molecular weight.

In the case of benzene, where the dielectric constant is approximately the same over a wide range of temperature,[25] the increase in molecular weight with decrease in temperature cannot be due to changes in the dielectric constant but to decrease in R_i. A semilogarithmic plot of the molecular weight against the reciprocal of the polymerization temperature gave a straight line whose slope corresponds to the difference in activation energy between propagation and initiation (the two reactions which control the molecular weight in this case) of 3.3 kcal./mole, as calculated from the equation, $d \ln M/dT = \Delta E/RT^2$.

Polymerization in Toluene and Benzene

The molecular weights obtained in toluene were higher than those obtained in petroleum ether (Table IX). The difference between the dielectric constants (toluene has dielectric constant of 2.4 at 20°C.)[25] is not enough to explain the increase. The increase in molecular weights is also connected with the nature of the polymerization. In petroleum ether, the polymerization is heterogeneous, and the "living" polystyrene precipitates. This decreases the contact between the growing end of the polymer and the monomer in solution. Meanwhile, this monomer can react with catalyst in solution, and new polymer chains start. In toluene, the "living" polystyrene remains in solution and can react with monomer more freely, thus leading to the higher molecular weights. The molecular weights in benzene (Table IX) are also higher than those in petroleum ether for the same reason.

When the catalyst is in ether and not in petroleum ether, the molecular weights obtained in toluene and benzene are lower, probably due to more participation of the catalyst in the polymerization.

Polymerization in Ether

In all the polymerizations studied in various solvents with the catalyst dissolved in ether, the molecular weights were either the same or less than those obtained with the catalyst dissolved in petroleum ether. It is known that in ether association of lithium alkyls occurs to a certain extent, although ether has a complexing ability being a Lewis base. Therefore, ether can reduce the association of the $(C_6H_5Li)_x$ relatively to petroleum ether, but, unlike tetrahydrofuran, is not strong enough to cause high solvation and complete dissociation into ions of the growing ion-pairs or of the phenyllithium. This fact seems to show that ether affects only the initiation step as can be seen from the following evidences: (*a*) low $\overline{DP}$ in ether; (*b*) slow polymerization; (*c*) low molecular weights in spite of the relatively high dielectric constant.

(*a*) The molecular weights obtained in ether were lower than those obtained in petroleum ether, i.e., the R_p/R_i ratio in ether is smaller, as required by an increase in R_i due to an easier initiation of the polymerization by the less associated catalyst.[1,3] Also, the fact that $\overline{DP}$ decreases sharply relatively to petroleum ether, shows, that, unlike R_i, R_p was not affected significantly on passing from petroleum ether to ether.

(*b*) The insignificant effect of ether on R_p may be seen from the relatively slow polymerization in ether (Run 308, Table IX), which is similar to that in petroleum ether (Run 193, Table IX), but much slower than that in tetrahydrofuran (Run 183, Table XV).

(*c*) It seems that the increase in R_p (or molecular weight) caused by increase of the dielectric constant is more effective when the solvation and the dissociation into ions of the growing ion-pairs is complete (Fig. 2). Now ether, leading to low molecular weights, although having a relatively

high dielectric constant (4.34 at 20°C.)[25] only proves this assumption to be true in this case too; its poor solvation of the growing ion-pairs does not affect R_p significantly, but increases R_i as explained.

The above considerations are nicely reflected from the results of the polymerizations in mixtures of ether and tetrahydrofuran (Table X, Figure 5). Addition of 1 vol.-% tetrahydrofuran (Run 319, Table X) increased greatly the molecular weight. This is due to the fact that R_i increased considerably due to preferred solvation by tetrahydrofuran of the growing end over that of phenyllithium, as was explained before. This effect is especially pronounced at very low tetrahydrofuran concentrations, since insufficient tetrahydrofuran is present for complete solvation of both the catalyst and the growing ends (at least two tetrahydrofuran molecules can complex with an R—Li).[1,3]

It is interesting to note that the molecular weight obtained in Run 319 (Table X) is as required by the dielectric constant of the polymerization mixture (approximately 4.3), as can be seen from Figure 2.

This initial increase in molecular weight at very low concentrations of tetrahydrofuran is different from what was found in petroleum ether, where initial addition of tetrahydrofuran led to considerable lowering in molecular weight. This is because ether has already caused solvation of the catalyst, and addition of tetrahydrofuran has a similar effect, as was found at tetrahydrofuran concentrations of 2–6 vol.-% by volume in the polymerizations carried out in petroleum ether–tetrahydrofuran mixtures (Fig. 1), where the molecular weights increased with increasing tetrahydrofuran concentration.

With higher concentrations of tetrahydrofuran (1.5–12 vol.-%), the molecular weight decreased due to increase in the initiation. This is due to a more available amount of tetrahydrofuran that can cause also solvation of the catalyst. At still higher tetrahydrofuran concentrations, the molecular weight increased continuously with increase in the tetrahydrofuran concentration due to increase in the dielectric constant.

References

1. O'Driscoll, K. F., and A. V. Tobolsky, *J. Polymer Sci.*, **35**, 259 (1959).
2. Welch, F. J., *J. Am. Chem. Soc.*, **81**, 1345 (1959).
3. Welch, F. J., *J. Am. Chem. Soc.*, **82**, 6000 (1960).
4. Kern, R. J., *Nature*, **187**, 410 (1960).
5. Braun, D., W. Betz, and W. Kern, *Makromol. Chem.*, **42**, 89 (1960).
6. Waack, R., and M. A. Doran, *Polymer*, **2**, 365 (1961).
7. Bamford, C. H., and A. D. Jenkins, *Proc. Roy. Soc. (London)*, **A216**, 515 (1953).
8. Gilman, H., and L. S. Miller, in *Organic Reactions*, R. Adams, Ed., Vol. VI, Wiley, New York, 1951, p. 253.
9. Talalaeva, T. V., and K. A. Kocheshkov, *Dokl. Akad. Nauk. SSSR*, **104**, 260 (1955).
10. Pepper, D. C., *J. Polymer Sci.*, **17**, 347 (1951).
11. LeFevre, R. J. W., *Dipole Moments*, Methuen, London, 1953, p. 35.
11. Ben-Dor, L., Ph.D. Thesis, Hebrew University, Jerusalem, 1959.

13. O'Driscoll, K. F., R. J. Boudreau, and A. V. Tobolsky, *J. Polymer Sci.*, **31**, 115 (1958).

14. Schreiber, H., *Makromol. Chem.*, **36**, 86 (1959).

15. Waack, R., A. Rembaum, J. D. Coombes, and M. Szwarc, *J. Am. Chem. Soc.*, **79**, 2026 (1957).

16. Lyssy, T., *Helv. Chim. Acta*, **42**, 2245 (1959).

17. Critchfield, F. E., J. A. Gibson, Jr., and J. L. Hall, *J. Am. Chem. Soc.*, **75**, 6044 (1953).

18. Hughes, E. D., and C. K. Ingold, *J. Chem. Soc.*, **1935**, 244.

19. Hine, J., *Physical Organic Chemistry*, McGraw-Hill, New York, 1956, p. 83.

20. Szwarc, M., *Fortschr. Hochpolymer. Forsch.*, **2**, 300 (1960).

21. Tobolsky, A. V., and C. E. Rogers, *J. Polymer Sci.*, **40**, 73 (1959).

22. Braude, E. A., *Progress in Organic Chemistry*, J. W. Cook, Ed., Vol. 3, Butterworths, London, 1955, p. 172.

23. Ingold, C. K., *Structure and Mechanism in Organic Chemistry*, Cornell Univ. Press, Ithaca, N. Y., 1953, p. 346.

24. George, J., H. Wechsler, and H. Mark, *J. Am. Chem. Soc.*, **72**, 3891 (1950).

25. *Handbook of Chemistry and Physics*, 41st Ed., Chemical Rubber Publishing Co., Cleveland, Ohio, 1959, p. 2513.

Résumé

On a étudié la polymérisation anionique du styrène par le phényllithium dans différents solvants. L'ordre de décroissance des poids moléculaires obtenus en fonction du solvant est: tétrahydrofuranne ≫ toluène > benzène > éther de pétrole > éther diéthylique. Les poids moléculaires par suite de l'absence de réaction de terminaison sont déterminés par le rapport de la vitesse de propagation et de la vitesse d'initiateur (R_p/R_i). Ces deux vitesses sont influencées par la constante diélectrique et le pouvoir de solvatation du solvant vis-à-vis du phényllithium et vis-à-vis de la chaîne en croissance; la solvattaion de la chaîne en croissance étant plus grande à cause de la stabilisation par résonance de l'anion styrylique. Ceci conduit au fait qu'en passant de l'éther de pétrole (constante diélectrique faible) au tétrahydrofuranne (relativement élevée et haut pouvoir solvatant), R_p décroît beaucoup plus que R_i conduisant à des poids moléculaires plus élevés. La polymérisation du styrène dans les mélanges éther de pétrole et tétrahydrofuranne a été étudiée par des additions de quantités croissantes de tétrahydrofuranne en maintenant les concentrations en catalyseur et en monomère constantes. Initialement (audessus de 2% en volume de tétrahydrofuranne) il y a une forte diminution dans le poids moléculaire due à une plus grande dissociation du phényllithium, accompagnée d'une augmentation correspondante de R_i. Par addition ultérieure de tétrahydrofuranne (jusqu'environ 25% en volume), le poids moléculaire augmente e atteint l'ordre obtenu dans l'éther de pétrole. Ceci est causé par une augmentation de R_p plus importante que R_i due à une plus grande solvatation de la fin de chaîne en propagation. À cette concentration relativement élevée en tétrahydrofuranne, on a une solvatation maximum et du catalyseur et de la fin de chaîne en croissance. Par addition de tétrahydrofuranne il y a une dépendance linéaire du poids moléculaire à la fois de la concentration du tétrahydrofuranne et de la constante diélectrique du système. L'éther donne les poids moléculaires les plus bas malgré sa constante diélectrique relativement élevée, due à la plus grande dissociation du catalyseur associé $(C_6H_5Li)_x$ conduisant à une efficacité plus importante du catalyseur (R_i plus grand). Le toluène et le benzène donne des poids moléculaires plus élevés que l'éther de pétrole bien que les constantes diélectriques soient approximativement du même ordre, par suite de la nature homogène de la polymérisation dans ces solvants si on les compare avec la polymérisation hétérogène dans l'éther de pétrole. Le poids moléculaire augmente avec la diminution de température dans divers solvants à cause de l'augmentation de la constante diélectrique et la diminution de R_i.

Zusammenfassung

Die anionische, durch Phenyllithium angeregte Polymerisation von Styrol wurde in verschiedenen Lösungsmitteln untersucht. Die erhaltenen Molekulargewichte nahmen in Abhängigkeit vom Lösungsmittel in folgender Reihenfolge ab: Tetrahydrofuran $\gg$ Toluol > Benzol > Petroläther > Diäthyläther. Das Molekulargewicht ist wegen des Fehlens eines Abbruchs durch das Verhältnis von Wachstumsgeschwindigkeit zu Startgeschwindigkeit (R_p/R_i) bestimmt. Beide Geschwindigkeiten werden durch die Dielektrizitätskonstante und Solvatationsfähigkeit des Lösungsmittels für Phenyllithium und das wachsende Kettenende beeinflusst; die Solvatisierung des wachsenden Kettenendes ist wegen der Resonanz des Styrylanions grösser. Das führt dazu, dass beim Übergang von Petroläther (niedrige Dielektrizitätskonstante) zu Tetrahydrofuran (relativ hohe Dielektrizitätskonstante und hohes Solvatisierungsvermägen) R_p viel stärker zunimmt a s R_i und so höhere Molekulargewichte entstehen. Die Polymerisation von Styrol in Gemischen von Petroläther und Tetrahydrofuran wurde durch Zusatz von steigenden Mengen von Tetrahydrofuran unter Konstanthaltung der Katalysator- und Monomerkonzentration untersucht. Anfänglich (bis zu 2 Vol. % Tetrahydrofuran) trat, durch die stärkere Dissoziation des Phenyllithiums bedingt, eine scharfe Abnahme des Molekulargewicths mit einem entsprechenden Anstieg von R_i auf. Bei weiterem Zusatz von Tetrahydrofuran (bis zu etwa 25 Vol.-%) nahm das Molekylargewicht zu und näherte sich dem in Petroläther erhaltenen. Die Ursache dafür liegt in einer stärkeren, durch die grössere Solvatisierung des wachsenden Ketgenendes bedingten, Zunahme von R_p gegen R_i. Bei dieser verhältnismässig hohen Tetrahydrofurankonzentration wird eine maximale Solvatisierung von Katalysator und wachsendem Kettenende erreicht. Bei weiterem Zusatz von Tetrahydrofuran besteht eine lineare Abhängigkeit des Molekulargewichts von der Tetranhdrofurankonzentration und von der Dielektrizitätskonstanten des Systems. Äther lieferte, ungeachtet seiner relativ hohen Dielektrizitätskonstanten, die niedrigsten Molekulargewichte; der Grund liegt in der stärkeren Dissoziation der Katalysatorassoziate $(C_6H_5Li)_x$, die zu einer grösseren Wirksamkeit des Katalysators (grösseres R_i) führt. In Toluol und Benzol entstanden höhere Molekulargewichte als in Petroläther, obgleich die Dielektrizitätskonstanten angenähert gleich sind; das ist durch den homogenen Verlauf der Polymerisation in diesen Lösungsmitteln, im Gegensatz zur heterogenen Polymerisation in Petroläther bedingt. Das Molekulargewitch nahm mit fallender Temperatur in verschiedenen Lösungsmitteln, wegen der Zunahme der Dielektrizitätskonstanten und der Erniedrigung von R_i zu.

Received February 26, 1962
Revised April 20, 1962

JOURNAL OF POLYMER SCIENCE: PART A VOL. 1, PP. 1839–1856 (1963)

Olefin Polymerizations and Polyolefin Molecular Weight Distribution

JAMES C. W. CHIEN, *Hercules Research Center Hercules Powder Company, Wilmington, Delaware*

Synopsis

A method for rapid determination of the nonuniformity coefficient, $\bar{M}_w/\bar{M}_n$, of linear polyethylenes and crystalline polypropylenes is described. The number-average molecular weight $\bar{M}_n$ was determined by counting the number of C^{14}-labeled alkyl groups introduced into the polymers during the initiation step. The weight-average molecular weight $\bar{M}_w$ was calculated from viscometric data. The errors in these calculations were estimated. The values of $\bar{M}_w/\bar{M}_n$ thus obtained for eleven samples of linear polyethylenes and three samples of crystalline polypropylenes are compared with the corresponding results obtained by polymer fractionations. The agreement was good for all the polyethylene and polypropylene samples studied except for three high viscosity polyethylene samples with high $\bar{M}_w$ values and low $\bar{M}_n$ values from fractionation data. The $\bar{M}_w/\bar{M}_n$ values were determined for polymer samples taken during ethylene polymerizations initiated by the $(C_5H_5)_2TiCl_2$–$(CH_3)_2AlCl$ system. This ratio at first decreased with the polymerization time, then reached a minimum as the concentration of growing chains reached a maximum. Comparison of polyethylene produced at various temperatures reveals that the width of polymer distribution decreases with rising polymerization temperatures. This decrease is attributed to the increase in the rates of initiation and termination and the higher activation energy for the termination processes. High catalyst concentrations yielded polyethylenes of broad distributions. At high catalyst concentrations, the concentrations of growing chains are also high. Consequently, more low molecular weight chains terminate early to give products with large $\bar{M}_w/\bar{M}_n$. On the other hand, increase of the Al/Ti ratio increases chain transfers giving polyethylenes having a low $\bar{M}_w/\bar{M}_n$. An additional effect of increasing the Al/Ti ratio is the decreased variation of $\bar{M}_w/\bar{M}_n$ with t. The $\bar{M}_w/\bar{M}_n$ values of crystalline polypropylene samples taken during polymerizations initiated by α-$TiCl_3$–$(C_2H_5)_2AlCl$ are also presented. They were high at the beginning of the polymerizations and decreased gradually to a lower constant value. At higher temperatures, this variation was less pronounced; and the $\bar{M}_w/\bar{M}_n$ values were lower than those for the polymers obtained at lower temperatures. The $\bar{M}_w/\bar{M}_n$ values were insensitive to experimental variables such as the catalyst concentrations, the Al/Ti ratios, and the monomer pressures in agreement with the kinetic results. The $\bar{M}_w/\bar{M}_n$ values of amorphous polypropylene samples taken during propylene polymerizations did not vary with t or with the other polymerization conditions. These results support the earlier kinetic interpretation that extensive chain transfers occur during the formation of amorphous polypropylenes.

INTRODUCTION

Numerous studies have been reported on the characterization of linear polyethylenes and crystalline polypropylenes. Tung[1] and Kaufman and Walsh[2] combined fractionation with some methods of molecular weight

determination to obtain relationships for $[\eta]$–$\bar{M}_n$ for linear polyethylenes, and Chiang[3] obtained the $[\eta]$–$\bar{M}_w$ relationship for Hi-fax polyethylene (trademark Hercules Powder Co.). Ciampa[4] reported an $[\eta]$–$\bar{M}_n$ expression for crystalline polypropylene; Chiang[5] obtained an $[\eta]$–$\bar{M}_w$ relationship for Pro-fax polypropylene (trademark Hercules Powder Co.). Wesslau[6] proposed a distribution function for linear polyethylene. Shyluk[7] demonstrated that the same distribution function may be used to describe Pro-fax polypropylene.

The procedures above are necessary to characterize the molecular weight distributions and intrinsic viscosity–molecular weight relationships of polymer systems. Thereafter, the knowledge of the nonuniformity coefficient, $\bar{M}_w/\bar{M}_n$, of a polymer is generally sufficient for process control, and for correlation with physical and mechanical properties. Taylor and Tung[8] used a turbidimetric method to determine $\bar{M}_w/\bar{M}_n$. Their empirical correlation remains to be verified. Blackmore and Alexander[9] combined infrared endgroup analysis and viscometry to obtain $\bar{M}_w/\bar{M}_n$. For some of the high viscosity fractions, the values of $\bar{M}_n$ calculated from methyl group and vinyl group analyses disagreed.

In this work, $\bar{M}_n$ was determined by the counting of the number of C^{14}-labeled alkyl groups in polymers introduced during the initiation step of the olefin polymerizations, and $\bar{M}_w$ was calculated from viscometric measurements. The results are compared with those obtained by polymer fractionation.

There have been several attempts to express $\bar{M}_w$ and $\bar{M}_n$ as a function of reaction time for vinyl polymerizations. These were mathematical treatments based upon *a priori* kinetics. Gold[10] discussed the case of first-order initiation and nonterminative polymerization. Kyner, Radock, and Wales[11] extended the treatment to include chain transfer with monomer. Neither was applied to actual systems. Using the radioactive tracer technique, Chien[12,13] followed the variation of $\bar{M}_n$ with reaction times for low-pressure ethylene and propylene polymerizations. In this paper the change of $\bar{M}_w/\bar{M}_n$ as a function of polymerization time is presented. The effects of polymerization conditions upon the molecular weight distribution of the polymers are examined.

DETERMINATIONS AND CALCULATIONS OF MOLECULAR WEIGHTS

Radioactive Tracer Determination of $\bar{M}_n$

Radioactive tracer determination of $\bar{M}_n$ is an extension of the method of endgroup analysis. Using C^{14}-labeled 2,2′-azobisisobutyronitrile, Arnett and co-workers[14] determined $\bar{M}_n$ for polymethyl methacrylates. Chien[12] found that polyethylenes prepared with the bis(cyclopentadienyl)titanium dichloride–dimethylaluminum chloride system contained an average of 1.07 C^{14}-methyl groups per molecule. In a similar study, the polypropylenes prepared with the α-$TiCl_3$–diethylaluminum chloride system also con-